BULGARIAN CHEMICAL COMMUNICATIONS

2008 Volume 40 / Number 4

Journal of the Chemical Institutes
of the Bulgarian Academy of Sciences
and of the Union of Chemists in Bulgaria

EDITORIAL

Bulgarian Chemical Communications dedicates gratefully this jubilee issue to Academician Professor D.Sc. Ivan Nikolov Juchnovski on the occasion of his 70th anniversary.

Academician Juchnovski has been working for more than 45 years in the field of basic research in the physical organic chemistry, molecular spectroscopy, quantum chemistry and correlational analysis, as well as in the applied research directions of highly productive and ecologically pure technologies for both galvanics and microplating. The two types of activities are very successful, realized on a high scientific, respectively technological level; they contribute to the establishing of the author's prestigious reputation both in Bulgaria and abroad.

Bulgarian Chemical Communications would like to thank all the colleagues, who wrote articles for this jubilee issue and wishes to Academician Juchnovski many happy anniversaries and fruitful years of work.

I. Binev
A. Popova

Bulgarian Chemical Communications, Volume 40, Number 4 (pp. 373–385) 2008

IVAN NIKOLOV JUCHNOVSKI

Academician, Professor, D.Sc., Master of Chemical Engineering

Biographical and professional data

Birth date: 12 August 1937
Birth place: Sofia, Bulgaria
Official address: Institute of Organic Chemistry with Centre of Phytochemistry, Acad. G.Bonchev St., Bld. 9, 1113 Sofia, Bulgaria
Tel.: (+359 2) 873 99 98; (+359 2) 9606 118
Fax: (+359 2) 931 00 18
e-mail: juchnovski@ orgchm.bas.bg
soa@orgchm.bas.bg

Education:
1961 – *Master* of Chemical Engineering (organic synthesis, pharmaceuticals and polymers).
Higher Institute of Chemical Technology, Sofia

Scientific degrees:
1968 – *Ph.D.* in organic chemistry, Institute of Organic Chemistry with Centre of Phytochemistry of the Bulgarian Academy of Sciences, Sofia
1982 – *D.Sc.* in theoretical organic chemistry, Institute of Organic Chemistry with Centre of Phytochemistry of the Bulgarian Academy of Sciences, Sofia.

Positions occupied
1961–1963 – *Assistant Professor* at the Organic Chemistry Department at the Higher Institute of Chemical Technology, Sofia
1963–1972 – *Junior scientist* at the Institute of Organic Chemistry with Centre of Phytochemistry of the Bulgarian Academy of Sciences, Sofia
1972–1984 – *Senior scientist* at the Institute of Organic Chemistry with Centre of Phytochemistry of the Bulgarian Academy of Sciences, Sofia
1963–1987 – *Lecturer* at the Department of Organic Chemistry, St. Kliment Ohridski University of Sofia
1979 – *Founder and Head* of the Laboratory of Structural Organic Analysis at the Institute of Organic Chemistry with Centre of Phytochemistry of the Bulgarian Academy of Sciences, Sofia
1984 – *Professor* of Physical Methods in the Organic Chemistry at the Institute of Organic Chemistry with Centre of Phytochemistry of the Bulgarian Academy of Sciences, Sofia
1989–1994 – *Director* of the Institute of Organic Chemistry with Centre of Phytochemistry of the Bulgarian Academy of Sciences, Sofia
1992–1999 – *President* of the National Science Fund at the Ministry of Education and Science
1990–1996 – *Vice President* of the Bulgarian Academy of Sciences
1991–1992 – *Chief Scientific Secretary* and *Vice President* of the Bulgarian Academy of Sciences
1996–2000, 2000–2004, 2004–2008 – *President* of the Bulgarian Academy of Sciences

© 2008 Bulgarian Academy of Sciences, Union of Chemists in Bulgaria

Honorary titles, awards, orders, medals

1970, 1972 – *Honorary awards*
– *For contributions to the technical progress* by the State Committee for Science and Technical Progress
– D*imitrov Award* for the creation of a technology for bright acidic copper electroplating

1980 – *Honorary Inventor* Title
1989 – *Corresponding Member* of the Bulgarian Academy of Sciences
1997 – *Academician (Full Member)* of the Bulgarian Academy of Sciences
1997 – *Marin Drinov* Honorary sign of the Bulgarian Academy of Sciences
1997 – *Honorary citizen* of the town of Sevlievo
1997 – *Honorary sign with a blue band* of St. Kliment Ohridski University of Sofia
1998 – Included in the *Golden Book* of inventors and innovators of the Patent Institute of the Republic of Bulgaria
– *Prof. Asen Zlatarov* Honorary medal of the Union of Chemists in Bulgaria
2001 – Honorary medal of the Federation of the Science-Technical Unions in Bulgaria
2004 – Honorary sign of the Union of Scientists in Bulgaria
– *Stara Planina* Order – first grade of the Republic of Bulgaria
– *Doctor Honoris Causa* of:
Paisiy Khilendarski University of Plovdiv;
Chernorizets Khrabar Free University of Varna;
University of Chemical Technology and Metallurgy, Sofia;
University of Kharkov, Republic of Ukraine;
– *St. St. Cyril and Methodius* Order – neck-line trimming of the Republic of Bulgaria;
– *Member of the European Academy of Sciences and Arts*, Paris;
– *Member of the Leibnitz Society*, Berlin.

Research activities and professional interests

The research fields of Academician I. N. Juchnovski are the electronic and steric structures of the conjugated organic compounds, and of their anionic derivatives (unstable species, intermediates in important organic reactions), studied by methods of vibrational spectroscopy, quantum chemistry and correlational analysis. His main basic research contributions, known world wide are in the field of the structures and infrared spectra of radical-anions and carbanions, as well as in the correlation analysis. The phenomena *Abnormally strong electronic interaction between functional groups* and *Abnormally high intensities in the infrared spectra of negative ions* are discovered by Academician I. N. Juchnovski; their theoretical interpretation is also given by him.

Academician I. N. Juchnovski has published more than 150 scientific articles, monographs and review papers. He has been supervisor of more than 15 Ph.D. students.

He has implemented a number of applied research achievements on highly productive and ecologically clean technologies for the general and specialized galvanotechnics, as well as for the microelectronics. Out of his 18 inventions, 15 have already been implemented as basic technologies for both the copper and zinc electroplating in more than one hundred large enterprises in Bulgaria and abroad.

LIST OF PUBLICATIONS

1. Certain relations between the physicochemical properties of the homologue compounds,
   I. Juchnovski,
   Ann. Inst. Chim. Technol., **9,** 153 (1962) (in Bulgarian).
2. Reaction of 2,3-diaryl and 2-aryl-3-alkylindenones with nitrogen oxides,
   B. Aleksiev, Ch. Ivanov, I. Juchnovski,
   Dokl. AN SSSR, **149,** 1315 (1963) (in Russian).
3. Stability and spectroscopic properties of intermediate products of the nitration of certain 2,3-disubstituted indenones,
   B. Aleksiev, Ch. Ivanov, I. Juchnovski,
   Dokl. AN SSSR, **150,** 89 (1963) (in Russian).
4. Infrared spectra of 2,3-disubstituted indenones. Carbonyl group frequencies in the infrared spectra of 2,3-disubstituted indenones,
   Ch. Ivanov, I. Juchnovski,
   Ann. Inst. Chim. Technol., **11,** 1 (1964) (in Bulgarian).
5. Some additions to the conjugation coefficients method,
   I. Juchnovski,
   Izv. Inst. Org. Chem., **1,** 109 (1964) (in Bulgarian).
6. Infrared spectra of 2,3-disubstituted indenones. II. Phenyl group frequencies in the region near 700 cm^{-1},
   Ch. Ivanov, I. Juchnovski,
   Ann. Inst. Chim. Technol., **12,** 71 (1965) (in Bulgarian).
7. Infrared spectra of 2,3-disubstituted indenones. III. Phenyl group frequencies in the 900–1700 cm^{-1} region,
   Ch. Ivanov, I. Juchnovski,
   Ann. Inst. Chim. Technol., **12,** 81 (1965) (in Bulgarian).
8. Resonance energy calculations of complex molecules on the basis of the conjugation coefficients method,
   I. Juchnovski,
   C. R. Acad. Bulg. Sci., **18,** 817 (1965) (in Russian).
9. Use of the conjugation coefficients method in the study of certain conjugated systems,
   I. Juchnovski,
   Izv. Inst. Org. Chem., **2,** 85 (1965) (in Russian).
10. Über die Frequenz der C≡N Gruppe konjugierter Nitrile in ihren IR Spektren.
    I. Juchnovski, B. Jordanov, M. Agova,
    Commun. Depart. Chem. Bulg. Acad. Sci., **2,** 13 (1965).
11. Polar effects transmission in conjugated systems. Frequency and integrated intensity of the C≡N group in the infrared spectra of substituted *trans*-α-cyanostilbenes,
    I. Juchnovski,
    Dokl. AN SSSR, **168,** 1117 (1966) (in Russian).
12. Über den Zusammenhang zwischen Bindungsordnung und Frequenz in den IR-Spektren Konjugierter Nitrile und Aldehyde,
    I. Juchnovski,
    C. R. Acad. Bulg. Sci., **19,** 1151 (1966).
13. Untersuchung der Schwächung des polaren Effekte der Substituenten auf die Frequenz der (C≡N) - Gruppe in Zimtnitrilen und deren Derivativen,
    I. Juchnovski,
    C. R. Acad. Bulg. Sci., **19,** 743 (1966).
14. Certain peculiarities of the of the resonance effects on the characteristic frequencies of the C=O and C≡N groups in the infrared spectra of molecules,
    I. Juchnovski,
    Teoret. Eksp. Khim., **3,** 123 (1967) (in Russian).
15. Frequency of the nitrile group in the infrared spectra of some carbanions,
    I. Juchnovski,
    Teoret. Eksp. Khim., **3,** 410 (1967) (in Russian).
16. Steric hindrance to the conjugation and its estimate by the nitrile group frequency in the infrared spectra of α,β-diarylacrylonitriles,
    I. Juchnovski,
    Zh. Strukt. Khim., **8,** 544 (1967) (in Russian).
17. Frequenz der Carbonylgruppe und ihres ersten Obertons in den infraroten Spektren der substituierten Zimtaldehyde und Benzaldehyde,

I. Juchnovski,
C. R. Acad. Bulg. Sci., **20,** 33 (1967).

18. Über einige Gesetzmässigkeiten in der Übertragung der polaren Effekte der Substituenten auf die Frequenz der Nitrilgruppe,
I. Juchnovski,
C. R. Acad. Bulg. Sci., **20,** 97 (1967).
19. Infrarote Spektren und Syntese einiger 2,3-disubstituierter 1,1'-Dicyanobenzofulvene.
I. Juchnovski, C. Ivanov, J. Vladovska,
C. R. Acad. Bulg. Sci., **20,** 449 (1967).
20. Physical Methods in the Organic Chemistry. A Textbook for University Students,
A. Trifonov, I. Juchnovski,
Sofia University, Sofia, 1968, (in Bulgarian).
21. Variation in the substituent effects on the infrared characteristic frequencies as a result of the lengthening of the conjugated system,
I. Juchnovski,
Dokl. AN SSSR, **186,** 878 (1969) (in Russian).
22. Use of the correlation of the nitrile group infrared frequencies with the bond orders to estimate the steric hindrances to the conjugation,
I. Juchnovski, Ts. Popov,
*Commun. Depart. Chem. Bulg. Acad. Sci., **2,*** 373 (1969) (in Russian).
23. IR-Spektren der Anion-Radikale von aromatischen Mononitrilen und Elektronenübergänge zwischen Anion-Radikalen und neutralen Molekülen,
I. Juchnovski, Ch. Tsvetanov, I. Panayotov,
Monatsh. Chem., **100,** 1980 (1969).
24. Über die Nitrierung substituierter Indenone. 6. Struktur der Zwischenprodukte,
B. Aleksiev, P. Nisanjan, I. Juchnovski,
Monatsh. Chem., **100,** 1400 (1969).
25. Übertragung des Polareffektes auf die Frequenzen der Carbonylgruppe in den trans-Zimtsäuren und anderen verwandten Systemen,
I. Juchnovski, N. Christov,
C. R. Acad. Bulg. Sci., **22,** 1401 (1969).
26. A study of some orotic acid derivatives and analogues by Hueckel's method of molecular orbitals. I. A theoretical study of the active site of orotidine-5'-phosphate pyrophosphorylase,
J. Kaneti, E. Golovinsky, I. Juchnovski, D. Genchev,
J. Theor. Biol., **26,** 19 (1970).
27. A study of some orotic acid derivatives and analogues by Hueckel's method of molecular orbitals. II. Analogues of orotic acid in the reaction with phosphoribosyl pyrophosphate,
E. Golovinsky, J. Kaneti, I. Juchnovski, D. Genchev,
J. Theor. Biol., **26,** 29 (1970).
28. Ausvertung der sterischen Hinderung von α,β-Diarylacrylnitrilen durch Korrelation polarogrophischer und HMO-LCAO - Angeben,
I. Juchnovski, Ts. Popov,
Monatsh. Chem., **100,** 337 (1970).
29. Elektronenstruktur und Eigenschaften einiger Beta-dicarbonyl Verbindungen. I. Struktur und Elektrinenspektren von 2-Aryliden-1,3-indandionen,
J. Kaneti, I. Juchnovski,
Commun. Depart. Chem. Bulg. Acad. Sci., **3,** 83 (1970).
30. Electronic substituent effects and carbonyl stretching frequencies of 2-arylmethylene-1,3-indandiones,
J. Kaneti, I. Juchnovski,
Tetrahedron, **26,** 4397 (1970).
31. Über die IR-Spektren der dinegativen Ionen einiger polycyclics Mononitrile und Elektronenübergänge zwischen Ionen und neutralen Molekülen,
I. Juchnovski, Ch. Tsvetanov, I. Panayotov,
Monatsh. Chem., **101,** 1271 (1970).
32. IR-Spektren der Ketyle einigen aromatischer Ketone und Elektroneübergänge zwischen Ketyl- und neutralen Keton- Molekülen,
I. Juchnovski, I. Raschkov, I. Panayotov,
Monatsh. Chem., **101,** 1712 (1970).
33. Vinyl polymerisation, initiated by metal complexes of aromatic nitriles,
I. Panayotov, Ch. Tsvetanov, I. Juchnovski,

Eur. Polymer J., **6,** 1625 (1970).

34. A model (MMO LCAO) investigation on the influence of the structure of the conjugated nitriles on the intensity on the infrared absorption band of the nitrile group,
    I. Juchnovski, C. Velev,
    Commun. Depart. Chem. Bulg. Acad. Sci., **4,** 333 (1971) (in Russian).
35. Substituent polar effects on the integral intensity of the C≡N group in some conjugated systems,
    I. Juchnovski, D. Dumanov, L. Mincheva,
    Commun. Depart. Chem. Bulg. Acad. Sci., **4,** 39 (1971) (in Russian).
36. Electronic structure of the rotational isomers of furfural,
    I. Juchnovski, J. Kaneti,
    Tetrahedron, **27,** 4269 (1971).
37. Etude de mecanisme de la polymerisation amorcée par les anion-radicaux et les bianions de cetones aromatiques a l'aide de la spectroscopie infrarouge,
    I. Panayotov, I. Rashkov, I. Juchnovski,
    Eur. Polymer J., **7,** 749 (1971).
38. Frequencies of the cyano group in the IR-Spectra of free, electrochemically generated anion-radicals of some aromatic nitriles,
    I. Juchnovski, I. Binev,
    C. R. Acad. Bulg. Sci., **24,** 483 (1971).
39. Infrared spectral data on strong intramolecular electron interaction in some anion-radicals containing CN group,
    I. Juchnovski, I. Binev,
    Chem. Phys. Lett., **12,** 40 (1971).
40. Relation between the electronic structure and infrared frequencies of the cyano group in alkali-metal complexes of some substituted benzonitriles,
    I. Juchnovski, I. Binev,
    J. Mol. Struct., **7,** 490 (1971)
41. Study (SCF, CI) on the intra-molecular charges transfer during excitation of n-substituted pyridine ions,
    N. Tyutyulkov, I. Juchnovski, K. Davarski,
    C. R. Acad. Bulg. Sci., **25,** 51 (1972).
42. Frequency of the nitrile group and electronic structure of the carbanions of some secondary saturated nitriles,
    I. Juchnovski, I. Binev,
    C. R. Acad. Bulg. Sci., **26,** 659 (1973).
43. Infrared and ultraviolet spectral study of some substituted trans-α-cyanostilbenes,
    I. Juchnovski, I. Binev,
    Commun. Depart. Chem. Bulg. Acad. Sci., **6,** 595 (1973).
44. The dependence of some characteristic frequencies of 2-arylmethylene-1,3-indanediones on their electronic structure. Steric effects and carbonyl coupling,
    I. Juchnovski, J. Kaneti,
    Commun. Depart. Chem. Bulg. Acad. Sci., **6,** 615 (1973).
45. Infrared spectra and structure of carbanions. III. Hammet study of the frequencies of the nitrile groups in intermediates formed by nucleophillic addition to trans-α-cyanostilbenes,
    I. Juchnovski, I. Binev,
    Tetrahedron Lett., 3645 (1974).
46. Infrared spectroscopic study on the deoxygenation of aromatic nitrile-N-oxides on their electrochemical reduction,
    I. Juchnovski, G.Andreev,
    Trav. Sci. Univ. Plovdiv, **13,** 143 (1975) (in Bulgarian).
47. Infrared spectra and structure of carbanions. V. Assignment of the nitrile group infrared bands of the phenylacetonitrile and acetonitrile lithium derivatives,
    I. Juchnovski, I. Binev,
    J. Organomet. Chem., **99,** 1 (1975).
48. Assignment of the infrared stretching frequencies of the nitro group in some nitroaromatic compounds and their ^{15}N labeled derivatives,
    I. Juchnovski, G. Andreev,
    C. R. Acad. Bulg. Sci., **29,** 1637 (1976).
49. Infrared spectral data on the structure of enamino-nitrile anions and the base catalysed dimerization of some saturated nitriles,
    I. Binev, R. Todorova, I. Juchnovski,
    C. R. Acad. Bulg. Sci., **29,** 1301 (1976).
50. Infrared spectra and structure of carbanions. IV**.** Carbanions - intermediates in nucleophillic addition reaction to α,β-diaril-cyanoethylenes,

I. Binev, I. Juchnovski,
Commun. Depart. Chem. Bulg. Acad. Sci., **9,** 33 (1976).

51. Infrared spectra and structure of carbanions. V. Transmission of the sustituent effects though a carbanionic center, I. Juchnovski, I. Binev, Ts. Kolev, *Tetrahedron Lett.,* 1519 (1976)**.**
52. Synthesis and structure of some bis-alkylammonium salts of 2,4-dinitro-3-phenyl glutaric acid dinitrile, Z. Demireva, I. Binev, I. Juchnovski, *Tetrahedron Lett.,* 1523 (1976).
53. Frequencies of the C=O stretching vibration in aromatic ketyl radicals, I. Juchnovski, Ts. Kolev, I. Binev, *C. R. Acad. Bulg. Sci.,* **30,** 1017 (1977).
54. Infrared spectra and structure of carbanions. VIII. Mono- and dialkalimetal derivatives of some bis(cyanomethyl) arenes, I. Juchnovski, V. Radomirska, I. Binev, E.Grekova, *J. Organomet. Chem.,* **128,** 139 (1977).
55. Infrared spectra and structure of carbanions. XI. Carbanions of arylacetonitriles. I. Binev, I. Juchnovski, Ts. Kolev, *Commun. Depart. Chem. Bulg. Acad. Sci.,* **10,** 76 (1977).
56. Infrared spectra and structure of carbanions. X. Dianion of 2,4-dinitro-3-phenyl-glutaronitrile, G. Andreev, Z. Demireva, I. Juchnovski, R. Kusmanova, I. Binev, *Commun. Depart. Chem. Bulg. Acad. Sci.,* **10,** 379 (1977).
57. Infrared spectra and structure of carbanions. XI. Estimation of σ^+ constants of anionic substituents, I. Juchnovski, I. Binev, *Tetrahedron,* **33,** 2993 (1977).
58. Infrared spectra and structure of carbanions. XII. Dimeric dianions from α,β-diaryl-acrylonitriles, I. Binev, I. Juchnovski, *J. Organomet. Chem.,* **141,** 123 (1977).
59. Infrared spectra and structure of carbanions. XIV. Isomeric carbanions adduct of some substituted cyano-polyenes, I. Binev, I. Juchnovski, *Bull. Soc. Chim. Belg.,* **86**, 793 (1977)**.**
60. IR Spectroscopic data on reversible character of dimerizotion of some α-aryl-β-phenyl-acrylonitrile anion-radicals, I. Juchnovski, I. Binev, *C. R. Acad. Bulg. Sci.,* **30,** 1977, 1419 (1977).
61. IR spectroscopic study on the stretching vibrations of the nitro group in anion-radicals of nitrobenzene and some isotope-labelled nitrobenzenes, I. Juchnovski, G.Andreev, *C. R. Acad. Bulg. Sci.,* **30**, 1021 (1977).
62. Optical spectra and electronic structure of anion-radicals. XI. Infrared study of the aromatic nitrile anion-radicals, I. Juchnovski, I. Binev, J. Kaneti, *Commun. Depart. Chem. Bulg. Acad. Sci*., **10,** 554 (1977).
63. Correlation of stretching vibration frequencies of nitro group in nitrobenzenes with substituent constants, I. Juchnovski, G.Andreev. *C. R. Acad. Bulg. Sci.,* **31,** 683 (1978).
64. Electronic structure and vibrational spectrum of acetonitrile complexes with lithium and sodium cations, I. Juchnovski, J. Dimitrova, *C. R. Acad. Bulg. Sci.,* **31,** 547 (1978).
65. IR and spectra and structure of carbanions. XIII. A study of the carbanions generated from acetonitrile, acetonitrile-d_3 and acetonitrile-^{15}N, I. Juchnovski, J. Dimitrova, I. Binev, J. Kaneti, *Tetrahedron,* **34,** 779 (1978).
66. IR spectroscopic study of anionic products derived from triphenyl-cyanoethylene and 1,1-diphenyl-2-2-dicyanoethylene, I. Juchnovski, I. Binev, *C. R. Acad. Bulg. Sci.,* **31,** 429 (1978).
67. Spectroscopic and theoretical study of arylmethylene malonodinitriles. I. Electronic spectra, J. Kaneti, D. Vitanov, I. Juchnovski, V. Juritsin, *Commun. Depart. Chem. Bulg. Acad. Sci.,* **11,** 273 (1978).
68. Structural effect on nitrile integrated intensities of α,β-diaryl cyanoethylenes: Hammet and quantum chemical approaches, I. Juchnovski, R. Kuzmanova, J.Tsenov, J. Kaneti, I. Binev,

Z. Naturforsch., **33b**, 557 (1978).
69. Optical spectra and electronic structure of anion-radicals. XII. IR study of the anion-radicals of N-substituted phthalimides and their isotope labelled derivatives,
I. Juchnovski, I. Binev, A. Fattah Nazir, J. Tsenov,
Commun. Depart. Chem. Bulg. Acad. Sci., **12,** 500 (1979).
70. Carbonyl group frequency in IR spectra of carbanions containing ethoxycarbonyl group,
I. Juchnovski, A. Fattah Nazir, I. Binev,
C. R. Acad. Bulg. Sci., **32,** 39 (1979)
71. Nitrile frequency and intensity-structure relationships of *trans*-1,2-diaryl-acrylonitriles; L.F.E.R. and quantum chemical approaches,
I. Binev, J. Kaneti, J. Tsenov, R. Kuzmanova, I. Juchnovski,
Commun. Depart. Chem. Bulg. Acad. Sci., **12,** 228 (1979).
72. Semiempirical calculation of force fields for molecules containing carbon-nitrogen bonds,
I. Juchnovski, J. Dimitrova, J. Kaneti,
Commun. Depart. Chem. Bulg. Acad. Sci., **12,** 97 (1979).
73. Spectroscopic and theoretical study of arylmethylene malononitriles. II. Frequencies and intensities of the nitrile groups: L.F.E.R. and Huckel MO approaches,
I. Binev, D. Vitanov, I. Juchnovski, J. Kaneti,
Commun. Depart. Chem. Bulg. Acad. Sci., **12,** 162 (1979).
74. Etude infrarouge sur la structure d'entités anioniques comprenant de groupes caractéristiques,
I. Juchnovski, I. Binev,
Organometalliques Fonctionells ambident. Rec. Comm., Colloques Franco-Bulgare, Tryavna, 1980, p. 144.
75. IR spectra and structure of carbanions. XVIII. A semiempirical study of carbanions of cyanoacetic acid derivatives,
J. Kaneti, A. Fattah Nazir, I. Binev, V. Radomirska, I. Juchnovski,
J. Mol. Struct., **68,** 11 (1980).
76. IR spectra and structure of carbanions. XIX. Anions containing ester, amide and carboxylato groups,
I. Juchnovski, A. Fattah Nazir, M. Sahatchieva, J. Kaneti, I. Binev,
Commun. Depart. Chem. Bulg. Acad. Sci., **13,** 269 (1980).
77. L.F.E.R. and simple HMO approaches to the study of the stretching frequencies of the nitro group in neutral and anionic nitrobenzenes,
I. Juchnovski, G. Andreev,
Commun. Depart. Chem. Bulg. Acad. Sci., **13,** 166 (1980).
78. Trends in the refining technologies of the copper electroplating,
S. Rashkov, D. Stoichev, L. Mirkova, I. Pojarliev, I. Juchnovski,
Proc. III Int. Conf. Corrosion Prevention, Warszawa, 1980, p. 107 (in Russian).
79. Transmission of substituents' polar effect to frequency of hydroxyl group in cinnamic acid,
I. Juchnovski, J. Vladovska,
C. R. Acad. Bulg. Sci., **33,** 71 (1980).
80. Effects of neutral and anionic substituents on the carbonyl stretching bands of substituted benzophenones,
I. Juchnovski, Ts. Kolev, I. Binev,
Spectrosc. Lett., **14,** 763 (1981).
81. IR spectra and structure of carbanions. XX. Strong ν_{CN} vibrational coupling in sodium malononitrile, its derivatives and isotopomers,
I. Juchnovski, V. Radomirska, I. Binev,
Commun. Depart. Chem. Bulg. Acad. Sci., **14,** 147-155 (1981).
82. 1,4-Benzodiazepine. 7. Über den Mechanismus der polarographischen Reduktion einiger Benzodiazepiniumbromide,
P. Kasandschieva, D. Mondeschka, I. Juchnovski, I. Nikolov,
Arch. Pharm., **314,** 493 (1981).
83. L.F.E.R. approach to the effects of neutral and charged substituents on IR frequencies and intensities. I. Substituted benzonitriles, determination of constants of anionic substituents,
I. Binev, R. Kuzmanova, J. Kaneti, I. Juchnovski,
Commun. Depart. Chem. Bulg. Acad. Sci., **14,** 470 (1981).
84. L.F.E.R. approach to the effects of neutral and anionic substituents on IR frequencies and intensities. II. Substituted benzophenones,
I. Binev, Ts. Kolev, I. Juchnovski,
Commun. Depart. Chem Bulg. Acad. Sci., **14,** 341 (1981).
85. Constantes des substituants anioniques,
I. Binev, I. Juchnovski,
Organometalliques fonctionnels Rec. Commun.,Coll. Franco-Bulgare C.N.R.S., Paris, 1982, p. 77.

86. Determination of constants of anionic subtituents based on nitrile infrared frequencies and intensities, I. Binev, R. Kuzmanova, J. Kaneti, I. Juchnovski, *J. Chem. Soc. Perkin Trans.* II**,** 1533 (1982).
87. IR Spectra of Cyano and Isocyano Group, I. Juchnovski, I. Binev, In: The Chemistry of Functional Group, Suppl. C., S. Patai and Z. Rappoport (Eds), John Wiley, New York, 1983, Chapt. 4, pp. 107-135.
88. Infrared spectra and structure of carbanions. XXII. Carbanions of *p*- and *m*-nitrophenyl nitromethanes, I. Juchnovski, G. Andreev, *Commun. Depart. Chem. Bulg. Acad. Sci.*, **15**, 339 (1982).
89. Effects of neutral and anionic substituents on the carbonyl stretching bands of substituted methylbenzoates, P. Wassileva, I. Binev, I. Juchnovski, *Spectrochim. Acta*, **39A**, 709 (1983).
90. Infrared spectra and structure of reduction products of p- and m-dinitrobenzenes and some ^{15}N-isotope-labelled dinitrobenzenes, I. Juchnovski, G. Andreev, *C. R. Acad. Bulg. Sci.*, **36,** 911 (1983).
91. IR-Spektroskopische Undersuchungen von Anion-Radikalen. XII. Anion- Radikale aromatischer Nitroverbindungen, I. Juchnovski, G. Andreev, *Commun. Depart. Chem. Bulg. Acad. Sci.*, **16,** 389 (1983).
92. IR-Spektren und Struktur von Carbanionen. XXIII. Carbanionen von arylaliphatischen Nitroverbindungen, I. Juchnovski, G. Andreev, *Commun. Depart. Chem. Bulg. Acad. Sci.*, **16,** 402 (1983).
93. C-N stretching and NO_2 deformation vibrations coordinate analysis of *m*-dinitrobenzene, *m*-dinitrobenzene-d_4, G. Andreev, B. Jordanov, I. Juchnovski, B. Schrader, *J. Mol. Struct.*, **115**, 375 (1984).
94. L.F.E.R. approach to the effects of neutral and anionic substituents on the CO bands of ring-substituted ethylbenzoates and acetophenones, I. Binev, P. Vassileva, Ts. Kolev, I. Juchnovski**,** *J. Mol. Struct.*, **114,** 1984, 371 (1984).
95. Normal coordinate analysis of *m*-dinitrobenzene-d_0, *m*-dinitrobenzene-d_4 and *m*-dinitrobenzene-(^{15}N,^{15}N), G. Andreev, B. Schrader, H. Takahashi, D. Bougeard, I. Juchnovski, *Can. J. Spectrosc.*, **29,** 145 (1984).
96. Vibrational spectra of *m*-dinitrobenzene, *m*-dinitrobenzene-d_4 and *m*-dinitrobenzene-(^{15}N, ^{15}N), G. Andreev, B. Schrader, H. Takahashi, D. Bougeard, I. Juchnovski, *Can. J. Spectrosc*., **29**, 139 (1984).
97. Infrared spectra and structure of products formed by electron transfer on some substituted acrylonitriles, I. Juchnovski, J. Tsenov, I. Binev, *J. Mol. Struct.*, **129,** 249 (1985).
98. L.F.E.R. approach to the effects of neutral and anionic substituents on infrared frequencies and intensities. IV. Substituted ethyl benzoates, I. Binev, A. Fattah Nazir, P. Vassileva, I. Juchnovski, *Commun. Depart. Chem. Bulg. Acad. Sci.*, **18,** 22 (1985).
99. Vibrational assignment of benzophenone and some of its isotopic species in the solid phase, Ts.Kolev, B. Nikolova, B. Jordanov, I. Juchnovski, *J. Mol. Struct***., 129,** 1 (1985).
100. Effects of neutral and anionic substitutents on the carbonyl stretching bands of ring-substituted acetophenones, I. Binev, Ts. Kolev, I. Juchnovski, *Can. J. Chem.*, **63,** 3149 (1985).
101. Infrared spectra of the anion-radicals of benzophenone and some of its isotopic isomers, I. Juchnovski, Ts. Kolev, I. Rashkov, *Spectrosc. Lett.*, **18,** 171 (1985).
102. Infrared spectra and structure of the anion-radicals of substituted benzophenones, I. Juchnovski, Ts. Kolev, *Spectrosc. Lett.*, **18,** 481 (1985).
103. Infrared spectra and configuration of anion radical and dianion of benzil and benzil- ^{18}O, I. Juchnovski, Ts. Kolev, *Spectrosc. Lett.*, **19,** 529 (1986).
104. Infrared study of anthraquinone-anion-radical and its ^{18}O labelled isomer,

I. Juchnovski, Ts. Kolev,
Spectrosc. Lett., **19,** 1183-1193 (1986)

105. Synthesis of molybdenum silica and cobalt-molybdenum silica catalysts and their catalytic activity in the hydrodesulphurization of thiophen,
A. Spozhakina, N. Kostova, I. Juchnovski, D. Shopov, T. Yurieva, T. Shochireva,
Appl. Catal., **39,** 333 (1988).
106. Some systematic deviations of the IR group frequencies from their correlations with substituent constants,
I. Juchnovski, J. Tsenov, J. Dimitrova, I. Binev,
Commun. Depart. Chem. Bulg. Acad. Sci., **23,** 502 (1990).
107. CNDO/2 analysis of the constants of anionic substituents, determined on the basis of infrared frequencies and intensies,
I. Juchnovski, J. Dimitrova, I. Binev,
C. *R. Acad. Bulg. Sci.,* **44,** 41 (1991).
108. The vibrational spectra of 9-fluorenone and some of its isotopic isomers,
Ts. Kolev, I. Juchnovski,
Spectrosc. Lett., **24,** 1023 (1991).
109. Structure of N-(4-cyanophenyl-phenyl)methylene aniline,
H. Preut, P. Bleckmann, Ts. Kolev, I. Juchnovski,
Acta Crystallogr., **C48,** 754 (1992).
110. Structure of 2-cyanobenzophenone,
H. Preut, Ts. Kolev, P. Bleckmann, I. Juchnovski,
Acta Crystallogr., **C48,** 938 (1992).
111. Crystal structure of 2-(4-nitrophenyl)-1-phenylethanone,
H. Preut, Ts. Kolev, P. Bleckmann, I. Juchnovski,
Acta Crysalogrt., **C48,** 1992, 1152 (1992).
112. Crystal structure of 1,4-dibenzoylbenzene,
Ts. Kolev, H. Preut, P. Bleckmann, I. Juchnovski,
Acta Crystallogr., **C48,** 1715 (1992).
113. Crystal structure of 2-(4-methylphenyl)-1H-indene-1,3(2H)-dione, ,
Ts. Kolev, H. Preut, P. Bleckmann, I. Juchnovski,
Acta Crystallogr., **C48,** 1547 (1992).
114. Unperturbed NO_2 stretching frequencies in the vibrational spectra of 1,4-dinitrobenzene,
G. Andreev, I. Juchnovski,
Appl. Spectrosc., **46,** 1304 (1992).
115. Reaction of phthalic anhydride with substituted dibenzoylketones: a novel synthesis of some substituted 5-hydroxy-6-arylbenzo(a)fluorenones,
I. Juchnovski, V. Aleksiev,
C. R. Acad. Bulg. Sci., **45,** 53 (1992).
116. Infrared spectra and transmission of substitutent effect through the arylazomethine groups in aromatic Schiff bases,
I. Juchnovski, V. Ognyanova, G. Andreev,
Spectrosc. Lett., **26**, 447 (1993).
117. Vibrational assignment of benzil and its oxigen-18 substituted derivative,
Ts. Kolev, I. Juchnovski,
Spectrosc. Lett., **26,** 1 (1993).
118. Infrared spectra of phthalic anhydride and its oxygen-18 substituted derivative,
I. Juchnovski, E. Velcheva, Ts. Kolev,
Spectrosc. Lett., **26,** 17 (1993).
119. Infrared spectra of benzophenone-ketyls. effects of meta and para-substituents on frequencies. correlation of ν_{CO} of substituted benzophenone-ketyls with the Hueckel P_{CO} bond order,
I. Juchnovski, Ts. Kolev, B. Stamboliyska,
Spectrosc. Lett., **26,** 67 (1993).
120. Vibrational assignment of N-phenylphtalimide and ^{15}N-phenylphtalimide,
Ts. Kolev, I. Juchnovski,
Spectrosc. Lett., **26,** 207 (1993).
121. Infrared spectra of aromatic Schiff base electron transfer products,
I. N. Juchnovski, V. Ognyanova, G. N. Andreev,
Spectrosc. Lett., **27,** 1299 (1994).
122. σ^+ Constants of charged substituents,
I. G. Binev, E. A. Velcheva, V. B. Radomirska, I. N. Juchnovski,
C. R. Acad. Bulg. Sci., **47,** 33 (1994).

123. IR spectra and structure of ethyl cyanoacetate and of its carbanion: an *ab initio* force field treatment,
B. A. Stamboliyska, E. A. Velcheva, Y. I. Binev, I. N. Juchnovski,
C. R. Acad. Bulg. Sci., **47,** 69 (1994).
124. Substituent effects on the isocyano group infrared frequencies and intensities of substituted phenyl isocyanides: the LFER approach,
I. N. Juchnovski, J. A. Tsenov,
Spectrosc. Lett., **28**, 211 (1995).
125. On the validity of the constants of ionic substituents: substituent effects on the cyano stretching frequencies and intensities of *trans*-α-phenyl-β-arylacrylonitriles,
I. G. Binev, E. A. Velcheva, I. N. Juchnovski,
Spectrochim. Acta, **A51**, 1871 (1995).
126. Infrared spectra and structure of phenylacetonitrile and of its carbanion: an *ab initio* force field treatment,
I. G. Binev, J. A. Tsenov, E. A. Velcheva, I. N. Juchnovski,
J. Mol. Struct., **344**, 205 (1995).
127. The *ab initio* force field treatment of the IR spectra and structure of 2-Acetyl-3,3-bis(dimethylamino)acrylonitrile: a strongly polarized ethylene,
I. G. Binev, J. A. Tsenov, E. A. Velcheva, Y. I. Binev, I. Juchnovski,
C. R. Acad. Bulg. Sci., **48,** No. 1, 65 (1995).
128. Vibrational assignment of N-benzylphtalimide and ^{15}N- benzylphtalimide,
Ts. Kolev, I. Juchnovski,
J. Mol. Struct., **349**, 377 (1995).
129. Crystal structure of (±)-*threo*-hydroxy-2,3-diphenylpropanoic acid dimethylamide,
Ts. Kolev, H. Preut, P. Bleckmann, I. Juchnovski,
Acta Crystallogr., **C51,** 1169 (1995).
130. Crystal structure of (±)-*threo*-hydroxy-2,3-diphenylpropanoic acid methyl ester,
Ts. Kolev, H. Preut, P. Bleckmann, I. Juchnovski,
Acta Crystallogr., **C51,** 1350 (1995).
131. L-(+)-α-bromobenzeneacetic acid (-)-mentyl ester,
Ts. Kolev, H. Preut, L. Koniczek, P. Bleckmann, I. Juchnovski, M. Mladenova,
Acta Crystallogr., **C51,** 1634 (1995).
132. Quantum-chemical study of the relation between electronic structure and IR spectra of neutral molecules, anion-radicals and dianions of aromatic nitriles,
Y. Dimitrova, I. Juchnovski,
Spectrosc. Lett., **28**, 937 (1995).
133. Infrared spectra and structure of alkane- and cycloalkanecarbonitriles and of their carbanions: an *ab initio* force field treatment,
I.N. Juchnovski, J.A. Tsenov, I.G. Binev,
Spectrochim. Acta Part **A, 52**, 1145 (1996).
134. Infrared spectra and structure of the isomeric (cyanophenyl)acetonitriles and of their carbanions: an *ab initio* force field treatment,
I. G. Binev, J. A. Tsenov, E. A. Velcheva , V. B. Radomirska, I. N. Juchnovski,
J. Mol. Struct., **378**, 133 (1996).
135. Quantum-chemical investigation of the electronic structure of the ionic derivatives of aromatic Schiff bases,
I. Juchnovski, V. Ognyanova, B. Stamlboliyska, G. N. Andreev,
C. R. Acad. Bulg. Sci., **50**, 51 (1997).
136. The infrared spectra and structure of 2-cyano-3-phenylpropenenitrile and of its sodium-metoxide adduct: an *ab initio* GF treatment,
I. N. Juchnovski, Y. I. Binev, B. A. Stamboliyska, I. G. Binev,
C. R. Acad. Bulg. Sci., **50**, 61 (1997).
137. The substituent effects on the isocyano group infrared frequencies and intensities of substituted phenyl isocyanides: an *ab initio* GF treatment.
J. A. Tsenov, I. N. Juchnovski,
C. R. Acad. Bulg. Sci., **50**, 35 (1997).
138. The infrared spectra and structure of benzylidenemalononitrile, its cyanide, metoxide and heptyamine adducts: experimental and *ab initio* studies,
I. G. Binev, Y. I. Binev, B. A. Stamboliyska, I. N. Juchnovski,
J. Mol. Struct., **435,** 235 (1997).
139. Vibrational assigment of *para*-dimethylaminobenzil and its ^{18}O substituted derivative,
V. Radomirska, Ts. Kolev, I. Juchnovski,
J. Mol. Struct., **408,** 409 (1997).

140. A*b initio* treatment of vibrational spectra and structure of free tricyanoethenolate anion and of its lithium and silver contact ion pairs,
I. N. Juchnovski, Y. I. Binev,
C. R. Acad. Bulg. Sci., **50**, 51 (1997).
141. IR spectral and structural changes of phenyl isocyanides and benzonitriles, accompanying their conversion into anion-radicals: *ab initio* and experimental studies,
J. A. Tsenov, I. G. Binev, I. N. Juchnovski
C. R. Acad. Bulg. Sci., **51,** 57 (1998).
142. Experimental and *ab initio* studies of IR spectra and structure of *trans*-benzylidenecyanacetamide and of its potassium cyanide (^{14}N and ^{15}N) adducts,
E. Velcheva, I. Bineva, I. Juchnovski,
C. R. Acad. Bulg. Sci., **51,** 41 (1998).
143. Vibrational spectra of 2-phenyl-indane-1,3-dione, its isotopic labelled derivatives and the corresponding carbanions,
Ts. Kolev, E. Velcheva, I. Juchnovski,
Spectrochim. Acta Part A, **54**, 1083 (1998).
144. Vibrational spectra of 3-benzylidenephthalide and its ^{18}O labelled derivative,
Ts. Kolev, E. Velcheva, I. Juchnovski,
Spectrochim. Acta Part A, **55,** 2477 (1999).
145. Vibrational spectra and structure of N-(4-cyanobenzylidene)-aniline, its^{15}N and D_5 isotopomers and their monomeric dianions: an experimental and *ab initio* study,
V. Ognyanova, G. N. Andreev, B. Stamlboliyska, I. N. Juchnovski,
J. Mol. Struct., **513,** 139 (1999).
146. IR spectra and structure of 2,5-pyrrolidinedione (succinimide) and of its nitranion: experimental and *ab initio* MO studies,
B. Stamboliyska, Y. Binev, V. Radomirska, J. Tsenov, I. Juchnovski,
J. Mol. Struct., **516,** 237 (2000).
147. The formation and isomerisation of sodium methoxide adducts of cinnamylidenemalononitrile, followed by IR spectra and *ab initio* force field calculations,
Y. Binev, I. Binev, I. Juchnovski,
J. Mol. Struct. (*Theochem*), **532,** 31 (2000).
148. A new approach to the detection and determination of *o*-chlorobenzylidene-malononitrile (CS) and its chemical relatives,
I. G. Binev, Y. I. Binev, I. N. Juchnovski,
Spectrosc. Lett., **35,** 285 (2002).
149. Correlation analysis of experimental *vs. ab initio* IR frequencies and intensities,
I. G. Binev, B. A. Stamboliyska, P. J. Vassileva-Boyadjieva, Y. I. Binev, E. A. Velcheva, J. A. Tsenov, Ch. Ts. Petkov, I. N. Juchnovski,
Bulg. Chem. Commun., **34,** 170 (2002).
150. IR studies in the substituted benzaldehyde series provide a new definition of sigma-plus constants of ionic substituents,
E. A. Velcheva, I. N. Juchnovski, I. G. Binev,
Spectrochim. Acta Part A, **59,** 1745 (2003).
151. Experimental and computational studies on the IR spectral and structural variations arising from the conversion of (2,4,6-trimethylphenyl)acetonitrile into carbanion,
M. K. Georgieva, N. B. Nedelchev, I. N. Juchnovski,
Bulg. Chem. Commun., **37**, 234 (2005).

INVENTIONS

by Academician I. N. Juchnovski and colleagues

1. A flux line for printed plates, Invention Certificate No. 14923/23.10.1969 (in Bulgarian).
2. An electrolysis cell for infrared spectroscopy, Invention Certificate No. 16928/25.03.1971 (in Bulgarian).
3. An additive with brightness forming and smoothing effect for bright acidic copper electroplating, Invention Certificate No. 20924/06.06.1973 (in Bulgarian).
4. A method for preparation of disodium-3-3'-dithiobis-propanesulfonate, Invention Certificate No. 19454/06.08.1973 (in Bulgarian).

5. A method for purification of disodium-3-3'-dithiobis-propanesulfonate, Invention Certificate No. 21484/30.05.1974 (in Bulgarian).
6. A safraninic polymer and method for its preparation, Invention Certificate No. 26832/30.05.1974 (in Bulgarian).
7. A sulfuric acid containing electrolyte for copper depositing in the production of two- and polylayer printed plates, Invention Certificate No. 20476/07.06.1974 (in Bulgarian).
8. Polysafranines with modified end groups, Invention Certificate No. 31897/1975.
9. An additive to electrolyte for acidic bright copper plating, Invention Certificate No. 27504/1978 (in Bulgarian).
10. An additive for acidic bright copper electroplating, Invention Certificate No. 21755/1975 (in Bulgarian).
11. A method for identification and quantitative determination of *o*-chloro-benzylidenemalononitrile, Invention Certificate No. 27283/12.01.1982 (in Bulgarian).
12. An electrolyte for bright cyanide- and chloride-free zinc plating, Invention Certificate No. 27305/13.04.1978 (in Bulgarian).
13. An alkaline electrolyte for bright zinc plating, Invention Certificate No. 43490/07.05.1979 (in Bulgarian).
14. A complex additive to weakly acidic electrolytes for zinc plating, Invention Certificate No. 54683/01.02.1983 (in Bulgarian).
15. An additive to sulfuric acid containing electrolyte for bright copper plating, Invention Certificate No. 32654/1978 (in Bulgarian).
16. An electrolyte for copper plating, USSR Invention Certificate No. 1058313/01.08.1983 (in Russian).
17. Complex additives and electrolytes to deposit bright coatings of zinc alloys. Invention Certificate No. 63360/12.06.1989 (in Bulgarian).
18. A reagent for extracting metals, Invention Certificate No. 69448/16.05.1985 (in Bulgarian).

SELECTED PUBLICATIONS

ON PROBLEMS OF THE SCIENCE AND THE BULGARIAN ACADEMY OF SCIENCES

A. I. N. Juchnovski, About Bulgarian Science and the Bulgarian Academy of Sciences, 13 Memorable Years, 1989–2003, Collection of Public Texts of the Author; Complier V. G. Christova, Marin Drinov Academic Publishing House, Sofia, 2003, 268 pp., (in Bulgarian).

This book-collection has appeared after consecutive discussions in the scientific community about the impact of science in Bulgaria, its financial collapse, the rapid decrease in the number of people engaged in science nowadays, its underestimated contributions when compared to the new active initiatives of the European Union for a united European Research Area.

A total of 91 selected publications were gathered in this book. Some of them had been printed in the newspapers and some had been presented to various audiences. Acad. I. Juchnovksi was participating actively in the events engaged in the development and protection of the scientific research in Bulgaria since 1989.

We have tried to select texts, which are of significant importance in order to create a better understanding of the author's ideas about the role of science in the country, during a critical situation; about the necessary government policy towards advanced scientific developments; about the different approaches to promote scientific research. Other included texts comprise sharp remarks against the hypocritical behaviour or pseudoscience, which the author does not accept at all. There are also publications that suggest deep and emotional devotion to all Bulgarian traditions and national characteristics, especially those that incorporate the country's legacy connected with the national will for education, science and progress. Following this process, we managed to prepare a collection of articles tracing back the development of the Bulgarian Academy of Sciences, Bulgarian science and education for the last 13 years. The book is written by a man who was involved in the events and, who knew the trends in science and university education, which he analyzed professionally. All of these texts represent the many difficulties and achievements, opportunities and struggles, that both the Bulgarian Academy of Sciences and the whole scientific community in Bulgaria have gone through during the period of complicated transition in our country, which has been looking for a bridge to pass over for some time now.

In this sense, the book will probably provoke an interest in researchers, direct participants in the events, and also in the educated reader, who wants to learn more about how Bulgarian science has survived and fought during the last 13 years (1989–2003).

B. Selected more recent publications on the same problems:

1. Preface (7–12 pp.) to the book by Academician E. P. Kruglyakov (Russian Acad. Sci.), Swindlers Posing as 'Scientists' (On the lying doctrines of certain modern scandalous pseudo-scientists), Marin Drinov Academic Press, Sofia, 2003, 297 pp (in Bulgarian).
2. The scientist must think honestly, Interview in the daily newspaper *Zemya*, 21.05.2003 (in Bulgarian).
3. Speech for the celebration of 24 May (the day of the Slavonic alphabet), 22.05.2003.
4. The nation must start to see scientific achievements, Interview in the daily newspaper *Duma*, 24.05.2003 (in Bulgarian).
5. People keep on going despite politics, Interview in the daily newspaper *Standart*, 26.05.2003 (in Bulgarian).
6. We have elected very good scientists, Interview in the daily newspaper *Trud*, 22.06.2003 (in Bulgarian).
7. The science is a productive force only within a working market economy, Interview in the daily newspaper *Sega*, 02.07.2003 (in Bulgarian).
8. The Bulgarian Academy of Sciences does not sanction scientists for media appearances, Interview in the daily newspaper *Sega*, 10.11.2003 (in Bulgarian).
9. The Bulgarian Academy of Sciences will do for the country what others are not capable of doing. In the evening you must be tired of creative work, not of conspiracy, Interview in the daily newspaper, *Duma*, 30.03.2004 (in Bulgarian).
10. Let us think more about Bulgaria, Interview, monthly chronicle *Az Buki*, 1–13.04.2004 (in Bulgarian).
11. Let us do what others cannot, Attachment Sofiyanets in the daily newspaper *Trud*, 23.04.2004 (in Bulgarian).
12. A day of intellectual inspiration and unity, Article in the newspaper *Za bukvite*, special edition, 24.05.2004 (in Bulgarian).
13. The government funds given for science are enough only for salaries, Interview in the daily newspaper *Sega*, 16.10.2004 (in Bulgarian).
14. The main purpose of Europe is to build a community of knowledge, Interview in the daily newspaper *Cherno more*, Varna, 08.11.2004 (in Bulgarian).
15. The antipode of knowledge, Interview in the daily newspaper *Duma*, 30.11.2004 (in Bulgarian).
16. The Bulgarian Secret Services were pressing us to treat cancer with arsenic, Interview in the daily newspaper *24 hours*, 30.11.2004 (in Bulgarian).
17. Fortune-tellers want to become academicians, Interview in the daily newspaper *Standart*, 18.12.2004 (in Bulgarian).
18. On the Pseudoscience. Brochure, edition of „Chernorizets Hrabar", Varna Free University, "Issue of Academic Forum", January, 2005 (in Bulgarian).
19. A report presented at the Forum "*Science for Bulgaria"*, 13–14.05.2005 (in Bulgarian).
20. The science is the engine for the economy, Interview in the daily newspaper *Duma*, 19.05.2005 (in Bulgarian).
21. An interview for Vera Mutaftchieva's new book, July 2005 (in Bulgarian).
22. An interview for Mira Mayer's book about Jews in Bulgaria, 08.08.2005 (in Bulgarian).
23. The Bulgarian Academy of Sciences and Morocco grasshoppers, A reply by the Bulgarian Academy of Sciences administration to the article by Prof. D. Draganov in the daily newspaper *24 hours*, 10.01.2006 (in Bulgarian).
24. Has the Bulgarian Academy of Sciences developed the poison for Georgi Markov? Nonsence!, Interview in the daily newspaper *Trud*, 03.04.2006 (in Bulgarian).
25. Welcoming speech to the conference "*Science evaluation"*, published in the daily newspaper *Duma* on 31.10.2006 (in Bulgarian).
26. We have to cut live flesh off the Academy to reform it, Interview in the daily newspaper *Monitor*, 06.04.2007 (in Bulgarian).
27. Lying about history is not an European idea (on the occasion of the widely discussed book "*Batak"*), Article in the daily newspaper *Duma*, 26.04.2007 (in Bulgarian).
28. We jump from one puddle into another one, Interview in the daily newspaper *Trud*, 24.05.2007, (in Bulgarian).
29. Why do you abuse leading scientific institutions? Article in the daily newspaper *Politika*, 7–13.09.2007 (in Bulgarian).
30. A new migration wave is expected. Interview in the daily newspaper *Trud*, 27.12.2007 (in Bulgarian).
31. Introduction words for the opening of the National Conference "Directions of differentiation and integration of scientific knowledge, codes of scientific specialities and disciplinary organization of the research in Bulgaria", 23–24.01.2008 (in Bulgarian).
32. I am fighting for a cause, not for a position. Interview in the daily newspaper *Duma*, 13.02.2008 (in Bulgarian).

I. Binev
A. Popova

Bulgarian Chemical Communications, Volume 40, Number 4 (pp. 386–396) 2008

Linear free energy relationships of the *gem*-dimethyl (*gem*-dialkyl) effect

I. B. Blagoeva, E. P. Ignatova-Avramova, A. H. Koedjikov, I. G. Pojarlieff*,
L. I. Proevska, V. T. Rachina, N. G. Vassilev

Institute of Organic Chemistry with Centre of Phytochemistry, Bulgarian Academy of Sciences, Acad. G. Bonchev St., Block 9, 1113 Sofia, Bulgaria

Dedicated to Academician Ivan Juchnovski on the occasion of his 70th birthday

Received May 26, 2008, Revised July 1, 2008

The *gem*-dimethyl effect, GDME, or dialkyl effect, defined by the acceleration of cyclization reactions or the retardation of ring-opening by substituents in the chain, can not be satisfactory predicted by means of Hammett linear free energy relationships, LFER, e.g. using Taft's E_S-values. The reason for this can be traced to the nature of the GDME. Examination of a large series of the reversible cyclization of 3-(3-phenylureido) acids showed that good LFER of the Leffler type, i.e. rates against equilibria of the same reaction, are obtained encompassing substituents at various position of the ring. The LFER defines a general *gem*-dimethyl effect; a few outliers are due to specific interactions arising in the transition states and not in the reactant or product. Extension to other reactions of the ring system was carried out in two ways: correlation of rates with the equilibrium constants of the acid catalyzed cyclization of ureido acids assumed as reference or correlating two series of reaction rates with similar transition states which can eliminate outliers due to specific transition state effects. The rates of alkaline hydrolysis of large number of dihydrouracils nicely illustrated the versatility of the two approaches.

The one pot Rodionov procedure readily provided several -amino acids with -alkyl substituents from the corresponding aldehydes and malonic acid. Most of the equilibrium and rate data for acid and base catalysed hydrolysis of 3-phenyldihydropyrimidine-2,4-diones are reported in this paper.

Key words: Linear free energy relationships, *gem*-dimethyl effect, rates and equilibrium constants, acid and base catalysed hydrolysis, dihydrouracils, -ureido acids.

INTRODUCTION

The quantitative prediction of substituent effects is widely used in the form of Quantitative Structure Activity Relationships, QSAR, [1] for drug design and related biological applications and Quantitative Structure Property Relationships, QSPR, for chemical and physical goals. An integral part of these methods are the Hammett Linear Free Energy Relationships, LFER, [2] based on equations of the type

$$\log(\frac{k_x}{k_o}) = \rho\sigma \qquad (1)$$

where describes the susceptibility of the reaction rate constant (or equilibrium constant or some other property) to polar effects of substituents while is the substituent constant based on substituent effects of a reference reaction. Soon LFER were extended to other types of effects.

The LFER are classified as "extrathermodynamic" because they are empirical and can be deduced from theoretical concepts such as the Marcus equation [3] which describes the variation of the potential with the reaction coordinate as a function of the energy of the reaction and the so called "intrinsic barrier", $G_o^{\ddagger}$, i.e. the energy of activation when the reaction energy G, is zero (for the sake of simplicity we assume G H). The equation predicts reduced kinetic barriers for exothermic reactions (low selectivity and early transition states) and increased kinetic barriers for endothermic reactions (high selectivity and late transition states). Under certain conditions the approximation for a LFER holds i.e. $G^{\ddagger} =$ G where $G = G_x - G_o$. The free energies and those of activation apply for the same reaction series whereby the intrinsic barrier remains the same. Such relationships are usually referred to as the Leffler relationships [4]. The first linear free energy relationship was discovered by Pedersen and Brønsted [5]. It correlates rates and pK's in general acid or base catalysis and presents a Leffler type LFER. The slopes or in the Brönsted linear correlations play a great role in study of reactivity because their values $0 <$ or > 1 have been shown by Leffler as well as by the Markus equation to measure directly the reaction coordinate in the transition state [6]. In

* To whom all correspondence should be sent:
E-mail: ipojarli@orgchm.bas.bg

© 2008 Bulgarian Academy of Sciences, Union of Chemists in Bulgaria

the Hammett equation the slopes compare the selectivity to substituent effects of an arbitrary reaction to a reference one and their values are not confined in the limits from zero to unity. The means of calibrating in terms of a Leffler equation have been discussed by A. Williams [7].

Seventy years after its conception as a quantitative description of polar effects, the Hammett equation and its applications have witness an immense proliferation and sophistication. One line of development is definition of substituent constants for all kind of effects. Those for steric effects, originally the E_S constants of Taft Jr. [8], have proved least useful because of deviations from linearity. This is not surprising bearing in mind that steric repulsion is dependent on twelve powers of r – the distance between the interacting atoms. In conformationally restricted transition states typical of cyclization and ring-opening reactions the situation becomes worse because the geometrical requirements become more specific and no longer correspond to those defining E_S – the steric hindrance arising in acid catalyzed hydrolysis of open-chain carboxylic esters. One of the few successful applications of E_S values in cyclizations or ring-opening was reported by Bruice and Bradbury [9a] who could correlate linearly the effect of 3-substituents in the hydrolysis of glutaric anhydrides with E_S. Palm [9b] has criticized their approach for using E_S for substituents removed from the reaction center and suggested inclusion of the interlinking chain to obtain more accurate description of the steric effects. Of course, another procedure would be to have separate series for the various positions with different 's. We however encountered the problem of specificity of the various ring positions in spite of assigning a unified set of E_S-values by treating part of the chain linked to the reaction center as the backbone of the substituent [10]. The steric effects in question were observed in the alkaline hydrolysis of dihydrouracils, Scheme 1.

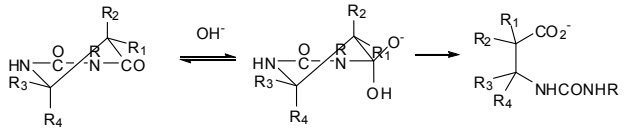

Scheme 1

We had assigned E_S-values to the substituents in the following manner:

When all R = H, E_S for Et was assumed; R^1 = Me: $E_S^{iPr,}$ $R^1 = R^2$ = Me: E_S^{tBu}; R^3 = Me: E_S^{nPr}; $R^3 = R^4$ =Me: E_S^{iBu}, $R^1 = R^4$ (or $R^1 = R^3$) = Me: E_S^{EtMeCH}. However, the available five points clearly defined two lines: one for 5-substituents (R^1 and R^2) and the other one for 6-substituents (R^3 and R^4). The data for the 5,6-dimethyl isomers appeared in between, Fig. 1.

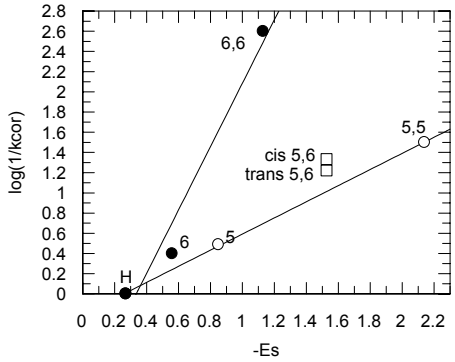

Fig. 1. Plot of $\log(1/k_{cor})$ where k_{cor} are the relative observed hydrolysis rate constants at pH 13 adjusted for ionization at 3-N against $-E$s (see text). Open circles: 5-methyl; closed circles: 6-methyl; squares 5,6-dimethyl. The point for R = H is common for both lines.

The deceleration by substituents in the 6th position is stronger (= 3.14, r = 0.981) than in the 5th position(= 0.80, r = 0.999). In the opposite reaction of cyclization of -ureido acids [11] substituents accelerate the reaction, the effect of - substituents being the stronger. Thus the greater retardation caused by 6-substituents is demonstration of the reverse *gem*-dimethyl effect.

The Thorpe-Ingold or *gem*-dimethyl (more generally dialkyl) effect is defined by the increase in both rate and equilibrium constants of cyclization reactions resulting from the introduction of substituents in the linking chain [12–14]. The nature of the effect has been the subject of a long controversy. It is best understood in terms of stain arising in the open-chain upon substitution which is released either by reduced ring bond angles in small rings or by diminishing the number of new gauche interactions because part of these are enforced upon the ring atoms [13].

Prediction of the GDME can be made by estimation of the strains involved [11], the best method for which is molecular mechanics [15].The strains released upon ring closure have to be overcome upon ring opening, an effect which is seldom recognized [16]. Further, in the case of reactions going through intermediates as the hydrolysis shown on Scheme 1, part of the strains due to the GDME arise in forming the intermediate because it is usually a looser structure than the parent ring [17].

The virtual inapplicability of steric constants to describe the GDME for varying positions in the ring prompted us to check whether Leffler type relations would provide a more coherent approach because a similar GDME is expected in the reaction equilibria and in the transitions states leading to these parti-

cular equilibria. We showed in an preliminary communication [18] that a log/log linear relationship does hold between the rates of acid catalyzed cyclization -(3-phenylureido)propionic acids to 3-phenyldihydrouracils and the respective equilibrium constants♥.

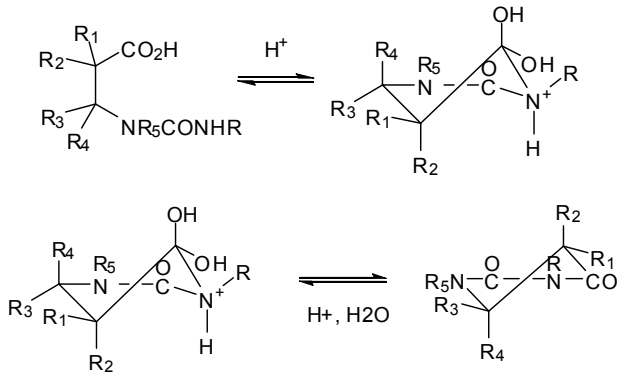

K_E = [DHU]/[UA] =.(k_{cycl}/k_{open}); $k^{rel} = k_x/k_o$
subscript *x* or *o* referring to substituted and unsubstituted derivative, respectively.

Scheme 2.

Linear fit of seven points produced the following equation:

$$\log k_{cycl}^{rel} = (0.35 \pm 0.03) \log K_E^{rel} \quad (r = 0.938) \quad (2)$$

Two neglected points deviated negatively by 0.5 log units; the deviations could be traced specifically to an axial methyl in position 5 of the tetrahedral intermediate or the transition state respectively.

The present paper reports extension of this correlation in two aspects:

a) enlarging the list of substituents in order to outline the permitted variation of structure;

b) correlating reactions of similar transition states and ring structure whereby transition state effects as the two above mentioned deviations can be avoided.

RESULTS AND DISCUSSION

Synthesis of β-amino acids, β-(3-phenylureido) acids and 3-phenyldihydrouracils

The Rodionov reaction [19] provides a convenient one pot procedure for -monosubstituted -alanines:

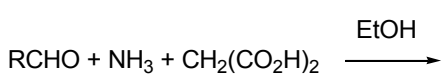

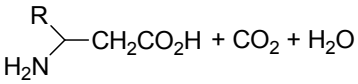

In the case of aliphatic aldehydes, the yields are usually low 20–30% which we found to be true for propanal and pivalaldehyde. However, with isobutyraldehyde a reasonable yield of 52% of the amino acid was obtained. The -substituted -alanines studied could be obtained in high yields by hydrogenation over PtO_2 of the respective -cyano esters and subsequent hydrolysis [20].

The 3-phenylureido acids were obtained by the standard Schotten-Baumann procedure with phenylisocyanate. Prolonged heating of the phenylureido acids upon recrystallization from water caused caused in some cases decomposition to amino acid and diphenylurea leading to lower m.p. Refluxing the ureido acids with dilute hydrochloric acids in water/ethanol produced the dihydrouracils. The cyclization can be complicated by several factors exemplified in the synthesis of the bicyclic dihydrouracils from the geometrical isomers of 2-(3-phenylureido)cyclohexane carboxylic acid. Adding more ethanol to augment solubility lead to a complex mixture from which the ethyl esters (according to elemental analysis and mass spectra) instead of dihydrouracils could be isolated. Prolonged reflux in 1:5 HCl solutions lead to some hydrolysis generating the parent amino acid. The appreciable reversibility of the cyclization reactions also complicated the isolation of the cyclic products. The reaction conditions were optimized by monitoring the reaction by means UV-spectrometry.

Kinetics of the reversible cyclization of 3-(3-phenylureido) acids and the Leffler linear free energy relationships between rate and equilibrium constants

The studied reactant and product pairs in the reversible cyclization of -phenylureido acids are designated by numbers in Table 1. The reaction kinetics were monitored by means of UV-spectrophotometry [20].

The phenylureido acids were chosen as substrates because the weak nucleofilicity of the -phenylureido group shifted the equilibria towards the open form and so a greater range of equilibrium constants could be determined by means of UV. Of the compounds listed on Table 1 the equilibrium could not be measured only with the , -dimethylalanine derivative (**11**) obviously showing the strongest GDME.

Fig. 2 shows the log/log plot of the relative rates of hydrolysis of 3-phenyldihydrouracils against the equilibrium constants.

♥ These N-phenyl derivatives allow a wide range of equilibrium constants to be determined by UV-spectrophotometry.

Table 1. Apparent equilibrium constants and rate constants, s^{-1}, for cyclization of 3-(3'-phenylureido)propanoic acids in 1 M H_2SO_4 at 70.0°C

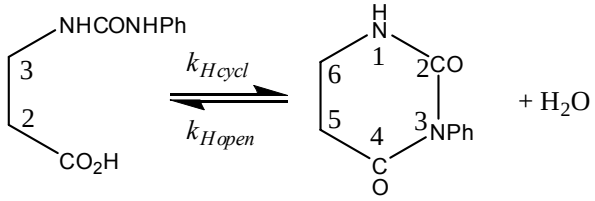

K_E = [DHU]/[UA]

#	Substituent	K_E	K_E^{rel}	$10^5 k_{Hcycl}$	k_{Hcycl}^{rel}	$10^5 k_{Hopen}$	k_{Hopen}^{rel}
1	None	0.337	1	2.56	1	7.79	1
2	2-Me	0.968	2.87	2.92	1.41	3.01	0.386
3	2-Et	0.814	2.42	2.23	0.871	2.73	0.350
4	2,2-diMe	3.10	9.20	1.40	0.574	0.452	0.058
5	2,2-diEt	7.30	21.7	0.601	0.235	0.0824	0.0106
6	3-Me	3.09	9.17	5.50	2.15	1.78	0.228
7	3-Et	2.11	6.42	4.51	1.76	2.16	0.277
8	3-isoPr	3.64	10.8	4.97	1.94	1.37	0.240
9	3-tert-Bu	5.56	16.5	3.07	1.20	2.97	0.381
10	3-Ph	1.35	4.01	2.71	1.06	2.01	0.258
11	3,3-diMe [a]	[a]		32.0	12.5		
12	R*,R*-2,3-diMe	12.4	36.9	8.11	3.17	0.650	0.0834
13	R*,S*-2,3-diMe	6.96	20.6	2.11	0.824	0.304	0.039
14	N-Me	7.33	21.7	85.7	33.5	11.7	1.50
15	*trans* 2,3-TM [b]	5.26	15.6	13.1	5.12	2.49	0.320
16	*cis* 2,3-TM [b]	23.2	68.8	3.01	1.18	7.71	0.989

[a] Equilibrium strongly shifted to the ring form and could not be measured. [b] TM = tetramethylene.

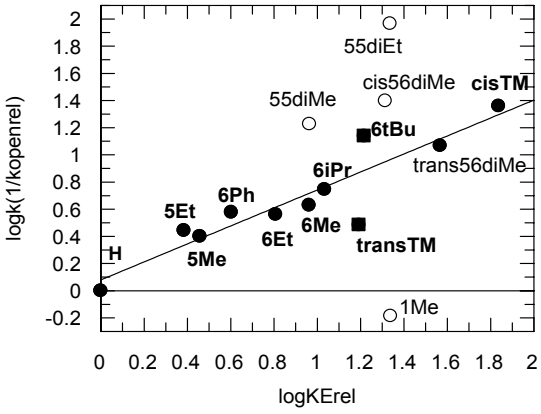

Fig. 2. Logarithmic plot of the relative rates of acid catalyzed hydrolysis of 3-phenyldihydrouracils against the relative equilibrium constants. Full circles and squares: data used in the linear fits, open circles: remaining data of Table 1.

This plot defines two types of substituent behaviour:

(a) The larger part (11 out of 15) exhibit the general GDME defined by its linear correlation with the GDME of the equilibrium between the open and ring forms:

$$\log(1/k_{Hopen}^{rel}) = \rho \log K_E^{rel} \qquad (3);$$

(b) the remaining substituents show deviations from linearity due to specific effects arising in the transition state.

The linear fit on Fig. 2 defines an equation** with following parameters:

$$\log(1/k_{Hopen}^{rel}) = (0.65 \pm 0.1) \log K_E^{rel} \quad (r = 0.909) \text{ (4a)}$$

Actually if the points denoted as squares are omitted the remaining 9 points give a linear relationship of much improved statistics with practically the same slope:

$$\log(1/k_{Hopen}^{rel}) = (0.66 \pm 0.05) \log K_E^{rel} \quad (r = 0.981) \text{ (4b)}$$

The greater scatter of the two points depicted as squares is not surprising – the *t*-butyl group is one of the most bulky groups while *trans*-5,6-tetramethylenedihydrouracil is a rigid structure. For these reasons the capacity for accommodating strains in the various species involved in pairs **9** and **15** could differ in some extent from the "better-behaved" substituents.

Comparison of Fig. 1 and Fig. 2 clearly shows the advantage of a Leffler relationship with respect

** ($1/k_{open}$) was chosen in order to deal with a positive slope.

to correlations of the GDME with Taft's *E*s constants – the points for substituents on C-atoms at different positions of the ring fall on the same line.

The data designated with open circles deviate strongly and can not be included in the correlations. Compounds 5,5-dimethylDHU, 5,5-diethylDHU, *cis*-5,6-dimethylDHU react more slowly than demanded by the LFER. All these necessarily have an axial 5-methyl group (in the last compound the alternate conformation with equatorial 5-methyl will give rise to the strong repulsion between axial 6-methyl and axial OH at 4-C, see Scheme 2, R^4 OH). 3-N is positively charged because of rate determining ureido group attack [21] and solvated respectively causing strong steric repulsion with an axial 5-substituent (Me or Et) (R^2 H, Scheme 2). This interaction is specific for the transition states of these compounds being absent in the product DHU bringing about deviation from linearity. A very large deviation but in the opposite direction (faster hydrolysis) is observed with 1-methylDHU. For the pair **14** K_E^{rel} is 21.7 showing considerable relaxation of strain in the ring form but contrary to the remaining cases, the transition from ring to the transition state is accompanied by greated release of strain indicated by k_{open}^{rel} is 1.5. Accordingly, $k_{cycl}^{rel} > K_E^{rel}$. These observations can be understood in terms of the bond angles in six-membered rings with planar segments. In the fully planar case, all these tend to be 120° because of the requirement for a sum of 720°. The smaller the planar segment the smaller the pressure for enforcing these angles because of the accommodation due to puckering [14]. In the product DHU ring planarity encompasses four atoms, while only two in the tetrahedral intermediate of Scheme 2 thus the squeeze exercised by the N-methyl group (R^5) will meet less resistance.

Correlation of systems with similar steric requirements

There are two obvious ways of expanding the correlations of the GDME to other reactions in dihydrouracil systems. One is to use the equilibrium series as a reference series in the way -values are defined for use in the Hammett equation. The other is to correlate rates of cyclizations or rates of ring opening of various derivatives, the common feature being the tetrahedral intermediates. The second procedure bears the promise of incorporating the cases of specific interactions in the transition states.

To test those two approaches, correlations with the rates for alkaline hydrolysis of 3-phenyldihydrouracils were attempted. These could be were measured in 0.01 M KOH for a lot of the compounds of Table 1 and supplemented with previously obtained second order rate constants. The data are listed in Table 2 which preserves the numbering of Table 1.

Table 2. Rates of alkaline hydrolysis of 3-phenyldihydropymidine-2,4-diones at 25.0°C I = 1 M (KCl).

#	Substituent	k_{OH} $dm^3 \cdot mol^{-1} \cdot s^{-1}$	k_{OH}^{rel}	$1/k_{OH}^{rel}$
1	None [a]	2.26	1	1
2	5-Me [b]	1.55	0.69	1.46
4	5,5-diMe [b]	0.453	0.200	5.00
5	5,5-diEt [c]	0.0165	0.00730	137
6	6-Me [b]	1.24	0.549	1.82
7	6-Et [c]	1.04	0.460	2.17
8	6-isoPr [c]	0.802	0.355	2.82
10	6-Ph [c]	0.800	0.354	2.82
11	6,6-diMe [b]	0.0127	0.00562	178
12	R*,R*-5,6-diMe [b]	0.373	0.165	6.06
14	1-Me [b]	1.44	0.637	1.57

[a] From Ref. 22; [b] From Ref. 23; [c] Measured in 0.01 M KOH and converted into second order rate constants by multiplication by 100 because hydrolysis 3-phenyldihydrouracils is 1st order in [KOH] [22].

Fig. 3 shows a log/log plot of the inverse relative constants for alkaline hydrolysis against the ureido acid = dihydrouracil equilibrium constants.

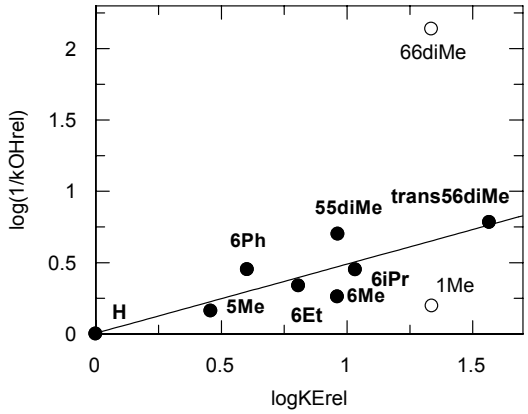

Fig. 3. Plot of $\log(1/k_{OH}^{rel})$ for the alkaline hydrolysis of 3-phenyldihydrouracils against $\log K_E^{rel}$

As readily seen the larger part of the points (8 out of ten) fit a linear relationship:

$$\log(1/k_{OH}^{rel}) = \rho \log K_E^{rel}, \quad = 0.48 \pm 0.12, \quad r = 0.853 \qquad (5)$$

The transition state is negatively charged, the 3-N atom is sp^2 hybridized and the planar segment consists of three atoms (Scheme 1). Compared to the positively charged transition state in acid the alkaline one has a ring geometry closer to that of the product dihydrouracil. This reduces the "specific" effects allowing the 5,5-dimethyl and the R*,R*-dimethyl derivative to be included in the common correlation. Exclusion of the former point, however, improves the linear fit (= 0.46, r = 0.900).

The second approach to correlate two reaction series with sterically similar transition states is demonstrated on Fig. 4 depicting a log/log plot of relative rates of ring opening under alkaline conditions against acid catalysis:

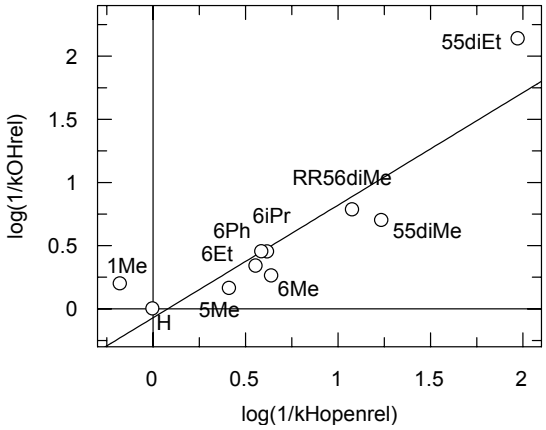

Fig. 4. Plot of $\log(1/k_{OH}^{rel})$ for the alkaline hydrolysis of 3-phenyldihydrouracils against $\log(1/k_{Hopen}^{rel})$.

All points fitted the equation

$$\log(1/k_{OH}^{rel}) = \rho \log(1/k_{Hopen}^{rel}), \quad = 0.89 \pm 0.15, \quad r = 0.906 \qquad (6)$$

which is a good achievement in itself taking into account the large variation in substitution.

An important application of Leffler type LFER is that the slopes, , measure the value of the internal reaction coordinate, IRC. These for acid and alkaline hydrolysis of dihydrouracils are 0.65 (Eqn. 4a) and 0.48 (Eqn. 5), respectively, indicating a more advanced transition state under acid catalysis. This agrees with the smaller than unity slope of the k_{OH}/k_H correlation (Eqn. 4) but quantitatively the agreement is not close. Actually when the strongly deviating points for 1-Me and 5,5-diMe are excluded from the correlation on Fig. 4, a line of slope of 0.65 (r = 0.939) obtains which is in much better agreement with the -values of Eqns. 2 and 3.

Because these hydrolysis reactions proceed through tetrahedral intermediates some elucidation is needed with regard to the meaning of the IRC. A convenient way is to assign 1 to the intermediate and zero to both reactants (the ring systems in our case) and products. With regard to steric effects to a large extent these are symmetrical on both sides of the intermediate♣. This allows conclusions to be drawn both in the cases of breakdown and of formation of tetrahedral intermediate. Rate determining in the alkaline hydrolysis of 3-phenyldihydrouracils is the attack of OH^- [22, 23], while in acid hydrolysis this is breaking of the C–N bond [21]. Thus = 0.48 for alkaline hydrolysis means that the C–O bond is 48% formed, while in the acid hydrolysis IRC for the breakdown of the C–N bond will be (1 – 0.65) i.e. the breaking will be 35%.

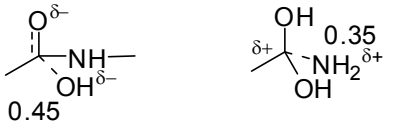

EXPERIMENTAL

Uncorrected melting points were measured in capillaries, IR spectra on a Specord IR 75 or Bruker IFS 113v instrument, UV spectra on a Specord UV-Vis or a UNICAM SP 800 spectrophotometer. Mass spectra EI on a JEOL JMS-D 300 spectrometer. The 1H NMR spectra on a Bruker DRX250 or a Avance II+ 600MHz instruments in DMSO-d_6 unless stated otherwise. ^{1}H-NMR signals were referenced TMS and coupling constants are given in Hz and without sign.

Materials

Inorganic reagents and buffer components were of analytical grade and were used without further purification. Potassium hydroxide solutions were prepared with CO_2-free distilled water. 3-(3-phenylureido)propanoic acid and its 2-methyl, 3-methyl, 2,2-dimethyl, 3,3-dimethyl, (R*,S*)-2,3-dimethyl derivatives as well as their cyclization products dihydropyrimidinediones have been described in Ref. 23. *cis*- and *trans*-2-Aminocyclohexane-carboxylic acid were obtained as described previously [24].

3-amino acids

-Monosubstituted -alanines were prepared essentially by the procedure developed by Rodionov and Zworykina [25] for 3-aminooctanoic acid.

3-Aminopentanoic acid. An ethanolic solution of ammonia (200 ml, 3.5% w/v) was added to propanal (16 g, 0276 mol) and malonic acid (28.7 g, 0.275 mol) in a round bottom flask under cooling with water. This was attached to a Liebig's condenser and the mixture slowly heated to 50–60°C and kept at this temperature for 2–3 h. The mixture was then brought to boiling and the oil remaining after ethanol was distilled off was heated further 3 h at 120°C on a glycerol bath. After cooling the oil (which hardens upon standing) was triturated with 200 ml diluted (1:3 v/v) hydrochloric acid. The mixture extracted three times with ether, the organic layer discarded. The water layer evaporated on a

♣ This applies to polar effects as well.

rotatory evaporator to dryness, adding twice some water and evaporating again to remove residual HCl. The residue dissolved in a minimal amount of water and passed through a column packed with the strong cation exchanger Wofatit KPS 200 I H^+-form. After washing the column with water to neutral reaction the amino acid was eluted with 1 L of diluted 1:10 v/v ammonia solution (ca. 1 M). The eluate evaporated to dryness gave an oil consisting of the amino acid according NMR, 6.8 g (yield 21%). Dissolved under reflux in 70 ml of dry ethanol and precipitated with 150 ml of dry ether to give 4.8 g (15%), m.p. 164–168°C decomp. ending at 185°C (lit. decomp. 160–165°C 185 clear [26]. ^{1}H NMR: (D_2O) 0.99 (t 3H 7.3), 1.69 (quintet 2H 7.3), 2.51 (2H AB octet of ABX 31.8 Hz, J_{AB} 16.6, J_{AX} 8.1, J_{BX} 4.2), 3.44 (m 1H).

3-Amino-4-methylpentanoic acid. iso-Butyraldehyde (23 g, 0.319 gmol) and 6 g of ammonia dissolved in 50 ml of EtOH were mixed under ice-cooling followed by 33.2 (0.32 gmol) of malonic acid. The mixture was heated gradually to 80°C and kept at this temperarue for 3 h. over a period of two hours the temperature of the bath was raised to 120°C and kept at this temperature 4 h until evolution of CO_2 ceased. After work up as above and recrystallization of the free amino acid from ca. 250 ml of ethanol 22.0 g (52%) were obtained, m.p. 195.5–197°C (lit. m.p. 197–197.5°C [27]).

3-amino-4,4-dimethylpentanoic acid. Pivalaldehyde (6.9 g 0.08 mol), 8.3 g (0.08 mol) of malonic acid and 12 ml of 10–12% ethanolic ammonia under the above procedure gave 1.7 g (15%) of the free amino acid. m.p. 224–225°C (from ethanol, Kofler). Anal. Calcd for $C_7H_{15}NO_2$: N, 9.65. Found: N, 9.76.

2-(aminomethyl)butanoic acid. The amino acid was obtained from ethyl 2-cyanobutanoate [27] by hydrogenation [28] over PtO_2 under 40 atm of H_2 at room temperature for 1 h and subsequent hydrolysis of the amino ester. Ethyl 2-(aminomethyl)butanoate, (10.3 g 0.07 mol), was refuxed in 10 ml of 1/1 HCl for 11 h. Two layers were formed, the oil decreasing in the course of the reaction. After cooling, the oil was extracted with ether. The water layer evaporated to dryness. To remove residual HCl twice small amounts of water were added and evaporated again. The free amino acid was obtained by means of a strong cation exchanger as described above in a 66% yield. Recrystallized from ethanol/water. Could not be obtained in an entirely pure state according to t.l.c. (on silica with mobile phase MeOH/$CHCl_3$ (4/1) presaturated with ammonia placed in a separate vessel). This product was further transformed into N-phenylcarbamoyl derivative with phenylisocyanate.

2-(aminomethyl)-2-ethylbutanoic acid. The amino acid was obtained by hydrogenation from ethyl 2-cyano-2-ethylbutanoate [29] as described above. Ethyl 3-amino-2-ethylbutanoate (12.1 g 0.07 mol) was refluxed for 9 h in 60 ml of 1/1 (v/v) HCl. Some oil extracted with ether and the aqueous layer evaporated to dryness *in vacuo* to give 7.6 g of the hydrochloride (59%). The free amino acid was obtained by means of a strong cation exchanger as described above in a 43% yield. Recrystallized from ethanol/water. The crystal plates transform into needles at 180°C which melt at 225–230°C. Gives one spot on t.l.c. on silica with mobile phase MeOH/$CHCl_3$ (4/1) presaturated with ammonia placed in a separate vessel. This product was further transformed into N-phenylcarbamoyl derivative with phenylisocyanate.

3-(3-phenylureido) acids

3-(3'-Phenylureido)pentanoic acid. 3-Aminopentanoic acid (3.80 g, 32.5 mmol) was dissolved in 4.9 ml of 1 M KOH. Under stirring and cooling with ice 4.6 g, 38.7 mmol, of phenylisocyanate were added. After an hour, the cooling bath was removed and the mixture stirred at room temperature until the smell of PhNCO disappeared. Some diphenylurea was filtered off and the filtrate acidified with HCl (1:1 v/v) on Kongo Red. An oil was obtained which solidified with some crystalline phase upon standing in the fridge, 6.6 g (86%). Recrystallized twice from water/ethatnol 2.7 g m.p. 147–147.5°C with decomp. (lit. m.p. 141.5°C [30]). NMR: The precise assignments of the ^{1}H and ^{13}C NMR spectra could be achieved on a 600 MHz instrument and were accomplished by measurement of 2D homonuclear correlation (COSY), DEPT-135 and 2D inverse detected heteronuclear (C–H) correlations (HSQC and HMBC).

The spin system including protons from $CH_3CH_2CH(NH–)CH_2–$ fragment was simulated and the parameters were iterated by program DAISY (included in the program package TOPSPIN 2.1) in order to obtain precise values for chemical shifts and coupling constants. The fragment was treated as $ABMNP_2X_3$ system.

= 0.861 (t, J = 7.4 Hz, 3H, CH_3), 1.445 (qdd, J = 7.4, 8.1, 13.6 Hz, 1H, A-part), 1.523 (dqdd, J = 0.2, 5.3, 7.4, 13.6 Hz, 1H, B-part), 2.395 (d, J = 6.3 Hz, 2H, C<u>H</u>$_2$COOH), 3.866 (dtdd, J = 5.3, 5.3, 8.1, 8.6 Hz, 1H, CH), 6.094 (d, J = 8.6 Hz, 1H, N<u>H</u>CH), 6.871 (tt, J = 1.1, 7.4 Hz, 1H, *p*-Ph), 7.201 (dd, J = 7.4, 8.5 Hz, 2H, *m*-Ph), 7.365 (dd, J = 1.1, 8.6 Hz, 2H, *o*-Ph), 8.456 (bs, 1H, N<u>H</u>Ph), 12.2 (bs, 1H, COOH).

^{13}C NMR (150 MHz, DMSO-d6, 25°C): = 10.20

(CH_3), 27.06 (CH_2), 39.06 ($\underline{C}H_2COOH$), 47.48 (CH), 117.38 (*o*-Ph), 120.83 (*p*-Ph), 128.52 (*m*-Ph), 140.43 (*i*-Ph), 154.60 (NHCONH), 172.71 (COOH).

4-methyl-3-(3'-phenylureido)pentanoic acid. Obtained as above from the respective amino acid and phenylisocyanate in a 93% yield. Recystallized from water/ethanol m.p.143–145°C with decomp. Anal. Calcd for $C_{13}H_{18}N_2O_3$: C, 62.38; H, 7.25. Found: C, 62.74; H, 7.44.

4,4-Dimethyl-3-(3'-phenylureido)pentanoic acid. Obtained as above from the respective amino acid and phenylisocyanate in an 80% yield. M.p. 188–192°C decomp. (from ethanol/water). ^{1}H NMR (CD_3CN) 1.00 (s 9H), 2.33 (q 1H 9.8, 15.1), 2.695 (q 1H 3.7, 15.1), 4.099 (m 1H), 4.11 (t 1H ~ 1.5 Hz) 5.35 (d 1H) 7.04 (app. t 1H) 7.33 (app. t 2H) 4.45 (app. d 2H). Anal. Calcd for $C_{14}H_{20}N_2O_3$: N, 10.60. Found: N, 10.32.

3-((3'-phenylureido)methyl)butanoic acid. 2-(aminomethyl)butanoic acid (0.3 g 2.6 mmol) was treated with phenylisocyanate as described above to give 0.36 g (60%) phenylureido acid, m.p. 145–148°C decomp. (from ethanol/water). ^{1}H NMR: 0.89 (t 3H 7.0); 1.50 (m 2H); 2.38 (quintet 1H 6.5); 3.24 (m 2H); 6.19 (t 1H 5) 6.89 (app. t 1H 7); 7.21 (app. t 2H 7); 7.36 (app. d 2H 7); 8.52 (s). Anal. Calcd. for $C_{12}H_{16}N_2O_3$: N, 11.86. Found: N, 11.36.

2-ethyl-2-((3-phenylureido)methyl)butanoic acid. 2-(aminomethyl)-2-ethylbutanoic acid (0.70 g 4.8 mmol) was treated with phenylisocyanate as described above to give 1.01 g (78%) phenylureido acid, m.p. 182–184°C with decomp. (from ethanol/water). ^{1}H NMR: 0.80 (t 6H 7.3); 1.50 (quartet 4H 7.3); 3.30 (d 2H 5.9); 6.02 (t 1H 5.9); 6.89 (app. t 1H 7); 7.22 (app. t 2H 7); 7.37 (app. d 2H 7); 12.41 (broad s). Anal. Calcd. for $C_{14}H_{20}N_2O_3$: N, 10.60. Found: 10.42.

(R,S*)-2-methyl-3-(3-phenylureido)butanoic acid. (R*,S*)*-3-Amino-2-methylbutanoic acid (1.17 g 0.01 mol) was treated with phenylisocyanate as described above to give 2.27 g (96%) phenylureido acid. Recrystallized by dissolving at room temperature in 1:1 water/ethanol and cooling, m.p. 181–181.5°C with decomp. Anal. Calcd. For $C_{12}H_{16}N_2O_3$: C, 61.00; H, 6.83; N, 11.84. Found: C, 60.82; H, 6.95; N, 11.31.

cis-2-(3-phenylureido)cyclohexane carboxylic acid. cis-2-Aminocyclohexane carboxylic acid (3.66 g 25.6 mmol) was treated with 3.62 ml of phenylisocyanate as described above to give 2.73 g (40%) phenylureido acid, m.p. 157–158°C from ethanol, one spot on t.l.c. on silica with petroleum ether/ethyl acetate/2-butanol 2/2/1, R_f 0.6. Anal. Calcd. for $C_{14}H_{18}N_2O_3$: N, 10.68. Found: 10.35.

trans-2-(3-phenylureido)cyclohexane carboxylic acid. trans-2-aminocyclohexane carboxylic acid (0.406 g 2.8 mmol) of was treated with 0.40 ml of phenylisocyanate as described above to give 0.609 g phenylureido acid, m.p. 196–199°C from ethanol/water, one spot on t.l.c. on silica with petroleum ether/ethyl acetate/2-butanol 2/2/1, R_f 0.3. Anal. Calcd. for $C_{14}H_{18}N_2O_3$: N, 10.68. Found: 10.80.

Dihydropyrimidine-2,4-diones

6-*Ethyl-3-phenyl-dihydropyrimidine-2,4-dione.* 3-Phenylureidopentanoic acid (0.60 g, 2.5 mmol) were refluxed for one hour in 5 ml of ethanol and 10 ml of 1:2 HCl. After concentrating the solution and cooling, the formed precipate was filtered and recrystallized from 10 ml of ethanol. Yield 0.28 g, 41%. M.p. 199–200°C (lit. [22] m.p. 192°C). ^{1}H NMR: 0.90 (t 3H 7), 1.53 (m 2H) 2.69 (2H AB octet of ABX 54 Hz, J_{AB} 16, J_{AX} 9.5, J_{BX} 5.5,), 3.50 (m 1H) 7.14 (app. d 2H), 7.38 (m 3H) 8.06 (s).

*6-*I*sopropyl-3-phenyl-dihydropyrimidine-2,4-dione*. 4-Methyl-3-(3'-phenylureido)pentanoic acid (2.0 g 8 mmol) in 50 ml 1:5 (v/v) HCl and 30 ml of ethanol were refluxed for 3 h. Upon cooling and recrystallization from ethanol 0.67 g (36%). M.p. 183–185°C. Anal. Calcd for $C_{13}H_{16}N_2O_2$: N, 12.06. Found: N, 12.27.

6-*tert.-Butyl-3-phenyl-dihydropyrimidine-2,4-dione*. 4,4-Dimethyl-3-(3'-phenylureido)-pentanoic acid (0.264 g 1 mmol) was refluxed for 8 h 8 ml of 1:1 (v/v) HCl to which 10 ml of ethanol have been added. A solution was obtained from which upon cooling 70 mg (38%) of the dihydrouracil precipitated as needles. The mother liquor contained a mixture of dihydrouracil and the initial ureido acid (t.l.c. on silica $CDCl_3$ as the eluent). M.p. 228–230°C. ^{1}H NMR: ($CDCl_3$) 1.03 (s 9H), 2.82 (m 2H; AB octet of ABX; lines of lower field quartet additionally split into doublets (^{14}J = 1.3 Hz to 1NH), 29 Hz, J_{AB} 16.4, J_{AX} 10.1, J_{BX} 4.9), 3.42 (octet 1H 10.1, 4.9. 1.7), 5.53 (m 1H unresolved) 7.17 (m 2H) 7.35–7.49 (m 3H). Anal. Calcd for $C_{14}H_{15}N_2O_2$: N, 11.37. Found: N, 11.12.

5-Ethyl-3-phenyl-dihydropyrimidine-2,4-dione. 2-Ethyl-2-((3-phenylureido)methyl)butanoic acid (0.472 g 2 mmol) were refluxed for 10 h in 15 ml of 1:1 (v/v) HCl. After cooling the homogenous solution was evaporated to dryness, adding water and repeating the process until HCl was removed. The residue was an oil consisting of a mixture of the reactant and product dihydropyrimidinedione. Attempts for separation by crystallization were unsuccessful. The oil was triturated with $CHCl_3$. The chloroform extract 160 mg was subjected to

preparative t.l.c. on 20×20 cm glass plates coated with silica. Eluted three times with diethyl ether. The slices containing the product were extracted with 500 ml of $CHCl_3$. The dry residue 120 mg subjected to analysis. M.p. 109–111°C Anal. Calcd for $C_{12}H_{14}N_2O_2$ N, 12.84. Found: N, 12.81.

5,5-Diethyl-3-phenyl-dihydropyrimidine-2,4-dione. 2-Ethyl-2-((3-phenylureido)methyl)butanoic acid (0.528 g 2 mmol) was refluxed for 10 h in a mixture of 15 ml 1:1 HCl and 5 ml ethanol. After cooling 0.4 g precipitated presenting a mixture of starting ureido acid and the cyclic product. The two show very similar R_f-values on t.l.c. and could be separated after multiple elution with ether. Pure dihydropyrimidine-2,4-dione was obtained by means of repeated recrystalliztion. UV monitoring of the cyclization showed that equilibrium is reached with a half-live of ca. 1 h at 90°C. M.p. 122–124°C Anal. Calcd for $C_{12}H_{14}N_2O_2$: N, 11.37. Found: N, 11.37.

cis-5,6-tetramethylene-3-phenyldihydropyrimidine-2,4-dione. *cis*-2-(3-phenylureido)cyclohexane carboxylic acid (0.203 g 0.78 mmol) in 360 ml of 1:6 HCl was stirred at 70°C for 14 h. The reaction course was followed by means of UV-spectral analysis in the following manner: Aliquots: 0.8 ml of the reaction solution were diluted to 25 ml with distilled water and the extinction measured at $_{max}$ = 238.5 of the phenylureido acid (the absorbance of dihydrouracils is negligible at this wave-length. Aliquot of the diluted sample was mixed with an equal volume of 0.1 M NaOH whereby the dihydrouracil was rapidly hydrolysed. The extinction of the hydrolysate should equal that of 1/2 of the initial ureido acid and can serve also to assess to any degradation to amino acid. Under the above conditions over 90% yield of the pyriminedione was estimated and no significant amounts of amino acid. As no precitate was formed after cooling, the reaction solution was evaporated to dryness washed with water to remove HCl and recrystallised from ethanol/water to give 0.113 g (59%) m.p. 219–220°C after second recrystallization. One spot on t.l.c. on silica with petroleum ether/ether/2-butanol 2/2/1 as the eluent

trans-5,6-tetramethylene-3-phenyldihydropyrimidine-2,4-dione. trans-2-(3-Phenylureido)cyclohexane carboxylic acid, 0.150 g 0.57 mmol, in 360 ml of 1:5 HCl were heated for 9 h at 65°C. The reaction mixture evaporated to ca 20 ml and left to crystallize. The precipitate filtered, dissolved in hot EtOH, treated with carbon and left to crystallize. 120 mg (86%) m.p. after second recrystallization in sealed capillary 260–261°C. Sublimates around 250°C in a Koffler apparatus.

cis-5,6-dimethyl-3-phenyldihydropyrimidine-2,4-dione. (R*,S*)-2-Methyl-3-(3-phenylureido)butanoic acid (0.52 g 2.2 mmol) in 15 ml 1:5 (v/v) HCl and 10 ml of ethanol were refluxed for 3 h. The solution concentrated and left to crystallize. The precipitate was recrystallized from ethanol/water to give 0.12 g (25%) of *cis*-dihydropyrimidinedione, m.p. 181–181.5°C. Anal. Calcd. for $C_{12}H_{14}N_2O_3$: C, 61.00, H, 6.83, N, 12.86. Found: C, 60.82, H, 6.95, N, 12.29.

trans-Ethyl 2-(3-phenylureido)cyclohexane carboxylate. *trans*-2-(3-Phenylureido)cyclohexane carboxylic acid (0.286 g 1.1 mmol) was refluxed in a mixture of 7 ml of 1:5 HCl and 8.5 ml of EtOH for 10 h. t.l.c. (ethyl acetate/petroleum ether/*n*-butanol 2/2/1) showed under UV a mixture of the initial ureido acid and a faster miving product. Upon cooling 96 mg of amino acid hydrochloride separated (ninhydrin reaction on t.l.c.). The mother liquor was evaporated to dryness and the residue dissolved in a mixture of water and ether and alkalized to pH 8 with aqueous ammonia. The ether layer yielded 80 mg product purified from admixture of the ureido acid by preparative t.l.c. with ether as the mobile phase. The extracted oil recrystallized from ethanol/water bright plates, m.p. 117–118°C. Anal. Calcd. for $C_{16}H_{22}N_2O_3$: N, 9.65. Found: 9.95. MS (chemical ionization) [M+1] 291 (fragments: 198, 172, 94).

cis-Ethyl 2-(3-phenylureido)cyclohexane carboxylate. *cis* 2-(3-phenylureido)cyclohexane carboxylic acid (0.450 g 1.7 mmol) was refluxed for 3 h in a mixture of 10 ml of 1:5 HCl and 6 ml of ethanol. Similar work up as with the *trans* isomer and preparative t.l.c. with ether/petroleum ether 1/1 gave 85 mg product which was recrystallized from methanol/water, m.p. 99–101°C. Anal. Calcd. for $C_{16}H_{22}N_2O_3$: N, 9.65. Found: 10.18. MS (chemical ionization) [M+1] 291 (fragments: 198, 172, 94).

Kinetic runs

The acid catalyzed reactions were carried out in 1 M H_2SO_4 at 70.0°C as described in Ref. 21 using two techniques: in the 10 mm stoppered quartz cells or in sealed ampoules for the slow reactions. The monitoring of both the cyclization and ring-opening reactions as well as the equilibrium concentrations was done at 238–240 nm which is $_{max}$ due to the phenylureido chromophore. The extent of further hydrolysis to amino acid was checked by means of alkaline hydrolysis of the product which restored the expected ureido acid absorption within experimental error. To this purpose, after completion of the reaction 1, 2 ml of the solution of the substrate in

1 M H_2SO_4 were diluted with 3 ml of 3 M KOH and 5 ml of water. At this alkalinity of 0.22 M the hydrolysis to the ureido acid is complete within several minutes and the absorption of the ureido acid salt can be compared to that of the acid because the extinctions are equal. Equilibria were reached starting from ureido acid and from dihydrouracil.

The rates of alkaline hydrolysis of the dihydrouracils were measured in 0.01 M KOH, I = 1 (KCl) at 25.0°C in the temperature controlled cell holder of the UNICAN SP 800 instrument using motors for fast scanning essentially as described in Ref. 23.

***Acknowledgement**: We thank the National Science Found of Bulgaria (Grant X-1408) for financial support.*

REFERENCES

1. C. D. Selassie in: Burger`s Medicinal Chemistry and Drug Discovery, 6th ed., D. J. Abraham, Ed., Vol. 1, Wiley, New York, pp. 1–48 (2003).
2. L. P. Hammett, Physical Organic Chemistry, McGraw Hill, New York, 1940.
3. R. A. Marcus, *J. Phys. Chem.,* **72**, 891 (1968).
4. J. E. Leffler, *Science*, **117,** 340 (1953).
5. J. N. Brønsted , K. Pedersen, *Z. Phys. Chem*., **108,** 185 (1924).
6. M. Page, A. Williams, Organic and Bio-organic Mechanisms, Longman, Singapore, 1997, p. 62–75.
7. A. Williams, *Acc. Chem. Res*., **17**, 425 (1984); A. Williams, *Adv. Phys. Org. Chem.,* **27**, 1 (1991).
8. J. Shorter, Advances in Linear Free Energy Relationships, N. B. Chapman, J. Shorter (Ed.), Plenum, London, Ch. 2, p. 71.
9. a. T. C. Bruice, W. C. Bradbury, *J. Am. Chem. Soc*., **87**, 4838 (1965). b. V. A. Palm, Osnovy Kolichestvennoi Teorii Organicheskikh Reaktsii, Khimiya, Leningrad, 1977, p. 236–237.
10. I. Pojarlieff, Z. Burgudjiev, I. Blagoeva, B. J. Kurtev, *Commun. Dept. Chem*. *Bulg. Acad. Sci*., **3,** 593 (1970).
11. I. B. Blagoeva, B. J. Kurtev, I. G. Pojarlieff, *J. Chem. Soc*., *Perkin Trans. 2*, 1115 (1979).
12. R. M. Beesley, C. K. Ingold, J. F. Thorpe, *J. Chem. Soc*., **113,** 1080 (1915); C. K. Ingold, *J. Chem. Soc*., **119**, 305 (1921); C. K. Ingold, S. Sako, J. F. Thorpe , *J. Chem. Soc.*, **120,** 1117 (1922).
13. T. C. Bruice, *Ann. Rev. Biochem.*, **45**, 331 (1976); A. G. Kirby, *Adv. Phys. Org. Chem.*, **17**, 183 (1980); R. E. Valter, *Usp. Khim.*, **51**, 1374 (1982); F. M. Menger, *Acc. Chem. Res.,* **18**, 128 (1985); L. Mandolini, *Adv. Phys*. *Org. Chem*., **22**, 1 (1986); T. C. Bruice, F. C. Lightstone, *Acc. Chem. Res.*, **32**, 127 (1999); M. E. Jung, G. Pizzi, *Chem. Rev.*, **105**, 1735 (2005).
14. J. Kaneti, A. J. Kirby, A. H. Koedjikov, I. G. Pojarlieff, *Org. Biomol. Chem*., **2**, 1098 (2004).
15. a. C. Danforth, A. W. Nicholson, J. C. James, G. M. Loudon, *J. Am. Chem. Soc.*, **98**, 4275 (1976); R. E. Winnans, C. F. Wilcox, Jr., *J. Am. Chem. Soc.*, **98**, 4281 (1976); b. P. M. Ivanov, I. G. Pojarlieff, *J. Chem. Soc., Perkin Trans*. *2*, 245 (1984); c. A. H. Koedjikov, P. M. Ivanov, I. G. Pojarlieff, *ARKIVOC,* **2**, 44 (2001); d. P. M. Ivanov, I. G. Pojarlieff, I. B. Blagoeva, C. Jaime, V. T. Angelova, A. H. Koedjikov, *J. Phys. Org. Chem*., **17**, 423 (2004).
16. I. B. Blagoeva, A. H. Koedjikov, I. G. Pojarlieff, E. J. Stankevic, *J. Chem. Soc., Perkin Trans*., *2*, 1077 (1984).
17. A. H. Koedjikov, I. B. Blagoeva, I. G. Pojarlieff, A. J. Kirby. *J. Chem. Soc., Perkin Trans. 2*, 2479 (1996).
18. I. B. Blagoeva, I. G. Pojarlieff, V. T. Rachina, *J. Chem. Soc., Chem. Comm*., 946 (1986).
19. I. L. Knunyantz, M. M. Shemyakin, Ed., V. M. Rodionov Izbannye Trudy, Akad. Nauk SSSR, Moscow, 1958; A. Lebedev, A. Lebedeva, V. Sheludyakov, E. Kovaleva, O. Ustinova, I. Kozhevnikov, *Russian J. Gen. Chem*., **75**, 1113 (2005); N. N. Romanova, *Russian J. Org. Chem.,* **39**, 692 (2003).
20. R. Schröter, in: Methoden der Organischen Chemie (Houben-Weyl) Georg Tieme, Stuttgart, 1957, 11/1, p. 557.
21. V. Rachina, I. B. Blagoeva, I. G. Pojarlieff, K. Yates, *Can. J. Chem*., **68**, 1676 (1990).
22. I. B. Blagoeva, I. G. Pojarlieff, *Compt. Rend. Acad. Bulg. Sci.,* **30,** 1043 (1977); M. Bergon, J.-P. Calmon, *C. R. Acad. Sci., Paris*, **233**, ser. C., 637 (1976).
23. I. B. Blagoeva, V. T. Rachina, I. G. Pojarlieff, *Compt. Rend. Acad. Bulg. Sci.,* **35,** 1499 (1982).
24. I.G. Pojarlieff, R.Z. Mitova-Cherneva, I. Blagoeva, B.J. Kurtev, *Compt. Rend. Acad. Bulg. Sci.*, **21,** 131 (1968).
25. V. M. Rodionov, V. K. Zvorykina, *Izv. AN SSSR, OKhN*, 216 (1943).
26. H. D. Dakin, *J. Biol. Chem.,* **99**, 531 (1933).
27. L. Birkofer, I. Stroch, *Chem. Ber*., **86**, 529 (1953).
28. E. R. Alexander, A. C. Cope, *J. Am. Chem. Soc*., **66**, 887 (1944).
29. J. H. Brothe, C. D. Wilson, *J. Am. Chem. Soc*., **68,** 449 (1946).
30. A. Anziegin, W. Gulewivich, *Z. Physiol. Chem*., **158**, 32 (1926).

гем-

(*гем-* A)

. . , . . - , . . , . . *,
. . , . . , . .

Институт по органична химия с център по фитохимия, Българска академия на науките, ул. „Акад. Г. Бончев“, бл. 9, 1113 София

Посветена на акад. Иван Юхновски по повод на 70-та му годишнина

26 2008 ., 1 2008 .

гем- , ,
,
, , . E_S- .
. 3-(3-)
, . .
, .
; ,
, .
:
-
.
” ”
„
.
.
- -
.
3- -2,4-
.

Bulgarian Chemical Communications, Volume 40, Number 3 (pp. 397–402) 2008

Brassica plants as a new source of food grade peptidases

M. D. Marinova*, B. P. Tchorbanov

Department of Biochemistry, Faculty of Biology, Sofia University "St. Kliment Ohridski", 8 Dragan Tzankov Blvd., 1164 Sofia, Bulgaria

Dedicated to Academician Ivan Juchnovski on the occasion of his 70th birthday

Received March 13, 2008, Revised March 30, 2008

Several plants of Brassica (cabbage, Brussels sprouts, kohlrabi, broccoli, cauliflower and Chinese cabbage) were screened for aminopeptidase and iminopeptidase activities using L-leucine-p-nitroanilide and proline-p-nitroanilide as substrates, respectively. Significant levels of aminopeptidase (40–160 μU/g) and iminopeptidase (40–100 μU/g) activities with seasonal variability were detected. The peptidases were precipitated from the native juice by ammonium sulfate saturation (25–70%) and separated by gel filtration chromatography on Sephadex G-200. The aminopeptidases (molecular weight ~60 kDa) predominantly hydrolyzed phenylalanine-p-nitroanilide as substrate, while the iminopeptidases (molecular weight ~200 kDa) were strongly specific to the applied substrate. The pH optima, 7–7.5 for aminopeptidases activities and 8–8.5 for iminopeptidases activities, were determined and they demonstrated a temperature optimum at 40 and 45ºC, respectively.

The edible biomass from Brassica plants is a new effective source of food grade exopeptidases meeting all the requirements with regard to contemporary ecological and economical concepts. The aminopeptidases and iminopeptidases can be used successfully for peptide modification under mild conditions during food processing, e.g. debittering of protein hydrolysates or in substrates with high Q-value.

Key words: Brassica plants, aminopeptidases, iminopeptidases, exopeptidases.

INTRODUCTION

Plant enzymes are essential for different biological processes and often meet all the requirements with regard to contemporary ecological and economical concepts. Aminopeptidases (EC 3.4.11) from plants have been isolated and characterized from various sources [1–5]. Most reports describe aminopeptidases from seeds and leaves. These enzymes catalyze the sequential removal of amino acids from the unblocked N-termini of peptides and proteins. In addition to their role in general protein and peptide metabolism, aminopeptidases have more specific functions. These include defense response to infection and wounding [6], protein maturation [7] and auxin transportation [8]. Imino-peptidases in plant kingdom (EC 3.4.13.8-9) are not so well investigated. Since plant aminopeptidases have little ability to release N-terminal proline-residues, iminopeptidases are important for the degradation of proline-containing peptides. Recently, the importance of proline-degrading proteolytic enzymes in celiac sprue treatment has been evaluated because of their unique ability to accelerate the decomposition of proline-rich gluten in the gut lumen [9].

The aim of this study was to describe aminopeptidase and iminopeptidase activities in Brassica plants, their separation by gel chromatography and to determine the optimal conditions for their application.

EXPERIMENTAL

Plant material

The edible parts of fresh Brassica plants – cabbage (Brassica oleracea var. capitata), Brussels sprouts (Brassica oleracea var. gemmifera), kohlrabi (Brassica oleracea var. gongylodes), cauliflower (Brassica oleracea var. botrytis) and broccoli (Brassica oleracea var. italica) and Chinese cabbage (Brassica pekinensis var. laxa), were used.

The L-amino acid-p-nitroanilides were purchased from Sigma, USA. All the other reagents were of analytical grade of purity. Sephadex G-200 was obtained from Pharmacia Biotech, Sweden.

Enzyme assay

The aminopeptidase activity using amino acyl-p-nitroanilides as substrates was assayed according to the procedure of Chrispeels and Boulter [10]. After incubation for 10 min at 30ºC in 0.05 M phosphate buffer (pH 7.0), the amount of liberated p-nitro-

* To whom all correspondence should be sent:
E-mail: daisy@orgchm.bas.bg

© 2008 Bulgarian Academy of Sciences, Union of Chemists in Bulgaria

aniline was measured at 410 nm on a spectrophotometer (UV-VIS spectrophotometer, Shimadzu 1240). The iminopeptidase activity was assayed spectrophotometrically at 410 nm in regard to L-proline-p-nitroanilide (Prop-NA) according to the approach of Yoshimoto and Tsuru [11] in 0.1 M Tris/HCl buffer (pH 8.0) for 20 min at 30ºC. One unit of enzyme activity was defined as the amount of enzyme releasing 1 µmol of p-nitroaniline per minute.

Protein determination

The amount of soluble protein was determined by the biuret reaction following precipitation with 20% (v/v) trichloroacetic acid (TCA). Bovine serum albumin (BSA) was used to prepare a standard curve [11].

Molecular weight determination

The molecular weights of the enzymes were determined by gel filtration on a Sephadex G-200 column (1.5×146 cm) using as elution medium 0.05 M sodium phosphate buffer at pH 7.5 containing 0.15 M NaCl. Cytochrome C (12 kDa), ovalbumin (45 kDa), bovine serum albumin (66 kDa) and ferritin (440 kDa) were used as standard proteins. The void volume was determined with Blue Dextran.

Enzyme purification

The fresh bio-mass of Brassicaceae plant was cut into pieces, milled and pressed giving a native juice. It was further precipitated with 25–75% ammonium sulphate (at 0°C), followed by centrifugation of the suspension at 6000×g for 30 min at 5ºC (MLW K24 D, Germany). The pellet was resolved in 0.05 M phosphate buffer at pH 7.5 containing 0.15 M NaCl (buffer A) and dialyzed against the same buffer for 4h. The suspension was then clarified by centrifugation at 4000×g for 15 min. The dialyzed solution (3 ml) was applied on a Sephadex G-200 column (1.5×146 cm) equilibrated with buffer A.

Enzyme assay

The exopeptidases were incubated at different temperatures from 15 to 60ºC. At various moments of time, 0.1-ml aliquots of aminopeptidase and iminopeptidase solutions were removed and assayed for activity against 1.5 mM L-leucine-p-nitroanilide (Leu-p-NA) and 0.8 mM Prop-NA, respectively, at 30ºC as it was described previously. The effect of pH optima on the aminopeptidase and iminopeptidase activities was determined using Leu-p-NA and Prop-NA as substrates, respectively, and 25 mM citrate-phosphate buffers (pH 5.0–7.0); 25 mM sodium phosphate buffer (pH 7.0–8.0); 25 mM Tris/HCl buffer (pH 8.5–9.0); and 25 mM glycine-NaOH buffers (pH 9.0–10.0) were used. Following the preincubation for 20 min, a 0.1-ml aliquot was removed and assayed against Leu-p-NA and Prop-NA.

RESULTS AND DISCUSSION

The Brassicaceae plants are a new source of food quality grade peptidases and the levels of the enzymes activities for different representatives are summarized in Table 1. It is seen that the plants of the Brassicaceae family grown during the summer-autumn period have higher exopeptidase activities than that of those grown during the winter-spring. The cabbage seems to be the most attractive source according to its price and the yield from the fresh juice. Moreover, cabbage leaves can be used successfully for preparative production of the enzymes.

Table 1. Aminopeptidase and iminopeptidase activities with seasonal variations in the crude extracts of edible parts from some representatives of Brassicaceae plants.

Brassicaceae plants	Crude juice from 1 kg biomass, ml	Amino-peptidase activity, µU/g	Imino-peptidase activity, µU/g
Cabbage	600	100–130	40–60
Brussel sprouts	200	110–160	100–80
Kohlraby	700	80–110	40–50
Broccoli	500	130–150	100–90
Cauliflower	500	100–120	40–70
Chinese cabbage	600	40–60	40–60

* The first digits showed the enzymes activities measured for winter-spring plants and the second digits – for summer-autumn plants. Aminopeptidase and iminopeptidase activities were determined using L-leucine-p-nitroanilide and proline-p-nitroanilide as substrates, respectively.

The high solution viscosity of all extracts from Brassicaceae plants hindered the filtration process as well as the concentration by ultrafiltration. The exopeptidases from crude extracts were precipitated with ammonium sulfate (25–70%), then the precipitates were resuspended in buffer A and the solutions obtained were further passed through a Sephadex G-200 column (Fig. 1). Under the chosen conditions, the iminopeptidase was separated readily from the aminopeptidase independently of the enzyme source. The elution volumes and the ratio between the two enzymes do not vary much in all cases. Using globular proteins as markers the molecular weights of the studied enzymes were evaluated – 60 ± 3 kDa for aminopeptidases and 200 ± 7 kDa for the iminopeptidases (Fig. 1).

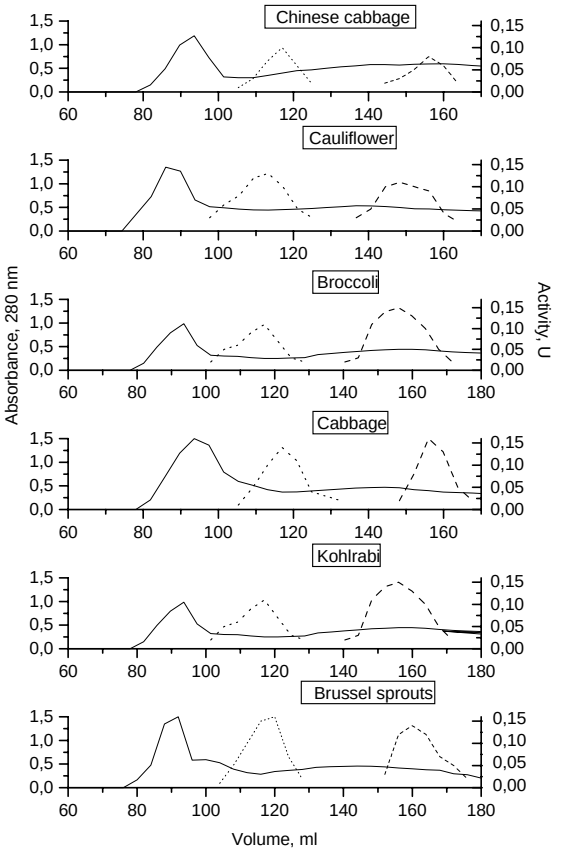

Fig. 1. Elution profiles (—) of exopeptidases from different plants of the *Brassicaceae* family at the outlet of G-200 column (1.5×146 cm), equilibrated with 0.05 M sodium phosphate buffer pH 7.5 containing 0.15 M NaCl. The aminopeptidases (---) and iminopeptidases (~ ~ ~) activities were assayed against L-leucine-*p*-nitroanilide and proline-*p*-nitroanilide, respectively.

During the tests with different L-aminoacyl-*p*-nitroanilides, it was found out that the aminopeptidases predominately hydrolyzed L-phenylalanine-*p*-nitroanilide as substrate while the iminopeptidases were strongly specific to the applied substrate. The action of the isolated enzymes was independent of the salt concentrations in the range 0–15% NaCl. The temperature of 35–45ºC and pH 7.5–8.5 appear to be optimal for the peptidases action (Fig. 2).

The initial characterization of the isolated aminopeptidases and iminopeptidases demonstrated that they closely resembled peptidases purified from other plant species [1]. The aminopeptidases are likely to belong to neutral aminopeptidases with preference to substrates with hydrophobic amino acids, as they have a neutral pH optima and they preferentially hydrolyzed L-phenylalanine-*p*-nitroanilide as substrate [12]. The iminopeptidases also possess most of the other plant iminopeptidases properties, such as an alkaline pH optimum, strong preference for hydrolyzing Pro-*p*-NA and high molecular weight [1, 12].

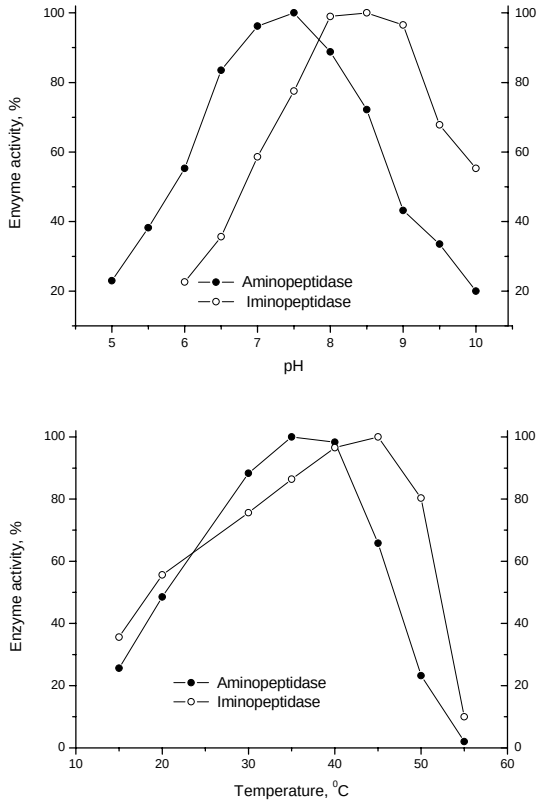

Fig. 2. (Top) pH optima of the aminopeptidases (full symbols) and iminopeptidases (open symbols). (Bottom) Temperature optima of the aminopeptidases (full symbols) and iminopeptidases (open symbols).

CONCLUSIONS

The obtained results manifest, that the edible parts of the *Brassicaceae* plants are real source of peptidases especially as unique combination of aminopeptidases and iminopeptidases. The aminopeptidase action demonstrates a higher specificity to the more hydrophobic substrate – phenylalanine-*p*-nitroanilide. The optimal pH and temperature for peptidase activity were studied and the enzymes could be succesfully employed in reducing the bitterness associated with hydrolysis of food proteins in order to obtain hydrolysates as anti-ageing food ingredients.

Acknowledgment: This work was supported by the Bulgarian National Science Fund (Project No. B-1305/2005).

REFERENCES

1. L. Walling, Y.-Q. Gu, in: Aminopeptidases (Molecular Biology Intelligence Unit), A. Taylor (ed.), Springer-Verlag, Germany, 1996, p. 173–206.
2. K. Arima, T. Uchikoba, M. Shimada, H. Yonezawa, M. Kaneda, Biosci. Biotech. Biochem. **64**,1055 (2000).

3. Y. Yamauchi, Y. Ejiri, K. Tanaka, B
65, 2802 (2001).
4. J. M. Couton, G. Sarah, F. W. Wagn
., **75**, 9 (1992).
5. A. Mikkonen,
., **84**, 393 (1992).
6. V. Pautot, F. M. Holzer, B. Reisch, L. L. Walling,
, **90**, 9906 (1993).
7. C. Giglione, A. Serero, M. Pierre, B. Boisson, T. Meinnel,
., **19**, 5916 (2000).
8. A. Murphy, W. A. Peer, L. Taiz
211, 315 (2000).
9. M. Siegel, T. M. Bethune, J. Gass, J. Ehren, J. Xia, A. Joannsen, B. T. Stuge, M. G. Gray, P. P. Lee, C. Knosla,
., **13**, 649 (2006).
10. M. J. Chrispeels, D. Boulte
55, 1031 (1975).
11. A. G. Gornall, C. J. Bardawill, M. M. David,
177, 751 (1949).
12. M. Marinova, A. Dolashki, F. Altenberend, S. Stevanovic, W. Voelter, B. Tchorbanov,
63c, 105 (2008).

РАСТЕНИЯТА ОТ СЕМ. КАТО ИЗТОЧНИК НА ХРАНИТЕЛНИ ПЕПТИДАЗИ

М. Д. Маринова*, Б. П. Чорбанов

Институт по органична химия с център по фитохимия, Българска академия на науките, ул. Акад. Г. Бончев, бл. 9 София

Посветена на акад. Иван Юхновски по повод на 7 та му годишнина

Постъпила на 13 март 2008г., Преработена на 30 март 2008г.

(Резюме)

Различни представители на растенията от сем. (бяло главесто зеле, брюкселско зеле, алабаш, броколи, карфиол и китайско зеле) бяха изследвани за аминопептидазна и иминопептидазна активност, използвайки като субстрати левцин-*p*-нитроанилид и пролин-*p*-нитроанилид. Бяха установени значителни нива на аминопептидазна (40–160 μU/g) и иминопептидазна (40–100 μU/g) активност със сезонна изменяемост. Екзопептидазите бяха утаени с амониев сулфат (25–70%) и разделени с помощта на гел-филтрационна хроматография на колона Sephadex G-200. Аминопептидазите (молекулна маса ~60 kDa) хидролизират предпочетено фенилаланин-*p*-нитроанилид, докато иминопептидазите (молекулна маса ~200 kDa) проявяват строга специфичност към използвания за скрининг субстрат. Бяха определени pH оптимумите за аминопептидазите 7–7.5 и за иминопептидазите 8–8.5, както и температурните им оптимуми – съответно 40 и 45°C.

Ядивните части на растенията от сем. са нов ефективен източник на хранителни екзопептидази, отговарящи на съвременните екологични и икономически норми. Аминопептидазите и иминопептидазите могат да бъдат успешно използвани за модифициране на пептиди при меки условия в процеса на обработка на храните напр. при обезгорчаване на белтъчни хидролизати от субстрати с висока Q-стойност.

Bulgarian Chemical Communications, Volume 40, Number 4 (pp. 401–408) 2008

Mechanism of the aminolysis of phenyl acetate: a computational study

S. Ilieva*, Y. Atanasov, B. Galabov*

Faculty of Chemistry, St. Kliment Ohridski University of Sofia
1, James Bourchier Blv., 1164 Sofia, Bulgaria

Dedicated to Academician Ivan Juchnovski on the occasion of his 70th birthday

Received November 30, 2007; Revised December 13, 2007

Density functional methods were applied in examining the possible mechanistic pathways for the reaction of phenyl acetate with ammonia. Transition state structures and energies were determined for concerted and neutral stepwise mechanisms. The general base catalysis of the process was also examined. The theoretical predictions reveal that the most favourable pathway of the reaction is through general base-catalysed neutral stepwise mechanism with the nucleophilic attack being the rate-determining stage. Comparisons are made with the energetics of the aminolysis for methyl formate and methyl benzoate. In the latter two esters, the energies of the first and second transition states, associated with the stepwise mechanism, are quite similar in magnitude. In contrast, in the case of phenyl acetate the transition state, associated with the nucleophilic attack (TS1), has distinctly higher energy than the elimination stage (TS2), and is the rate-determining stage of the reaction. The much lower energy of TS2 in phenyl acetate is attributed to the higher stability of the leaving group.

Key words: ester aminolysis, phenyl acetate, mechanism; density functional theory.

INTRODUCTION

The ester aminolysis is an important reaction for both biochemistry and organic chemistry. It is the usual process in the generation of amide functional groups in proteins and peptides [1–9]. The kinetics and mechanism of the reaction has been the subject of numerous experimental [10–19] and theoretical studies [20–33]. These studies have focused on the influence of various factors on the rate and mechanism of the reaction. The detailed understanding of the chemistry of the process – mechanism, reactivity, and catalysis – is, therefore, of importance for both chemistry and biology. The theoretical and experimental results obtained so far indicate that the reaction can proceed *via* two probable paths: concerted and step-wise neutral mechanisms. The particular mechanistic pathway for a pair of ester and amine would depend on the structure of reactants, the presence of excess amine, and the nature of solvent. The aim of the present study is to apply methods of computational quantum chemistry in studying the mechanism of ester aminolysis in the case of phenyl acetate. Ammonia was used as a model reactant.

Phenyl acetate and several ring-substituted derivatives have been popular models for a number of experimental studies on the aminolysis process [10e, 34–40]. Jencks and Carriuolo [34] investigated the reaction of phenyl acetate with several amines in aqueous solution and found out that the process proceeds under general base catalysis. Oleinik *et al.* [37] studied the kinetics of the aminolysis of *p*-nitrophenyl acetate and 2,4-dinitrophenyl acetate by a number of aliphatic amines in various solvents. The kinetic results indicated that the transition state associated with the rate-determining stage of the reaction varies from reactant-like to similar in structure to a tetrahedral intermediate depending on the nature of the participating ester or amine. Lee and co-workers [38] investigated the kinetics of the aminolysis of substituted in the aromatic ring phenyl acetates by benzyl amine in dimethyl sulfoxide solution. Rajarathnam *et al.* [39, 40] examined the kinetics of the aminolysis of *meta* and *para* ring-substituted phenyl acetates by imidazole in aqueous medium.

It was of interest to compare the energy profiles of the aminolysis of phenyl acetate with previously reported results for methyl formate [29a] and methyl benzoate [29d]. In this way it would be possible to assess the influence of aromatic substitution at both sides of the ester grouping on the energy characteristics of the aminolysis reaction.

COMPUTATIONAL METHODS

The computations were carried out with the Gaussian 98 [41] program package. Stable structures and transition states along the reaction pathway were fully optimised by applying B3LYP

* To whom all correspondence should be sent:
E-mail: Galabov@chem.uni-sofia.bg

© 2008 Bulgarian Academy of Sciences, Union of Chemists in Bulgaria

method [42, 43] in conjunction with the 6–31G+(d,p) [44, 45] basis set. The critical points were further characterized by analytic computations of harmonic vibrational frequencies at the same level/basis set. Transition state structures were located by the traditional transition state optimisation using the Berny algorithm [46] and then checked by intrinsic reaction coordinate (IRC) computations [47] at the same level of theory. Single point computations at the MP2/6–31+G(d,p) [48] and MP2/cc-pVTZ [49] level were performed for more precise energy predictions.

The effects of solvent were predicted by using the Polarized Continuum Model (PCM) [50] incorporated in the Gaussian package. Single point PCM//B3LYP/6-31+G(d,p) computations were performed for estimating the change in energy profile of the reaction in presence of water and the aprotic solvent acetonitrile. The standard dielectric constants for water and acetonitrile implemented in the Gaussian program were employed.

RESULTS AND DISCUSSION

As already emphasized in the introductory section, the experimental and theoretical results accumulated so far showed two most likely pathways for the ester aminolysis reaction: concerted and neutral stepwise mechanisms. Theoretical computations have revealed that a step-wise mechanism involving the formation of zwiterionic intermediates is unlikely [29b]. These two possibilities are explored here in studying the reaction of phenyl acetate with ammonia. The manner of attack by the nucleophile differs in the two mechanisms. For the concerted pathway, the initial nucleophilic attack is along the C–O ester bond, while for the stepwise route the reaction begins with an orientation of an N-H bond from NH_3 along the carbonyl C=O bond.

Concerted mechanism

In the case of the concerted pathway the reaction consists of one step, in which all bond-forming and breaking processes occur in concert. The nucleophilic ammonia molecule attaches to the eletrophilic carbonyl carbon atom from the ester, accompanied by a proton transfer from the ammonia molecule to the oxygen atom of the ester C–O single bond. Thus, the transition state for the concerted mechanism (designated **CTS**) involves simultaneous creation of a C–N bond, cleavage of the C–O bond and a proton transfer from ammonia to the oxygen atom. The transition structure involved in the concerted pathway of the aminolysis of phenyl acetate is presented in Fig. 1. The main vectors of the imaginary vibrational frequency of the transition state **CTS** are also shown in Fig. 1 and correspond to a proton transfer between the nitrogen and the oxygen atoms and to the cleavage of the C–O ester bond, and the formation of the C–N bond. The distance between the carbonyl carbon and the ester oxygen in the transition state structure is significantly longer, 2.044 Å, than in the reactant phenyl acetate, 1.378 Å. The nitrogen-carbon bond is close to formation with a distance of 1.605 Å in **CTS** compared with 1.369Å in the product acetamide.

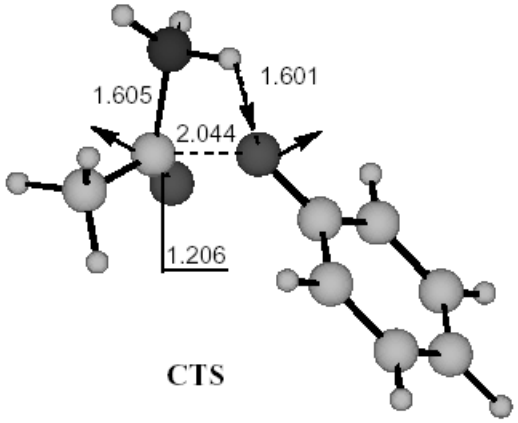

Fig. 1. B3LYP/6-31+G(d,p) optimised structure for the concerted transition state structure **CTS** for the uncatalysed aminolysis of phenyl acetate. The arrows in the transition state structure **CTS** indicate the normal coordinate with an imaginary frequency.

Stepwise mechanism

The stepwise pathway for the aminolysis of phenyl acetate is an addition-elimination process accompanied by proton transfer processes that maintain the neutrality of the structures. The transition state structures along the stepwise pathway of phenyl acetate aminolysis are presented in Fig. 2.

The first step of the reaction is the addition of an N-H bond from the ammonia molecule to the carbonyl double bond in phenyl acetate and formation of a tetrahedral imtermediate (Fig. 2). This addition takes place through a transition state **TS1**. The main vectors of the imaginary vibrational frequency for **TS1** are shown in Fig. 2 and correspond mainly to a proton transfer from the nucleophile NH_3 to the carbonyl oxygen. The hybridisation of the electrophilic carbonyl carbon atom converts from sp^2 to sp^3 during the process. The C=O double bond becomes longer (1.335 Å for **TS1**) and an alcohol-amine is obtained as an intermediate. A new C–N bond is created with a length of 1.560 Å in the transition state **TS1**.

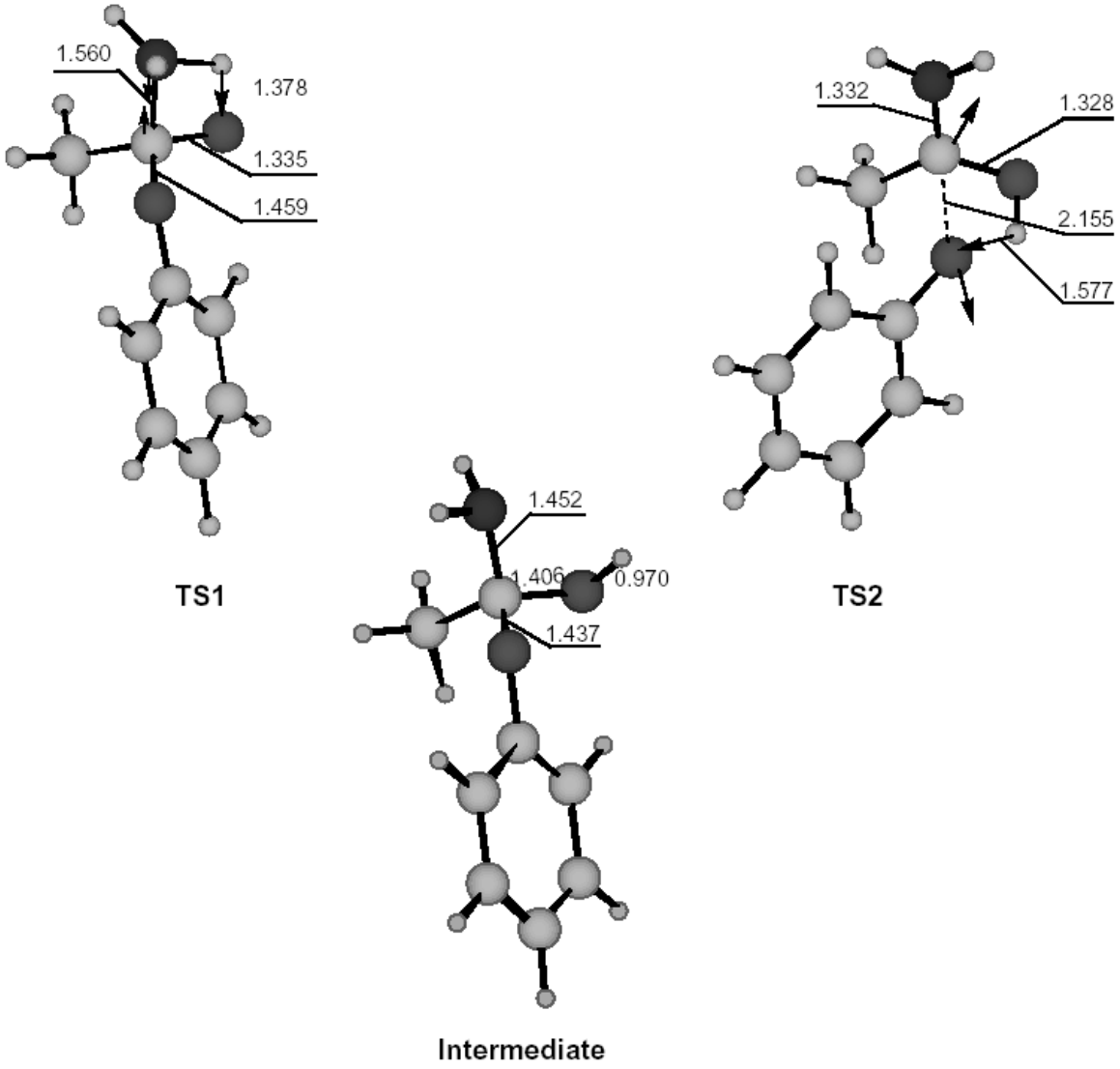

Fig. 2. B3LYP/6-31+G(d,p) optimised structures of the intermediate and transition states for the stepwise pathway of the uncatalysed aminolysis of phenyl acetate. The arrows associated with the transition state structures **TS1** and **TS2** indicate the respective normal coordinates with imaginary frequency.

The second step of the reaction is the conversion of the tetrahedral intermediate into aminolysis products. The intermediate converts to the products acetamide and phenol through the transition state **TS2**. This stage of the process involves the breaking of the C–O ester single bond and simultaneous restoration of the C=O bond following a proton transfer between the two oxygen atoms. The main components of the transition vector for the second transition state (**TS2)** correspond to the proton transfer process and cleavage of the ester C–O ester single bond (Fig. 2).

The relative energies of the structures along the concerted and stepwise pathways computed at different levels of theory are summarized in Table 1. It can be seen that the DFT computations predict the concerted mechanism to be more favourable than the stepwise pathway. The higher-level MP2 quantum mechanical computations show the same trend. The presence of a solvent, simulated here by PCM//B3LYP/6-31+G(d,p) computations (Table 1), does not significantly affect the energetics of the process. The theoretical predictions for the effect of CH_3CN and H_2O reveal that the overall trends in the energy profile of the aminolysis of phenyl acetate are not affected significantly by these solvents. These theoretical findings are in qualitative agreement with earlier results for the aminolysis of methylthioacetate [25] and methyl formate [29a]. The latter studies showed that the energies of the transition states for the stepwise and concerted pathways are quite close.

Table 1. Relative to reactants energies in kcal/mol for the stationary point structures along the concerted and stepwise mechanisms for the uncatalysed and catalysed aminolysis of phenyl acetate

Structure [a]	B3LYP/ 6-31+G(d,p)	MP2/ 6-31+G(d,p)// B3LYP/ 6-31+G(d,p)	MP2/ cc-pVTZ// B3LYP/ 6-31+G(d,p)	MP2/ cc-pVTZ// B3LYP/ 6-31+G(d,p)	PCM// B3LYP/ 6-31+G(d,p)	B3LYP/ 6-31+G(d,p)	MP2/ 6-31+G(d,p)// B3LYP/ 6-31+G(d,p)	MP2/ cc-pVTZ// B3LYP/ 6-31+G(d,p)
	Uncatalysed in gas phase			Uncatalysed in solvent		Catalysed in gas phase		
				CH_3CN	H_2O			
CTS	32.33	30.61	30.56	29.71	27.40	22.31	18.83	18.83
TS1	42.19	38.44	36.88	43.11	40.12	18.43	12.47	11.18
TS2	25.18	27.33	26.98	25.30	20.67	6.53	4.78	4.43
P	–5.49	–0.93	–2.08	–7.30	–13.88	–5.49	–0.93	–2.08

a - See text for symbols.

General base catalysis

The catalytic effects of a second ammonia molecule on the concerted and stepwise mechanisms of the aminolysis of phenyl acetate were next examined. The potential energy surfaces for the two reaction pathways were searched by applying the B3LYP/6–31+G(d,p) method. The theoretically estimated energies of the transition states for the concerted and stepwise pathways for the catalysed aminolysis of phenyl acetate are given in the last column of Table 1. In the case of ester aminolysis, the activation barriers were earlier found to result mainly from unfavourable proton transfer geometries [21]. This deduction is also supported by the present computational results for the directions of the transition vectors, characterizing the **CTScatal, TS1catal** and **TS2catal** structures. These structures are shown in Fig. 3 and reveal that all steps along the concerted and stepwise pathways involve proton transfers. The role of the catalyst in the process is to facilitate the proton transfer, thus lowering the energy barrier. In the case of the general base-catalysed aminolysis the stepwise mechanism has lower activation barrier (18.43 kcal/mol) than the concerted pathway (22.31 kcal/mol). The higher level calculations confirm that conclusion.

The energies of principal critical structures along the reaction pathways for the uncatalysed and catalysed aminolysis of methyl benzoate are illustrated in Fig. 4.

Comparison of the aminolysis process for methyl formate, methyl benzoate and phenyl acetate

As mentioned earlier, one of the aims of this study is to analyse the factors that determine the different energetics of the aminolysis reactions of aliphatic and aromatic esters. In the latter, the phenyl ring can be directly bonded to the carbonyl functionality, as in the case of methyl benzoate, or at the site of the ester oxygen atom in the phenyl acetate. In a previous study [29d] we showed that, in general terms, the ester aminolysis follows similar energy profiles for methyl esters of aliphatic (methyl formate) and aromatic (methyl benzoate) acids. In these esters the energy differences between the concerted and stepwise mechanisms are relatively small, approximately 2 kcal/mol in the case of methyl formate and 3 kcal/mol for the methyl benzoate aminolysis in the gas phase. The present theoretical computations for the aminolysis of phenyl acetate predict an energy profile with a pronounced difference between concerted and stepwise pathways. In all three cases the catalytic role of a second ammonia molecule makes the stepwise mechanism energetically more preferable. In the two previously studied systems (methyl formate and methyl benzoate), the two transition states **TS1** and **TS2** for both uncatalysed and catalysed processes have very similar energies at different level of computations. As can be seen from Fig. 4 the nucleophilic attack is definitely the rate-determining stage for both uncatalysed and catalysed aminolysis of phenyl acetate. This feature can be associated with the higher stability of PhO^- compared to CH_3O^- as leaving groups.

In the cases of methyl esters of aliphatic and aromatic acids, the concerted mechanism is energetically slightly more favourable for the uncatalysed process, but the stepwise pathway is preferred when general base catalysis is available. The small energy differences between concerted and stepwise processes are, very possibly, behind the experimentally established shifts upon substitution between the two mechanistic pathways in certain ester systems [16]. In contrast, in the case of phenyl acetate the energy differences between the two mechanisms are well pronounced as can be seen from Fig. 4.

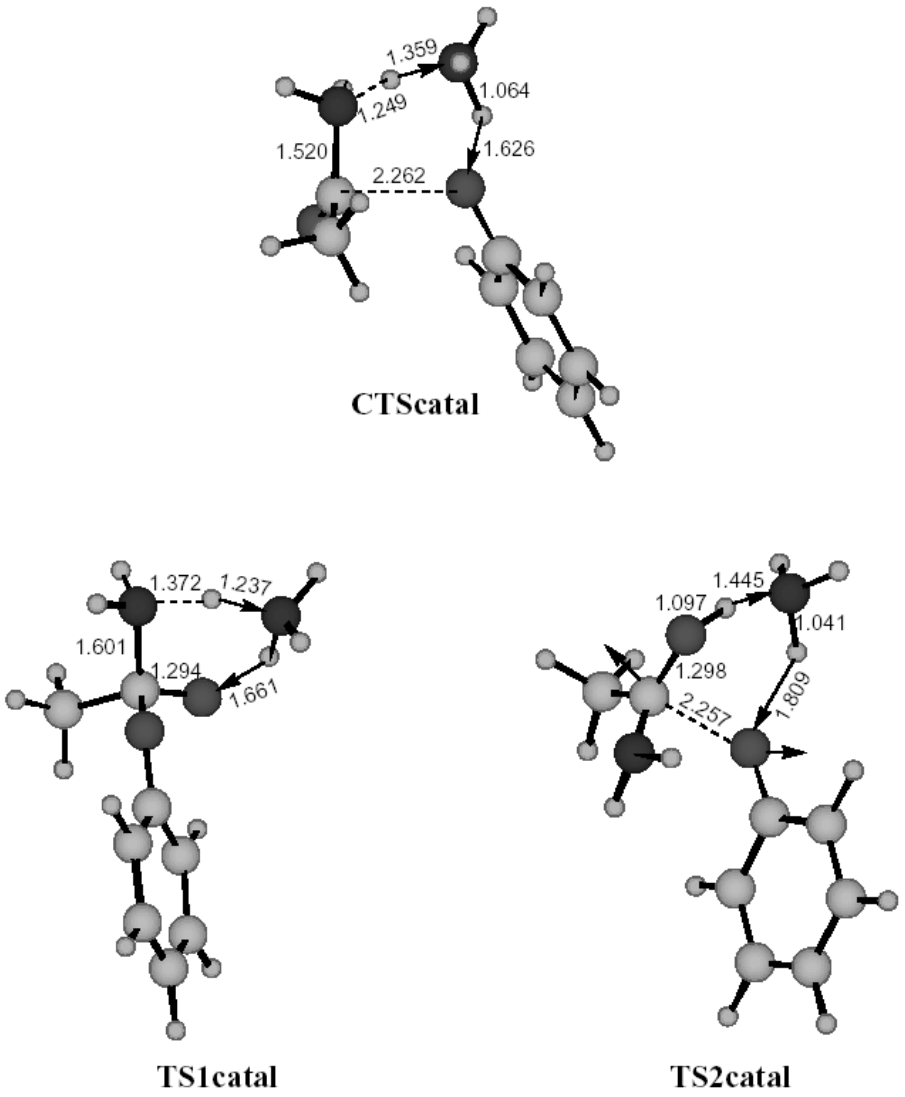

Fig. 3. B3LYP/6-31+G(d,p) optimised structures of the transition states for the catalysed aminolysis of methyl benzoate. The arrows in the transition state structures **CTScatal, TS1catal** and **TS2catal** indicate the respective normal coordinates with one imaginary vibrational frequency.

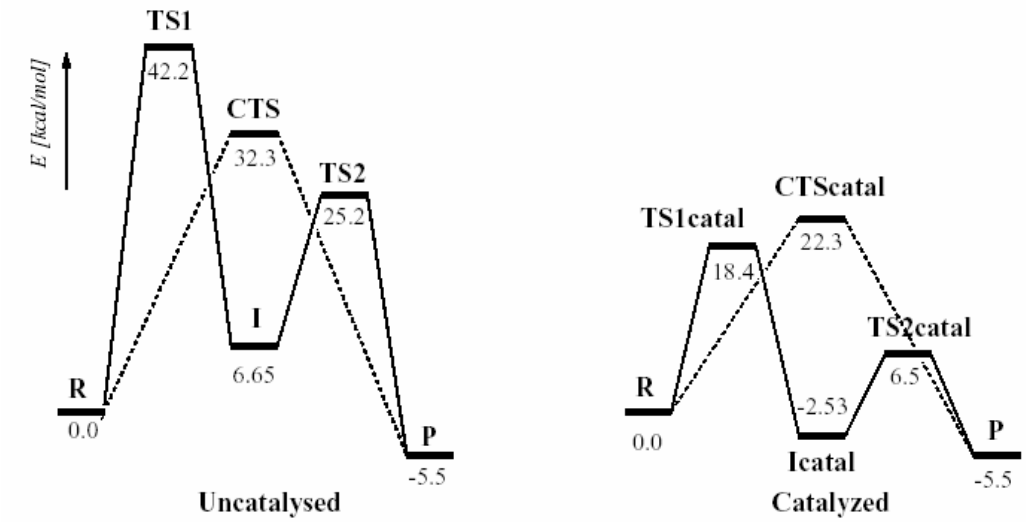

Fig. 4. Energy diagram for the uncatalysed and catalysed aminolysis of phenyl acetate from B3LYP/6-31+G(d,p) computations.

CONCLUSIONS

Density functional methods were applied in examining the possible mechanistic pathways for the reaction of phenyl acetate with ammonia. Transition state structures and energies were determined for concerted and neutral stepwise mechanisms. The general base catalysis of the process was also examined. The theoretical predictions reveal that the catalytic process results in considerable energy savings and the most favourable pathway of the reaction is through general base-catalysed neutral stepwise mechanism with the nucleophilic attack being the rate-determining stage. The structure and transition vectors of the transition states indicate that the catalytic role of ammonia is realized by facilitating the proton transfer processes. Comparisons are made with the energetics of the aminolysis for methyl formate and methyl benzoate. In the latter two esters, the energies of the first and the second transition states, associated with the stepwise mechanism, are quite similar in magnitude. In contrast, in the case of phenyl acetate the transition state, associated with the nucleophilic attack (**TS1**), has distinctly higher energy than the elimination stage (**TS2**), and is the rate-determining stage of the reaction. The much lower energy of **TS2** in phenyl acetate is attributed to the higher stability of the leaving group.

***Acknowledgement**: This research was supported by the National Science Fund (Bulgaria), Grant VU-X 04/05.*

REFERENCES

1. N. Ban, P. Nissen, J. Hanssen, P. B. Moore, T. Steitz, *Science*, **289**, 905 (2000).
2. P. Nissen, J. Hanssen, N. Ban, P. B. Moore, T. Steitz, *Science*, **289**, 920 (2000).
3. G. W. Muth, L. Ortoleva-Donnely, S. A. Strobel, *Science*, **289**, 947 (2000).
4. S. Nakano, D. M. Chadalavada, P. C. Bavilacqua, *Science*, **287**, 1493 (2000).
5. A. Barta, S. Dorner, N. Polacek, *Science*, **291,** 203 (2001).
6. A. Fersht, Structure and Mechanism in Protein Science, W. H. Freeman and Company, New York, 1999.
7. (a) I. Alfonso, V. Gotor, *Chem. Soc. Rev*., **33,** 201 (2004); (b) V. Fernandes-Gotor, V. Gotor, *Curr. Org. Chem*., **10,** 1125 (2006).
8. D. Suárez, K. M. Merz, *J. Am. Chem. Soc*., **123,** 7687 (2001).
9. (a) M. A. Rangelov, G. N. Vayssilov, D. D. Petkov, *Org. Biomol. Chem.*, **3,** 737 (2005); (b) M. A. Rangelov, G. N. Vayssilov, V. M. Yomtova, D. D. Petkov, *J. Am. Chem. Soc.*, **128,** 4964 (2006); (c) S. G. Bayryamov, M. A. Rangelov, A. P. Mladjova, G. N. Vayssilov, V. Yomtova, D. D. Petkov, *J. Am. Chem. Soc*., **129,** 5790 (2007).
10. (a) J. F. Bunnett, G. T. Davis, *J. Am. Chem. Soc.*, **82,** 665 (1960); (b) W. P. Jencks, J. Carriuolo, *J. Am. Chem. Soc.*, **82,** 675 (1960); (c) T. C. Bruice, M. F. Mayahi, *J. Am. Chem. Soc.*, **82,** 3067 (1960); (d) W. P. Jencks, M. Gilchrist, *J. Am. Chem. Soc.*, **88,** 104 (1966); (e) T. C. Bruice, A. Donzel, R. W. Huffman, A. R. Butler, *J. Am. Chem. Soc.*, **89,** 2106 (1967); (f) G. M. Blackburn, W. P. Jencks, *J. Am. Chem. Soc.*, **90,** 2638 (1968); (g) G. A. Rogers, T. C. Bruice, *J. Am. Chem. Soc.*, **95,** 4452 (1973); (h) G. A. Rogers, T. C. Bruice, *J. Am. Chem. Soc.*, **96,** 2473 (1974); (i) A. Williams, *Acc. Chem. Res.*, **22,** 387 (1989).
11. A. Arcelli, C. Concilio, *J. Org. Chem*., **61,** 1682 (1996).
12. (a) E. A. Castro, *Chem. Rev.*, **99,** 3505 (1999); (b) E. A. Castro, L. Leandro, N. Quesieh, J. G. Santos, *J. Org. Chem*., **66,** 6130 (2001); (c) E. A. Castro, A. Galvez, L. Leandro, J. G. Santos, *J. Org. Chem*., **67,** 4309 (2002); (d) E. A. Castro, M. Andujar, P. Campodonico, J. G. Santos, *Int. J. Chem. Kinet*., **34,** 309 (2002); (e) E. A. Castro, P. Campodonico, A. Toro, J. G. Santos, *J. Org. Chem*., **68,** 5930 (2003); (f) E. A. Castro, M. Andujar, A. Toro, J. G. Santos, *J. Org. Chem*., **68,** 3608 (2003); (g) D. D. Sung, I. S. Koo, K. Yang, I. Lee, *Chem. Phys. Lett.*, **426,** 280 (2006).
13. (a) H. K. Oh, S. K. Kim, I. H. Cho, H. W. Lee, I. Lee, *J. Chem. Soc. Perkin Trans. 2*, 2306 (2000); (b) H. K. Oh, M. H. Ku, H. W. Lee, I. Lee, *J. Org. Chem*., **67,** 8995 (2002); (c) H. K. Oh, M. H. Ku, H. W. Lee, I. Lee, *J. Org. Chem*., **67,** 3874 (2002); (d) H. W. Lee, A. K. Guha, C. K. Kim, I. Lee, *J. Org. Chem*., **67,** 2215 (2002); (e) H. K. Oh, J. Y. Lee, H. W. Lee, I. Lee, *New J. Chem*., **26,** 473 (2002); (f) H. J. Koh, S. J. Kang, C. J. Kim, H. W. Lee, I. Lee, *Bull. Korean Chem. Soc*., **24,** 925 (2003); (g) H. B. Song, M. H. Choi, I. S. Koo, H. K. Oh, I. Lee, *Bull. Korean Chem. Soc.*, **24,** 91 (2003); (h) D. D. Sung, I. S. Koo, K. Yang, I. Lee, *Chem. Phys. Lett.*, **426,** 280 (2006).
14. (a) I. H. Um, J. S. Min, J. A. Ahn, H. J. Hahn, *J. Org. Chem*., **65,** 5659 (2000); (b) I. H. Um, S. E. Lee, H. J. Kwon, *J. Org. Chem*., **67,** 8999 (2002); (c) I. H. Um, E. J. Lee, J. P. Lee, *Bull. Korean Chem. Soc.*, **23,** 381 (2002); (d) I. H. Um, J. A. Seok, H. T. Kim, S. K. Bae, *J. Org. Chem*., **68,** 7742 (2003); (e) I. H. Um, J. Y. Hong, J. J. Kim, O. M. Chae, S. K. Bae, *J. Org. Chem*., **68,** 5180 (2003); (f) I. H. Um, H. R. Park, E. Y. Kim, *Bull. Korean Chem. Soc.*, **24,** 1251 (2003); (g) I. H. Um, J. Y. Hong, J. A. Seok, *J. Org. Chem*., **70,** 1438 (2005); (h) I. H. Um, J. Y. Lee, M. Fujio, Y. Tsuno, *Org. Biomol. Chem.*, **4,** 2979 (2006); (i) I. H. Um, S. J. Hwang, M. H. Baek, E. J. Park, *J. Org. Chem*., **71,** 9191 (2006).
15. (a) E. A. Castro, C. L. Santander, *J. Org. Chem*., **50,** 3595 (1985); (b) E. A. Castro, J. L. Valdivia, *J. Org. Chem*., **51,** 1668 (1986); (c) E. A. Castro, G. B.

Steinfort, *J. Chem. Soc. Perkin Trans. 2*, 453 (1983); (d) E. A. Castro, J. Bessolo, R. Aguayo, J. G. Santos, *J. Org. Chem*., **68,** 8157 (2003).
16. I. H. Um, K. H. Kim, H. R. Park, M. Fujio, Y. Tsuno, *J. Org. Chem*., **69,** 3937 (2004).
17. T. C. Bruice, S. J. Benkovic, Bioorganic Mechanisms, Vol. 1, W.A. Benjamin Inc., New York, 1966.
18. W. P. Jencks, Catalysis in Chemistry and Enzymology, McGraw Hill, New York, 1969.
19. M. Page, A. Williams, Organic and Bioorganic Mechanisms, Longman, Harlow, 1997.
20. T. Oie, G. H. Loew, S. K. Burt, J. S. Binkley, R. D. McElroy, *J. Am. Chem. Soc.*, **104**, 6169 (1982).
21. L. Wang, H. Zipse, *Liebigs Ann.*, 1501 (1996).
22. H. Zipse, L. Wang, K.N. Houk, *Liebigs Ann*., 1511 (1996).
23. J. F. Marlier, B. A. Haptonsall, A. J. Johnson, K. A. Sacksteder, *J. Am. Chem. Soc.*, **119,** 8838 (1997).
24. H. Adalstensson, T. C. Bruice, *J. Am. Chem. Soc.*, **120**, 3440 (1998).
25. W. Yang, D. G. Drueckhammer, *Org. Lett*., **2**, 4133 (2000).
26. R. A. J. O'Hair, N. K. Androutsopoulos, *Org. Letters*, **2,** 2567 (2000).
27. C. K. Kim, H. G. Li, H. W. Lee, C. K. Sohn, Y. I. Chun, I. Lee, *J. Phys. Chem. A*, **104,** 104 (2000).
28. D. A. Singleton, S.R. Merrigan, *J. Am. Chem. Soc.*, **122,** 11035 (2000).
29. (a) S. Ilieva, B. Galabov, D. G. Musaev, K. Morokuma, H. F. Schaefer, *J. Org. Chem*., **68**, 1496 (2003); (b) S. Ilieva, B. Galabov, D. G. Musaev, K. Morokuma, *J. Org. Chem*., **68,** 3406 (2003); (c) S. Ilieva, Y. Atanasov, V. Kalcheva, B. Galabov, J. Mol. Struct. (Theochem), **633,** 49 (2003); (d) B. Galabov, Y. Atanasov, S. Ilieva, H. F. Schaefer, *J. Phys. Chem. A*, **109,** 11470 (2005).
30. Y. H. Wang, J. W. Zou, B. Zhang, Z. Min, G. X. Hu, K. W. Zheng, *Chin. Chem. Lett*., **16,** 705 (2005).
31. H. E. Maoxia, D. Feng, J. U. Xie, Z. Cai, *J. Theor. Comp. Chem*., **4,** 383 (2005).
32. R. Z. Liao, W. J. Ding, J. G. Yu, W. H. Fang, R. Z. Liu, *J. Phys. Chem. A*, **111,** 3184 (2007).
33. L. Jin, Y. Wu, Y. Xue, Y. Guo, D. Q. Xie, G. S. Yan, *Acta Chim. Sinica*, **64,** 873 (2006).
34. W. P. Jencks, J. Carriuolo, *J. Am. Chem. Soc.*, **82,** 675 (1960).
35. L. R. Fedor, T. C. Bruice, K. L. Kirk, J. Meinwald, *J. Am. Chem. Soc.*, **88,** 108 (1966).
36. T. C. Bruice, A. Donzel, R. W. Huffman, A. R. Butler, *J. Am. Chem. Soc.*, **89,** 2106 (1967).
37. N. M. Oleinik, L. M. Livinenko, L. P. Kurchenko, S. E. Terekhova, Zh. P. Gelbina, *J. Org. Chem*. *USSR (English Transl.)*, **43,** 2304 (1975).
38. H. J. Koh, S. I. Kim, B. C. Lee, I. Lee, *J. Chem. Soc. Perkin Trans. 2*, 1353 (1996).
39. D. Rajarathnam, T. Jeyakumar, P. A. Nadar, *Int. J. Chem. Kin*., **34,** 366 (2002).
40. D. Rajarathnam, T. Jeyakumar, P. A. Nadar, *Int. J. Chem. Kin*., **37,** 211 (2005).
41. M. J. Frisch, G.W. Trucks, H. B. Schlegel, G. E. Scuseria, M. A. Robb, J. R. Cheeseman, V. G. Zakrzewski, J. A. Montgomery, R. E. Stratmann, J. C. Burant, S. Dapprich, J. M. Millam, A. D. Daniels, K. N. Kudin, M. C. Strain, O. Farkas, J. Tomasi, V. Barone, M. Cossi, R. Cammi, B. Mennucci, C. Pomelli, C. Adamo, S. Clifford, J. Ochterski, G. A. Petersson, P. Y. Ayala, Q. Cui, K. Morokuma, D. K. Malick, A. D. Rabuck, K. Raghavachari, J. B. Foresman, J. Cioslowski, J. V. Ortiz, B. B. Stefanov, G. Liu, A. Liashenko, P. Piskorz, I. Komaromi, R. Gomperts, R. L. Martin, D. J. Fox, T. Keith, M. A. Al-Laham, C. Y. Peng, A. Nanayakkara, C. Gonzalez, M. Challacombe, P. M. W. Gill, B. G. Johnson, W. Chen, M. W. Wong, J. L. Andres, M. Head-Gordon, E. S. Replogle, J. A. Pople, Gaussian 98 (Revision A.7), Gaussian Inc., Pittsburgh, PA, 1998.
42. (a) A. D. Becke, *J. Chem. Phys.*, **98,** 5648 (1993); (b) C. Lee, W. Yang, R. G. Parr, *Physical Review B*, **37,** 785 (1988).
43. G. A. Petersson, T. G. Tensfeldt, J. A. Montgomery Jr., *J. Chem. Phys.*, **94,** 6091 (1991).
44. P. C. Hariharan, J. A. Pople, *Theo. Chim. Acta*, **28,** 213 (1973).
45. T. Clark, J. Chandrasekhar, G. W. Spitznagel, P. v. R. Schleyer, *J. Comp. Chem.*, **4**, 294 (1983).
46. C. Peng, P. Y. Ayala, H. B. Schlegel, M. J. Frisch, *J. Comp. Chem.*, **17,** 49 (1996).
47. C. Gonzalez, H. B. Schlegel, *J. Chem. Phys.*, **90,** 2154 (1989).
48. M. J. Frisch, M. Head-Gordon, J. A. Pople, *Chem. Phys. Lett.*, **166,** 281 (1990).
49. R. A. Kendall, T. H. Dunning Jr., R. J. Harrison, *J. Chem. Phys.*, **96,** 6796 (1992).
50. (a) S. Miertus, E. Scrocco, J. Tomasi, *Chem. Phys*., **55,** 117 (1981); (b) V. Barone, M. Cossi, J. Tomasi, *J. Comput. Chem.*, **19,** 404 (1998).

ТЕОРЕТИЧНО ИЗСЛЕДВАНЕ НА МЕХАНИЗМА НА АМИНОЛИЗАТА НА ФЕНИЛАЦЕТАТ

С. Илиева*, Я. Атанасов, Б. Гълъбов*

Химически факултет, Софийски университет „Св. Климент Охридски“,
бул. „Джеймс Баучер“ № 1, София 1164

Посветена на акад. Иван Юхновски по повод на 70-та му годишнина

Постъпила на 30 ноември 2007 г.; Преработена на 13 декември 2007 г.

(Резюме)

Проведено е теоретично изследване на механизма на реакцията на аминолиза на фенилацетат. Стабилните структури и преходните състояния в хода на реакцията са оптимизирани на ниво B3LYP/6-31G+(d,p) за синхронен и стъпков механизъм, след което са охарактеризирани чрез изчисляване на хармоничните вибрационни честоти на съответното ниво/базисен набор. Преходните състояния са проверени чрез IRC изчисления. За по-точно определяне на енергията на състоянията са проведени MP2/6-31+G(d,p)//B3LYP/6-31+G(d,p) и MP2/cc-pVTZ//B3LYP/6-31+G(d,p) изчисления. Ефектът на разтворителя е изследван чрез метода PCM (Polarized Continuum Model). Проведени са PCM//B3LYP/6-31+G(d,p) изчисления във водна среда и в присъствие на апротонен разтворител ацетонитрил.

Получените резултати показват, че енергетично най-изгоден е процесът на базично катализирана аминолиза, протичащ в 2 стадия (стъпков механизъм), като скорост-определящ е първият етап на нуклеофилна атака и формиране на тетраедричен интермедиат. Направено е сравнение в енергетиката на аминолизата на метилбензоат и метилформиат. За двата метилови естери на мравчената и бензоената киселини енергиите на първото и второто преходни състояния, свързани със стъпковия механизъм, са близки. При фенилови естери на оцетната киселина първото преходно състояние (TS1), свързано с нуклеофилната атака, е доста по-високо енергетично от второто (TS2), което е свързано с етапа на елиминиране. По-ниската енергия на TS2 при аминолиза на фенилацетат може да се обясни с по-голямата стабилност на напускащата група в този случай.

Bulgarian Chemical Communications, Volume 40, Number 4 (pp. 409–417) 2008

One-pot solvent-free synthesis of symmetrical azines under microwave irradiation

S. P. Simeonov[1], V. B. Kurteva[1,*], R. P. Bontchev[2]

[1] *Institute of Organic Chemistry, Bulgarian Academy of Sciences, Acad. G. Bonchev St., Block 9, 1113 Sofia, Bulgaria*
[2] *Cabot Corporation, 5401 Venice Ave. N. E., Albuquerque, NM 87113, USA*

Dedicated to Academician Ivan Juchnovski on the occasion of his 70th birthday

Received November 29, 2007, Revised January 11, 2008

Fast, efficient and environmentally benign solvent-free one-pot procedures for the synthesis of symmetrical aryl and heteroaryl azines under microwave irradiation were developed. The main advantages of these synthetic approaches are the serious energy saving in comparison with the conventional heating and that they avoid the use of the toxic and dangerous for the environment hydrazine. The transformations go *via* semicarbazone or carbazate intermediates, which convert to azine with different rate depending on the conditions and the type of aromatic substituents. It was shown that the methods are effective when aryl aldehydes without substituents or with electrodonating ones are used. In contrast, if an electrowithdrawing group exists in the aldehyde molecule, no azine formation was observed and the intermediately formed semicarbazone or carbazate are the only reaction product. It was found that the carbazate route is preferable, particularly when a hydroxyl group exists in the aromatic subunit. The two-step procedure applied to the semicarbazone path was shown to be unfavourable in general. The *E,E*-configuration of the products was confirmed by X-ray analysis of a selected sample.

Key words: Azine, semicarbazone, carbazate, microwaves, solventless, X-ray.

INTRODUCTION

Compounds having azine moiety have displayed a broad spectrum of biological activity profiles such as antitumor [1–4], antibacterial [5–8], anti-inflammatory [9], antimalarial dyes (Janus Green B, Indoline Blue, etc.) [10], anticonvulsant [11], selective allosteric modulators of the metabotropic glutamate receptors subtype 5 (mGluR5) [12], insect growth regulators [13] and many others. Polynuclear platinum complexes with bridging linkers are described as cisplatin analogues, which are expected to overcome the resistance problem of the latter due to a significantly different way of binding DNA adducts. Among the complexes possessing rigid bridging ligands, azines have shown induction of apoptosis, implying considerable anticancer potential [14, 15]. They are important sintons for various cycloaddition reactions [16–20] and ligands in coordination chemistry [21–30]. In addition, both azines and transformation intermediates described in this paper (semicarbazones and carbazates) are widely used for the isolation and characterisation of carbonyl compounds and for their protection during synthesis [31].

Azines are well-known compound ever since 19th century but only a limited number of synthetic pathways is applied for their preparation. The classical scheme is based on a reaction of aldehydes with the highly toxic hydrazine [32, 33]. Semicarbazide has been also applied as a reagent in a two-step procedure involving thermolysis of the intermediately formed semicarbazones at high temperature, above 250ºC [34, 35]. It was found [35] that the reaction occurs through reactive *N*-substituted isocyanate intermediates which undergo $\pi^{2s}+\pi^{2a}$ cycloaddition to the relatively unstable isocyanate dimmer followed by threefold extrusion. The proposed mechanism has been supported by detection of the decomposition products and by trapping the reactive isocyanate intermediates with nucleophiles. The hard conditions of semicarbazone pathway have been overcome by performing the transformation *via* a *t*-butyl carbazate intermediate and using HCl/AcOH in the second step [36].

Microwave-assisted reactions achieve rate enhancement, higher yields and better selectivity with respect to the conventional heating [37–46]. The efficient, clean and economic solvent-free technique [47–51], which avoids hazards of solution phase reactions, is an environmentally benign condition preventing release of reaction products into the environment. To the best of our knowledge, there are no records in the literature on the one-pot procedure for conversion of aldehydes to azines *via* semicarbazones and carbazates and only one record on microwave-assisted azine synthesis by applying hydrazine sulfate as a reagent [52].

* To whom all correspondence should be sent:
E-mail: vkurteva@orgchm.bas.bg

© 2008 Bulgarian Academy of Sciences, Union of Chemists in Bulgaria

One-pot solvent-free protocols for the preparation of symmetrical azines under microwave irradiation are presented herein. The methods are fast, efficient, and avoid the use of the toxic and dangerous for the environment hydrazine.

RESULTS AND DISCUSSION

A series of symmetrically aryl-substituted azines (**5a**–**5j**) were prepared from aromatic aldehydes in a solvent-free protocol under microwave irradiation (MWI). In an attempt to avoid the use of the toxic and environmentally hazardous hydrazine, two different reagents were applied, namely semicarbazide hydrochloride (**2**, R=NH_2) and *t*-butyl carbazate (**2**, R = OBu^t). In a typical reaction, mixtures of an aromatic aldehyde (**1**) and a reagent (**2**) were irradiated in a domestic household microwave oven in open vessels yielding the target azines, as shown in Scheme 1.

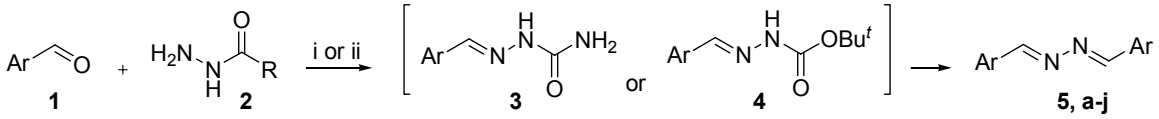

R = NH_2 (i), OBu^t (ii)

Ar = 2-OH-1-naphthyl (**a**), 4-OHPh (**b**), 2-OHPh (**c**), 2-OH-3-MeOPh (**d**), 3,4-$(MeO)_2$Ph (**e**), 4-MePh (**f**), 4-Me_2NPh (**g**), 2-furfuryl (**h**), 2-thiophenyl (**i**), ferrocenyl (**j**)

Scheme 1. Synthesis of azines **5a**-**5j**. i) Method A: **2** hydrochloride, R = NH_2 (2 equiv), MWI; ii) Method B: **2**, R = OBu^t (2 equiv), MWI.

The target azines **5** were obtained with different rates depending on the reagent used, the power and the type of aromatic substituents as shown in Table 1. The reaction duration and the power were selected according to the concrete transformation behaviours followed by TLC; overheating and decomposition being detected in many cases. The products were separated from the reaction inter-mediates or decomposition products by high performance flash chromatography.

Semicarbazide hydrochloride (2, R=NH_2), an inexpensive commercially available material, was first used as a reagent. An overheating was detected by TLC at 800 W resulting in complex reaction mixtures, while a slow graduate azine formation was observed at varying the power (Table 1, method A). However, a complete and clean conversion cannot be achieved on a reasonable time-scale. Nevertheless, the method is very fast and thus leads to a serious energy saving in comparison with the conventional heating, where high temperatures are required to reach azine formation above 250ºC.

In an attempt to increase the reaction yields, the transformation was carried out with immobilized on solid support reagents. Different solids were tested as supports, such as silica gel, alumina oxides, celite, but better conversion was not achieved.

Tert-butyl carbazate (**2**, R = OBu^t) was also tested in the transformation studied. As can be seen from Table 1 (method B), good to excellent yields were achieved for most of the examples, in contrast to the conversion *via* semicarbazone. The results show that in general carbazate is preferred over semicarbazide as a reagent in this reaction. The latter conclusion is effectively illustrated on an example of 2-hydroxy substituted aldehydes. While the corresponding azines **5a**, **5c** and **5d** were obtained in good to excellent yields *via* carbazates, much lower conversions were achieved by method A (72–98%, entries 2, 6, 8 *vs* 17–63%, entries 1, 5, 7). The formation of 4-hydroxy azine **5b** appears as a frontier case. It was obtained quantitatively *via* carbazate (entry 4), while no product was isolated by method A (entry 3). No conversion was detected at low power and the intermediately formed semicarbozone was isolated, while decomposition took place above 440 W.

The results in Table 1 show that the presence of a polar electrodonating group seems to be essential for the reactivity, the effect being most clearly exhibited if the substituent is at *p*-position with respect to the aldehyde function. A possible explanation of the latter could be an increasing of the energy absorption caused by the polar group and/or electronic effects of the substituents. As can be seen, quantitative conversions were achieved *via* carbazate with aldehydes **1b** and **1g** possessing a single polar substituent in *p*-position (entries 4 and 14), while the *o*-substituted products **5a** and **5c** were isolated in a bit lower yield (entries 2 and 6). The better conversion to disubstituted product **5d** in comparison with **5a** and **5c** (entry 8 *vs* entries 2 and 6) could be due to a surplus energy absorbed by the second polar group. The behaviour of aldehyde **1e**, where the extra energy absorbed resulted in an overheating and decomposition even at relatively low power (entry 10), is

in accordance with the given suggestion. The product **5e** contains an additional polar group with respect to **5b** and *p,m*-substituents instead of *o,m*- in comparison with **5d**. The results *via* semicarbazone intermediate are in agreement with that pattern; an overheating for **5b** and **5e** and graduate formation of **5a**, **5c** and **5d**.

The presence of a hydroxyl group in *o*-position leads to serious lack of solubility of azines **5a** and **5c** thus creating problems in their isolation. This very low solubility is due to H-bonding between *o*-hydroxyl group and nitrogen, which is clearly demonstrated by the absence of a band for OH in their IR spectra. In the case of **5d** the H-bonding between OH and OMe is stronger than OH…N, while a strong band for free OH group exists in the IR spectrum of **5b**. The NMR data for O*H* and C*H*=N protons present an additional confirmation of the presence and direction of the H-bonding. The downfield shifting of the O*H* proton resonances of **5a**, **5c** and **5d** with respect to **5b** (11.08 ppm, 10.61 ppm and 11.57 ppm *vs* 9.70 ppm, respectively) show that the hydroxyl groups are H-bonded. On the other side, the C*H*=N resonances are downfielded only in the case of **5a** and **5c** (9.70 ppm and 9.88 ppm, respectively) indicating that the nitrogen in **5d** (C*H*=N of 8.44 ppm) is not H-bonded.

Table 1. Microwave synthesis of symmetrical aryl azines **5**.

Entry		Aryl azine	Synthetic scheme [a]	Reaction time, min	MWI power, W	Yield, [b] %
1	**5a**	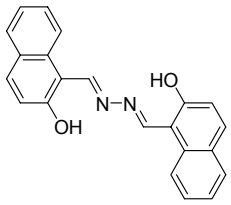	A	5	800	45
2			B	5	800	81
3	**5b**	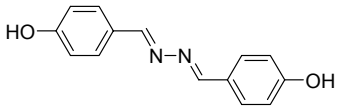	A	2-15	300-800	-
4			B	5	800	99
5	**5c**	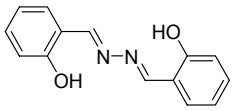	A	5	600	17
6			B	5	800	72
7	**5d**	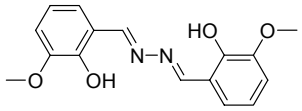	A	10	800	63
8			B	5	800	98
9	**5e**	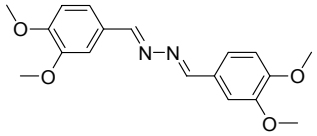	A	2	600	49
10			B	5	600	35
11	**5f**	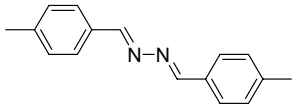	A	2	440	55
12			B	5	800	67
13	**5g**	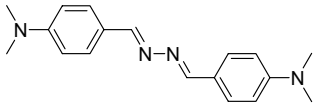	A	2	600	75
14			B	5	800	99
15	**5h**	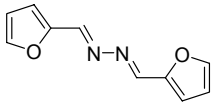	A	1	800	11
16			B	5	800	43
17	**5i**	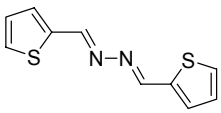	A	2	440	34
18			B	5	600	70
19	**5j**	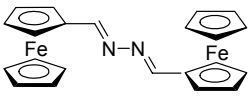	A	2-5	440-800[c]	<10
20			B	2-5	440-800	<5

[a] Method A: Preparation *via* semicarbazone **3**; Method B: Preparation *via* carbazate **4**. [b] After high performance flash chromatography on silica gel.
[c] In consecutive 30 sec intervals.

Ferrocenyl azine **5j** presents an exception of the general pattern of behaviour. An overheating was observed even at low power by both methods (entries 19, 20) resulting in complex mixtures. Moreover, the yields of the product were not reproducible. These facts are most probably due to the presence of iron in the molecule.

No azine formation was detected from 4-cyanobenzaldehyde and 4-nitrobenzaldehyde by both methods even at 800 W and the corresponding intermediates, semicarbazones or carbazates, were isolated. These results are an indication that no transformation takes place if electrowithdrawing substituents exist in the aromatic ring of the starting aldehyde. When 3,4-dihydroxybenzaldehyde was used even at low power, the corresponding azine was detected as a component of a complex polymers-containing reaction mixture, which shows that polyphenols are not stable enough upon the reaction conditions used.

The slower conversion rate of method A compared to method B gave us the idea to transform the former scheme as a two-step protocol for the synthesis of the selected products. Semicarbazones **3** were obtained in high yields (above 90%) by irradiating aqueous solutions of an aldehyde and semicarbazide hydrochloride in a microwave oven applying 800 W power for 5 min. After simple filtration the products were irradiated with microwaves in the absence of a solid support but no transformation was detected. The reaction vessels were only slightly warmed up at the end of the treatment, which is an indication that semicarbazones **3** do not absorb sufficient energy. When performing the reaction with pre-immobilized on silica gel or basic alumina semicarbazones, azine formation was observed but at much slower reaction rate compared to the direct protocol (Scheme 1, Table 1: method A), which makes the latter a preferable reaction scheme in all cases. In an attempt to obtain ferrocenyl azine **5j** in a reasonable scale and reproducible results, the two-step protocol was applied on both pathways A and B by using silica gel and basic alumina as solid supports. However, an overheating was again observed and no product was isolated.

X-ray Crystallography and Structure Description

Crystals of bis(3,4-dimethoxyphenyl)azine **5e** suitable for X-ray analysis were grown by slow diffusion of hexane into chloroform solutions of the product. The asymmetric unit of **5e** consists of two crystallographically independent $C_{18}H_{20}N_2O_4$ molecules, Figure 1, which are arranged in slabs parallel to the *ac* plane, Figure 2. No solvent molecules have been identified and located in the structure. All atoms fully occupy general (2a: x,y,z) positions. The C–C, C–N and C–O distances are typical for such compounds and range between 1.365(2)–1.457(3) Å (C–C), 1.359(2)–1.438(2) Å (C–O), 1.278(2)–1.285(2) Å (C–N) and 1.410(2)–1.412(2) Å (N–N), respectively.

Fig. 1. Asymmetric unit, thermal ellipsoids (50% probability level) and labeling scheme of **5e**.

Fig. 2. Unit cell and space filling of 5e.

CONCLUSIONS

In conclusion, a series of symmetrical aryl and heteroaryl azines was obtained in solvent-free one-pot protocols under microwave irradiation. Semicarbazide hydrochloride and *t*-butyl carbazate were applied as reagents, thus avoiding the use of the toxic and dangerous for the environment hydrazine. The methods are very fast, which leads to a serious energy saving in comparison with the conventional heating. It was found that the rate of the azine formation is strongly dependent on the conditions and the type of aromatic substituents. It has been shown that the methods are effective when aryl aldehydes without substituents or with electro-donating ones are used. In contrast, if an electro-withdrawing group exists in the aldehyde molecule, no azine formation has been observed and the intermediately formed semicarbazone or carbazate are the only reaction products. It was observed that the carbazate route is preferable, particularly when a hydroxyl group exists in the aromatic moiety. The two-step procedure applied to the semicarbazone path was shown to be unfavourable in general. The *E,E*-configuration of the products was confirmed by X-ray analysis of a selected sample.

EXPERIMENTAL SECTION

General Procedures

All reagents were purchased from Aldrich, Merck and Fluka and were used without any further purification. The microwave irradiated reactions (MWI) were performed in a domestic household oven Panasonic NN-S255W. Merck silica gel 60 (0.040–0.063 mm) and BDH basic active aluminium oxide Brockmann grade 1 were employed as solid supports. Fluka silica gel/TLC-cards 60778 with fluorescent indicator 254 nm were used for TLC chromatography and R_f-values determination. The purifications were carried out on a Biotage Horizon^{TM} HPFC system on silica gel. The melting points were determined in capillary tubes on a MEL-TEMP 1102D-230 VAC apparatus without corrections. The IR spectra were taken on a Bruker IFS 113v as KBr discs and were quoted in cm^{-1}. The NMR spectra were recorded on a Bruker AVANCE DRX 250 spectrometer, the chemical shifts were quoted in ppm in δ-value against tetramethylsilane (TMS) as internal standard and the coupling constants were calculated in Hz. The low-resolution mass spectra were carried out on a HP 5973 Mass Selective Detector.

Synthesis of aryl azines ***5***

General procedure: A mixture of an aldehyde (1 mmol) and semicarbazide hydrochloride (2 mmol, method A) or *t*-butyl carbazate (2 mmol, method B) was irradiated in a microwave oven. The crude product was purified by high performance flash chromatography on silica gel without work-up.

The reaction conditions and yields are summarized in Table 1.

Azine ***5a*** [53]. Flash chromatography (CH_2Cl_2), R_f 0.86; m. p. 290–293ºC decomp. (Ref. [53] > 290 ºC); IR: 421.2, 755.4, 788.4, 797.8, 834.2, 871.2, 956.0, 1143.0, 1167.6, 1184.7, 1215.6, 1242.8, 1283.2, 1321.4, 1418.3, 1467.6, 1580.6, 1604.8, 1622.1, 2923.6, 3055.2; ^{1}H NMR ($CDCl_3$:CF_3COOH 3:1): 7.30 (d, 2H, J 9.0, C*H*-3 of Ar), 7.50 (dd, 2H, J 7.1, 8.1, C*H*-7 of Ar), 7.68 (ddd, 2H, J 1.2, 7.1, 8.5, C*H*-6 of Ar), 7.81 (d, 2H, J 8.1, C*H*-8 of Ar), 8.07 (d, 2H, J 9.0, C*H*-4 of Ar), 8.23 (d, 2H, J 8.5, C*H*-5 of Ar), 9.70 (s, 2H, C*H*=N), 11.08 (bs, O*H*, overlapped with COO*H* of CF_3COOH); ^{13}C NMR ($CDCl_3$:CF_3COOH 3:1): 106.43 (C_{quat}-1), 118.08 (*C*H of Ar), 120.11 (*C*H of Ar), 126.13 (*C*H of Ar), 128.98 (C_{quat}), 130.27 (*C*H of Ar), 130.69 (*C*H of Ar), 132.79 (C_{quat}), 141.76 (*C*H of Ar), 157.90 (*C*H=N), 163.29 (C_{quat}-2); MS: (EI+) m/z 340 (M^+, 72) , 323 (M-OH, 34), 170 (½ M^+, 100), 115 (Ar, $C_9H_7^+$, 52).

Azine ***5b*** [54]. Flash chromatography (CH_2Cl_2:MeOH 95:5), R_f 0.36 (CH_2Cl_2:MeOH 90:10); m. p. 258–259ºC (Ref. [55] 268ºC); IR: 516.3, 521.4, 625.1, 812.7, 827.9, 841.8, 1167.1, 1230.4, 1264.4, 1285.1, 1303.6, 1382.3, 1393.7, 1449.0, 1514.3, 1563.9, 1592.3, 1607.9, 1623.3, 2526.0, 2591.9, 2943.9, 3338.0; ^{1}H NMR ($CDCl_3$:DMSO 2:1): 6.79 (d, 4H, J 8.6, C*H*-2 and C*H*-6 of Ar), 7.58 (d, 4H, J 8.6, C*H*-3 and C*H*-5 of Ar), 8.45 (s, 2H, C*H*=N), 9.69 (bs, 2H, O*H*,

exchangeable signal); ^{13}C NMR ($CDCl_3$:DMSO 2:1): 115.52 (*C*H-2 and *C*H-6 of Ar), 125.09 (C_{quat}-4), 129.70 (*C*H-3 and *C*H-5 of Ar), 159.85 (C_{quat}-1), 160.52 (*C*H=N).

Azine ***5c*** [34]. Flash chromatography (CH_2Cl_2), R_f 0.14; m. p. 209–211ºC (Ref. [34] 213–214ºC); IR: 459.2, 683.6, 751.9, 785.3, 894.3, 1198.0, 1207.1, 1223.2, 1237.6, 1278.4, 1317.0, 1331.1, 1388.1, 1488.0, 1572.6, 1624.8, 2639.1, 2752.9, 3043.9; ^{1}H NMR ($CDCl_3$:CF_3COOH 10:1): 7.02 (m, 4H, C*H* of Ar), 7.56 (m, 4H, C*H* of Ar), 9.88 (d, 2H, J 0.6, C*H*=N), 10.61 (bs, 2H, O*H*, exchangeable signal); ^{1}H NMR ($CDCl_3$:CF_3COOH 3:1): 7.18 (m, 4H, *C*H-3 and *C*H-5 of Ar), 7.57 (dd, 2H, J 1.6, 8.0, C*H*-6 of Ar), 7.69 (ddd, 2H, J 1.6, 7.3, 8.7, C*H*-4 of Ar), 8.98 (s, 2H, C*H*=N), 11.69 (bs, O*H*, overlapped with COO*H* of CF_3COOH); ^{13}C NMR ($CDCl_3$:CF_3COOH 10:1): 117.76 (*C*H-3 or *C*H-5 of Ar), 120.26 (*C*H-3 or *C*H-5 of Ar), 120.71(C_{quat}-1), 134.18(*C*H-4 or *C*H-6 of Ar), 137.59 (*C*H-4 or *C*H-6 of Ar), 161.77 (C_{quat}-2), 197.39 (*C*H=N); ^{13}C NMR ($CDCl_3$:CF_3COOH 3:1): 114.23 (C_{quat}-1), 118.03 (*C*H-3 or *C*H-5 of Ar), 122.69 (*C*H-3 or *C*H-5 of Ar), 136.06 (*C*H-4 or *C*H-6 of Ar), 139.94 (*C*H-4 or *C*H-6 of Ar), 160.49 (C_{quat}-2), 164.58 (*C*H=N).

Azine ***5d*** [56]. Flash chromatography (CH_2Cl_2), R_f 0.47; m. p. 192–193ºC (Ref. [56] 196ºC); IR: 733.0, 745.4, 778.3, 838.7, 963.8, 1077.6, 1092.4, 1219.9, 1250.6, 1263.2, 1321.1, 1440.0, 1469.6, 1491.8, 1578.2, 1623.1, 2229.4, 2840.8, 2928.6, 3421.4; ^{1}H NMR ($CDCl_3$): 3.93 (s, 6H, OC*H*$_3$), 6.88–7.03 (m, 6H, 6C*H* of Ar), 8.70 (s, 1H, C*H*=N), 11.57 (bs, 1H, O*H*, exchangeable); ^{13}C NMR ($CDCl_3$): 56.16 (O*C*H$_3$), 110.59 (*C*H of Ar), 115.03 (*C*H of Ar), 117.29 (C_{quat}-1), 119.40 (*C*H of Ar), 124.01 (*C*H of Ar), 148.30 (C_{quat}), 149.63 (C_{quat}), 164.80 (*C*H=N); after addition of KOH: ^{1}H NMR ($CDCl_3$:DMSO-d_6 5:1): 3.75 (s, 6H, OC*H*$_3$), 6.50 (dd, 2H, J 7.5, 7.8, C*H*-5 of Ar), 6.75 (d, 2H, J 7.5, C*H* of Ar), 7.04 (d, 2H, J 7.8, C*H* of Ar), 8.81 (s, 1H, C*H*=N); ^{13}C NMR ($CDCl_3$:DMSO-d_6 5:1): 55.63 (O*C*H$_3$), 78.68 (*C*H of Ar), 113.28 (*C*H of Ar), 114.96 (C_{quat}), 118.54 (C_{quat}), 122.06 (*C*H of Ar), 127.61 (C_{quat}), 149.98 (C_{quat}), 161.92 (*C*H=N), 217.83 (*C*=O); HMQC cross-peaks: 3.752/55.63, 6.496/116.65, 6.750/113.28, 7.043/122.06, 8.811/161.92; MS (EI+) m/z 300 (M^+, 100), 283 (M-OH, 38), 150 (½ M^+, 100), 135 (½ M^+-CH_3, 28), 108 (½ M^+-CH_3-CHN, 27), 65 (Ar, $C_5H_5^+$, 27).

Azine ***5e*** [57]. Flash chromatography (CH_2Cl_2:NH_4OH 100:0.1), R_f 0.27; m. p. 189–190ºC (Ref. 195ºC [58], 193ºC [59]); IR: 617.5, 650.1, 753.9, 810.4, 866.1, 957.4, 1015.9, 1034.6, 1140.8, 1157.1, 1238.0, 1258.5, 1270.4, 1312.9, 1343.3, 1420.1, 1442.0, 1463.7, 1507.8, 1579.2, 1597.9, 1622.7, 2019.5, 2838.9, 2928.4, 2961.0, 3000.7, 3420.1; ^{1}H NMR ($CDCl_3$): 3.94 (s, 6H, OC*H*$_3$), 3.975 (s, 6H, OC*H*$_3$), 6.91 (d, 2H, J_{56} 8.3, C*H*-5 of Ar), 7.25 (dd, 2H, J_{26} 1.9, J_{56} 8.3, C*H*-6 of Ar), 7.54 (d, 2H, J_{26} 1.9, C*H*-2 of Ar), 8.60 (s, 2H, C*H*=N); ^{13}C NMR ($CDCl_3$): 55.90 (O*C*H$_3$), 108.65 (*C*H of Ar), 110.59 (*C*H of Ar), 123.90 (*C*H of Ar), 127.19 (C_{quat}), 149.31 (C_{quat}), 151.74 (C_{quat}), 161.14 (*C*H=N).

Azine ***5f*** [60]. Flash chromatography (CH_2Cl_2), R_f 0.66; m. p. 146–148ºC (Ref. [61] 153ºC); IR: 505.8, 817.8, 864.2, 969.2, 1176.1, 1211.1, 1290.3, 1303.5, 1321.0, 1511.7, 1568.6, 1608.6, 1621.5, 2857.9, 2915.0, 2939.6, 2996.4, 3030.3; ^{1}H NMR ($CDCl_3$): 2.40 (s, 6H, C*H*$_3$), 7.25 (d, 4H, J 8.1, C*H*-3 and C*H*-5 of Ar), 7.73 (d, 4H, J 8.1, C*H*-2 and C*H*-6 of Ar), 7.74 (s, 1H, C*H*=N); ^{13}C NMR ($CDCl_3$): 21.61 (*C*H$_3$), 128.47 (*C*H of Ar), 129.50 (*C*H of Ar), 131.40 (C_{quat}), 141.57 (C_{quat}), 161.88 (*C*H=N).

Azine ***5g*** [62]. Flash chromatography (CH_2Cl_2), R_f 0.59; m. p. 231–232ºC (Ref. [62] 226–228ºC); IR: 522.5, 814.4, 948.2, 1064.3, 1178.8, 1228.1, 1302.0, 1365.6, 1430.2, 1443.4, 1522.6, 1551.8, 1602.7, 2802.0, 2911.7; ^{1}H NMR ($CDCl_3$): 3.03 (s, 12H, NC*H*$_3$), 6.72 (d, 4H, J 8.9, C*H*-2 and C*H*-6 of Ar), 7.70 (d, 4H, J 8.9, C*H*-3 and C*H*-5 of Ar), 8.57 (s, 2H, C*H*=N); ^{13}C NMR ($CDCl_3$): 40.16 (N*C*H$_3$), 111.67 (*C*H-2 and *C*H-6 of Ar), 128.18 (C_{quat}-4), 129.85 (*C*H-3 and *C*H-5 of Ar), 152.07 (C_{quat}-1), 160.77 (*C*H=N); MS (EI+): m/z 294 (M^+, 100), 266 (M^+-2N, 31), 250 (M^+-$N(CH_3)_2$, 17), 206 (M^+-$2N(CH_3)_2$, 46), 147 (½ M^+, 47), 132 (½ M^+-CH_3, 29), 117 (½ M^+-$2CH_3$, 27), 105 (½ M^+-CHN-CH_3, 17), 65 (Ar, $C_5H_5^+$, 16).

Azine ***5h*** [63]. Flash chromatography (CH_2Cl_2), R_f 0.36; m. p. 87–90ºC (Ref. [63] 111–112ºC); IR: 515.1, 591.4, 735.6, 750.6, 805.3, 882.1, 888.0, 929.4, 950.5, 1023.2, 1077.8, 1098.8, 1147.1, 1153.3, 1217.6, 1263.2, 1271.7, 1291.1, 1392.9, 1470.5, 1547.3, 1575.6, 1641.9, 2963.0, 3077.5, 3101.4, 3136.0, 3149.8; ^{1}H NMR ($CDCl_3$): 6.50 (dd, 2H, J 1.8, 3.5, C*H*-4 of Ar), 6.86 (dd, 2H, J 0.6, 3.5, C*H*-3 of Ar), 7.56 (d, 2H, J 1.8, C*H*-5 of Ar), 8.49 (s, 2H, C*H*=N); ^{13}C NMR ($CDCl_3$): 112.18 (*C*H-3 of Ar), 116.73 (*C*H-4 of Ar), 145.71 (*C*H-5 of Ar), 149.26 (C_{quat}-2 of Ar), 150.82 (*C*H=N).

Azine ***5i*** [64]. Flash chromatography (CH_2Cl_2), R_f 0.42; m. p. 150–152ºC (Ref. 154ºC [65], 151–152ºC [66], 157.5–158.5ºC [67]); IR: 498.7, 724.1, 765.1, 833.7, 858.0, 950.4, 1041.6, 1166.0, 1212.5, 1235.5, 1253.8, 1273.5, 1327.0, 1368.2, 1420.9, 1511.7, 1537.8, 1609.2, 1696.8, 2966.5, 3007.8, 3081.0, 3099.7, 3248.3; ^{1}H NMR (DMSO): 7.21 (dd, 2H, J 3.7, 5.1, C*H*-4 of Ar), 7.63 (dd, 2H, J 1.0, 3.7, C*H*-5 of Ar), 7.56 (ddd, 2H, J 1.0, 1.0, 4.9 C*H*-3 of Ar), 8.86 (s, 2H, C*H*=N); ^{13}C NMR (DMSO):

128.18 (*C*H of Ar), 130.91 (*C*H of Ar), 133.71 (*C*H of Ar), 138.32 (C_{quat}-2 of Ar), 155.72 (*C*H=N).

Azine ***5j*** [68]. Flash chromatography (CH_2Cl_2), R_f 0.55; m. p. 243–244ºC (Ref. [68] 245ºC); ^{1}H NMR (DMSO-d_6:$CDCl_3$ 5:1): 4.18 (s, 10H, C*H* of ferrocene), 4.42 (t, 4H, J 1.8, C*H* of ferrocene), 4.65 (t, 4H, J 1.8, C*H* of ferrocene), 7.98 (s, 2H, C*H*=N); ^{13}C NMR (DMSO-d_6:$CDCl_3$ 5:1): 67.04 (2×*C*H of ferrocene), 68.83 (5×*C*H of ferrocene), 69.65 (2×*C*H of ferrocene), 79.74 (C_{quat} of ferrocene), 143.74 (*C*H=N); MS (EI+): m/z 424 (M^+, 100), 396 (M^+-2N, 16), 212 (½ M^+, 74), 198 (½ M^+-NH, 79), 185 (ferrocene$^+$, 47), 56 (Fe, 57).

Two-step protocols for the preparation of azines ***5***

A mixture of ferrocene carbaldehyde (1 mmol) and semicarbazide hydrochloride **2** (R = NH_2, 2 mmol) or *t*-butyl carbazate **2** (R = OBu^t, 2 mmol) in water (30 ml) was irradiated in a microwave oven for 2–5 min with a power of 440 W. The crystals formed after cooling were filtered off and dried in air. To a solution of thus prepared semicarbazone **3** or carbazate **4** (1 mmol) in acetone (5 ml) silica gel (2 g) or basic alumina (2 g) was added and the solvent was removed *in vacuo*. The mixture was irradiated in a microwave oven. The product was purified by high performance flash chromatography on silica gel.

Crystal structure determination of compound ***5e***

A prismatic colourless crystal 0.41×0.12×0.08 mm in size was mounted on a SMART X-ray diffractometer with a 1K CCD area detector. Data were collected at room temperature using graphite-monochromatized Mo-K_α radiation (λ = 0.71073 Å). A hemisphere of data (1271 frames at 5 cm detector distance) was collected using a narrow-frame method with scan widths of 0.30º in ω and an exposure time of 30 s/frame. The first 50 frames were measured again at the end of the data collection to monitor instrument and crystal stability. Analysis of the frames showed negligible decay during data collection. The data were integrated using a Bruker SAINT software package with a narrow frame algorithm [69] yielding a total of 10262 reflections of which 4650 independent and 3641 with I > 10σ(I). The SADABS program was used for the absorption correction [70]. The final cell constants were based on 1562 reflections with *I* > 10σ(I). The structure was solved by direct methods and refined by full matrix least-squares techniques with the SHELX97 software package [71]. The observed reflection conditions (h0l; 00l: l = 2n) indicated Pc (#7) and P2/c (#13) as the only possible space groups. The initial solution in the higher symmetry S.G. resulted in an unsatisfactory model. Initial solution in Pc resulted in R-factor of c.a. 10% and the refinement was consequently carried out in the lower symmetry S.G. First, all non-hydrogen atoms have been found and assigned from the Fourier maps and their thermal parameters refined anisotropically. Next, the hydrogen atoms have been added to the refinement as riding models and their thermal parameters refined isotropically. After the refinement con-verged, a close examination of the solution as well as a test using the PLATON program confirmed the lack of possible higher symmetry [72]. Main crystallographic details are listed in Table 2. Full crystallographic data for this paper in cif-format can be obtained free of charge from the Cambridge Crystallographic Data Centre [73].

Table 2. Crystal data and structure refinement for **5e**.

Empirical formula	$C_{18}H_{20}N_2O_4$
Formula weight	328.35
Temperature	293(2) K
Wavelength	0.71073 Å
Crystal system, S.G.	Monoclinic, P1c1 (#7)
Unit cell dimensions	a = 11.3601(10) Å
	α = 90 deg.
	b = 18.8367(17) Å
	β = 92.858(4) deg.
	c = 8.4068(8) Å
	γ = 90 deg.
Volume, Z	1690.8(3) Å^3, 4
Calculated density	1.290 g/cm^3
Absorption coefficient	0.092 mm^{-1}
F(000)	696
Crystal size	0.41×0.12×0.08 mm
θ range for data collection	1.91 to 22.98 deg.
Limiting indices	$-9 \le h \le 9$, $-20 \le k \le 19$, $-12 \le l \le 12$
Reflections collected/unique	10262/4650 [R(int) = 0.0202]
Refinement method	Full-matrix least-squares on F^2
Data / parameters	4650/431
Goodness-of-fit on F^2	1.023
Final R indices [I>2σ(I)]	[a]R1 = 0.0303, [b]Rw2 = 0.0763
R indices (all data)	R1 = 0.0337, Rw2 = 0.0785
Largest diff. peak and hole	0.151 and –0.144 e·Å^{-3}

[a] $R1 = \Sigma \mid |F_o| - |F_c| / \Sigma |F_o|$ (based on reflections with I > 2σ(I));
[b] $R_w = [\Sigma w(|F_o| - |F_c|)^2 / \Sigma w |F_o| 2]^{1/2}$;
$w = 1/[\sigma^2(F_o^2) + (0.0511P)^2 + 0P]$; $P = [\mathrm{Max}(F_o^2, 0) + 2F_c^2]/3$ (all data).

REFERENCES

1. W. J. Haggerty, C. C. Cheng, *J. Med. Chem.*, **13**, 574 (1970).
2. J. R. Dimmock, P. Kumar, J. W. Quail, U. Pugazhenthi, J. Yang, M. Chen, R. S. Reid, T. M. Allen, G. Y. Kao, S. P. C. Cole, G. Batist, J. Balzarini, E. De Clercq**,** *Eur. J. Med. Chem.*, **30**, 209 (1995).
3. A. I. Khodair, P. Bertrand**,** *Tetrahedron*, **54**, 4859 (1998).
4. H. I. Gul, M. Gul, J. Vepsälainen, E. Erciyas, O. Hänninen**,** *Biol. Pharm. Bull.*, **26**, 631 (2003).
5. Y. Sawa , M. Hoten**,** *Sen'i Gakkaishi*, **57**, 153 (2001).
6. I. A. Danish, K. R. Prasad, *Acta Pharmac.*, **54**, 133

(2004).
7. H. I. Gul, F. Sahin, M. Gul, S. Ozturk, K. O. Yerdelen**,** *Arch. Pharm. Chem. Life Sci.*, **338**, 335 (2005).
8. M. N. Kumaraswamy, V. P. Vaidya**,** *Indian J. Heterocyclic Chem.*, **14**, 193 (2005).
9. R. W. Lange**,** *Curr. Opin. Anti-inflamm. Immunomod. Investig. Drugs*, **2**, 338 (2000).
10. J. L. Vennerstrom, M. T. Makler, C. K. Angerhofer, J. A. Williams**,** *Antimicrob. Agents Chemother.*, **39**, 2671 (1995).
11. H. I. Gul, U. Calis, J. Vepsalainen, *Arzneim. Forsch.*, **54**, 359 (2004).
12. J. O'Brien, W. Lemaire, T.-B. Chen, R. S L. Chang, M. A. Jacobson, S. N. Ha, C. W. Lindsley, H. J. Schaffhauser, C. Sur, D. J. Pettibone, P. J. Conn, D. L. Williams, Jr.**,** *Mol. Pharmacol.*, **64**, 731 (2003).
13. M. Eberle, S. Farooq, A. Jeanguenat, D. Mousset, A. Steiger, S. Trah, W. Zambach, A. Rindlisbacher**,** *Chimia*, **57**, 705 (2003).
14. S. Komeda, G. V. Kalayda, M. Lutz, A. L. Spek, Y. Yamanaka, T. Sato, M. Chikuma, J. Reedijk, *J. Med. Chem.*, **46**, 1210 (2003).
15. G. V. Kalayda, S. Komeda, K. Ikeda, T. Sato, M. Chikuma, J. Reedijk**,** *Eur. J. Inorg. Chem.*, 4347 (2003).
16. R. Grashey, in: 1,3-Dipolar Cycloaddition Chemistry, A. Padwa (ed.), John Wiley and Sons, New York, 1984, Vol. 1, p. 733.
17. A. A. Aly, M. A.-M. Gomaa, *Can. J. Chem.*, **83**, 57 (2005).
18. H. Zachová, S. Man, M. Nečas, M. Potáček**,** *Eur. J. Org. Chem.*, 2548 (2005).
19. B. B. Snider, J. F. Grabowski, R. W. Alder, B. M. Foxman, L. Yang, *Can. J. Chem.*, **84**, 1242 (2006).
20. S. D. Sharma, R. D. Anand, G. Kaur**,** *J. Indian Chem. Soc.*, **83**, 1273 (2006).
21. J. R. Dilworth, *Coord. Chem. Rev.*, **21**, 29 (1976).
22. J. Chatt, J. R. Dilworth, R. L. Richards, *Chem. Rev.*, **78**, 589 (1978).
23. M. Sate, J. H. Enemark, in: Nitrogen Fixation. The Chemical-Biochemical-Genetic-Interface, A. Moiler, W. E. Newton (eds.), Plenum, New York, 1983, p. 301.
24. R. A. Henderson, G. J. Leigh, C. J. Pickett, *Adv. Inorg. Chem.*, **27**, 197 (1983).
25. J. A. McCleverty**,** *Transition Met. Chem.*, **12**, 282 (1987).
26. G. J. Leigh**,** *J. Mol. Catal.*, **47**, 363 (1988).
27. P. S. Braterman (ed.), Reactions of Coordinated Ligands, Plenum, New York, 1989.
28. A. E. Shilov, in: Perspectives in Coordination Chemistry, A. F. Williams, C. Floriani, A. E. Merbach (eds.), VCH, Baset, Switzerland, 1992, p. 233.
29. G. J. Leigh, *Acc. Chem. Res.*, **25**, 177 (1992).
30. W. R. Browne, R. Hage, J. G. Vos, *Coord. Chem. Rev.*, **250**, 1653 (2006).
31. T. W. Greene, P. G. M. Wuts, Protective Groups in Organic Synthesis, John Wiley, New York, 1991.
32. D. Kolbah, D. Korunčev, in: Methoden der Organischen Chemie, Houben-Weyl, Thieme Verlag, Stuttgart, 1967, Vol. 10, part 2, p. 89.
33. S. Dayagi, Y. Degani, in: The Chemistry of the Carbon-Nitrogen Double Bonds, S. Patai (ed.), Interscience, New York, 1970, Ch. 2, p. 61.
34. W. Borsche, *Ber.*, **34**, 4297 (1901).
35. S. N. Shah, N. K. Chudgar, *Molecules*, **5**, 657 (2000).
36. A. Obreza, U. Urleb, *Acta Chim. Slov.*, **49**, 605 (2002).
37. S. Caddick**,** *Tetrahedron*, **51**, 10403 (1995).
38. S. Deshayes, M. Liagre, A. Loupy, J.-L. Luche, A. Petit**,** *Tetrahedron*, **55**, 10851 (1999).
39. P. Lidstrom, J. Tierney, B. Wathey, J. Westman**,** *Tetrahedron*, **57**, 9225 (2001).
40. A. Kirschning, H. Monenschein, R. Wittenberg**,** *Angew. Chem., Int. Ed.*, **40**, 650 (2001).
41. A. Loupy, Microwaves in Organic Synthesis, Wiley-VCH, Weinheim, 2002.
42. A. Katritzky, S. Singh**,** *Arkivoc*, 68 (2003, **xiii**).
43. M. Taylor, B. Atri, S. Minhas, Developments in Microwave Chemistry, Evalueserve, 2005.
44. C. O. Kappe, A. Stadler, Microwaves in Organic and Medicinal Chemistry, Wiley-VCH, Weinheim, 2005.
45. J. Tierney, P. Lidström (eds.), Microwave Assisted Organic Synthesis, Blackwell Publishing, Oxford, 2005.
46. E. S. H. El Ashry, A. A. Kassem, *Arkivoc*, 1 (2006, **ix**).
47. A. Loupy, A. Petit, J. Hamelin, F. Texier-Boullet, P. Jacquault, D. Mathe**,** *Synthesis*, 1213 (1998).
48. R. S. Varma**,** *Green Chem.*, **1**, 43 (1999).
49. R. S. Varma**,** *Pure Appl. Chem.*, **73**, 193 (2001).
50. R. S. Varma, Advances in Green Chemistry: Chemical Syntheses Using Microwave Irradiation, R. Astra Zaneca Research Foundation, Kavitha Printers, Bangalore, India, 2002.
51. R. S. Varma, Microwave Technology – Chemical Synthesis Application, Kirk-Othmer Encyclopedia of Chemical Technology, J. Wiley & Sons, Inc., New York, 2003.
52. H. Loghmani-Khouzani, M. M. M. Sadeghi, J. Safari, M. S. Abdorrezaie, *J. Chem. Res. (S)*, 80 (2001).
53. L. Gattermann, T. von Horlacher, *Ber.*, **32**, 284 (1899).
54. Aldrich S780278; CAS Number: 5466-23-9.
55. D. Vorländer, *Ber.*, **39**, 803 (1906).
56. A. P. Terent'ev, E. G. Rukhadze, G. P. Talyzenkova, G. V. Panova, *Zh. Obschch. Khim.*, **36**, 1590 (1966).
57. Aldrich S529869; CAS Number: 17745-86-7.
58. L. Gattermann, *Ann.*, **357**, 313 (1907).
59. H. C. Barany, E. A. Braude, M. Pianka, *J. Chem. Soc.*, 1898 (1949).
60. Aldrich S542636; CAS Number: 4702-76-5.
61. L. B. Howard, G. E. Hilbert, W. R. Wiebe, V. L. Gaddy, *J. Am. Chem. Soc.*, **54**, 3628 (1932).
62. T. Curtius, A. Bertho, *J. Prakt. Chem.*, **125**, 23 (1930).
63. G. Manunni, C. Carta-Satta, *Gazz. Chim. Ital.*, **29** (II), 467 (1899).
64. Aldrich S927147; CAS Number: 24523-46-4.
65. L. Gattermann, *Justus Liebigs Ann. Chem.*, **393**, 215 (1913).

66. E. Grischkewitsch-Trochimowski, I. Mazurewitsch, *Zh. Russ. Fiz.-Khim. Obsht.*, **44**, 570 (1912).
67. R. E. Miller, F. F. Nord, *J. Org. Chem.*, **16**, 1720 (1951).
68. P. J. Graham, R. V. Lindsey, G. W. Parshall, M. L. Peterson, G. M. Whitman, *J. Am. Chem. Soc.*, **79**, 3416 (1957).
69. Saint Plus, v. 7.01, Bruker Analytical X-ray, Madison, WI, 2003.
70. G. M. Sheldrick: SADABS, v. 2.10. Program for Empirical Absorption Correction of Area Detector Data, University of Gottingen, Gottingen, Germany, 2003.
71. G. M. Sheldrix: SHELX97 (Includes SHELXS97, SHELXL97, CIFTAB) - Programs for Crystal Structure Analysis (Release 97-2). Institüt für Anorganische Chemie der Universität, Tammanstrasse 4, D-3400 Göttingen, Germany, 1998.
72. A. L. Spek: PLATON, A Multipurpose Crystallographic Tool, Utrecht University, Utrecht, The Netherlands, 1998.
73. The crystallographic data for the azine **5e** were deposited at the Cambridge Crystallographic Data Centre and allocated the deposition number CCDC 649185. Copies of the data can be obtained, free of charge, on application to CCDC, 12 Union Road, Cambridge CB2 1EZ, UK; http://www.ccdc.cam.ac.uk/data_request/cif, CCDC 649185; fax: +44 1223 336033; e-mail: deposit@ccdc.cam.ac.uk.

ЕДНОСТАДИЕН СИНТЕЗ НА СИМЕТРИЧНИ АЗИНИ ПОД ДЕЙСТВИЕ НА МИКРОВЪЛНИ В ОТСЪСТВИЕ НА РАЗТВОРИТЕЛИ

Св. Симеонов[1], В. Б. Куртева[1,*], Р. П. Бончев[2]

[1] *Институт по органична химия с център по фитохимия, Българска академия на науките, ул. „Акад. Г. Бончев“, блок 9, 1113 София*
[2] *Кабот корпорейшън, 5401 Венайс ав. , С.-И. Албукерк, NM 87113, САЩ*

Посветена на акад. Иван Юхновски по повод на 70-та му годишнина

Постъпила на 29 ноември 2007, Преработена на 11 януари 2008 г.

Разработени са бързи, ефикасни и благоприятни за околната среда едностадийни процедури за синтез на симетрични арил и хетероарил азини под действие на микровълни в отсъствие на разтворители. Основните предимства на тези синтетични схеми са сериозната икономия на енергия в сравнение с реакциите при конвенционално нагряване и избягването на употребата на токсичния и вреден за околната среда хидразин. Трансформациите протичат през семикарбазонен или карбазатен междинен продукт, който се превръща в азин с различна скорост в зависимост от реакционните условия и вида на заместителите в ароматното ядро. Показано е, че методите са ефективни при използване на ароматни алдехиди без заместители или с електронодонорни заместители. Обратно, при наличие на електроно-акцепторни групи в молекулите на алдехидите не се наблюдава образуване на азини, а се изолират единствено междинно образуваните семикарбазони или карбазати. Намерено е, че карбазатният път е предпочетен, особено при наличие на хидроксилна група в ароматната част. Семикарбазонният път е проведен и по двустадийна процедура и е показано, че едностадийната е предпочетен като цяло. *E,E*-Конфигурацията на продуктите е потвърдена посредством рентгеноструктурен анализ на подбрана проба.

Bulgarian Chemical Communications, Volume 40, Number 4 (pp. 418–425) 2008

Hydrogen bonding in ionic systems of 1,5,7-triazabicyclo[4.4.0]dec-5-ene (TBD) with 4-cyanophenol: *ab initio* and DFT studies of their structures

Y. Dimitrova*

Department of Structural Organic Analysis, Institute of Organic Chemistry with Centre of Phytochemistry, Bulgarian Academy of Sciences, Acad. G. Bonchev St., Block 9, 1113 Sofia, Bulgaria

Dedicated to Academician Ivan Juchnovski on the occasion of his 70th birthday

Received December 11, 2007; Revised January 14, 2008

The structures of the hydrogen-bonded systems of 1,5,7-triazabicyclo[4.4.0]dec-5-ene (TBD) with one and two 4-cyanophenol molecules have been investigated employing *ab initio* and DFT calculations at different basis sets. The calculations show that the optimised structures of the studied systems are cyclic. The calculated values of the dissociation energy and the changes of the atomic charges upon hydrogen bonding for the studied hydrogen-bonded systems confirm their ionic structures. The hydrogen bonding of TBD with one and two 4-cyanophenol molecules leads to changes in the structural (bond lengths and angles) and vibrational (vibrational frequencies and infrared intensities) characteristics of the monomers. It was established that the TBD molecule is considerably deformed upon hydrogen bonding, while the deformation of the 4-cyanophenol molecules is smaller. The ab initio and DFT predicted vibrational spectra for the complexes TBD: 4-cyanophenol (1:1 and 1:2) demonstrate the ionic character of the forming hydrogen-bonded systems.

Key words: hydrogen-bonded complexes; TBD; 4-cyanophenol; structures; *ab initio*; DFT.

INTRODUCTION

It is known that the organic ions are very important in organic synthesis as powerful synthons and the knowledge of their structure can be used for the understanding of their reactivity [1, 2]. The variations in the IR spectra caused by the changes in the structures of the neutral molecules into ions (carbanions, anion-radicals, dianionis, *etc*.) are useful information for studying the mechanism and kinetics of the chemical reaction in which the ions play role as intermediates. The contribution in these studies of Juchnovski *et al*. [3–11] is indisputable.

The ionic systems are very interesting also in the context of the hydrogen bonding. Hydrogen bonds in which either the donor or the acceptor is an ion play an important role in aqueous chemistry and in biological systems. It is, therefore, not surprising that these systems have often been studied by theoretical and experimental methods in the last few years [12–18]. The primary interest is in the structural data as the number of molecules that will fit around an ion, the structure of clusters containing several molecules and the equilibrium distances and angles of these systems. Empirical modeling of ionic systems is not trivial since nonadditivity is expected to be important and so the modern quantum-chemical methods have an important role in calibrating such models.

Since phenol is a prototype among many hydrogen-donating aromatics, the studies of clusters of phenol with hydrogen-accepting molecules are contributed to the investigation of structures, vibrational spectra and dynamics of various hydrogen-bonded systems [19–22]. In previous studies [23, 24] the complexes between phenols and a range of strong N-bases have been studied extensively by FTIR spectroscopy in order to understand the nature of the intermolecular hydrogen bonds and the structures of the hydrogen-bonded chains. The hydrogen-bonded complexes between 1,5,7-triazabicyclo[4.4.0]dec-5-ene (TBD) and 4-CNPhOH are studied by FTIR spectroscopy [23]. The formation of cyclic hydrogen-bonded structures between TBD and 4-CNPhOH molecules was observed in chloroform. In this connection the objects of this study are the ionic hydrogen-bonded systems of 1,5,7-triazabicyclo[4.4.0]dec-5-ene (TBD) with one and two 4-CNPhOH molecules. The aim of the study is, firstly, to establish the most stable structures of the studied hydrogen-bonded systems, secondly, to study the nature of the hydrogen bonding and charge rearrangement in the monomers forming a complex, and finally to estimate the changes in the structural and vibrational characteristics upon hydrogen bonding.

* E-mail: dimj@orgchm.bas.bg

© 2008 Bulgarian Academy of Sciences, Union of Chemists in Bulgaria

CALCULATIONS

The *ab initio* and DFT calculations with various basis sets using the GAUSSIAN 03 series of programs [25] have been performed in order to study the structural and vibrational features of the ionic hydrogen-bonded systems formed between 4-CNPhOH and TBD. It is important to note that the density functional methods for electronic structure calculations [26–28] contain semiempirical elements based on properties of atoms and simple molecules. Prior to routine application in a given field such as hydrogen bonding [29–31], they have to be checked against experimental measurements and more established quantum chemical approaches at least for some prototype systems [32]. The density functional calculations in this work were carried out in the framework of Kohn-Sham density-functional theory [26] (DFT) with the nonlocal gradient-corrected exchange-correlation functional of Becke and Lee, Yang and Parr including partially exact HF-exchange (BLYP) [33]. The combination of *ab initio* and DFT calculations in the studies of hydrogen-bonded systems is very useful in order to obtain better knowledge of hydrogen-bonded structures, their stability and vibrational features.

The dissociation energy calculated by ab initio and DFT calculations can be used for the estimation of the stability of the hydrogen-bonded systems between two and more partners. The supermolecular variation method determines dissociation energy (ΔE) as a difference between the energy of the complex and the energies of the isolated molecules. For complexes **1** and **2,** shown in Figures 1 and 2 the dissociation energy is calculated by Eqns (1) and (2):

$$\Delta E_{\text{com.1}} = E_{\text{com.1}} - (E_{\text{TBD}} + E_{\text{4-CNPhOH}}) \qquad (1)$$

$$\Delta E_{\text{com.2}} = E_{\text{com.2}} - (E_{\text{TBD}} + 2E_{\text{4-CNPhOH}}) \qquad (2)$$

where E_{TBD} and $E_{\text{4-CNPhOH}}$ are the energies of the isolated monomers in their own basis set and $E_{\text{com.}\mathbf{1}}$, $E_{\text{com.}\mathbf{2}}$ are the energies of the complexes.

Further, to compare the calculated results of the dissociation energy with the respective experimental ones the effect of the zero-point energy (ZPE) should be taken into account. *Ab initio* calculations yield the total molecular electronic energy of the hypothetical vibrationless state at 0K. To convert this energy (U^0_0) to an enthalpy at 298.15K it is necessary to make correction for the zero-point energy ($E_{\text{zp vib}}$) by using the enthalpy function, ($H^0_{298} - H^0_0$):

$$\Delta H^0_{298} = (U^0_0) + \Delta(E_{\text{zp vib}}) + \Delta(H^0_{298} - H^0_0) \qquad (3)$$

$$E_{\text{zp vib}} = 0.5\text{h}\sum\nu_i \qquad (4)$$

The zero-point energy is calculated from Eqn. (4) and the enthalpy function is obtained by standard statistical thermodynamic procedures, using the optimised geometries to provide structural constants.

The zero-point vibrational energy correction for the studied complex can be defined as a difference between the calculated zero-point vibrational energy of the complex and the zero-point energies of the monomers:

$$\Delta E_{\text{zp vib}} = E_{\text{zp vib.}}(\text{com.}) - (E_{\text{zp vib}}(\text{TBD}) + E_{\text{zp vib}}(\text{4-CNPhOH})) \qquad (5)$$

RESULTS AND DISCUSSION

Hydrogen-bonded structures and their stabilities

Full geometry optimization was made with GAUSSIAN 03 series of programs [25] for the studied hydrogen-bonded systems between TBD and 4-CNPhOH: complex **1** (1:1) and complex **2** (1:2). The optimized structures of complexes **1** and **2** with BLYP/6-31+G(d,p) calculations are shown in Figures 1 and 2. As can be seen the optimized structures are cyclic. In Table 1 are shown the optimum values of the total energy and the selected optimized geometric parameters for free and complexed TBD and 4-CNPhOH, obtained from BLYP/6-31+G(d,p) calculations.

The complex **1** (1:1) has optimum geometry for H…O distance between TBD and 4-CNPhOH molecules 1.665 Å ($H_8…O_1$ and $H_{25}…O_1$). The hydrogen bonds $H_8…O_1$ and $H_{25}…O_1$ for complex **2** (1:2) are weaker and longer than the hydrogen bonds for complex **1,** moreover these hydrogen bonds are with different lengths namely R ($H_8…O_1$) is shorter and stronger than R ($H_{25}…O_1$) (see Table 1). The hydrogen bond for complex **2** formed between 4-CNPhOH molecules: $O_1…H_{45}$ is the strongest.

The changes of the geometrical parameters from monomers to a complex are defined in order to investigate the influence of the hydrogen bonding on the structural parameters of the monomers TBD and 4-CNPhOH. It is seen that the bond lengths and angles for complexes **1** and **2**, shown in Figs. 1 and 2 are perturbed from their values in the monomers. The most sensitive to the complexation are the bonds taking part in the hydrogen bonding. The calculations show that the changes in the geometrical parameters of the TBD molecule are larger than the changes of 4-CNPhOH molecules. The most sensitive to the formation of hydrogen bonds for complexes **1** and **2** are the following bonds: $C_2–O_1$, $C_2–C_3$, $N_{15}–C_{24}$, $N_{23}–C_{24}$ and $N_{23}–H_{25}$. The bonds $C_2–C_3$, $N_{15}–C_{24}$ and $N_{23}–H_{25}$ are lengthened in

the complexes, while the bonds C_2–$O_1$and N_{23}–C_{24} are shortened upon formation of the hydrogen bonds. The bond O_{38}–H_{45}, taking part in the strongest hydrogen bond O_1…H_{45} for complex **2**, is very sensitive to the hydrogen bonding. In the complex it becomes longer in comparison with its value in the monomer (4-CNPhOH).

Table 1. Selected optimized geometric parameters for free and complexed TBD and 4-CNPhOH, obtained from BLYP/6-31+G(d,p) calculations.

Parameter[a]	Monomers	Complex **1**	Complex **2**
Bond length, Å			
C_2–O_1	1.379	1.322 (–0.057)	1.343 (–0.036)
C_2–C_3	1.412	1.436 (0.022)	1.428 (0.016)
C_3–C_4	1.401	1.396 (–0.005)	1.398 (–0.003)
C_4–C_5	1.418	1.424 (0.006)	1.421 (0.003)
C_5–C_{13}	1.437	1.432 (–0.005)	1.434 (–0.003)
C_{13}–N_{14}	1.178	1.181 (0.003)	1.179 (0.001)
H_8–N_{15}	-	1.065	1.051
N_{15}–C_{16}	1.457	1.469 (0.012)	1.473 (0.016)
N_{15}–C_{24}	1.304	1.352 (0.048)	1.355 (0.051)
N_{23}–C_{24}	1.393	1.352 (–0.041)	1.357 (–0.036)
C_{22}–N_{23}	1.457	1.469 (0.012)	1.473 (0.016)
N_{19}–C_{24}	1.389	1.376 (–0.013)	1.369 (–0.020)
N_{23}–H_{25}	1.017	1.065 (0.048)	1.043 (0.026)
O_{38}–H_{45}	0.978	-	1.033 (0.055)
O_{38}–C_{39}	1.379	-	1.356 (–0.023)
C_{39}–C_{40}	1.412	-	1.420 (0.008)
C_{40}–C_{41}	1.401	-	1.397 (–0.004)
C_{41}–C_{42}	1.418	-	1.422 (0.004)
C_{42}–C_{50}	1.437	-	1.435 (–0.002)
C_{50}–N_{51}	1.178	-	1.179 (0.001)
O_1…H_8	-	1.665	1.755
O_1…H_{25}	-	1.665	1.833
O_1…H_{45}	-	-	1.573
Angle (º)			
H_8…O_1…H_{25}	-	75.1	69.6
H_8…O_1…H_{45}	-	-	103.0
H_8–N_{15}–C_{24}	-	113.5	113.4
N_{15}–C_{24}–N_{23}	116.5	117.5 (1.0)	117.3 (0.8)
C_{24}–N_{23}–H_{25}	111.7	113.5 (1.8)	113.0 (1.3)
E^{tot}(a.u.)	–399.610848[b] –438.619198[c]	–838.282014	–1237.914464

[a] See Figs. 1 and 2 for numbering of atoms; [b] E^{tot} for 4-CNPhOH; [c] E^{tot} for TBD; In the parenthesis are given the changes of the parameters from monomer to a complex.

The changes in the angles N_{15}–C_{24}–N_{23} and C_{24}–N_{23}–H_{25}, taking part in the hydrogen bonding for complexes **1** and **2,** are also estimated. The calculations show that these angles become larger in the complexes in comparison with their monomer values. Bearing in mind the changes in the geometrical parameters for complexes **1** and **2** it can be concluded that the TBD molecule is considerably deformed upon hydrogen bonding, while the deformation of the 4-CNPhOH molecules is smaller.

The next step in the study is to estimate the stability of the hydrogen-bonded systems between TBD and 4-CNPhOH: complex **1** (1:1) and complex **2** (1:2), shown in Figs. 1 and 2. The dissociation energies, uncorrected and corrected with zero-point energy differences are calculated by *ab initio* and DFT calculations with different basis sets. The results from the calculations are presented in Table 2. The corrected dissociation energy (–24.55 kcal·mol^{-1}) calculated with BLYP/6-31G(d,p) calculations for complex **2** (per one 4-CNPhOH molecule) are in a very good agreement with the experimentally measured heat of formation [6]: –23.42 kcal·mol^{-1}. This agreement confirms the reliability of the determined ionic structure of complex **2**: TBD: 4-CNPhOH (1:2). In agreement with the classification of the hydrogen-bonded systems, given in [37], the calculated values of the dissociation energy for the studied hydrogen-bonded systems confirm their ionic structures.

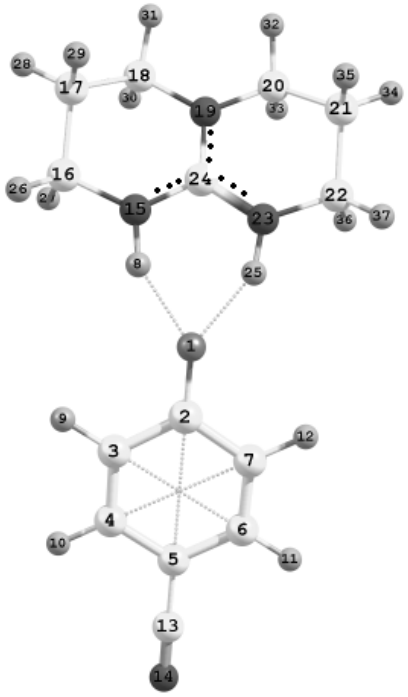

Fig. 1. Optimized structure with BLYP/6-31+G(d,p) calculations and atomic numbering for the hydrogen-bonded systems TBD:4-CNPhOH (1:1).

Charge distribution upon hydrogen bonding

The next aim in this study is to determine the influence of hydrogen bonding on the charge distribution in the studied hydrogen-bonded ionic systems. In this connection the atomic charges (q_i) for the free and complexed TBD and 4-CNPhOH are calculated by BLYP/6-31+G(d,p) calculations, using Mulliken population analysis. In Table 3 are included the atomic charges (q_i) and the changes of the atomic charges (Δq_i) upon hydrogen bonding:

$$\Delta q_i = q_i^{complex} - q_i^{monomer} \qquad (6)$$

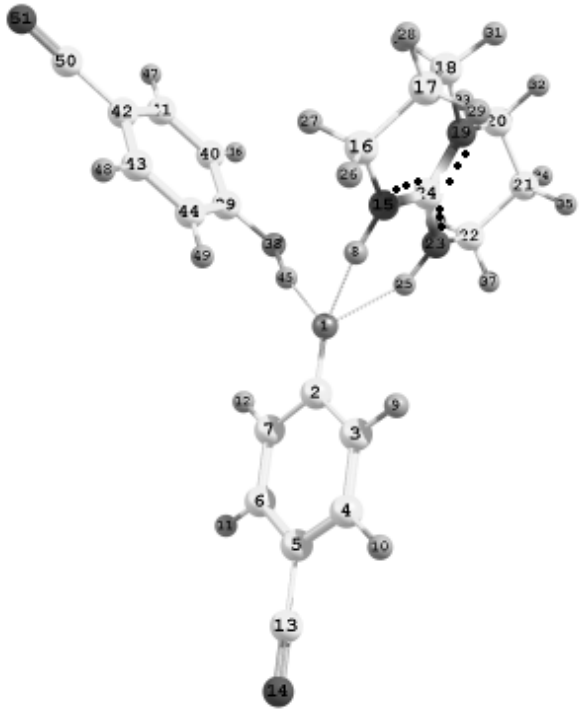

Fig. 2. Optimized structure with BLYP/6-31+G(d,p) calculations and atomic numbering for the hydrogen-bonded systems TBD:4-CNPhOH (1:2).

The calculations show that the most sensitive to the complexation are the atoms, taking part in the hydrogen bonding. The hydrogen bond formations between TBD and 4-CNPhOH lead to more considerable charge rearrangement for the TBD molecule than for the 4-CNPhOH molecules. In complexes **1** and **2** the oxygen atom O(1) (from 4-CNPhOH) acts as acceptor of electric charge. Its negativity increases significantly in the complexes in comparison with the corresponding negativity in the monomer. At the same time, the hydrogen atom H(8) (from OH group of 4-CNPhOH), the carbon atom C(39) and the hydrogen atom H(25) (from TBD) become more positive in the complex.

The changes of the atomic charges (Δq_i) upon hydrogen bonding for complex **1** (1:1) and complex **2** (1:2) show large proton polarizability of the hydrogen bonds within these complexes, i.e. hydrogen-bonded systems with ionic character are formed. It is important to note that in complex **2**, the 4-CNPhOH molecule with retained O–H group is subjected to a very strong charge rearrangement. The negativity of carbon atoms C(40), C(42) and C(44) is larger than the corresponding negativity of carbon atoms C(3), C(4) and C(5) in the 4-CNPhOH molecule which O-H group is strongly polar due to the formation of the $O^-\ldots H^+N$ hydrogen bonds with proton transfer, i.e. of the polar structure.

Changes in the vibrational frequencies and infrared intensities arising from the hydrogen bonding

The infrared (IR) spectroscopic signature of the hydrogen bond formation is the shift to the lower frequency and the increase in intensity of the stretching vibrations of the monomer bonds involving in hydrogen bonding. It is known that the *ab initio* and DFT predicted values of the vibrational frequencies depend on the method and the basis set used for the calculations. The frequencies from the calculations with larger basis sets give reasonable prediction of the experimental values, if the vibrations have small anharmonicity.

The prediction of the vibrational characteristics (vibrational frequencies and infrared intensities) of the hydrogen-bonded systems by *ab initio* and DFT calculations at different levels [34–43] has become widely employed in order to elucidate the influence of hydrogen bonding on the vibrational spectra of the monomers forming a complex. In the hydrogen-bonded system, the geometrical symmetry of the monomers often changes under perturbation [11]. The vibrational mixing, derived by a perturbation approach, is the counterpart of the orbital mixing.

Table 2. Dissociation energies ΔE (uncorrected and corrected), zero-point energy differences ΔE_{zpve} in kcal/mol and hydrogen bond distances R in Å for the hydrogen-bonded complexes **1** (1:1) and **2** (1:2), shown in Figures 1 and 2.

Complex	Basis set	ΔE_{uncor}	ΔE_{zpve}	ΔE_{cor}	R, Å
1:1	SCF/6-31G(d,p)	–29.284	2.017	–27.267	1.748 ($O_1\ldots H_8$) 1.723 ($O_1\ldots H_{25}$)
	BLYP/6-31G(d,p)	–35.109	1.522	–33.587	1.632 ($O_1\ldots H_8$) 1.632 ($O_1\ldots H_{25}$)
	BLYP/6-31+G(d,p)	–32.610	1.796	–30.814	1.665($O_1\ldots H_8$) 1.665 ($O_1\ldots H_{25}$)
1:2	SCF/6-31G(d,p)	–45.647 (–22.823)[a]	3.603	–42.044 (–21.022)[a]	1.831 ($O_1\ldots H_8$) 1.860 ($O_1\ldots H_{25}$) 1.693 ($O_1\ldots H_{45}$)
	BLYP/6-31G(d,p)	–52.493 (–26.246) [a]	3.397	–49.096 (–24.548) [a]	1.772 ($O_1\ldots H_8$) 1.799 ($O_1\ldots H_{25}$) 1.561($O_1\ldots H_{45}$)

a In the parenthesis is given the dissociation energy per one 4-CNPhOH molecule.

Table 3. Mulliken charges (q_i) for free and complexed TBD and 4-CNPhOH, obtained from BLYP/6-31+G(d,p) calculations.

[a]No.	[a]Atom	q_i			Δq_i	
		Monomers	Comp. 1:1	Comp. 1:2	Comp. 1:1	Comp. 1:2
1	O	–0.1367	–0.7213	–0.7846	–0.5845	–0.6479
2	C	–0.2160	–0.2788	–0.3331	–0.0628	–0.1172
3	C	0.4984	0.4812	0.2064	–0.0173	–0.2920
4	C	–0.3986	–0.5182	–0.3918	–0.1196	0.0068
5	C	0.8384	0.7890	0.6290	–0.0494	–0.2094
6	C	–0.3414	–0.5182	–0.3050	–0.1768	0.0365
7	C	0.5687	0.4812	0.5489	–0.0876	–0.0199
8	H	0.0000	0.3855	0.3771	0.3855	0.3771
9	H	0.0000	0.0830	0.0888	0.0830	0.0888
10	H	0.0000	0.1095	0.1157	0.1095	0.1157
11	H	0.0000	0.1095	0.1183	0.1095	0.1183
12	H	0.0000	0.0830	0.1098	0.0830	0.1098
13	C	–0.2671	–0.2679	–0.2664	–0.0008	0.0007
14	N	–0.5457	–0.5970	–0.5834	–0.0512	–0.0376
15	N	–0.3761	–0.3388	–0.1309	0.0373	0.2452
16	C	–0.2059	–0.0575	–0.0586	0.1484	0.1473
17	C	–0.4477	–0.3986	–0.4842	0.0491	–0.0365
18	C	0.0402	–0.0769	0.0158	–0.1171	–0.0244
19	N	–0.2306	–0.1769	–0.0978	0.0537	0.1327
20	C	0.0909	–0.0769	–0.0015	–0.1678	–0.0924
21	C	–0.4256	–0.3987	–0.4590	0.0270	–0.0333
22	C	–0.1970	–0.0575	–0.0202	0.1395	0.1769
23	N	–0.3591	–0.3388	–0.1529	0.0204	0.2063
24	C	0.1685	0.0768	–0.4070	–0.0917	–0.5755
25	H	0.2962	0.3855	0.3677	0.0893	0.0715
26	H	0.1282	0.1536	0.1526	0.0254	0.0244
27	H	0.1282	0.1490	0.1663	0.0208	0.0381
28	H	0.1431	0.1523	0.1592	0.0092	0.0161
29	H	0.1431	0.1679	0.1716	0.0248	0.0286
30	H	0.1321	0.1533	0.1659	0.0212	0.0338
31	H	0.1321	0.1428	0.1470	0.0107	0.0150
32	H	0.1337	0.1428	0.1471	0.0091	0.0134
33	H	0.1337	0.1533	0.1629	0.0196	0.0292
34	H	0.1524	0.1523	0.1565	0.0000	0.0041
35	H	0.1524	0.1679	0.1716	0.0156	0.0192
36	H	0.1337	0.1490	0.1737	0.0153	0.0400
37	H	0.1337	0.1536	0.1528	0.0199	0.0190
38	O	–0.1367	-	–0.4773	-	–0.3406
39	C	–0.2160	-	0.3977	-	0.6136
40	C	0.4984	-	–0.2473	-	–0.7457
41	C	–0.3986	-	–0.1438	-	0.2548
42	C	0.8384	-	0.2714	-	–0.5670
43	C	–0.3414	-	0.0097	-	0.3511
44	C	0.5687	-	–0.1035	-	–0.6722
45	H	0.0000	-	0.4553	-	0.4553
46	H	0.0000	-	0.1101	-	0.1101
47	H	0.0000	-	0.1232	-	0.1232
48	H	0.0000	-	0.1191	-	0.1191
49	H	0.0000	-	0.1210	-	0.1210
50	C	–0.2671	-	–0.0885	-	0.1786
51	N	–0.5457	-	–0.5755	-	–0.0298

[a]See Figs. 1 and 2 for numbering of atoms.

Table 4. Calculated and experimental vibrational characteristics (ν in cm^{-1}, A in $km \cdot mol^{-1}$) for the hydrogen-bonded complexes 1 and 2.

Mode	Exp. [23]		SCF/6-31G(d,p)				BLYP/6-31G(d,p)			
			Complex **1**		Complex **2**		Complex **1**		Complex **2**	
	ν/Δν	*A*/Δ*A*	ν/Δν	A/Δ*A*	ν/Δν	*A*/Δ*A*	ν/Δν	*A*/Δ*A*	ν/Δν	*A*/Δ*A*
$\nu(H_8–N_{15})$	-	-	3388/ –543	3597.0/ 3547.3	3611/ –320	2955.7/ 2906.0	2726/ –815	5491.1/ 5469.9	3101/ –440	3031.9/ 3010.7
$\nu(N_{23}–H_{25})$	-	-	3299/ –632	81.1/ 31.4	3513/ –418	381.8/ 332.1	2552/ –989	86.3/ 65.1	2975/ –566	513.1/ 491.9
$\nu(O_{38}–H_{45})$	3318/ –270	vs	-	-	3546/ –621	1128.7/ 1011.6	-	-	3010/ –432	1186.1/ 1138.8
$\nu(C_{13}\equiv N_{14})$	2204/ –36	s	2569/ –32	244.3/ 168.8	2581/ –20	201.2/ 126.1	2217/ –19	181.9/ 138.2	2225/ –11	158.3/ 114.5
$\nu(C_{50}\equiv N_{51})$	2204/ –36	s	-	-	2591/ –10	113.0/ 37.5	-	-	2228/ –8	87.2/ 43.5
$\nu(O_1…H_8)$			174	0.7	182	3.3	136	11.6	149	17.7
$\nu(O_1…H_{25})$			169	0.9	183	8.2	128	0.2	137	8.3
$\nu(O_1…H_{45})$			-	-	118	6.7	-	-	116	6.7

The shifts in the vibrational frequencies ($\Delta\nu_i$) upon formation of the hydrogen-bonded complexes **1** (TBD:4-CNPhOH (1:1)) and **2** (TBD:4-CNPhOH (1:2)) have been calculated by *ab initio* and DFT calculations with 6-31G(d,p) basis set. The predicted frequency shift for each vibration is:

$\Delta\nu_i = (\nu_i^{complex} - \nu_i^{monomer})$,

The changes in the infrared intensities (ΔA_i) upon hydrogen bond formation are also estimated using ab initio and DFT calculations.

$\Delta A_i = A_i^{complex} - A_i^{monomer}$

The predicted changes in the vibrational frequencies and infrared intensities for the modes more sensitive to the complexation are shown in Table 4 together with the experimentally observed [23] shifts.

The predicted vibrational spectra for the complexes of TBD with one and two 4-CNPhOH molecules by *ab initio* and DFT calculations demonstrate the ionic character of the forming hydrogen-bonded systems. In the vibrational spectra of the complexes two N–H stretching vibrations appear: $\nu(N_{23}–H_{25})$ and $\nu(N_{15}–H_8)$. The calculations show that these two vibrations are very sensitive to complexation: their vibrational frequencies are shifted to lower wavenumbers and their IR intensities dramatically increase in comparison with the corresponding values for the N–H stretching vibration in the non-hydrogen-bonded TBD molecule. This fact confirms the participation of the $N_{23}–H_{25}$ and $N_{15}–H_8$ bonds in the hydrogen bonding.

The predicted vibrational spectra for the hydrogen-bonded systems of TBD with two 4-CNPhOH molecules show that one 4-CNPhOH molecule takes part in the hydrogen bonding as non-ionic. The stretching $\nu(O_{38}–H_{45})$ vibration of the hydrogen-bonded O–H group is shifted to lower frequencies and its IR intensity increases considerably upon hydrogen bonding. This result is in agreement with the assumption of P. Przybyski *et al*. [23] for the formation of the $O^-…H^+$ hydrogen bonds with proton transfer, i.e. of the polar structure. The changes in the vibrational characteristics of the stretching $\nu(C\equiv N)$ vibrations confirm also the polar structures of the studied hydrogen-bonded systems. The vibrational frequencies of $\nu(C\equiv N)$ in the complexes are shifted to lower wavenumbers indicating that the electron density at the C≡N group is decreased due to the formation of $O^-…H^+$ hydrogen bonds. As can be seen from the results in Table 4, the predicted changes in the vibrational characteristics for the stretching $\nu(C\equiv N)$ vibrations are in a good agreement with the experimentally measured [23].

The hydrogen bonding between TBD and one 4-CNPhOH molecule (complex **1**) leads to arising of two stretching intermolecular vibrations: $\nu(O_1^-…H_8^+)$ and $\nu(O_1^-…H_{25}^+)$. The predicted frequencies for these vibrations are very near: 169–174 cm^{-1} (SCF/6-31G(d,p) calculations) and 136–128 cm^{-1} (BLYP/6-31G(d,p) calculations). The calculated IR intensities for these vibrations are low.

For the hydrogen-bonded system between TBD and two 4-CNPhOH molecules (complex **2**) three stretching intermolecular vibrations are predicted: $\nu(O_1^-…H_8^+)$, $\nu(O_1^-…H_{25}^+)$ and $\nu(O_1^-…H_{45})$. As well as for complex **1**, the predicted vibrational frequencies for the vibrations $\nu(O_1^-…H_8^+)$ and $\nu(O_1^-…H_{25}^+)$ are very near and their IR intensities are low. The $\nu(O_1^-…H_{45})$ vibration is calculated with lower frequency in comparison with the vibrations $\nu(O_1^-…H_8^+)$ and $\nu(O_1^-…H_{25}^+)$. This phenomenon could be explained with the charge rearrangement upon hydrogen bonding, namely that the hydrogen bond formations between TBD and 4-CNPhOH lead to more considerable charge rearrangement for the TBD molecule than for the 4-CNPhOH molecules.

CONCLUSSIONS

The main results in this study are:

- The calculated values of the dissociation energy for the hydrogen-bonded systems TBD: 4-CNPhOH (1:1 and 1:2) confirm their ionic structures.

- The changes of the atomic charges (Δq_i) upon hydrogen bonding show large proton polarizability of the hydrogen bonds within these complexes, i.e. hydrogen-bonded systems with ionic character are formed.

- *Ab initio* and DFT predicted vibrational spectra for the complexes of TBD with one and two 4-CNPhOH molecules demonstrate the ionic character of the formed hydrogen-bonded systems.

Acknowledgements: *The research is supported by the Bulgarian National Science Fund, contract X-1510. This financial support is gratefully acknowledged.*

REFERENCES

1. M. Szwarc, *Progr.Phys.Org.Chem.,* **6**, 323 (1968).
2. S. Arseniadis, K. S. Kyler, D. S. Watt, *Org. React.,* **31** (1984).
3. I. Juchnovski, I. Binev, in: The Chemistry of Functional Group, Suppl. C, Wiley, New York, 1983, Ch. 4.
4. I. Juchnovski, DSc. Thesis, Inst. Org. Chem., Bulg. Acad. Sci., Sofia, 1983.
5. I. Juchnovski, I. Binev, J. Kaneti, *Commun.Depart.*

Chem. Bulg. Acad. Sci., **10**, 554 (1977).
6. I. Juchnovski, J. S. Dimitrova, I. G. Binev, J. Kaneti, *Tetrahedron*, **34**, 779 (1978).
7. I. Juchnovski, J. S. Dimitrova, J. Kaneti, *Commun. Dept. Chem. Bulg. Sci.*, **12**, 97 (1979).
8. I. Juchnovski, J. S. Dimitrova, *C. R. Acad. Bulg. Sci.,* **31**, 547 (1978).
9. Y. Dimitrova, I. Juchnovski, *Spectrosc. Lett.,* **28**, 937 (1995).
10. Y. Binev, J. A. Tsenov, I. N. Juchnovski, I. G. Binev, *J. Mol. Struct.*, **625**, 207 (2003).
11. M. K. Georgieva, N. B. Nedelchev, I. N. Juchnovski, *Bulg. Chem. Commun.,* **37**, 235 (2005).
12. D. Hadzi, Theoretical Treatment of Hydrogen Bonding, John Wiley and Sons, New York, 1997.
13. Y. Dimitrova, *J. Mol. Struct. (Theochem),* **334,** 215 (1995).
14. Y. Dimitrova, *J. Mol. Struct. (Theochem),* **343**, 25 (1995).
15. M. C. Buzzeo, L. N. Zakharov, A. L. Rheingold, L. H. Doerrer, *J. Mol. Struct.,* **657**, 19 (2003).
16. J. P.Castaneda, G. S. Denisov, S. Yu. Kucherov, V. M. Scheiber, A. V. Shurukhina, *J. Mol. Struct.,* **660**, 25 (2003).
17. R. Maiti, K. Nagarajan, S. Sarkar, *J. Mol. Struct.,* **656**, 169 (2003).
18. K. Mierzwicki, Z. Latajka, *Chem. Phys.*, **265**, 301 (2001).
19. Y. Dimitrova, *J. Mol. Struct. (Theochem),* **455**, 9 (1998).
20. Y. Dimitrova, *Spectrochim. Acta, Part A,* **55**, 999 (1999).
21. Y. Dimitrova, *J. Mol. Struct. (Theochem),* **499**, 207 (2000).
22. Y. Dimitrova, *Spectrochim.Acta, Part A,* **60**, 3049 (2004).
23. P. Przybylski, G. Wojciechnowski, B. Brzezinski, G. Zundel, F. Bartl, *J. Mol. Struct.* **661-662,** 171 (2003).
24. G. Wojciechnowski, G, Schroeder, G. Zundel, B. Brzezinski, *J. Phys. Chem. A* **104,** 7469 (2000).
25. M. J. Frisch, G. W. Trucks, H. B. Schlegel, G. E. Scuseria, M. A. Robb, J. R. Cheeseman, J. A. Montgomery, Jr., T. Vreven, K. N. Kudin, J. C. Burant, J. M. Millam, S. S. Iyengar, J. Tomasi, V. Barone, B. Mennucci, M. Cossi, G. Scalmani, N. Rega, G. A. Petersson, H. Nakatsuji, M. Hada, M. Ehara, K. Toyota, R. Fukuda, J. Hasegawa, M. Ishida, T. Nakajima, Y. Honda, O. Kitao, H. Nakai, M. Klene, X. Li, J. E. Knox, H. P. Hratchian, J. B. Cross, C. Adamo, J. Jaramillo, R. Gomperts, R. E. Stratmann, O. Yazyev, A. J. Austin, R. Cammi, C. Pomelli, J. W. Ochterski, P. Y. Ayala, K. Morokuma, G. A. Voth, P. Salvador, J. J. Dannenberg, V. G. Zakrzewski, S. Dapprich, A. D. Daniels, M. C. Strain, O. Farkas, D. K. Malick, A. D. Rabuck, K. Raghavachari, J. B. Foresman, J. V. Ortiz, Q. Cui, A. G. Baboul, S. Clifford, J. Cioslowski, B. B. Stefanov, G. Liu, A. Liashenko, P. Piskorz, I. Komaromi, R. L. Martin, D. J. Fox, T. Keith, M. A. Al-Laham, C. Y. Peng, A. Nanayakkara, M. Challacombe, P. M. W. Gill, B. Johnson, W. Chen, M. W. Wong, C. Gonzalez, J. A. Pople, Gaussian 03, Revision B.04, Gaussian, Inc., Pittsburgh PA, 2003.
26. R. G. Parr, W. Yang, Density-Functional Theory of Atoms and Molecules, Oxford University Press, Oxford, 1989.
27. R. G. Parr, W. Yang, *Annu. Rev. Phys. Chem.,* **46**, 701 (1995).
28. J. K. Labanowski, J. W. Andzelm, Density Functional Methods in Chemistry, Springer, Berlin, 1991.
29. P. Schuster (Ed.), Hydrogen Bonds, Topics in Current Chemistry, Vol. 120, Springer, Berlin, 1984.
30. G. A.Jeffrey, W. Saenger, Hydrogen Bonding in Biological Structures, Springer, Berlin, 1991.
31. R. Ludwig, F. Weinhold, T.C. Farrar, *J. Chem. Phys.,* **102**, 5118 (1995).
32. M. C. Holthausen, C. Heinemann, H. H. Cornehl, W. Koch, H. Schwartz, *J. Chem. Phys.,* **102**, 4931 (1995).
33. A. D. Becke, *J. Chem. Phys.,* **98**, 5648 (1993).
34. T. Bürgi, M., Schütz, S. Leutwyler, *J. Chem. Phys.,* **103**, 6350 (1995).
35. M. Gerhards, K. Kleinermanns, *J. Chem. Phys.,* **103**, 7392 (1995).
36. Ch. Jacoby, W. Roth, M. Schmitt, Ch. Janzen, D. Spangenberg, K. Kleinermanns, *J. Phys. Chem. A,* **102**, 4471 (1998).
37. D. Hadzi, Theoretical Treatment of Hydrogen Bonding, John Wiley and Sons, New York, 1997.
38. J. E. Del Bene, M. J. T. Jordan, *Intern. Rev. Phys. Chem*., **18**, 119 (1999).
39. J. Smets, W. McCarthy, G. Maes, L. Adamowicz, *J. Mol. Struct*., **476**, 27 (1999).
40. Y. Dimitrova, *Recent Res. Dev. Phys. Chem*., **3**, 133 (1999).
41. Y. Dimitrova, *Recent Res. Dev. Phys. Chem*., **6**, 127 (2002).
42. Y. Dimitrova, *Spectrochim. Acta, Part A,* **60**, 2457 (2004).
43. Y. Dimitrova, *Spectrochim. Acta, Part A,* **60**, 3049 (2004).
44. T. Hirano, T. Taketsugu, Y. Kurita, *J. Phys. Chem*., **98**, 6936 (1994).

ВОДОРОДНО СВЪРЗВАНЕ В ЙОННИ СИСТЕМИ НА 1,5,7-ТРИАЗАБИЦИКЛО[4.4.0]ДЕЦ-5-ЕН С 4-ЦИАНОФЕНОЛ. ИЗСЛЕДВАНИЯ НА СТРУКТУРИТЕ ИМ С МЕТОДИТЕ *AB INITIO* И ТФП

Й. Димитрова

Лаборатория „Структурен органичен анализ“, Институт по органична химия с център по фитохимия, Българска академия на науките, ул. „Акад. Г. Бончев“ бл. 9, 1113 София

Посветена на акад. Иван Юхновски по повод на 70-та му годишнина

Постъпила на 11 декември 2007 г.; Преработена на 14 януари 2008 г.

(Резюме)

Изследвани са структурите на водородно-свързаните системи на 1,5,7-триазабицикло[4.4.0]дец-5-ен (ТБД) с една и две молекули 4-цианофенол посредством *ab initio* и ТФП пресмятания с различни базисни набори. Пресмятанията показват, че оптимизираните структури на изследваните системи са циклични. Изчислените стойности на енергията на свързване и промените в атомните заряди под действие на водородното свързване за изследваните водородно-свързани системи потвърждават техните йонни структури. Водородното свързване на ТБД с една и две молекули 4-цианофенол води до промени в структурните (дължини на връзки и ъгли) и вибрационните (вибрационни честоти и интензивности на инфрачервените ивици) характеристики на мономерите. Установено е, че молекулата на ТБД е значително деформирана под действие на водородното свързване, докато деформацията на молекулите на 4-цианофенола е по-малка. Предсказаните с *ab initio* и ТФП вибрационни спектри за комплексите ТБД: 4-цианофенол (1:1 и 1:2) доказват йонния характер на образуваните водородно-свързани системи.

Bulgarian Chemical Communications, Volume 40, Number 3 (pp. 426– 432) 2008

Theoretical study of structures and stability of hydrogen-bonded systems between pyridine-3-carboxamide (nicotinamide) and DMSO

L. I. Daskalova, Y. Dimitrova*

Department of Structural Organic Analysis, Institute of Organic Chemistry with Centre of Phytochemistry, Bulgarian Academy of Sciences, Acad. G. Bonchev St., Block 9, 1113, Sofia, Bulgaria

Dedicated to Academician Ivan Juchnovski on the occasion of his 70th birthday

Received December 11, 2007; Revised January 16, 2008

The structures and stability of hydrogen-bonded complexes between nicotinamide and DMSO are studied by *ab initio* and DFT calculations at various basis sets. Full geometry optimization was made of the complexes studied. According to the energy analysis, the complex between (Z)-nicotinamide and two molecules DMSO is more stable by 1.91–2.68 kcal·mol^{-1} than the complex, formed between (E)-nicotinamide and two molecules DMSO. This result is in agreement with their coexistence, found experimentally. The changes in the geometrical parameters and charge distribution of the monomers upon hydrogen bonding have been studied.

Key words: hydrogen-bonded nicotinamide-DMSO complexes, *ab initio*, DFT.

INTRODUCTION

Hydrogen bonds constitute an area of research that is a typical interdisciplinary field concerning physicist as well as chemists and biologists. The structure and dynamics of the hydrogen-bonded complexes has become of greater and greater interest to chemists in a variety of fields. The elucidation of the structure and energetics of the hydrogen-bonded complexes pertains to the understanding of intermolecular interactions and a concerted application of experimental and theoretical methods can be used to obtain a clear picture of hydrogen-bonded structures [1–5].

Pyridine-3-carboxamide (nicotinamide) is known as a component of the vitamin B complex as well as a component of a coenzyme, nicotinamide adenine dinucleotide. Vitamin B_3 plays a crucial role in biological oxidative chemistry. Therefore, the structure of nicotinamide has been the subject of many experimental [6–8] and theoretical studies [7–11]. The amide group in nicotinamide can adopt a variety of tautomeric and rotameric structures in addition to forming interesting molecular associations *via* hydrogen bonding [12].

In a recent study [10] the solvent effects of DMSO on the vibrational spectrum of nicotinamide have been estimated on the basis of spectroscopic measurements. The authors [10] suppose the formation of hydrogen bonds between nicotinamide and DMSO. In this connection, the objects of the present study are the hydrogen-bonded complexes formed between nicotinamide and DMSO. The aim of the study is to establish the most stable structures of the hydrogen-bonded complexes and to estimate the influence of the hydrogen bonding on the structural parameters and charge distribution in the monomers using *ab initio* and DFT calculations at various basis sets.

METHODS

The structural and geometrical features of the hydrogen-bonded complexes of nicotinamide with DMSO were studied by *ab initio* and DFT calculations with various basis sets: 6-31G(d,p), 6-31+G(d,p), 6-311++G(d,p) using GAMMESS software [13] and CAUSSIAN 98 series of programs [14]. The density functional calculations were carried out in the framework of the Kohn-Sham density functional theory [15] with Becke exchange functional coupled with the Lee-Yang-Parr correlation [16].

RESULTS AND DISCUSSION

Dissociation energy

As is noted in previous studies [7–10], the nicotinamide molecule can exist in two conformers: NA(Z) and NA(E) (See Fig. 1). The conformational population in nicotinic acid derivatives was studied by Kuthan *et al*. [9] *via* dipole moment measurements in benzene solution together with theoretical moments of their CNDO/2 models, following earlier measurements of Purcell and co-workers [17, 18].

* To whom all correspondence should be sent:
E-mail: dimj@orgchm.bas.bg

© 2008 Bulgarian Academy of Sciences, Union of Chemists in Bulgaria

By means of microwave spectroscopy Vogelsanger *et al*. [7] detected both the NA(E) and NA(Z) conformer of nicotinamide in the gas-phase and found that (E)-conformer is more stable than (Z)-conformer. The calculated *ab initio* and DFT energy difference between the molecular conformers NA(E) and NA(Z) of 2.92–4.14 kJ·mol^{-1} is low and this results is in agreement with their coexistence, found experimentally [10]. NA(E) was found to be prevalent in solutions [9, 17], in the gas-phase [7], and the conformation in the monocrystal is firmly NA(E) [6].

The complexation between NA(Z) nicotinamide and two molecules DMSO leads to the formation of complex **1**, and the hydrogen bonded systems between NA(E) nicotinamide and two molecules DMSO is marked as complex **2** (see Fig. 2).

Full geometry optimization has been performed for the complexes studied by *ab initio* and DFT (BLYP) calculations with various basis sets: 6-31G(d,p), 6-31+G(d,p) and 6-311++G(d,p) using the GAUSSIAN 98 series of programs [14]. In Fig. 2 are shown the optimized structures of complexes **1** and **2** with BLYP/6-311++G(d,p) calculations. As can be seen, the hydrogen bonding between (E)-nicotinamide and two DMSO molecules leads to the formation of a fully cyclic structure (complex **2**), while the hydrogen-bonded system between (Z)-nicotinamide and two DMSO molecules (complex **1**) is open with one DMSO molecule.

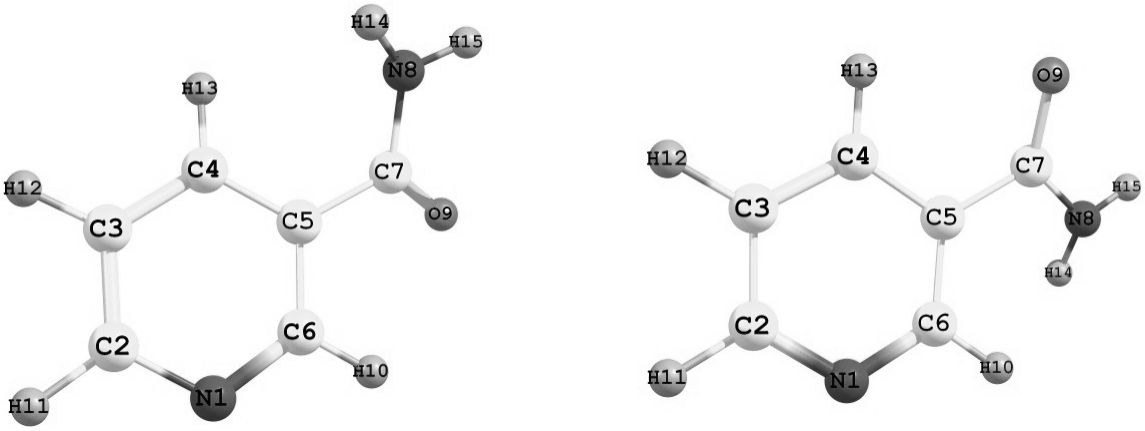

NA(Z) NA(E)

Fig. 1. Optimized by BLYP/6-311++G(d,p) calculations structures of the conformers of nicotinamide molecule.

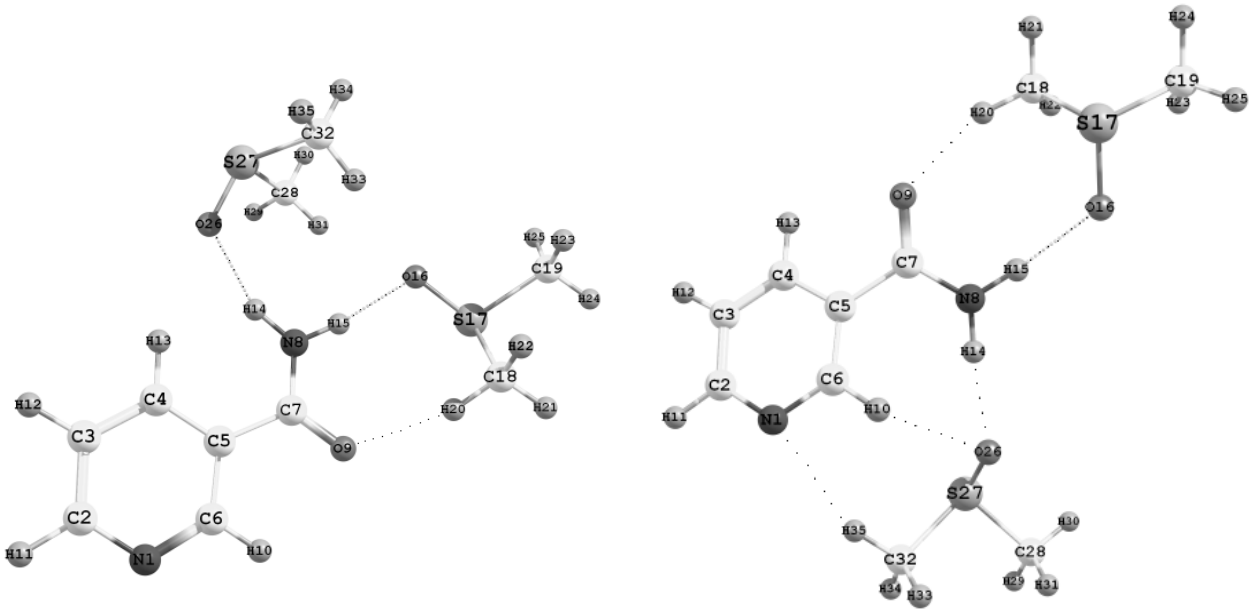

Complex **1** Complex **2**

Fig. 2. Optimized structures by BLYP/6-311++G(d,p) calculations for the hydrogen-bonded: (Z)-nicotinamide with two molecules DMSO (complex **1**); (E)-nicotinamide with two molecules DMSO (complex **2**).

The dissociation energy is used for estimation of the stability of hydrogen-bonded systems between two and more partners. The supramolecular variation method determines dissociation energy (ΔE) as a difference between the energy of the complex and the energies of the isolated molecules.

$$\Delta E = E_{\text{com.}} - (E_1 + E_2 + E_3\ldots) \quad (1)$$

where E_1, E_2, $E_3\ldots$ are the energies of the isolated monomers in their own basis set and $E_{\text{com.}}$ is the energy of the complex.

The supramolecular approach is theoretically able to provide dissociation energy at any accuracy, however, only if a sufficiently large basis set and a sufficiently high level of correlation are used. For the exact determination of the interaction energy in the supramolecular approach the consideration of zero-point energies is very important.

The zero-point vibrational energy correction for the studied complexes can be defined as a difference between the calculated zero-point vibrational energy of the complex and the zero-point energies of the monomers:

$$\Delta E_{\text{zp vib}} = E_{\text{zp vib.}}(\text{com.}) - (E_{\text{zp vib}}(1) + E_{\text{zp vib}}(2) + E_{\text{zp vib}}(3)\ldots) \quad (2)$$

The dissociation energies, uncorrected and corrected with zero-point energy differences are calculated by *ab initio* and DFT calculations with different basis sets. The results from the calculations are presented in Table 1.

As can be seen from the data of ΔE (uncorrected and corrected with ΔE(zp vib), the calculated values of the dissociation energy with *ab initio* SCF and DFT (BLYP) calculations at 6-31G(d,p) basis set are very close, while the calculated values with BLYP calculations with larger basis sets, including s and p diffuse functions (6-31+G(d,p) and 6-311++G(d,p)), are smaller by about 20%.

The following comments can be made on the basis of the corresponding energy values:

a). According to all calculation performed, complex **1** is by 1.91–2.68 kcal·mol^{-1} more stable than complex **2**.

b). The calculated energy difference between the complexes is very small. This result is in agreement with their coexistence, found experimentally.

In Table 1 are presented also the optimised values of the hydrogen bonds formed between (Z)-nicotinamide and two molecules DMSO (complex **1**) and (E)-nicotinamide and two DMSO molecules (complex **2**). For complex **1** the calculated values of the $O_{16}\ldots H_{15}$ is much longer than for complex **2**. On the contrary, the hydrogen bond $O_{26}\ldots H_{14}$ for complex **1** is shorter than in complex **2**. In complex **2** this hydrogen bond is bifurcated and involves also H_{10}. Bearing in mind the optimized values of the hydrogen bonds of the complexes, it could be concluded that the hydrogen bond $O_{26}\ldots H_{14}$ in complex **1** is the strongest. The optimized values of the hydrogen bonds show that complex **1**, with stronger hydrogen bonds, is more stable than complex **2**.

Changes in geometrical parameters upon hydrogen bonding

The optimized geometrical parameters by BLYP/6-311++G(d,p) calculations for the both complexes, as well as for the monomers are presented in Tables 2 and 3. In order to estimate the accuracy of the calculations, the optimized geometrical parameters of the monomers are compared with the available experimental data [6–8]. In this case, as well as in the previous studies [5, 20–23] is observed a good agreement between experimental and DFT calculated geometrical parameters. The crystal structure determined by X-ray and neutron diffraction [6] shows that nicotinamide takes a non-planar (E)-form, in which the dihedral angle $C_6C_5C_7N_8$ is 22º. In the crystal of nicotinamide adenine dinucleotide (NAD) the conformation of the nicotinamide is similar to that of (E)-nicotinamide [24, 25]. In the study of Vogelsanger *at al*. [7] the dihedral angle $C_6C_5C_7N_8$ of the (E) and (Z) conformers was estimated to be 14(2)º and 158(2)º, respectively. Our calculations at BLYP/6-311++G(d,p) gave essentially the same values: 21º (E-form) and 156º (Z-form). By complexation the non planar (Z)-nicotinamide converts into a planar complex **1**: the dihedral angle $C_6C_5C_7N_8$ is 173º. For complex **2** this angle takes nearly the same value *via* non bonded nicotinamide: 24º (Tables 2 and 3).

Our aim is to estimate the influence of hydrogen bonding on the structural parameters of nicotinamide (Z and E) and DMSO. For this aim, the changes in the geometrical parameters from monomers to a complex are defined. It is seen from the results in Tables 2 and 3 that the optimized values of the bond lengths and angles for complex **1** and complex **2** are slightly perturbed from their values in the monomers. The calculated changes (Δ) in the structural parameters show that the formation of the hydrogen-bonded systems results in changes in the bond lengths and angles. These changes concern the atomic groups taking part directly in the formation of hydrogen bonds or situated in immediate vicinity to them. Upon formation of hydrogen bonds, the bonds: N_8H_{14}, N_8H_{15} and $O_{26}S_{27}$ are lengthened in the complexes. The bond lengths of the adjacent atomic groups are shortened.

Table 1. Dissociation energies ΔE (uncorrected and corrected), zero-point vibrational energy differences ΔE_{zpve} in kcal/mol and intermolecular distances in Å for the hydrogen-bonded complexes between DMSO and nicotinamide.

Complex [a]	Basis set	$\Delta E_{uncorr.}$	ΔE_{zpve}	ΔE_{corr}	R $O_{16}\ldots H_{15}$	R $O_{26}\ldots H_{14}$	R $O_{26}\ldots H_{10}$	R $O_{9}\ldots H_{20}$	R $N_{1}\ldots H_{35}$
Complex **1**	HF/6-31G(d,p)	–22.32	2.27	–20.05	2.035	1.998	-	2.328	-
	BLYP/6-31G(d,p)	–23.66	2.40	–21.25	1.985	1.924	-	2.184	-
	BLYP/6-31+G(d,p)	–17.12	2.05	–15.06	2.001	1.953	-	2.242	-
	BLYP/6-311++G(d,p)	–18.09	2.09	–16.00	1.982	1.943	-	2.240	-
Complex **2**	HF/6-31G(d,p)	–19.46	2.09	–17.37	2.015	2.071	2.464	2.378	2.817
	BLYP/6-31G(d,p)	–20.87	2.28	–18.59	1.932	2.020	2.414	2.287	2.534
	BLYP/6-31+G(d,p)	–15.38	2.14	–13.24	1.968	2.025	2.527	2.309	2.657
	BLYP/6-311++G(d,p)	–16.36	2.27	–14.09	1.945	1.998	2.461	2.293	2.693

a - For the structures see Fig. 2.

Table 2. Calculated geometries for free and complexed nicotinamide NA(Z) and DMSO (1:2) by DFT (BLYP/6-311++G(d,p)) calculations.

Parameter [a]	Monomers		Complex **1**	Δ^h Change of the parameters
	Experiment	BLYP/6-311++G(d,p)	BLYP/6-311++G(d,p)	BLYP/6-311++G(d,p)
Bond lengths [b]				
N_1C_2	1.330 [d]	1.351	1.350	0.001
N_1C_6	1.328 [d]	1.346	1.348	0.002
C_2C_3	1.402 [d]	1.403	1.401	–0.002
C_3C_4	1.400 [d]	1.401	1.403	0.002
C_4C_5	1.404 [d]	1.408	1.409	0.001
C_5C_6	1.407 [d]	1.412	1.412	0.000
C_5C_7	1.497 [d]	1.511	1.517	0.006
C_7O_9	1.216 [d]	1.233	1.249	0.016
C_7N_8	1.366 [d]	1.387	1.359	–0.028
N_8H_{14}	1.022 [d]	1.015	1.025	0.010
N_8H_{15}	1.022 [d]	1.017	1.025	0.008
$O_{16}S_{17}$	1.531(5) [e]	1.534	1.555	0.021
$S_{17}C_{18}$	1.775(8) [e]	1.872	1.856	–0.016
$S_{17}C_{19}$	1.821(11) [e]	1.872	1.861	–0.011
$C_{18}H_{20}$	1.531(5) [e]	1.096	1.100	0.004
$O_{26}S_{27}$	1.775(8) [e]	1.534	1.547	0.013
$S_{27}C_{28}$	1.821(11) [e]	1.872	1.866	–0.006
$S_{27}C_{32}$	1.531(5) [e]	1.872	1.866	–0.004
Angle [c]				
$H_{14}N_8H_{15}$	-	116.97	116.06	–0.91
$H_{14}N_8C_7$	121.3(21) [d]	121.14	125.48	4.34
$H_{15}N_8C_7$	118.5(21) [d]	116.08	118.31	2.23
$N_8C_7O_9$	123.1 [d]	121.94	122.33	0.39
$C_7C_5C_4$	117.1 [d]	124.04	124.47	0.43
D $C_6C_5C_7N_8$	**158.0** [g]	**156.14**	**172.58**	**16.44**
$O_{26}S_{27}C_{28}$	106.7(40) [e]	107.10	107.24	0.14
$C_{28}S_{27}C_{32}$	97.4(40) [e]	96.02	96.39	0.37
$O_{16}S_{17}C_{18}$	106.7(40) [e]	107.10	106.70	–0.40
$C_{18}S_{17}C_{19}$	97.4(40) [e]	96.02	97.58	1.56

a - See Figs. 1 and 2, for numbering of atoms; b - In Å; c - In degree; d - Ref. [8]; e - Ref. [19]; f - Ref. [6]; g - Ref. [7];
Δ^h = parameter^{complex} – parameter^{monomer}

The changes in the angles from monomers to a complex are also estimated. The data in Tables 2 and 3 show that in complexes **1** and **2** the angles taking part in the hydrogen bonding are the most sensitive to complexation. The angles $H_{14}N_8C_7$, $H_{15}N_8C_7$, $N_8C_7O_9$ and $C_7C_5C_4$ from nicotinamide in complexes **1** and **2** become larger in comparison with their values in the monomer. The angles $C_{28}S_{27}C_{32}$ and $C_{18}S_{17}C_{19}$ from DMSO are also sensitive to complexation. Their values in the complexes are also larger in comparison with the monomer values. The dihedral angle $C_6C_5C_7N_8$ is the most sensitive to complexation. Its value in complex **1** changes by 16.4º and in the complex **2** by 3.2º. The remaining geometrical parameters of the monomers (nicotinamide and DMSO) in complexes **1** and **2** are either unchanged or changed slightly upon formation of hydrogen bonds. The results from the calculations show that the changes in the angles for complex **1** are more substantial than for the complex **2** (See Tables 2 and 3).

Table 3. Calculated and experimental geometries for free and complexed nicotinamide NA(E) and DMSO (1:2) by DFT (BLYP/6-311++G(d,p)) calculations.

Parameter [a]	Monomers		Complex **2**	Δ^h Change of the parameters
	Experiment	BLYP/6-311++G(d,p)	BLYP/6-311++G(d,p)	BLYP/6-311++G(d,p)
Bond lengths [b]				
N_1C_2	1.328 [d]	1.349	1.350	0.001
N_1C_6	1.328(6) [d]	1.348	1.351	0.004
C_2C_3	1.404 [d]	1.405	1.404	–0.001
C_3C_4	1.397 [d]	1.398	1.399	0.002
C_4C_5	1.404 [d]	1.408	1.406	–0.001
C_5C_6	1.406(4) [d]	1.410	1.409	–0.002
C_5C_7	1.498(8) [d]	1.513	1.520	0.007
C_6H_{10}	1.074 [f]	1.094	1.090	–0.004
C_7O_9	1.216(5) [d]	1.234	1.248	0.015
C_7N_8	1.362(12) [d]	1.383	1.359	–0.024
N_8H_{14}	1.022 [d]	1.015	1.024	0.010
N_8H_{15}	1.022 [d]	1.017	1.030	0.013
$O_{16}S_{17}$	1.531(5) [e]	1.534	1.547	0.013
$S_{17}C_{18}$	1.775(8) [e]	1.872	1.859	–0.013
$S_{17}C_{19}$	1.821(11) [e]	1.872	1.864	–0.008
$C_{18}H_{20}$	1.09 [e]	1.096	1.097	0.001
$O_{26}S_{27}$	1.531(5) [e]	1.534	1.546	0.012
$S_{27}C_{28}$	1.775(8) [e]	1.872	1.863	–0.009
$S_{27}C_{32}$	1.821(11) [e]	1.872	1.863	–0.009
Angle [c]				
$H_{14}N_8H_{15}$	-	117.55	118.36	0.81
$H_{14}N_8C_7$	121.3(21) [f]	121.85	123.25	1.40
$H_{15}N_8C_7$	118.5(21) [f]	116.59	118.13	1.54
$N_8C_7O_9$	123.1 [d]	121.91	123.51	1.60
$C_7C_5C_4$	117.0 [d]	118.36	118.97	0.62
D $C_6C_5C_7N_8$	**14.0 [g]**	**20.64**	**23.79**	**3.15**
$O_{26}S_{27}C_{28}$	106.7(40) [e]	107.10	105.78	–1.32
$C_{28}S_{27}C_{32}$	97.4(40) [e]	96.02	97.13	1.11
$O_{16}S_{17}C_{18}$	106.7(40) [e]	107.10	106.87	–0.23
$C_{18}S_{17}C_{19}$	97.4(40) [e]	96.02	97.36	1.34

a - See Figs. 1 and 2, for numbering of atoms; b - In angstroms; c - In degree; d - Ref. [8]; e - Ref. [19]; f - Ref. [6]; g - Ref. [7]; Δ^h = parameter^{complex} – parameter^{monomer}.

Charge distribution

It is known from our previous studies [20–23] that the hydrogen bonding leads to charge rearrangement in the monomers forming a complex. Our aim was to determine the influence of hydrogen bonding on charge distribution in the studied hydrogen-bonded complexes between nicotinamide and DMSO, shown in Figure 2 (complex **1** and complex **2)**. In this connection, the atomic charges (q_i) for the monomers (nicotinamide and DMSO) and for the both complexes have been calculated by BLYP/6-311++G(d,p) calculations, using the Mulliken population analyses. The data are shown in Tables 4 and 5. In these tables are also included the changes of the atomic charges (Δq_i) upon hydrogen bonding: $\Delta q_i = q_i^{complex} - q_i^{monomer}$.

It was established that the most sensitive to complexation are the atoms, taking part in hydrogen bonding. In the complexes studied the atoms S_{17}, S_{27}, C_6, C_7 and N_8 act as acceptors of electric charge. The negativity of these atoms increases significantly in the complexes in comparison with the corresponding negativity in the monomers. At the same time, the carbon atoms C_4 and C_5 and the hydrogen atoms H_{14} and H_{15} become more positive in the complexes. The results from the calculations show that the changes in the charges (Δq_i) of the atoms taking part in hydrogen bonding depend on the strength of the hydrogen bonds. As can be seen from the results for Δq_i in Tables 4 and 5, the hydrogen bond formation between nicotinamide and DMSO lead to charge rearrangements of the monomers.

Table 4. Mulliken charges (q_i)) for free and complexed nicotinamide NA(Z) and DMSO (1:2) obtained by BLYP/6-31++G(d,p) calculations.

No	Atom [a]	Monomers	Complex **1**	Δq_i [b]
1	N	–0.018	–0.021	–0.003
2	C	–0.349	–0.326	0.022
3	C	–0.016	–0.208	–0.192
4	C	–0.163	–0.018	0.145
5	C	0.842	1.493	0.651
6	C	–0.497	–0.509	–0.012
7	C	–0.409	–1.218	–0.810
8	N	–0.303	–0.417	–0.113
9	O	–0.293	–0.327	–0.033
10	H	0.211	0.206	–0.005
11	H	0.166	0.165	–0.001
12	H	0.163	0.172	0.009
13	H	0.155	0.207	0.052
14	H	0.212	0.340	0.129
15	H	0.299	0.336	0.038
16	O	–0.446	–0.405	0.041
17	S	0.531	0.408	–0.123
18	C	–0.535	–0.522	0.013
19	C	–0.535	–0.425	0.109
20	H	0.178	0.216	0.038
21	H	0.130	0.143	0.014
22	H	0.184	0.175	–0.010
23	H	0.184	0.173	–0.011
24	H	0.130	0.144	0.015
25	H	0.178	0.174	–0.004
26	O	–0.446	–0.393	0.053
27	S	0.531	0.366	–0.165
28	C	–0.535	–0.512	0.023
29	H	0.178	0.182	0.004
30	H	0.130	0.141	0.011
31	H	0.184	0.224	0.040
32	C	–0.535	–0.541	–0.006
33	H	0.183	0.264	0.081
34	H	0.130	0.140	0.010
35	H	0.178	0.174	–0.004

a - See Figs. 1 and 2, for numbering of atoms;
b - $\Delta q_i = q_i^{complex} - q_i^{monomer}$.

Table 5. Mulliken charges (q_i) for free and complexed nicotinamide NA(E) and DMSO (1:2) obtained by BLYP/6-31++G(d,p) calculations

No	Atom [a]	Monomers	Complex **2**	Δq_i [b]
1	N	–0.017	0.051	0.067
2	C	–0.339	–0.147	0.192
3	C	–0.057	–0.171	–0.114
4	C	–0.015	0.136	0.151
5	C	0.839	1.625	0.786
6	C	–0.654	–1.556	–0.902
7	C	–0.356	–0.683	–0.326
8	N	–0.298	–0.491	–0.193
9	O	–0.304	–0.350	–0.046
10	H	0.152	0.166	0.014
11	H	0.169	0.168	–0.001
12	H	0.167	0.180	0.013
13	H	0.201	0.214	0.014
14	H	0.220	0.337	0.117
15	H	0.295	0.473	0.178
16	O	–0.446	–0.454	–0.008
17	S	0.531	0.492	–0.039
18	C	–0.535	–0.574	–0.039
19	C	–0.535	–0.453	0.081
20	H	0.178	0.228	0.050
21	H	0.130	0.134	0.004
22	H	0.184	0.181	–0.004
23	H	0.178	0.168	–0.010
24	H	0.130	0.134	0.005
25	H	0.184	0.181	–0.003
26	O	–0.446	–0.477	–0.031
27	S	0.531	0.509	–0.022
28	C	–0.535	–0.482	0.053
29	H	0.178	0.177	–0.001
30	H	0.130	0.141	0.011
31	H	0.184	0.183	–0.001
32	C	–0.535	–0.533	0.002
33	H	0.184	0.182	–0.002
34	H	0.130	0.133	0.003
35	H	0.178	0.180	0.002

a - See Figs. 1 and 2, for numbering of atoms;
b - $\Delta q_i = q_i^{complex} - q_i^{monomer}$.

CONCLUSION

In the present study the structures and stability of the hydrogen-bonded complexes between nicotinamide and DMSO have been investigated using *ab initio* and DFT calculations. The main results of the study are:

1. The hydrogen bonding between (E)-nicotinamide and two DMSO molecules leads to the formation of a cyclic structure (complex **2**), while the hydrogen-bonded system between (Z)-nicotinamide and two DMSO molecules (complex **1**) is open with one DMSO molecule.

2. According to the calculated values of the dissociation energy, complex **1** is more stable than complex **2** by 1.91–2.68 kcal·mol^{-1}

3. The calculated changes (Δ) in the structural parameters show that the formation of the hydrogen-bonded systems results in changes in the bond lengths and angles. These changes concern the atomic groups taking part directly in the formation of the hydrogen bonds or situated in immediate vicinity to them. The most sensitive to complexation is the dihedral angle $C_6C_5C_7N_8$. Its value in complex **1** changes by 16.4º and in complex **2** by 3.2º.

4. In the studied complexes, the atoms S_{17}, S_{27}, C_6, C_7 and N_8 act as acceptors of electric charge. The negativity of these atoms increases significantly in the complexes in comparison with the corresponding negativity in the monomers. At the same time, the carbon atoms C_4 and C_5 and the hydrogen atoms H_{14} and H_{15} become more positive in the complexes.

Acknowledgements: *The financial support by the Bulgarian National Science Fund under contract X-1510 is gratefully acknowledged.*

REFERENCES

1. J. Blair, *Chem. Phys. Lett*., **154**, 531 (1989).
2. D. Hadzi, Theoretical treatment of hydrogen bonding, John Wiley and Sons, England, 1997.
3. J. E. Del Bene, I. Shavitt, Intermolecular interaction: From van der Waals to strongly bound complexes, S. Scheiner (ed.), Wiley, Chichester, West Sussex, 1997, p. 157–179.
4. Y. Dimitrova, *Rec. Res. Dev. Phys. Chem*., **3**, 133 (1999).
5. Y. Dimitrova, *Rec. Res. Dev. Phys. Chem*., **6**, 127 (2002).
6. Y. Miwa, T. Mizuno, K. Tsuchido, T. Taga, I. Iwata, *Acta Cryst. Part B*, **55**, 78 (1999).
7. B. Vogelsanger, R. D. Brown, P. D. Godfrey, A. P. Pierlot, *J. Mol. Spectrosc*., **145**, 1 (1991).
8. T. Takeshima, H. Takeushi, T. Eguawa, S. Konaka, *J. Mol. Struct*., **644**, 197 (2003).
9. J. Kuthan, L. Musil, V. Jehlicka, *Coll. Czechoslov. Chem. Commun*., **42**, 283 (1977).
10. E. A. Velcheva, L. I. Daskalova, I. G. Binev, *Bulg. Chem. Commun*., **36**, 230 (2004).
11. E. A. Velcheva, L. I. Daskalova, *J. Mol. Struct.,* **741**, 85 (2005).
12. R. A. Olsen, L. Liu, N. Ghaderi, A. Johns, M. Hatcher, L. J. Mueller, *J. Am. Chem. Soc*., **125**, 10125 (2003).
13. M. W. Schmidt, K. K. Baldridge, J. A. Boatz, S. T. Elbert, M. S. Gordon, J. H. Jensen, S. Koseki, N. Matsunaga, K. A. Nguyen, S. J. Su, T. L. Windus, M. Dupuis, J. A. Montgomery, *J. Comput. Chem*., **14**, 1347 (1993).
14. M. J. Frisch, G. W. Trucks, H. B. Schlegel, G. E. Scuseria, M. A. Robb, J. R. Cheeseman, V. G. Zakrzewski, J. A. Montgomery, Jr., R. E. Stratmann, J. C. Burant, S. Dapprich, J. M. Millam, A. D. Daniels, K. N. Kudin, M. C. Strain, O. Farkas, J. Tomasi, V. Barone, M. Cossi, R. Cammi, B. Mennucci, C. Pomelli, C. Adamo, S. Clifford, J. Ochterski, G. A. Petersson, P. Y. Ayala, Q. Cui, K. Morokuma, D. K. Malick, A. D. Rabuck, K. Raghavachari, J. B. Foresman, J. Cioslowski, J. V. Ortiz, A. G. Baboul, B. B. Stefanov, G. Liu, A. Liashenko, P. Piskorz, I. Komaromi, R. Gomperts, R. L. Martin, D. J. Fox, T. Keith, M. A. Al-Laham, C. Y. Peng, A. Nanayakkara, C. Gonzalez, M. Challacombe, P. M. W. Gill, B. Johnson, W. Chen, M. W. Wong, J. L. Andres, M. Head-Gordon, E. S. Replogle and J. A. Pople, Gaussian 98, Revision A.7, Gaussian Inc., Pittsburgh, PA (1998).
15. W. Kohn, L. Sham, *J. Phys. Rev. A*, **140**, 1133 (1965).
16. A. D. Becke, *J. Chem. Phys*., **104**, 1040 (1996).
17. W. P. Purcell., J. A. Singer, *J. Phys. Chem*., **69**, 4097 (1965).
18. W. P. Purcell, *J. Phys. Chem*., **68**, 2666 (1964).
19. R. Thomas. C. Shoemaker, K. Eriks, *Acta Cryst*., **21**, 12 (1966).
20. Y. Dimitrova, *J. Mol. Struct. (Theochem),* **532**, 41 (2000).
21. Y. Dimitrova, L. I. Daskalova, *J. Mol. Struct. (Theochem),* **756**, 73 (2005).
22. Y. Dimitrova, J. A. Tsenov, *Spectrochim. Acta, Part A,* **68**, 454 (2007).
23. Y. Dimitrova, L. I. Daskalova, *J. Mol. Struct*., *(Theochem),* **823**, 65 (2007).
24. B. Gillot, C. Lecomte, A. Cousson, C. Schert, C. Jelsch, *Acta Crystallogr. C*, **56**, 726 (2000).
25. B. Gillot, C. Lecomte, A. Cousson, C. Schert, C. Jelsch, *Acta Crystallogr. D*, **57**, 981 (2001).

ТЕОРЕТИЧНО ИЗСЛЕДВАНЕ НА СТРУКТУРИ И СТАБИЛНОСТ НА ВОДОРОДНО-СВЪРЗАНИ СИСТЕМИ МЕЖДУ ПИРИДИН-3-КАРБОКСАМИД (НИКОТИНАМИД) И ДМСО

Л. Ив. Даскалова, Й. Димитрова*

Лаборатория „Структурен органичен анализ“, Институт по органична химия с център по фитохимия, Българска академия на науките, ул. „Акад. Г. Бончев“ бл. 9, 1113 София

Посветена на акад. Иван Юхновски по повод на 70-та му годишнина

Постъпила на 11 декември 2007 г.; Преработена на 16 януари 2008 г.

(Резюме)

Структурата и стабилността на водородно-свързаните комплекси между никотинамида и ДМСО са изследвани посредством *ab initio* и ТФП пресмятания с различни базисни набори. Съгласно анализа на енергиите на свързване комплексът между (Z)-никотинамида и две молекули ДМСО е по-стабилен с 1.91–2.68 kcal·mol^{-1} от комплекса, образуван между (E)-никотинамида и ДМСО. Този резултат е в съгласие с експериментално установеното съществуване на двете форми в разтвор. Изследвани са промените в геометричните параметри и разпределението на зарядите при мономерите под действие на водородното свързване.

Bulgarian Chemical Communications, Volume 40, Number 4 (pp. 433–439) 2008

Experimental and DFT studies on IR spectral and structural changes arising from the conversion of 1H-indole-2,3-dione (isatin) into azanion

E. A. Velcheva*, P. J. Vassileva-Boyadjieva, I. G. Binev

Department of Structural Organic Analysis, Institute of Organic Chemistry with Centre of Phytochemistry, Bulgarian Academy of Sciences, Acad. G. Bonchev St., Block 9, 1113 Sofia, Bulgaria

Dedicated to Academician Ivan Juchnovski on the occasion of his 70th birthday

Received December 17, 2007; Revised January 25, 2008

IR spectral and structural changes, arising from the conversion of 1H-indole-2,3-dione (isatin) into azanion have been studied by IR spectra and quantum chemical calculation within the Onsager self-consistent reaction field (SCRF), using a density functional theory (DFT) method at the B3LYP/6-31++G** level. A good agreement has been found between experimental and scaled theoretical IR frequencies. In agreement between theory and experiment, the conversion causes a 109 cm^{-1} decrease in the α-carbonyl stretching frequency, 24 cm^{-1} decrease in the β-carbonyl stretching frequency and other essential IR spectral variations. The same theoretical method has given good descriptions both of steric and electronic structures of isatin. According to the computations, the changes in natural bond orbital (NBO) charges indicate that the $0.76e^-$ of the new (azanionic) charge of the azanion are delocalized within the aromatic residue and azanionic center.

Key words: IR, DFT B3LYP, structure, 1H-indole-2,3-dione, (isatin), azanion.

INTRODUCTION

1H-Indole-2,3-dione (isatin) was discovered in the nineteenth century as an oxidation product of pigment indigo [1] and first prepared synthetically by Sandmayer in 1919 [2]. Isatin was found in mammalian body fluids and tissues, isolated as an endogenous compound in 1988 [3] and reported to possess a wide range of central nervous system activities [4, 5], as well as to inhibit the neuroblastoma cell line proliferation at submicromolar concentrations; the potential utility of isatin as antitumor agent was also discussed [6]. Isatin class compounds are used mainly as precursors in dyes manufacturing (including hair dye) and in analytical chemistry [7]. The synthetic versatility of isatin has led to the extensive use of this compound in synthesis of pharmaceuticals, herbicides, *etc*. Schiff bases of isatin were reported to possess interesting pharmaceutical properties [8], such as anti-HIV [9] and anticonvulsant [10] ones. Isatin and its derivatives have also been used as ligands for complexation with various metal ions and the biological activities of these complexes were investigated [11–13]. It was found, that the structural properties of substituted isatins could be related with their biological activity.

The cristal structure of isatin was determined in 1950 [14], but because of the low accuracy of the data, it was redeterminated later [15, 16]. Contrary to the parent molecule, there are no structural data on its azanion.

The vibrational spectra of isatin have previously been studied [17–19]. The assignment of most of the observed frequencies has been assumed on the basis of IR and Raman spectra and dichroism of the single crystal [17]. The proton-donor ability of isatine when its H-form participated in complexes with organic bases were investigated by IR spectroscopy [18]. *Ab initio* theoretical as well as experimental data on the FTIR spectra of isatin and its 5-substituted analogues in the solid state were reported recently [19]. Authors' attempts to isolate solid alkali isatinate for the purpose of spectral comparison with the theoretical results for isatinato anion were unsuccessful [19].

We report in the present paper the experimental infrared spectrum of isatin azanion and determine the spectral and structural changes, arising from the conversion of isatin into the corresponding azanion by means of both quantitative IR spectra and DFT calculations.

EXPERIMENTAL

The isatin azanion (counter ion Na^+) was prepared by adding 0.09 and 0.2 $mol \cdot l^{-1}$ solutions of the parent isatin in DMSO-d_6 to excess of dry alkali-metal methoxide-d_3, obtained by reacting CD_3OD (Merck, 99% at enrichment), under argon. The con-

* To whom all correspondence should be sent:
E-mail: ev@orgchm.bas.bg

© 2008 Bulgarian Academy of Sciences, Union of Chemists in Bulgaria

version was practically complete (no bands of the parent compound were seen in the spectra after metalation). Organic anions are not soluble in common spectroscopic solvents and react with some of them, so the use of polar aprotic solvents (usually DMSO or DMSO-d_6) [20–29] is necessary in these cases.

The IR spectra were recorded on a Bruker IFS 113v FTIR spectrometer in a CaF_2 cell of 0.13 mm path length, at a resolution of 1 cm^{-1} and 50 scans.

COMPUTATIONS

The quantum chemical calculations were performed using the GAUSSIAN-98 program package [30]. We employed B3LYP (Becke's three-parameter method [31] using the correlation functional of Lee, Yang and Parr [32] and standard 6-31++G** basis set. The stationary points found on the molecular potential energy hypersurfaces were characterized using standard harmonic vibrational analyses. Use of the above basis set in the computations has recently given better or equally good structural predictions, compared to other basis sets for both molecules and/or anions [27–29, 33] (and references therein). No scaling in the density functional force field was done. To estimate the effect of a polar medium (DMSO) on the fundamental vibrational frequencies and intensities of the species studied we applied the Onsager SCRF method [34, 35] and DFT at the same level of theory (B3LYP/6-31++G**). In order to improve the visual representation of the calculated IR spectra in the figures, the calculated absorption lines were replaced by Lorentz functions with a half-width of 10 cm^{-1} by the SimOpus program [36] (see Fig. 2).

RESULTS AND DISCUSSION

Energy analysis

Optimized total energies (E^{tot}), Gibbs free energies (G) and vibrational zero-point energies (*VZPE*) calculated for the species studied in the gas state and DMSO solution are given in Table 1.

The deprotonation energy (E^D) of isatin was calculated as a difference between the *ZPVE*-corrected total energies ($E^{tot.}_{corr.}$) of the azanion and molecule: $\Delta E^{tot.}_{corr.} = E^{tot.}_{corr.}$ (anion) – $E^{tot.}_{corr.}$ (molecule) (Table 1).

The E^D values are related to the gas-phase acidities of Broensted acids and could also be used as an approximate measure of their pKa values in polar aprotic solvents [37]. There is a fair linear correlation between gas-phase ΔG_{acid} and DMSO pKa values for 97 C–H acids of various structures [38]. We have recently found a linear correlation between B3LYP/6-31++G** $\Delta E^{tot.}_{corr.}$ and pK_a (solvent DMSO) for a series of C–H, N–H and O–H acids containing cyano and/or carbonyl groups [33]:

$$pK_a(DMSO) = 0.11507\ \Delta E^{tot.}_{corr.}\ [kJ\cdot mol^{-1}] - 150.04.$$

This equation has successfully been used to estimate pK_a's of moderate [33, 39] and superstrong [40] organic acids. We did not find in the literature any pK_a (DMSO) data for isatin. The calculated E^D value is not away from those of *p*-hydroxyacetophenone (1383.6 $kJ\cdot mol^{-1}$) [25] and of *p*-hydroxybenzonitrile (1402.11 $kJ\cdot mol^{-1}$) [21], so the title compound should be a moderately weak Broensted N–H acid. In fact, pKa of *p*-hydroxyacetophenone is 11.9 (DMSO) [41] and 8.05 (H_2O) [41]; the corresponding values of *p*-hydroxybenzonitrile are 13.1 and 7.97, respectively [42, 43]. Having in mind the above equation and the B3LYP/6-31++G** $\Delta E^{tot.}_{corr.}$ of 1400.1 $kJ\cdot mol^{-1}$ (Table 1 the last line), we can calculated pK_a(DMSO) of isatin near 11.07.

Correlation analysis

We obtained the following linear correlation between theoretical and experimental IR frequencies of isatin: $\nu_{exp} = 0.9343\ \nu_{theor} + 64.45$ (cm^{-1}); correlation coefficient R = 0.9998; standard deviation s.d. = 13.5; number of data points n = 15. According to Jaffe's classification [44], the correlation is excellent, with 1 > R > 0.99. We shall use it for correlational scaling of the theoretical frequencies in the next section.

Table 1. Total energies (E), Gibbs free energies (G), zero-point vibrational energies (ZPVE) of isatin and its azanion.

	Gas-phase			DMSO solution		
Species	E, a.u.	G, a.u.	ZPVE, $kJ\cdot mol^{-1}$	E, a.u.	G, a.u.	ZPVE, $kJ\cdot mol^{-1}$
Molecule	–513.095037	–513.012950	302.29	–513.102387	–513.020158	302.51
Azanion	–512.547945	–512.479470	266.01	–512.560381	–512.491463	266.96
$\Delta E^{tot.}_{corr.} = E^{tot.}_{corr.}$ (azanion) – $E^{tot.}_{corr.}$ (molecule)			1400.11			1387.48

Spectral analysis

Tables 2 and 3 contain theoretical and experimental IR data for isatin and its azanion, respectively. We can find there a good agreement between experimental and scaled theoretical IR frequencies. The mean absolute deviations between them are 9.6 cm^{-1} for isatine and 10.5 cm^{-1} for its azanion. These values are within the corresponding mean deviation intervals of 9–20 and 9–24 cm^{-1}, typical for DFT calculations for series of molecules and anions, containing cyano and/or carbonyl groups [23–29] (and references therein).

We can state the following further comments on the results in Table 2:

- ν_{N-H} at 3444 cm^{-1}(solvent carbon tetrachloride) corresponds to hydrogen-bond free N–H groups. The ν_{N-H} band (solvent DMSO) is broad and complex, due to the formation of strong N–H....O=S hydrogen bonds between isatine and solvent.
- carbonyl stretchings $\nu_{C=O}$ at 1740 cm^{-1} with shoulder at 1757 cm^{-1} correspond to α-C=O and β-C=O groups. According to the calculations there is a vibrational interaction between the two carbonyl grups. The higher-frequency mode can be described as asymmetrical stretch of the –(C=O)–(C=O)– fragment, where the $\nu(\alpha$-C=O) coordinate is predominant. The lower-frequency mode corresponds to the symmetrical stretch of the same fragment; in this case $\nu(\beta$-C=O) coordinate is predominant.
- The δ_{N-H} coordinate is strongly delocalized, taking part in vibrations Nos. 12–15 of isatin (Table 2).

Table 2. Theoretical (SCRF model) and experimental (DMSO-d_6) IR data for isatin.

No.	B3LYP/6-31++G**			Approximate	Experimental data[b]	
	N, cm^{-1}	N, cm^{-1} [c]	A, $km \cdot mol^{-1}$	Description [a]	N, cm^{-1}	A, $km \cdot mol^{-1}$
1.	3638	3464	81.0	ν_{NH}	3444[d]	
2.	3223	3075	3.9	ν_{PhH}		
3.	3213	3066	6.3	ν_{PhH}	3074	5.1
4.	3205	3059	0.3	ν_{PhH}		
5.	3200	3054	2.2	ν_{PhH}		
6.	1811	1757	387.1	$\nu_{\alpha-(C=O)}, \nu_{\beta-(C=O)}$	1757	68.8
7.	1789	1736	877.9	$\nu_{\beta-(C=O)}, \nu_{\alpha-(C=O)}$	1740	216.8
8.	1657	1612	693.6	$\nu_{Ph}, \nu_{PhH}, \delta_{PhNC}$	1621	110.2
9.	1639	1596	94.3	ν_{Ph}, δ_{PhH}	1611	12.1
10.	1517	1482	40.4	$\delta_{PhH}, \nu_{Ph},$	1487	3.1
11.	1500	1466	147.8	δ_{PhH}, ν_{Ph}	1470	43.5
12.	1408	1380	73.6	$\delta_{NH}, \delta_{PhH}, \delta_{CNC}$	1398	2.2
13.	1359	1334	110.0	$\nu_{Ph}, \delta_{NH}, \delta_{PhH}, \delta_{PhNC}$	1328	28.2
14.	1310	1289	76.2	$\nu_{Ph}, \delta_{NH}, \delta_{PhH}, \delta_{PhNC}$	1289	12.1
15.	1265	1246	19.0	$\delta_{NH}, \delta_{PhH}, \delta_{PhNC}$	1218	8.3
16.	1215	1200	25.1	$\delta_{PhH}, \nu_{Ph}, \delta_{PhCC}$	1199	11.9
17.	1205	1190	106.4	$\delta_{NCC}, \delta_{PhH}, \delta_{Ph}$	1189	10.5
18 [f].	1175	1162	51.8	$\delta_{Ph}, \delta_{PhH}, \delta_{NCC}$	1147	2.8

[a] Vibrational modes: ν, stretching; δ, in-plane bendings; [b] Measured after having decomposed the complex bands into components; [c] Scaled, according to the correlation equation $\nu_{exp}=0.9343\ \nu_{theor} + 64.45$ (cm^{-1}); correlation coefficient R = 0.9998; standard deviation s.d. = 13.5; number of data points n = 15; [d] in carbon tetrachloride; [f] Followed by 24 lower-frequency normal vibrations.

Table 3. Theoretical (SCRF model) and experimental (DMSO-d_6) IR data for isatin azanion.

No.	B3LYP/6-31++G**			Approximate Description [a]	Experimental data[b]	
	N, cm^{-1}	N, cm^{-1} [c]	A, $km \cdot mol^{-1}$		N, cm^{-1}	N, cm^{-1} [c]
1.	3206	3060	30.4	ν_{PhH}	3057	2.3
2.	3190	3045	53.5	ν_{PhH}	3050	5.1
3.	3175	3031	8.0	ν_{PhH}	3045	2.3
4.	3171	3027	26.0	ν_{PhH}	3042	2.5
5.	1748	1698	578.6	$\nu_{\beta-(C=O)}$	1716	119.3
6.	1682	1636	206.1	$\nu_{\alpha-(C=O)}, \nu_{Ph}, \delta_{PhNC}, \delta_{PhH}$	1648	74.3
7.	1621	1579	1186.7	$\nu_{Ph}, \delta_{PhH}, \delta_{CCC}, \nu_{\alpha-(C=O)}$	1600	248.6
8.	1593	1553	1011.6	$\nu_{Ph}, \delta_{PhH}, \delta_{CCN}$	1568	134.7
9.	1503	1468	200.8	$\delta_{Ph}, \delta_{PhH}$	1470	61.7
10.	1463	1431	356.9	$\delta_{PhH}, \delta_{Ph}$	1439	92.7
11.	1341	1318	140.3	$\delta_{PhH}, \delta_{Ph}$	1320	42.5
12.	1330	1307	407.4	$\delta_{PhH}, \delta_{PhNC}$	1291	31.1
13.	1262	1244	112.4	$\delta_{PhNC}, \delta_{PhH}, \delta_{Ph}$	1243	16.5
14.	1244	1227	225.3	$\delta_{PhNC}, \delta_{PhH}, \delta_{Ph}$	1224	18.7
15.	1199	1185	3.1	$\delta_{PhH}, \delta_{PhCC}, \delta_{Ph}$	1210	13.8
16 [d].	1153	1142	181.8	$\delta_{PhH}, \delta_{Ph}, \nu_{NCC}$	1133	32.5

[a-c] See footnotes to Table 2. [d] Followed by 23 lower-frequency normal vibrations.

The conversion of isatin into azanion is accompanied by the following essential changes in the IR spectrum (cf. Tables 2, 3 and Figs. 1, 2):

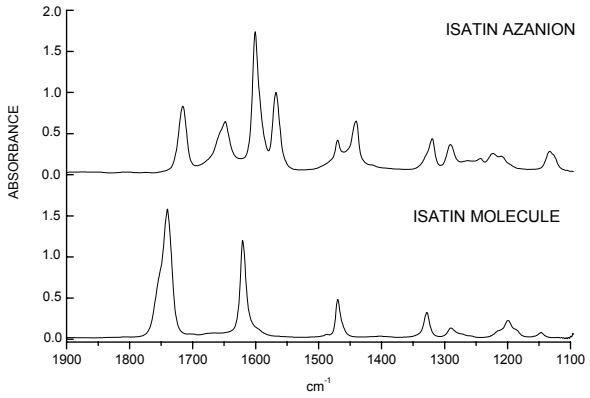

Fig. 1. IR spectra of isatin and isatin azanion in DMSO-d_6 (0.09 $mol \cdot l^{-1}$)

- The absence of a N–H group in the azanion cancels the N–H vibration and the influence of the δ_{N-H} coordinate on the lower-frequency vibrations (cf. above).
- Due to the strong direct resonance between the α-carbonyl group and azanionic center $\nu_{\alpha-C=O}$ frequency undergoes an essential lowering: calculated 121 cm^{-1}, measured 109 cm^{-1}. The computations predict participation of $\nu_{\alpha-C=O}$ coordinate also in vibration No. 7.
- Again due to the resonance, indirect in this case, the β-carbonyl stretching frequency undergoes a lowering, but not so strong: calculated 39 cm^{-1}, measured 24 cm^{-1}.
- In agreement between theory and experiment, the conversion of the molecule into azanion causes 2-fould increase in the integrated intensity of the 8a-type phenylene ring band.

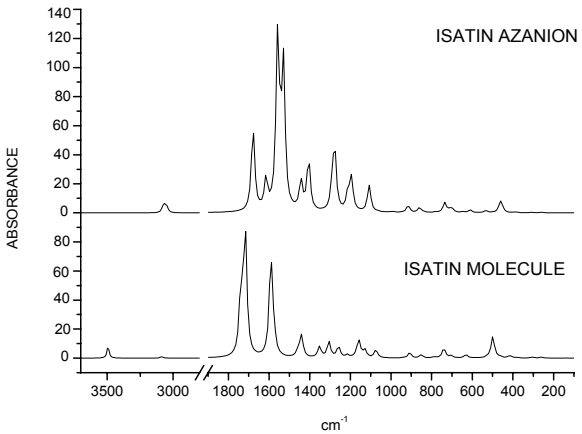

Fig. 2. Theoretical (B3LYP 6-31++G**, SCRF) IR spectra of isatin and isatin azanion.

Structural analysis

Theoretical and experimental steric structural parameters of the species studied are compared in Table 4. The comparison of calculated with X-ray values for the molecule shows a good agreement between them. The mean absolute deviations are: m.a.d. = $n^{-1}\sum|R_i(theor)-R_i(exp.)|$ of 0.0408 Å and m.a.d. = $n^{-1}\sum|A_i(theor)-A_i(exp.)|$ of 0.71°.

Table 4. Theoretical and experimental bond lengths R (Å) and angles A (°) in the isatin molecule and its azanion.

	B3LYP/6-31++G**			X-ray [a]
	molecule	azanion	Δtheor.(ion-mol)	molecule
R(1,2) [b]	1.3848	1.3594	**–0.0254**	1.3553
R(1,11)	1.4043	1.374	**–0.0303**	1.4073
R(1,16)	1.0104	-	-	0.943
R(2,3)	1.2110	1.2349	**0.0239**	1.2203
R(2,4)	1.5747	1.5958	**0.0211**	1.5623
R(4,5)	1.2119	1.2238	**0.0119**	1.2113
R(4,6)	1.4717	1.4643	–0.0074	1.4593
R(6,7)	1.3936	1.3906	–0.0030	1.3883
R(6,11)	1.4100	1.4315	**0.0215**	1.4013
R(7,8)	1.3981	1.4008	0.0027	1.3824
R(7,12)	1.0857	1.0887	0.0030	0.973
R(8,9)	1.4019	1.4105	0.0086	1.4044
R(8,13)	1.0849	1.0868	0.0019	0.983
R(9,10)	1.4027	1.3952	0.0075	1.3903
R(9,14)	1.0861	1.0893	0.0032	0.963
R(10,11)	1.3898	1.4139	**0.0241**	1.3743
R(10,15)	1.0856	1.0868	0.0012	0.923
m.d.a. [c]	*0.0408*			
A(2,1,11)	112.13	106.9567	**–5.1767**	111.42
A(2,1,16)	122.73	-	-	121.2
A(11,1,16)	125.13	-	-	127.2
A(1,2,3)	127.14	128.7038	1.5569	127.62
A(1,2,4)	104.86	109.2387	**4.3752**	105.82
A(3,2,4)	127.98	122.0575	**–5.9321**	126.62
A(2,4,5)	124.43	126.8649	2.4338	123.62
A(2,4,6)	104.89	103.0657	–1.8338	104.92
A(5,4,6)	130.66	130.0694	–0.5999	131.42
A(4,6,7)	131.37	132.5628	1.1849	132.42
A(4,6,11)	107.78	104.7719	–3.0107	107.22
A(7,6,11)	120.83	122.6653	1.8258	120.43
A(6,7,8)	118.61	119.0714	0.4531	118.72
A(6,7,12)	119.85	119.7708	–0.0866	120.02
A(8,7,12)	121.52	121.1577	–0.3666	121.2
A(7,8,9)	119.98	118.9368	–1.0496	119.91
A(7,8,13)	120.20	120.8127	0.6059	121.2
A(9,8,13)	119.80	120.2505	0.4437	119.2
A(8,9,10)	121.94	122.4936	0.5511	122.02
A(8,9,14)	119.29	118.7754	–0.5210	119.2
A(10,9,14)	118.76	118.7309	–0.0302	119.2
A(9,10,11)	117.48	119.2392	1.7571	117.2
A(9,10,15)	120.90	121.1289	0.2287	119.2
A(11,10,15)	121.61	119.6318	–1.9859	123.2
A(1,11,6)	110.32	115.9669	**5.6460**	110.7
A(1,11,10)	128.54	126.4395	–2.1083	127.5
m.d.a.[c]	*0.71*			

[a] Ref. 16. [b] For atom numbering see Scheme 1. [c] Mean absolute deviation between theoretical and experimental values.

There are not in the literature any experimental (X-ray or other) data for the isatine azanion structure. Having in mind the low m.a.d values for the molecule we assume that the structural parameters, calculated by the same method for its azanion should also be adequate. So, we could estimate the steric structure charge, caused by the conversion of isatine into azanion:

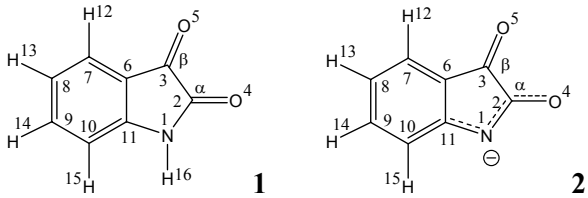

Scheme 1. Atom numbering of the isatin **1** and its azanion **2.**

Like in many other cases [27–29] (and reference therein), the **1→2** conversion causes strong bond length changes *at* and *next to* the anionic center (Table 4, Δ values in bold). They are strong shortenings of the N^1C^{11} and N^1C^2 bonds and strong lengthenings of the C^2O^3 and C^6C^{11} bonds.

Bond lengthenings take place of the C^2C^4 and C^4O^5 bonds. The C^2C^4 bond in isatin (Table 4) is one of the longest *α*–dicarbonyl bond reported [15, 16] and probably responsible for cleavage of the five-membered ring in alkali media.

The strongest bond angle changes caused by the **1→2** conversion correspond to the 5-membered ring.

The natural bond orbital (NBO) net electric charges q_i on atoms of the species studied are listed in Table 5. The net charges distribution over fragments of the species studied are as follows: –0.003, 0.075, 0.125 and –0.197, for the *β*-carbonyl group, *α*-carbonyl group, phenylene ring and amido group, respectively, of the isatin molecule, and –0.086, –0.083, –0.165 and –0.665 for *β*-carbonyl group, *α*-carbonyl group, phenylene ring and azanionic centre, respectively, of the isatine azanion.

Table 5. Calculated NBO atomic charges (q) for isatin and its azanion (For atom numbering see Scheme 1).

Atom [a]	*q*(molecule)	*q*(azanion)
N^1	–0.645	–0.665
C^2	0.613	0.556
O^3	–0.538	–0.639
C^4	0.482	0.483
O^5	–0.484	–0.569
C^6	–0.202	–0.245
C^7	–0.151	–0.180
C^8	–0.265	–0.335
C^9	–0.178	–0.213
C^{10}	–0.277	–0.296
C^{11}	0.199	0.209
H^{12}	0.259	0.230
H^{13}	0.247	0.217
H^{14}	0.246	0.216
H^{15}	0.248	0.231
H^{16}	0.447	

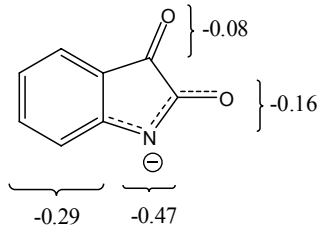

Scheme 2. The natural bond orbital (NBO) azanionic changes distribution over fragments of the isatin azanion.

The differences $\Delta q_i = q_i(\text{anion}) - q_i(\text{molecule})$ are quite informative to show the distributions of the new (carbanionic, azanionic, *ect*.) electric charges in anions [23–29] (and references therein). We can see in Scheme 2, that according to the computations $0.08e^-$, $0.16e^-$ and $0.29e^-$ of the new azanionic charge are delocalized over the *β*-carbonyl group, *α*-carbonyl group and phenylene ring, respectively, and $0.47e^-$ of it is remain localized at the azanionic center.

CONCLUSION

We found in this study a good agreement between theoretical and experimental IR data for both the isatin molecule **1** and its azanion **2**. Use of the same theoretical method and basis set made it possible to describe well both the steric and electronic structure of the molecule **1**. On the basis of these results we assumed that the structural predictions for the azanion **2** should also be adequate.

Acknowledgements: *The financial support by the Bulgarian National Science Fund under contract Chem.-1510 is gratefully acknowledged.*

REFERENCES

1. O. Erdmann, *J. Prakt. Chem.*, **24**, 1 (1841).
2. T. Sandmayer, *Helv. Chim. Acta*, **2**, 234 (1919).
3. V. Glover, J. M. Halket, P. J. Watkins, A. Clone, B. L. Goodwin, M. Sandler, *J. Neurochem.*, **51**, 656 (1988).
4. S. K. Bhattacharya, V. Glover, I. McIntyre, G. Oxenkrug, M. Sandler, *Neurosci. Lett*., **92**, 218 (1982).
5. S. K. Bhattacharya, S. K Mitra, S. B. Acharya, *J. Psychopharmacol*., **5**, 202 (1991).
6. A. Cane, M. C. Tournaire, D. Barritault, M. Crumeyrolle-Arias, *Biochem. Biophys. Res. Commun.*, **276**, 379 (2000).
7. The Merck Index, 13 Edn., Merck & Co. Inc., Whitehouse Station, N.J., USA, 2001.
8. A. A. Jarrahpour, D. Khalili, *Molbank*, M437 (2005).
9. S. N. Pandeya, D. Sriram, G. Nath, E. De Clercq, *Arzneimittel Forschun./Drug Res.*, **50**, 55 (2000).
10. S. K. Sridhar, S. N. Pandeya, J. P. Stables, S. K. Armes, *Eur. J. Pharm. Sci.*, **16**, 129 (2002).
11. A. M. A. Hassaan, *Transit. Met. Chem.,* **15**, 283 (1990).
12. A. Garcia-Raso, J. J. Fiol, E. Molins, A. M. Calafat, P. A. Marzilli, L. G. Marzilli, *Metal-Based Drugs,* **2**, 81 (1995).
13. P. Naumov, F. Atanasova, *Bull. Chem. Thechnol. Macedonia,* **19**, 1 (2000).
14. G. H. Goldschmidt, F. J. Llewellyn, *Acta Cristallogr*., **3**, 294 (1950).
15. M. H. Palmer, A. J. Blake, R. O. Gould, *Chem. Phys*., **115**, 219 (1987).
16. M. A. Frolova, V. N. Kravtsov, V. N. Biyushkin, Y. M. Chumakov, O. N. Belkova, T. I. Malynovskii, *Zh. Strukt. Khim*., **29**, 155 (1988).
17. A. Bigatto, V. Galasso, *Spectrochim. Acta,* **35 A**, 725 (1979).
18. B. N. Narziev, N. Mulloev, *J. Struct. Chem*., **40**, 481 (1999).
19. P. Naumov, F. Atanasova, *Spectrochim. Acta,* **57 A**, 469 (2001).
20. I. N. Juchnovski, I. G. Binev, in: The Chemistry of Functional Groups, Suppl. C, S. Patai, Z. Rappoport (Eds), Wiley, New York, 1983, Ch. 4.
21. V. Ognyanova, J. Petrov, G. N. Andreev, *Spectrosc. Lett*., **30**, 933 (1997).
22. G. N. Andreev, O. K. Argirov, V. Ognyanova, *J. Mol. Struct*., **516**, 238 (2000).
23. I. G. Binev, P. J. Vassileva-Boyadjieva, Y. I. Binev, *J. Mol. Struct*., **447**, 235 (1998).
24. Y. I. Binev, Ch. T. Petkov, L. Pejov, *Spectrochim. Acta Part A*, **56**, 1949 (2000).
25. P. J. Vassileva-Boyadjieva, E. A. Velcheva, Y. I. Binev, *Bulg. Chem. Commun*., **37**, 313 (2005).
26. M. K. Georgieva, P. N. Angelova, I. G. Binev, *J. Mol. Struct*., **692**, 23 (2004).
27. D. Popova, M. K. Georgieva, O. I. Petrov, K. V. Petrova, E. A. Velcheva, *Int. J. Quant. Chem.,* **107,** 1752 (2007).
28. L. I. Daskalova, E. A. Velcheva**,** I. G. Binev, *J. Mol. Struct*., **826**, 198 (2007).
29. E. A. Velcheva, B. A. Stamboliyska, *J. Mol. Struct*., (2007) in press.
30. M. J. Frisch, G. W. Trucks, H. B. Schlegel, G. E. Scuseria, M. A. Robb, J. R. Cheeseman, V. G. Zakrzewski, J. A. Montgomery, Jr., R. E. Stratmann, J. C. Burant, S. Dapprich, J. M. Millam, A. D. Daniels, K. N. Kudin, M. C. Strain, O. Farkas, J. Tomasi, V. Barone, M. Cossi, R. Cammi, B. Mennucci, C. Pomelli, C. Adamo, S. Clifford, J. Ochterski, G. A. Petersson, P. Y. Ayala, Q. Cui, K. Morokuma, D. K. Malick, A. D. Rabuck, K. Raghavachari, J. B. Foresman, J. Cioslowski, J. V. Ortiz, A. G. Baboul, B. B. Stefanov, G. Liu, A. Liashenko, P. Piskorz, I. Komaromi, R. Gomperts, R. L. Martin, D. J. Fox, T. Keith, M. A. Al-Laham, C. Y. Peng, A. Nanayakkara, C. Gonzalez, M. Challacombe, P. M. W. Gill, B. Johnson, W. Chen, M. W. Wong, J. L. Andres, M. Head-Gordon, E. S. Replogle, J. A. Pople, Gaussian 98, Revision A.7, Gaussian, Inc., Pittsburgh PA, 1998.
31. A. D. Becke, *Phys. Rev. A*, **38**, 3098 (1988).
32. C. Lee, W.Yang, R. G. Parr, *Phys. Rev. B*, **37,** 785 (1988).

33. M. K. Georgieva, E. A. Velcheva, *Int. J. Quant. Chem.,* **106,** 1316 (2006).
34. M. W. Wong, M. J. Frisch, K. B. Wiberg, *J. Am. Chem. Soc*., **113**, 4776 (1990).
35. O. Tapia, O. Goscinski, *Mol. Phys*., **29**, 1653 (1975).
36. Y. I. Binev, Ph.D. Thesis, Inst. Org. Chem., Bulgarian Academy of Sciences, Sofia, 2000.
37. V. M. Vlasov, L. A. Oshkina, *Org. React*., **28**, 47 (1993).
38. I. A. Koppel, J. Koppel, V. Pihl, I. Leito, M. Mishima, V. M. Vlassov, L. M. Yagupolski, R. W. Taft, *J. Chem. Soc. Perkin Trans.,* **2**, 1125 (2000)
39. L. I. Daskalova, *J. Mol. Struct*., in press.
40. J. A. Tsenov, S. S. Stoyanov, I. G. Binev, *Bulg. Chem. Commun.,* **37**, 361 (2005).
41. A. P. Kreshkov, N. Sh. Aldarova, A. I. Tarassov, V. A. Vasnyev, S. V. Vinogradova, M. V. Slavgorodska, T. I. Mitaishvili, V. V. Korshak, *Org. Reactivity,* **7**, 279 (1970).
42. J. K. Ellington, E. M.Arnet, *J. Am. Chem. Soc.,* **110**, 7778 (1988).
43. A. Fini, P. De Maria, A. Guarnjeri, L. Varoli, *J. Pharm. Sci*., **76**, 48 (1987)
44. H. H. Jaffe, *Chem. Rev*., **53**, 191 (1953).

ЕКСПЕРИМЕНТАЛНО И ТФП ИЗСЛЕДВАНЕ НА ИЧ СПЕКТРАЛНИ И СТРУКТУРНИ ПРОМЕНИ ПРОИЗТИЧАЩИ ОТ ПРЕВРЪЩАНЕТО НА 1Н-ИНДОЛ-2,3-ДИОН (ИЗАТИН) В АЗАНИОН

Ев. А. Велчева*, П. Ж. Василева-Бояджиева, Ив. Г. Бинев

Лаборатория „Структурен органичен анализ“, Институт по органична химия с център по фитохимия, Българска академия на науките, ул. „Акад. Г. Бончев“, бл. 9, 1113 София

Посветена на акад. Иван Юхновски по повод на 70-та му годишнина

Постъпила на 17 декември 2007 г.; Преработена на 25 януари 2008 г.

(Резюме)

ИЧ спектрални и структурни промени, произтичащи от превръщането на 1Н-индол-2,3-дион (изатин) в азанион са изследвани чрез спектроскопски експерименти и B3LYP/6-31++G** пресмятания в рамките на модела на Онзагер. Намерено е добро съответствие между експериментални и скалирани ИЧ честоти. В съгласие между теория и експеримент, превръщането предизвиква 109 cm^{-1} понижение на α-карбонилната валентна честота, 24 cm^{-1} понижение на β-карбонилната валентна честота и други същетвени спектрални промени. Същия теоретичен метод дава добро описание на пространствената и електронна структура на изатина. Според изчисленията, $0.76e^{-}$ (NBO) от новия (азанионен) заряд на аниона е делокализиран в ароматния остатък и азанионния център.

Bulgarian Chemical Communications, Volume 40, Number 3 (pp. 440–444) 2008

UV-VIS absorption and fluorescent characteristics of some substituted in the styril fragment synthetic chalcones

D. I. Ivanova, I. I. Timtcheva*, B. A. Stamboliyska, D. I. Batovska

Institute of Organic Chemistry with Centre of Phytochemistry, Bulgarian Academy of Sciences, Sofia 1113, Bulgaria

Dedicated to Academician Ivan Juchnovski on the occasion of his 70th birthday

Received December 17, 2007; Revised May 9, 2008

The photophysical properties of a number of synthetic chalcones in different media at 293K are investigated. The effect of the substituents in *p*-position of ring B of the studied chalcones on the deactivation processes of their singlet electronically excited state is discussed. It is found that in the case of the *p*-dimethyl-amino substituted compound the relationship between the fluorescent Franck-Condon transition energy and of the fluorescence quantum yield as well, and the ET(30) constants of the solvents is strongly influenced by the proton donating ability of the solvent. These experimental results indicate formation of intermolecular hydrogen bonded solute - solvent complexes in the fluorescent excited state at room temperature in protic solvents. Formation of different tautomeric forms of *p*-hydroxy substituted chalcone in different media is observed as well.

Key words: chalcones, UV-VIS absorption, fluorescence, DFT.

INTRODUCTION

Investigation on the relationship between the structure of electronically excited states of conjugated organic molecules and their absorption and fluorescent properties is one of the main problems of molecular photophysics. Nevertheless, the great number of experimental and theoretical data that is available in the literature specific characteristics for a particular group of compounds is observed in many cases. This holds for the conjugated organic compounds containing hetero-atoms in particular. Their electronic system includes nπ* levels that play decisive role in the processes of radiative and nonradiative deactivation of the electronically excited states [1, 2].

Chalcones are natural oxygen-containing aromatic compounds that belong to the group of flavonoids with an open γ-pyrone cycle connecting two benzene fragments. In nature they occur mainly in plants and are also present in food products of plant origin such as propolis, wine, beer, fruit juices and tea. The low content of chalcones in natural raw material and their proved wide-range physiological activities are the reason for the increased interest towards the preparation of new synthetic chalcones with desired properties for application in medicine [3–5]. The synthetic chalcones studied in the present paper possess strong growth inhibitory activity towards the major human pathogen *Candida albicans* [6].

EXPERIMENTAL AND COMPUTATIONS METHODS

Absorption spectra were scanned on a UV-VIS Spectrophotometer Perkin Elmer Lambda 25 and the fluorescence spectra – on a Perkin Elmer LS 55 spectrofluorimeter. The fluorescence quantum yield (Q_F) was determined relative to that of the dye Rhodamine 6G (Q_F = 0.95 in ethanol) [7]. All measurements were performed at room temperature. The solvents used are of fluorescent grade.

The ground state geometry of two tautomers of *p*-hydroxy chalchon (hydroxy and oxo) were optimized by applying density functional theory (DFT) at the B3LYP/6-311+G** level. The nature of the potential energy surfaces was determined using harmonic vibrational analyses. The absence of imaginary frequencies confirmed that the stationary points correspond to minima on the potential energy surfaces. Self-consistent reaction field (SCRF) theory was employed to optimize the tautomers in the aqueous phase. The optimized geometries were used to compute electronic vertical singlet transition energies at the time-dependent density functional theory (TDDFT) level using the B3LYP functional. All calculations were performed using GAUSSIAN 98 suite of program [8].

RESULTS AND DISCUSSION

The investigated compounds are presented in Table 1. The longest wavelength absorption maxima of the studied chalcones in ethanol at room tempe-

* To whom all correspondence should be sent:
E-mail: iltim@orgchm.bas.bg

© 2008 Bulgarian Academy of Sciences, Union of Chemists in Bulgaria

rature are in the region of 33000–23000 cm^{-1} and move to the red with increasing the solvent polarity passing from benzene through acetonitrile to ethanol. The molar absorptivity in ethanol is between 12000 and 30000 $L \cdot mol^{-1} \cdot cm^{-1}$. The type of the substituent in *p*-position of the phenyl ring B has a strong influence on the energy of the longest wavelength absorption Frank-Condon transitions. A bathochromic shift by 3500 cm^{-1} is observed upon increasing its electron donating ability in the sequence methyl-, methoxy- and hydroxy- group. On the contrary, the cyano group possessing strong electron withdrawing abilities increases the energy of the S_0-S_1 absorption transition by 400 cm^{-1}. The presence of dimethylamino group in *p*-position of ring B leads to the appearance of a second red shifted absorption band in ethanol with a maximum around 23000 cm^{-1}. This experimental result could be explained by the strong charge transfer transition between the electron withdrawing carbonyl group and the electron donating dimethylamino one in the molecule of compound **5** [9] (Table 2).

Table 1. Investigated compounds.

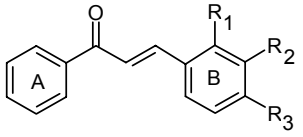

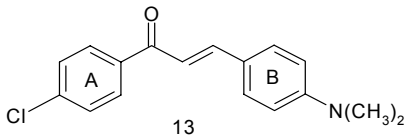

13

Ccompound	R_1	R_2	R_3
1	H	H	H
2	H	H	CH_3
3	H	H	OCH_3
4	H	H	OH
5	H	H	$N(CH_3)_2$
6	H	H	Cl
7	H	H	CN
8	OH	H	H
9	H	OH	H
10	H	OH	OH
11	H	- O – CH_2 – O -	
12	H	OCH_3	OCH_3

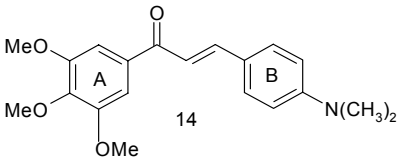

14

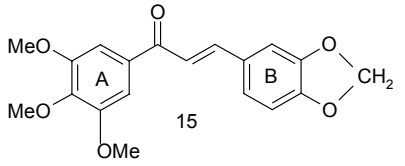

15

Table 2. Absorption characteristics of the investigated chalcones at 293 K: $\tilde{\nu}_{ABS}$ – energy of the longest wavelength absorption Franck-Condon transitions in cm^{-1}; ε ($L \cdot mol^{-1} \cdot cm^{1}$) – molar absorptivity. The numbers of the compounds correspond to those given in Table 1.

Compound	Benzene	Acetonitrile	Ethanol	
	$\tilde{\nu}_{ABS}$	$\tilde{\nu}_{ABS}$	$\tilde{\nu}_{ABS}$	ε
1	32790	32260	32050	13000
2	31250	30960	30490	19350
3	29590	29410	28990	17510
4	29760	29410	28570	13330
5	24510	24390	28270	26000
			23260	
6	31750	32260	31750	12850
7	33330	32790	32470	12000
8	29410	28990	28170	14800
9	32790	32470	32790	15000
10	28570	28170	27030	14860
			sh 23410	
11	28170	28170	28090	16380
12	28170	27930	27620	17100
13	24270	23810	23260	24320
14	24100	23920	23260	30000
15	28410	27780	27620	17200

In the case of compounds **4** and **10** (Table 1), where the substituent R_2 is a hydroxyl group, a specific interaction with protic solvents in S_0 state is observed (Fig. 1) that is most probably due to the oxo-hydroxy tautomerism of these compounds [10].

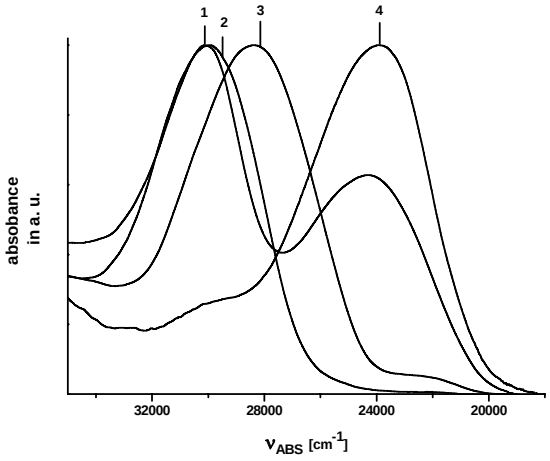

Fig. 1. Absorption spectra of compound **4** in solution at 293 K in: benzene - curve 1; ethanol - curve 2; water at pH 7 - curve 3; water at pH 9 - curve 4.

The assignment of the bands between 33000 and 20000 cm^{-1} to the absorption of the hydroxy and the oxo form is performed on the basis both of experimental results in benzene, ethanol, water at pH 7 and water at pH 9, and quantum chemical calculations as well.

The longest wavelength absorption band of **4** in benzene has a maximum at 29760 cm^{-1}. It could be related to the presence of a hydroxy form. A new bathochromicaly shifted band with maximum at

around 24000 cm^{-1} appears in ethanol and water at pH 7. It could be assigned to the possible formation of another tautomeric form of *p*-hydroxy substituted chalcones – namely an oxo form. Equilibrium between oxo and hydroxy tautomeric forms in ethanol and water (pH 7) is observed, while in water at pH 9 the oxo tautomeric form is mainly present. Computed transitions energies were found in a good agreement with the corresponding experimental data as well. Calculation predicts singlet π–π* electron transition at 29400 cm^{-1} for hydroxy and at 24800 cm^{-1} for oxo tautomeric forms, respectively.

In order to explain the obtained experimental results a detailed theoretical study of the molecular geometry of the species studied was performed. The solvent effect was studied by SCRF theory. The relative stability of the hydroxy and oxo tautomers in gas phase and in water (ε = 78.39) was determined. Comparison of the energy values of the studied tautomers indicates that in gas phase the hydroxy tautomer is more stable by 15.7 kcal/mol, while in water solution the oxo tautomer is only slightly less stable (less than 1 kcal/mol). Therefore, it could be concluded that *p*-OH chalcones will be present mainly in their hydroxy tautomeric form in gas phase while in aqueous media both hydroxy and oxo forms exist. The obtained results are in good agreement with the corresponding experimental ones.

The unsubstituted chalcone does not fluoresce in solution at room temperature. The absence of fluorescence is due to the fact that its longest wavelength absorption transition lies around 27 000 cm^{-1} and like in the case of other carbonyl-containing compounds is of S_0–$S_1(n\pi^*)$ type [11]. This transition cannot be observed in the absorption spectrum of compound ***1*** as it is overlapped by an intensive S_0–$S_1(\pi\pi^*)$ band. Radiation $S_1(n\pi^*)$–(S_0) transitions in carbonyl compounds are forbidden and that is why the compound does not have a fluorescence of its own [1].

The presence of electron donating substituent in p-position of ring B such as methoxy- or hydroxy-group leads to a bathochromic shift of the longest wavelength absorption transition. The energy of lowest lying $S_1(\pi\pi^*)$ and $S_1(n\pi^*)$ levels becomes similar. These compounds do not fluoresce in aprotic solvents. However, in protic solvents the so-called "activated fluorescence" [1, 2, 12] with maxima in the range of 25000–23000 cm^{-1} and low fluorescent quantum yields is observed.

In the case of the *p*-dimethylamino substituted in ring B chalcone a specific interaction with protic solvents in excited state is observed, namely formation of intermolecular solute-solvent hydrogen bonds (Fig. 2).

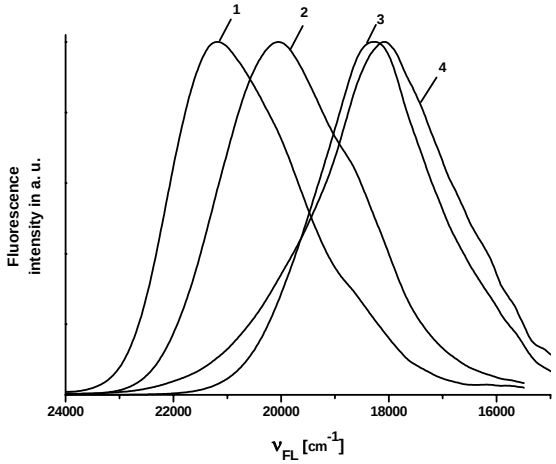

Fig. 2. Fluorescent spectra of compound **5** in solution at 293K in: benzene - curve 1; ethylacetat - curve 2; acetonitrile - curve 3; ethanol - curve 4.

The fluorescent maximum of compound **5** moves to the red with increasing the polarity and proton donating ability of the solvents. The fluorescent quantum yield increases with increasing the solvent polarity in the case of aprotic solvents. On the contrary, the Q_F decreases drastically in protic solvents in comparison to aprotic ones despite their high polarity.

The assumption for formation of hydrogen bonds in excited state is confirmed by the investigations on the relationship between the ET(30) constants of the solvents and the energy of the fluorescent maxima and the Q_F value, respectively [13].

Two different linear correlations – one for protic and one for aprotic solvents – for the relationship between the energy of the fluorescent transition and ET(30) constants of the solvents are observed. The presence of two different linear correlations shows that the nature of the fluorescent species in protic and in aprotic solvents is different [14, 15] (Fig. 3).

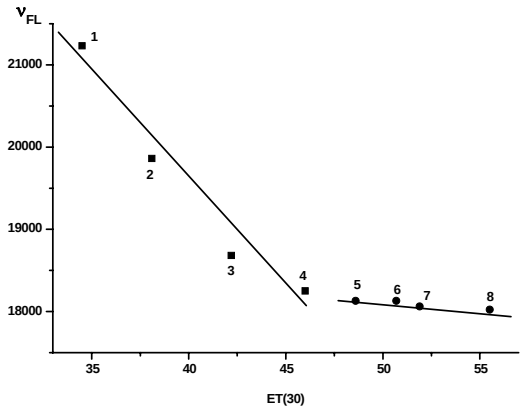

Fig. 3. Energy of the fluorescent maxima ν_{FL} in cm^{-1} of compound **5** *vs* the solvent polarity parameter ET(30) in: benzene - 1; ethylacetate - 2; acetone - 3; acetonitrile - 4; *n*-buthanol - 5; *i*-propanol - 6; ethanol - 7; methanol - 8.

In corroboration of the assumption for formation of intermolecular hydrogen bonds is the presence of two linear correlations ET(30) /Q_F that are obtained for protic and aprotic solvents, respectively. The quenching of fluorescence in protic solvents is most probably due to vibrations of the hydrogen bonds between the molecules of the solute and the protic solvent in excited state, thus acting as an additional channel for radiationles deactivation (Fig. 4).

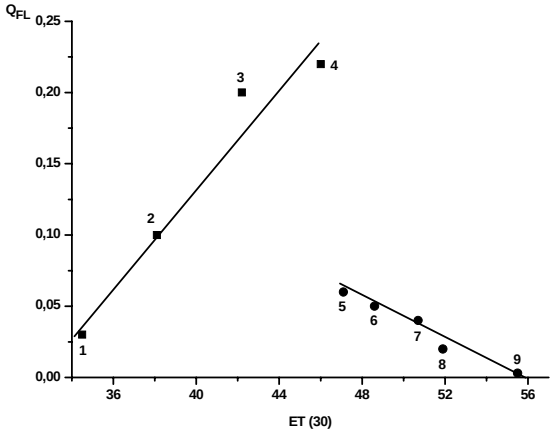

Fig. 4. Fluorescent quantum yield QFL of compound **5** vs the solvent polarity parameter ET(30) in: benzene - 1; ethylacetate - 2; acetone - 3; acetonitrile - 4; *n*-buthanol - 5; *i*-buthanol - 6; *i*-propanol - 7; ethanol - 8; methanol – 9.

CONCLUSIONS

It is shown that the nature of the substituent in *p*-position of the benzene ring B has a strong influence on the position of the longest wavelength absorption maxima of the investigated chalcones. The presence of electron donating groups like methoxy- and hydroxy- ones leads to its bathochromic shift, while the introduction of electron withdrawing substituent, namely cyano group leads to a blue shift of this maximum. The occurrence of strong charge transfer in the case of *p*-dimethylamino-substituted chalcone is observed. The ability of *p*-hydroxy-substituted chalcone to exist in different tautomeric forms, namely oxo and hydroxy ones, in solvents of different polarity and proton donating ability is proved by experimental data and quantum chemical calculations. The main fluorescent characteristics of the studied chalcones are determined at room temperature and it is shown that the absence of fluorescence in some cases is due to the fact that their lowest lying S_1 state is of $n\pi^*$ type. A specific interaction – formation of intermolecular hydrogen bonds in excited state between the *p*-dimethyl-amino-substituted chalcone and protic solvents is proved on the basis of the relationship between the energy of the Fluorescent Frank Condon transition and the ET(30) constants of the solvents.

Acknowledgement: *The financial support by the Bulgarian Council of Scientific Research for Project X–1514 is politely acknowledged.*

REFERENCES

1. J. B. Birks, Photophysics of Aromatic Molecules, Wiley-Interscience, London, 1970.
2. J. R. Lakowicz, Principles of Fluorescence Spectroscopy, Plenum Press, 1986.
3. L. Ni, Ch. Meng, J. Sikorski, *Expert Opinion,* **14**, 1669 (2004).
4. J.-C. Stoclet, T. Chataigneau, M. Ndiaye, M.-H. Oak, J. El. Bedoui, M. Chataigneau, V. B. Schini-Kerth, *Eur. J. Pharm.,* **500**, 299 (2004).
5. F. A. Tomas-Barberan, M. N. Clifford, *J. Sci. Food Arg*., **80**, 1073 (2000).
6. D. Batovska, S. Parushev, A. Slavova, I. Tsvetkova, M. Ninova, H. Najdenski, *Eur. J. Med. Chem*., **42**, 87 (2007).
7. C. Zander, K-H. Drexhage, *Adv. Photochem.,* **20**, 59 (1995).
8. M. Frisch, G. Trucks, H. Schlegel, G. Scuseria, M. Robb, J. Cheeseman, V. Zakrzewski, J. Montgomery, R. Stratmann, J. Burant, S. Dapprich, J. Millam, A. Daniels, K. Kudin, M. Strain, O. Farkas, J. Tomasi, V. Barone, M. Cossi, R. Cammi, B. Mennucci, C. Pomelli, C. Adamo, S. Clifford, J. Ochterski, G. Petersson, P. Ayala, Q. Cui, K. Morokuma, D. Malick, A. Rabuck, K. Raghavachari, J. Foresman, J. Cioslowski, J. Ortiz, A. Baboul, B.Stefanov, G. Liu, A. Liashenko, P. Piskorz, I. Komaromi, R. Gomperts, R. Martin, D. Fox, T. Keith, M. Al-Laham, C. Peng, A. Nanayakkara, C. Gonzalez, M. Challacombe, P. Gill, B. Johnson, W. Chen, M. Wong, J. Andres, C. Gonzalez, M. Head-Gordon, E. Replogle, J. Pople, *Gaussian 98*, revision A.7; Gaussian, Inc.; Pittsburgh, PA, 1998.
9. C. A. Parker, Photoluminescence of solutions, Elsevier Publishing Company, 1968.
10. F. Miquel, Memories Presentes a la Siciete Chique, **214,** 1369 (1961).
11. R. X. Nurmuhametov, Absorption and Luminescence of Aromatic Compounds, Khimia, Moskow, 1971 (in Russian).
12. P. Nikolov, F. Fratev, St. Minchev, *Z. Naturforsch.,* **A 38,** 200 (1983).
13. K. Dimroth, C. Reichardt, T. Siepmann, F. Bohlmann, *Liebigs Ann. Chem.,* **661,** 1 (1963).
14. P. Nikolov, I. Timcheva, *J. Photochem. Photobiol. A: Chemistry,* **131,** 23 (2000).
15. D. Noukakis, P. Suppan, *J. Luminescence,* **47,** 285 (1991).

АБСОРБЦИОННИ И ФЛУОРЕСЦЕНТНИ ХАРАКТЕРИСТИКИ В УВ-ВИДИМАТА ОБЛАСТ НА НЯКОИ ЗАМЕСТЕНИ В СТИРИЛНИЯ ФРАГМЕНТ СИНТЕТИЧНИ ХАЛКОНИ

Д. И. Иванова, Ил. И. Тимчева*, Б. А. Стамболийска, Д. И. Бътовска

Институт по Органична химия с Център по фитохимия, Българска академия на науките, ул. „акад. Г. Бончев“, бл. 9, София 1113

Посветена на акад. Иван Юхновски по повод на 70-та му годишнина

Постъпила на 17 декември 2007 г.; Преработена на 9 май 2008 г.

(Резюме)

Изучени са фотофизичните отнасяния в различни по полярност и протонодонорни свойства разтворители при 293К на една група синтетични халкони. Проследен е ефектът на природата на заместителя на *p*-място във фенилното ядро B на изследваните халкони върху процесите на дезактивация на възбудените им синглетни електронни състояния. Установено е, че в случая на *p*-диметиламино-заместеният халкон протонодонорните свойства на разтворителите оказват съществено влияние върху зависимостите между енергията на флуоресцентния Франк Кондонов преход и флуоресцентния квантов добив от една страна и ET(30) константата на разтворителите от друга. Тези експериментални резултати са индикация за формирането на свързани с междумолекулни водородни връзки комплекси между разтвореното вещество и протния разтворител във възбудено състояние при стайна температура. На базата на експериментални резултати от абсорбционните спектри в УВ-видимата област в различни разтворители и на квантово-химични пресмятания е доказано наличието на различни тавтомерни форми на *p*-хидрокси заместения халкон.

Bulgarian Chemical Communications, Volume 40, Number 4 (pp. 445–449) 2008

Theoretical study of the conformational preference of N-[(4-aminophenyl) sulphonyl]acetamide (sulphacetamide) and its azanion

B. A. Stamboliyska*, A. D. Popova, E. A. Velcheva

Department of Structural Organic Analysis, Institute of Organic Chemistrywith Centre of Phytochemistry, Bulgarian Academy of Sciences, Acad. G. Bonchev St., Block 9, 1113 Sofia, Bulgaria

Dedicated to Academician Ivan Juchnovski on the occasion of his 70th birthday

Received December 18, 2007; Revised January 25, 2008

The potential energy surfaces of N-[(4-aminophenyl)sulphonyl]acetamide (sulphacetamide) and its azanion have been explored with DFT calculation at the B3LYP/6-31G* level of theory. All conformational isomers have been located. Three torsion angles (C–C–S–N, C–S–N–C, and S–N–C=O) are used in describing the conformations of the species examined. The preferred structures obtained by the scan for molecule (∠C–C–S–N, 90°; ∠C–S–N–C, 60° and ∠S–N–C=O, 0°) and azanion (∠C–C–S–N, –90°; ∠C–S–N–C, 60° and ∠S–N–C=O, 0°) were optimized at the B3LYP/6-31++G** level. The results of the optimized molecular structure are presented and compared with the experimental X-ray diffraction. The geometry changes caused by the conversion of the molecule into azanion have also been estimated.

Key words: sulphacetamide, azanion, conformers, DFT.

INTRODUCTION

N-[(4-Aminophenyl)sulfonyl]acetamide (sulphacetamide) belongs to the important class of sulpha drugs, which are well-known as antimicrobial agents. The structural resemblance between the sulphanilamide grouping and *p*-aminobenzoic acid enables the sulphanilamide to block folic acid synthesis in bacteria, which accounts the antibacterial action of these drugs [1, 2]. Sulphacetamide is of considerable interest as a highly soluble sulphonamide which does not cause crystalluria, and its sodium salts are extensively used in cases of ophthalmic infections, giving solutions which do not irritate the delicate eye tissues [3]. Detailed knowledge of the structure of the species studied is an obligatory prerequisite for understanding its biological activity. Theoretical investigations were performed with the aim to provide an insight into structure-activity relationships. CNDO/2 calculations have been used to represent the changes in the electronic structure of a series of sulphanilamides on going to their anionic, imidic and amidic form and to obtain correlations between theoretically calculated values and biological activity parameters [4]. It was found that the anionic forms appear to give the dominant contributions to the biological potency of these compounds. The increase in the charge on the nitrogen atom was associated with the increase in the experimental pK_a and also in a decrease of the bacteriostatic activity [5]. It was suggested that acidity of sulphonamido group, and the factors affecting it, are key features ruling the physico-chemical properties which modulate the sulphonamide bioactivity [6]. A conformational analysis of sulphonamide-type compounds illustrates that active molecules have relatively larger torsion energy barriers [7].

The molecular structure of sulphacetamide has not received the attention one could reasonably expect. We found in the literature only one quantum chemical study where selected geometrical parameters of the sulphacetamide molecule and its anionic form were presented [6]. By single crystal X-ray diffraction was determined the crystal and molecular structure of sulphacetamide [8], sodium sulphacetamide monohydrate [9] and silver sulphacetamide [10].

Since the characterization of the most stable conformers of sulphacetamide and the factors which contribute to their relative stability are essential for a complete understanding of its biological properties, we used in this article the density functional theory (DFT) in order to perform structural analysis of both sulphacetamide and its azanionic form.

THEORETICAL AND COMPUTATIONAL METHODS

DFT computations of the studied species were performed using the GAUSSIAN-98 program

* To whom all correspondence should be sent:
E-mail: bs@orgchm.bas.bg

© 2008 Bulgarian Academy of Sciences, Union of Chemists in Bulgaria

package [11]. We employed the B3LYP functional, which combines Becke's three - parameter non-local exchange with the correlation functional of Lee, Yang and Parr [12, 13], adopting a 6-31G* basis set. The conformational analysis of the molecule and its anion was carried out by varying the torsion angles τ_1, τ_2 and τ_3 from 0° up to 360° in step of 18° with relaxation of the system (see Scheme 1). The minima obtained by the scan for both species were optimized at B3LYP/6-31++G** level. For each structure, the stationary points found on the molecular potential energy hypersurfaces were characterized using standard analytical harmonic vibrational analysis. The absence of negative frequencies, as well as of negative eigenvalues of the second-derivative matrix, confirmed that the stationary points correspond to minima on the potential energy hypersurfaces.

RESULTS AND DISCUSSION

Sulphacetamide and its azanion have a large degree of conformational mobility due to the three single bonds C–S–N–C. In order to characterize conformational states, the potentional energy profiles for internal rotations around these single bonds were calculated. Three torsion angles (τ_1, τ_2 and τ_3) are used here to describe the conformations of the species examined (see Scheme 1).

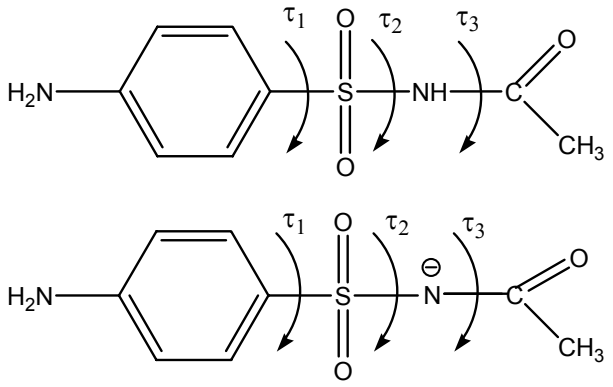

Scheme 1.

The smaller of the two C–C–S–N torsion angles between the aniline ring and S–N bond is marked as τ_1. Figure 1 presents the calculated potential energy profiles for internal rotation around the Ph–S bond for sulphacetamide and its anion. B3LYP calculations predict the existence of two stable conformations both in molecule and azanion: **1** (C–C–S–N, 90°) and **2** (C–C–S–N, –90°). Comparison of the energy values of these conformers indicates that structure **1** with $\tau_1 \cong 90$ is the lowest in energy for the molecule and it is the least stable for the azanion. However, in both cases the estimated conformational energy differences are very small (0.3 kJ·mol^{-1} for molecule and 0.7 kJ·mol^{-1} for azanion). These τ_1 values lie in a characteristic range (between 70 and 120°) reported in literature by analyzing of the geometries of many independent sulphonamide fragments [14, 15]. This angle for sulphacetamide has been experimentally found to be 114.5° [8]. The calculated energy barriers (about 21 and 17 kJ·mol^{-1} for molecule and azanion, respectively) are higher than the energies of the rotation of the aromatic rings which respect to the sulphonamido group for sulphanilamide [6].

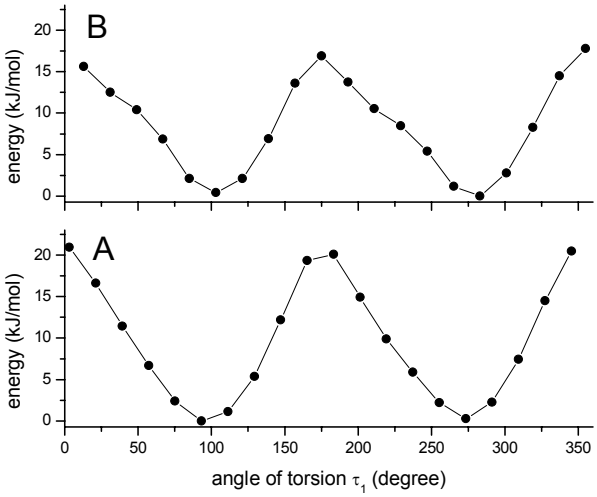

Fig. 1. Conformation potential energy curves for the rotation around Ph-S bond of sulphacetamide molecule (A) and its azanion (B).

The dependence of the total energy on the central torsion angle, C–S–N–C (called τ_2, Scheme 1) is depicted in Figure 2. Internal rotation around the S–N bond, in the molecule and in azanion, also leads to a conformational isomerism. Three stable conformers were predicted both in the molecule and azanion: **1** (C–S–N–C, 60°) and **2** (C–S–N–C, –60°) and **3** (C–S–N–C, 180°). The conformers **1** and **2** were predicted to have relative energies within *ca.* 0.3 and 0.1 kJ·mol^{-1} for molecule and azanion, respectively, and then being expected to contribute significantly to the gas-phase conformation equilibrium. Conformers **3** in both molecule and azanion were found to be of no practical interest, because their energies are higher by more than 23 and 13 kJ·mol^{-1}, respectively than the energies of **1** and **2** conformers.

Conformation potential energy curves for the rotation around N–C bond of sulphacetamide molecule and its azanion are given in Figure 3. The S–N–C=O torsion angle is referred to as τ_3. Two possible conformers were located: **1** (S–N–C=O, 0°) and **2** (S–N–C=O, 180°). In this case, however, the

estimated conformational energy differences in the molecule are very small (<1 kJ·mol^{-1}) and no conclusive answer regarding the relative stability of the different conformers can be extracted by taking into consideration only the theoretical results. According to X-ray diffraction the τ_3 value is 7.2° [8]. Comparison of the energy values of these conformers in azanion indicates that conformer **2** is less stable by 10 kJ·mol^{-1} than conformer **1** in the gas state. In general, conformations **1** are within the range of (τ_3, 0–20) observed for secondary amides [15].

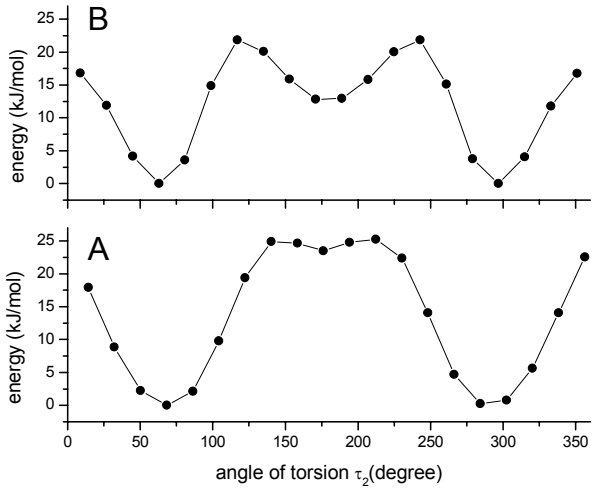

Fig. 2. Conformation potential energy curves for the rotation around S-N bond of sulphacetamide molecule (A) and its azanion (B).

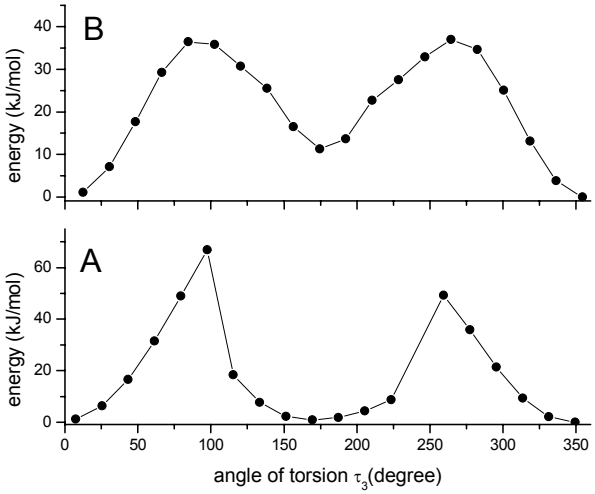

Fig. 3. Conformation potential energy curves for the rotation around N-C bond of sulphacetamide molecule (A) and its azanion (B).

The minima obtained by the scan for molecule and azanion were optimized at B3LYP/6-31++G** level. The relevant conformations are depicted in Scheme 2. All calculated geometry parameters of the most stable conformer for the molecule are presented in Table 1. The molecular structure data of sulphacetamide [8] determined by single crystal X-ray analyses are listed, too. According to X-ray data, the sulphur and amino nitrogen atoms are lying in the phenilene ring plane. The one of the sulphonyl oxygen is almost coplanar with the phenilene ring (<OSCC = 3.5), while the other is out of this plane (<OSCC = 44.7). The fragment containing S, N, C, C, O atoms is also planar and the dihedral angle between this plane and is 90.9. Similar results have been theoretically estimated for the isolated sulphacetamide molecule. As can be seen, there is a good agreement between the experimental and the theoretical structural parameters (the mean absolute deviations are 0.03Å for bond length and 1.0º for bond angle). The largest individual deviation of 0.076 Å corresponds to the S–N bond, whose N-atom participated directly in intermolecular interaction in the crystal state. The theoretical method used predicts correctly the N_8–C_9 and N_{14}–C_1 bond lengths which are in agreement with trigonal hybridization of the nitrogen atoms and with a C_9–C_{11} bond length close to the expected Csp^2–Csp^3 distances. The carbonyl distance C_9–O_{10} is equivalent to that of a partially double bond as the O atom is involved. In agreement between theory and experiment there are deviations of the phenyl ring bond lengths C_2–C_3 and C_5–C_6 from the remaining ones (Table 1). Similar partially quinoidal structures were observed in *p*-aminobenzoic acid [16], *p*-sulphanilamide [17] and *p*-sulphathiazole [18].

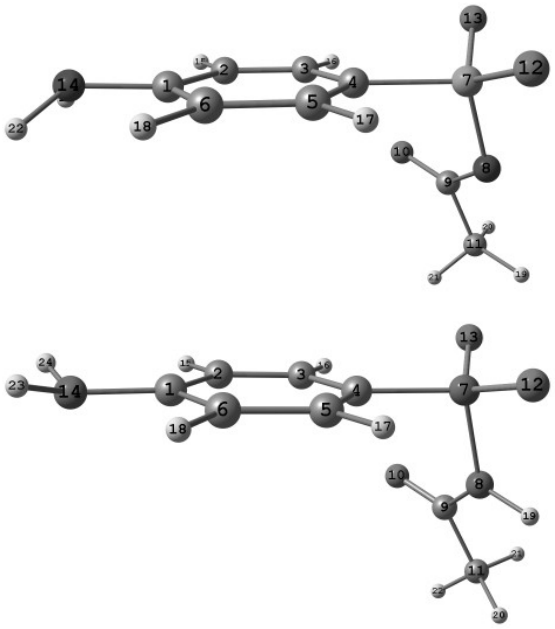

Scheme 2. Lowest energy conformer of neutral sulphacetamide (*down*) and its azanion (*up*) with atom numbering scheme.

Table 1. Theoretical and experimental values of bond lengths (Å), angles (degrees) and selected torsion angles (degrees) in the molecule of sulphacetamide.

Geometry parameters	B3LYP	X-ray [a]	Δ [b]
Bond lengths			
$R(C_1C_2)$	1.410	1.387(5)	0.023
$R(C_2C_3)$	1.384	1.372(5)	0.012
$R(C_3C_4)$	1.400	1.380(4)	0.020
$R(C_4C_5)$	1.400	1.385(4)	0.015
$R(C_5C_6)$	1.389	1.355(5)	0.034
$R(C_6C_1)$	1.410	1.405(4)	0.005
$R(S_7C_4)$	1.775	1.749(3)	0.026
$R(N_8S_7)$	1.729	1.653(3)	0.076
$R(C_9N_8)$	1.388	1.363(4)	0.025
$R(O_{10}C_9)$	1.219	1.216(5)	0.003
$R(C_{11}C_9)$	1.518	1.488(5)	0.030
$R(O_{12}S_7)$	1.469	1.419(5)	0.050
$R(O_{13}S_7)$	1.459	1.425(5)	0.034
$R(N_{14}C_1)$	1.384	1.366(5)	0.018
m.d. [c]	-	-	0.027
Bond angle			
$<(C_1C_2C_3)$	120.8	120.2(2)	0.6
$<(C_2C_3C_4)$	119.4	120.8(3)	1.4
$<(C_3C_4C_5)$	120.8	119.3(3)	1.5
$<(C_4C_5C_6)$	119.6	120.3(3)	0.7
$<(C_1C_6C_5)$	120.5	121.0(3)	0.5
$<(C_2C_1C_6)$	118.9	118.3(3)	0.6
$<(S_7C_4C_5)$	119.2	119.7(2)	0.5
$<(O_{12}S_7C_4)$	109.2	110.0(1)	0.8
$<(O_{13}S_7C_4)$	109.5	109.1(1)	0.4
$<(N_8S_7C_4)$	105.5	105.5(1)	0
$<(N_8S_7O_{12})$	101.1	103.2(1)	2.1
$<(N_8S_7O_{13})$	108.4	109.9(1)	1.5
$<(C_9N_8S_7)$	126.3	124.8(2)	1.5
$<(O_{10}C_9N_8)$	122.4	120.1(2)	2.3
$<(C_{11}C_9N_8)$	114.4	115.0(3)	0.6
$<(C_{11}C_9O_{10})$	123.2	124.8(3)	1.6
m.d.[c]			1.04
Torsion angle			
$<(N_8S_7C_4C_3)$	87.8	66.0	
$<(O_{12}S_7C_4C_3)$	164.2	134.8	
$<(O_{13}S_7C_4C_3)$	28.8	3.5	
$<(C_9N_8S_7O_{12})$	–47.1	–61.6	
$<(C_9N_8S_7O_{13})$	146.5	171.4	
$<(O_{10}C_9N_8S_7)$	10.1	7.2	
$<(C_{11}C_9N_8S_7)$	–169.3	–172.0	
$<(C_4S_7N_8C_9)$	68.2	55.8	

[a]Ref. 8; [b] Algebraic deviations between theoretical and experimental value; [c]Mean absolute deviation.

Certain geometry parameters (bond lengths and bond angles), calculated for the isolated azanion and sodium sulphacetamide monoxydrate determined by single crystal X-ray analyses, are compared in Table 2. The mean absolute deviation (m.a.d.) between the theoretical and experimental bond length is 0.020. This result can be considered as very good with m.a.d. values comparable to the average error for carbanions, oxyanions, azanions [19–22] and references therein. The theoretical method used predicts quite correctly also the bond angles (m.a.d. = 0.6º). The calculations predict that the largest structural deviations, caused by the molecule→azanion conversion, should be manifested as shortenings of the S–N and N–C bonds and lengthenings of the Ph–S, C=O, S=O bonds.

Table 2. Theoretical and experimental values of bond lengths (Å) and angles (degrees) in the azanion of sulphacetamide.

Geometry Parameters	B3LYP	X-ray [a]	Δ [b]
Bond lengths			
$R(C_1C_2)$	1.404	1.400(9)	0.004
$R(C_2C_3)$	1.394	1.382(9)	0.012
$R(C_3C_4)$	1.397	1.393(9)	0.004
$R(C_4C_5)$	1.396	1.392(10)	0.004
$R(C_5C_6)$	1.396	1.382(9)	0.014
$R(C_6C_1)$	1.403	1.387(9)	0.016
$R(S_7C_4)$	1.819	1.763(6)	0.056
$R(N_8S_7)$	1.641	1.603(5)	0.038
$R(C_9N_8)$	1.354	1.349(9)	0.005
$R(O_{10}C_9)$	1.247	1.247(7)	0
$R(C_{11}C_9)$	1.534	1.498(9)	0.036
$R(O_{12}S_7)$	1.484	1.444(6)	0.040
$R(O_{13}S_7)$	1.483	1.453(4)	0.030
$R(N_{14}C_1)$	1.414	1.394(8)	0.020
m.d. [c]	-	-	0.020
Bond angle			
$<(C_1C_2C_3)$	120.8	120.5(6)	0.3
$<(C_2C_3C_4)$	119.9	119.8(6)	0.1
$<(C_3C_4C_5)$	119.9	120.0(6)	0.1
$<(C_4C_5C_6)$	120.3	119.9(6)	0.4
$<(C_1C_6C_5)$	120.4	120.7(5)	0.3
$<(C_2C_1C_6)$	118.9	119.1(6)	0.2
$<(S_7C_4C_5)$	119.3	120.4(5)	1.1
$<(O_{12}S_7C_4)$	104.6	-	0
$<(O_{13}S_7C_4)$	106.3	107.7(3)	1.4
$<(N_8S_7C_4)$	108.3	107.3(3)	1
$<(N_8S_7O_{12})$	106.2	105.6(3)	0.6
$<(N_8S_7O_{13})$	114.0	113.5(3)	0.5
$<(C_9N_8S_7)$	120.0	121.5(4)	1.5
$<(O_{10}C_9N_8)$	129.5	-	0
$<(C_{11}C_9N_8)$	112.3	114.1(5)	1.8
$<(C_{11}C_9O_{10})$	118.2	119.3(3)	1.1
m.d. [c]			0.65
Torsion angle			
$<(N_8S_7C_4C_3)$	–94.9	145.0	
$<(O_{12}S_7C_4C_3)$	162.0	165.3	
$<(O_{13}S_7C_4C_3)$	37.8	22.5	
$<(C_9N_8S_7O_{12})$	–55.2	–55.2	
$<(C_9N_8S_7O_{13})$	174.7	179.2	
$<(O_{10}C_9N_8S_7)$	5.6	0.2	
$<(C_{11}C_9N_8S_7)$	–175.6	–179.3	
$<(C_4S_7N_8C_9)$	62.8	64.9	

[a] Refs. 9, 10; [b] Algebraic deviations between theoretical and experimental value; [c] Mean absolute deviation.

Acknowledgement: *The useful discussion with Prof. I. G. Binev, D.Sc., and the financial support by the Bulgarian Council of Scientific Research for Project Chem. – 1510 are politely acknowledged.*

REFERENCES

1. R. B. Silverman, The Organic Chemistry of Drug

Design and Drug Action, Academic Press, New York, 1992.
2. M. Wolff, Burger's Medicinal Chemistry, Wiley & Sons, New York, 1979.
3. Drug Information Handbook, Lexi-Comp, Hudson, OH, 2002, p 1100.
4. P. G. Benedetti, S. Quartieri, A. Rastelli, *J. Mol. Struct*., **85**, 45 1981.
5. E. C. Foernzler, A. N. Martin, *J. Pharm. Sci.,* **56**, 608 (1967).
6. J. R. B. Gomes, P. Gomes, *Tetrahedron*, **61**, 2705 (2005).
7. C. Soriano-Correa, R. O. Esquivel, R. P. Sagar, *Int. J. Quantum. Chem*., **94**, 165 (2003).
8. A. K. Basak, S. K. Mazumdar, *Cryst. Struct. Comm*., **11**, 1609 (1982).
9. H. C. Petel, T. P. Singh, *Acta Crystallogr*., **C43**, 844 (1987).
10. M. Ghosh, A. K. Basak, S. K. Mazumdar, *Acta Crystallogr*., **C46**, 1223 (1990).
11. M. J. Frisch, G. W. Trucks, H. B. Schlegel, G. E. Scuseria, M. A. Robb, J. R. Cheeseman, V. G. Zakrzewski, J. A. Montgomery, Jr., R. E. Stratmann, J. C. Burant, S. Dapprich, J. M. Millam, A. D. Daniels, K. N. Kudin, M. C. Strain, O. Farkas, J. Tomasi, V. Barone, M. Cossi, R. Cammi, B. Mennucci, C. Pomelli, C. Adamo, S. Clifford, J. Ochterski, G. A. Petersson, P. Y. Ayala, Q. Cui, K. Morokuma, D. K. Malick, A. D. Rabuck, K. Raghavachari, J. B. Foresman, J. Cioslowski, J. V. Ortiz, A. G. Baboul, B. B. Stefanov, G. Liu, A. Liashenko, P. Piskorz, I. Komaromi, R. Gomperts, R. L. Martin, D. J. Fox, T. Keith, M. A. Al-Laham, C. Y. Peng, A. Nanayakkara, C. Gonzalez, M. Challacombe, P. M. W. Gill, B. Johnson, W. Chen, M. W. Wong, J. L. Andres, M. Head-Gordon, E. S. Replogle, J. A. Pople, *Gaussian 98*, Revision A.7, Gaussian, Inc., Pittsburgh PA, 1998
12. A. D. Becke, *J. Chem. Phys.*, **98** (1993) 5648.
13. C. Lee, W. Yang, R. G. Parr, *Phys. Rev.*, **B37** (1988) 785.
14. A. Kalman, M. Czugler, G. Argay, *Acta Crystallogr*., **B37**, 868 (1981).
15. D. A. Adsmond, D. J. V. Grant, *J. Pharm. Sci*., **90**, 2058 (2001)
16. F. T. Lai, E. N. Marsh, *Acta Crystallogr*., **22**, 885 (1967).
17. A. M. O'Connel, E. N. Maslen, *Acta Crystallogr*., **22**, 134 (1967).
18. G. J. Kruger, G. Gafner, *Acta Crystallogr*., **B27**, 134 (1971).
19. L. Daskalova, I. Binev, *Int. J. Quantum. Chem*., **106**, 1338 (2006).
20. Y. G. Binev, M.K. Georgieva, L. Daskalova, *Spectrochim. Acta,* **60**, 2601 (2004).
21. L. I. Daskalova, E. A. Velcheva, I. G. Binev *J. Mol. Struct.,* **826**, 198 (2007).
22. A. Popova, M.K. Georgieva, O. I. Petrov, K. V. Petrova, E. A. Velcheva, *Int. J. Quant. Chem.,* **107**, 1752 (2007).

ТЕОРЕТИЧНО ИЗСЛЕДВАНЕ НА КОНФОРМАЦИОННИТЕ ПРЕДПОЧИТАНИЯ НА N-[(4-АМИНОФЕНИЛ)СУЛФОНИЛ]АЦЕТАМИД (СУЛФАЦЕТАМИД) И НЕГОВИЯ АЗАНИОН

Б. А. Стамболийска*, А. Д. Попова, Е. А. Велчева

Лаборатория „Структурен органичен анализ", Институт по органична химия с център по фитохимия, Българска академия на науките, ул. „Акад. Г. Бончев", бл. 9, 1113 София

Посветена на акад. Иван Юхновски по повод на 70-та му годишнина

Постъпила на 18 декември 2007 г.; Преработена на 25 януари 2008 г.

(Резюме)

Потенциалните енергетични повърхности на N-[(4-аминофенил)сулфонил]ацетамид (сулфацетамид) и неговия азанион са изследвани чрез теорията на фукционала на плътността на ниво B3LYP/6-31G*. Три торзионни ъгъла (C–C–S–N, C–S–N–C и S–N–C=O) са използвани за описанието на възможните конформациите на изследваните частици. Предпочетените структури получени при сканирането за молекулата (∠C–C–S–N, 90°; ∠C–S–N–C, 60° и ∠S–N–C=O, 0°) и азаниона (∠C–C–S–N, –90°; ∠C–S–N–C, 60° и ∠S–N–C=O, 0°), са оптимизирани на ниво B3LYP/6-31++G**. Оптимизираните структурни параметри за молекулата и азаниона за сравнени с експерименталните рентгеноструктурни данни. Установени са геометричните промени, произтичащи от превръщането на молекулата в анион.

Bulgarian Chemical Communications, Volume 40, Number 4 (pp. 450–455) 2008

Computational study of the electronic spectra of some B–N dyes

S. M. Bakalova[1], J. Kaneti[1,2]*, O. Castaño[2]

[1] *Institute of Organic Chemistry with Centre of Phytochemistry, Bulgarian Academy of Sciences, 1113 Sofia, Bulgaria*
[2] *Department of Physical Chemistry, Universidad de Alcalá, 28871 Alcalá de Henares (Madrid), Spain*

Dedicated to Academician Ivan Juchnovski on the occasion of his 70th birthday

Received December 21, 2007; Revised January 17, 2008

Boron "complexes" of dipyrromethenes (BDP) have found wide application as excellent optoelectronic materials and luminescent chemo- and bio-sensors since the very end of the past century. Their high absorption coefficients and fluorescence quantum yields in the VIS spectral region are augmented by outstanding resistance to photodegradation. Presently, a large amount of empirical, unstructured knowledge on the relationships between molecular structure and spectroscopic parameters of BDP dyes has been accumulated. High level correlated calculations, CISD with size consistency corrections, reproduce fairly well the energies of lowest pyrromethene singlet excited states, but have a prohibitively high computational cost and do not satisfactorily predict substituent effects, Stokes' shifts, and solvent effects on either absorption or emission.

We apply a recently proven semiempirical CISD AM1 methodology to study excited state energies and substituent effects on pyrromethene chromophores, parallel to TD DFT computations of the Frank-Condon absorption and emission transition energies. This combination of methodologies is a robust approach to the rational search for new compounds within the relatively novel class of boron-containing optical materials.

Key words: borindacene dyes, fluorescence, AM1, B3LYP and B2PLYP calculations.

INTRODUCTION

The search for new classes of heterocyclic compounds as fluorescent indicators and laser dyes is a challenging and rapidly advancing area. Pyrrolo-boraheterocycles such as [2,3-a,5,6-a]bis-pyrrolo-1,1-difluoro-[1,2,6]-boradiazine, or 4,4-difluoro-borindacene **1**, BDP, Scheme 1, [5–7] have a number of convenient properties, in particular an outstanding resistance to photodegradation, high molar absorptivities and high fluorescence quantum yields. BDP dyes have found interesting applications as optoelectronic materials, laser active media and molecular chemo- and bio-sensors. [8–12].

There is indeed some remote topological similarity between borindacenes and triphenylmethane dyes, e.g. rhodamines as well as fluorescein, which has probably contributed to the rapid commercialization of the new heterocycles under the trademark BODIPY® [11, 12], but hardly to the understanding of structural and electronic factors behind the observed photophysical properties. The latter factors have been thoroughly studied with rhodamines, [4] while the introduction of the scarcely known boron atom into the seemingly aromatic [5–12] boraheterocycles renders a wide unexplored area open to imagination and research.

X-ray structural as well as computational studies in general confirm the supposedly aromatic structure of pyrrolo-boraheterocycles [1, 2, 10]. The rather numerous computational papers however provide no detailed description of the nature of the excited states and, in particular, of the fluorescent states. Knowledge of structural changes and electronic distributions of the latter geometry relaxed excited states is necessary for the description of such quantities as emission wavenumbers and Stokes' shifts. This information could signifycantly amplify the capacity for rational search for and design of new compounds with promising photophysical and photochemical properties as fluorescent probes for biological assays. Notably, solvent effects on both absorption and emission maxima of BDP are minimal [5–7] and they will not be considered in the present study.

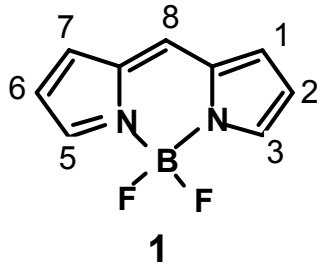

1

Scheme 1. Structural sketch of the parent 4,4-difluoro-*s*-borindacene.

* To whom all correspondence should be sent:
E-mail: kaneti@orgchm.bas.bg

© 2008 Bulgarian Academy of Sciences, Union of Chemists in Bulgaria

COMPUTATIONAL DETAILS

To model the well known electron excitation – emission cycle of Jablonski [3], Scheme 2, we use a computational cycle consisting of the following steps:

1. Semiempirical CISD calculation of the equilibrium geometry of the S_0 electronic state of the molecules with full geometry relaxation.

2. Single point semiempirical CISD, as well as TD DFT calculations of the S_1 energy at the S_0 geometry, relating the results to vertical Frank-Condon $S_0 \rightarrow S_1$ absorption transition energies.

3. Semiempirical CISD calculation of the equilibrium geometry of the S_1 (or, possibly, T_1) electronic state with full geometry relaxation.

4. Single point semiempirical CISD and TD DFT calculations of the S_0 energy at the S_1 (or, possibly, the T_1) geometry and relating the transition energies to the corresponding vertical $S_1 \rightarrow S_0$ and $T_1 \rightarrow S_0$ emission energies.

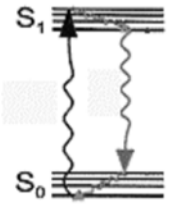

Scheme 2. The simplified Jablonski cycle, used in the computational modelling.

While having so far used semiempirical AM1 method in all steps of the model computational cycle, we are aware of its deficiencies, in particular its inability to reproduce simultaneously the qualitative trends in substituent and solvent effects on both electronic absorption and emission spectra for any given chemical compound or series of compounds. Apparently the same situation exists also with TD DFT or TD HF or nonempirical MO CIS calculations of electronic spectra [4]. The reasons for the present computational situation are clear: absorption spectra can be routinely reproduced as vertical electron excitation energies from the ground molecular electronic states. However, CIS and TD DFT geometry optimizations of excited electronic states are troublesome and unreliable due to their multireference nature [4]. Therefore, we take the liberty to carry out semiempirical CISD geometry optimizations of electronic states of interest, and use TD DFT at the latter semiempirical geometries to obtain the vertical transition energies for electron excitation as well as emission processes. The calculated TD DFT energies for the ground and lowest excited molecular electronic states are corrected for dynamic electron correlation using the recently introduced double-hybrid functional B2PLYP [13], which uses the "resolution of identity" methodology to introduce perturbational MP2 corrections to the standard generalized gradient (GGA) DFT energy [13, 14]. All CISD AM1 computations are performed with MOPAC 93 with c.i. = 5 open (2,2) EF for the semiempirical geometry optimizations [15]. Despite the semiempirical nature of AM1, CISD geometry optimizations are still very laborious. We persisted with the optimization process until reducing the calculated gradient norm below 1 kcal/Å or radian. For the TD B2PLYP 6-311++G(2d,2p) single point energy calculations we use ORCA [16] at the optimized AM1 geometries.

RESULTS AND DISCUSSION

Electronic transition energies of medium size molecules are so far among the most problematic properties to reproduce by quantum mechanical calculations, giving at best a precision of e.g. 0.2 eV for electronic absorption energies, and in quite a few cases much worse [17]. Recent high basis set level TD DFT computations have shown convergence to significantly better precision, e.g. below 0.05 eV relative to the experiment, using augmented triple zeta basis sets and explicit treatments of solvent effects on electron transition energies. [17]. The computational cost of these calculations is however still too high for routine screening of large batches of essentially unknown heterocyclic structures for the desired photophysical and photochemical properties. Our goal is rather a pragmatic search for a satisfactory, robust approach for the prediction of electronic absorption and emission energies, as well as their solvent dependence. Such an approach, a methodology or combination of methodologies, would ultimately lead to the ability to rationalize the search for new molecules with suitable photophysical and optoelectronic properties.

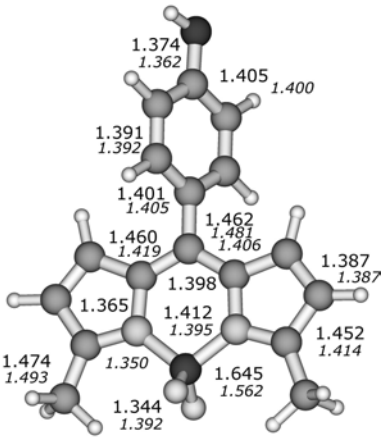

Fig. 1: CISD AM1 and B3LYP/6-31G* (*italics*) ground state geometries of 8-[4'-hydroxyphenyl]-4,4-difluoro-*s*-borindacene. Bond lengths are given in Å.

A prerequisite condition for the use of combined computational methodologies as rational search tools is the consistency of computed molecular parameters. In the present case, we note that CISD AM1 and B3LYP/6-31G* geometries of borindacene derivatives are reasonably close, with bond length differences usually below 0.02 Å, Fig. 1. For the shown borindacene derivative, the only more significant differences in calculated bond lengths between AM1 and B3LYP/6-31G* are for B–N, 1.645 vs. 1.562 Å, and B–F, 1.344 vs. 1.392 Å. The calculated rotation angle of the 8-aryl fragment relative to the borindacene is 56° (AM1), resp. 53°, (DFT).

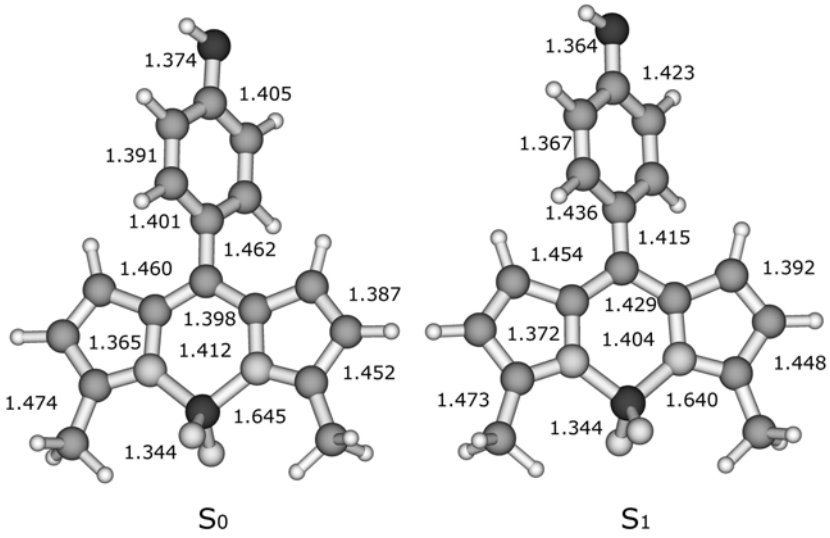

Fig. 2. CISD AM1 ground S_0 and first excited S_1 singlet state geometries of 8-[4'-hydroxyphenyl]-4,4-difluoro-*s*-borindacene. Bond lengths are given in Å.

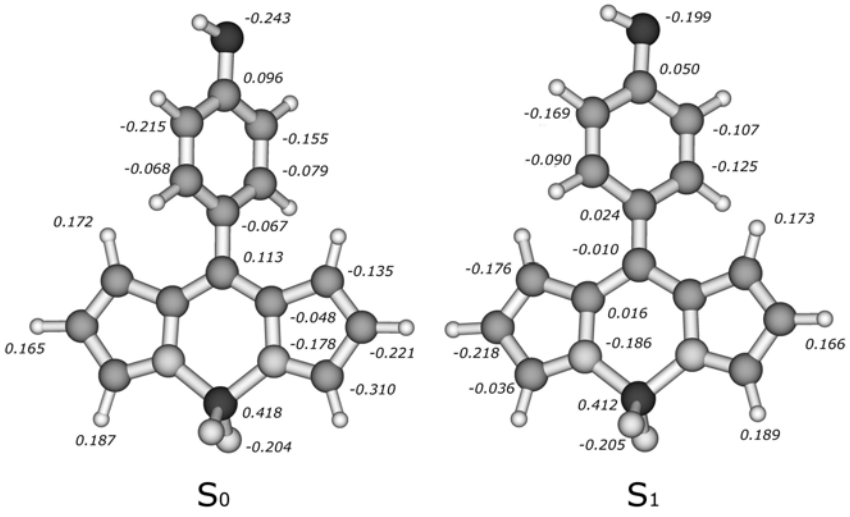

Fig. 3. CISD AM1 atomic point charges of 8-[4'-hydroxyphenyl]-4,4-difluoro-*s*-borindacene in the ground S_0 and first excited S_1 singlet states.

Some understanding of the nature of electronic transitions in 8-aryl-BDP dyes can be gained by comparison of their geometries in the ground S_0 and excited S_1 electronic states. Bond length values calculated at the CISD AM1 semiempirical MO level are compared in Fig. 2 for the 4'-hydroxyphenyl derivative. In the S_1 geometry of the aryl fragment one observes some indication of bond length redistribution typical of intramolecular charge transfer (ICT) dye molecules. However, these changes do not clearly characterize the underlying electron density redistribution taking place upon excitation from the S_0 to the S_1 state. Computed CISD AM1 atomic point charges of the ground S_0 and excited S_1 state are shown in Fig. 3.

Similar to geometry changes, the point charge redistribution in case of S_0–S_1 excitation does not clearly reflect the ICT pattern, widely discussed in relation to traditional dyes [6, 10]. Therefore, to clarify the nature of the lowest energy electron excitations in 8-aryl borindacenes, we consider explicitly the molecular orbitals taking part in the process (Fig. 4).

Fig. 4. Molecular orbitals of 8-[4'-hydroxyphenyl]-4,4-difluoro-borindacene, taking part in lowest electronic excitations. The approximate C_{2v} symmetry is apparent.

Table 1: Longest wavelength absorption and fluorescence emission maxima (ν) of 8-aryl substituted 3,5-dimethyl-4,4-difluoro-s-borindacenes, together with the respective Stokes' shifts (Δν) in cyclohexane [5–7] and calculated vertical electron transition energies (E), 10^3 cm^{-1}. Also given are the fluorescence quantum yields ϕ and theoretical oscillator strength *F*, derived from the B2PLYP/6-311++G(2d,2p) calculations.

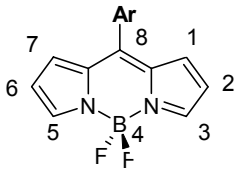

Aryl	ν_{abs}	ν_{em}	Δν	ϕ	E_{abs}		*F*	E_{em}		*F*
					AM1	B2PLYP		AM1	B2PLYP	
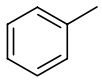	19.53	19.08	0.447	0.29	23.85	24.15	0.80	19.69	22.35	0.68
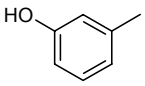	19.53	19.05	0.484	0.25	23.60	24.12	0.81	19.30	22.18	0.67
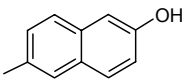	19.53	19.08	0.556	0.17	25.43	24.05	0.78	21.00	22.03	0.61
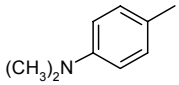	19.69	19.31	0.454	0.15	24.89	24.02	0.76	18.59	22.65	0.66
								21.16	23.28	0.60
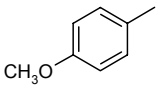	19.61	19.19	0.414	0.42	24.60	23.95	0.74	20.09	22.75	0.80
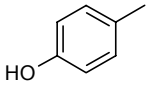	19.61	19.19	0.414	0.45	24.60	24.29	0.81	20.19	22.85	0.69
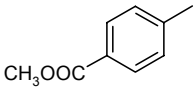	19.42	18.76	0.656	0.073	23.70	23.81	0.78	19.45	21.12	0.60
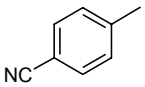	19.34	18.55	0.789	0.038	23.78	23.66	0.77	19.14	21.00	0.59

TD DFT calculations reveal a common characteristic of all three computed lowest singlet excited states. In all the 8-aryl-4,4-difluoro-borindacene molecules investigated computationally these states are dominated by electron excitations from consecutive highest occupied orbitals to the lowest unoccupied orbital. The corresponding CI expansions are regularly dominated up to 90% and more by excitations from HOMO to LUMO, S_1; from HOMO-1 to LUMO, S_2; and from HOMO-2 to LUMO, S_3, Fig. 4. Orbital distributions of the three highest occupied MO's together with the LUMO, also reveal a relatively little absolute dipole moment change upon corresponding electron excitations, but significant change of dipole moment directions.

Substituents at position 8 of 4,4-difluoroborindacenes preserve the C_{2v} local symmetry of the parent molecule and thus provide a clear insight into the nature of electronic transitions. $S_0 \rightarrow S_1$ excitation in BODIPY® molecules is accompanied by

intense electron density reorganization from peripheral pyrrolic fragments towards the local C_2 symmetry axis and, in the case of π-electron withdrawing substituents as CN and $COOCH_3$ in the 8-aryl fragment, also to the electron acceptor substituent along the same twofold symmetry axis. This explains the calculated high oscillator strengths for the lowest energy excitations of these compounds and the observed high molar absorptivities [6, 10].

Particularly revealing are the predicted in agreement with experiment substituent effects on absorption and emission Frank-Condon transition energies, Table 1. Electron withdrawing substituents in the aryl fragment at position 8 stabilize the S_1 excited state by drawing the electron density to the central bora-heterocycle, thereby shifting both the $S_0 \rightarrow S_1$ and the $S_1 \rightarrow S_0$ electronic transitions in the direction to the red. Vice versa, π -electron donating substituents in the aryl fragment at position 8 destabilize the S_1 state by drawing electronic density away from the symmetry axis, which results in a blue shift of the electronic transitions. Due to the nonplanar arrangement of 8-aryl substituents relative to the borindacene, the mentioned electronic effects are relatively small. Nevertheless, the above observations are completely opposite to the traditional electronic substituent effects on the absorption or emission Frank-Condon energies of classical ICT organic chromophores like 4-dimethylaminobenzonitrile, or 2-propionyl-6-dimethylamino-naphthalene, PRODAN [1].

The results in Table 1 clearly reflect the trends outlined above based on considerations of BODIPY® orbitals. However, calculated absorption Frank-Condon energies are higher than experimental values by roughly 0.5 eV, or ca. 4000 cm^{-1}, i.e. a much worse result than recent B3LYP and PBE0 predictions [17]. This failure of single point TD B2PLYP/AM1 calculations to predict electronic absorption spectra is possibly due to obsolete boron atom parameterization in the original version of AM1 [18], now abandoned in the recent versions of MOPAC and superseded by PM3 and PM6 [15, 19]. Another possible reason for the faulty representation of BODIPY® ground electronic states may be the inability of semiempirical calculations to represent B–N bonding and its participation in the π-electronic system of borindacenes correctly. The latter conjecture is based on the fact that the largest discrepancy between AM1 and B3LYP/6-31G* geometries of borindacenes, almost 0.1 Å, refers exactly to the B–N bond length. Further complete B2PLYP studies of borindacenes will certainly bring clarity to this point.

A considerably better relationship is obtained between theoretical B2PLYP/6-311++G(2d,2p)//CISD AM1 and experimentally observed emission Frank-Condon energies, Fig. 5. While the absolute differences between the latter values and calculated $S_1 \rightarrow S_0$ vertical transition energies are still high, in the range of 0.3 eV (2500 cm^{-1}) and the slope of the linear relationship is relatively high, the vanishing intercept certainly indicates that CISD AM1 geometries of the emitting state, S_1 in the case of BODIPY®, represent qualitatively correctly the structural changes upon excitation. This result is another argument in favour of our computational approach in modeling the "simplified Jablonsky cycle", Scheme 2, in the spectroscopic and theoretical study of molecular excited electronic states.

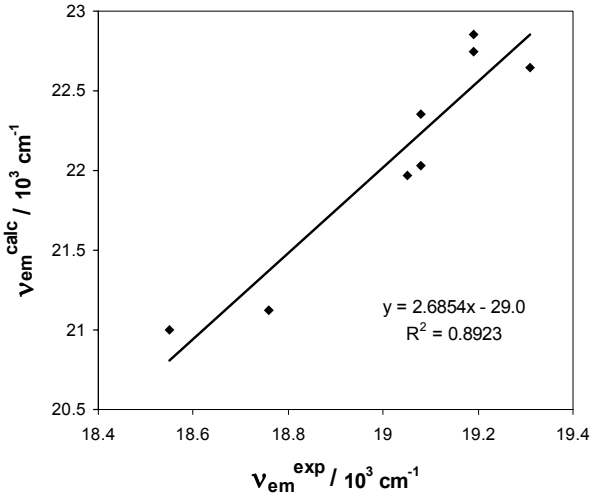

Fig. 5. The linear relationship between experimental and calculated single point B2PLYP 6-311++G(2d,2p)//CISD AM1 fluorescence emission energies.

Apparently, one more argument in the favour of our "reduced model of Jablonsky cycle" is the predicted dual emission of 8-[4'-dimethylaminophenyl]-4,4-difluoro-borindacene, coming from closely lying adjacent S_1 and S_2 excited electronic states (Table 1). As it was stated in the above orbital analysis, the S_2 state is dominated by the HOMO-1 to LUMO excitation, Fig. 4, and should thus be a true charge transfer electronic state. Dual fluorescence of 4'-aminophenyl borindacenes has indeed been observed experimentally [6], the relative intensity of the two bands depending on the solvent and certainly deserving further more detailed theoretical analysis.

CONCLUSION

A satisfactory linear relationship between calculated single point B2PLYP/6-311++G(2d,2p)//CISD AM1 $S_1 \rightarrow S_0$ emission energies and experimental fluorescence Frank-Condon energies of B–N containing 8-aryl-4,4-difluorobora-*s*-indacene dyes, BODIPY®, is in favour of the qualitative correctness of our recently introduced computational

approach modeling a "simplified Jablonsky cycle" to study structures and energies of excited molecular electronic states. However, in the studies of atypical B–N molecules at the boundary between organic and inorganic species, failure of semiempirical descriptions of corresponding ground electronic states cannot be excluded.

REFERENCES

1. J. R. Lakowicz, Principles of Fluorescence Spectroscopy, 2nd edn., Kluwer, NY, 1999, pp. 63–93.
2. P. Acebal, S. Blaya, L. Carretero, *Chem. Phys. Lett.,* **374**, 206-214 (2003).
3. S. Bakalova, J. Kaneti, *Spectrochim. Acta A,* **56**, 1443 (2000).
4. A. Dreuw, M. Head-Gordon, *Chem. Rev.,* **105**, 4009 (2005).
5. W. Qin, M. Baruah, A. Stefan, M. van der Auweraer, N. Boens, *Chem. Phys. Chem.,* **6**, 2343 (2005).
6. W. W. Qin, M. Baruah, M. van der Auweraer, F. C. De Schryver, N. Boens, *J. Phys. Chem. A,* **109**, 7371 (2005).
7. M. Baruah, W. W. Qin, N. Basaric, W. M. De Borggraeve, N. Boens, *J. Org. Chem.,* **70**, 4152 (2005).
8. J. B. Prieto, F. L. Arbeloa, V. M. Martinez, T. A. Lopez, F. Amat-Guerri, M. Liras, I. L. Arbeloa, *Chem. Phys. Lett.,* **385**, 29 (2004).
9. J. B. Prieto, F. L. Arbeloa, V. M. Martinez, I. L. Arbeloa, *Chem. Phys.,* **296**, 13 (2004).
10. F. L. Arbeloa, J. Banuelos, V. Martinez, T. Arbeloa, I. L. Arbeloa, *Internat. Rev. Phys. Chem*., **24**, 339 (2005).
11. Bioprobes 25: New Probes and Applications, Molecular Probes Inc., Eugene, Oregon, 1997.
12. R. P. Haugland, Handbook of Fluorescent Probes and Research Chemicals, 9th edn.; Molecular Probes Inc., Eugene, OR, 2002.
13. S. Grimme, *J. Chem. Phys.,* **124**, 034108 (2006).
14. S. Grimme, F. Neese, *J. Chem. Phys.,* **127**, 154116 (2007).
15. J. J. P. Stewart, *J. Mol. Model.,* **13**, 1173 (2007). MOPAC2007, J. J. P. Stewart, Stewart Computational Chemistry, Colorado Springs, CO, USA, 2007**,** HTTP://OpenMOPAC.net.
16. F. Neese, ORCA, University Bonn, 2007.
17. D. Jacquemin, E. A. Perpete, G. E. Scuseria, I. Giofini, C. Adamo, *J. Chem. Theory Comput.,* 4, 123 (2008).
18. M. J. S. Dewar, C. Jie, E. G. Zoebish, *Organometallics,* **7**, 513 (1988).
19. J. J. P. Stewart, *J. Mol. Model.,* **10**, 155 (2004).

ИЗЧИСЛИТЕЛНО МОДЕЛИРАНЕ НА ЕЛЕКТРОННИТЕ СПЕКТРИ НА НЯКОИ БАГРИЛА, СЪДЪРЖАЩИ ВРЪЗКАТА B–N

Сн. М. Бакалова[1], Х. Ян. Канети[1,2]*, Об. Д. Кастаньо[2]

[1] *Институт по органична химия с център по фитохимия, Българска академия на науките, ул. „Акад. Г. Бончев", Блок 9, 1113 София*

[2] *Департамент по физикохимия, Университет Алкала, 28871 Алкала де Енарес, Мадрид, Испания*

Посветена на акад. Иван Юхновски по повод на 70-та му годишнина

Постъпила на 21 декември 2007 г.; Преработена на 17 януари 2008 г.

(Резюме)

Борните „комплекси" на дипирометени, БДП, намират широко приложение като превъзходни оптоелектронни материали и луминесцентни хемо- и биосензори от самия край на миналия век. Те имат високи моларни абсорбционни коефициенти и флуоресцентни квантови добиви във видимата област, както и изключителна фотостабилност. Досега е натрупан голям обем емпирични неструктурирани факти за връзката между молекулна структура и спектроскопски параметри на БДП багрила. Пресмятанията на високо ниво, CISD с корекции за съразмерност на вълновите функции, отчитат задоволително енергиите на най-ниските синглетни възбудени състояния на пирометени, но имат твърде висока цена в изчислителни ресурси и не възпроизвеждат ефектите на заместителя, Стоксовите отмествания и ефектите на разтворителя както върху абсорбцията, така и върху емисията.

Ние прилагаме един наскоро въведен полуемпиричен CISD AM1 подход за изчисляване на енергиите на възбудените състояния и ефектите на заместителя при пирометенови хромофори, съвместно с TD DFT пресмятания на енергиите на Франк-Кондоновите абсорбционни и емисионни преходи. Това съчетание на методики е удобен подход за рационално търсене на нови съединения в сравнително новия клас бор-съдържащи оптични материали.

Bulgarian Chemical Communications, Volume 40, Number 4 (pp. 456–463) 2008

Solid-state IR-LD spectroscopy of L-tryptophan-containing dipeptides L-tryptophyl-L-methionine (H-Trp-Met-OH), L-methionyl-L-tryptophan (H-Met-Trp-OH) and glycyl-L-tryptophan dihydrate (H-Gly-Trp-OH.2H_2O)

B. B. Koleva

St. Kliment Ohridsky Sofia University, Faculty of Chemistry, 1, J. Bourchier, Blv., 1164 Sofia, Bulgaria

Dedicated to Academician Ivan Juchnovski on the occasion of his 70th birthday

Received January 2, 2008, Revised January 11, 2008

IR-spectroscopic and structural elucidation of L-tryptophan-containing dipeptides L-tryptophyl-L-methionine (H-Trp-Met-OH), L-methionyl-L-tryptophan (H-Met-Trp-OH) and glycyl-L-tryptophan dihydrate (H-Gly-Trp-OH.2H_2O) by means of solid-state linear dichroic IR- (IR-LD) spectroscopy of orientated colloid suspensions in nematic host is performed. A correlation structure-spectroscopic property of the latter compound is done, comparing IR-LD and known single crystal X-ray diffraction data. Quantum chemical *ab initio* and DFT calculations of H-Trp-Met-OH/H_2O and H-Met-Trp-OH/H_2O systems support is made in addition to the IR-LD spectroscopic analysis.

Key words: L-tryptophyl-L-methionine (H-Trp-Met-OH), L-methionyl-L-tryptophan (H-Met-Trp-OH), glycyl-L-tryptophan dehydrate, solid-state linear polarized IR-LD spectroscopy, quantum chemical calculations.

INTRODUCTION

Tryptophan-containing peptides are intensively studied during the last years, due to their possibility to recognize and cleave DNA at apurinic sites [1]. On the other side the aromatic interactions in tryptophan-containing peptides have been also studied [2]. A series of small peptides has been structurally investigated by single crystal X-ray diffraction [2]. As a part of systematic spectroscopic and structural elucidation of small peptides, their salts and metal complexes have been studied [3–15] by means of solid-state IR-LD spectroscopy of orientated colloids in nematic mesophase [16–19], herein included L-tryptophane containing dipeptides as L-tryptophyl-L-methionine (H-Trp-Met-OH) and L-methionyl-L-tryptophan (H-Met-Trp-OH) (Scheme 1). The conclusions about the structures of the above stated dipeptides are supported by the additionally performed IR-LD characterization of glycyl-L-tryptophan dihydrate (H-Gly-Trp-OH.2H_2O), shown in Scheme 1. The crystal structure of H-Gly-Trp-OH.2H_2O has been determined by single crystal X-ray diffraction [20], thus allowing a comparison between spectroscopic and structural data, i.e. correlation between structure-optical properties.

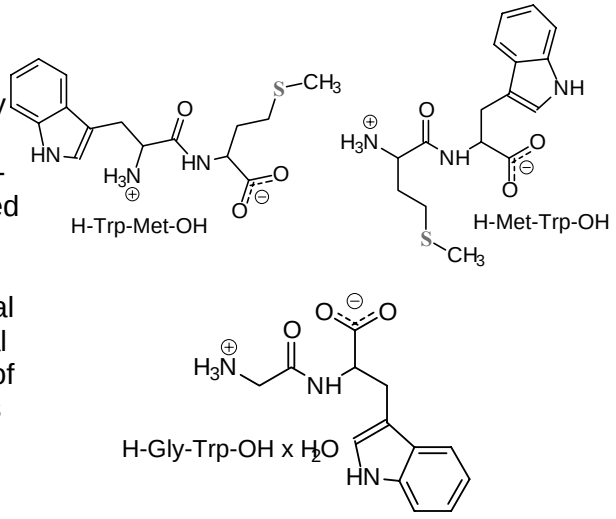

Scheme 1. Chemical diagram of dipeptides H-Trp-Met-OH, H-Met-Trp-OH and H-Gly-Trp-OH.2H_2O.

EXPERIMENTAL

Both peptides are “Bachem” (Switzerland) products. The H-Gly-Trp-OH.2H_2O is obtained by the procedure described in [20]. The purity of the studied compound was proved by mass spectrometry (ESI) and ^{1}H-NMR.

The IR-spectra were measured on a THERMO NICOLET 6700 FTIR-spectrometer (4000–400 cm^{-1}, 1 cm^{-1} resolution, 200 scans) equipped with a Specac wire-grid polarizer. The non-polarized solid-state IR spectra were recorded using KBr disk

* E-mail: BKoleva@chem.uni-sofia.bg

© 2008 Bulgarian Academy of Sciences, Union of Chemists in Bulgaria

technique. The orientated samples were obtained as a colloid suspension in a nematic host (ZLI 1695, Merck), using the method described in [16–19]. The application of colloid suspensions in nematic liquid crystal host allows IR-spectroscopic and structural elucidation of embedded solid particles, which was demonstrated in series of papers dealing with characterization of inorganic compounds and glasses [21], organic and coordination compounds (see Refs. 3–19). It has been found out [19] that a partial orientation (15–20%) of suspended particles (Scheme 2), adequate for the recording of reasonable linearly polarized IR-spectra is achieved, when 5 ± 1% by weight of the given solid compound, with particle size within the limits 0.3–0.9 μm, is mixed with a nematic liquid crystal substance (ZLI 1695, ZLI 1538 or MLC 6815) suitable for IR spectroscopy and the obtained slightly viscous suspension is phase pressed between two KBr plates. They are roughened in one direction prior to use with fine sandpaper (C800) (size 5 μm). The KBr-plates and pressed suspension are moved repeatedly with 3 μm/s for 100 times. The optimal cell thickness is 100 μm. The validation of this orientation solid-state method in regard to accuracy and precision, the influence of the liquid crystal medium on peak positions and integral absorbances of the guest molecule bands have been represented [17,18]. The reological model, the nature and balance of the forces in the nematic liquid crystal suspension system, the mathematical model, and morphology of the suspended particles are discussed [19].

Scheme 2. Electron microscopic data of the colloid suspension in nematic host.

The interpretation of the non-polarized and polarized infrared spectra includes determination of the position (ν_i) and integral absorbances (A_i) for each i-peak by deconvolution and curve fitting at a 50:50% ratio of Lorentzian to Gaussian peak functions. Usually χ^2 factor varies within 0.00013–0.00008 (in our case 1.2×10^{-5}–2.3×10^{-4}) and 2000 iterations [17, 18]. The mean values of two treatments were compared by the Student-test. The experimental IR-spectral patterns were acquired and processed by means of the GRAMS/AI 7.01 IR spectroscopy (Thermo Galactic, USA) and the STATISTICA for Windows 5.0 (StatSoft, Inc., Tulsa, OK, USA) program packages.

Spectroscopic and structural results by orientation technique presented here were obtained using the known "reducing-difference procedure" designated as "stepwise reduction" for polarized IR-spectra interpretation. This method was initially suggested by Thulstrup and Eggers for the interpretation of polarized UV-spectra [22]. The procedure involves consecutive elimination of the spectral bands of a given polarization by subtracting the perpendicular spectrum multiplied by a coefficient from the parallel one. This procedure was extended by Spanget-Larsen [23] and by Korte and Lampen [24] to include samples orientated in stretched polyethylene and in nematic solution, respectively. A systematic analysis of this approach and its application to IR-band assignment according to their symmetry appurtenance was developed by Jordanov and co-workers [25–28] for polarized IR-LD spectra in nematic liquid crystal solution. The method consists of subtraction of the perpendicular spectrum, ($IR_\perp$, resulting from a 90° angle between the polarized light beam electric vector and the orientation of the sample) from the parallel one ($IR_\parallel$) obtained with a co-linear mutual orientation. The recorded difference ($IR_\parallel$-$IR_\perp$) spectrum divides the corresponding parallel ($A_\parallel$) and perpendicular ($A_\perp$) integrated absorbencies of each band into positive values originating from transition moments, which form average angles with the orientation direction ($\mathbf{n}$) between 0° and 54.7° (magic angle), and negative ones corresponding to transition moments between 54.7° and 90°. In the reducing-difference procedure, the perpendicular spectrum multiplied by the parameter c, is subtracted from the parallel one and c is varied until at least one band or a set of bands is eliminated. The simultaneous disappearance of these bands in the obtained reduced IR-LD spectrum ($IR_\parallel$-$cIR_\perp$) indicates co-linearity of the corresponding transition moments, thus yielding information regarding the mutual disposition of the molecular fragments.

The optimization of the structures of the peptides in the systems peptide/H$_2$O was carried out by DFT calculations (B3LYP) at 6-31+G** basis set using the Gaussian 98 and Dalton 2.0 program packages [29, 30]. The visualization of the output files is done by ChemCraft 5.0 [31]. The methodology for exploring the conformational energy landscape described in [32, 33] was used in our case too. The scheme first creates all possible conformers by rotating around the flexible bonds according to a set

of suitable step sizes and then employs a hierarchy of increasingly more accurate electronic structure methods. For every structure the stationary points found on the molecule potential energy hyper-surfaces were characterized using standard analytical harmonic vibrational analysis. The absence of imaginary frequencies, as well as of negative eigenvalues of the second-derivative matrix, confirmed that the stationary points correspond to minima of the potential energy hyper-surfaces. The calculations of vibrational frequencies and infrared intensities were checked to establish which kind of performed calculations agrees best with the experimental data.

RESULTS AND DISCUSSION

The non-polarized IR-spectra of the dipeptides are depicted in Figs. 1.1A and 1.1B. The IR-characteristic band assignment is listed in Table 1. The NH stretching vibration ν_{NH}) is observed within 3326–3446 cm^{-1} range. The indole stretching $\nu_{NH(In)}$, usually observed as a strong band [8, 9, 15, 34–36] is obtained within 3409–3424 cm^{-1}. In all cases the asymmetric and symmetric stretching vibrations of NH_3^+ group (ν^{as}_{NH3+} and ν^{s}_{NH3+}) are observed as a broad band within wide 3200–2000 cm^{-1} ranges with highest frequency sub maxima about 3200 cm^{-1}. The IR-spectroscopic region 1800–1450 cm^{-1} is characterized with overlapping absorption bands of bending NH_3^+, Amide I ($\nu_{C=O}$), ν^{as}_{COO-}, δ_{NH} (Amide II) and indole in-plane (i.p.) vibrations (Table 1). In 800–400 cm^{-1} region are described and assigned to the out-of-plane (o.p.) bending vibrations of indole ring, bending vibrations of COO–-group and Amide IV-VI vibrations. The last ones are observed usually within the regions γ_{NH} (Amide V) 735 ± 60 cm^{-1}, $\delta_{C=O}$ (Amide IV) 695 ± 75 cm^{-1} and $\gamma_{C=O}$ (Amide VI) 600 ± 70 cm^{-1}, respectively [37]. Usually the indole o.p. mode about 740 cm^{-1} is characterized by strongest intensity within the discussed IR-spectroscopic region [8, 9, 15, 34–36]. Other characteristic IR-bands of latter structural fragment correlated well with the data for previously studied tryptophan-containing peptides [8, 9, 15] and of L-tryptophan [34–36]. The IR-spectroscopic patterns are preliminaryly deconvoluted and curve fitted with a view to determine the band positions and integral absorbances. As reference procedure a second derivative analysis is also applied. The IR-characteristic bands of COO–-fragment are assigned as well by an independent way, studying the IR-characteristics of corresponding protonated forms of the peptides.

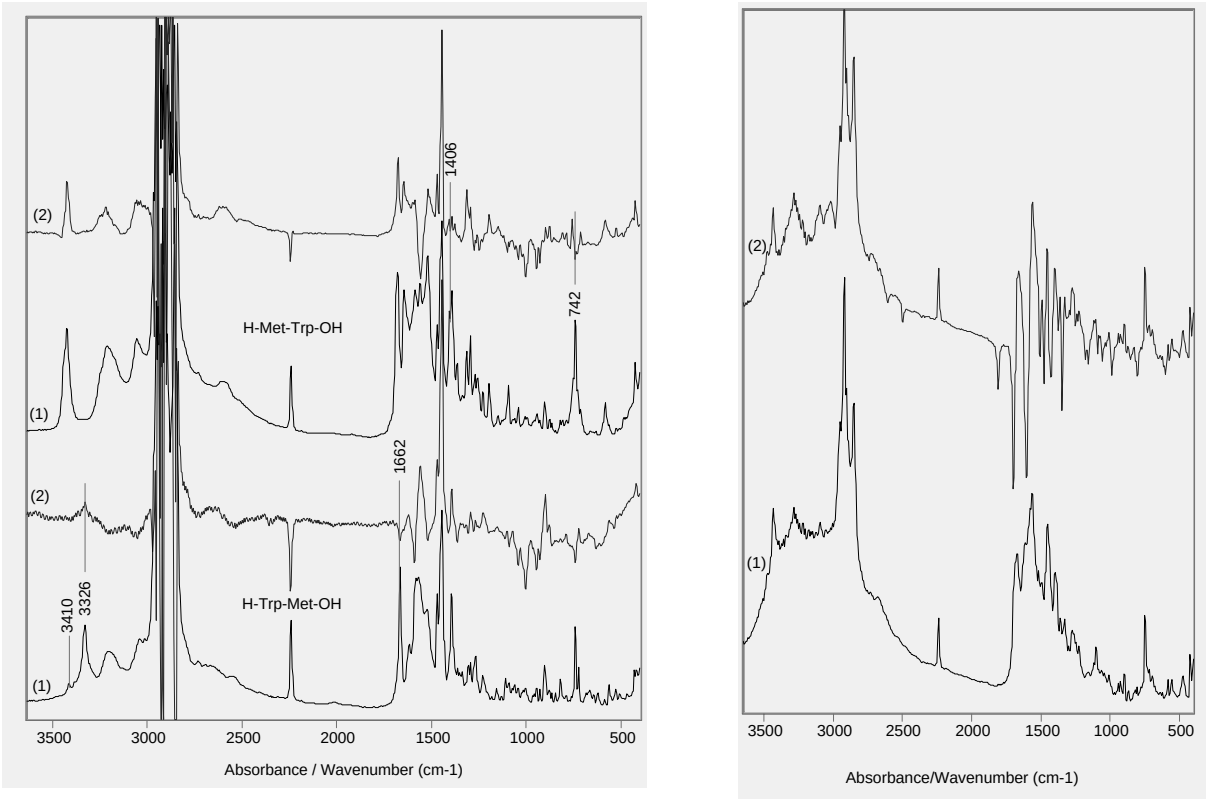

A B

Fig. 1. Non-polarized IR (1) and difference IR-LD (2) spectra of H-Trp-Met-OH, H-Met-Trp-OH(A) and H-Gly-Trp-OH.2H_2O (B).

Table 1. IR-characteristic bands of L-tryptophyl-L-methionine (H-Trp-Met-OH), L-methionyl-L-tryptophan (H-Met-Trp-OH) and glycyl-L-tryptophan dihydrate (H-Gly-Trp-OH.2H_2O) in solid-state.

Assignment	H-Trp-Met-OH ν, cm^{-1}	H-Met-Trp-OH ν, cm^{-1}	H-Gly-Trp-OH.2H_2O ν, cm^{-1}
ν_{NH}	3326	3446	3430
$\nu_{NH(In)}$	3409	3424	3419
$\nu_{OH(H2O)}$	-	-	3280
ν^{as}_{NH3+}, ν^{s}_{NH3+} Sub. maximum	3190	3208	3210
δ_{NH3+}	1675	1685	1689
$\nu_{C=O}$ (Amide I)	1662	1675	1673
δ^{as}_{NH3+}	1623	1643	1617
Indole i.p.	1612, 1469, 1265	1615, 1465, 1265	1610, 1465, 1265
ν^{as}_{COO-}	1581	1615	1563
δ_{NH} (Amide II)	1521	1508	1540
ν^{s}_{COO-}	1396	1406	1395
ν_{C-N}/δ_{NH} (Amide III)	1257	1260	1255
ν_{N-C}	1000	1008	1010
Indole o.p.	738, 424	742, 420	750, 424
$\nu_{S-C(H3)}$	721	723	718
δ_{COO-}	684	661	696
ρ_{COO-}	505	484	468
γ_{NH} (Amide V)	651	665	474
$\delta_{C=O}$ (Amide IV)	580	640	576
$\gamma_{C=O}$ (Amide VI)	526	560	553

The assignment given in Table 1 is experimentally proved by the possibilities of the IR-LD spectroscopy of orientated colloid suspensions stated below. Moreover, for the dipeptides L-tryptophyl-L-methionine (H-Trp-Met-OH) and L-methionyl-L-tryptophan (H-Met-Trp-OH) crystallographic data are not available.

Similar to other peptide systems [3–15] a significant degree of macro-orientation of suspended particles is obtained [17–19], thus resulting in a reasonable interpretation of the polarized IR-spectra.

In the IR-spectrum H-Trp-Met-OH the $\nu_{NH(In)}$ stretching vibration typical for indole ring is low intensive band (Table 1), which can be explained with the participation of the $N_{In}H$ group in intermolecular interactions in solid-state. The intensive band at 1662 cm^{-1} ($\nu_{C=O,}$ Amide I) stretching vibration and the corresponding γ_{NH} one are eliminated in difference IR-LD spectrum (Fig. 1A.2), indicating a co-linear orientation of the transition moments. The last result supposed a *trans*-configuration of the O=C–NH fragment. The low-intensive bands at 1675 cm^{-1} and 1623 cm^{-1} are assigned as δ^{as}_{NH3+} and δ^{s}_{NH3+}, while the intensive band at 1581 cm^{-1} to ν^{as}_{COO-}. The discussed bands are overlapped with the low-intensive maxima in the 1600–1450 cm^{-1} typical for in-plane vibrations of indole ring (Table 1). Only the band at 1469 cm^{-1} is well defined. Its elimination leads to a disappearance of the band at 721 cm^{-1}, typical for $\nu_{S–C(H3)}$ of L-methyonyl-side chain [6, 7, 10, 38–40]. This fact supposed a co-linear disposition of both transition moments (Scheme 3). The elimination of the intensive band at 740 cm^{-1} (out-of-plane mode of indole ring) with the band of $\nu^{as}_{COO–}$ (1581 cm^{-1}) at equal dichroic ratio also indicates a collinear orientation of the corresponding transition moments, which is realized in the frame of the proposed structure of H-Trp-Met-OH, shown in Scheme 3. The intensive band at 1396 cm^{-1} belongs to $\nu^{s}_{COO–}$. The experimentally proposed structure of the dipeptide correlated well with the theoretically approximated model of the system dipeptide/water. A torsion angle of 179.3° of the

The difference IR-LD spectrum of H-Met-Trp-OH (Fig. 1A.2) is characterized by eliminated bands at 1406 cm^{-1} (ν^{s}_{COO-}) and 742 cm^{-1} (o.p. mode of indole ring), thus assuming a collinear orientation of their transition moments. In contrast to H-Trp-Met-OH, in this case the NH-stretching region is characterized by pairs of bands at 3446 cm^{-1} and 3424 cm^{-1} (ν_{NH} and $\nu_{NH(In)}$) stretching vibrations. The consequent eliminations of these bands result in a disappearance of the maxima at 1685 cm^{-1} (ν^{as}_{NH3+}) and 1675 cm^{-1} (Amide I) (Figs. 2.2 and 2.3). This result can be observed when the HN–C=O amide fragment possesses cisoide-configuration. The band at 723 cm^{-1} ($\nu_{S-C(H3)}$) is eliminated with the bands of ν_{NH}, proposing a co-linearity of these transition moments as well. The predicted geometry of the dipeptide is supported by the theoretical structure with E_{rel} of 0.7 kJ/mol, where a dihedral angle of 8.6(1)° of HN–C=O fragment is obtained. On the other side the transition moments of ν_{NH} and $\nu_{S-C(H3)}$ close an angle of 2.6(2)°, indicating their co-linearity. The calculated angle between the transition moments of $\nu_{NH(In)}$ and Amide I of 5.2(1)° is in accordance with the obtained elimination of last two bands at different dichroic ratio (Figs. 2.2 and 2.3). In the frame of the optimized electronic structure of H-Met-Trp-OH the o.p. mode of indole and ν^{s}_{COO-} close an angle of 7.8(3)°. These data also support the experimentally proposed structure of the dipeptide. An experimental evidence of the cisoide-configuration of the amide fragment in this dipeptide follows from the obtained cyclic dipeptide in strongly acidic medium, in contrast to H-Trp-Met-OH, where a hydrochloride salt is obtained. Similar results have been observed in the case of other tryptophan-containing dipeptides, where the cyclic product has been characterized spectroscopically [20].

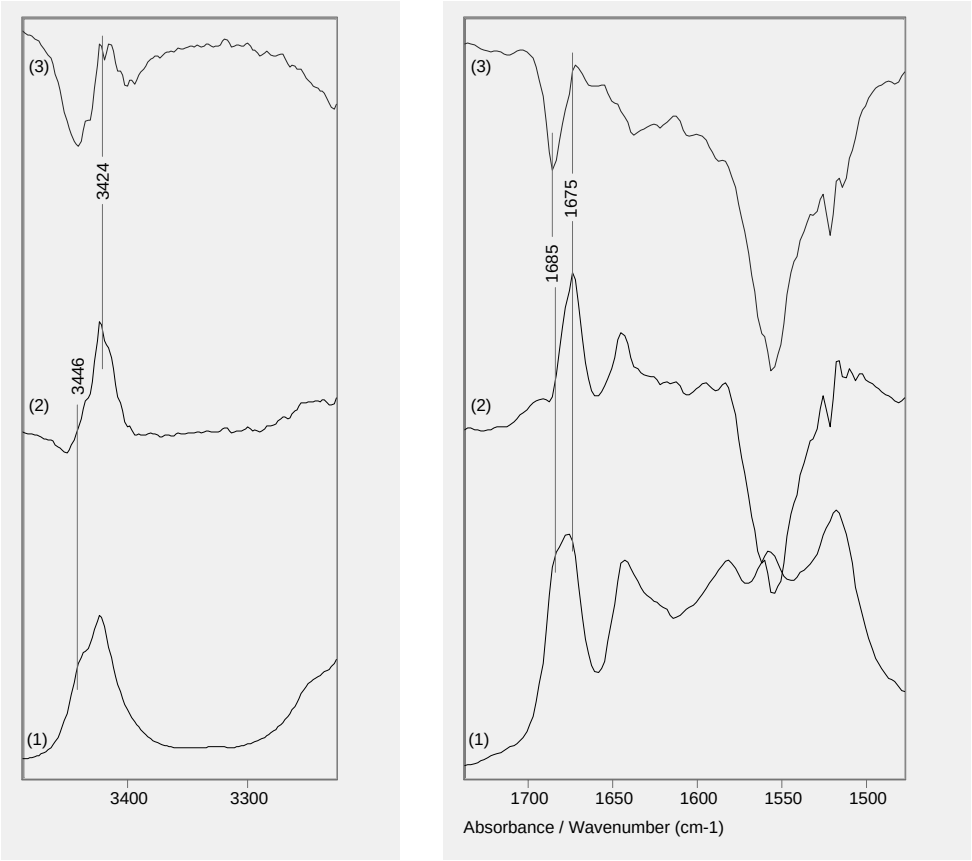

Fig. 2. Non-polarized IR (1) and reduced IR-LD spectra of H-Met-Trp-OH after elimination of the bands at 3446 cm^{-1} (2) and 3424 cm^{-1} (3).

The characterization of the dipeptide H-Gly-Trp-OH.$2H_2O$ is carried out, comparing the IR-spectroscopic data and the known crystalline structure [20]. H-Gly-Trp-OH.$2H_2O$ crystallizes in $P2_12_12_1$ space group and the unit cell contains two peptide molecules, perpendicularly orientated (Scheme 4). The amide HN–C=O fragment is flat trans-configurated with a dihedral angle of 177.4(9)° [20]. For this reason the elimination of the bands of ν_{NH} and $\nu_{C=O}$ (Amide I) at equal dichroic ratio is observed (Fig. 3A.2). The transition moments of indole o.p. modes of the two molecules close an angle of 64.6(4)°, while those of the amide fragment – 68.6(2)°, respectively (Scheme 4). It is valid for o.p. vibrations

of amide fragment. In all cases the consequent elimination of the bands at 750 cm^{-1} or 553 cm^{-1} leads to disappearance of the maxima at 424 cm^{-1} and 474 cm^{-1}, respectively. In all cases the observation of second peaks of the same symmetry class are observed. As for example the bands at 754 cm^{-1} and 750 cm^{-1} are eliminated at different dichroic ratio (Fig. 3B.2). The phenomenon has been described in a series of papers on the IR-band assignment, by means of the method represented here, describing the systems crystallizing in different space groups and containing non-equivalent molecules in the unit cell [10, 11].

Acknowledgements: The author wishes to thank Prof. T. Kolev (Institute of Organic Chemistry with Centre of Phytochemistry, Bulgarian Academy of Sciences) for the possibility to use Gaussian 98 program and Prof. T. Spassov (Sofia University "St. Kliment Ohridski") for the electron microscopic data.

Scheme 4. Unit cell of dl-Gly-Trp-OH.2H_2O.

REFERENCES

1. 1. T. Behmoaras, J.-J. Toulmé, C. Hélène, Nature, **292**, 858 (1981).
2. 2. A. Sengupta, R. Mahalaksmhi, N. Shamala, P. Balaram, J. Pept. Res., **65**, 113 (2005).
3. 3. B. B. Ivanova, M. Mitewa, J. Coord. Chem., **57**, 217 (2004).
4. 4. B. B. Ivanova, M. G. Arnaudov, Prot. Pept. Lett., **13**, 889 (2006).
5. B. B. Ivanova, J. Mol. Struct., **782**, 122 (2006).
6. B. B. Ivanova, M. G. Arnaudov, Spectrochim. Acta, **65A**, 56 (2006).
7. B. B. Ivanova, M. G. Arnaudov, St. Todorov, W. S. Sheldrick, H. Mayer-Figge, Struct. Chem., **17**, 49 (2006).
8. B. B. Ivanova, Spectrochim. Acta, **64A**, 931 (2006).
9. B. B. Ivanova, Spectrochim. Acta. Part A, (2007) in press. DOI: http://dx.doi.org/10.1016/j.saa.2007.09.005.
10. B. B. Ivanova, T. Kolev, S. Y. Zareva, Biopolymers, **82**, 587 (2006)
11. B. B. Koleva, T. M. Kolev, M. Spiteller, Biopolymers, **83**, 498 (2006).
12. B. B. Ivanova, J. Coord. Chem., **58(7)**, 587 (2005).
13. T. Kolev. B. B. Ivanova, S. Y. Zareva, J. Coord. Chem., **60**, 109 (2007).
14. B. B. Koleva, Ts. Kolev, S. Y. Zareva, M. Spiteller, J. Mol. Struct., **831**, 165 (2007).
15. B. B. Koleva, Ts. Kolev, M. Spiteller, Inorg. Chim. Acta, **360**, 2224 (2007).
16. B. B. Ivanova, M. G. Arnaudov, P. R. Bontchev, Spectrochim. Acta, **60**, 855 (2004).
17. B. B. Ivanova, D. L. Tsalev, M. G. Arnaudov, Talanta, **69**, 822 (2006).
18. B. B. Ivanova, V. D. Simeonov, M. G. Arnaudov, D. L. Tsalev, Spectrochim. Acta, **67A**, 66 (2007).
19. B. B. Koleva, T. Kolev, V. Simeonov, T. Spassov, M. Spiteller, Colloids Surf. (2007) submitted.
20. T. J. Emge, A. Agrawal, J. P. Dalessio, G. Dukovic, J. A. Inghrim, K. Janjua, M. Macaluso, L. L. Robertson, T. J. Stiglic, Y. Volovik, M. M. Georgiadis, Acta Crystallogr., **C56**, e469 (2000).
21. Ts. Kolev, B. Koleva, B. Shivachev, Inorg. Chim. Acta, (2007) in press. doi:10.1016/j.ica.2007.10.030
22. E. W. Thulstrup, J. H. Eggers, Chem. Phys. Lett., **1**, 690 (1996).
23. J. Spanget-Larsen, SPIE, **1575**, 404 (1992).
24. E. H. Korte, P. Lampen, Private communications, 1988.
25. B. Jordanov, R. Nentchovska, B. Schrader, J. Mol. Struct., **297**, 401 (1993).
26. B. Jordanov, B. Schrader, J. Mol. Struct., **347**, 389 (1995).
27. M. Belhakem, B. Jordanov, J. Mol. Striuct., **218**, 309 (1990).
28. M. Rogojerov, D. Kolev, B. Jordanov, J. Mol. Striuct., **349**, 447 (1995).
29. M. J. Frisch, G. W. Trucks, H. B. Schlegel, G. E. Scuseria, M. A. Robb, J. R. Cheeseman, V. G. Zakrzewski, J. A. Montgomery Jr., R. E. Stratmann, J. C. Burant, S. Dapprich, J. M. Millam, A. D. Daniels, K. N. Kudin, M. C. Strain, Ö. Farkas, J. Tomasi, V. Barone, M. Cossi, R. Cammi, B. Mennucci, C. Pomelli, C. Adamo, S. Clifford, J. Ochterski, G. A. Petersson, P. Y. Ayala, Q. Cui, K. Morokuma, P. Salvador, J. J. Dannenberg, D. K. Malick, A. D. Rabuck, K. Raghavachari, J. B. Foresman, J. Cioslowski, J. V. Ortiz, A. G. Baboul, B. B. Stefanov, G. Liu, A. Liashenko, P. Piskorz, I. Komáromi, R. Gomperts, R. L. Martin, D. J. Fox, T. Keith, M. A. Al-Laham, C. Y. Peng, A. Nanayakkara, M. Challacombe, P. M. W. Gill, B. Johnson, W. Chen, M. W. Wong, J. L. Andres, C. Gonzalez, M. Head-Gordon, E. S. Replogle, J. A. Pople, Gaussian 98, Gaussi Inc., Pittsburgh, PA (1998).
30. "DALTON, a molecular electronic structure program, Release 2.0 (2005), http://www.kjemi.uio.no/software/dalton/dalton.html "
31. G. A. Zhurko, D. A. Zhurko, ChemCraft: Tool for Treatment of Chemical Data, Lite version build 08 (2005).
32. D. Toroz, T. Van Mourik, Molec. Phys., **105**, 209 (2007).
33. D. Toroz, T. Van Mourik, Molec. Phys., **104**, 559 (2006).
34. X. Cao, G. Fischer, J. Phys. Chem. A **103**, 9995 (1999).
35. C. Snoek, R. T. Kroemer, M. R. Hockridgea, J. P. Simons, Phys. Chem. Chem. Phys., **3**, 1819 (2001).
36. B. C. Dian, A. Longarte, T. S. Zwier, J. Chem. Phys., **118**, 6 (2003).
37. N. Roeges, A Guide to the Complete Interpretation of Infrared Spectra of Organic Structures, J. Wiley, N.Y. (1993).
38. X. Cao, G. Fischer, J. Phys. Chem. A, **106**, 41 (2002).
39. D. T. Rosa, J. A. K. Bauer, M. J. Baldwin, Inorg. Chem., **40**, 1606 (2001).
40. B. B. Koleva, Vibr. Spectrosc., **44**, 30 (2007).

ТВЪРДОТЕЛНА ЛИНЕЙНО-ДИХРОИЧНА ИЧ СПЕКТРОСКОПИЯ НА L-ТРИПТОФАН-СЪДЪРЖАЩИ ДИПЕПТИДИ L-ТРИПТОФИЛ-L-МЕТИОНИН (H-TRP-MET-OH), L-МЕТИОНИЛ-L-ТРИПТОФАН (H-MET-TRP-OH) И ГЛИЦИЛ-L-ТРИПТОФАН ДИХИДРАТ (H-GLY-TRP-OH.2H_2O)

Б. Б. Колева

Софийски университет „Св. Климент Охридски“, Химически факултет, Катедра „Аналитична химия“, 1164 София

Посветена на акад. Иван Юхновски по повод на 70-та му годишнина

Постъпила на 2 януари 2008г., Преработена на 11 януари 2008г.

(Резюме)

С помощта на линейно-дихроичния ИЧ-спектрален анализ на ориентирани проби в твърдо състояние като суспензии в нематичен течен кристал бе проведено ИЧ-спектрално и структурно охарактеризиране на L-триптофан-съдържащите дипептиди L-триптофил-L-метионин (H-Trp-Met-OH), L-метионил-L-триптофан (H-Met-Trp-OH) и глицил-L-триптофан дихидрат (H-Gly-Trp-OH.2H_2O). Зависимостта структура–спектрални свойства бе изследвана чрез сравнителен анализ на данните от ИЧ спектроскопия с тези, получени чрез рентгенова дифракция от монокристален образец на H-Gly-Trp-OH.2H_2O. В допълнение са представени резултати от квантово-химични пресмятания на ab initio и ТФП нива на теория за системите дипептид/H_2O.

Bulgarian Chemical Communications, Volume 40, Number 4 (pp. 464–468) 2008

Application of diffusion-ordered spectroscopy for the analysis of cancer related biological samples

G. I. Ivanova[1,2]*, E. J. Cabrita[1], R. O´Connor[3], A. J. Eustace[3], D. F. Brougham[3,4]

[1] *REQUIMTE/CQFB - Departamento de Química, Faculdade de Ciências e Tecnologia, Universidade Nova de Lisboa, 2829-516 Caparica, Portugal*
[2] *Institute of Organic Chemistry with Centre of Phytochemistry, Bulgarian Academy of Sciences, 1113 Sofia, Bulgaria*
[3] *National Institute of Cellular Biotechnology, Dublin City University, Dublin 9, Ireland*
[4] *School of Chemical Sciences, Dublin City University, Dublin 9, Ireland*

Dedicated to Academician Ivan Juchnovski on the occasion of his 70th birthday

Received January 2, 2008; Revised January 19, 2008

A preliminary application of diffusion-ordered spectroscopy (DOSY) for separation, identification and characterisation of metabolites of human lung carcinoma cell extracts, exhibiting different levels of multi-drug resistance (MDR) is reported. The results show the presence of at least three lipid components of different sizes in the lipophilic extracts which can not be identified by one- and two-dimensional NMR techniques. A number of metabolites in the hydrophilic extracts of human lung carcinoma cell lines are successfully separated by different diffusivities. The appearance in the DOSY spectra of different metabolites with the same diffusion coefficient is consistent with them being chemically bound together.

Key words: cells; composition; NMR, diffusion; DOSY.

NMR spectroscopy is a powerful technique for the investigation of the metabolite composition of biological samples: biofluids, tissues and tissue extracts. Proton NMR spectra of tissues are usually extremely complex due to the large number of components in the samples, resulting in spectra with complex line shapes and significant overlap of the resonance signals. The tissue extracts, both hydrophilic and lipophilic, yield NMR spectra with enhanced resolution, improving the possibility for detailed metabolite identification and structural characterization [1–3].

Pulsed field gradient spin echo NMR spectroscopy can be used for investigating diffusion phenomena in solution [4, 5]. Mixture analysis continues to be one of the most challenging pursuits in analytical science. Diffusion-ordered spectroscopy (DOSY) allows the separation of components of different molecular size through differences in their diffusion coefficients and can be a powerful tool for mixture analysis. The diffusion coefficients of the components are dependent on their individual physical properties, such as the size and shape of the molecules as well as the temperature and viscosity of the solutions. In high resolution diffusion-ordered spectroscopy (DOSY), differences in the diffusion coefficient between species are sufficient to allow the spectrum of an intact mixture to be decomposed into the subspectra of individual components. Therefore, the DOSY technique offers a route whereby the components in complex biological systems such as tissue and tissue extracts might be separated and hence identified [5–7].

The aim of the present study has been to apply diffusion-ordered spectroscopy (DOSY) for separation and identification of the metabolites of human lung carcinoma cell extracts, exhibiting different levels of multi-drug resistance (MDR). The human lung carcinoma cell extracts, both hydrophilic and lipophilic, have been studied.

EXPERIMENTAL

Cancer cell lines

The cell lines studied include the parent cell line DLKP (a human squamous non-small cell lung carcinoma) and the resistant daughter cell line DLKP-A5F. DLKP cells express a small amount of the multidrug resistance. The lipophilic (L) and hydrophilic (H) extracts of the parent cell line DLKP (a human squamous cell lung carcinoma) and resistant daughter cell line DLKP-A5F were prepared according to a slightly modified methodology published in the literature [8]. The extraction procedure was performed on a number of 1×10^7 cells per NMR sample on a crushed ice bath at 4ºC. Cells were trypsinised, counted and pelleted into a

* To whom all correspondence should be sent:
E-mail: g.ivanova@dq.fct.unl.pt

© 2008 Bulgarian Academy of Sciences, Union of Chemists in Bulgaria

1.5 ml eppendorf tube. 500 µl of a 2:1 (v/v) ratio of ice cold methanol-chloroform were added and the pellet resuspended using a vortex. The tube was mixed for 10 min on a blood tube mixer. 500 µl of ice cold 1:1 (v/v) chloroform water mixture were added and again mixed using a vortex. The eppendorf tube was floated in a sonicating bath and sonicated for 10 min. The tube was centrifuged in a microfuge at 13000 rpm for 5 min. The top and bottom layers were removed to separate eppendorf tubes taking care not to disturb the pelleted debris. The solvent was evaporated using a centrifugal concentrator (MaxiPrep, Holten) and the tubes placed in a darkened box in a freezer for later analysis.

NMR spectroscopy

The NMR spectra were recorded on a Bruker AvanceII 600 spectrometer, equipped with a cryo probe and pulse gradient units, capable of producing magnetic field pulsed gradients in the z-direction of 56.0 G/cm.

^{1}H NMR spectroscopy of lipophilic cell extracts

Standard 1D ^{1}H NMR spectra of the lipophilic cell extracts (10 mg), in deuterated chloroform were recorded at 300K, using 30º pulses. The solvent resonance peak at 7.26 ppm has been used as a chemical shift reference. Magnitude mode gradient-COSY spectra with double quantum filter, gradient pulses for selection, gradient ratio 16:12:40 and relaxation delay 1.5 s were performed. A total 2K data points in F_2 and 256 data points in F_1 over a spectral width of 4000 Hz were collected using 32 transients and 16 dummy scans. ^{1}H/^{1}H total correlation (TOCSY) spectra were recorded with 2K data points, spectral width 4000 Hz, relaxation delay 2 s, MLEV-17 sequence with a mixing time of 80 ms. A total 256 data points in F_1 were collected using 32 transients and 16 dummy scans.

^{1}H NMR spectroscopy of hydrophilic cell extracts

1D ^{1}H NMR spectra of hydrophilic cell extracts (7 mg) in D_2O were recorded at 300K and 0.1% solution of TSP in D_2O as an external chemical shift reference, using a presaturation during the relaxation delay. Two-dimensional ^{1}H/^{1}H COSY (correlated spectroscopy) and ^{1}H/^{1}H TOCSY (total correlated spectroscopy) have been acquired in a phase sensitive mode. In both cases, 64 transients per increment and 256 increments were collected into 2K data points and relaxation delay 2 s. The spectral width in both dimensions was 5000 Hz. The TOCSY NMR spectra were recorded by use of MLEV-17 spin lock scheme for proton-proton transfer with a mixing time of 60 ms.

Diffusion-ordered NMR spectroscopy

The DOSY experiments were acquired using the bipolar pulse longitudinal eddy current delay (BPPLED) pulse sequence [9] and presaturation during the relaxation delay for the samples of hydrophilic extracts (in D_2O). Typically, in each experiment a number of 32 BPPLED spectra of 32K data points were collected, with a duration of the magnetic field pulse gradients (δ) of 2.2–3.0 ms, diffusion times (Δ) of 100–200 ms and an eddy current delay set to 5 ms. The pulse gradient (g) has been incremented from 2 to 95% of the maximum gradient strength in a linear ramp. The experiments were acquired at a temperature of 298K and air flow of 535 l/h, in 3 mm NMR tubes. NMR tubes of 3 mm size were used to increase samples concentration and suppress the temperature induced convection currents due the smaller diameter as compared to 5 mm tubes in the diffusion experiments.

RESULTS

Typical ^{1}H NMR spectra of intact cancer cells (for comparison), their lipophilic and hydrophilic extracts are presented in Figure 1. The signal assignment of the spectra (Figure 1B and C) is based on the analysis of 1D and 2D (^{1}H/^{1}H COSY and ^{1}H/^{1}H TOCSY) spectra and is in agreement with the literature data [10–12]. The main resonances observed in the spectra of lipophilic extracts (B) are those from fatty acids (saturated and unsaturated), choline, cholesterol and glycerol backbone moieties. In the ^{1}H NMR spectra of the hydrophilic extracts, the anticipated resonances of water-soluble cell metabolites (amino acids and other organic acids and bases) have been observed. The characteristic resonance signals of some of the major metabolites found in the samples are shown in Figure 1.

In the 2D DOSY (600 MHz) spectra of the lipophilic extracts of the lung carcinoma cell lines studied, four groups of proton resonance signals characterized by a distinct self-diffusion coefficient have been observed (Fig. 2A, B).

The analysis of the spectra shows that the lipids extracted from both lung carcinoma cell lines contain at least three lipid components classified according to their self-diffusion coefficients and respectively different molecular size and molecular weight aromatic fractions. The diffusion coefficients of the separated components are presented in Table 1. As depicted from the 2D DOSY plots, the results in table 1 show that on the base of the measured diffusion coefficients, differences in the composition of the cellular extracts could be estimated. The presence of cholesteryl esters of fatty acids has been detected

in both mixture components of DLKP_L (log$D$ = –9.02 and log$D$ = –9.23 m^2/s), but only in one of the components of DLKP5fA_L (log$D$ = –9.17 m^2/s). The results suggest the presence of high molecular weight free fatty acids and/or hydrocarbons (log$D$ = –9.32 m^2/s).

2D DOSY (600 MHz) spectra of the hydrophilic extracts in D_2O are presented in Fig. 3. The spectra are dominated by the resonance signals of myo-Inositol (myo-I), choline (Cho), creatine (Cr), glutamine (Glu)/glutatione (Glt). The signal overlap in the spectral area between 3.30 and 4.30 ppm as well as the low intensity of some components in the high field spectral area have hampered a more detailed analysis of the DOSY spectra.

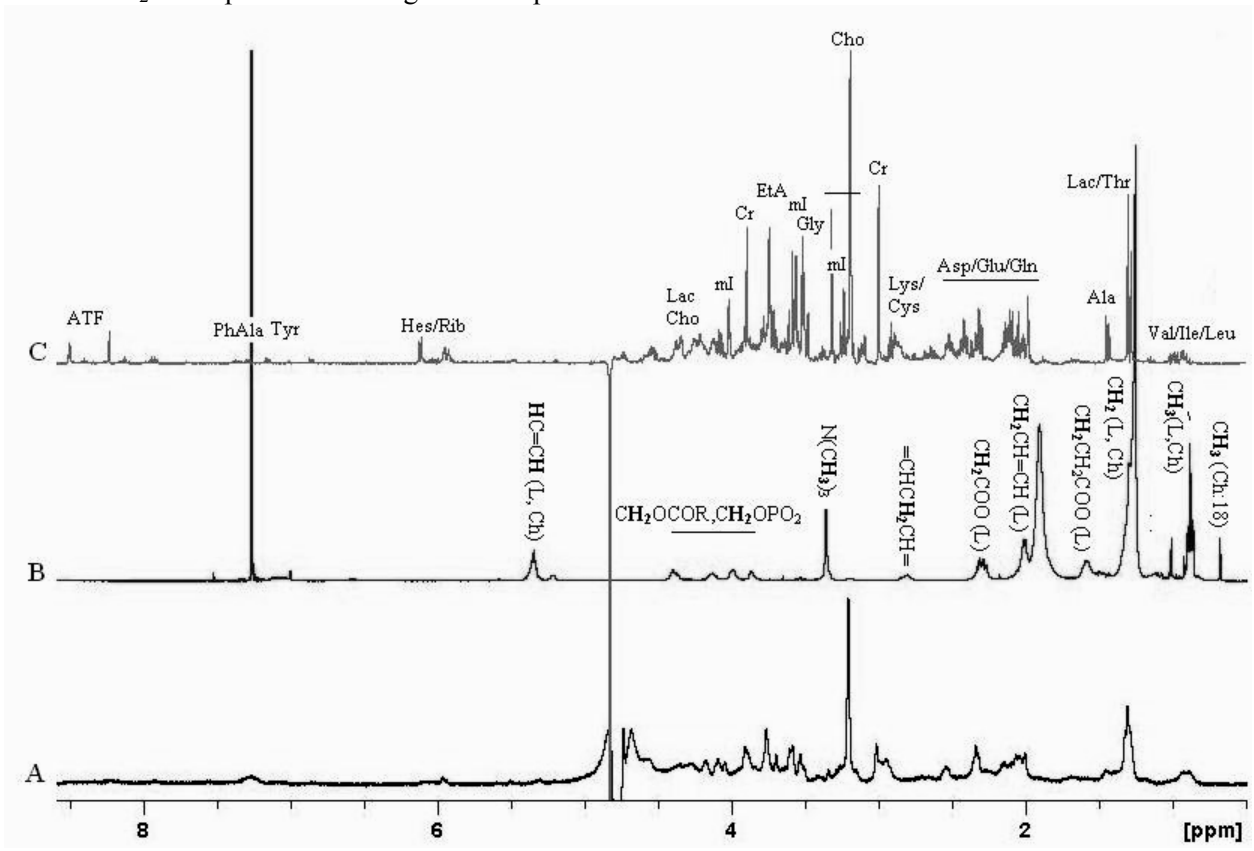

Fig. 1. Typical ^{1}H NMR spectra of intact DLKP lung carcinoma cells (A) and their lipophilic (B) and hydrophilic (C) extracts.

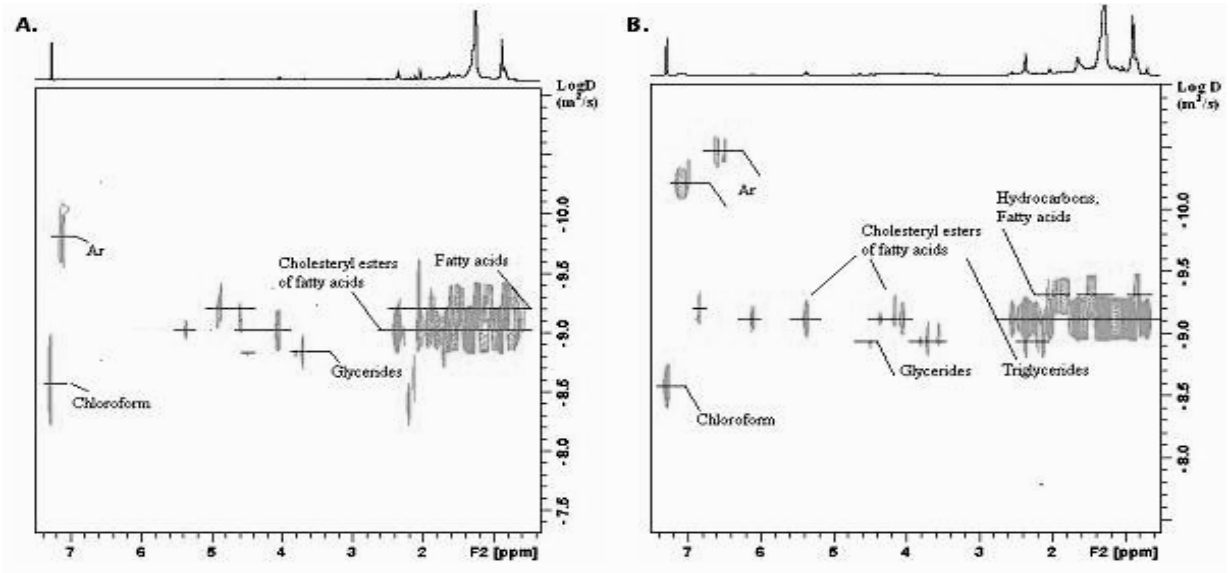

Fig. 2. 600 MHz 2D DOSY spectra of lipophilic extracts of DLKP (A) and DLKP5fA (B) cancer cells in $CDCl_3$, and Δ = 200 ms; δ = 3.0 ms; TD = 32k .

The decay of the methyl resonances of the amino acids has been usually utilized to determine their D values. The analysis of the spectra of the hydrophilic extracts DLKP_W and DLKP5fA_W has shown that some of the characteristic signals of metabolites present in the samples can be separated in the DOSY experiment, according to their distinct diffusion coefficients. However, an estimation of the differences in the cellular composition requires further studies in order to improve the resolution in the diffusion dimension. Experimental conditions such as those concerning the influence of pH, temperature and/or application of complexation agents can be explored. Another option to increase the resolution in the diffusion dimension is the spread of chemical shifts in a 2nd frequency dimension (^{1}H or ^{13}C), creating a pseudo 3D experiment like COSY-DOSY or HSQC-DOSY.

Further studies exploring these possibilities are ongoing in order to improve the resolution in the diffusion dimension of DOSY spectra of complex biological samples.

Table 1. Measured self-diffusion coefficients of the separated components of lipophilic extracts of DLKP_L and DLKP5fA_L.

Composition	DLKP_L	DLKP5fA_L
	D* 10^9 [m^2/s]	D* 10^9 [m^2/s]
Chloroform	2.45	3.31
Un	3.98	1.99
Glycerides	1.48	1.15
CholE/FA	9.55	6.76
CholE/FA	5.89	4.79
Ar	1.48	4.79
Ar	9.12	1.58

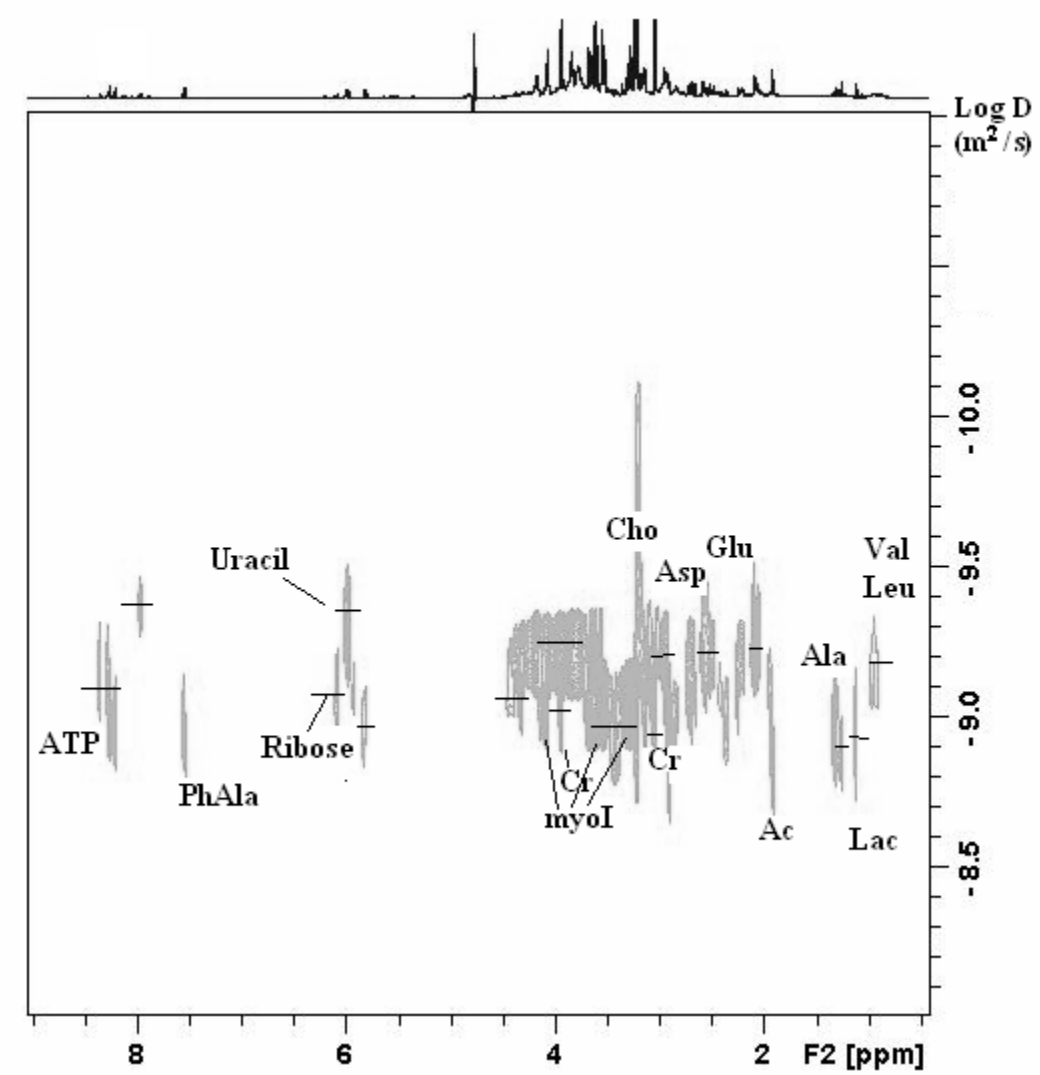

Fig. 3. 600 MHz 2D DOSY NMR spectra of hydrophilic extracts of DLKP5fA cancer cells in D_2O and Δ =100 ms; δ = 2.2 ms; TD = 32k.

CONCLUSION

The preliminary results presented here show that Diffusion-Ordered NMR Spectroscopy (DOSY) can be a powerful tool for separation and spectral characterisation of the components of complex mixtures, such as tissue extracts. The DOSY techniques can be used as a tool to distinguish between components in a mixture due to the differences in their relative diffusion coefficient values. The diffusion coefficient measurements of cell extracts allow an additional chemical and physical characterization of individual components, in term of their diffusivities, size and shape of the molecules.

***Acknowledgements**: G. I. Ivanova acknowledges FCT-Portugal for the grant SFRH/BPD/24930/2005.*

REFERENCES

1. M. Bloom, K. T. Holmes, C. E. Mountford, P. G. Williams, *J. Magn. Reson*., **69**, 73 (1986).
2. C. E. Mountford, S. Doran, C. L. Lean, P. Russell, *Chem.Rev*., **104**, 3677 (2004).
3. T. L. Whitehead, T. Kieber-Emmons, *Prog. NMR Spectr*., **47**, 165 (2005).
4. C. S. Johnson, *Progr. NMR Spectr*., **34**, 203 (1999).
5. J. S. Gounarides, A. Chen, M. J. Shapiro, *J. Chromatogr. B*, **725**, 79 (1999).
6. Y. Cohen, L. Avram, L. Frish, *Angew. Chem., Int. Ed*., **44**, 520 (2005).
7. B. Antalek. *Conc. Magn. Reson*., **14**, 225 (2002).
8. J. E. Le Belle, N. G. Harris, S. R. Williams, K. K. Bhakoo, *NMR Biomed*.,**15**, 37 (2002).
9. D. Wu, A. Chen, C. S. Johnson. *J. Magn. Reson. Ser. A*, **115**, 260 (1995).
10. U. Sharma, A. Mehta, V. Seenu, N. R. Jagannathan, *Magn. Reson. Imag*., **22**, 697 (2004).
11. V. Govindaraju, K. Young, A. A. Maudsley, *NMR Biomed*., **13**, 129 (2000).
12. N. J. Waters, E. Holmes, C. J. Waterfield, R. D. Farrant, J. K. Nicholson, *Biochem. Pharmacol*., **64**, 67 (2002).

ПРИЛОЖЕНИЕ НА ДИФУЗИОННО ПОДРЕДЕНА СПЕКТРОСКОПИЯ ЗА АНАЛИЗ НА РАКОВИ БИОЛОГИЧНИ ПРОБИ

Г. Ив. Иванова[1,2]*, Еур. Ж. Кабрита[1], Р. О´Конор[3], Ал. Дж. Юстасе[3], Д. Ф. Броухам[3,4]

[1] Катедра по химия, Научен и технологичен факултет, Нов университет на Лисабон, 2829-516 Капарика, Португалия
[2] Институт по органична химия с център по фитохимия, Българска академия на науките, 1113 София
[3] Национален институт по клетъчна биотехнология, Университет на град Дъблин, Дъблин 9, Ирландия
[4] Химически факултет, Университет на град Дъблин, Дъблин 9, Ирландия

Посветена на акад. Иван Юхновски по повод на 70-та му годишнина

Постъпила на 2 януари 2008 г.; Преработена на 19 януари 2008 г.

(Резюме)

Използвана е дифузионно подредена ЯМР спектроскопия за разделяне, откриване и характеризиране на метаболити в екстракти на човешки белодробни ракови клетки, проявяващи различна степен на резистентност към лекарства (мулти-лекарствена резистентност). Резултатите показват, че в липидните екстракти присъстват най-малко три липидни компонента с различен размер, които не могат да бъдат идентифицирани посредством традиционните едномерни и двумерни ЯМР техники. Метаболитите присъстващи в хидрофилните екстракти на човешки белодробни ракови клетки са успешно разделени на базата на разлика в техните дифузионни свойства. Появата на различни метаболити с еднакви коефициенти на дифузия в дифузионно подредените ЯМР спектри, са доказателство за наличието на химична връзка между тях.

Bulgarian Chemical Communications, Volume 40, Number 4 (pp. 469–476) 2008

Preparation of novel chitosan-containing micro- and nanofibrous materials by electrospinning

M. G. Spasova, D. P. Paneva, N. E. Manolova, I. B. Rashkov*

Laboratory of Bioactive Polymers, Institute of Polymers, Bulgarian Academy of Sciences, 1113 Sofia, Bulgaria

Dedicated to Academician Ivan Juchnovski on the occasion of his 70th birthday

Received January, 4, 2008; Revised January 16, 2008

Electrospinning is an efficient and versatile technique for fabrication of nanofibres. This article presents a condensed overview of this technique, with emphasis on chitosan-based nanofibrous materials. For the first time two easily feasible and efficient approaches for preparation of micro- and nanofibrous materials containing the natural polymer chitosan were proposed. The first approach relied upon electrospinning of chitosan and a non-ionogenic polymer mixed solutions. The mean diameters of the nanofibres were in the range of 40–290 nm. The second approach consisted of coating of electrospun poly(L-lactide) or poly(L-lactide)/poly(ethylene glycol) nanofibrous mats with chitosan. Particular potential applications of these novel materials in the biomedical field such as drug delivery systems and wound dressings were evaluated.

Key words: chitosan, electrospinning, nanofibres, drug delivery, wound healing.

INTRODUCTION

Polymer fibres are applied in a wide variety of industrial fields [1]. Electrospinning is a cutting edge technique that allows producing continuous polymer fibres with submicron diameters. While the conventional techniques like spinning from melt or solution provide fibres with diameters in the range of 5–500 μm, the electrospinning allows producing polymer fibres with diameters in the nanoscale range. Because of their inherent large specific surface area and the small pore size in nanofibrous materials, the electrospun mats may find a variety of applications, e.g. in military protective clothing and filter applications, for non-traumatic wound dressings, in drug delivery carriers, as tubular shapes for blood vessels and nerve regeneration, 3D-scaffolds for bone and cartilage regeneration, in cosmetics, in nanosensors (thermal, piezoelectric, biochemical and fluorescence optical chemical sensors), or in electronics [2]. At present the electrospinning is recognized as the most efficient technique for preparation of significant in length fibres having diameters in the micro- and nanoscale [2, 3]. Moreover, the transfer from laboratory to industrial scale can be easily achieved. In the recent years, the electrospinning process gains particularly increasing interest as illustrated in Figure 1, which shows the number of scientific publications that are focused on electrospinning per year and the publications distribution in Europe.

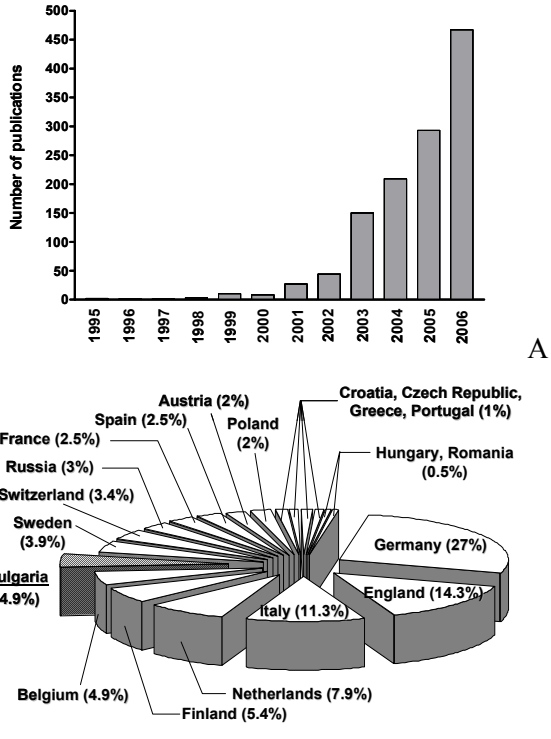

Fig. 1. Number of scientific publications per year (1995–2006) (A) and distribution of publications in Europe for 2007 (B) on electrospinning (source: Science Citation Index, SCI®).

Typically, a laboratory set-up is used for electrospinning since complete electrospinning apparatuses are not yet marketed. Schematic illustration of the electrospinning process and photographs of electrospinning set-up are shown in Figure 2.

* To whom all correspondence should be sent:
E-mail: rashkov@polymer.bas.bg

© 2008 Bulgarian Academy of Sciences, Union of Chemists in Bulgaria

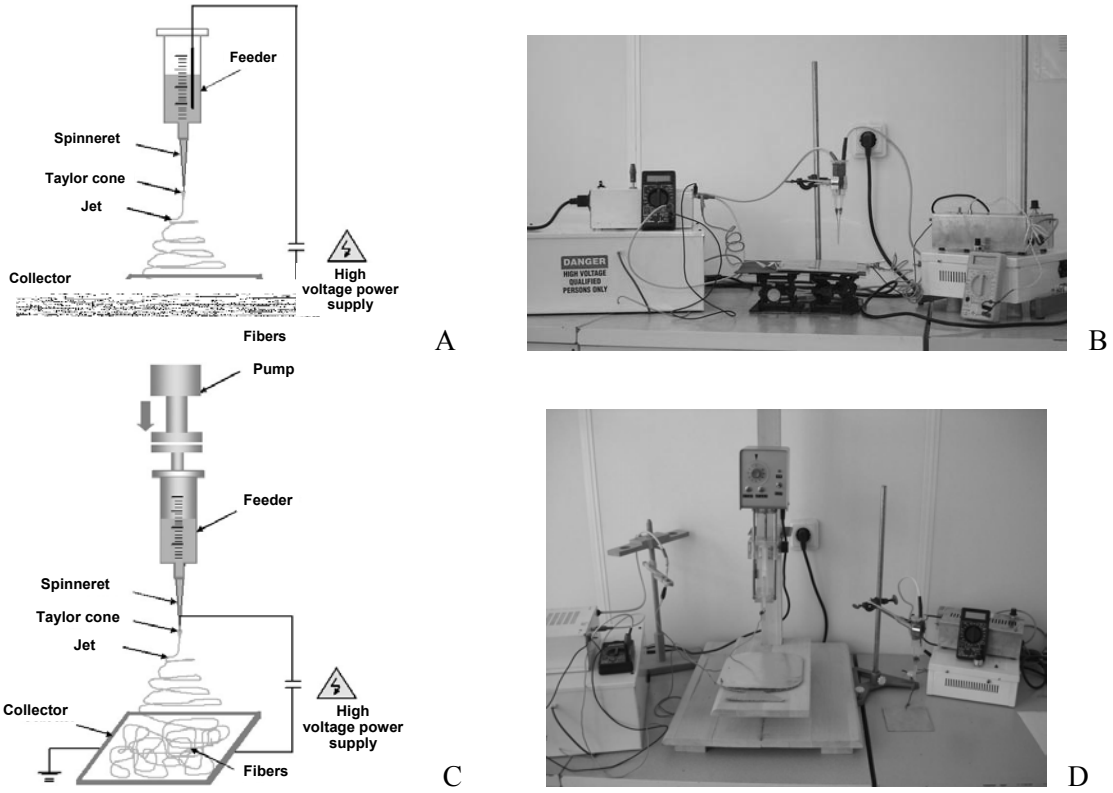

Fig. 2. Electrospinning set-up: A) and C) Schematic illustration; B) and D) Laboratory set-up: The high voltage electrode is immersed in the polymer solution (A and B); the high voltage electrode is connected to the spinneret (C and D).

The electrospinning involves the application of a strong electrostatic field to a polymer solution. The high voltage electrode is immersed in the polymer solution or connected to the spinneret. The electrostatic field deforms the pendant droplet of the polymer solution at the capillary tip into a conical shape known as Taylor cone. When the applied field strength exceeds a threshold value, the electrostatic forces overcome the surface tension, and a fine charged jet is ejected to move towards a ground plate acting as a counter electrode. Due to the high viscosity of the polymer solution and the presence of entanglements, the jet remains stable and is not transformed into droplets. The solvent begins to evaporate immediately after the jet is formed. As a result, thin polymer fibres are deposited on the counter electrode.

Many parameters have an effect on the electrospinning process. These parameters include (a) solution properties such as viscosity, elasticity, conductivity, and surface tension, (b) process variables such as feeding rate, hydrostatic pressure, electric potential at the capillary tip, and the gap (distance between the tip and the collecting screen), and (c) ambient parameters such as solution temperature, humidity, and air velocity [2]. Despite of the great number of variables that affect the process, some models describing the electrospinning process have been put forward [4–6]. A simplified model for predicting the diameter of electrospun fibres was proposed as well [7]. Last, but not least, criteria for complex evaluation of the morphology and alignment of electrospun polymer micro- and nanofibres were systematized [8].

More than hundred polymers have already been electrospun [2, 9]. The significant interest in electrospinning of biocompatible and biodegradable polymers is mainly due to the possibility to obtain scaffolds that mimic the extracellular matrix of native tissues and organs [10]. Nanofibrous scaffolds of aliphatic biodegradable polyesters, such as polylactide (PLA), polyglycolide, poly(ε-caprolactone), poly(lactide-*co*-glycolide), poly(L-lactide-*co*-caprolactone), have been successfully electrospun [11–15]. There is also an increasing interest in use of natural polymers for preparation of nanofibrous matrixes. However, fabrication of nanofibres of natural polymers by electrospinning is still a challenge [2].

Chitosan is regarded as the natural polymer, which is the most attracting for use in nanofibrous materials. The interest on preparation of chitosan-based polymer materials is mainly provoked by its numerous beneficial properties in terms of its potential application in biomedical field [16]. Chitosan is a polysaccharide, which is typically produced by partial *N*-deacetylation of the abundant natural

polymer chitin. Chitosan may be considered as a polyelectrolyte built of (1→4)-linked 2-acetamido-2-deoxy- -D-glucopyranose and 2-amino-2-deoxy- -D-glucopyranose residues. During the past few years, particularly increased attention has been paid on the development of optimal conditions for preparation of chitosan-containing nanofibres by electrospinning [17–28]. Electrospinning has been successfully applied to prepare nanofibrous materials with antibacterial and/or haemostatic activity [17–20, 22, 29, 30], nanofibrous scaffolds for tissue engineering [31], as well as hybrid nanofibres of biocompatible polymers and fullerenes [32, 33] or magnetic nanoparticles [23].

Herein we summarize two novel approaches proposed by us for successful preparation of chitosan-containing micro- and nanofibrous materials applying the electrospinning technique. Some possibilities for the application of these materials in the biomedical field have been estimated.

EXPERIMENTAL PART

Materials

Chitosan from crab shells ($\overline{M}$ v = 540 000 g/mol, deacetylation degree 80%, Sigma), poly(ethylene oxide) (PEO, $\overline{M}$ v = 800 000 g/mol, Badimol® Dimitrovgrad, Bulgaria), poly(L-lactide) (PLLA, $\overline{M}$ w = 152 000 g/mol, Fluka) and poly(ethylene glycol) (PEG, mol. wt. range 1 900–2 200, Fluka) were used.

Preparation and characterization of chitosan/PEO nanofibres and chitosan-coated PLLA or PLLA/PEG fibres

The electrospinning of chitosan/PEO mixed aqueous solutions in absence/presence of the model drug potassium 5-nitro-8-quinolinolate (K5N8Q) is described in details elsewhere [17]. PLLA and PLLA/PEG fibres were prepared as already described [22, 31]. The electrospinning was performed using the electrospinning set-up presented in Figure 2B. Chitosan-coated PLLA and PLLA/PEG mats were prepared by immersion of the mats in aqueous chitosan solution (0.05%, pH 5) followed by crosslinking of the natural polymer in glutaraldehyde vapours [22]. The morphology of the electrospun mats was observed by scanning electron microscopy (SEM) and evaluated in terms of the previously reported criteria for complex evaluation of electrospun mats [8] using Image J software [34] by measuring 20 fibres from each SEM image. The antibacterial and antimycotic activity of chitosan/PEO and (chitosan-coated) PLLA or PLLA/PEG mats was tested against Gram-negative bacteria (*Escherichia coli*), Gram-positive bacteria (*Staphylococcus aureus*) and the fungus *Candida albicans* [17, 22]. Platelet and erythrocyte adhesion were monitored by direct SEM observation of blood cells adhered on the surfaces of mats that had been in contact with whole human blood [22].

RESULTS AND DISCUSSION

Preparation of chitosan/PEO nanofibres

Until 2004, all attempts to prepare chitosan-containing fibres by electrospinning have been unsuccessful [2]. Our preliminary experiments to electrospin chitosan alone from its aqueous solutions also failed. We assumed that the impossibility chitosan to form a continuous spinning jet (a prerequisite for successful electrospinning of polymers) is due to its polyelectrolyte behaviour and chains rigidity in aqueous solutions. Having in mind our previous studies on the rheological behaviour of chitosan/PEO mixed solutions [35] we suggested that the adding of a non-ionogenic flexible polymer would facilitate the chitosan electrospinning. Chitosan-containing nanofibres were successfully electrospun from chitosan/PEO mixed solutions at a weight ratios of chitosan/PEO equal to or less than 1 [17]. SEM micrographs of the nanofibres obtained at different weight ratios chitosan/PEO are shown in Figure 3. The nanofibres electrospun from mixed solutions at a weight ratio of chitosan/PEO = 0.05–0.33 and total polymer concentration of 5% were cylindrical with mean diameters in the range of 200–250 nm. On increasing the chitosan content, the fibre diameters decreased. The nanofibres prepared at a weight ratio of 1/1 and total polymer concentration of 3% have significantly smaller mean diameter (ca. 40 nm) and bead-like defects. On further increasing the chitosan content (chitosan/PEO = 4) fibres did not spun and only ‘tailed’ beads were formed. The necessity of adding an excess of PEO to the chitosan solution (PEO in an amount higher than the equimolar one) might be attributed to the possibility of formation of a complex between PEO and chitosan resulting in an uncoiling of the PEO macromolecules and their orientation along the chitosan chains. The possibility of formation of a chitosan/PEO complex with composition close to the stoichiometric one has been previously shown [35].

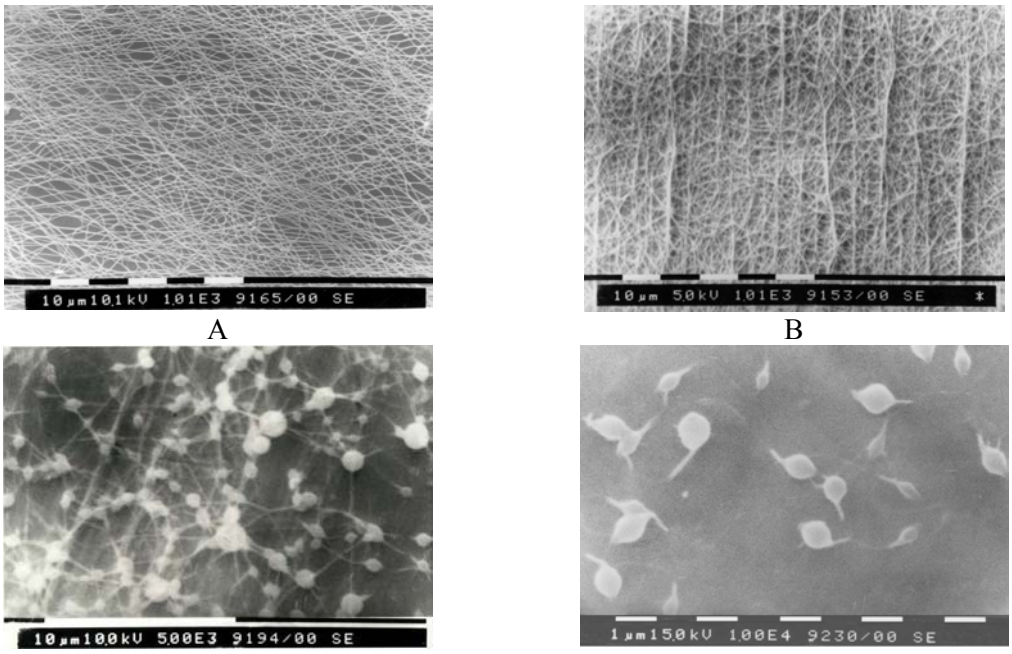

Fig. 3. SEM micrographs of nanofibres electrospun from chitosan/PEO mixed solutions obtained at applied field strength of 1 kV/cm and chitosan/PEO weight ratios: 0.18; ×1 000 (A), 0.33; ×1 000 (B) (total polymer concentration – 5%); 1.0; ×5 000 (C), 4.0; ×10 000 (D) (total polymer concentration – 3%).
Reproduced from Spasova *et al*. [17] by permission of e-Polymers.

Further, the possibility to incorporate a model drug into the chitosan-containing fibres was studied. Potassium 5-nitro-8-quinolinolate (K5N8Q) was selected because of its wide-spectrum antimicrobial and antimycotic activity. Considerable decrease in the mean fibre diameter (ca. 70 nm) was observed. It was attributed to the ability of K5N8Q to form charged ions in aqueous solutions. The incorporation of this model drug resulted in obtaining of nanofibres that possess antibacterial and antimycotic activity as evidenced by the performed microbiological tests.

The obtained results revealed the possibility natural polymers with inherent polyelectrolyte behaviour in aqueous solutions to be electrospun into nanofibres in the presence of non-ionogenic polymers with flexible chains. This approach has been confirmed by the preparation of chitosan-containing fibres in the presence of PEO [17, 24] or poly(vinyl alcohol) [25], as well as in the presence of silk fibroin using formic acid as a common solvent [26]. The use of trifluoracetic acid as a solvent has allowed the electrospinning of chitosan alone [25, 27, 28]. Applying the approach of electrospinning of mixed solutions of chitosan and non-ionogenic polymers allowed nanofibres containing chitosan derivatives to be obtained as well [18–21]. The solubility in aqueous medium of the obtained nanofibres however may limit some of their possible applications, especially when a contact of the nanofibrous materials with body fluids is envisaged. The preparation of water-insoluble fibres of chitosan or its derivatives by chemical- [27], thermal- [18, 21] or photo-crosslinking [19, 20] was reported. The antibacterial activity of nanofibrous materials of quaternized derivatives of chitosan revealed the potential of these new materials to be used as wound dressings [19, 20]. Moreover, very recently the preparation of magnetic nanofibres by electrospinning of a chitosan derivative and magnetite nanoparticles applying the same approach was shown [23].

Preparation of chitosan-coated PLLA or PLLA/PEG micro- and nanofibres

Poly(L-lactide) (PLLA) has numerous advantages as poly(.-hydroxy acid) for wide range of applications in the medical field and especially in implantology because of its bioresorbability and favourable physico-mechanical properties [36]. It is easily electrospun into micro- and nanofibres [11, 37]. However, the hydrophobic nature of the polyesters induces adhesion of pathogenic microorganisms onto implants prepared thereof [38]. In consequence, formation of bacterial biofilm which can lead to implant failure is possible. Thus, incorporation of suitable substances into the PLLA materials preventing the bacterial biofilm formation is required. One of the widely used methods of inhibiting adhesion of pathogenic microorganisms on hydrophobic surfaces is to impart certain hydro-

philicity to the material by physical or chemical incorporation of polyethylene glycol (PEG) [39]. Recently, we have shown that the incorporation of PEG up to 30% in PLLA fibres during the electrospinning process allows tuning the hydrophilicity of the obtained materials thus providing a convenient tool for modulation of the cellular response [31]. The electrospun PLLA and PLLA/PEG mats are promising scaffolds for cell proliferation and for tissue regeneration. Despite the repelling effect of PEG against pathogenic microorganisms it cannot kill them. It is expected that further modification of polyester-containing materials with polymers that possess inherent antibacterial activity can allow the preparation of devices hav153 e regeneration. Despite the repelling effect of PEG against pathogenic microorganisms it cannot kill them. It is expected that further modification of polyester-containing materials with polymers that possess inherent antibacterial activity can allow the preparation of devices hav153 e regeneration. Despite the repelling effect of PEG against pathogenic microorganisms it cannot kill them. It is expected that further modification of polyester-containing materials with polymers that possess inherent antibacterial activity can allow the preparation of devices hav153 e regeneration. Despite the repelling effect of PEG against pathogenic microorganisms it cannot kill them. It is expected that further modification of polyester-containing materials with polymers that possess inherent antibacterial activity can allow the preparation of devices hav153 e regeneration. Despite the repelling effect of PEG against pathogenic microorganisms it cannot kill them. It is expected that further modification of polyester-containing materials with polymers that possess inherent antibacterial activity can allow the preparation of devices hav153 e regeneration. Despite the repelling effect of PEG against pathogenic microorganisms it cannot kill them. It is expected that further modification of polyester-containing materials with polymers that possess inherent antibacterial activity can allow the preparation of devices hav153 e regeneration. Despite the repelling effect of PEG against pathogenic microorganisms it cannot kill them. It is expected that further modification of polyester-containing materials with polymers that

PEG aBantn 9yuk.leprnst pah2aga8esris devathi]TJ0vesris devath.h2vee.09eIt iirtheeIt iirtrc TDm aecihas6r-ct

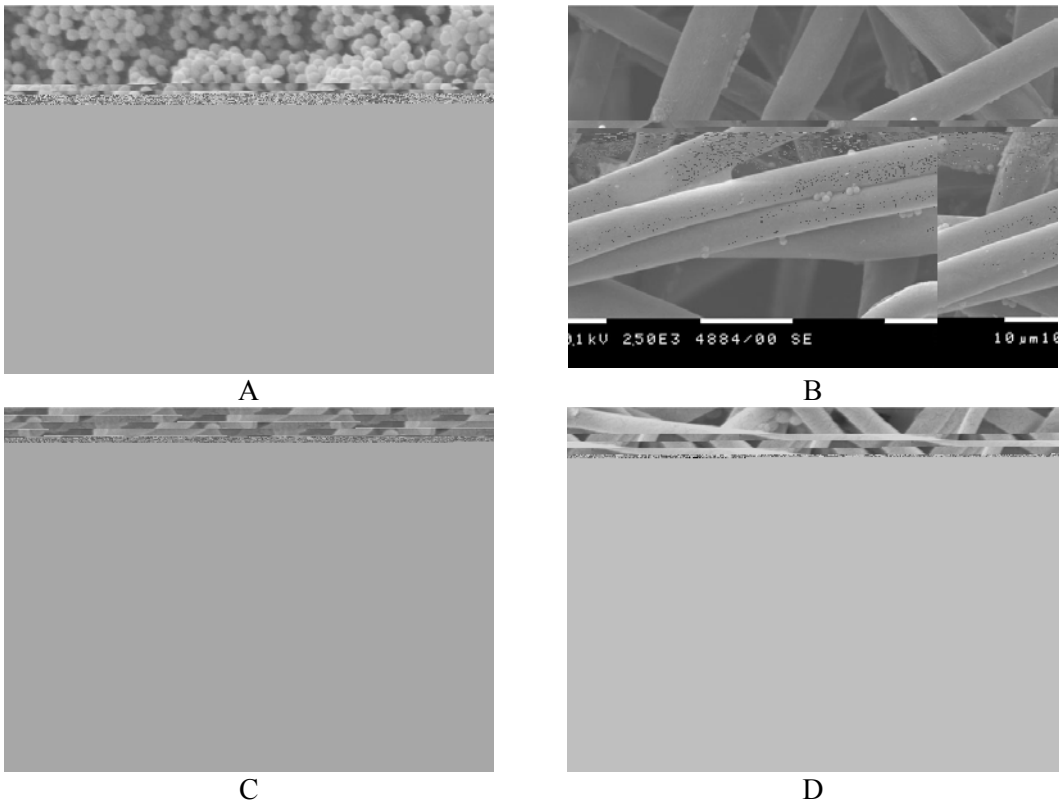

Fig. 5. SEM micrographs of *S. aureus* cells adhered on PLLA mat: pristine (A) and triple-coated with chitosan (crosslinked) (B); PLLA/PEG (70/30) mat: pristine (C) and triple-coated with chitosan (crosslinked) (D). Reproduced from Spasova *et al.* [22] by permission of Wiley-VCH Verlag GmbH & Co. KGaA, Germany.

As expected a significant number of adhered cells are observed on the PLLA mats (more than 200 cells per 100 mm^2). Triple coating of PLLA mats with chitosan led to a significant decrease in the number of adhered cells to ca. 5 cells per 100 mm^2. The increased hydrophilicity of PEG-containing fibres decreased the number of adhered bacterial cells (e.g., from more than 200 cells on the PLLA mat to 26 cells on the PLLA/PEG mat). Chitosan coating also resulted in significant decrease in the number of the adhered cells on the PLLA/PEG mat; the cell number was ca. 5 cells per 100 mm^2, which is the same as for chitosan-coated PLLA mats. The suppressing of the pathogenic cells adhesion combined with the haemostatic properties of the chitosan-coated PLLA and PLLA/PEG mats renders them very promising for use as wound dressings.

CONCLUSION

It has been shown that formation of defect-free chitosan nanofibres by electrospinning of chitosan aqueous solutions is feasible when poly(ethylene oxide) is added to the spinning solution. The incorporation of antimicrobial drug in the fibres imparts microbicidal activity of the nanofibrous materials. Novel non-woven textiles are easily prepared by coating PLLA or PLLA/PEG mats with chitosan. The chitosan-coated materials possess haemostatic and antibacterial activity, and thus are promising candidates for healing applications enabling rapid cessation of bleeding and regeneration of injured tissue.

The propounded simple and efficient approaches for preparation of chitosan-containing nanofibrous materials by electrospinning are easily extendable for other polymer systems. The electrospinning of aqueous solutions of polyelectrolytes is facilitated by incorporation of a non-ionogenic polymer. The beneficial properties of a polymer used for preparation of a scaffold with tuned properties may be easily combined with the properties of a second polymer using a combination of the electrospinning and coating techniques. The potential applications of the obtained nanofibrous mats are diversified by incorporation of bioactive substances thus obtaining novel materials with tuned biological activity.

Acknowledgements: *Financial support from the National Fund of Scientific Research (Grant NANOBIOMAT, NT 4-01/04) is acknowledged. The authors thank Dr. N. Markova (Institute of Microbiology, Bulgarian Academy of Sciences) and Dr. D. Danchev (Department of Haemostasis, Military Medical Academy, Sofia) for their help in pe-*

rforming the biological tests. The authors thank Dr. N. Malinowski (Central Laboratory of Photoprocesses, Bulgarian Academy of Sciences) for providing the SCI data.

REFERENCES:

1. K. H. Lee, H. Y. Kim, M. S. Khil, Y. M. Ra, D. R. Lee, *Polymer*, **44**, 1287 (2003).
2. Z.-M. Huang, Y.-Z. Zhang, M. Kotaki, S. Ramakrishna, *Composites Sci. Techn*., **63**, 2223 (2003).
3. A. Greiner, J. H.Wendorff, *Angew. Chem. Int. Ed*., **46**, 5670 (2007).
4. D. H. Reneker, A. L. Yarin, H. Fong, S. J. Koombhongse, *Appl. Phys*., **87**, 4531 (2000).
5. M. M. Hohman, M. Shin, G. Rutledge, M. P. Brenner, *Phys. Fluids*, **13**, 2221 (2001).
6. Y. M. Shin, M. M. Hohman, M. P. Brenner, G. C. Rutledge, *Polymer*, **42**, 9955 (2001).
7. G. Peev, M. Spasova, R. Mincheva, I. Rashkov, *J. Theor. Appl. Mechanics*, **36**, 43 (2006).
8. M. Spasova, R. Mincheva, D. Paneva, N. Manolova, I. Rashkov, *J. Bioact. Compat. Polym*., **21**, 465 (2006).
9. D. Li, Y. Xia, *Adv. Mater.*, **16**, 1151 (2004).
10. G. L. Bowlin, K. J. Pawlowski, J. D. Stitzel, E. D. Bowland, D. G. Simpson, J. B. Fenn, G. E. D. Wnek, in: "Tissue Engineering and Biodegradable Equivalents: Scientific and Clinical Applications", K.-U. Lewandrowski, D. L. Wise, M. J. Yaszemski, J. D. Gresser, D. J. Trantolo, D. E. Altobelli, (Eds), Marcel Dekker, Inc., N.Y., 2002, chapter 9, p. 165–178.
11. M. Bognitzki, W. Czado, T. Frese, A. Schaper, M. Hellwig, M. Steinhart, A. Greiner, J. H. Wendorff, *Adv. Mater*., **13**, 70 (2001).
12. K. Kim, M.Yu, X. Zong, J. Chin, D. Fang, Y. Seo, B. Hsiao, B. Chu, M. Hadjiargyrou, *Biomater.*, **24**, 4977 (2003).
13. H. Yoshimoto, Y. M. Shin, H. Terai, J. P. Vacanti, *Biomater.*, 24, 2077 (2003).
14. W. J. Li, C. T. Laurencin, E. J. Caterson, R. S. Tuan, F. K. Ko, *J. Biomed. Mater. Res*., **60**, 613 (2002).
15. X. M. Mo, C. Y. Xu, M. Kotaki, S. Ramakrishna, *Biomater*., 25, 1883 (2004).
16. R. N. Tharanathan, F. S. Kittur, *Crit. Rev. Food. Sci. Nutr*., **43**, 61 (2003).
17. M. Spasova, N. Manolova, D. Paneva, I. Rashkov, *e-Polymers*, no. 056, 1 (2004).
18. R. Mincheva, N. Manolova, D. Paneva, I. Rashkov, *J. Bioact. Compat. Polym*., **20**, 419 (2005).
19. M. Ignatova, K. Starbova, N. Markova, N. Manolova, I. Rashkov, *Carbohydr. Res*., **341**, 2098 (2006).
20. M. Ignatova, N. Manolova, I. Rashkov, *Eur. Polym. J*., **43**, 1112 (2007).
21. R. Mincheva, N. Manolova, I. Rashkov, *Eur. Polym. J*., **43**, 2809 (2007).
22. M. Spasova, D. Paneva, N. Manolova, Ph. Radenkov, I. Rashkov, *Macromol. Biosci.*, **8**, 153 (2008).
23. R. Mincheva, O. Stoilova, H. Penchev, T. Ruskov, I. Spirov, N. Manolova, I. Rashkov, *Eur. Polym. J*., **44**, 615 (2008).
24. B. Duan, C. Dong, X. Yuan, K. Yao, *J. Biomater. Sci., Polym. Ed*., **15**, 797 (2004).
25. K. Ohkawa, D. Cha, H. Kim, A. Nishida, H. Yamamoto, *Macromol. Rapid Commun*., **25**, 1600 (2004).
26. W. H. Park, L. Jeong, D. I. Yoo, S. Hudson, *Polymer*, **45**, 7151 (2004).
27. J. D. Schiffman, C. L. Schauer, *Biomacromolecules*, **8**, 594 (2007).
28. J. D. Schiffman, C. L. Schauer, *Biomacromolecules*, **8**, 2665 (2007).
29. M. Ignatova, N Manolova, I. Rashkov, *Eur. Polym. J.*, **43**, 1609 (2007).
30. M. Ignatova, N. Markova, N. Manolova, I. Rashkov, *J. Biomat. Sci. Polym. Ed*. **19**, 373 (2008).
31. M. Spasova, O. Stoilova, N. Manolova, G. Altankov, I. Rashkov, *J. Bioact. Compat. Polym*., **22**, 62 (2007).
32. O. Stoilova, C. Jérôme, C. Detrembleur, A. Mouithys-Mickalad, N. Manolova, I. Rashkov, R. Jérôme, *Chem. Mater*., **18**, 4917 (2006).
33. O. Stoilova, C. Jérôme, C. Detrembleur, A. Mouithys-Mickalad, N. Manolova, I. Rashkov, R. Jérôme, *Polymer*, **48**, 1835 (2007).
34. W. S. Rasband, Image J, U. S. Nat. Inst. Health, Bethesda, Maryland, USA, http://rsb.info.nih.gov/ij/ (1997-2006).
35. A. Nikolova, N. Manolova, I. Rashkov, *Polym. Bull*., 41, 115 (1998).
36. L. S. Nair, C. T. Laurencin, *Progr. Polym. Sci*. **32**, 762 (2007).
37. E. R. Kenawy, G. L. Bowlin, K. Mansfield, J. Layman, D. G. Simpson, E. H. Sanders, G. E. Wenk, *J. Control. Rel*. **81**, 57 (2002).
38. L. G. Harris, L. Mead, E. Muller-Oberlander, R. G. Richards, *Eur. Cell. Mater*., **10**, 24 (2005).
39. A. Razatos, T. Ong, F. Boulay, D. L. Elbert, J. A. Hubell, M. M. Sharma, G. Georgiou, *Langmuir,* **16**, 9155 (2000).
40. Y. Chung, Y. Su, C. Chen, G. Jia, H. Wang, J. Wu, J. Lin, *Acta Pharmacol. Sin*., **25**, 932 (2004).
41. H. S. Whang, W. Kirsh, Y. H. Zhu, C. Z. Yang, S. M. Hudson, *J. Macromol. Sci., Polym. Rev*., **45**, 309 (2005).
42. D. Paneva, N. Manolova, I. Rashkov, D. Danchev, *J. Bioact. Compat. Polym.*, **20**, 133 (2005).
43. R. Mincheva, N. Manolova, D. Paneva, I. Rashkov, *Eur. Polym. J*., **42**, 858 (2006).

I H E M Q : < : G G ? : G H < K D B L H A - : K G T > T J @ : S F B B D J - H B G : G H < E : D G ? K L B F : L ? J B : E K Q J ? ? A E ? D L J H H < E : D G Y < : G ?

F. = KiZkh\>ZI. IZg_\Z ?f FZghe,hBZ;. JZrdh\

Лаборатория „Биологично активни полимери“, Институт по полимери, Българска академия на науките, 1113 София

Посветена на акад. Иван Юхновски по повод на 70-та му годишнина

Ihkltibegz4 ygmz2008]; Ij_jZ[hl_gz6 ygmz2008]

(J _ a x)f _

? e _ d l j h h \ e Z d g y \ i Z h g b _ a l h h ^ b l _ b e g _ Z k g h k t s _ k l \ b f _ Z o g b a l Z h e m q Z \ g Z Z g _ o g e Z d g L Z Z a b
i m [e b d Z i g j _ b y k l Z \ e h y [a Z h j h k \ _ l g g Z l h a b _ l h ^ d Z l h k h [_ g g h b f Z g _ b h l ^ _ e _ g g Z g Z g h \ e Z d g _ k l b
f Z l _ j b Z g e Z h k g h \ Z g l Z Z o b l h a Z g Z t j \ b i t l k Z j _ ^ e h ` _ ^ g \ b Z e _ k g h k t s _ k l \ b i h b ^ o h ^ a Z Z h e m q Z \ Z g _
g Z f b d j - h b g Z g h \ e Z d g Z _ k _ j b b Z _ k e b ^ t j ` Z s i j b j h ^ g b h y e b f _ j b l h a Z t g j \ b y l i h ^ o h k ^ _ h k g h \ Z g \ Z Z
_ e _ d l j h h \ e Z d g g Z k \ f Z _ g _ j g Z b a l \ h g j b Z o b l h a b Z g g _ c h g h] i h g e _ g f . _ K j _ ^ g b k l _ h c g h k g l Z b Z f _ l t j Z
g Z g Z g h \ e Z d \ g Z Z _ l b Z f l _ ` ^ m 0 b 290 nm. < l h j b y i l h ^ o h k ^ _ k t k l h \ b i h d j b \ Z g Z _ e _ d l j h h \ e Z d g _ g b
g Z g h \ e Z d g f _ Z k l h b \ _ h l i h e (b - e Z d l) b f b e b i h e (b - e Z d l) b i ^ h e b _ l b e _ g] e k b o d h b k e h a Z - g p _ g _ g k Z
i h l _ g p b Z e g j j b l e _ h ` _ g b g Z l _ a l g h \ b f Z l _ j b Z \ e b [e Z k l g Z [b h f _ ^ b p b g b Z h Z k i _ p b Z e g y b g h l h
i j b e h ` _ g d b Z _ l k b b k l _ a b Z ^ h k l Z \ g g Z e _ _ d Z j k l \ k j g b ^ k l b Z l Z i h d j b l h a Y e _ q _ g g b Z _ Z g b

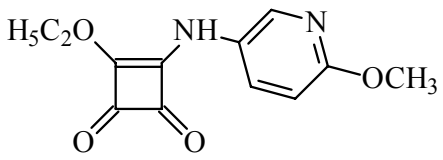

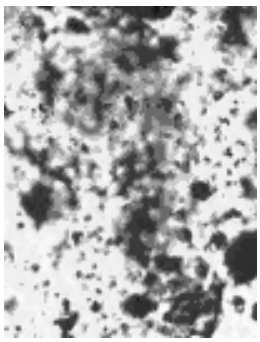

Yellow solid phase 1.

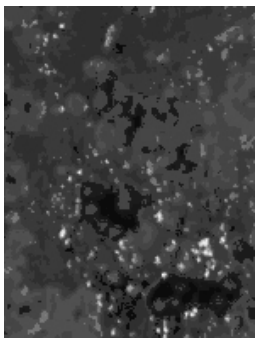

Red solid phase 2.

Scheme 1. Chemical diagram of compound studied; solid phases 1 and 2.

EXPERIMENTAL

Synthesis

The starting compound, 5-amino-2-methoxy-pyridin ester amide of squaric acid ethyl ester (solid phase 1) was synthesized according to the procedure described in [4]. IR and UV-Vis spectroscopy confirmed the purity of the compound. The most intensive signal in the mass spectrum is that of the peak at *m/z* 249.29, corresponding to the singly charged cation $[C_{12}H_{13}N_2O_4]^+$ with a molecular weight of 249.24. The solid phase 2 was obtained by heating of solid phase 1 at 200ºC at Pt-crucible. It was also obtained after heating of the starting compound in glass capillary. Our attempts to receive suitable single crystals of this phase have failed due to the formation of solid phase 1 after dissolving of the solid phase 2.

Materials and methods

IR-spectroscopic measurements within 4000–400 cm^{-1} range were obtained on a Thermo Nicolet 6700 FT-IR spectrometer (resolution 1 cm^{-1}, 250 scans). A Specac wire-grid polarizer was used. Oriented solid samples were obtained as a colloid suspension in a nematic liquid crystal of the 4'-cyano-4'-alkylbicyclohexyl type (ZLI 1695, Merck), mesomorphic at room temperature. Its weak IR-spectrum permits recording of the guest-compound IR-bands in the whole 4000–400 cm^{-1} range. The isolated nitrile stretching IR-band at 2236 cm^{-1} serves additionally as an orientation indicator. The effective orientation of the samples was achieved through the new procedure described in [5–8]. The procedure for the position (v_i) and integral absorbances (A_i) determination for each *i*-peak has been carried out by deconvolution and curve-fitting procedures at 50:50% ratio of Lorentzian to Gaussian peak functions, γ^2 factors about 10^{-5} and 2000 iterations [7, 8]. The means of two treatments were compared by Student *t*-test. The experimental IR-spectral patterns have been acquired and processed by GRAMS/AI 7.01 IR spectroscopy (Thermo Galactic, USA) and STATISTICA for Windows 5.0 (StatSoft, Inc., Tulsa, OK, USA) program packages. The theoretical approach, experimental technique for preparing the samples, procedures for polarized IR-spectra interpretation and the validation of this new linear-dichroic infrared (IR-LD) orientation solid-state method for accuracy and precision have been presented. The influence of the liquid crystal medium on peak positions and integral absorbances of the guest molecule bands, the rheological model, the nature and balance of the forces in the nematic liquid crystal suspension system, and morphology of the suspended particles have been also discussed [6–8].

Spectroscopic and structural results were obtained by the orientation technique [5–8] using the known reducing-difference procedure designated as "stepwise reduction" for polarized IR-spectra interpretation. This method was primarily suggested by Thulstrup and Eggers for polarized UV-spectral interpretation [9]. The procedure consists in consecutive elimination of the spectral bands of a given polarization by means of subtracting the perpendicular spectrum multiplied by a coefficient from the parallel one. This procedure was extended by Spanget-Larsen [10] and by Korte and Lampen [11] to samples orientated in stretched polyethylene and nematic solution, respectively. A systematic analysis of this approach and its application to IR-bands assignment according to their symmetry appurtenance was developed by B. Jordanov and co-workers [12–15] for polarized IR-spectra in nematic liquid crystal solution. The method consists of subtraction of the perpendicular spectrum, (IR_s, resulting from a 90º angle between the polarized light beam electric vector and the orientation of the sample) from the parallel one (IR_p) obtained with a co-linear mutual orientation. The recorded *difference* (IR_p–IR_s) spectrum divides the corresponding parallel (A_p) and perpendicular (A_s) integrated absorbencies of each band into positive values originating from transition moments, which form average angles with the orientation direction ( ) between 0º and 54.7º (magic angle), and negative ones corresponding to transition moments between 54.7º and 90º. In the *reducing-difference procedure*, the perpendicular spectrum multiplied by the parameter ***c***, is subtracted from the parallel one and ***c*** is varied until at

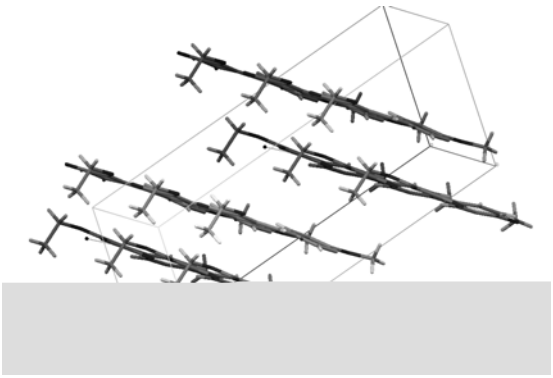

Scheme 2. Hydrogen bonding in solid phase 1.

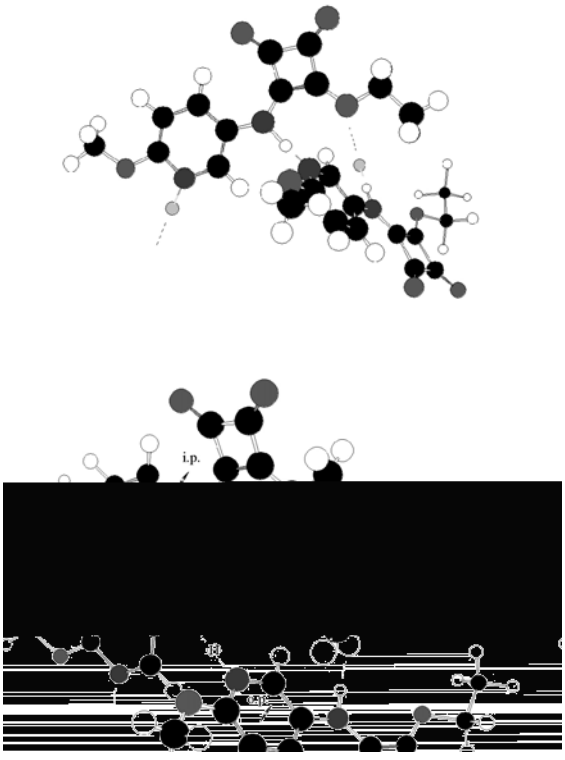

Scheme 3. Intermolecular interactions in solid phase 2.

Moreover, the absence of well-defined isolated band of ν_{NH}, typical for solid phase 1, and an observation of the broad band within 3500–2500 cm^{-1} as well as the intensive broad band at 1587 cm^{-1}, typical for full or partially charged amines, proposed strong intermolecular NH…N_{Py}, which has been observed in a series of papers dealing with protonated heterocyclics [18–20] or in 4-aminopyridinium hemiperchlorate, where the NH bonds in the NH…N interaction is equalized and H- is fixed at an equal distance of both the N-atoms [21]. Additional confirmation of the last assumption follows as well from the obtained more than 100 nm batochromic sift of λ_{max} in the solid red phase, typical for push-pull systems [1–3].

The above stated vibrational assignment is experimentally proved by the polarized IR-spectroscopic study. Moreover, an interesting result is obtained in addition. In contrast to solid phase 1, where the elimination of o.p. modes leads to a total vanishing of the corresponding IR-bands of same symmetry class [4], the elimination of the corresponding bands in solid phase 2 as well as the $\nu^{s}_{C=O(Sq)}$ stretching modes leads to an observation of second bands of same symmetry class. As can be seen the elimination of each of the well-defined by deconvolution and curve-fitting procedures bands at 1803 and 1795 cm^{-1} leads to an observation of numbering maximum (Figs. 3.2 and 3.3).

Fig. 3. Curve-fitted IR-spectrum (1) of solid phase 2 (χ^2 values less then 8×10^{-4}) within 1850–1650 cm^{-1} and reducing IR-LD spectra after elimination of the bands at 1803 cm^{-1} (2) and 1795 cm^{-1} (3).

On the other hand, the elimination of the bands about 1600 and 835 cm^{-1} at equal dichroic ratio in

addition confirms the assumption stated above, due to in the frame of one isolated molecule is impossible to be eliminated IR-bands with i.p. and o.p. symmetry classes. This phenomenon has been observed in systems, where the unit cell contains mutual perpendicular oriented molecules [22, 23]. These results proposed that the second phase 2 is characterized by infinite zig-zag chains of molecules, connected by strong NH..N_{Py} hydrogen bonds (Scheme 3). In the frame of these chains the molecule of 5-amino-2-methoxypyridin ester amide of squaric acid ethyl ester is with low influenced conformation, because of our thermal analysis, shows only a small thermal process at 94ºC with shape, indicating a second order phase transformation, explained by the liberation of a rotation around the C–N bond [4].

CONCLUSION

By means of linear-polarized IR-spectroscopy of oriented colloid suspensions in nematic host, the IR-spectroscopic and structural elucidation of the high temperature solid phase of 5-amino-2-methoxypyridine ester amide of squaric acid is preformed. In contrast to the solid phase obtained at room temperature, where a pseudo-layered structure is stabilized by intermolecular NH…O=C intermolecular hydrogen bonds with length of 2.955 Å [4], in the high temperature phase strong NH…N_{Py} interactions are predominant. As a result of the solid phase transition, the layered structure is distorted and infinite zig-zag chains are typical.

Acknowledgments: *This work has been supported financially by the Bulgarian National Fund of Scientific Research, Contract X– 1510.*

REFERENCE

1. D. Chemla, J. Zyss, Nonlinear Optical Properties of Organic Molecules and Crystals, Vol. 1, D. Chemla, J. Zyss (Eds), Academic Press, New York, 1987, pp. 23–187.
2. H. Nalwa, T. Watanabe, S. Miyata, Nonlinear Optics of Organic Molecules and Polymers, H.S. Nalwa, S. Miyata, (Eds.) CRC Press, Boca Raton, 1997, pp. 89–329.
3. J. J. Wolf, R. Wortmann, *Adv. Phys. Org. Chem*, (1999) 121.
4. T. Kolev, B. B. Koleva, T. Spassov, E. Cherneva, M. Spiteller, H. Mayer-Figge, W. S. Sheldrick, *J. Mol. Struct*., (2007), (in press), doi:10.1016/j.molstruc. 2007.05.005.
5. B. B. Ivanova, M. G. Arnaudov, P. R. Bontchev, *Spectrochim. Acta*, , 855 (2004).
6. B. B. Ivanova, D. L. Tsalev, M. G. Arnaudov, *Talanta*, , 822 (2006).
7. B. B. Ivanova, V. D. Simeonov, M. G. Arnaudov, D. L. Tsalev, *Spectrochim Acta*, , 66 (2007).
8. B. B. Koleva, T. Kolev, V. Simeonov, T. Spassov, M. Spiteller, *J. Inclusion Phenom. Macrocyclic Chem.*, , 319 (2008).
9. E. W. Thulstrup, J. H. Eggers, *Chem. Phys*. *Lett*., 690 (1996).
10. J. Spanget-Larsen, *SPIE*, , 404 (1992).
11. E. H. Korte, P. Lampen, Private communications (1988).
12. B. Jordanov, R. Nentchovska, B. Schrader, *J. Mol. Struct*., , 401 (1993).
13. B. Jordanov, B. Schrader, *J. Mol. Struct*, , 389 (1995).
14. M. Belhakem, B. Jordanov*, J. Mol. Striuct*., , 309 (1990).
15. M. Rogojerov, D. Kolev, B. Jordanov, *J. Mol. Striuct*., , 447 (1995).
16. S. G. de Miranda, P. A. M. Vazquez, *J. Braz. Chem. Soc*., 3 (2002).
17. H. Torii, M. Tasumi, *J. Mol. Struct*. *(Theochem)*, , 15 (1995).
18. B. B. Ivanova, *Spectrochim. Acta, Part A*, , 58 (2005).
19. B. B. Ivanova, M. G. Arnaudov, H. Mayer-Figge, *Polyhedron*, , 1624 (2005).
20. B. B. Koleva, T. Kolev, T. Tsanev, St. Kotov, H. Mayer-Figge, R. W. Seidel, W. S. Sheldrick, *J. Mol. Struct., (*2007), (in press) DOI: http://dx.doi.org/ 10.1016/j.molstruc.2007.09.006
21. P. Teulon, R. G. Delaplane, I. Olovsson, J. Rozière, *Acta Cryst*., , 479 (1985).
22. B. B. Koleva, E. N. Trendafilova, M. G. Arnaudov, W. S. Sheldrick, H. Mayer-Figge, *Trans. Met. Chem*., , 866 (2006).
23. B. B. Ivanova, H. Mayer-Figge, *J. Coord. Chem*., 653 (2005).

ПОЛАРИЗАЦИОННО ИЧ-СПЕКТРАЛНО ИЗСЛЕДВАНЕ НА ВИСОКОТЕМПЕРАТУРНАТА „ЧЕРВЕНА“ ФАЗА НА 5-АМИНО-2-МЕТОКСИПИРИДИН ЕСТЕР АМИД НА ЕТИЛОВИЯ ЕСТЕР НА КВАДРАТНАТА КИСЕЛИНА

Е. Д. Чернева[1], Ц. М. Колев[1,2]*

[1] *Институт по органична химия с център по фитохимия, Българската академия на науките, ул. „Акад. Г. Бончев“, бл. 9, 1113 София,*
[2] *Пловдивски университет, Катедра „Органична химия“, ул. „Цар Асен“ № 24, 4000 Пловдив*

Посветена на акад. Иван Юхновски по повод на 70-та му годишнина

Постъпила на 6 януари 2008 г.; Преработена на 19 март 2008 г.

(Резюме)

В наша предишна работа бе установено, че съединението 5-амино-2-метоксипиридин естер амид на етиловия естер на квадратната киселина се стабилизира в две твърди фази в зависимост от температурата. Така наречената „жълта“ фаза изкристализира при температура T = 298K и се характеризира с нецентросиметрична пространствена група *Cc,* а молекулите образуват псевдослоеста структура посредством междумолекулни NH…O=C водородни връзки (2.955 Å). Втората, аморфна „червена“ фаза се получава в резултат на фазов преход при температура от 200ºC. Нейното спектрално охарактеризиране бе извършено използвайки възможностите на поляризационната ИЧ-спектроскопия на ориентирани колоидни суспензии в нематичен течен кристал.

Bulgarian Chemical Communications, Volume 40, Number 4 (pp. 483–490) 2008

Spectroscopic elucidation of hydrogensquarate and ester amide of squaric acid of 2-cloro-3-amino-pyridine

Ts. D. Tsanev[1], Ts. M. Kolev[1,2]*

[1] *Department of Structural Organic Analysis, Institute of Organic Chemistry with Centre of Phytochemistry, Bulgarian Academy of Sciences, Acad. G. Bonchev St., Block 9, 1113 Sofia, Bulgaria*
[2] *Plovdiv University, Department of Organic Chemistry, 24 Tzar Assen St., Plovdiv 4000, Bulgaria*

Dedicated to Academician Ivan Juchnovski on the occasion of his 70th birthday

Received January 6, 2008; Revised March 19, 2008

Novel derivatives of squaric acid with 2-chloro-3-amino-pyridine, i.e. hydrogensquarate and ester amide of squaric acid are synthesized, isolated and spectroscopically characterized in solution and in solid-state. Methods as conventional and linear polarized IR-spectroscopy of oriented colloid suspensions, UV-spectroscopy, ^{1}H- and ^{13}C-NMR, mass spectrometry (positive and negative ESI, FAB, HPLC tandem MS/MS), TGV and DSC methods are used. Quantum chemical *ab initio* and DFT calculations are performed, supporting the obtained optical experimental data.

Key words: IR-LD spectroscopy, colloid suspension, spectroscopic elucidation, 2-cloro-3-amino-pyridine ester amide of squaric acid ethyl ester, hydrogensquarate, UV-, ^{1}H- and ^{13}C-NMR, HPLC ESI MS/MS, quantum chemistry.

INTRODUCTION

Aminopyridines are bioactive *N*-heterocyclic tertiary amines that increase the strength of the nerve signal [1], exerting their action by inhibiting the voltage-dependent K^+-channels [2] and hence maintain the presynaptic action potential. In this form, the calcium influx is enhanced, leading to an increase in the release of neurotransmitter [3]. Due to their ability to facilitate nerve transmission, aminopyridines have been applied to reverse anaesthesia and muscle relaxation [4]. In addition, they have been proposed as drugs for the treatment of multiple sclerosis [5], *myasthenia gravis* [6], spinal cord injuries [7], botulism [8] and Alzheimer's disease [9]. Aminopyridines are weak bases, p*K*a ~9.0, and thus they can exist both as the neutral or cationic protonated form at physiological pH [10]. For these reasons, in series of papers we have investigated the structure-spectroscopic properties correlation of protonated forms of different substituted aminopyridines [11–14]. Now, we present spectroscopic and structural elucidation of hydrogensquarate (**1**) and ester amide of squaric acid (**2**) of 2-chloro-3-amino-pyridine (Scheme 1). For halogen-substituted aminopyridines has been proved the action on mammalian non-myelinated nerve fibres [15]. Both in solution and in solid state the compounds are characterized by means of conventional and linear polarized IR-spectroscopy of solids, oriented as a colloid suspension in nematic host, ^{1}H- and ^{13}C-NMR, positive and negative ESI mass spectrometry (MS), FAB MS, hybrid method HPLC tandem MS/MS, UV-spectroscopy, TGV and DSC methods. Quantum chemical calculations at DFT, MP2 and CIS level of theory and 6-31++G** basis set are employed for predicting and supporting experimentally observed optical properties of the compounds studied.

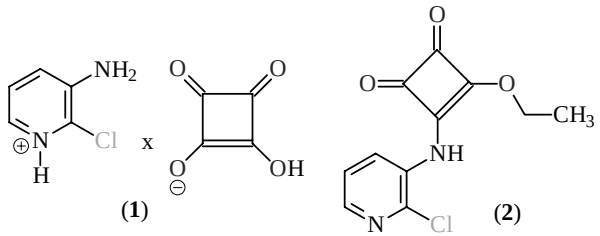

Scheme 1. Chemical diagram of compounds studied.

Experimental

Synthezis

2-chloro-3-amino-pyridine was purchased from Riedel de Haën (Germany). The hydrogensquarate salt (**1**) was obtained according to the following procedure: 2-chloro-3-amino-pyridine (0.1286 g) was dissolved in 20 ml methanol. An aqueous solution (20 ml) of squaric acid (0.1140 g) was added by continuous stirring and heating (T = 50ºC) for 3h. After two weeks at ambient conditions a yellow precipitate was formed. It was filtered, washed with methanol and dried under P_2O_5 at 25ºC. (Found: C,

* To whom all correspondence should be sent:
E-mail: kolev@orgchm.bas.bg; kolev@uni-plovdiv.bg

© 2008 Bulgarian Academy of Sciences, Union of Chemists in Bulgaria

44.59; H, 2.90; N, 11.50; [$C_9H_7N_2O_4Cl$] calcd.: C, 44.56; H, 2.91; N, 11.55 %).

Ester amide of squaric acid of 2-chloro-3-amino-pyridine (**2**) was synthesized as follows: equimolar amounts of 2-chloro-3-amino-pyridine (0.1286 g) and ethyl ester of squaric acid (1 mmol) in 20 ml ethanol (95%) were mixed by continuous stirring at room temperature for 30 h. The formed yellow precipitate was filtered, washed with ethanol and dried under P_2O_5 at 25ºC. (Found: C, 52.50; H, 3.60; N, 11.10; [$C_{11}H_9N_2O_3Cl$] calcd.: C, 52.29; H, 3.59; N, 11.09%).

The TGV and DSC data for (**1**) and (**2**) in the temperature range of 300–500K show an absence of the included solvent molecules in the both compounds.

Materials and methods

Conventional and polarized IR-spectra were measured on a Thermo Nicolet OMNIC FTIR-spectrometer (4000–400 cm^{-1}, 2 cm^{-1} resolution, 200 scans) equipped with a Specac wire-grid polarizer. Non-polarized solid-state IR spectra were recorded using the KBr disk technique. The oriented samples were obtained as a colloid suspension in a nematic liquid crystal ZLI 1695. Its self-absorption bands are shown in Fig. 1. The theoretical approach, experimental technique for preparing the samples, procedures for polarized IR-spectra interpretation and the validation of this new linear-dichroic infrared (IR-LD) orientation solid-state method for accuracy and precision has been presented in [16–19]. The influence of the liquid crystal medium on peak positions and integral absorbances of the guest molecule bands, the rheological model, the nature and balance of the forces in the nematic liquid crystal suspension system, mathematical model, and morphology of the suspended particles also been discussed [16–19].

The *positive and negative ESI mass* spectra were recorded on a Fisons VG Autospect instrument employing 3-nitrobenzylalcohol (Sigma-Aldrich) as the matrix.

Ultraviolet (UV) spectra were recorded on a Tecan Safire Absorbance/Fluorescence XFluor 4 V 4.40 spectrophotometer operating between 190 and 900 nm, using solvents such as water, methanol, dichloromethane, tetrahydrofurane, acetonitrile, acetone, 2-propanol and ethyl acetale (all Uvasol, Merck products) in concentration of 2.5×10^{-5} M, using 0.0921 cm quarz cells.

HPLC-MS/MS analysis. The analyses of the samples were performed with a Thermo Finnigan surveyor LC-Pump. Compounds were separated on a Luna C18 column (150×2 mm, 4 μm particle size) from Phenomenex (Torrance, CA, USA). The mobile phase consisted of water + 0.1% HCOOH (A) and acetonitrile + 0.1% HCOOH (B) using a gradient program. The compound was detected via UV and a TSQ 7000 (Thermo Electron Corporation, Dreieich, Germany) mass spectrometer. The spectra were obtained using the TSQ 7000 equipped with an ESI ion source and operated at the following conditions: capillary temperature 180ºC; sheath gas 60 psi and spray voltage 4.5 kV. 1 mg/ml of the sample was dissolved in acetonitrile and injected into the ion source by an auto sampler (Finnigan Surveyor). The obtained data were processed using the Excalibur 1.4 software. The molecular mass was determined using FAB mass spectra, measured on a Fusion VG Autospect instrument employing 3-nitrobenzyl alcohol as a matrix.

Quantum chemical calculations were performed with GAUSSIAN 98 and Dalton 2.0 program packages [20, 21]. The output files were visualized by means of the ChemCraft program [22]. The geometries of N_{py} protonated form of 2-cloro-3-amino-pyridine and the corresponding ester amide of squaric acid with 2-cloro-3-amino-pyridine were optimized at two levels of theory: second-order Moller-Pleset perturbation theory (MP2) and density functional theory (DFT) using the 6-31++G** basis set. The DFT method employed is B3LYP, which combines Backe's three-parameter non-local exchange function with the correlation function of Lee, Yang and Parr. Molecular geometries of the studied species were fully optimized by the force gradient method using Bernys' algorithm. For every structure, the stationary points found on the molecule potential energy hypersurfaces were characterized using standard analytical harmonic vibrational analysis. The absence of the imaginary frequencies, as well as of negative eigenvalues of the second-derivative matrix, confirmed that the stationary points correspond to minima of the potential energy hypersurfaces. The calculations of vibrational frequencies and infrared intensities were checked to establish which kind of performed calculations agree best with the experimental data. In our cases the DFT method provides more accurate vibrational data, as far as the calculated standard deviations of respectively 12 cm^{-1} (B3LYP) and 17 cm^{-1} (MP2) corresponding to groups, which do not participate in intra- or intermolecular interactions, are concerned. So, the B3LYP/6-31++G** data are presented for above discussed modes, where a modification of the results using the empirical scaling factor 0.9614 is made to achieve better correspondence between the experimental and theoretical values. The UV spectra in the gas phase and in ethanol solution were obtained by CIS/6-

31++G** and TD-DFT calculations.

The *thermal analyses* were performed in the 300–500K region on a Differential Scanning Calorimeter Perkin-Elmer DSC-7, and a Differential Thermal Analyzer DTA/TG (Seiko Instrument, model TG/DTA 300). The experiments were carried out with scanning rate of 10 K/min under an argon atmosphere.

The *elemental analysis* was carried out according to the standard procedures for C and H (as CO_2, and H_2O) and N (by the Duma's method).

RESULTS AND DISCUSSION

The non polarized IR-spectra of (**1**) and (**2**) are depicted in Fig. 1. The 3500–300 cm^{-1} IR-spectroscopic region of the first compound is characterized by a series of maxima (Fig. 2), which can be assigned as follows: 3410 cm^{-1} (ν^{as}_{NH2}), 3323 cm^{-1}/ 3202 cm^{-1} (ν^{s}_{NH2}) and the band within 3100–3000 cm^{-1} – to in-plane (i.p.) CH-stretching vibrations of pyridine ring. The observation of Fermi resonance spitted band of ν^{s}_{NH2} has been previously observed in pyridinium derivatives [23–25]. When a given NH_2-group participates in asymmetric intermolecular interactions NH_2…X, the ν^{s}_{NH2} is observed as two bands, which are eliminated at equal dichroic

cular interactions NH

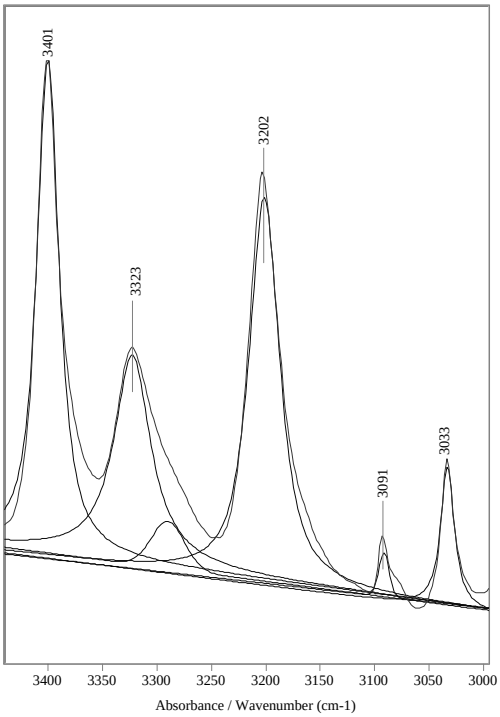

Fig. 2. Curve-fitted IR-spectrum of (**1**) within 3450–3000 cm^{-1} IR-region (χ^2 value is 4×10^{-5}).

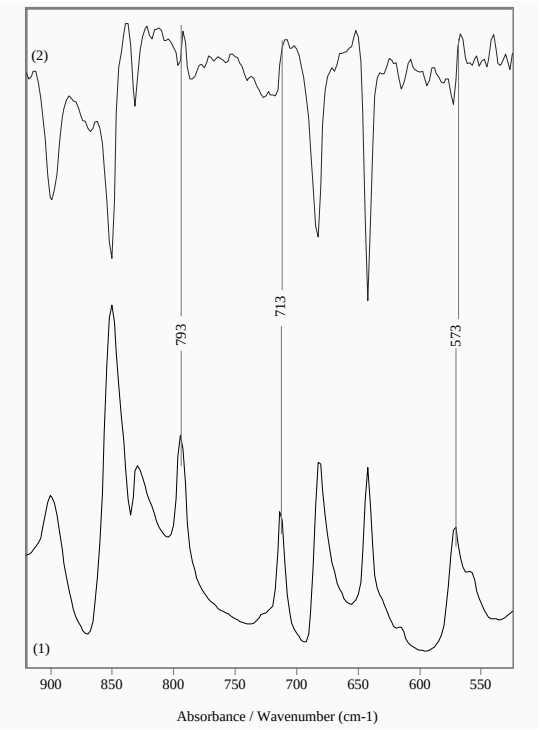

Fig. 3. Non-polarized IR- (1) and reduced IR-LD (2) spectrum of (**1**) after elimination of the band at 713 cm^{-1}.

The IR-spectrum of (**2**) in solid-state is characterized with an intensive band at 3225 cm^{-1} belonging to ν_{NH} stretching vibration. The symmetric and asymmetric stretching modes of squarate fragment are low- and high-frequency shifted and are observed at 1798 and 1704 cm^{-1}. The intensive band at 1564 cm^{-1} corresponds to $\nu_{C=C}$ stretching vibration. The i.p. pyridine modes are observed at 1640, 1607 and 1500 cm^{-1} and are eliminated at equal dichroic ratio (Fig. 4.2). The values are typical for pyridinium derivatives [27].

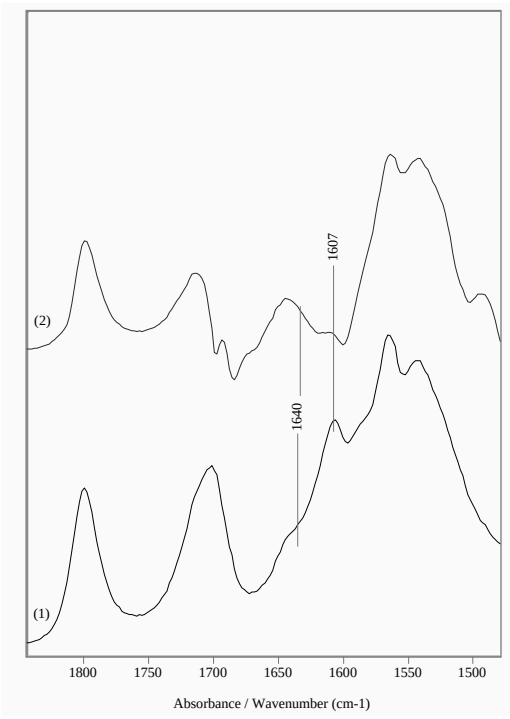

Fig. 4. Non-polarized IR- (1) and reduced IR-LD (2) spectrum of (**2**) after elimination of the band at 1607 cm^{-1}.

The experimentally observed IR-spectroscopic data are supported by theoretical quantum chemical spectra (Fig. 5). Comparison between the theoretical and experimental values shows a difference less then 2 cm^{-1} for i.p. vibrations of pyridine ring, 7 cm^{-1} for o.p. modes and within 10–17 cm^{-1} for ν_{NH} and $\nu\varepsilon_{C=O}$ stretching vibrations of squaric acid residues. These data can be explained with the participations of these groups in intermolecular interactions, typical in solid state and are similar for other ester amides of squaric acid [28, 29].

UV-spectra

The UV-spectra of 2-cloro-3-amino-pyridine, its hydrogensquarate and ester-amide of squaric acid are depicted in Fig. 6. The compounds are characterized with a band at 277 nm (ε = 10000–9865 $l\cdot mol^{-1}\cdot cm^{-1}$). Both in the N_{py} protonatated form (**1**) and in ester amide (**2**) the complex band does not affect significantly. The charge transfer band over than 350 nm (ε = 10178–12561 $l\cdot mol^{-1}\cdot cm^{-1}$) is batochromic shifted as a result of protonation or formation of the ester-amide derivative (Fig. 6). In contrast to protonated forms of 4-aminopyridine [30] and 3,4-diaminopyridine [12], the N_{py} protonation in 2-cloro-3-amino-pyridine does not affect the aromatic character of pyridine ring. These

results are predicted theoretically as well where our TD-DFT calculations in ethanol solution give better results, after a comparison with corresponding CIS data. The corresponding values are 377 nm (E = 4.21 eV, f = 0.0032) of 2-cloro-3-amino-pyridine, 390 nm (E = 5.11 eV, f = 0.1056) of N_{py} protonated form and 401 nm (E = 6.67 eV, f = 0.2546) in (**2**), respectively.

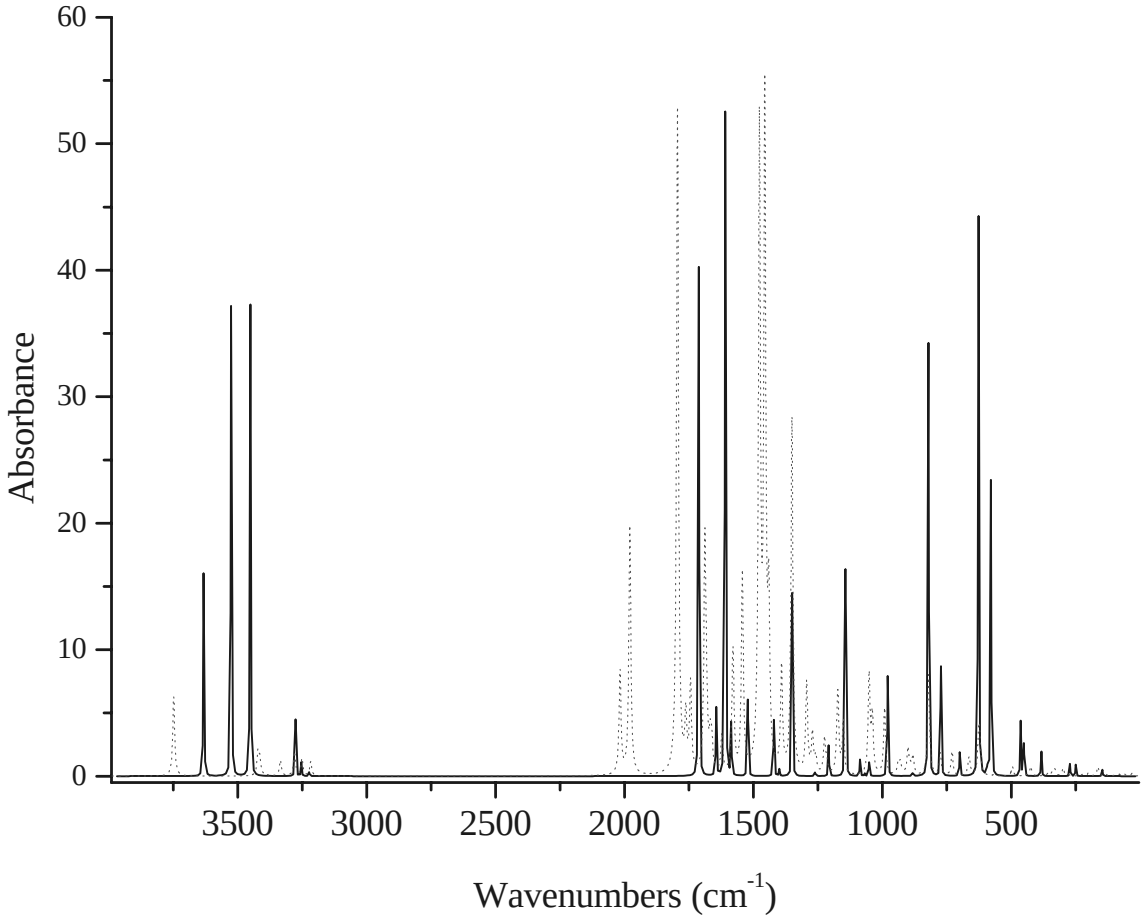

Fig. 5. Non-scaled theoretical IR-spectra of protonated 2-cloro-3-amino-pyridine (solid line) and 2-cloro-3-amino-pyridine ester amide of squaric acid (dot line).

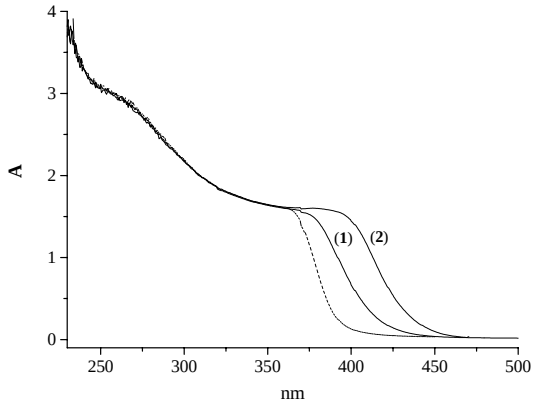

Fig. 6. UV-spectra of 2-cloro-3-amino-pyridine (dot line) its hydrogensquarate (**1**) and ester amide of squaric acid (**2**).

HPLC ESI MS/MS data

The positive ESI mass spectrum of (**1**) shows a peak at *m/z* 129.44 corresponding to singly charged $[C_5H_5N_2Cl]^+$ with molecular weight of 129.57. The negative spectrum is characterized with peak at m/z 113.2, belonging to anion $[C_4HO_4]^-$ with a molecular weight of 113.05.

The ESI mass spectrum of (**2**), shown in Fig. 7, is characterized with a peak at *m/*z of 257.1, corresponding to singly charged cation $[C_{11}H_{10}N_2O_3Cl]^+$ with a molecular weight of 253.66. The next fragmentation of chlorine leads to an observation of the signal at *m/z* 217.1. The peak at *m/z* 163.1 corresponds to $[C_8H_7N_2O_2]^+$ with a molecular weight of 163.16.

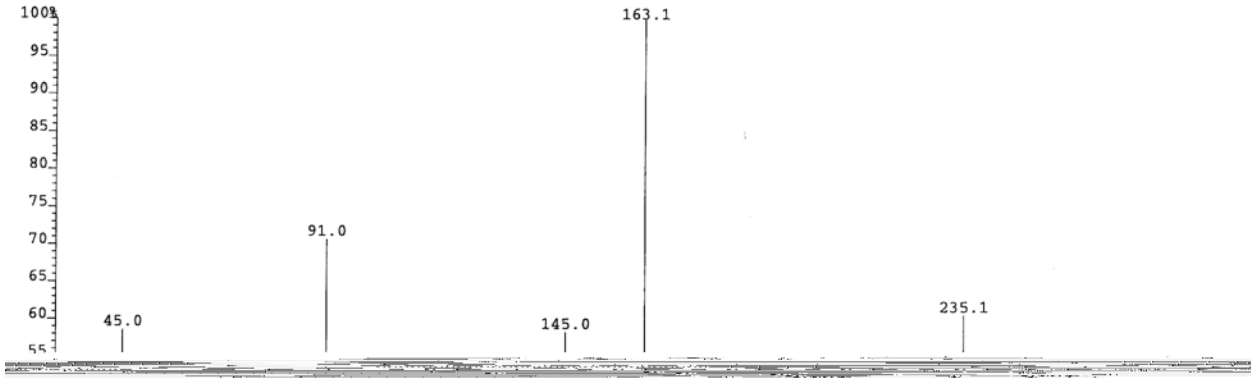

Fig. 7. ESI MS spectrum of (**2**).

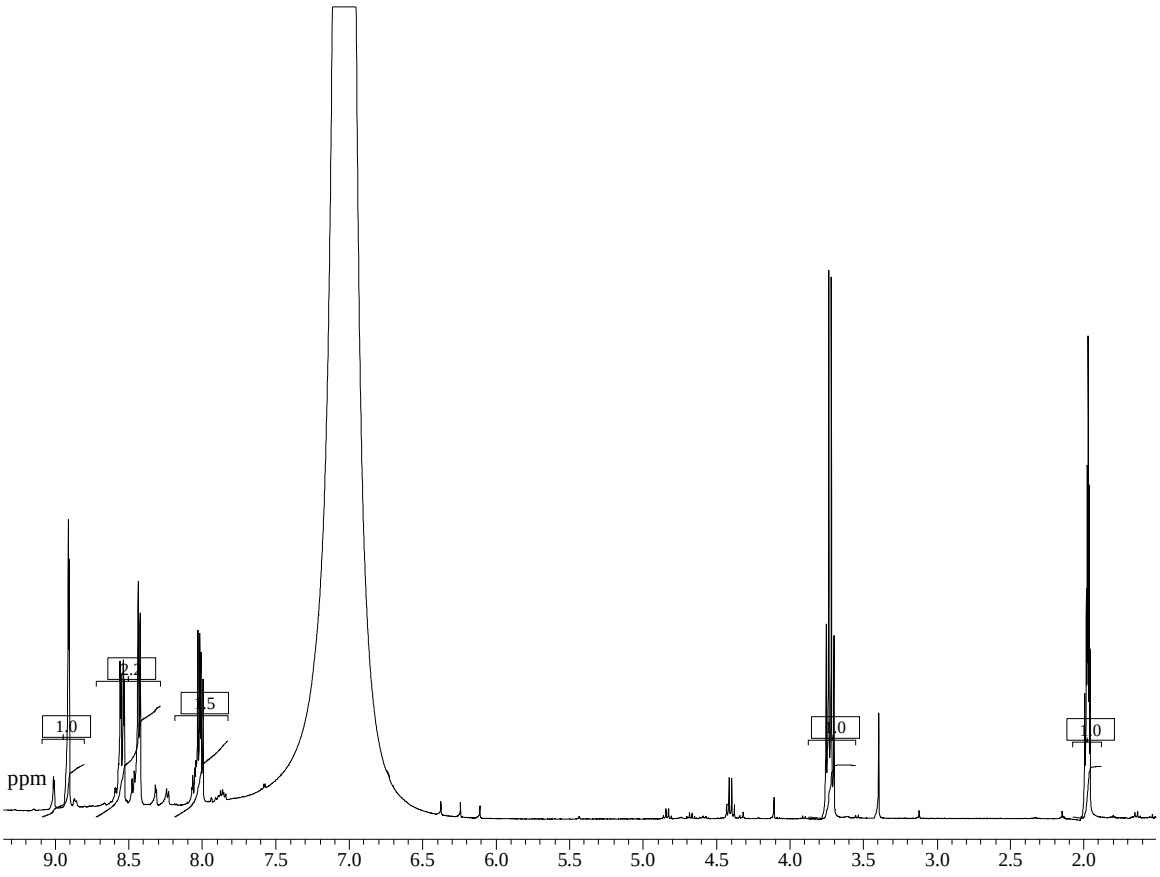

Fig. 8. ^{1}H-NMR spectra of (**2**).

^{1}H and ^{13}C-NMR data in solution

^{1}H- and ^{13}C-NMR spectra chemical shift signals are low affected as a result of protonation in the case of (**1**) or formation of the ester amide derivative – in (**2**) (Fig. 8). The chemical shift signals are observed at 8.01 ppm (H4), 8.40 ppm (H5) and 8.88 ppm (H6), respectively. This result also supports the UV-spectroscopic ones, i.e. the protonation affected the aromatic character of pyridine in insignificant level. In (**2**) are observed additionally chemical signals for C**H**$_2$ (3.7 ppm) and C**H**$_3$ (2.1 ppm). ^{13}C-NMR spectroscopic data of (**1**) and (**2**) show that the chemical signals of C2 are observed about 60.0 ppm. Other signals C3–C6 are within the range of 42.9–55.6 ppm, respectively. Four signals in the ^{13}C-NMR spectra about 170.0, 177.5, 178.0 and 179.0 ppm, belong to squaric acid residues in (**1**) and (**2**), respectively.

CONCLUSION

Hydrogensquarate and ester amide of squaric acid of 2-chloro-3-amino-pyridine are synthesized, isolated and spectroscopically characterized in solution and in solid-state by means of conventional and linear polarized IR-spectroscopy of oriented colloid suspensions, UV-spectroscopy, ^{1}H- and ^{13}C-NMR, positive and negative ESI, FAB, HPLC tandem mass spectrometry (MS/MS), TGV and DSC methods. Quantum chemical *ab initio* and DFT calculations are performed, supporting the obtained optical experimental data. The correlation between the structure optical and magnetic properties of the newly synthesized compounds is performed. The effect of N_{py} protonation and the formation of the ester amide with squaric acid on the optical and magnetic properties of the 2-chloro-3-amino-pyridine specie/fragment in both the compounds are elucidated by a comparison of the properties of starting compound.

Acknowledgements*: The authors thank the Assoc. Prof. B. Koleva (St. Kliment Ohridski Sofia University) for the using of Dalton 2.0 program and helpful discussion. This work has been supported financially by Bulgarian National Fund of Scientific Research, Contract X– 1510.*

REFERENCES

1. J. Molgo, M. Lemeignan, F. Peradejordi, P. Lechat, *J. Pharmacol. Paris*., **16,** 109 (1985).
2. G. E. Kirsch, T. Narahashi, *Biophys. J*., **22,** 507 (1978).
3. J. Molgo, M. Lemeignan, P. Lechat, F. Peradejordi, *Eur. J. Med. Chem*., **20**, 149 (1985).
4. C. Carlsson, I. Rosen, E. Nilsson, *Acta Anaesthesiol. Scand*., **27**, 87 (1993).
5. S. R. Schwid, M. D. Petrie, M. P. McDermott, D. S. Tierney, D. H. Maso, A. D. Goodman, *Neurology*, **48**, 817 (1997).
6. K. M. McEvoy, A. J. WindebankN, J. R. Daube, P. A. Low, *N. Engl. J. Med*., **321**, 1567 (1989).
7. J. L. Segal, S. R. Brunnemann, *Pharmacotherapy*, **17**, 415 (1997).
8. L. C. Sellin, *Med. Biol*., **59**, 11 (1981).
9. M. Davidson, J. H. Zemishlany, R. C. Mohs, *Biol. Psychiatry*, **23**, 485 (1988).
10. H. Meves, Y. Pichon, *J. Physiol. Lond*., **251**, 60P (1979).
11. B. B. Koleva, T. Tsanev, T. Kolev, H. Mayer-Figge, W. S. Sheldrick, *Acta Cryst*., **E63**, o3356 (2007)
12. B. B. Koleva, T. Kolev, T. Tsanev, St. Kotov, H. Mayer-Figge, R. W. Seidel, W. S. Sheldrick, *J. Mol. Struct*., (2007), (in press). DOI: http://dx.doi.org/10.1016/j.molstruc.2007.09.006.
13. B. B. Koleva, T. Kolev, T. Tsanev, St. Kotov, H. Mayer-Figge, R. W. Seidel, W. S. Sheldrick, *Struct. Chem*., (2007) (in press).
14. B. B. Koleva, T. Kolev, R. W. Seidel, T. Tsanev, H. Mayer-Figge, M. Spiteller, W. S. Sheldrick, *Spectrochim. Acta, Part A*, (2007) (in press).
15. A Den Hertog, P Biessels, J Van den Akker, S Agoston, A. S Horn, *Eur. J. Pharmacol*., **142**, 115 (1987).
16. B. B. Ivanova, M. G. Arnaudov, P. R. Bontchev, *Spectrochim. Acta*, **60**, 855 (2004).
17. B. B. Ivanova, D. L. Tsalev, M. G. Arnaudov, *Talanta,* **69**, 822 (2006).
18. B. B. Ivanova, V. D. Simeonov, M. G. Arnaudov, D. L. Tsalev, *Spectrochim. Acta*, **67A**, 66 (2007).
19. B. B. Koleva, T. Kolev, V. Simeonov, T. Spassov, M. Spiteller, *J. Inclus. Phenom*., (2008) in press.
20. M. J. Frisch, G. W. Trucks, H. B. Schlegel, G. E. Scuseria, M. A. Robb, J. R. Cheeseman, V. G. Zakrzewski, J. A. Montgomery Jr., R. E. Stratmann, J. C. Burant, S. Dapprich, J. M. Millam, A. D. Daniels, K. N. Kudin, M. C. Strain, Ö. Farkas, J. Tomasi, V. Barone, M. Cossi, R. Cammi, B. Mennucci, C. Pomelli, C. Adamo, S. Clifford, J.

All other chemicals were of analytical grade and used without further purification.

Preparation of magnetic chitosan beads

Two types of magnetic chitosan beads – with *in situ* prepared or pre-formed nanosized magnetite – were prepared. For preparation of chitosan beads with *in situ* prepared nanosized magnetite, further denoted as Ch/Fe_3O_4 (*in situ*), solution containing 40 ml of 0.4% chitosan solution in 0.4 M HCl, 0.05 M $FeCl_2$ and 0.1 M $FeCl_3$ was prepared. The obtained homogeneous solution was filtered and dropped through capillary (diameter 0.5 mm) into ammonium hydroxide precipitation bath (2.9 M NH_3), containing 0.026 M Na_2SO_3. The prepared Ch/Fe_3O_4 (*in situ*) beads were kept in the precipitation bath for 24 h and then were repeatedly washed with deionized water to neutral reaction of the aqueous phase. A part of the beads were crosslinked with glutaraldehyde (GA) in aqueous solution of GA (0.03 M) at mole ratio [GA]:[aminoglucoside units] = 5:1 at 28°C for 1 h. The crosslinked beads were washed repeatedly for removing any unreacted crosslinking agent. The beads, before and after crosslinking, were dried to constant weight at room temperature.

For comparison, beads with pre-formed magnetite were prepared. For convenience, these beads are further denoted as Ch/Fe_3O_4. In a typical run, preformed dispersion of magnetic nanoparticles was prepared as previously described [7]. Briefly, 1 ml of degassed solution of $FeCl_2$ (2 M $FeCl_2$ in 2 M HCl, 0.002 mol) and 4 ml of degassed solution of $FeCl_3$ (1 M $FeCl_3$ in 2 M HCl, 0.004 mol) were mixed under nitrogen and vigorously stirred. Then 50 ml degassed solution of 0.7 M NH_3 was added dropwise under nitrogen. Magnetite, as a black precipitate was immediately formed and after repeatedly washing by degassed water, magnetite suspension (14 mg/ml) was prepared by ultrasonic dispersion in degassed water. Then, under vigorous stirring, 10 ml of preformed suspension were added to 10 ml of 3% chitosan solution in 1% CH_3COOH. The obtained homogeneous viscous chitosan suspension was dropped through a capillary (diameter 0.5 mm) into 5% NaOH, thus causing formation of coacervate chitosan beads. After 24 h staying in the precipitation bath, they were repeatedly washed with deionized water to neutral reaction of the aqueous phase. The prepared Ch/Fe_3O_4 beads were cross-linked in aqueous solution of GA (0.03 M) at 28°C for 1 h at a mole ratio [GA]:[aminoglucoside units] = 5:1.

Characterization

Beads surface and core morphology was observed by scanning electron microscope (SEM) Jeol JSM-5510. Specimens, preliminary freeze-dried, were placed on the sample holders and vacuum-coated with gold in Jeol JFC-1200 fine coater. The IR-spectra were taken with a FTIR Bruker Vector 22 spectrophotometer on a KBr plate. Thermogravimetric analyses (TGA) were carried out under nitrogen with a TA Instruments Q500 thermogravimetric analyzer in the 25–1000°C range, at a 10 °C/min rate (HiRes method). The equilibrium swelling degree (α_{eq}) of the magnetic beads was determined gravimetrically by immersion of dry and previously weighed beads in buffer solutions (pH 4, 7 and 9 and constant ionic strength I = 0.1) at 25°C. Then, the beads were weighed at regular intervals of time after gentle removing of the excess of buffer solution. The procedure was repeated until reaching a constant weight of the swollen beads. The α_{eq} was estimated by the equation: $\alpha_{eq} = [(w_{eq} - w_d)/w_d]\times 100$ (in %), where w_{eq} and w_d were the weights of the sample in equilibrium swollen and in dry state, respectively. The results are averages from three measurements. Phase composition and particle size of the Ch/Fe_3O_4 (*in situ*) beads were studied by X-ray powder diffraction (XRD) analysis. XRD spectra were recorded at room temperature with computer controlled D8 Bruker Advance powder diffractometer with a filtered Cu-K_α radiation and a scintillation registration. Data were collected in the 2θ range from 5 to 85° with a step 0.02° and counting time of 1 s/step. The magnetization of the Ch/Fe_3O_4 (*in situ*) beads was measured with a vibrating-sample magnetometer by applying an increasing magnetic field. Dry beads were fixed in quartz holders, which were placed in the magnetometer. The Mössbauer spectroscopy analysis was performed in a transmission mode with conventional constant acceleration spectrometer at 300 and 77K. A ^{57}Co source in an Rh matrix with a diameter of the activity spot of 5 mm was used. The spectra were fitted using continuously magnetic field distribution and quadrupole splitting distribution. The isomer shifts of the spectra are referred to the centroid of α-Fe foil reference spectrum at room temperature. The dried beads were pulverized in a mortar, mixed with PVA powder (glue substance) and pressed into a disk.

RESULTS AND DISSCUSION

Preparation and characterization of magnetic chitosan beads

One-pot preparation of magnetic chitosan beads comprised *in situ* prepared nanosized magnetite by combining the sol-gel and simple coacervation methods. Simultaneous formation of the nanosized

magnetite and beads, which occurs during the extrusion of the mixed chitosan, $FeCl_2$ and $FeCl_3$ solution into the alkaline precipitation bath, is due to the following reaction:

$$\underset{\text{pH = 1}}{\text{Chit}-NH_3^+ + Fe^{2+} + 2Fe^{3+} + 8OH^-} \longrightarrow \underset{\text{pH > 10}}{\text{Chit}-NH_2 + FeO.Fe_2O_3 + 4H_2O}$$

During the capillary extrusion of the chitosan/$FeCl_2$/$FeCl_3$ solution into ammonium hydroxide bath, the conversion of the water-soluble protonated form ($–NH_3^+$) of chitosan to the water-insoluble neutral ($–NH_2$) form takes place. This leads to the simultaneous formation of beads and co-precipitation of $FeCl_2$ and $FeCl_3$, thus forming nanosized magnetite (Fe_3O_4). For comparison of the obtained Ch/Fe_3O_4 (*in situ*) beads, coacervate chitosan beads with pre-formed magnetite were prepared. This is a two-step process including preliminary preparation of nanosized magnetic suspension, followed by adding of this suspension to chitosan solution and subsequent extrusion of the obtained chitosan suspension into alkaline precipitation bath. This way of preparation (using Fe_3O_4 suspension) is more advantageous than involving magnetite powder since it allows better homogenization of the solution and thus minimizes the losses of magnetic material during the extrusion process.

The morphology of the beads surface and core was observed by SEM after freeze-drying. As seen from the SEM micrographs (Fig. 1), the surface of the prepared beads is smooth, while their cross-section reveals highly porous structure, characteristic of chitosan. The measurements showed that the pore size of the Ch/Fe_3O_4 beads (45 μm) was considerably larger than that of Ch/Fe_3O_4 (*in situ*) beads (1.8 μm).

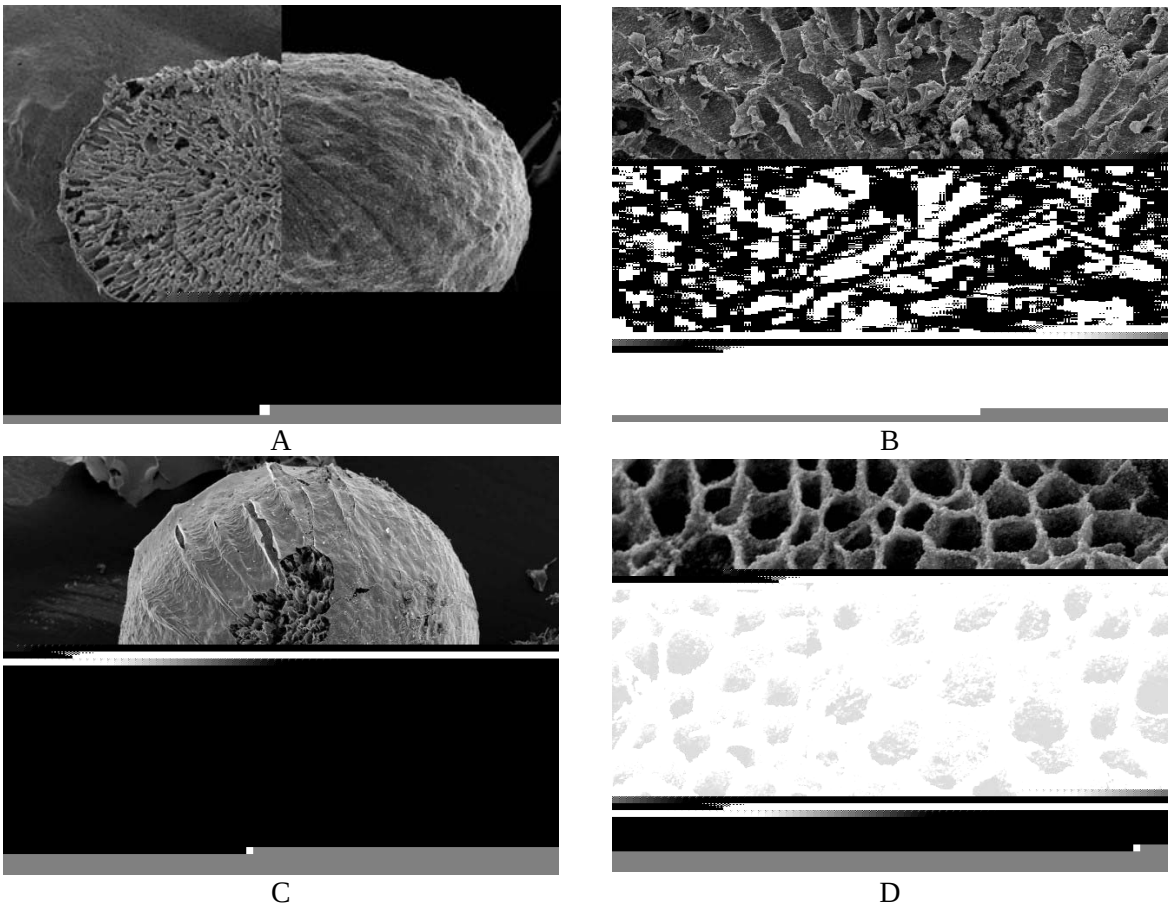

Fig. 1. SEM micrographs of freeze-dried magnetic chitosan beads: Ch/Fe_3O_4 ×40 (A) and ×150 (B); Ch/Fe_3O_4 (*in situ*) ×70 (C) and ×5 000 (D).

The IR spectra of the beads showed the following characteristic for chitosan bands: in the range of 3500–3300 cm^{-1} (NH- and OH-stretching vibrations), the bands due to its saccharide structure – at 1153 cm^{-1} (OH-bending), 1068 cm^{-1} (–C–O–C– stretching vibrations) and 1030 cm^{-1} (OH-bending)

and for Amide I at 1634 cm^{-1}. A new band in the low-frequency region (570–588 cm^{-1}), due to the iron oxide skeleton (–Fe–O– stretching vibrations), is an evidence for presence of magnetite in the beads [8].

The changes which occur after thermal treatment of Ch/Fe_3O_4 (*in situ*) beads were estimated by TGA (Fig. 2). The most considerable destruction (approximately 32% weight losses) was observed in the range of 150–780°C. As seen, the first decomposition stage started at 150°C and ended at 420°C with weight loss of 15.8% from the sample initial weight. The second stage continued up to 780°C with weight losses of 15.9%. Clearly, these two stages correspond to the thermal decomposition of chitosan, which usually starts at 250°C and ends at 650°C [9].

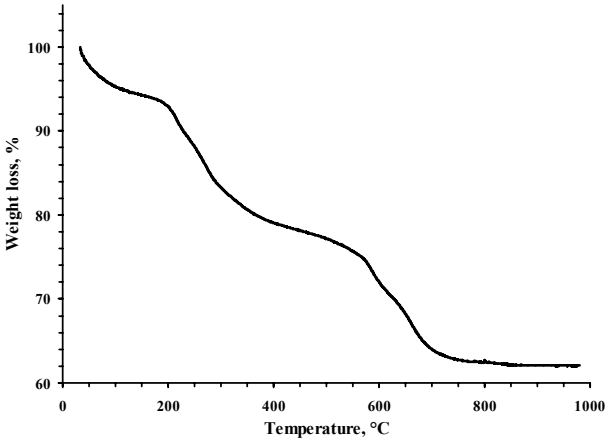

Fig. 2. TGA thermogram of dried Ch/Fe_3O_4 (*in situ*) beads

The successful preparation of Ch/Fe_3O_4 (*in situ*) beads enriched in Fe_3O_4 has been evidenced by all these previous experiments. Moreover, the one-pot preparation of Ch/Fe_3O_4 (*in situ*) beads provides an additional possibility for their stabilization which is favored by the complex formation between amino groups of chitosan and iron ions [10, 11]. Therefore, the formation of physical network during the extrusion process leads to collapse of chitosan gel, thus decreasing the pore size of Ch/Fe_3O_4 (*in situ*) beads compared to Ch/Fe_3O_4 one. These peculiarities of the one-pot preparation of Ch/Fe_3O_4 (*in situ*) beads determine different behaviour of the beads at different pH values. The dependence of the equilibrium swelling degree (α_{eq}) of the Ch/Fe_3O_4 (*in situ*) and Ch/Fe_3O_4 beads on the pH (4, 7 and 9) of the medium is presented in Table 1. As seen, the highest α_{eq} value (exceeding 1000%) was attained in acidic medium for the Ch/Fe_3O_4 (*in situ*) beads. After 6 h at pH 4 the Ch/Fe_3O_4 (*in situ*) beads fragmented, thus hampering the determination of α_{eq} at this pH value. At pH 4 Ch/Fe_3O_4 beads dissolved in comparison with Ch/Fe_3O_4 (*in situ*). As seen (Table 1), the Ch/Fe_3O_4 (*in situ*) and Ch/Fe_3O_4 beads swelled slightly at pH 7 and pH 9, besides Ch/Fe_3O_4 (*in situ*) swelled less than Ch/Fe_3O_4 beads.

Table 1. Dependence of the equilibrium swelling degree (α_{eq}) of different magnetic chitosan beads on pH; 25°C; I = 0.1.

Beads	α_{eq}, %		
	pH = 4	pH = 7	pH = 9
Ch/Fe_3O_4 (*in situ*)	1300 [a]	24	16
Ch/Fe_3O_4 (*in situ*)/GA	212	16	15
Ch/Fe_3O_4	[b]	125	162
Ch/Fe_3O_4/GA	255	64	41

[a] the beads are fragmented after 6 h; [b] the beads are dissolved.

As mentioned above, due to the formation of physical network by interaction between the amino groups of chitosan and iron ions in Ch/Fe_3O_4 (*in situ*) the pore size decreased thus decreasing the water uptake in the beads. After chemical crosslinking with glutaraldehyde (GA), both beads types were stable in acidic medium and reached equilibrium swelling degree for 24 h. Obviously, non-crosslinked beads swelled to a greater extent compared to the crosslinked ones and the α_{eq} values were higher in acidic than in neutral or alkaline solutions (Table 1). For example, at pH 7 the α_{eq} decreased in the order: Ch/Fe_3O_4 > Ch/Fe_3O_4/GA > Ch/Fe_3O_4 (*in situ*) > Ch/Fe_3O_4 (*in situ*)/GA. For the beads, crosslinked with GA, α_{eq} decreased in the order: pH 4 > pH 7 > pH 9.

The obtained results show the advantages of the one-pot preparation of magnetic chitosan beads. Further, the magnetic properties of the beads were studied.

Magnetic properties of the prepared magnetic chitosan beads

The presence only of magnetite (Fe_3O_4) phase was confirmed by XRD analysis of dried Ch/Fe_3O_4 (*in situ*) beads (Fig. 3). The iron oxide phase was identified from the XRD patterns by the peak positions at 18.2 (111), 30.0 (220), 35.5 (311), 43.1 (400), 53.4 (422), 57.0 (511), 63 (440) and 73.9 (533), which were in agreement with magnetite standard data.

The mean particle size of the formed in the beads ferromagnetic particles was 12 nm, as calculated by the Scherer's equation. It has been reported that Fe_3O_4 particles with size lower than 20 nm are superparamagnetic [12]. Therefore, it might be assumed that a part of the magnetite, formed *in situ* in the beads, is in superparamagnetic state.

Magnetization of the Ch/Fe_3O_4 (*in situ*) beads as a function of internal magnetic field was measured

by vibrating-sample magnetometer (Fig. 4). As seen, the saturation of magnetization could not be reached even at maximum internal magnetic field of 6 kOe. At H = 0, the magnetization curve showed almost immeasurable coercivity (H_c = 100 Oe) and remanence (M_r = 1.2 ± 0.2 emu/g). These low values of H_c and M_r showed that magnetic particles formed in Ch/Fe_3O_4 (*in situ*) beads were in superpara-magnetic state [13].

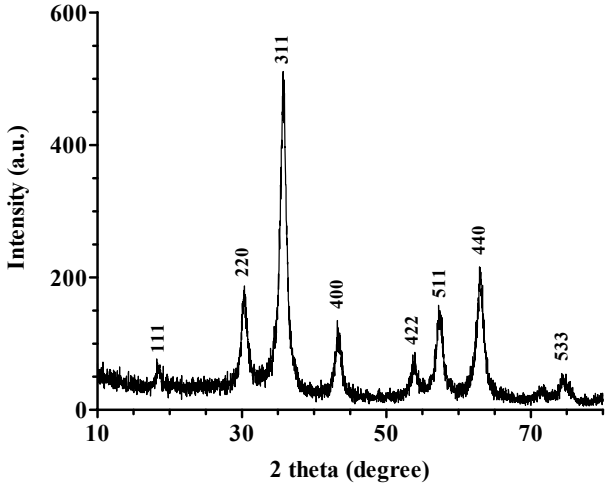

Fig. 3. XRD patterns of the dried Ch/Fe_3O_4 (*in situ*) beads.

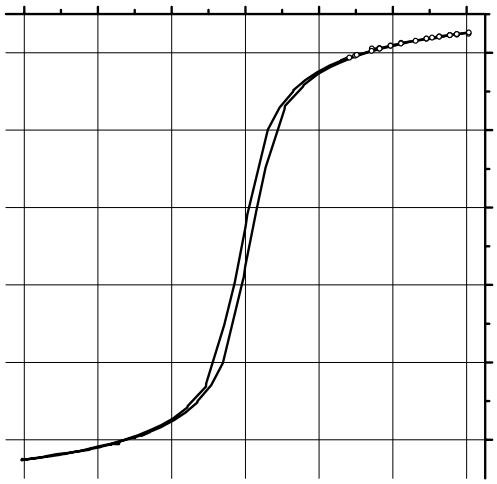

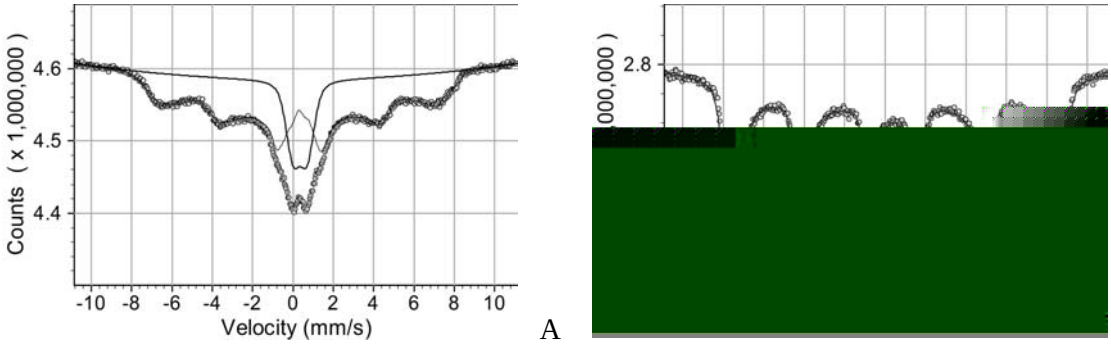

Fig. 5. Mössbauer spectra of dried Ch/Fe_3O_4 (*in situ*) beads recorded at 300K (A) and 77K (B).

Table 2. Mössbauer parameters [a] of dried Ch/Fe_3O_4 (*in situ*) beads.

Sample	T [b], K	SXT	IS, mm/s	H_{avr}, kOe	σH, kOe	H_{max}, kOe	QS_{avr}, mm/s	QS_{area}, %
Ch/Fe_3O_4 (*in situ*)	300	I	0.30	296	-	436	0.78	18.7
		II	0.68	276	-	430		
	77	I	0.44	422	53	504	-	0
		II	0.37	403	52	498		

[a] isomer shift (IS); average magnetic field at the site of the Fe nucleus (H_{avr}); dispersion of magnetic hyperfine-field distribution (σH); maximum value of magnetic hyperfine-field distribution (H_{max}); average quadrupole splitting (QS_{avr}); relative spectral area of quadrupole doublets distribution (QS_{area}); [b] T (K) - temperature in K degrees.

As seen, the results are close to literature data for maghemite [15] implying that topotactic oxidation of magnetite has taken place during storage. At room temperature the Mössbauer spectra of bulk magnetite and maghemite are quite different. When the material is in the form of nanoparticles the crucial parameter of the Mössbauer spectra to distinguish between two possible iron oxides is the isomer shift. Moreover, the isomer shift is typically ≥ 1.0 mm/s for Fe^{2+}, while 0.3–0.4 mm/s for Fe^{3+}. Therefore, the values of isomer shift of Ch/Fe_3O_4 (*in situ*) presented in Table 2 suggest an average valence of iron close to Fe^{3+}.

CONCLUSIONS

The combination of the sol-gel method with those of simple coacervation is successfully used for one-pot preparation of chitosan beads with *in situ* involved nanosized magnetite. Compared to the beads with pre-formed nanosized magnetite, these with *in situ* prepared magnetite are more stable in acidic medium. The size of the *in situ* prepared magnetite is 12 nm, as proved by the XRD calculations and by the low values of saturated magnetization. The measurements of the magnetization and the Mössbauer analyses showed that the magnetic particles formed in the beads existed in superparamagnetic state and a part of them was in intermediate state between superparamagnetic and ferrimagnetic one. Therefore, the herein one-pot prepared Ch/Fe_3O_4 (*in situ*) beads are promising magnetic materials.

***Acknowledgement**: This work was supported by the Grant CH-1414 from the Bulgarian National Science Fund of Ministry of Education and Science.*

REFERENCES

1. K. Arai, T. Kinumaki, T. Fujita, *Bull. Tokai Reg. Fish Res. Lab.*, **56**, 89 (1968).
2. C. Peniche, W. Argüelles-Monal, H. Peniche, N. Acosta, *Macromol. Biosci.*, **3**, 511 (2003).
3. F.-L. Mi, T.-B. Wong, S.-S. Shyu, S.-F. Chang, *J. Appl. Polym. Sci.*, **71**, 747 (1999).
4. J. Zhang, S. Zhang, G. Wu, W. Wang, S. Gao, J. Zhang, Y. Wang, *J. Bioactive Compatible Polym.*, **22**, 429 (2007).
5. E. Denkbaş, E. Kiliçay, C. Birlekseven, E. Öztürk, *React. Funct. Polym.*, **50**, 225 (2001).
6. D. Paneva, O. Stoilova, N. Manolova, I. Rashkov, *e-Polymers*, no. **060** (2004).
7. R. Mincheva, O. Stoilova, H. Penchev, T. Ruskov, I. Spirov, N. Manolova, I. Rashkov, *Eur. Polym. J.*, **44**, 615 (2008).
8. H. Ma, X. Qi, Y. Maitani, T. Nagai, *Int. J. Pharm.*, **333**, 177 (2007).
9. J. Zhi, Y. Wang, Y. Lu, J. Ma, G. Luo, *React. Funct. Polym.*, **66**, 1552 (2006).
10. M. Rinaudo, A. Domard, in: Chitin and chitosan, G. Skajak-Braek, T. Anthonsen, P. Sanford (eds.), Elsevier, London, 1989, p. 71.
11. S. C. Bhatia, N. Ravi, *Biomacromolecules*, **1**, 413 (2000).
12. M. A. M. Gijs, *Microfluid Nanofluid*, **1**, 22 (2004).
13. B. Li, D. Jia, Y. Zhou, Q Hu, W. Cai, *J. Magnetism Magnet. Mater.*, **306**, 223 (2006).
14. L. Neel, *Ann. Geophys.*, **5**, 99 (1949).
15. G. M. Da Costa, E. De Grave, L. H. Bowen, P. M. A. De Bakker, R. E. Vandenberhe, *Clays and Clay Minerals*, **43**, 562 (1995).

ЕДНОЕТАПНО ПОЛУЧАВАНЕ НА МАГНИТНИ ХИТОЗАНОВИ СФЕРИ

О. Стоилова[1], Хр. Пенчев[1], Т. Русков[2], Ив. Спиров[2], Н. Манолова[1], Ил. Рашков[1]*

[1] *Лаборатория „Биологично активни полимери“, Институт по полимери, Българска академия на науките, ул. Акад. „Г. Бончев“, бл. 103А, 1113 София,*
[2] *Лаборатория по Мьосбауерова спектроскопия и ниска активност, Институт за ядрени изследвания и ядрена енергетика, Българска академия на науките, бул. „Цариградско шосе“ 72, 1784 София,*

Посветена на акад. Иван Юхновски по повод на 70-та му годишнина

Постъпила на 7 януари 2008 г.; Преработена на 30 януари 2008 г.

(Резюме)

Предложен е нов едноетапен метод за получаване на магнитни хитозанови сфери, включващ *in situ* получени магнитни наночастици. Основното предимство на предложения метод е получаването на феромагнитен материал едновременно с формирането на хитозановите сфери като това става чрез комбинирането на два метода – зол-гел метода и капилярната екструзия. В допълнение, намерени са подходящите условия за ефективно включване на предварително получена суспензия от магнитни наночастици в хитозанови сфери без загуба на магнитен материал по време на екструзията на разтвора. Нещо повече, зол-гел методът позволява включването на значителни количества магнетит в сферите. Равновесната степен на набъбване на получените сфери зависи от pH на средата. Оптичната и сканираща електронна микроскопия разкриват силно порестата структура на сферите. Измерването на намагнитеността на сферите показва, че насищане не се достига дори при максимално външно магнитно поле от 6 kOe. Мьосбауеровите анализи показват, че *in situ* получените магнитни наночастици са в суперпарамагнитно състояние и част от тях са в междинно състояние – между суперпарамагнитно и феримагнитно.

Bulgarian Chemical Communications, Volume 40, Number 4 (pp. 498–504) 2008

A theoretical investigation on the structure, electronic spectra and nonlinear optical properties of pyridinium-betaines of squaric acid

B. A. Stamboliyska*, D. Y. Yancheva, Ts. M. Kolev

Department of Structural Organic Analysis, Institute of Organic Chemistry with Centre of Phytochemistry, Bulgarian Academy of Sciences, Acad. G. Bonchev St., Block 9, 1113 Sofia, Bulgaria

Dedicated to Academician Ivan Juchnovski on the occasion of his 70th birthday

Received January 17, 2008; Revised January 29, 2008

A theoretical investigation is carried out to estimate the structure and properties of six pyridinium-betaines of squaric acid and the dependence of their nonlinear optical (NLO) response on the structural modification. The ground-state geometries of all studied pyridinium-betaines of squaric acid were optimized at the HF/6-311G(d,p) level of theory. The vertical singlet transition energies were computed at the CIS and at the TD-DFT level by using the optimized geometries. The electron charge distributions, the vibrational and electronic spectra were analyzed in order to describe the charge transfer in the molecules and the related electronic transitions. The molecular NLO properties were discussed in terms of electron structure parameters and estimated based on the two-level model. The best performance was found for acceptor substituted pyridinium-betaines of squaric acid.

Key words: Organic NLO materials, UV-Vis, quantum chemical calculations, molecular structure.

INTRODUCTION

The nonlinear optics (NLO) has been a field of intensive research over the last two decades due to the great prospect for developing of new electronic devices and communication technologies based on NLO-effects such as optical frequency doubling, electro-optical modulation, optical rectification, self-focusing, and photorefractivity [1–4]. For the realization of the different optical functions new highly-effective materials should be applied and the organic materials offer many advantages such as great variety, flexible structure, lower cost and easier fabrication for example [5–12].

In the search for strategies aimed at rational design of new organic NLO materials, a number of theoretical models for evaluation of the molecular hyperpolarizabilities have been defined [1–4]. The most widely applied one, the so-called "two-level model", describes the first molecular hyperpolarizability (β) in electron structure terms. It is suggested that β could be optimized via synthesis of NLO-phores exhibiting excited states close in energy to the ground states, large oscillator strengths for the corresponding electron transition, and as a result of the transition – a large difference between the dipole moments in ground state and in excited state. In the framework of the two-level model, the π-conjugated molecules with strong donor and acceptor groups seem to be the most promising candidates for NLO applications. The electron structure affects also the transparency, the thermal stability and some other features of the material, important from technical point of view.

Optical (UV-vis) and electro-optical absorption measurement (EOAM) techniques allow experimental determination of the electron structure parameters involved in the two-level model [13, 14]. On the other hand, the experimental measurements are often hampered by practical limitations, so it may be of practical use if the same characteristics could be estimated based on structural parameters determined directly by quantum-chemical methods. By elucidating the microscopic structure – NLO property relationship the computational evaluations may be used to model the NLO-activity of the molecules.

In the present paper, we represent a detailed computational analysis of the NLO properties of six pyridinium-betaines of squaric acid. For our purposes, we analyzed the ground state and excited state structures, vibrational spectra, electronic transitions and molecular NLO properties and we compared the obtained data to the corresponding experimental values. The dependence of the electronic parameters involved in the two-level model on structural modification in the elucidated molecules has also been studied.

* To whom all correspondence should be sent:
E-mail: bs@orgchm.bas.bg

© 2008 Bulgarian Academy of Sciences, Union of Chemists in Bulgaria

COMPUTATIONAL DETAILS

The ground-state geometries of all studied pyridinium-betaines of squaric acid were optimized at the HF level of theory by employing the 6-311G(d,p) basis set. The vertical singlet transition energies were computed at the CIS (configuration interaction singles) and at the TD-DFT (time-dependent density functional theory) level by using the optimized geometries. The geometries of the lowest singlet excited state were also optimized at the CIS level. The nature of the stationary point was analyzed by vibrational frequency calculation both in the ground state and in the excited state. To estimate the dipole moments in the excited state we have performed the population analysis using the CI density. All calculations were performed using GAUSSIAN 98 suite of programs [15]. It is well known that linear scaling is needed for the CIS transition energies to compare the energies with the corresponding experimental data. A factor of 0.72 has been found to be satisfactory ([16] and references therein]), and we have used the same scaling factor in this case also.

RESULT AND DISCUSSION

Molecular geometry and electronic charge distribution in ground state

The bond lengths in the ground state computed at HF level for all studied molecules are plotted in Scheme 1 along with the atomic numbering. In the cases of molecules with C_{2v} symmetry only one of the equal bond lengths is shown in Scheme 1 for simplicity.

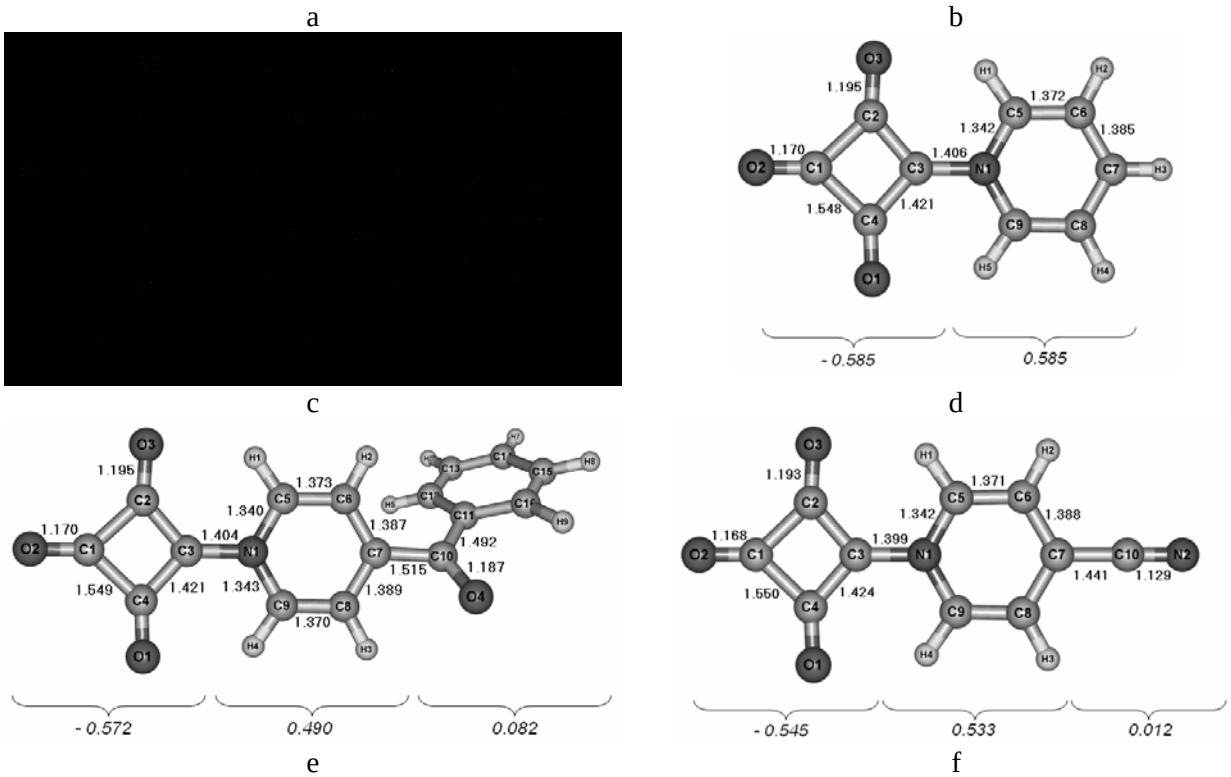

Scheme 1. Theoretical (HF/6-311G**) bond lengths in the ground state (Å) and NBO charges over fragments of the studied pyridinium-betaines of squaric acid.

All the theoretically found bond lengths and angles are in a very good agreement with the X-ray refinement values from previous crystallographic studies [17–19]. The ground state geometry of the squaric and pyridinium ring is almost constant within the elucidated series and the calculated interatomic distances vary within very narrow ranges. For all structures, the C_1–O_2 bond is predicted to be nearly double in character, which is in accordance with the single crystal data, and its bond length has an average value around 1.170 Å. As a result of the negative charge delocalization the remaining two squarate carbonyl groups C_2–O_3 and C_4–O_1 have identical bond lengths within the range 1.193–1.199 Å. For the same reason, two of the C–C bonds in the squaric ring (C_2–C_3 and C_3–C_4) are considerably shorter.

The heterocycle has partially quinoidal character, most clearly expressed in the 4-dimethylamino derivative. In comparison to the other structures, the latter has the shortest C_5–C_6 and C_8–C_9 bonds and respectively the longest C_6–C_7 and C_7–C_8 bonds. The interatomic distance between the squaric and pyridinium fragment is found to be sensitive to the substitution and it shows variation of 0.012 Å within the elucidated series, gradually decreasing in the order:

4-N$(CH_3)_2$ > 4-CH_3 ~ 4-C$(CH_3)_3$ > H > 4-COC_6H_5 > > 4-CN.

The bigger part of the molecule is virtually flat including the carbonyl groups, the squaric ring and the heterocycle, and in some cases – even the non-hydrogen atoms of the substituents, which is an indication of the strong conjugation between the fragments. It is known from the X-ray diffraction studies that the squaric and pyridinium ring in 4-sustituted pyridinium-betaines of squaric acid show negligible deviation from the planarity [17–19], whereas in 2- and 3-substituted derivatives the dihedral angle between their two planes differs significantly i.e. the conjugation is strongly decreased by substitution at 2- and 3-position [20].

The NBO model was chosen for calculation of the atomic charges of the studied species. In order to illustrate the charge transfer (CT) in the ground state, the calculated charges were summarized over fragments as shown in Scheme 1. The molecules were regarded as constituted of three fragments – cyclobutenedione moiety (acceptor part), pyridinium ring (donor part) and substituent. The substituent is expected to increase or decrease the donor properties of the pyridinium ring by its own electron releasing or withdrawing ability and thus to influence the CT in the molecule. Following this approach, the most favourable degree of conjugation could be achieved by varying the substituent nature.

The excellent acceptor properties of the squaric fragment are revealed by the complete localization of the negative charge on the fragment, even in the presence of cyano or benzoyl group in the pyridinium ring.

The electron deficiency in the heterocycle is decreasing in the order: 4-N$(CH_3)_2$ > 4-C$(CH_3)_3$ ~ ~ 4-CH_3 > 4-COC_6H_5. As it could be seen from the values depicted in Scheme 1, longer alkyl chains as substituents do not contribute significantly to the increase in the positive charge on the pyridinium ring.

Given the strong conjugation and the aromatic character of the system, not surprisingly the substituents releasing or withdrawing electrons through mesomeric effects influence to a greater extent the CT than those acting through inductive effects. To summarize, the introduction of a donor substituent leads to a larger displacement of the electron density from the heterocycle to the squarate fragment.

Vibrational spectra

In accordance with the minor structural differences found in the ground state geometry, the vibrational spectra of the studied species closely resemble one another. The most characteristic IR region (2000–800 cm^{-1}) is represented in Figure 1 with experimental and theoretical IR bands of selected pyridinium-betaines of squaric acid.

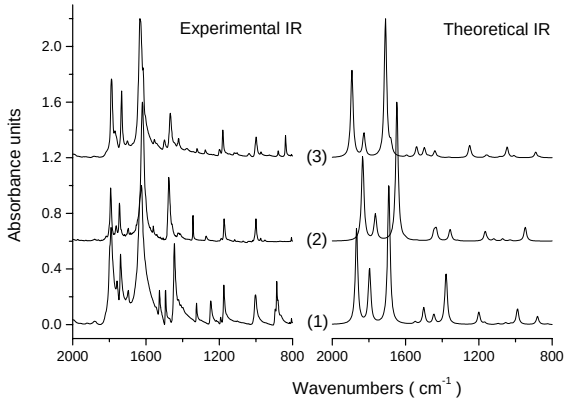

Fig. 1. Solid state experimental (left) and theoretical (right) IR spectra of selected pyridinium-betaines of squaric acid: (1) 4-CN; (2) H; (3) 4-CH_3;

The quantum-chemical calculations predict accurately the frequency range and the intensity of the characteristic vibrational modes [21–23]. In general the most intensive bands in the vibrational spectra of the pyridinium-betaines of squaric acid are between 1800 and 1615 cm^{-1}, and they correspond to stretching vibrations of the carbonyl groups of the

squaric ring. The band for stretching vibration of the formal double bond C_1–O_2 is observed at the highest frequency in this region and it is followed by the symmetric ν^s(C⎓O) and antisymmetric ν^{as} (C⎓O) stretching vibrations of C_2–O_3 and C_4–O_1. In the case of carbonyl substitution in the pyridinium ring, as for example in the 4-benzoyl compound, an additional band appears in the same spectral region. The stretching vibration $\nu(C_3–N_1)$ is found in the experimental spectra at ca. 1420 cm^{-1} (theoretically predicted at ca. 1400 cm^{-1}) and its frequency is higher than the value observed for other similar pyridinium-betaines [24] due to the partially quinoidal character of this bond.

Molecular geometry in excited state

The unsubstituted, the dimethylamino- and the cyano-substituted derivatives best exemplify the differences caused by the substitution in the pyridinium ring and hence these three compounds have been used for description of the structural changes observed in excited state. Selected computed structural parameters in excited state are shown in Scheme 2. All bond lengths vary within larger ranges than in ground state and the geometry of the squaric and pyridinium fragments are much more affected by the presence of donor and acceptor groups.

There is a general trend toward lengthening of the C_1–O_2 bond, but to a different extent depending on the substituent. On the other hand, in all cases C_2–O_3 and C_4–O_1 bonds become shorter by 0.011 Å resulting in a completely new geometry of the cyclobutenedione moiety with one single and two double carbonyl bonds. In the case of the 4-cyano derivative equal bond lengths are observed for the three squaric C–O groups. The C–C bond distances in the squaric ring show a similar tendency, but they are less pronounced and the overall geometry of the cycle is preserved.

A notable difference is observed regarding the bond length of C_3–N_1 not only compared with the ground state, but between the species studied in excited state as well. In comparison with the ground state, the bond has decreased its length, but again to a much different degree in the three cases. The largest decrease is found for the 4-cyano compound, where it is shorter by 0.054 Å.

The pyridinium cycle also undergoes a structural modification, although not so dramatically expressed as in the above-discussed cases. The quinoidal character of the latter fragment is less expressed in excited state in the 4-dimethylamino compounds and more expressed in the 4-cyano pyridinium-betaine of squaric acid. It is interesting to note that the bond distances between the pyridinium ring and the substituents are also affected – in opposite directions. Same fact has been established for other pyridinium dertivatives as well [25–27].

Thus, the excited state geometry shows major differences compared to the ground state one, but it is not possible to describe them as purely aromatic and quiniod-like as it is defined typically in long-chain push-pull NLO-phores. The changes depend specifically on the donor and acceptor groups and cannot be generalized; however, it is quite evident that the substituent influence is particularly strong in the excited state.

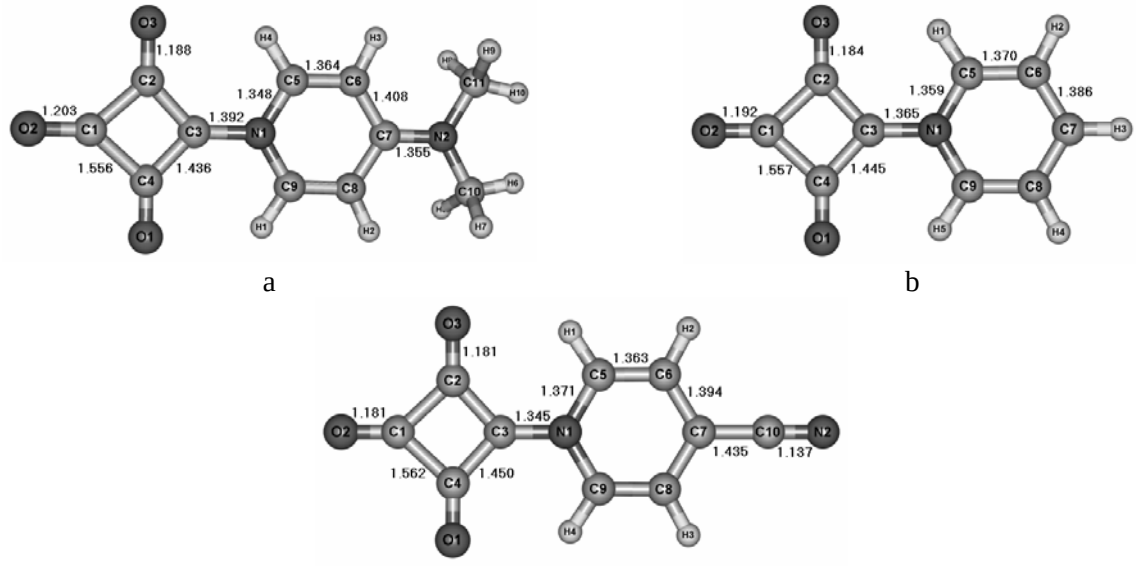

Scheme 2. Theoretical (CIS/6-311G**) bond lengths (Å) in the excited state of selected pyridinium-betaines of squaric acid.

Electronic spectra, dipole moments in ground and excited state and nonlinear optical properties

The electron charge distribution over fragments indicates that a strongly polarized system is present with negative and positive moieties of the molecule in immediate vicinity without any linking chain between them. So, although it is very useful in many cases, here it is impossible to determine the bond length alternation (BLA) and the c^2 parameter cannot be used for description of the ground state polarization and for showing the relationship between the electron distribution and the ground-state properties. For that reason, the NLO behaviour and the degree of the CT will be estimated based on dipole moments in ground and excited state (μ_g and μ_e) and the difference between them ($\Delta\mu = \mu_e - \mu_g$), energy of the electronic transition (ΔE), and oscillator strength of the electronic transition (f). These are the parameters involved in the two-level model: $\beta \sim \Delta\mu.f^2/\Delta E^2$, according to which large molecular hyperpolarizabilities β are related to a dominant CT excitation from the donor to the acceptor part of the molecule [1–4].

Consequently, the first step in our quantum-chemical evaluation of the NLO properties was to investigate the electronic transitions of the species studied. We used TD-DFT and CIS methods to calculate ΔE and f, and in order to find which one of the methods gives better description of the optical properties of the compounds, we compared the obtained theoretical data to experimental EOAM values in nonpolar solvent 1,4-dioxane [28]. A summary of the calculation results and the corresponding experimental parameters is represented in Table 1. Excitation to the first excited state gives rise to an intense absorption in the visible region characterized by transition energy predicted by the CIS method between 3.30 and 2.74 eV, and 3.17–2.83 by TD-DFT respectively. There is a progressive decrease in ΔE, expressed in a considerable bathochromic shift, when the the donor substituents in the pyridinium ring are replaced by acceptor groups. The calculated ΔE values reproduce quite accurately the experementally observed values, although the solvent effects were not considered in the theoretical evaluation.

Upon varying the substitution nature, the ground-state dipole moments significantly change decreasing more than twice from the most donating (17.8 D for 4-$N(CH_3)_2$) to the most electron withdrawing group (7.5 D for 4-CN). According to the two-level model, a large difference between the dipoles in the ground and excited state is a sign of large β. Hence, we determined the excited state dipole moments of the six compounds – for all the compounds a negative difference was found as a result of their less polar structure in excited state. The two acceptor substituted derivatives show the largest difference between the dipole moments in the ground and excited state. Experimentally the decrease of the dipole moments upon excitation was characterized by solvatochromic elucidation of the CT band [29]. Altough the CIS and the TD-DFT calculations overestimated the ground and excited state dipole moments, the variation of μ_g and $\Delta\mu$ values are in good agreement with the experimentally determined values.

As it was given above according to the two-level model, higher β values should be expected based on larger $\Delta\mu$ and f and smaller ΔE. The difference between the dipole moments in the ground and excited state and the oscillator strengths of the CT transition are predicted by both computational methods as being highest for the acceptor substituted compounds. These two compounds exhibit the lowest-wavelength CT transitions as well and subsequently they should be expected to show the highest first molecular hyperpolarizability within the series.

Table 1. Theoretically calculated dipole moments in the ground and excited states (μ_g and μ_e), difference between the ground and excited state dipole moments ($\Delta\mu$), energy of the electronic transition (ΔE), oscillator strength of the electronic transition (f), and the corresponding experimental parameters [25].

Substituent	CIS					TD-DFT		Experiment				
	μ_g, D	μ_e, D	$\Delta\mu$, D	E, eV	f	E, eV	f	μ_g, D	μ_e, D	$\Delta\mu$, D	E, eV	μ_{ge}, D
4-$N(CH_3)_2$	17.8	14.2	–2.8	3.30	0.85	3.17	0.51	12.5	11.3	–1.2	3.33	6.8
4-CH_3	13.5	10.3	–3.2	3.13	0.63	3.14	0.41	10.0	5.4	–4.6	3.32	5.2
4-$C(CH_3)_3$	14.1	10.6	–3.4	3.14	0.69	3.14	0.46	10.1	5.7	–4.4	3.31	5.0
H	12.4	9.2	–3.2	3.09	0.57	3.15	0.37	9.7	4.9	–4.8	3.16	4.8
4-COC_6H_5	12.6	8.2	–4.4	2.83	0.81	2.83	0.55	8.9	1.2	–7.7	2.95	5.8
4-CN	7.5	3.3	–4.2	2.74	0.78	2.93	0.52	6.1	0.9	–5.2	2.81	5.2

CONCLUSION

A theoretical study on the molecular NLO efficiency of a series of squaric acid based chromophores was carried out. The molecular NLO properties depend strongly on the nature of the substituents. The theoretical methods used reproduce accurately the experimentally observed ΔE values and the variation of μ_g and $\Delta\mu$, although the solvent effects were not considered in the theoretical evaluation. On the basis of the established electronic structure, the large difference between the dipole moments in the ground and excited state and the intensive low-lying absorption maxima in the visible UV region best performance should be expected for the acceptor substituted chromophores.

Acknowledgements: *The financial support by the Bulgarian National Science Fund (Contract X-1510) is gratefully acknowledged.*

REFERENCES

1. J. Wolff, R. Wortmann, *Adv. Phys. Org. Chem*., **32**, 121 (1999).
2. H. Nalwa, S. Miyata, in: Nonlinear Optics of Organic Molecules and Polymers, H. Nalwa, S. Miyata (Eds.), CRC Press. Inc., Boca Ratton, 1997, Ch. 4.
3. H. S. Nalwa, T. Watanabe, S. Miyata, *Opt. Mater*., **2**, 73 (1993).
4. B. Champagne, D. Bishop, *Adv. Chem. Phys*., **126**, 41 (2003).
5. D. F. Aeton, *Science*, **253**, 281 (1991).
6. S. Gilmour, R. A. Montgomery, S. R. Marder, L.-T. Cheng, A. K.-Y. Jen, Y. Cai, J. W. Perry, L. R. Dalton, *Chem. Mater*., **6**, 1603 (1994).
7. D. M. Burland, R. D. Miller, C. A. Walsh, *Chem. Rev*., **94**, 31 (1994).
8. T. J. Marks, M. A. Ratner, *Angew. Chem. Int*. *Ed.*, **34**, 155 (1995).
9. W. Lin, S. Yitzchaik, A. Malik, M. K. Durbin, A. G. Richter, G. K. Wong, P. Dutta, T. J. Marks, *Angew*. *Chem. Int*. *Ed.*, **34**, 1497 (1995).
10. T. Yamashiki, S. Fukuda, K. Tsuda, T. Gotoh, *Appl. Phys. Lett*., **83**, 605 (2003).
11. X. Zheng, S. Wu, R. Sobolewski, R. Adam, M. Mikulics, P. Kordoš, M. Siegel, *Appl. Phys. Lett*., **82**, 2383 (2003).
12. M. Sliwa, S. Letard, I. Malfant, M. Nierlich, P. G. Lacroix, T. Asahi, H. Masuhara, P. Yu, K. Nakatani, *Chem. Mater*., **17**, 4727 (2005).
13. W. Liptay, in: Excited States, Dipole Moments and Polarizabilities of Molecules in Excited Electronic States, E. C. Lim (ed.), vol. 1, Academic Press, New York, 1974, p.129.
14. R. Wortmann, K. Elich, S. Lebus, W. Liptay, P. Borowicz, A. Grabowska, *J. Chem. Phys*., **96**, 9724 (1992).
15. M. J. Frisch, G. W. Trucks, H. B. Schlegel, G. E. Scuseria, M. A. Robb, J. R. Cheeseman, V. G. Zakrzewski, J. A. Montgomery, Jr., R. E. Stratmann, J. C. Burant, S. Dapprich, J. M. Millam, A. D. Daniels, K. N. Kudin, M. C. Strain, O. Farkas, J. Tomasi, V. Barone, M. Cossi, R. Cammi, B. Mennucci, C. Pomelli, C. Adamo, S. Clifford, J. Ochterski, G. A. Petersson, P. Y. Ayala, Q. Cui, K. Morokuma, D. K. Malick, A. D. Rabuck, K. Raghavachari, J. B. Foresman, J. Cioslowski, J. V. Ortiz, A. G. Baboul, B. B. Stefanov, G. Liu, A. Liashenko, P. Piskorz, I. Komaromi, R. Gomperts, R. L. Martin, D. J. Fox, T. Keith, M. A. Al-Laham, C. Y. Peng, A. Nanayakkara, C. Gonzalez, M. Challacombe, P. M. W. Gill, B. Johnson, W. Chen, M. W. Wong, J. L. Andres, C. Gonzalez, M. Head-Gordon, E. S. Replogle, J. A. Pople, Gaussian 98, Revision A.7, Gaussian, Inc., Pittsburgh PA, 1998.
16. A. M. K. Shuhla, J. Leszczynski, *J. Phys. Chem*. *A*, **107**, 5538 (2003).
17. T. Kolev, D. Yancheva, D. C. Kleb, M. Schurmann, H. Preut, P. Bleckmann, *Z. Krist. NCS*, **216**, 65 (2001).
18. T. Kolev, D. Yancheva, M. Schurmann, D. C. Kleb, H. Preut, M. Spiteller, *Acta Cryst*., **E58**, o1267 (2002).
19. T. Kolev, D. Yancheva, B. Shivachev, R. Petrova, *Acta Cryst*., **E63**, o3259 (2007).
20. I. Uçar, A. Bulut, O. Yeşilel, M. Odabaşoglu, O. Büyükgüngör, *Acta Cryst*., **C61**, o148 (2005).
21. T. M. Kolev, D. Y. Yancheva, B. A. Stamboliyska, *Spectrochim. Acta*, **59**, 1805 (2003).
22. T. M. Kolev, B. A. Stamboliyska, D. Y. Yancheva, V. Enchev, *J. Mol. Struct*., **191**, 241 (2004).
23. T. Kolev, B. Stamboliyska, D. Yancheva, *Chem. Phys*., **324**, 489 (2006).
24. M. Szafran, J. Koput, *J. Mol. Struct*., **381**, 157 (1996).
25. Y. Yang, B. Champagne, *J. Phys. Chem*., **107A**, 3942 (2003).
26. T. Kolev, B. B. Koleva, M. Spiteller, W. S. Sheldrick, H. Mayer-Figge, *J. Phys. Chem*., **111A**, 10084 (2007).
27. B. B. Koleva, T. Kolev, R. W. Seidel, H. Mayer-Figge, M. Spiteller, W. S. Sheldrick, *J. Phys. Chem*. *A,* (2008) in press.
28. T. Kolev, D. Yancheva, B. Stamboliyska, M. Dimitrov, R. Wortmann, *Chem. Phys*., **348**, 45 (2008).
29. T. Kolev, D. Yancheva, S. Stoyanov, *Adv. Funct. Mater*., **14**, 799 (2004).

ТЕОРЕТИЧНО ИЗСЛЕДВАНЕ НА СТРУКТУРАТА, ЕЛЕКТРОННИТЕ СПЕКТРИ И НЕЛИНЕЙНИТЕ ОПТИЧНИ СВОЙСТВА НА ПИРИДИН-БЕТАИНИТЕ НА КВАДРАТНАТА КИСЕЛИНА

Б. А. Стамболийска*, Д. Я. Янчева, Ц. М. Колев

Лаборатория „Структурен органичен анализ“, Институт по органична химия с център по фитохимия, Българска академия на науките, ул. „Акад. Г. Бончев“, бл. 9, 1113 София

Посветена на акад. Иван Юхновски по повод на 70-та му годишнина

Постъпила на 17 януари 2008 г.; Преработена на 30 януари 2008 г.

(Резюме)

Строежът и свойствата на шест пиридин-бетаини на квадратната киселина и зависимостта на техните нелинейно-оптични характеристики от структурните промени са изследвани посредством теоретичен анализ. Структурите на всички изследвани пиридин-бетаини са оптимизирани на HF/6-311G(d,p) ниво на теория. Синглетната енергия на прехода е пресметната на нива CIS и TD-DFT. Разпределението на заряда, вибрационните и електронни спектри са анализирани за да се опишат преноса на заряд в молекулата и свързаните с това енергии на прехода. Молекулните нелинейно-оптични свойства са определени на базата на „модела на две нива“ като е установено, че те са най-добри при акцепторно-заместените пиридин-бетаини на квадратната киселина.

Bulgarian Chemical Communications, Volume 40, Number 4 (pp. 505–511) 2008

Molecular mechanics (MM3(π)) conformational analysis of molecules containing conjugated π-electron fragments: a molecular tweezer

M. I. Kotev, P. M. Ivanov*

Laboratory of Physical Organic and Computational Chemistry, Institute of Organic Chemistry with Centre of Phytochemistry, Bulgarian Academy of Sciences, Acad. G. Bonchev St., Block 9, 1113 Sofia, Bulgaria

Dedicated to Academician Ivan Juchnovski on the occasion of his 70th birthday

Received January 17, 2008; Revised February 15, 2008

The conformations of a molecular tweezer formed by two aromatic chiral molecules, bonded and separated, by a conjugated spacer, were studied with molecular mechanics. This molecule contains conjugated π-electron fragment and necessitates special treatment with the MM3(π) modeling protocol. Comparison was made with results from the standard MM3 scheme and semiempirical and *ab initio* MO, and DFT quantum-mechanical methods. The CONFLEX conformational search procedure was used for finding low-energy conformations. Although one and the same cluster of conformations for the molecular tweezer is strongly preferred when using the two molecular mechanics modeling protocols (MM3 and MM3(π)), differences were obtained in the geometries of the lowest-energy conformations.

Key words: molecular tweezer, conformational analysis, molecular mechanics, MM3(π), CONFLEX search.

INTRODUCTION

We reported recently results from molecular mechanics study of the preferred conformations of tylosin [1, 2] and leucomycin-V [3]. We emphasized in these studies the dependency of the results on the molecular mechanics protocol used and the completeness of the conformational search. A thorough search for the lowest energy conformations based on the CONFLEX [4–6] procedure as a searcher and the MM3(92) force field [7–10] as a molecular mechanics model was performed. Two problems are of particular importance when molecular mechanics is used for modeling the conformations of large molecules: (i) the proper choice of a force field for modeling the system under study; (ii) reliable and efficient conformational search of low-energy conformations when many degrees of freedom for intramolecular rotations determine the conformational flexibility of the molecule. A specific characteristic and an advantage of the Allinger's MM3 force field is that an extension of the force field, MM3(π) [11, 12], has been devised to model molecules with conjugated π-electron fragments.

As an overall result of methodological signifycance from an earlier study [3] is the differences that manifest two very similar molecules, leucomycin-V and its 9-epi isomer (they differ only by the chirality of the C(9) macroring carbon atom), when comparative studies are carried out using the MM3 and MM3(π) molecular mechanics modeling protocols. This prompted us to extend further our study by examining also the conformations of a molecular tweezer containing conjugated π-electron spacer – di-(R,R)-1-[10-(1-hydroxy-2,2,2-trifluoroethyl)-9-anthryl]-2,2,2-trifluoroethyl muconate (**1**). A cautionary note is made in the present report regarding the execution of conformational search/minimization studies in the case of cooperative movements of the atoms on potential energy surface of small slope – molecules like **1**, where aromatic rings are present [13].

The chiral molecular tweezer (**1**) (Fig. 1) was synthesized recently. It contains conjugated π-electron spacer and behaves as an excellent chiral solvating agent (CSA) [14]. CSA are optically pure compounds that after binding pairs of enantiomers produce diastereomeric associates with different NMR spectra. Common CSAs can usually participate in hydrogen bonds or π interactions. Some non-cyclic compounds with flexibly-sized cavities, which are frequently termed molecular tweezers or clips, proved to be effective as synthetic receptors. This kind of compounds is characterized by having two planar aromatic groups, separated by a semi-rigid spacer, which enhances the selective binding with aromatic guests by π interactions [15]. Molecular tweezers are studied also in relation to elucidating the mechanisms of the recognition of

* To whom all correspondence should be sent:
E-mail: ivanov@bas.bg

© 2008 Bulgarian Academy of Sciences, Union of Chemists in Bulgaria

sequence information in high-molar mass copolymers by small molecules of complementary structure [16]. Intensive research is carried out on such systems during the last two decades [17–50].

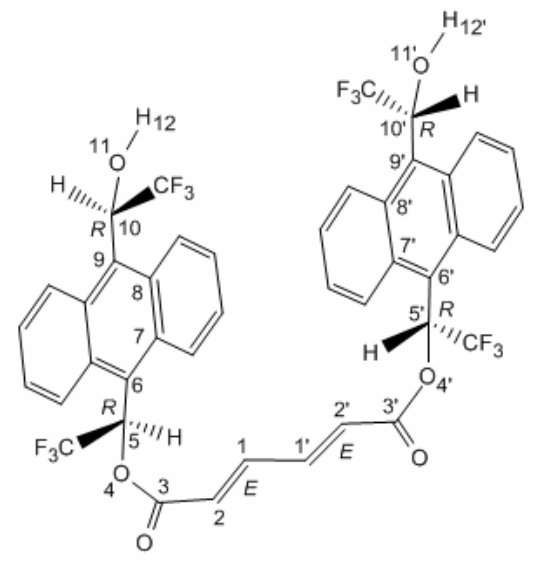

Dihedral angle	
D_1	1-2-3-4
D_2	1'-2'-3'-4'
D_3	2-3-4-5
D_4	2'-3'-4'-5'
D_5	3-4-5-6
D_6	3'-4'-5'-6'
D_7	4-5-6-7
D_8	4'-5'-6'-7'
D_9	8-9-10-11
D_{10}	8'-9'-10'-11'
D_{11}	9-10-11-12
D_{12}	9'-10'-11'-12'
D_{13}	2-1-1'-2'

Fig.1. Numbering of the atoms in di-(R,R)-1-[10-(1-hydroxy-2,2,2-trifluoroethyl)-9-anthryl]-2,2,2-trifluoroethyl muconate (**1**) and the definition of dihedral angles.

METHOD AND COMPUTATIONAL DETAILS

The version 3.6 of CONFLEX [4–6] was used. A gradual increase to a search limit of 4.0 kcal·mol^{-1} for **1** determined the energy range from which the initial structures for the search were selected [4-6]. The variable torsional angles (Fig. 1), which were used for conformation comparison when eliminating identical conformers are: D1 = 1 – 2 – 3 – 4, D2 = 1' – 2' – 3' – 4', D3 = 2 – 3 – 4 – 5, D4 = 2' – 3' – 4' – 5', D5 = 3 – 4 – 5 – 6, D6 = 3' – 4' – 5' – 6', D7 = 4 – 5 – 6 – 7, D8 = 4' – 5' – 6' – 7', D9 = 8 – 9 – 10 – 11, D10 = 8' – 9' – 10' – 11', D11 = 9 – 10 – 11 – 12', D12 = 9' – 10' – 11' – 12', D13 = 2 – 1 – 1' – 2'. Nine dihedrals describe the geometry of the π-conjugated bridge and these are the angles which were used for cluster analysis in Table 1 [because of the preferred s-trans conformation for this fragment of the π-spacer, D13 is always about 180º degrees, a letter-code ***A*** (*vide infra*)]. The default values of the options were used when the steric energies and the dihedral angles were compared in the redundancy test, e.g. 3N/100 kcal·mol^{-1} (N – the number of atoms) allowance for the comparison of steric energies in the first stage, and 10.0º allowance for the comparison of dihedral angles in the final stage. The whole set of conformations were subjected to a cluster analysis [51, 52] and the structures resulted sorted into 2 clusters (Table 1). Unique conformations were processed with the π-version of the MM3(92) program [10–12]. This approach is more economical than the direct search with the computational scheme for modeling conjugated π-electron segments in the molecule. In addition, an independent CONFLEX/MM3(π) search/minimization study was also executed. The block-diagonal Newton-Raphson minimization procedure was used [10]. Electrostatic interactions were estimated with the value 2.0 of the dielectric parameter.

RESULTS AND DISCUSSION

Computed conformational data for 1 are summarized in Table 1. They include average steric energies and populations of clusters and a letter-code representation of the important dihedral angles (Table 1). For the sake of compactness of the presentation we used a letter-code designations of dihedral angles as given in Fig. 2 [1]. Letter ***G*** designates a dihedral angle in the range from 20 to 100º, ***G*** - from 100 to 150º, ***A*** - from 150º to –150º, *etc*.

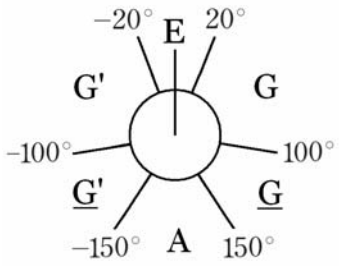

Fig. 2. Designation of dihedral angles.

Table 1. Cluster analysis of low-energy conformations of di-(R,R)-1-[10-(1-hydroxy-2,2,2-trifluoroethyl)-9-anthryl]-2,2,2-trifluoroethyl muconate (**1**) [a].

Clusters	Dihedral angles								Number of conformations	ΔE_0 [b]		ΔEav [c]	Population [d]
	D1	D2	D3	D4	D5	D6	D7	D8		MM3	MM3(π)		
I	A	A	G	G	G'	G'	G	G	460	0.0	0.0	0.9	0.990
II	A	E	A	A	G'	G'	G	G	85	3.6	4.0	4.4	0.010

a - Units are kcal·mol^{-1}; b - Relative steric energy of the lowest-energy conformation of the cluster. CONFLEX search has been carried out with the MM3 protocol. Search limit 4.0 kcal·mol^{-1} was used. The final set of coordinates for the lowest-energy conformations of each cluster was subjected to MM3(π) minimization. The independent CONFLEX/MM3(π) was executed with search limit 1.5 kcal·mol^{-1}; c - Average steric energy of the cluster; d - At 300K.

We have emphasized in our previous work [2, 3] the importance of using at the final stage of the minimization the version of MM3 devised to model molecules with conjugated π-electron fragments. Such a kind of treatment required the dienone portion of tylosin [2] and the diene fragment of leucomycin-V [3]. The overall result from the present study on **1** is that the conjugated π-electron spacer of the molecular tweezer **1** necessitates MM3(π) treatment. The concavely arranged host geometry of the two anthracene rings bound with the chiral $CHOHCF_3$ groups is important for the selective binding with aromatic or other guests. The conformational equilibrium and the C2 symmetry of **1** make it impossible to study its global geometry using NMR experiments [14]. Molecular mechanics modeling is of particular usefulness in such situations. Although one and the same cluster of conformations is strongly preferred when using the two molecular mechanics modeling protocols (CONFLEX/MM3 and CONFLEX/MM3(π)), significant differences of the geometries for the π-bridge portion were obtained in the lowest-energy conformations (Fig. 3, A, B and Table 2, data in 'bold'). These differences in the geometries did not appear however when using CONFLEX/MM3 search with subsequent MM3(π) minimization (Tables 1 and 2). We had to carry out an independent CONFLEX/MM3(π) search/minimization study (Fig. 3, B). This is purely "technical" artifact that originates from the block-diagonal Newton-Raphson minimization procedure in MM3 that may not always produce completely converged results for molecules containing aromatic rings, as they present cases with cooperative movements of the atoms on a surface of small slope [13].

Attempting further to interpret the results, we compared the geometries derived with molecular mechanics with semiempirical molecular orbital (SE-MO) [53–55] and *ab initio* MO (RHF/6-31G*), ant DFT (hybrid functionals B3LYP and MPW1K with basis set 6-31G*) [56] methods (Table 2). The CONFLEX/MM3 and CONFLEX/MM3(π) optimized geometries of the lowest-energy conformations (Fig. 3, A and B) served as starting structures for the AM1, PM3, and Hartree-Fock computations. The ab initio MO optimized structure was used as starting geometry for the DFT calculations. Gaussian 98 was used for all quantum-mechanical computations [56]. Significantly different final geometries were obtained (Fig. 3). The spacer of the muconate (**1**) connecting the two chiral arms is now flatter compared with the geometries from the molecular mechanics modeling, i.e. the tweezer does not possess enough flexibility and the two arms of the clip are positioned more distant from each other (Fig. 3, C–H). This result is not unexpected because the SE-MO, HF *ab initio* MO and standard DFT methods cannot model enough satisfactorily dispersion interactions and the system lacks forces that could deform the linear spacer. Structures C and D (AM1) have the same geometry of the conjugated spacer, but differ by the rotation of the $CHOHCF_3$ groups. Similar is the geometry of E, whereas the geometry of F (PM3) is completely different in comparison with all low-energy forms obtained after the CONFLEX search. Quite probably, the *syn* disposition of the anthracene rings in this case does not correspond to a local minimum on the PM3 potential energy surface. The present case, muconate **1**, illustrates the different behaviour of the two SE-MO methods (cases D and F), as well as the importance of proper choice of the starting geometry (cases A and B). Except for PM3, all other quantum-mechanical methods produce symmetrical geometries (Table 2). The DFT optimized clips are more opened compared with the structures obtained with the other modeling protocols (compare G and H on Fig. 3 and the torsion angles D5, D6 in Table 2). It is gratifying, however, that in the prevailing number of cases cavities are produced after the optimizations with the SE-MO, *ab initio* MO and DFT methods (cases C, D, E, G, and H).

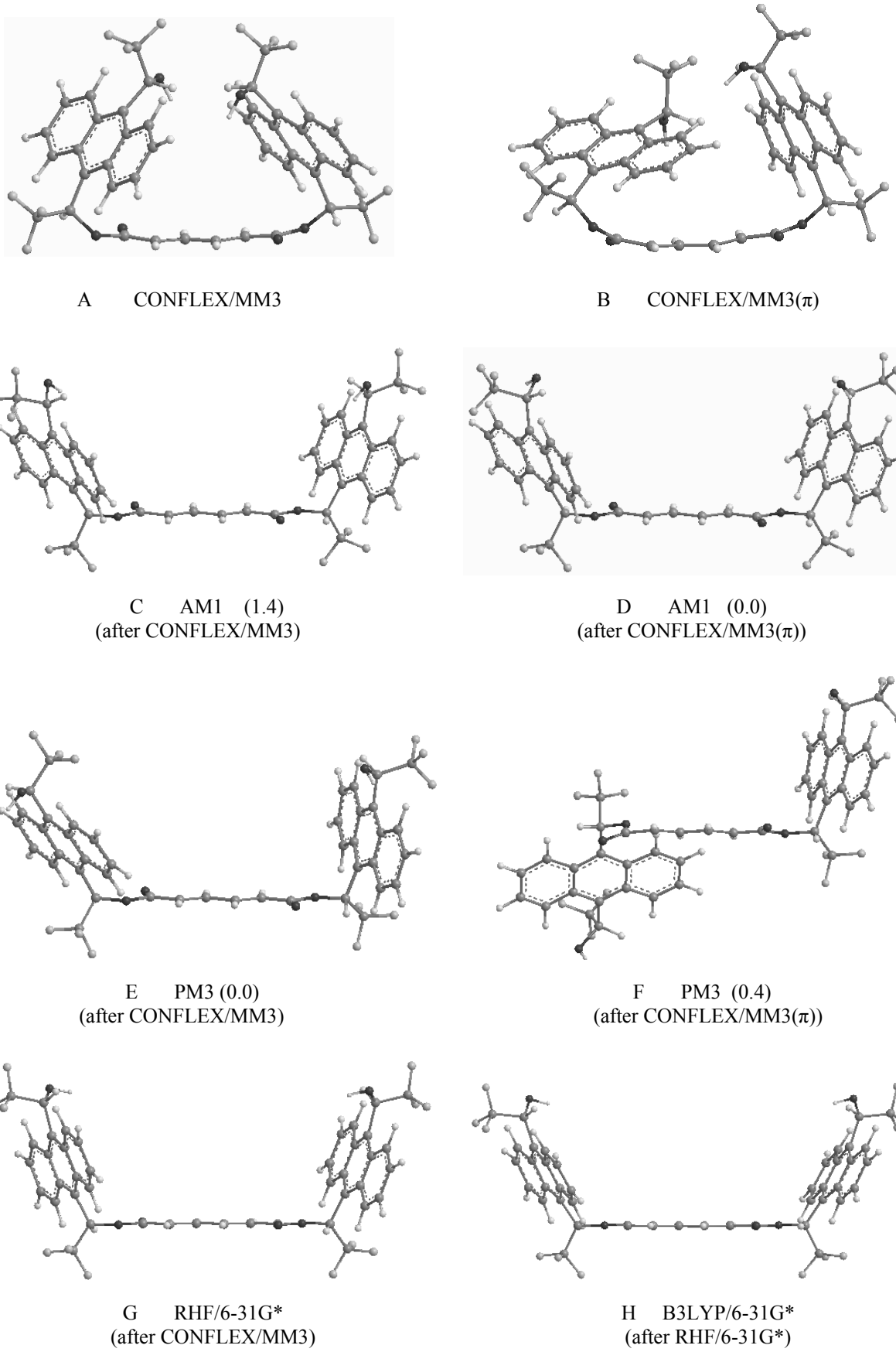

A CONFLEX/MM3

B CONFLEX/MM3(π)

C AM1 (1.4)
(after CONFLEX/MM3)

D AM1 (0.0)
(after CONFLEX/MM3(π))

E PM3 (0.0)
(after CONFLEX/MM3)

F PM3 (0.4)
(after CONFLEX/MM3(π))

G RHF/6-31G*
(after CONFLEX/MM3)

H B3LYP/6-31G*
(after RHF/6-31G*)

Fig. 3. Optimized geometries of the lowest-energy conformations of **1**. Relative AM1 and PM3 energies (in kcal·mol^{-1}) are given in parentheses.

Table 2. Comparison of the geometries (dihedral angles in degrees) of the lowest-energy conformations of **1** obtained with different methods.

Method	D1	D2	D3	D4	D5	D6	D7	D8	D9	D10	D11	D12	D13
A [a] - CONFLEX/MM3 [b]	–174.6	–174.9	142.1	143.1	–62.1	–62.9	136.4	136.6	138.1	137.9	–61.9	–61.0	–175.0
B - CONFLEX/MM3(π) [c]	–153.9	–174.6	138.1	144.3	–54.2	–76.3	138.9	136.3	141.1	137.9	–62.8	–69.1	–167.7
MM3(π) [d]	–170.4	–172.0	141.0	142.2	–63.8	–65.1	136.6	136.8	138.1	137.9	–62.6	–61.3	–174.0
C - AM1 [e]	179.1	179.1	179.9	179.9	–114.1	–114.1	143.9	143.9	143.0	143.0	–25.0	–25.0	179.7
D - AM1 [f]	179.9	179.9	179.2	179.2	–115.3	–115.3	144.4	144.3	127.5	127.5	49.4	49.4	–179.8
E - PM3 [g]	177.7	–179.7	178.2	178.2	–110.7	–94.6	145.0	133.1	144.8	127.8	–62.8	55.9	–179.3
F - PM3 [h]	–27.6	–179.2	175.9	178.2	–100.2	–94.2	145.9	133.1	143.9	127.8	–64.5	56.0	179.3
G - RHF/6-31G* [i]	179.5	179.5	180.0	180.0	–103.5	–103.6	139.4	139.4	140.1	140.1	–52.3	–52.3	179.8
RHF/6-31G* [j]	179.4	179.4	180.0	108.0	–103.7	–104.3	139.4	139.3	140.1	140.1	–52.2	–52.3	179.8
H - B3LYP/ 6-31G* [k]	–179.5	–179.5	–179.2	–179.2	–119.0	–119.0	138.7	138.7	140.0	140.0	–40.0	–40.0	–179.5
MPW1K/6-31G* [l]	–179.7	–179.7	–179.5	–179.5	–118.8	–118.8	138.3	138.3	139.7	139.7	–35.2	–35.2	–179.5

a - The structures A-H are given in Fig. 3; b - CONFLEX/MM3 search; c - CONFLEX/MM3(π) search; d - MM3(π) optimization after CONFLEX/MM3 search. The lowest-energy structure obtained in this way practically preserves its starting geometry (A) and it is not given on Fig. 3; e - AM1 optimized geometry after CONFLEX/MM3 search; f - AM1 optimized geometry after CONFLEX/MM3(π) search; g - PM3 optimized geometry after CONFLEX/MM3 search; h - PM3 optimized geometry after CONFLEX/MM3(π) search; i - RHF/6-31G* optimized geometry after CONFLEX/MM3 search; j - RHF/6-31G* optimized geometry after CONFLEX/MM3(π) search. HF optimized examples show identical geometries (energies) and only one structure is given in Fig. 3; k - B3LYP/ 6-31G* optimized geometry after RHF/6-31G*; l - MPW1K/6-31G* optimized geometry after RHF/6-31G*. Both DFT optimized structures are with the same geometries.

The lowest-energy MM3(π) structure of cluster II (Table 1) was also optimized with the SE-MO, and *ab initio* MO and DFT methods. The geometries obtained resemble structure F in Fig. 3. The *anti* disposition of the chiral clips (cluster II) is disfavoured energetically by about 1–2 kcal·mol^{-1} in all cases.

CONCLUSIONS

Although one and the same cluster of conformations of **1** is strongly preferred when using the two molecular mechanics modeling protocols, significant differences were obtained in the geometries of the lowest energy conformations (Fig. 3, A and B). Both the molecular mechanics and quantum-mechanical methods confirm the prevalence of conformation that can easily adapt to a small molecule substrate by formation of a chiral cavity [14].

***Acknowledgement**: The National Science Fund of Bulgaria is acknowledged for the financial support (project X-1406).*

REFERENCES

1. P. M. Ivanov, *J. Mol. Struct.*, **440**, 121 (1998).
2. P. M. Ivanov, *J. Mol. Struct.*, **606**, 217 (2002).
3. M. I. Kotev, P. M. Ivanov, *Chirality*, **20**, 400 (2008).
4. H. Goto, E. Osawa, *J. Mol. Struct.* (*Theochem*), **285**, 157 (1993).
5. H. Goto, E. Osawa, *J. Chem. Soc. Perkin Trans 2*, 187 (1993).
6. E. Osawa, H. Goto, M. Yamato, in: Computer Aided Innovation of New Materials, M. Doyama, J. Kihara, M. Tanaka, R. Yamamoto (Eds.), Elsevier Sci. Publ. BV (North-Holland), Amsterdam, 1993, p. 845.
7. N. L. Allinger, Y. H. Yuh, J. H. Lii, *J. Am. Chem. Soc.*, **111**, 8551 (1989).
8. J. H. Lii, N. L. Allinger, *J. Am. Chem. Soc.*, **111**, 8566 (1989).
9. J. H. Lii, N. L. Allinger, *J. Am. Chem. Soc.*, **111**, 8576 (1989).
10. MM3(92), Technical Utility Corporation, 235 Glen Village Court, Powell, OH 43065.
11. N. L. Allinger, F. Li, L. Yan, J. C. Tai, *J. Comput. Chem.*, **11**, 868 (1990).
12. N. L. Allinger, S. Rodriguez, K. Chen, *J. Mol. Struct.* (*Theochem*), **260**, 161 (1992).
13. P. M. Ivanov, *QCPE Bull.*, **6**, 6 (1986).
14. M. Palomino-Schätzlein, A. Virgili, S. Gil, C. Jaime, *J. Org. Chem.*, **71**, 8114 (2006).
15. M. Harmata, *Acc. Chem. Res.*, **37**, 862 (2004).
16. H. M. Colquhoun, Z. Zhu, Ch. J. Cardin, Y. Gab, M. G. B. Drew, *J. Am. Chem. Soc.*, **129**, 16163 (2007).
17. S. C. Zimmerman, M. Mrksich, M. Baloga, *J. Am. Chem. Soc.*, **111**, 8528 (1989).
18. J. F. Blake, W. L. Jorgensen, *J. Am. Chem. Soc.*, **112**, 7269 (1990).
19. L. Sharma, *J. Inclusion Phenom. Mol. Recognit. Chem.*, **31**, 161 (1998).
20. F.-G. Klärner, U. Burkert, M. Kamieth, R. Boese, J. Benet-Buchholz, *Chem. Eur. J.*, **5**, 1700 (1999).
21. F.-G. Klärner, J. Panitzky, D. Preda, L. T. Scott, *J. Mol. Model.*, **6**, 318 (2000).
22. H. Kurebayashi, T. Haino, S. Usui, Y. Fukazawa, *Tetrahedron*, **57**, 8667 (2001).
23. S. P. Brown, T. Schaller, U. P. Seelbach, F. Koziol, C. Ochsenfeld, F.-G. Klärner, H. W. Spiess, *Angew. Chem. Int. Ed.*, **40**, 717 (2001).
24. R. Ruloff, U. P. Seelbach, A. E. Merbach, F.-G. Klärner, *J. Phys. Org. Chem.*, **15**, 189 (2002).
25. O. P. Kryatova, A. G. Kolchinski, E. V. Rybak-Akimova, *J. Incl. Phenom. Macrocycl. Chem.*, **42**, 251 (2002).
26. J. S. Disch, R. J. Staples, T. E. Concolino, T. E. Haas,

E. V. Rybak-Akimova, *Inorg. Chem.*, **42**, 6749 (2003).
27. F.-G. Klärner, B. Kahlert, *Acc. Chem. Res.*, **36**, 919 (2003).
28. C.-P. Du, J.-S. You, X.-Q Yu, C.-L. Liu, J.-B. Lan, R.-G. Xie, *Tetrahedron: Asymmetry*, **14**, 3651 (2003).
29. H. M. Colquhoun, Z. Zhu, *Angew. Chem. Int. Edit.*, **43**, 5040 (2004).
30. N. C. Gianneschi, S.-H. Cho, S. B. T. Nguyen, C. A. Mirkin, *Angew. Chem. Int. Ed.*, **43**, 5503 (2004).
31. A. Petitjean, R. G. Khoury, N. Kyritsakas, J.-M. Lehn, *J. Am. Chem. Soc.*, **126**, 6637 (2004).
32. A. F. Jalbout, C. A. Morgado, L. Adamowicz, *Chem. Phys. Lett.*, **383**, 317 (2004).
33. F.-G. Klärner, J. Polkowska, J. Panitzky, U. P. Seelbach, U. Burkert, M. Kamieth, M. Baumann, A. E. Wigger, R. Boese, D. Blaeser, *Eur. J. Org. Chem.*, **7**, 1405 (2004).
34. H. Iwamoto, N. Takahashi, T. Maeda, Y. Hidaka, Y. Fukazawa, *Tetrahedron Lett.*, **46**, 6839 (2005).
35. H. Nemoto, T. Kawano, N. Ueji, N. Sakamoto, T. Araki, N. Miyoshi, I. Suzuki, M. Shibuya, *Tetrahedron Lett.*, **46**, 551 (2005).
36. M. Parac, M. Etinski, M. Peric, S. Grimme, *J. Chem. Theory Comput.*, **1**, 1110 (2005).
37. 37. M. Fokkens, T. Schrader, F.-G. Klärner, *J. Am. Chem. Soc.*, **127**, 14415 (2005).
38. T. Korenaga, Y. Kawauchi, T. Kosaki, T. Ema, T. Sakai, *Bull. Chem. Soc. Jpn.*, **78**, 2175 (2005).
39. M. Lobert, H. Bandmann, U. Burkert, U. P. Büchele, V. Podsadlowski, F.-G. Klärner, *Chem. Eur. J.*, **12**, 1629 (2006).
40. V. Balzani, H. Bandmann, P. Ceroni, C. Giansante, U. Hahn, F.-G. Klärner, U. Müller, W. M. Müller, C. Verhaelen, V. Vicinelli, F. Vögtle, *J. Am. Chem. Soc.*, **128**, 637 (2006).
41. F.-G. Klärner, B. Kahlert, A. Nellesen, J. Zienau, C. Ochsenfeld, T. Schrader, *J. Am. Chem. Soc.*, **128**, 4831 (2006).
42. R. Chhabra, J. Sharma, Y. Liu, H. Yan, *Nano Lett.*, **6**, 978 (2006).
43. X.-X. Peng, H.-Y. Lu, T. Han, C.-F. Chen, *Org. Lett.*, **9**, 895 (2007).
44. T. Schaller, U. P. Büchele, F.-G. Klärner, D. Bläser, R. Boese, S. P. Brown, H. W. Spiess, F. Koziol, J. Kussmann, C. Ochsenfeld, *J. Am. Chem. Soc.*, **129**, 1293 (2007).
45. P. Degen, T. Optenhostert, H. Rehage, C. Verhaelen, M. Lange, J. Polkowska, F.-G. Klärner, *Langmuir*, **23**, 11611 (2007).
46. E. Scamporrino, P. Mineo, S. Dattilo, D. Vitalini, E. Spina, *Macromol. Rapid Comm.*, **28**, 1546 (2007).
47. J. Zienau, J. Kussmann, F. Koziol, C. Ochsenfeld, *Phys. Chem. Chem. Phys.*, **9**, 4552 (2007).
48. J. M. Hermida-Ramon, C. M. Estevez, M. Carlos, *Chem. Eur. J.*, **13**, 4743 (2007).
49. J. L. Katz, B. J. Geller, P. D. Foster, *Chem. Commun.*, **10**, 1026 (2007).
50. D. Margetic, R. N. Warrener, D. N. Butler, D. Officer, *Theor. Chem. Acc.*, **117**, 239 (2007).
51. H. Goto, Y. Kawashima, M. Kashimura, S. Morimoto, E. Osawa, *J. Chem. Soc. Perkin Trans 2*, 1647 (1993).
52. E. Osawa, H. Goto, T. Hata, E. Deretey, *J. Mol. Struct.* (*Theochem*), **398-399**, 229, (1997).
53. M. J. S. Dewar, E. G. Zoebisch, E. F. Healy, J. J. P. Stewart, *J. Am. Chem. Soc.*, **107**, 3902, (1985).
54. M. J. S. Dewar, E. G. Zoebisch, *J. Mol. Struct. (Theochem)*, **180**, 1, (1988).
55. J. J. P. Stewart, *J. Comp. Chem.*, **10**, 209, (1989).
56. M. J. Frisch, G. W. Trucks, H. B. Schlegel, G. E. Scuseria, M. A. Robb, J. R. Cheeseman, V. G. Zakrzewski, J. A. Montgomery, Jr., R. E. Stratmann, J. C. Burant, S. Dapprich, J. M. Millam, A. D. Daniels, K. N. Kudin, M. C. Strain, O. Farkas, J. Tomasi, V. Barone, M. Cossi, R. Cammi, B. Mennucci, C. Pomelli, C. Adamo, S. Clifford, J. O chterski, G. A. Petersson, P. Y. Ayala, Q. Cui, K. Morokuma, D. K. Malick, A. D. Rabuck, K. Raghavachari, J. B. Foresman, J. Cioslowski, J. V. Ortiz, A. G. Baboul, B. B. Stefanov, G. Liu, A. Liashenko, P. Piskorz, I. Komaromi, R. Gomperts, R. L. Martin, D. J. Fox, T. Keith, M. A. Al-Laham, C. Y. Peng, A. Nanayakkara, C. Gonzalez, M. Challacombe, P. M. W. Gill, B. Johnson, W. Chen, M. W. Wong, J. L. Andres, C. Gonzalez, M. Head-Gordon, E. S. Replogle, J. A. Pople, Gaussian 98, Revision A.7, Gaussian, Inc., Pittsburgh PA, 1998.

МОЛЕКУЛНО-МЕХАНИЧЕН (ММ3(π)) КОНФОРМАЦИОНЕН АНАЛИЗ НА МОЛЕКУЛИ СЪДЪРЖАЩИ СПРЕГНАТИ π-ЕЛЕКТРОННИ ФРАГМЕНТИ: МОЛЕКУЛНА ПИНСЕТА

М. И. Котев, П. М. Иванов*

Лаборатория „Физична органична и изчислителна химия“, Институт по органична химия с център по фитохимия, Българска академия на науките, ул. „Акад. Г. Бончев“, блок 9, 1113 София

Посветена на акад. Иван Юхновски по повод на 70-та му годишнина

Постъпила на 17 януари 2008 г.; Преработена на 15 февруари 2008 г.

(Резюме)

С молекулна механика бяха проучени конформациите на молекулна пинсета (**1**), съдържаща две ароматни хирални щипки, свързани помежду си със спрегнат мостови фрагмент. Използван е ММ3(π) протокол за молекулно-механично моделиране и е направено сравнение с резултати от стандартния ММ3 метод, както и с полуемпирични, *ab initio* MO и DFT квантовомеханични методи. За конформационно търсене на нискоенергетични конформери е използван CONFLEX алгоритъма. Резултатите от ММ3 и ММ3(π) разглежданията показват, че **1** има силно предпочитание към един и същ клъстер от конформери, но геометриите на най-нискоенергетичните конформации, получени с двата протокола, се различават.

Bulgarian Chemical Communications, Volume 40, Number 4 (pp. 512–519) 2008

Experimental IR, and computational *ab initio* and DFT B3LYP studies on spectral and structural changes, caused by the conversion of methyl cyanoacetate into carbanion

A. D. Popova[1,*] , Y. I. Binev[2], P. J. Vassileva-Boyadjieva[1], I. G. Binev[1]

[1] *Institute of Organic Chemistry with Centre of Phytochemistry, Bulgarian Academy of Sciences, Acad. G. Bonchev St., Block 9, 1113 Sofia, Bulgaria*
[2] *Instituto de Investigação Cientifica Tropical, Rua da Junqueira, 86–1, 1300-344 Lisboa, Portugal*

Dedicated to Academician Ivan Juchnovski on the occasion of his 70th birthday

Received January 24, 2008, Revised March 27, 2008

Spectral and structural changes, caused by the conversion of methyl cyanoacetate molecule into carbanion, have been studied applying a combined IRS experimental/*ab initio*, DFT computational approach. A good agreement has been found between experimental and scaled B3LYP/6-31++G** vibrational frequencies; the relationship between the corresponding band intensities has been only qualitative. In agreement between theory and experiment, the conversion of methyl cyanoacetate into carbanion causes strong decreases in the cyano and carbonyl stretching frequencies (with 109 and 127 cm^{-1}, respectively), a dramatic integrated intensity increase (51.3 fold) of the cyano stretching band and other essential IRS changes. According to both steric and electronic structure computations, the carbonyl group is conjugated with the carbanionic center more strongly than the cyano group. Except the methyl group hydrogen atoms, the whole carbanion is planar.

Key words: IR spectra, *ab initio* HF, DFT B3LYP method, structure, methyl cyanoacetate, carbanion.

INTRODUCTION

Methyl cyanoacetate $NC–CH_2–COOCH_3$ was first prepared by Walden in the twenties of 20th century; the detailed description of this synthesis was reported in 1934 in the patent of I. G. Farbenindustrie [1]. Methyl cyanoacetate is used nowadays as precursor in industrial synthesis of pharmaceuticals, herbicides and fungicides, cyanoacrylic polymers, dies for leather and polyesters, etc. [2, 3] (and references therein).

Vibrational spectra of methyl cyanoacetate have repeatedly been studied [2–10]; a part of these studies has been related to real and possible conformers of the molecule [2–5, 6, 9, 10]. This problem has also been approached by computational methods: PCILO [8], *ab initio* HF/4-21G [9], HF/6-31 G [2], MP2/6-31 G, DFT B3LYP 6-31G* [3], VDZ and MP2/6-31++G** [10]. All the used methods have predicted both little energy differences between the conformers and low energy barriers of the corresponding conformational conversions.

The vibrational spectra or structure of the carbanion of methyl cyannoacetate have not been studied either experimentally or theoretically, so the aim of the present studies is: (a) to obtain data for the carbanion and (b) to compare them with those for the molecule. This comparison will make it possible to determine spectral and structural changes accompanying the conversion of methyl cyanoacetate molecule into carbanion, using both experimental and computational methods.

EXPERIMENTAL

Methyl cyanoacetate (Aldrich, spectroscopic purity grade) was used without any additional purification. Its carbanion was prepared by adding dimethyl sulfoxide (DMSO/ DMSO-d_6) solutions of the parent compound to excess of dry $CD_3O^-Na^+$ under argon, and collecting the clear carbanion solution with a syringe-filter. We prepared the sample of $CD_3O^-Na^+$ itself by reacting CD_3OD (Fluka, 99 at.% enrichment) with Na and evapo-rating the excess of methanol *in vacuo*. The methyl cyanoacetate reacted with $CD_3O^-Na^+$ to form the carbanion in DMSO/DMSO-d_6 promptly (within 1–2 min) and practically completely: no bands of the parent compound were seen in the spectra after metalation. The IR spectra were recorded on a Bruker IFS 113v and Tensor 27 Standard System FTIR spectrophotometers in a CaF_2 cell of 0.129 mm path length, at a resolution of 1 cm^{-1} and 64 scans.

* To whom all correspondence should be sent:
E-mail: ani_popova@orgchm.bas.bg

© 2008 Bulgarian Academy of Sciences, Union of Chemists in Bulgaria

COMPUTATIONS

The *ab initio* force field computations (full optimization) of the studied species were performed using the GAMESS software [11] at the Hartree-Fock HF/6-31++G** level. The GAUSSIAN 98 program package [12] was used for the same procedure within the same basis set, but applying the Density Functional Theory (DFT). This theory was the groundwork of a series of cost-effective methods to approximate electron correlation effects [13]. We applied the B3LYP functional, which combined Becke's three-parameter nonlocal exchange with the correlation functional of Lee, Yang and Parr [14, 15], adopting a 6-31++G** basis set without any symmetry restrictions. For every structure, the stationary points found on the molecular potentional energy supersurfaces (PEHS) were characterized using the standard harmonic vibrational analysis. The absence of any irrational frequencies or negative eigenvalues in the second-derivative matrix confirmed that the stationary points corresponded to global minima on PEHS [13]. The use of 6-31++G** basis sets both in *ab initio* and in DFT computations has recently resulted in better or equally good structural predictions, compared with other basis sets both for molecules and for anions [16–20] (and references therein). No scaling in the ab initio or density functional theory force fields was done. A standard least-squares program was used to calculate the single-parameter linear regression indices.

RESULTS AND DISCUSSION

Conformational and energy analysis

The most stable conformations of the studied species are shown in Fig. 1. In these cases "s-cis" and "s-trans" indicate the co-position of the CN and CO groups. The energies of the studied species can be seen in Table 1. In a qualitative agreement with the results of earlier computations (see Introduction), the molecular conformer **1** is slightly more stable, by 1.10 kJ·mol^{-1}, than **2**. It is known [2, 4] that only the thermodynamically most stable **1** exists in the crystalline state; in the gas and liquid phase the methyl cyanoacetate exists as mixture of the two main conformers of similar energies **1** and **2** [2]. Reva *et al*. [10] have recently found on the basis of IR spectra of methyl cyanoacetate, isolated in low temperature inert gas matrices, that the results of the conformational cooling depend on:

i) the nature of the matrix gas host;
ii) the relative energies ΔE and the corresponding barriers;
iii) the dipole moments of the conformers;
iv) the temperature. For example, an increase in the temperature from 20 to 40 K results in a radical change of the conformational ratio [10].

According to our calculations (Table 1), the carbanion **3** is only by 0.57 kJ·mol^{-1} more stable than **4**. The deprotonation energy of a given Broensted acid can be defined [18, 20] (and references therein) as $E^{D} = E^{corr.}$ (anion) – $E^{corr.}$ (molecule) (for the most stable conformers of these species). Georgieva and Velcheva have recently found that E^{D}'s correlate fairly well with pKa values of Broensted acids, containing cyano or carbonyl groups, in DMSO solvent, according to Eqn. 1 [18]:

$$\text{pKa (DMSO)} = 0.11507\, E^{D}\,(\text{B3LYP/6-31++G}^{**}) - 150.04 \quad (1)$$

Table 1. Total energies E (in hartree) and differences between them ΔE (in kJ·mol^{-1}) of the species studied.

No.	Species	E (native)	E (corrected) [a]	ΔE [a, b]
1	Molecule s-trans 1	–360.642650	–360.553883	0
2	Molecule s-cis 2	–360.642134	–360.553463	1.10
3	Carbanion CH^- s-trans 3 [c]	–360.095170	–360.019854	1402.09
4	Carbanion CH^- s-cis 4 [c]	–360.094768	–360.019637	1402.66
5	Carbanion CH_2^- s-cis 5 [d]	–360.012041	–359.938965	1614.47
6	Carbanion CH_2^- s-trans 6 [d]	–360.011197	–359.938174	1616.54

[a] With corrections for zero-point vibrational energies (ZPVE).
[b] $\Delta E = E_n - E_1$. [c] Deprotonated in the methylene group.
[d] Deprotonated in the methyl group.

So, having in mind $E^{corr.}$ of **1** and **3** in Table 1, we can estimate pKa (DMSO) of methyl cyanoacetate to be near 11.3. Hence, this compound should be a moderately strong carbon acid, like dicyanomethane, 5,5-dimethylcyclohexane-1,3-dione and α-phenylsulfonyl acetophenone, whose pKa (DMSO) are 11.0, 11.2 and 11.4, respectively [21]. It was clear a priori that deprotonation in the methyl group of methyl cyanoacetate should be very disadvantageous. However, the data in Table 1 make it possible to estimate how much compound **5** is less stable than **3**. So, according to our calculations, **5** is by 213.37 kJ·mol^{-1} less stable than **3**, i.e. (having in mind Eqn. 1) the deprotonation of methyl cyanoacetate in the methyl group should correspond to a very weak C–H acid, with pKa (DMSO) equal to 35.7. This hypothetic C–H "acid" should have a pKa by 24.4 units higher (or an acidity by 24.4 orders of magnitude lower) than that of methyl cyanoacetate.

Correlation analysis

Comparison of B3LYP/6-31++G** vibrational frequencies, calculated for the conformer **1** with those measured experimentally in DMSO/DMSO-d_6 solvent gave the following linear correlation (Eqn. 2):

$$\nu_{(exp.)} = 0.92771\nu_{(exp.)} + 72.2 \quad (cm^{-1}) \qquad (2)$$

Correlation coefficient R = 0.99986, Standard deviation S. D. = 13.82 cm^{-1}; Number of data points n = 15.

According to Jaffe's classification [22], this correlation is *excellent*, as 0.99 < R < 1.00. We shall use Eqn. 2 for correlational scaling of the theoretical vibrational frequencies of the species studied in this work. As it was stated in Alcolea's review article [23] (and references therein), use of scaling equations instead of scale factors gave better results, especially in the low-frequency region. Correlational scaling is still used nowadays [3, 17, 20, 24–29] (and references therein).

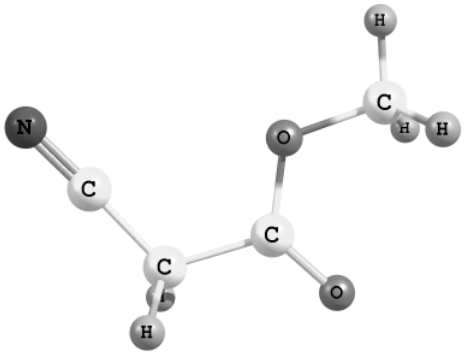

Molecule s-trans **1**

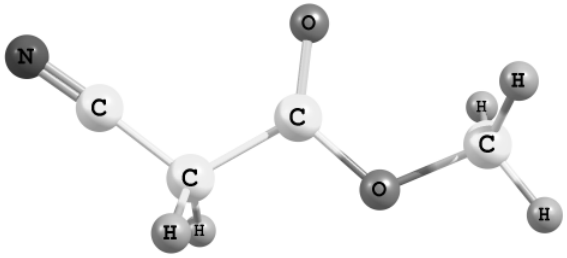

Molecule s-cis **2**

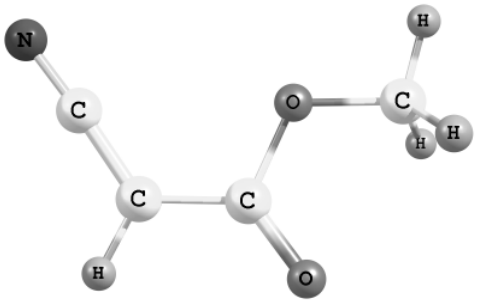

Carbanion CH^- s-trans **3**[a]

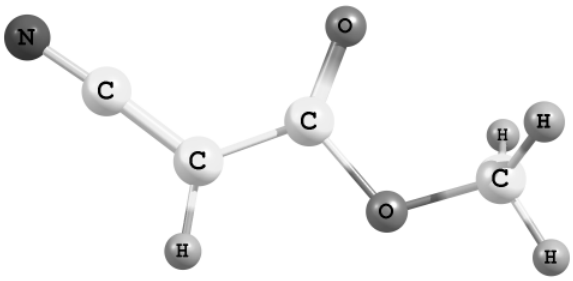

Carbanion-CH^- s-cis **4**[a]

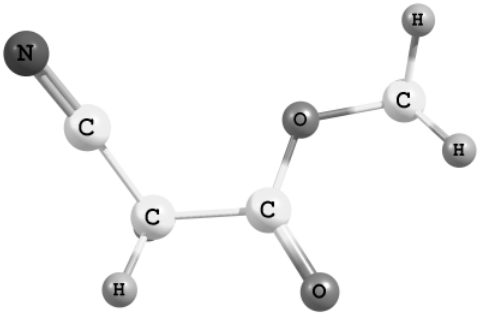

Carbanion CH_2^- s-trans **6**[b]

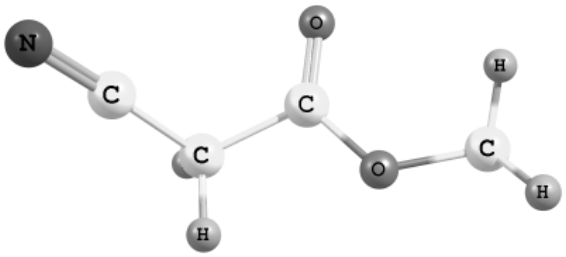

Carbanion CH_2^- s-cis **5**[b]

Fig. 1. DFT/B3LYP 6-31++G** conformers of the molecule and carbanions of methylcyanoacetate. [a] Deprotonated in the methylene group. [b] Deprotonated in the methyl group.

Spectral analysis

Table 2 contains IRS data for the methyl cyanoacetate *molecule*. A good agreement between experimental and scaled theoretical frequencies can be seen there. The mean absolute deviation

$$m.a.d. = n^{-1}\sum_{i=1}^{n}\left|\nu_{theor}^{i} - \nu_{exp}^{i}\right|$$

is 8.7 cm^{-1}, a little bit lower (i.e. better value) than the interval of 9–20 cm^{-1}, typical for the DFT calculations for molecules containing cyano or carbonyl groups [20, 28–31] (and references therein). The approximate description of the vibrations in Table 2 is not far from those of the authors [2, 4]. The cyano stretching band shows no peculiarity: high $\nu_{C\equiv N}$ frequency and low $A_{C\equiv N}$ intensity, as the cyano group is not conjugated. As it can be expected, the stretching vibration of the carbonyl group is represented by a very strong band (see also Fig. 2). The various CH_3 and CH_2 bendings are listed below in Table 2 (Nos, 8–12, 14). A moderate band at 1211 cm^{-1} corresponds to the ν_{COC}^{as} vibration in methyl cyanoacetate molecule. There are cases where this band is comparable in intensity to the $\nu_{C=O}$ one [32].

Table 2. Theoretical (B3LYP 6-31++G (d,p) and experimental (solvent DMSO/DMSO-d_6) IRS frequencies (cm^{-1}) and integrated intensities ($km \cdot mol^{-1}$) of methyl cyanoacetate.

No	B3LYP 6-31++G (d, p)				Experimental data [a]	
	ν	ν [b]	A	Approximate description [c]	ν	A
1	3186	3028	9.7	$\nu_{CH_3}^{as}$	3039[d]	2.0
2	3154	2998	13.9	$\nu_{CH_3}^{as}$	3012[d]	4.0
3	3104	2952	0.4	$\nu_{CH_3}^{as}$	2955	11.4
4	3071	2921	24.9	$\nu_{CH_3}^{s}$	2932[d]	4.8
5	3065	2916	3.5	$\nu_{CH_2}^{s}$	2897	1.8
6	2375	2275	5.6	$\nu_{C\equiv N}$	2256	3.0
7	1825	1766	236.8	$\nu_{C=O}$	1749	151.2
8	1500	1464	11.0	$\delta_{CH_3}^{as}$	– [e]	–
9	1489	1453	9.8	$\delta_{CH_3}^{as}$	1448	vw
10	1475	1441	13.9	$\delta_{CH_3}^{as}$	1439	12.2
11	1446	1413	19.8	$\delta_{CH_2}^{sc}$	1403	7.9
12	1364	1338	103.7	τ_{CH_2}, ν_{CCC}, $\delta_{CH_3}^{s}$	1343	34.2
					1268 [f]	m
13	1226	1209	291.2	ν_{COC}^{as}, $\delta_{CH_2}^{wag}$, $\delta_{CH_3}^{as}$,	1211	55.0
14	1225	1209	3.2	$\delta_{CH_2}^{rock}$	1211	55.0
15	1200	1185	115.6	τ_{CH_3}, ν_{COC}, $\delta_{CH_2}^{wag}$	1183	44.3
16 [g]	1174	1161	0.9	$\delta_{CH_2}^{tw}$	– [e]	–

[a] Measured after having decomposed the complex bands into components; relative intensity: m, moderate; vw, very weak. [b] Scaled, according to correlation equation 2. [c] Vibrational modes: υ, stretching; δ, in-plane bending; τ, torsion. Superscripts: s, symmetrical; as, asymmetrical; sc, scissoring; rock, rocking; wag, wagging; tw, twisting. [d] Solvent $CDCl_3$. [e] We did not detect this band. [f] The origin of this band is not clear. [g] Followed by 14 lower-frequency vibrations.

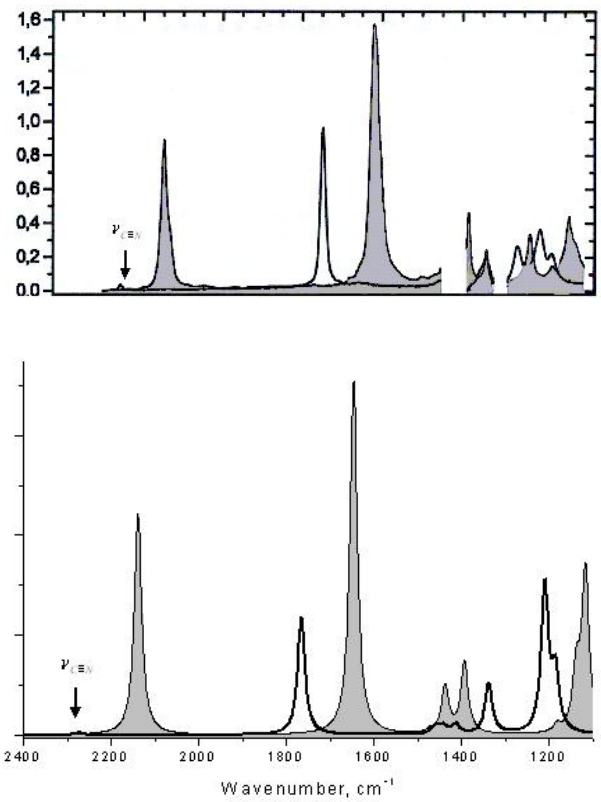

Fig. 2. Theoretical (bottom) and experimental (top) IR spectra of methyl cyanoacetate and its carbanion (solvent DMSO, counter ion Na^+, shaded).

We can see in Table 3 IRS data for the carbanion of methyl cyanoacetate. Like in the previous case, the agreement between experimental and scaled theoretical IRS frequencies is good. The main absolute deviation between them is only 8.1 cm^{-1}, lower than the corresponding interval of 9–25 cm^{-1}, typical for DFT calculations of frequencies for anions containing cyano or carbonyl groups [20, 28–31] (and references therein).

In agreement between theory and experiment, the conversion of methyl cyanoacetate into carbanion results in the following IR spectral changes (cf. Tables 2, 3 and Fig. 2).

- Strong decrease in $\nu_{C\equiv N}$: predicted 136 cm^{-1}, measured 109 cm^{-1}.
- Dramatic intensification of the corresponding IR band: calculated 79.0 fold measured 51.3 fold.
- Strong decrease in the $\nu_{C=O}$ frequency: predicted 119 cm^{-1}, measured 127 cm^{-1}.
- Increase in the intensity of the corresponding IR band: predicted 3.0 fold, measured 2.0 fold.
- Decrease in the ν^{as}_{COC} frequency: calculated 91 cm^{-1}, measured 56 cm^{-1}, as well as other IR spectral variations.

STRUCTURAL ANALYSIS

We did not found in the literature any experimental data on the *steric structure* of either methyl cyanoacetate or its carbanion. According to our calculations the conversion of the molecule into carbanion causes essential steric structure variations (Table 4), which take place *at* the carbanionic center and *next to* it. This rule is also valid for bond angles (Table 4).

Table 4. Selected B3LYP/6-31++G (d,p) bond lengths R (Å), bond angles A (degrees) and dihedral angles D (degrees) of methyl cyanoacetate and its carbanion.

Indices [a]	Molecule	Carbanion	Δ [b]
R (1,2)	1.16	1.18	0.02
R (2,3)	1.46	1.40	–0.06
R (3,4)	1.53	1.41	–0.12
R (4,5)	1.21	1.24	0.03
R (4,6)	1.35	1.42	0.07
R (6,7)	1.45	1.42	–0.03
A (1,2,3)	177.6	177.0	–0.6
A (2,3,4)	113.6	123.1	9.5
A (3,4,5)	126.0	130.7	4.7
A (5,4,6)	125.0	118.6	–6.4
A (4,6,7)	115.8	114.7	–1.1
D 3 (2,4,8)	121.8	180.0	58.2
D 4 (3,5,6)	180.0	180.0	0
D 4 (5,6,7)	0.0	–0.1	–0.1

[a] Atom numbering according to Scheme 1.
[b] Δ = Index (anion) – Index (molecule) (Å or degrees).

For example, $|\Delta R(C–CO)|$ is twice larger than $|\Delta R(C–CN)|$ $|\Delta R(C=O)|$, is also larger than $|\Delta R(C\equiv N)|$, so it seems that the carbonyl group is more strongly conjugated with the carbanionic center than the cyano group. The largest bond angle deviation ΔA corresponds to C3, to indicate the transformation of the tetrahedral CH2 group of the molecule into a trigonal –CH group in the carbanion. The analysis of the dihedral angle changes shows that except for the methyl group hydrogen atoms, the whole carbanion is planar (Table 4, cf. Scheme 1).

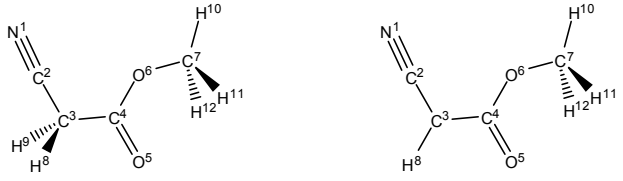

1 **3**

Scheme 1. Atom numbering of methyl cyanoacetate molecule **1** and its carbanion **3** within our both HF/and B3LYP/ 6-31++G** calculations.

Table 3. Theoretical (B3LYP++G(d,p)) and experimental (solvent DMSO/DMSO–d_6, counter ion Na^+) IRS frequencies (υ in cm^{-1}) and integrated intensities (A in $km \cdot mol^{-1}$) of methyl cyanoacetate carbanion.

No.	B3LYP++G(d,p)				Experimental data [a]	
	ν	ν [b]	A	Approximate description [c]	ν	A
1	3203	3043	8.5	ν_{CH^-}	– [d]	–
2	3093	2942	57.7	$\nu^{as}_{CH_3}$	2945	vw
3	3065	2916	66.8	$\nu^{as}_{CH_3}$	2907	vw
4	3010	2865	120.8	$\nu^{s}_{CH_3}$	2840	vw
5	2228	2139	442.6	$\nu_{C\equiv N}$	2147	153.8
6	1698	1647	706.8	$\nu_{C=O}$	1622	299.1
7	1509	1472	6.5	$\nu^{as}_{CH_3}$	1469	6.2
8	1472	1438	89.7	$\delta^{s}_{CH_3}$	1440	m
9	1472	1438	3.93	$\delta^{as}_{CH_3}$	1440	m
10	1425	1394	143.7	$\delta^{s}_{CH_3}$, δ_{CH^-}	1389	24.2
					1239[e]	w
11	1197	1183	14.9	τ_{CH_3} , δ_{CH^-} , ν_{COC}	1185	4.1
12	1169	1157	0.3	τ_{CH_3}	– [d]	-
13	1149	1139	117.7	τ_{CH_3} , ν_{COC} , δ_{CH^-}	1135	47.8
14 [f]	1127	1118	322.9	ν^{as}_{COC} , δ_{CH^-} , τ_{CH_3} , ν_{CCC} ,	1127	30.7

[a] Measured after having decomposed the complex bands into components; relative intensity: m, moderate; vw, very weak. [b] Scaled, according to correlation equation 2 (Table 2). [c] Vibrational modes: ν, stretching; δ, in-plane bending; τ, torsion. Superscripts: s, symmetrical; as, asymmetrical. [d] These bands were not detected in the experimental spectrum. [e] The origin of this band is not clear. [f] Followed by 13 lower-frequency vibrations.

We shall demonstrate the changes in the *electronic structure* of methyl cyanoacetate molecule, caused by its conversion into carbanion, on the basis of data on bond orders and net electric charges. The bond order variations (Table 5) are in agreement with the corresponding bond length changes (shorter bonds → higher bond orders, cf. Table 4). The largest (in absolute values) bond order changes (Table 5, values in bold) take place again at and next to the carbanionic center. The changes $|\Delta P(3,4)|$ and $|\Delta P(4,5)|$ are larger than $|\Delta P(2,3)|$ and $|\Delta P(1,2)|$, respectively. So, we can say as above that according to the computations, the carbonyl group is conjugated with the carbanionic center more strongly than the cyano one.

The net electric charges q_i of fragments of the molecule and carbanion of methyl cyanoacetate are shown in Scheme 2. The electric charge changes $\Delta q_i = q_i(\text{anion}) - q_i(\text{molecule})$ are usually quite informative to demonstrate the distribution of the new charge (carbanionic, azanionic, etc.) between individual fragments of anions [19, 33] (and references therein). According to the calculations (cf. Scheme 2), the anionic charge in the studied carbanion is distributed, as follows: 0.22, 0.26 and 0.13 e^- are delocalized over the cyano, carbonyl and methoxy groups, respectively, and 0.39 e^- of it remain localized in the carbanionic center. Δq(C=O) is larger than Δq(C≡N) i. e. the carbonyl group seems again to be better conjugated with the carbanionic center than the cyano one.

Table 5. *Ab initio* HF 6-31++G(d,p) bond orders *P* of methyl cyanoacetate molecule and carbanion.

Bonds [a]	Molecule	Carbanion	ΔP [b]
$C^1{\equiv}N^2$	2.89	2.82	–0.07
C^3–H^8	0.94	0.96	0.02
C^3–H^9	0.94	- [c]	– [c]
O^6–C^7	0.77	0.87	0.1
C^2–C^3	0.91	1.13	0.22
C^4–O^6	0.99	0.82	–0.17
C^3–C^4	0.95	1.34	0.39
$C^4{=}O^5$	1.84	1.62	–0.22
C^7–H^{10}	0.97	0.98	0.01
C^7–H^{11}	0.96	0.97	0.01
C^7–H^{12}	0.96	0.97	0.01

[a] Atom numbering according to Scheme 2. [b] $\Delta P = P_{\text{anion}} - P_{\text{molecule}}$. The largest $|\Delta P|$ values are given in bold. [c] There is no C^3–H^9 bond in the carbanion.

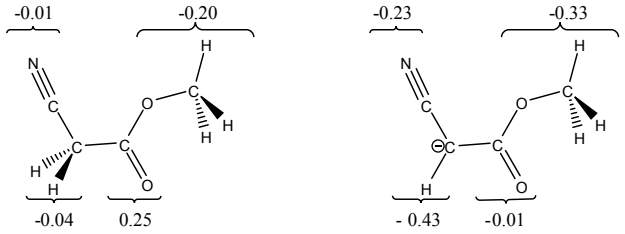

1 **3**

Scheme 2. Natural Bond Orbital (NBO) net electric charges q_i over fragments of the most stable conformers of methyl cyanoacetate molecule **1** and carbanion **3**.

CONCLUSIONS

We found in this work a good agreement between experimental and B3LYP/6–31++G** data on the essential spectral changes, caused by the conversion of methyl cyanoacetate into the carbanion. So, we anticipate that the structural variations, computed by same method, should also be adequate.

***Acknowledgements**: The financial support by the Bulgarian Fund of Scientific Research for Project Chem. – 1510 is gratefully acknowledged.*

REFERENCES

1. I. G. Farbenindustrie, D. D. R., 640509 (1934).
2. J. M. F. Neta, R. Fausto, *J. Mol. Struct*., **443**, 41 (1998).
3. I. D. Reva, S. V. Ilieva, R. Fausto, *Phys. Chem. Chem. Phys*., **3**, 4235 (2001).
4. S. W Charles, G. I. L. Jones, N. L. Owen, *J. Chem. Soc. Faradey Trans. II*, **69**, 1454 (1973).
5. D. Sinha, J. E. Katon, *Can. J. Chem*., **52**, 3057 (1974).
6. R. G. Makitra, T. A. Protsaylo, I. E. Boldeskul, Z. Z. Rozhkova, *Zh. Prikl. Spektrosk*., **37**, 784 (1982).
7. R. Prasad, Y. K. Mishra, R. K. Gupta, *Indian J. Chem*, **29A**, 618 (1990).
8. C. Maury, J. Petrissans, *J. Mol. Struct*., **246**, 267 (1991).
9. S. J. Leibowitz, J. Laane, C. Van Alenoy, B. J. Van der Veken, *J. Mol. Struct*., **248**, 251 (1991).
10. I. D. Reva, S. G. Stepanian, L. Adamowicz, R. Fausto, *Chem. Phys. Lett*., **374**, 631 (2003).
11. M. W. Schmidt, K. K. Baldridge, J. A. Boatz, S. T. Elbert, M. S. Gordon, J. H. Jensen, S. Koseki, N. Matsunaga, K. A. Nguyen, S. J. Su, T. L. Windus, M. Dupuis, J.A. Montgomery, *J. Comput. Chem*., **14**, 1347 (1993).
12. M. J. Frisch, G. W. Trucks, H. B. Schlegel, G. E. Scuseria, M. A. Robb, J. R. Cheeseman, V. G. Zakrzewski, J. A. Montgomery, Jr., R. E. Stratmann, J. C. Burant, S. Dapprich, J. M. Millam, A. D. Daniels, K. N. Kudin, M. C. Strain, O. Farkas, J. Tomasi, V. Barone, M. Cossi, R. Cammi, B. Mennucci, C. Pomelli, C. Adamo, S. Clifford, J. Ochterski, G. A. Petersson, P. Y. Ayala, Q. Cui, K. Morokuma, D. K. Malick, A. D. Rabuck, K. Raghavachari, J. B. Foresman, J. Cioslowski, J. V. Ortiz, A. G. Baboul, B. B. Stefanov, G. Liu, A. Liashenko, P. Piskorz, I. Komaromi, R. Gomperts, R. L. Martin, D. J. Fox, T. Keith, M. A. Al-Laham, C. Y. Peng, A. Nanayakkara, C. Gonzalez, M. Challacombe, P. M. W. Gill, B. Johnson, W. Chen, M. W. Wong, J. L. Andres, M. Head-Gordon, E. S. Replogle, J. A. Pople, *Gaussian 98*, Revision A.7, Gaussian, Inc., Pittsburgh PA, 1998.
13. T. M. Kolev, E. A. Velcheva, B. A. Stamboliyska, *Int. J. Quant. Chem*., **102**, 1069 (2005).
14. A. D. Becke, *J. Chem. Phys*. **98**, 5648 (1993).
15. C. Lee, W. Yang, G. R. Parr, *Phys. Rev. B*, **37**, 1316(2006).
16. M. K. Georgieva, O. I. Petrov, K. V. Petrova, A. D. Popova, E. A. Velcheva, *C. R. Acad. Bulg. Sci*., **58**, 561 (2005).
17. E. A. Velcheva, G. I. Nikolova, O. I. Petrov, *Bulg. Chem. Commun*., **38**, 263 (2006).
18. M. K. Georgieva, E. A. Velcheva, *Int. J. Quant. Chem*., **106**, 1316 (2006).
19. A. D. Popova, M. K. Georgieva, O. I. Petrov, K. V. Petrova, E. A. Velcheva, *Int. J. Quant. Chem*., **107**, 1752 (2007).
20. L. I. Daskalova, *J. Mol. Struct. (THEOCHEM)*, **848**, 9 (2008)
21. F. G. Bordwell, *Acc. Chem. Res*., **21**, 456 (1988).
22. H. H. Jaffe, *Chem. Rev*., **53**, 191 (1953).
23. M. Alcolea Palafox, *Resent Res. Develop. Phys. Chem*., **2**, 213 (1998).
24. M. K. Georgieva, *Bulg. Chem. Commun*., **32**, 195 (2003).
25. O. Sala, N. S. Gonsalves, L. K. Nada, *J. Mol. Struct*., **565–566**, 411 (2001).
26. M. Alcolea Palafox, V. K. Rastogi, L. Mittal, *Int. J. Quant. Chem*., **94**, 198 (2003).
27. M. K. Georgieva*, J. Mol. Struct*., **691**, 71 (2004).
28. M. K. Georgieva, P. J. Vassileva-Boyadjieva, P. N. Angelova, *Bulg. Chem. Commun*., **37**, 366 (2005).
29. L. I. Daskalova, E. A. Velcheva, I. G. Binev*, J. Mol. Struct*., **826,** 198 (2007).
30. M. K. Georgieva, N. B. Nedelchev, I. N. Juchnovski, *Bulg. Chem. Commun*., **37,** 235 (2005).
31. P. J. Vassileva-Boyadjieva, E. A. Velcheva, Y. I. Binev, *Bulg. Chem. Commun*., **37**, 313 (2005).
32. G. N. Andreev, Molecular spectroscopy, Plovdiv University Press, 1999 (in Bulgarian).
33. E. A. Velcheva, B. A. Stamboliyska, *J. Mol. Struct*., (2007) in press.

ЕКСПЕРИМЕНТАЛНИ ИЧ И ТЕОРЕТИЧНИ *AB INITIO* ХФ И ТФП B3LYP ИЗСЛЕДВАНИЯ НА СПЕКТРАЛНИТЕ И СТРУКТУРНИТЕ ПРОМЕНИ, ПРИЧИНЕНИ ОТ ПРЕВРЪЩАНЕТО НА МЕТИЛЦИАНОАЦЕТАТА В КАРБАНИОН

Ан. Д. Попова[1,*], Юр. Ив. Бинев[2], П. Ж. Василева-Бояджиева[1], Ив. Г. Бинев[1]

[1] *Институт по органична химия с център по фитохимия, Българска академия на науките, ул. „Акад. Г. Бончев“, бл. 9, 1113 София*
[2] *Институт по тропически изследвания, ул. „Жункейро“ № 86-1, 1300-344 Лисабон, Португалия*

Посветена на акад. Иван Юхновски по повод на 70-та му годишнина

Постъпила на 24 януари 2008 г., Преработена на 27 март 2008 г.

(Резюме)

Спектралните и структурни промени, причинени от превръщането на метилцианоацетата в карбанион са изследвани с помощта на комбиниран ИЧ експериментален/*ab initio*, ТФП теоретичен подход. Установено е добро съответствие между експерименталните и скалираните B3LYP/6–31++G** вибрационни честоти; връзката между съответните интензивности на ИЧС ивици е само качествена. В съгласие между теория и експеримент, превръщането на метилцианоацетата в карбанион води до силно понижение на честотите на валентните трептения на циано- и на карбонилната групи (със 109 и 127 cm^{-1}, съответно), драстично повишение на интегралната интензивност (51.3 пъти) на вибрационната ивица на цианогрупата и други съществени промени в ИЧС спектър. В съгласие с изчислената пространствена и електронна структура, карбонилната група е спрегната по-здраво с карбанионния център в сравнение с цианогрупата. С изключение на водородните атоми на метиловата група, целият карбанион е планарен.

Bulgarian Chemical Communications, Volume 40, Number 4 (pp. 520–525) 2008

IR spectral and structural changes, caused by the conversion of 4-cyanobenzamide into azanion: a combined experimental/computational approach

J. A. Tsenov*, S. S. Stoyanov, I. G. Binev

Department of Structural Organic Analysis, Institute of Organic Chemistry with Centre of Phytochemistry, Bulgarian Academy of Sciences, Acad. G Bonchev St., Block 9, 1113 Sofia, Bulgaria

Dedicated to Academician Ivan Juchnovski on the occasion of his 70th birthday

Received January 25, 2008; Revised March 20, 2008

A combined IR experimental/DFT computational approach has been applied to follow the spectral and structural changes, caused by the conversion of 4-cyanobenzamide into azanion. The conversion has shown a weak effect on the cyano stretching band ν(C≡N) and strong effects on both amide ν(C=O) and ν(C–N) stretching bands. According to the computations, the two latter vibrational modes are strongly delocalized in the azanion and participate essentially in a few vibrations each. Again according to the computations, the strong structural changes, caused by the conversion, take place *at* and *next to* the azanionic center; the non-planar 4-cyanobenzamide molecule turns into a planar azanion.

Key words: IR spectra, *ab initio* HF; DFT B3LYP, structure, 4-cyanobenzamide, azanion.

INTRODUCTION

4-cyanobenzamide **1** in Scheme 1 was first prepared by partial hydrolysis of 1,4-dicyanobenzene in 1912 [1]. This compound is mentioned nowadays mainly in relation with *Thetrahymena Pyriformis* [2, 3].

Ten years ago Ognianova *at al*. reported about a 76–180 cm^{-1} interval of decrease in the carbonyl stretching frequencies $\nu_{C=O}$ of 23 amides, accompanying their conversion into azanions (4-cyanobenzamide was not studied) [4]. It is known on the other hand that conversion of nitriles into anions results in very essential decrease in the cyano stretching frequency $\nu_{C\equiv N}$ and strong, in certain cases dramatic increase in the integrated intensity $A_{C\equiv N}$ of the corresponding IR bands [5–7] (and references therein). This rule is valid for anions where the cyano group is in resonance with the anionic center, even in cases they are quite distant. In the azanions (**2, 3** in Scheme 1) of 4-cyanobenzamide, the cyano group and the azanionic center are distant and there is no formal resonance between them. So, the molecule/azanion pair of 4-cyanobenzamide is an interesting example of weakly interacting cyano group and anionic center, i.e. with a presumed weak effect of the molecule → azanion conversion on the C≡N group spectral and structural characteristics. Another indication to this presumption is the low (absolute) value of –0.23 for the σ^+ constant of the $CONH^-$ group.

EXPERIMENTAL

We prepared 4-cyanobenzamide from 4-cyanobenzoic acid *via* 4-cyanobenzoyl chloride:

$$4\text{-}NC(C_6H_4)COOH \xrightarrow[-SO_2,\ -HCl]{SOCl_2} 4\text{-}NC(C_6H_4)COCl$$

$$4\text{-}NC(C_6H_4)COCl \xrightarrow[-HCl]{NH_3.aq.} 4\text{-}NC(C_6H_4)CONH_2$$

The first reaction was carried out (60 min at 80ºC) in the presence of catalytic amounts of N,N-dimethylformamide, then the excess of $SOCl_2$ was evaporated *in vacuo*. The second reaction was accomplished by cold ammonia (20% by weight water solution) under cooling. The white residue of 4-cyanobenzamide was washed with 1% (by weight) cold aqueous NaOH solution and with cold water, then recrystallized from water in the presence of a few drops of ammonia. M.p. 225–226ºC; lit. m.p. 225–228ºC [9].

4-Cyanobenzamide azanion was prepared by adding dimethyl sulfoxide (DMSO/DMSO-d_6) solution of the parent compound to excess of dry $CD_3O^-Na^+$ under argon, stirring and collecting the clear azanion solution with a syringe-filter. We prepared the sample of dry $CD_3O^-Na^+$ itself by reacting CD_3OD (Fluka 99% at enrichment) with Na and evaporating the excess of methanol *in vacuo*. 4-Cyanobenzamide reacted with $CD_3O^-Na^+$ to form azanion in DMSO/DMSO-d_6 promptly (within 3–4 min) and practically completely: no bands of the parent compound were shown in the spectra after

* To whom all correspondence should be sent:
E-mail: soa@orgchm.bas.bg

© 2008 Bulgarian Academy of Sciences, Union of Chemists in Bulgaria

metalation. The IR spectra were recorded on a Bruker IFS113v and Tensor 27 FTIR spectrometers in a CaF_2 cell of 0.129 mm path length, at a resolution of 1 cm^{-1} and 64 scans.

COMPUTATIONS

The *ab initio* force field computations (full optimization) of the species studied were performed using the GAMESS software [10] at the Hartree-Fock HF/6-31++G** level. The GAUSSIAN 98 program package [11] was used for the same procedure within the same basis set, but applying the Density Functional Theory (DFT). This theory was the groundwork of a series of cost-effective methods to approximate electron correlation effects [12]. We applied the B3LYP functional which combined the Becke's three-parameter non-local exchange with the correlation functional of Lee, Yang and Parr [13, 14], adopting a 6-31++G** basis set without any symmetry restrictions. For every structure, the stationary points found on the molecular potentional energy surfaces (PEHS) were characterized using the standard harmonic vibrational analysis. The absence of irrational frequencies or negative eigenvalues in the second derivative matrix confirmed that the stationary points corresponded to global minima on PEHS [13]. The use of 6–31++G** basis sets in both *ab initio* and DFT computations has recently resulted in better or equally good structural predictions, compared to other basis sets for both molecules and anions [7, 15, 16] (and references therein). No scaling in the *ab initio* or density functional theory force fields was done. A standard least-squares program was used to calculate the single-parameter linear regression indices.

RESULTS AND DISSCUSSION

Energy analysis

The molecule of 4-cyanobenzamide can exist as one conformation **1** only; two conformations are in principle possible for its azanion, **2** and **3** (Fig. 1, Scheme 1). The energies of the species studied are compared in Table 1. It is seen there that the energy difference between the two anionic conformers of 31.01 $kJ \cdot mol^{-1}$ is quite essential, so we can *a priori* assume that the isolated conformer **2** should be strongly predominant over **3.**

Table 1. B3LYP/6-31++G** zero-point vibrational energy (ZPVE) corrected total energies ($E^{corr.}$ in hartree) of the 4-cyanobenzamide molecule **1** and of its azanions **2** and **3**, as well as their differences (ΔE in $kJ \cdot mol^{-1}$).

Species	Conformers [a]	$E^{corr.}$	ΔE [b]
molecule	**1**	–493.102417	0.00
azanion	**2**	–492.558760	1427.37
azanion	**3**	–492.546949	1458.38

a See in Scheme 1; b - $\Delta E = E_n - E_1$.

The deprotonation energy of a given Broensted acid can be defined [7, 16] (and references therein) as $E^D = E^{corr.}(\text{anion}) - E^{corr.}(\text{molecule})$ (for the most stable comformers of these species). Georgieva and Velcheva have recently found that E^D's correlate fairly well with pKa's of Broensted acids, containing cyano or carbonyl groups, in DMSO solvent, according to Eqn. 1 [7].

$$\text{pKa(DMSO)} = 0.11507E^D(\text{B3LYP/6-31++G**}) - 150.04 \quad (1)$$

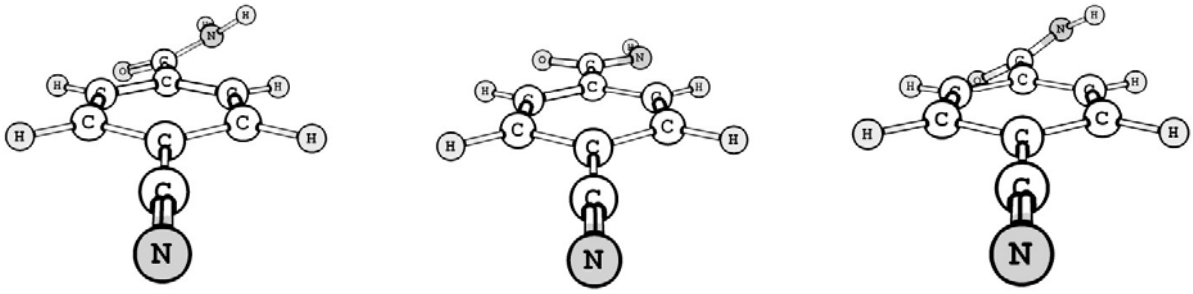

1 **2** **3**

Fig. 1. B3LYP/6-31++G** optimized structures of the studied species.

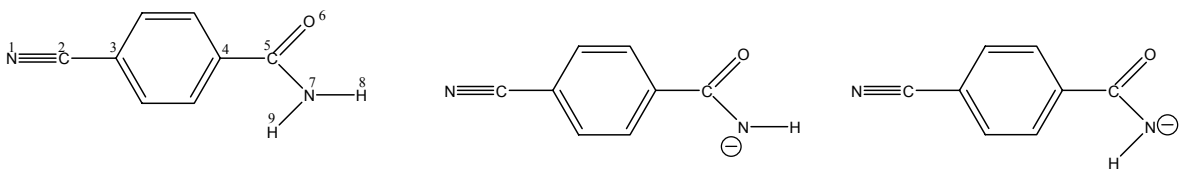

1 **2** **3**

Scheme 1. Possible conformers of the molecule (**1**) and azanion (**2, 3**) of 4-cyanobenzamide.

So, having in mind $E^{corr.}$ of **1** and **2** in Table 1, we can estimate pKa (DMSO) of 4-cyanobenzamide near 14.2. Hence, 4-cyanobenzamide should be a moderately weak N–H acid, like e.g. 1,2,3-triazole, uracil or succinimide; their pKa's (DMSO) are 13.9, 14.1 and 14.6, respectively [17].

Correlation analysis

We compared B3LYP/6-31++G** vibrational frequencies for the parent molecule **1** with those measured experimentally in DMSO/DMSO-d_6 solvent. Thus, we obtained the following linear correlation (Eqn. 2):

$$\nu(\text{exp.}) = 0.92757\nu(\text{theor.}) + 74.7\ (\text{cm}{-}1) \quad (2)$$

Correlation coefficient R = 0.99968; Standard deviation S. D. = 23.4 cm^{-1}; Number of data points n = 12.

According to the Jaffe's classification [18], this correlation is *excellent*, with $0.99 < R < 1.00$. Eqn. 2 can be used for correlational scaling of theoretical vibrational frequencies of species studied in this work. It is known [19] (and references therein) that use of scaling equations instead of scale factors gives better results, especially in the low-frequency region. Correlational scaling is still used nowadays [15, 16, 20–24] (and references therein).

We tested Eqn. 2 in the following way:

i) We scalled the B3LYP/6-31++G** frequencies of the anionic conformers **2** and **3**, and compared them with the experimental frequentcies of the azanion, measured in DMSO/DMSO-d_6.

ii) We calculated the mean absolute deviations, m.a.d. = $n \sum_{i=1}^{n} | \nu^{i}_{theor.} - \nu^{i}_{\boldsymbol{exp.}} |$ and obtained values of 9.6 and 11.8 cm^{-1} for **2** and **3**, respectively. Thus, we can say that, like the isolated azanion (Table 1), the DMSO solvated **2** predominates over the DMSO solvated **3**.

Spectral analysis

Theoretical and experimental IR data for 4-cyanobenzamide molecule (**1** in Scheme 1) are compared in Table 2. We can see there a good agreement between experimental and scaled theoretical frequencies. M.a.d. between them is 17.8 cm^{-1}, which value lies within the interval of 9–20 cm^{-1}, typical for the DFT calculations for molecules containing cyano or carbonyl groups [5, 16, 24–27] (and references therein). We preferred to include in Table 2 the frequencies $\nu^{as}(NH_2)$, $\nu^{s}(NH_2)$ and $\delta^{sciss}(NH_2)$, measured in $CDCl_3$, as the stretching frequencies of $–XH_n$ groups (X = O, N at al.), measured in DMSO, are strongly underestimated, and the bending ones are moderately overestimated [28], obviously due to strong $–XH_n$ - - - $O=S(CH_3)_2$ hydrogen bonds, which effects can be estimated only qualitatively within the Onzeger's approach [29]. There are no peculiarities of the cyano stretching band: moderately high frequency ν(C≡N) and intensity A(C≡N), as the cyano and phenylene groups are in resonance. As it can be expected [28] the carbonyl stretching band ν(C=O) is very strong, the strongest one in the spectrum. A strong band corresponds to the ν(C−N) vibration (No 14 in Table 2). Its frequency of 1385 cm^{-1} is very close to ν(C−N) of pyridine-3-carboxamide, 1381 cm^{-1} (solvent DMSO-d_6) [26].

We compare in Table 3 theoretical and experimental IR data for the *azanion* of 4-cyanobenzamide (**2** in Scheme 1). The agreement between experimental and scaled theoretical frequencies is essentially better than above. M.a.d. between them is 9.6 cm^{-1} only, close to the lower limit of the corresponding integral of 9–25 cm^{-1}, typical for DFT calculations of vibrational frequencies for anions containing cyano or carbonyl groups [5, 16, 24–27] (and references therein). The following spectral changes take place as a result of the conversion of 4-cyanobenzamide into azanion:

iii) The computational method used predicts only qualitatively the changes in the cyano stretching band characteristics, *viz.*: ν(C≡N) decrease, predicted 33 cm^{-1}, measured 5 cm^{-1} only; A(C≡N) increase, predicted 7.1 fold, measured 1.7 fold only.

iv) According to the computations, the ν(C=O) vibrational mode in the azanion is delocalized, taking essential parts in vibrations Nos. 7–9 in Table 3. If we take into account the average frequency values of $\nu(C=O)^{teor.}$ = 1569 cm^{-1} and $\nu(C=O)^{exp.}$ = 1572 cm^{-1} we could estimate ν(C=O) decrease of: predicted 135 cm^{-1}, measured 114 cm^{-1}. Further, if we assume the total integrated intensities of the corresponding IR bands $\sum_{i=1}^{3}{}^{theor.} A_i(C=O)$ = 538.8 and $\sum_{i=1}^{3}{}^{exp.} A_i(C=O)$ = 188.7 $km \cdot mol^{-1}$ as a measure of the azanionic A(C=O), we should estimate the A(C=O) increase as: predicted 1.6 fold, measured 1.8 fold. For comparison we calculated as above the changes in the ν(C=O) IR band, accompanying the molecule → azanion conversion in the case of pyridine-3-carboxamide (data from ref. 26). We obtained in this manner ν(C=O) decrease: calculated 132 cm^{-1}, measured 122 cm^{-1} and A(C=O) increase: calculated 1.4 fold, measured 1.4 fold.

v) The ν(C–N) mode is strongly delocalized in the azanion: it participates to vibrations Nos. 8, 9, 16 and 17 (Table 3).

vi) Again, according to the calculations, some statement is valid for the new δ(CNH⁻) mode: it takes essential parts in vibrations Nos. 12, 16, 17 and 18 (Table 3).

Table 2. Theoretical (B3LYP/6-31++G**) and experimental (DMSO/DMSO-d_6) frequencies (ν in cm^{-1}) and integrated intensities (*A* in $km \cdot mol^{-1}$) of 4-cyanobenzamide molecule.

No	B3LYP/6-31++G**				Experimental data [a]	
	ν	ν [b]	A	Approximate description [c]	ν	*A*
1	3728	3533	43.3	$\nu^{as}(NH_2)$	3528 [d]	m
2	3594	3408	54.4	$\nu^{s}(NH_2)$	3413 [d]	m
3	3228	3069	1.5	ν(PhH)	3095	8.1
4	3218	3060	2.1	ν(PhH)	3081	5.1
5	3212	3054	1.0	ν(PhH)	[e]	-
6	3197	3040	4.7	ν(PhH)	3001	vw
7	2337	2242	32.4	ν(C≡N)	2230	13.4
8	1756	1704	340.5	$\nu(C{=}O) + \delta^{sciss}(NH_2)$	1686	106.3
9	1657	1612	5.6	ν(Ph) + δ(Ph) + δ(Ph−H)	[e]	-
10	1625	1582	158.8	$\delta^{sc}(NH_2)$	1602[d]	m
11	1601	1560	5.8	ν(Ph) + δ(Ph) + ν(Ph−H)	1561	5.7
12	1540	1503	0.7	δ(PhH) + ν(Ph−CO) + ν(Ph−CN)	[e]	-
13	1437	1408	15.1	δ(PhH) + δ(Ph)	1407	0.81
14	1370	1345	253.4	ν(C−N) + ν(Ph−CO) + ν(Ph−CN)	1385	76.3
15	1339	1317	29.0	δ(PhH) + δ(Ph)	1291	7.6
16	1332	1310	4.8	δ(PhH) + δ(Ph)	[e]	-
17	1223	1209	1.4	δ(PhH) + ν(Ph−CN)	[e]	-
18	1206	1193	1.7	δ(PhH)	[e]	-
19	1141	1133	8.6	δ(PhH) + $\delta(NH_2)$	[e]	-
20 [f]	1138	1130	0.6	δ(PhH) + ν(CO)	[e]	-

a - Measured after having decomposed the complex bands into components. Relative intensities: m, moderate: w, weak: v, very; b - Scaled, according to correlation Eqn. (1); c - Vibrational modes: ν, stretching; δ, in-plane bendings: superscripts: s, symmetrical; as, asymmetrical; sc, scissoring; d - Solvent $CDCl_3$; e - These bands, expected as weak ones, were not detected in the experimental spectrum; f - Followed by 25 lower-frequency vibrations.

Table 3. Theoretical (B3LYP/6-31++G**) and experimental (DMSO/DMSO-d_6, counter ion Na^+) frequencies (ν in cm^{-1}) and integrated intensities (*A* in $km \cdot mol^{-1}$) of 4-cyanobenzamide azanion.

№	B3LYP/6-31++G**				Experimental data [a]	
	ν	N [b]	A	Approximate description [c]	ν	*A*
1	3447	3272	24.0	$\nu^{s}(NH^-)$	[e]	-
2	3219	3060	5.2	ν(PhH)	3084	vw
3	3210	3052	7.8	ν(PhH)	[e]	-
4	3183	3027	12.9	ν(PhH)	3050	0.4
5	3182	3026	15.9	ν(PhH)	3039	5.2
6	2301	2209	227.4	ν(C≡N)	2225	22.4
7	1634	1590	87.0	ν(Ph) + δ(PhH) + ν(C=O)	1602	3.3
8	1623	1580	323.3	ν(C=O) + δ(PhH) + ν(C–N)	1581	77.5
9	1576	1537	128.5	ν(Ph) + ν(C=O) + ν(C–N)	1533	107.9
10	1518	1483	8.5	δ(PhH) + ν(Ph) +ν(Ph–CO)	1497	10.5
11	1429	1400	0.6	δ(PhH) + ν(Ph) + ν(Ph–CN)	1400	16.7
12	1389	1363	94.2	δ(CNH⁻) + ν(Ph–CO) + δ(OCN)	1358	42.5
13 [d]	1343	1321	10.2	ν(Ph)	[e]	–
14	1310	1290	0.7	δ(PhH)	1291	1.0
15	1211	1198	18.3	ν(Ph–CN) + ν(Ph) + δ(PhH)	1206	vw
16	1197	1185	44.8	δ(CNH⁻) + δ(PhH) + ν(C–N)	1180	vw
17	1180	1169	41.3	δ(PhH) + δ(CNH⁻) + ν(C–N)	[e]	-
18	1127	1120	1.2	ν(Ph–CO)+ δ(PhH) + δ(CNH⁻)	1128	41.0
19 [e]	1107	1102	8.9	δ(PhH) + ν(Ph)	[e]	–

a - Measured after having decomposed the complex bands into components. Relative intensities: w, weak: v, very; b - Scaled, according to correlation Eqn. (1); c - Vibrational modes: ν, stretching; δ, in-plane bendings: superscripts: s, symmetrical; as, asymmetrical; sc, scissoring; d - These bands, expected as weak ones, were not detected in the experimental spectrum; e - Followed by 23 lower-frequency vibrations.

Structural analysis

There are no experimental data on the *steric structure* of either 4-cyanobenzamide or its azanion in literature. According to our computations, the conversion of the molecule into azanion causes certain essential steric structure variations (Table 4). It is seen in Table 4 that the largest R changes are the shortening of R(5, 6) with 0.044 Å lenghting of R(5, 7) with 0.048 Å. The A changes correspond to A(6, 5, 7) (8.2º) and A(5, 7, 8) (–9.8º). So, the largest changes both in bond lengths and bond angles take place *at* and *next to* the anionic center. The effects of the molecule → azanion conversion on the R(C≡N), R(C–C(N)) and A(CCN) are by 1–2 orders weaker. The analysis of dihedral angles in Table 4 shows that the non-planar 4-cyanobenzamide molecule turns into a planar azanion.

The changes in the *electronic structure* of 4-cyanobenzamide, caused by its conversion into azanion, can be demonstrated on the basis of data on bond orders and net electronic charges. The bond order variations (Table 5) are in agreement with the corresponding bond length changes (higher orders correspond to shorter bonds, under equal other conditions cf. Table 4).

Table 4. Selected B3LYP/6-31++G** bond lengths R (Å), bond angles A (degrees) and dihedral angle D (degrees) of 4-cyanobenzamide molecule 1 and its azanion 2.

Indices [a]	Molecule	Azanion	Δ [b]
R(4, 5)	1.507	1.530	0.023
R(5, 6)	1.227	1.271	**0.044**
R(5, 7)	1.370	1.322	**–0.048**
R(7, 8)	1.010	1.024	0.014
R(2, 3)	1.436	1.432	–0.004
R(1, 2)	1.163	1.167	0.004
A(4, 5, 7)	116.6	113.7	–2.9
A(6, 5, 7)	121.9	130.1	**8.2**
A(5,7,8)	116.3	106.5	**–9.8**
A(10, 3, 2)	120.1	120.3	0.2
A(3, 2, 1)	179.9	180.0	0.1
D(11, 4, 5, 7)	–21.7	0.0	**21.7**
D(12, 4, 5, 6)	–21.5	0.0	**21.5**
D(6, 5, 7, 8)	6.3	0.0	–6.3

a - Atom numbering according to Scheme 1; b - Δ = Index (anion) – Index (molecule) (Å or degrees). The largest |Δ| values are given in bold.

Scheme 2 contains values of net electric charges q_i over fragments of molecule **1** and azanion **2**. The electric charge changes $\Delta q_i = q_i(\text{anion}) - q_i(\text{molecule})$ are usually quite informative to demonstrate the distribution of the new (carbanionic, azanionic, *etc*.) charge between individual fragments of anions [22, 30] (and references therein). According to our calculations, the anionic charge in 4-cyanobenzamide azanion is distributed, as follows: 0.07, 0.29 and 0.11 e^- are delocalized over the cyano, phenylene and carbonyl groups, respectively, and 0.53 e^- of it remain localized in the azanionic center. The Δq_i value of the cyano group is the least one within all Δq_i to confirm the weak effect of the molecule → azanion conversion on the C≡N group of 4-cyanobenzamide (cf. above).

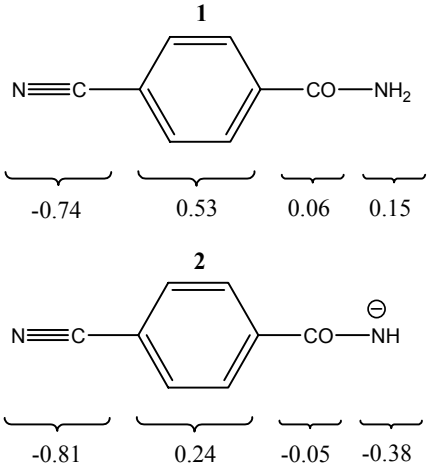

Scheme 2. Natural Bond Orbital (NBO) net electric charges q_i over fragments of molecule **1** and azanion **2** of 4-cyanobenzamide.

Table 5. *Ab initio* HF/6-31G** bond orders P of 4-cyanobenzamide and its azanion

Bonds [a]	Molecule	Azanion	ΔP [b]
$C^2{\equiv}N^1$	2.901	2.926	0.025
$C^2–C^3$	0.992	0.998	0.006
$C^5{=}O^6$	1.812	1.547	**–0.265**
$C^4–C^5$	0.973	0.926	–0.047
$C^5–N^7$	1.048	1.647	**0.599**
$N^7–H^8$	0.884	0.937	0.053

a - Atom numbering according to Scheme 1; b – $\Delta P = P_{\text{anion}} - P_{\text{molecule}}$. The largest |ΔP| values are given in bold.

CONCLUSIONS

We found on the basis of both experimental and computational IR data that the effect of the conversion of 4-cyanobenzamide into azanion on the cyano group was weak. This statement was confirmed by the analysis both of steric and electronic structures, computed for the species studied.

***Acknowledgements**: The financial support by the Bulgarian Council of Scientific Research for Project Chem. – 1510 is gratefully acknowledged.*

REFERENCES

1. M. Pfannl, O. Dafert, *Monat. Chem.*, **33,** 485 (1912).
2. M. T. D. Crolin, T. W. Schultz, *Chem. Res. Toxicol.*, **14**, 1284 (2001).
3. M. T. D. Crolin, N. Manda, J. R. Steward, G. D. Sinks, T. W. Schultz, *Chem. Res. Toxicol.*, **14**, 1498 (2001).

4. V. Ognianova, J. Petrov, G. N. Andreev, *J. Mol. Struct.*, **598**, 27 (1997).
5. M. K. Georgieva, N. B. Nedelchev, I. N. Juchnovski, *Bulg. Chem. Commun.*, **37,** 235 (2005).
6. B. A. Stamboliyska, *Bulg. Chem. Commun.*, **37**, 289 (2005).
7. M. K. Georgieva, E. A. Velcheva, *Int. J. Quant. Chem.*, **106,** 1316 (2006).
8. I. G. Binev, E. A. Velcheva, V. B. Radomirska, I. N. Juchnovski, *Compt. Rend. Acad. Bulg. Sci.*, **47**, 33 (1994).
9. C. Crisostomo, M. G. Crestani, J. J. Garcia, *J. Mol. Catal. A*, **266**, 139 (2007).
10. M. W. Schmidt, K. K. Baldridge, J. A. Boatz, S. T. Elbert, M. S. Gordon, J. H. Jensen, S. Koseki, N. Matsunaga, K. A. Nguyen, S. J. Su, T. L. Windus, M. Dupuis, J. A. Montgomery, *J. Comput. Chem.*, **14** 1347 (1993).
11. M. J. Frisch, G. W. Trucks, H. B. Schlegel, G. E. Scuseria, M. A. Robb, J. R. Cheeseman, V. G. Zakrzewski, J. A. Montgomery, Jr., R. E. Stratmann, J. C. Burant, S. Dapprich, J. M. Millam, A. D. Daniels, K. N. Kudin, M. C. Strain, O. Farkas, J. Tomasi, V. Barone, M. Cossi, R. Cammi, B. Mennucci, C. Pomelli, C. Adamo, S. Clifford, J. Ochterski, G. A. Petersson, P. Y. Ayala, Q. Cui, K. Morokuma, D. K. Malick, A. D. Rabuck, K. Raghavachari, J. B. Foresman, J. Cioslowski, J. V. Ortiz, A. G. Baboul, B. B. Stefanov, G. Liu, A. Liashenko, P. Piskorz, I. Komaromi, R. Gomperts, R. L. Martin, D. J. Fox, T. Keith, M. A. Al-Laham, C. Y. Peng, A. Nanayakkara, C. Gonzalez, M. Challacombe, P. M. W. Gill, B. Johnson, W. Chen, M. W. Wong, J. L. Andres, M. Head-Gordon, E. S. Replogle, J. A. Pople, Gaussian 98, Revision A.7, Gaussian Inc., Pittsburgh, PA, 1998.
12. T. M. Kolev, E. A. Velcheva, B. A. Stamboliyska, *Int. J. Quant. Chem.*, **102**, 1069 (2005).
13. A. D. Becke, *J. Chem., Phys.*, **98**, 5648 (1993).
14. C. Lee, W. Yang, G. R. Parr, *Phys. Rev. B*, **37**, 785 (1988).
15. E. A. Velcheva, G. I. Nikolova, O. I. Petrov, *Bulg. Chem. Commun.*, **38**, 263 (2006).
16. L. I. Daskalova, *J. Mol. Struct. (THEOCHEM)*, **848**, 9 (2008)
17. F. A. Bordwell, *Acc. Chem. Res.*, **21**, 456 (1988).
18. H. H. Jaffe, *Chem. Rev.*, **53**, 191 (1953).
19. M. Alcolea Palafox, *Recent Res. Develop. Phys. Chem.*, **2**, 213 (1996).
20. I. D. Reva, S. V. Ilieva, R. Fausto, *Phys. Chem. Chem. Phys.*, **2**, 4235 (2001).
21. E. A. Velcheva, P. J. Vassileva-Boyadjieva, I. G. Binev, *Bulg. Chem. Commun.*, **40**, 423 (2008).
22. A. D. Popova, M. K. Georgieva, O. I. Petrov, K. V. Petrova, E. A. Velcheva. *Int. J. Quant. Chem.*, **107**, 1752 (2007).
23. A. D. Popova, Y. I. Binev, P. J. Vassileva-Boyadjieva, I. G. Binev, *Bulg. Chem. Commun.*, **40**, 502 (2008).
24. S. S. Stoyanov, A. D. Popova, J. A. Tsenov, *Bulg. Chem. Commun.*, **40** (2008), in pess.
25. M. K. Georgieva, P. J. Vassileva-Boyadjieva, P. N. Angelova, *Bulg. Chem. Commun.*, **37**, 66 (2005).
26. L. I. Daskalova, E. A. Velcheva, I. G. Binev, *J. Mol. Struct.*, **826**, 1987 (2007).
27. P. J. Vassileva-Boyadjieva, E. A. Velcheva, Y. I. Binev, *Bulg. Chem. Commun.*, **37**, 313 (2005).
28. G. N. Andreev, Molecular Spectroscopy, Plovdiv University Press, 1999 (in Bulgarian).
29. E. A. Velcheva, L. I. Daskalova, I. G. Binev, *Bulg. Chem. Commun.*, **36**, 230 (2004).
30. E. A. Velcheva, B. A. Stamboliyska, *J. Mol. Struct.*, (2007), in press.

ИЧ-СПЕКТРАЛНИ И СТРУКТУРНИ ПРОМЕНИ, ПОРОДЕНИ ОТ ПРЕВРЪЩАНЕТО НА 4-ЦИАНОБЕНЗАМИД В АЗАНИОН. КОМБИНИРАН ЕКСПЕРИМЕНТАЛНО-ТЕОРЕТИЧЕН ПОДХОД

Й. Ан. Ценов*, С. С. Стоянов, Ив. Г. Бинев

„ o a “, , , . „ . . “ . 9, 1113

. 70-

Постъпила на 25 януари 2008 г.; Преработена на 20 март 2008 г.

(Резюме)

Приложен е комбиниран ИЧ експериментален/DFT теоретичен подход за проследяване на спектралните и структурни промени, породени от превръщането на 4-цианобензамид в азанион. Ефектът на превръщането се проявява слабо върху валентното трептение на ν(C≡N) и силно върху двете амидни ν(C=O) и ν(C–N) валентни трептения. Според изчисленията последните две форми на трептения са силно делокализирани в азаниона и по същество всяко от тях участва в няколко трептения. Отново според изчисленията, превръщането в азанион поражда значителни промени в структурата при и азанионния център; непланарната молекула на 4-цианобензамида преминава в планарен азанион.

Bulgarian Chemical Communications, Volume 40, Number 4 (pp. 526–531) 2008

Ab initio SCF study of the barrier to internal rotation in N,N-dimethylcinnamamides

N. G. Vassilev*

Institute of Organic Chemistry with Centre of Phytochemistry, Bulgarian Academy of Sciences, Acad. G. Bonchev St., Block 9, 1113 Sofia, Bulgaria

Dedicated to Academician Ivan Juchnovski on the occasion of his 70th birthday

Received January 28, 2008; Revised January 30, 2008

The barrier to internal rotation around the amide C–N bond in R–C_6H_4–CH=CH–C(O)N$(CH_3)_2$ (R = *p*-NO_2, *m*-NO_2, *m*-Cl, *p*-Cl, *m*-OCH_3, H, *p*-CH_3, *p*-OCH_3) was studied at the MP2(fc)/6-31+G*//6-31G* level of theory. The solvent effect was estimated using polarizable continuum model (PCM) and the free energies of activation were compared with the NMR data in $CHCl_3$. For all studied compounds the *anti* transition state (*anti* TS) is more stable and determines the rotational barrier. A linear relationship is established linking the barrier heights and the shift of C–N bond order difference between *anti* TS and ground state (GS) upon substitution in the aromatic ring.

Key words: N,N-dimethylcinnamamides, barrier to internal rotation, *ab initio* SCF study.

INTRODUCTION

The great interest for the amide functional group in chemistry is mainly related to its occurrence as a building block in peptides and proteins. The internal rotation about the amide C–N bond in amides and thioamides has been intensively studied experimentally by NMR spectroscopy in gas [1–7] and in the liquid phase [8]. The experimental results were used to judge theoretical methods of calculating barrier heights [9]. The origin of the C–N rotational barrier, its relation to amide resonance and its response to the medium have received much attention in the last years [10–25].

Recently, the electronic effect of polar substituents on the barrier of internal rotation around the amide carbon-nitrogen bond in *p*-substituted acetanilides [26, 27] and thioacetanilides [28] were studied at the B3LYP/6-31G(d,p) level. Several linear relationships were established linking the barrier heights with structural and electronic parameters that characterize the amide and thioamide grouping. The results obtained are consistent with the views for a classical amide resonance as being the origin of higher rotational barriers in thioamides than in amides.

Here we present our *ab initio* calculation of barrier to internal rotation about C–N bond in N,N-dimethylcinnamamides, which were studied by dynamic NMR spectroscopy [29, 30]. The aim of this study is to analyze the influence of phenyl substituents remote effects on the barrier of internal rotation around the amide C–N bond in these compounds. On the other hand, the interest to cinnamamides, namely coumaric amides, increases in the last years because of potential antioxidant activity of these compounds [31, 32].

METHODS

The *ab initio* SCF calculations were performed using the package GAMESS [33]. The complete geometry optimization was carried out using the 6-31G* basis sets. The molecules were assumed to have C1 symmetry in the ground state (GS) and CS symmetry in the transition states (TS). The bond order analysis was done at the HF/6-31G* level of theory as it is implemented in program GAMESS for closed shells by Giambiagi [34] and Mayer [35]. For recent review about bond orders see ref. [36]. The energies were then calculated at the MP2(fc)/6-31+G*//6-31G* level of theory. In calculating the vibrational energies, the vibrational frequencies were scaled by 0.89 [37]. In each case 7 (TS) or 8 (GS) scaled frequencies below 500 cm^{-1} were treated as rotations (E = RT/2) [37]. The imaginary frequency for the transition states is ignored in all thermodynamics calculations. The effect of solvent on the relative stabilities of the GS and TS was studied using the polarized continuum model (PCM) proposed by Tomasi *et al*. [38]. In our investigations only the electrostatic contributions were taken into account utilizing single point PCM calculations at HF/6-31G* level of theory.

* E-mail: niki@orgchm.bas.bg

© 2008 Bulgarian Academy of Sciences, Union of Chemists in Bulgaria

RESULTS AND DISCUSSION

Geometry optimization

The heavy-atom framework of the studied molecules in GS was found to be essentially planar and close to C_S symmetry. The transition state geometries of the studied amides (Fig. 1) were optimized in C_S symmetry. This approach usually yields transition states, but for some of our structures additional refining of saddle point was necessary in order to locate TS structure with only one imaginary frequency. The calculated energies for GS, *anti* and *syn* TS, are presented in Table 1. The *anti* TS is much more stable in all cases. Therefore, *anti* TS of the studied compounds give the main contribution to the rotational barrier.

The most significant structural changes in the process of rotation towards the transition states are that the nitrogen is pyramidalized and the C–N bond lengthens from 1.357–1.361 to 1.427–1.431 Å (Table 2). The C=O bond length shortens by 0.01–0.02 Å only, which indicates that the carbonyl group is relatively unaffected by this rotation. The C–C bond between carbonyl group and double bond decreases also slightly in the process of rotation from GS to *anti* TS. This can be explained by the decrease of conjugation. The C=C double bond is almost not affected by the rotation.

In the case of *m*-NO_2, *m*-Cl, *m*-OCH_3 derivatives, they are two conformations depending on the orienttation of aryl substituent against C=C double bond. The more stable conformation of *m*-NO_2 and *m*-Cl is the *synclinar* conformation, while in case of *m*-OCH_3 derivative the *antiperiplanar* conformation is more stable.

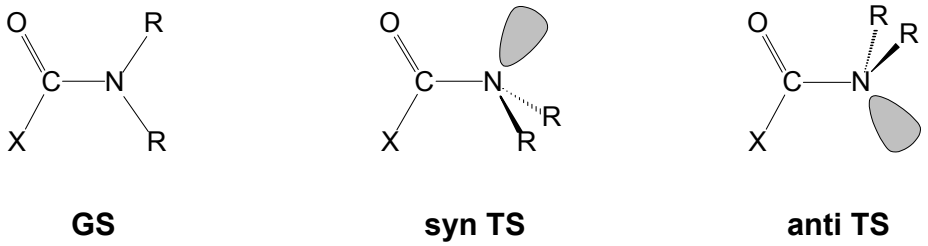

Fig. 1. Conformations of the studied amides X = R–C_6H_4–CH=CH (R = *p*-NO_2, *m*-NO_2, *m*-Cl, *p*-Cl, *m*-OCH_3, H, *p*-CH_3, *p*-OCH_3)

Table 1. Calculated Electronic energies E_e^o for the studied amides RC_6H_4–CH=CH–$CON(CH_3)_2$ in Hartrees.

R	State	ZPE [b]	HF/6-31G*	MP2(fc)/6-31+G*//6-31G*	PCM/6-31G* (ε = 4.9) [c]
p-NO_2	GS	132.54	–756.898270	–759.204688	–9.025
p-NO_2	*anti* TS	132.28	–756.879231 [a]	–759.183975 [a]	–7.799
p-NO_2	*syn* TS	132.10	–756.872329	–759.178001	–9.312
m-NO_2	GS	132.54	–756.898605	–759.203737	–8.943
m-NO_2	*anti* TS	132.30	–756.879322 [a]	–759.183409 [a]	–7.887
m-NO_2	*syn* TS	132.12	–756.872720	–759.177756	–9.186
m-Cl	GS	124.75	–1012.326958	–1014.222284	–6.525
m-Cl	*anti* TS	124.52	–1012.308192 [a]	–1014.202267 [a]	–5.340
m-Cl	*syn* TS	124.33	–1012.301472	–1014.196209	–6.735
p-Cl	GS	124.74	–1012.327078	–1014.221772	–6.566
p-Cl	*anti* TS	124.53	–1012.308572 [a]	–1014.202103 [a]	–5.329
p-Cl	*syn* TS	124.33	–1012.301713	–1014.195886	–6.748
m-OCH_3	GS	150.12	–667.307444	–669.382656	–7.290
m-OCH_3	*anti* TS	149.89	–667.288887 [a]	–669.362644 [a]	–6.183
m-OCH_3	*syn* TS	149.71	–667.282214	–669.357077	–7.443
H	GS	130.38	–553.427464	–555.187857	–7.121
H	*anti* TS	130.18	–553.409162 [a]	–555.168490 [a]	–5.711
H	*syn* TS	129.99	–553.402390	–555.162334	–7.390
p-CH_3	GS	146.68	–592.465061	–594.359397	–6.362
p-CH_3	*anti* TS	146.50	–592.446874 [a]	–594.340710 [a]	–5.197
p-CH_3	*syn* TS	146.31	–592.440104	–594.334565	–6.570
p-OCH_3	GS	150.15	–667.308843	–669.381867	–7.454
p-OCH_3	*anti* TS	149.96	–667.290747 [a]	–669.363369 [a]	–6.327
p-OCH_3	*syn* TS	149.78	–667.283988	–669.357231	–7.687

a - more stable TS; b - ZPE is reported in kcal/mol at the HF/6-31G* level scaled by 0.89; c - Energy change from gas phase to solvent in kcal/mol.

Table 2. Selected bond lengths, bond orders and imaginary frequencies calculated at HF/6-31G* level of theory for the studied amides R–C_6H_4–CH=CH–CON$(CH_3)_2$.

R	State	r_{C-N}, Å	$r_{C=O}$, Å	$r_{C=C}$, Å	r_{C-C}, Å	Bond Order C–N	*Iv*, cm^{-1}
p-NO_2	GS	1.357	1.206	1.325	1.498	1.054	
p-NO_2	*anti* TS	1.431	1.192	1.327	1.487	0.929	104.0i
p-NO_2	*syn* TS	1.427	1.188	1.326	1.496	0.990	87.3i
m-NO_2	GS	1.357	1.207	1.325	1.497	1.054	
m-NO_2	*anti* TS	1.431	1.192	1.327	1.486	0.930	103.3i
m-NO_2	*syn* TS	1.427	1.188	1.327	1.495	0.944	88.0i
m-Cl	GS	1.358	1.207	1.326	1.495	1.048	
m-Cl	*anti* TS	1.432	1.193	1.328	1.484	0.926	101.8i
m-Cl	*syn* TS	1.429	1.189	1.327	1.493	0.943	87.4i
p-Cl	GS	1.359	1.207	1.326	1.495	1.046	
p-Cl	*anti* TS	1.433	1.193	1.329	1.483	0.925	101.0i
p-Cl	*syn* TS	1.429	1.189	1.328	1.492	0.941	87.3i
m-OCH_3	GS	1.359	1.207	1.326	1.494	1.044	
m-OCH_3	*anti* TS	1.434	1.193	1.329	1.482	0.924	101.2i
m-OCH_3	*syn* TS	1.430	1.189	1.328	1.491	0.940	86.4i
H	GS	1.360	1.207	1.327	1.493	1.043	
H	*anti* TS	1.434	1.193	1.329	1.481	0.923	99.8i
H	*syn* TS	1.430	1.189	1.329	1.490	1.003	86.7i
p-CH_3	GS	1.360	1.207	1.328	1.492	1.041	
p-CH_3	*anti* TS	1.434	1.194	1.330	1.480	0.922	99.0i
p-CH_3	*syn* TS	1.431	1.189	1.329	1.489	0.938	86.6i
p-OCH_3	GS	1.361	1.208	1.328	1.491	1.039	
p-OCH_3	*anti* TS	1.435	1.194	1.331	1.479	0.922	97.6i
p-OCH_3	*syn* TS	1.431	1.190	1.330	1.488	0.937	86.4i

Comparison of calculated activation parameters and experimental data

Calculation of the vibrational frequencies confirmed the assignment of the *anti* and *syn* forms as transition states and allowed computation of the enthalpy, entropy and free energy changes at 298K. The thermodynamic results for the isomerisation of the studied amides are presented in Table 3. In the present case, $\Delta H^{\neq}$(0 K) is calculated as a sum of the changes in the energies and the zero-point vibrational energy (ZPE) differences while $\Delta H^{\neq}$(298 K) involves a correction for the difference in heat capacity of GS and TS. The scaled frequencies were used also for the entropy calculation. From the calculated free energies $\Delta G^{\neq}$(298 K) and using Eyring equation, one obtains the respective rate constants for both *syn* and *anti* TS. The effective rate constant is a sum of the rate constants through the two transition states. In the studied molecules the contribution of *syn* TS is negligible. The effective free energy $\Delta G^{\neq}_{eff}$(298K), which is in turn calculated from the effective rate constant, can be corrected by the energy change from gas phase to solvent (Table 1) and compared with NMR data in $CHCl_3$. It is seen from Table 3 that the rotational barriers for the studied compounds in chloroform were reproduced very satisfactory at this level of theory. There is also a good relation between experimental activation entropies, $\Delta S^{\neq}$(298K) and calculated ones for *m*-Cl, *m*-OCH_3 and nonsubstituted cinnamamide. Recently, the barriers of rotation around C–N bond in gas phase of simple amides and tioamides were well reproduced at MP2(fc)/6-31+G*//6-31G* level of theory, as well [20, 21, 25].

Effect of substituents on the rotational barrier

In order to study the effect of nonbonded interactions on the barrier heights we examined the following reaction both in ground state and in the two possible transition states:

$$H–CO–N(CH_3)_2 + R–CO–NH_2 \rightarrow$$

$$\rightarrow H–CO–NH_2 + R–CO–N(CH_3)_2$$

This approach was explored before to estimate the difference in repulsion between R and the CH_3 group, the difference in repulsion between R and the amide lone pair and the difference in repulsion between oxygen and amide lone pair [20, 21, 25]. The calculated electronic energies of the studied amides RC_6H_4–CH=CH–$CONH_2$, ZPE and ΔH^o of the above model reaction are presented in Table 4. All values for ΔH^o are small enough to conclude that there is not significant difference in nonbonded interactions in GS and TS's and these results are not able to explain the difference in barrier heights.

Table 3. Thermodynamic results for the isomerization of the studied amides R–C_6H_4–CH=CH–$CON(CH_3)_2$ in the gas phase and in $CHCl_3$.

R	Parameter	anti TS	*syn* TS	Experimental
p-NO_2	$\Delta H^{\neq}$(0K)	12.74	16.31	
	$\Delta H^{\neq}$(298K)	11.76	15.18	16.9 ± 0.4 [a] (18.13 ± 0.1) [b]
	$\Delta S^{\neq}$(298K)	–7.42	–8.39	0.4 ± 1.3 [a] (3.99 ± 0.5) [b]
	$\Delta G^{\neq}$(298K)	13.97	17.68	
	$\Delta G^{\neq}_{eff}$(298K)	13.96 (15.35) [c]		16.80 ± 0.06 [a] (16.94 ± 0.01)
m-NO_2	$\Delta H^{\neq}$(0K)	12.52	15.88	
	$\Delta H^{\neq}$(298K)	11.55	14.77	16.5 ± 0.8 [a]
	$\Delta S^{\neq}$(298K)	–8.51	–7.04	–0.1 ± 2.6 [a]
	$\Delta G^{\neq}$(298K)	14.09	16.87	
	$\Delta G^{\neq}_{eff}$(298K)	14.08 (15.29) [c]		16.58 ± 0.07 [a]
m-Cl	$\Delta H^{\neq}$(0K)	12.33	15.94	
	$\Delta H^{\neq}$(298K)	11.36	14.24	14.0 ± 0.3 [a]
	$\Delta S^{\neq}$(298K)	–8.90	–16.63	–7.7 ± 1.1 [a]
	$\Delta G^{\neq}$(298K)	14.01	21.59	
	$\Delta G^{\neq}_{eff}$(298K)	14.01 (15.34) [c]		16.33 ± 0.02 [a]
p-Cl	$\Delta H^{\neq}$(0K)	12.13	15.83	
	$\Delta H^{\neq}$(298K)	11.15	14.72	17.9 ± 1.4 [a] (17.15 ± 0.1) [b]
	$\Delta S^{\neq}$(298K)	–10.02	–8.44	5.6 ± 4.6 [a] (2.16 ± 0.4) [b]
	$\Delta G^{\neq}$(298K)	14.14	17.24	
	$\Delta G^{\neq}_{eff}$(298K)	14.13 (15.58) [c]		16.25 ± 0.07 [a] (16.51 ± 0.01) [b]
m-OCH_3	$\Delta H^{\neq}$(0K)	12.33	15.64	
	$\Delta H^{\neq}$(298K)	11.36	14.53	14.4 ± 0.7 [a]
	$\Delta S^{\neq}$(298K)	–7.67	–8.29	–5.9 ± 2.2 [a]
	$\Delta G^{\neq}$(298K)	13.65	17.00	
	$\Delta G^{\neq}_{eff}$(298K)	13.64 (15.02) [c]		16.19 ± 0.06 [a]
H	$\Delta H^{\neq}$(0K)	11.95	15.63	
	$\Delta H^{\neq}$(298K)	10.99	14.52	14.1 ± 0.6[a](17.22 ± 0.1)[b]
	$\Delta S^{\neq}$(298K)	–10.77	–9.35	–6.8 ± 1.9[a](2.76 ± 0.2)[b]
	$\Delta G^{\neq}$(298K)	14.20	17.31	
	$\Delta G^{\neq}_{eff}$(298K)	14.19 (15.60) [c]		16.16 ± 0.04 [a] (16.39 ± 0.01)
p-CH_3	$\Delta H^{\neq}$(0K)	11.55	15.21	
	$\Delta H^{\neq}$(298K)	10.57	14.10	17.1 ± 2.1 [a] (18.04 ± 0.2) [b]
	$\Delta S^{\neq}$(298K)	–11.25	–10.18	4.8 ± 7.1 [a] (5.89 ± 0.6) [b]
	$\Delta G^{\neq}$(298K)	13.92	17.14	
	$\Delta G^{\neq}_{eff}$(298K)	13.91 (15.33) [c]		15.72 ± 0.09 [a] (16.29 ± 0.01) [b]
p-OCH_3	$\Delta H^{\neq}$(0K)	11.42	15.09	
	$\Delta H^{\neq}$(298K)	10.44	13.98	16.9 ± 0.2 [a] (17.8 ± 0.1) [b]
	$\Delta S^{\neq}$(298K)	–10.53	–9.66	3.4 ± 0.9 [a] (5.84 ± 0.4) [b]
	$\Delta G^{\neq}$(298K)	13.58	16.86	
	$\Delta G^{\neq}_{eff}$(298K)	13.57 (14.93) [c]		15.93 ± 0.04 [a] (16.06 ± 0.01) [b]

a - Solution data ref. [29]; b - Solution data ref. [30]; c - Values in parenthesis includes $CHCl_3$ solvation correction of energy from Table 1.

The calculated free energy of activation $\Delta G^{\neq}$(298K) for *anti* TS increases with increasing electron withdrawal of the phenyl substituent and follows almost the same trend as the experimental free energies of activation (Table 3).

The remote substituent effect in the studied compound has a pure electronic origin and therefore can be estimated by the influence on the bond order of the C–N bond. The calculated bond orders for both ground and transition states are presented in Table 2. Figure 2 presents the relationship between C–N bond order difference and calculated energy barrier ΔE of the studied amides, $\Delta E = E$(*anti* TS) – E(GS). The correlation coefficient is not perfect (ρ = 0.924), but we have to take into account the shortness of the basis set and the relative low level of theoretical calculations. The experimental free energies didn't correlate better with the C–N bond order differences. This fact can be explained with the experimental errors and relative low remote substituent effects. The attempt to correlate the $\Delta G^{\pm}_{eff}$(298 K) values with three sets of empirical reactivity parameter leads to correlation coefficients between 0.902 and 0.953 [29].

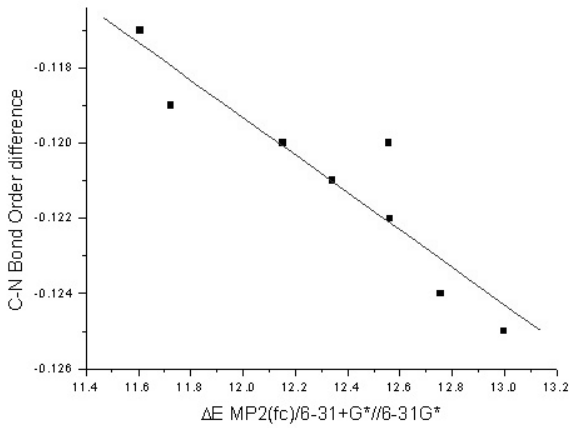

Fig. 2. Relationship between C–N bond order difference (*anti*-TS – GS) and calculated Δ*E* of the studied amides, Δ*E* = *E*(*anti*-TS) – *E*(GS), y = –0.0595x – 0.00499

Table 4. Calculated electronic energies E_e^o for the studied amides R–C_6H_4–CH=CH–$CONH_2$ in Hartrees and ΔH^o of following reaction: H–CO–$N(CH_3)_2$ + + X–CO–NH_2 → → H–CO–NH_2 + X–CO–$N(CH_3)_2$

R	State	ZPE [b]	HF/6-31G*	ΔH^o, kcal/mol
p-NO_2	GS	98.61	–678.846099	–0.18
p-NO_2	*anti* TS	98.39	–678.823888[a]	–0.06
p-NO_2	*syn* TS	98.22	–678.816434	–0.28
m-NO_2	GS	98.51	–678.846494	–0.04
m-NO_2	*anti* TS	98.42	–678.823937[a]	–0.09
m-NO_2	*syn* TS	98.24	–678.817022	–0.16
m-Cl	GS	90.84	–934.275021	–0.05
m-Cl	*anti* TS	90.64	–934.252896[a]	–0.04
m-Cl	*syn* TS	90.46	–934.245904	–0.08
p-Cl	GS	90.87	–934.275183	–0.07
p-Cl	*anti* TS	90.65	–934.253320[a]	–0.01
p-Cl	*syn* TS	90.46	–934.246129	–0.09
m-OCH_3	GS	116.26	–589.255656	–0.01
m-OCH_3	*anti* TS	116.01	–589.233639[a]	–0.01
m-OCH_3	*syn* TS	115.85	–589.226786	–0.01
H	GS	96.54	–475.375722	0
H	*anti* TS	96.31	–475.353943[a]	0
H	*syn* TS	96.13	–475.346971	0
p-CH_3	GS	112.85	–514.413359	0.02
p-CH_3	*anti* TS	112.63	–514.391672[a]	0.01
p-CH_3	*syn* TS	112.45	–514.384741	0.04
p-OCH_3	GS	116.33	–589.257170	0.02
p-OCH_3	*anti* TS	116.10	–589.235553[a]	0.01
p-OCH_3	*syn* TS	115.92	–589.228691	0.08

a - more stable TS; b - ZPE is reported in kcal/mol at the HF/6-31G* level scaled by 0.89

CONCLUSION

The free energy of activation of substituted cinnamamides were reproduced very well using MP2(fc)/6-31+G*//6-31G* energies and PCM/6-31G* energy change from gas phase to chloroform. For all studied compounds the *anti* transition state (*anti* TS) is more stable and determines the rotational barrier. The remote effect of phenyl substituens in the studied compound has pure electronic origin, which was demonstrated by the relationship between C–N bond order difference and calculated energy barrier.

Acknowledgements: *Financial support by the Bulgarian National Science Foundation (Grant X-1408) is acknowledged with gratitude. Thanks are due to Dr. Valentin Dimitrov for the inspiration of this study.*

REFERENCES

1. C. B. LeMaster, *Prog. Nucl. Magn. Reson. Spectrosc.,* **31**, 119 (1997).
2. A. N. Taha, N. S. True, *J. Phys. Chem. A*, **104**, 2985 (2000).
3. A. N. Taha, S. M. Neugebauer-Crawford, N. S. True, *J. Phys. Chem. A*, **104**, 7957 (2000).
4. C. L. LeMaster, C. B. LeMaster, N. S. True, *J. Am. Chem. Soc.*, **121**, 4478 (1999).
5. A. N. Taha, S. M. Neugebauer Crawford, N. S. True, *J. Am. Chem. Soc.*, **120**, 1934 (1998).
6. A. N. Taha, S. M. Neugebauer Crawford, N. S. True, *J. Phys. Chem. A*, **102**, 1425 (1998).
7. S. M. Neugebauer Crawford, A. N. Taha, N. S. True, C. B. LeMaster, *J. Phys. Chem. A*, **101**, 4699 (1997).
8. W. E. Stewart, T. H. Siddal, III, *Chem. Rev.*, **70**, 517 (1970).
9. C. H. Langley, N. L. Allinger, *J. Phys. Chem. A*, **106**, 5638 (2002).
10. K. B. Wiberg, K. E. Laidig, *J. Am. Chem. Soc*, **109**, 5935 (1987).
11. M. W. Wong, K. B. Wiberg, *J. Phys. Chem.*, **96**, 668 (1992).
12. E. M. Duffy, D. L. Severance, W. L. Jorgensen, *J. Am. Chem. Soc*, **114**, 7535 (1992).
13. K. B. Wiberg, C. M. Breneman, *J. Am. Chem. Soc*, **114**, 831 (1992).
14. K. B. Wiberg, C. M. Hadad, P. R. Rablen, J. Cioslowski, *J. Am. Chem. Soc*, **114**, 8644 (1992).
15. M. Feigel, T. Strassner, *J. Mol. Struc. THEOCHEM*, **102**, 33 (1993).
16. K. B. Wiberg, P. R. Rablen, *J. Am. Chem. Soc*, **117**, 2201 (1995).
17. K. B. Wiberg, P. R. Rablen, D. J. Rush, T. A. Keith, *J. Am. Chem. Soc*, **117**, 4261 (1995).
18. K. E. Laidig, L. M. Cameron, *J. Am. Chem. Soc.*, **118**, 1737 (1996).
19. D. Lauvergnat, P. C. Hiberty, *J. Am. Chem. Soc*, **119**, 9478 (1997).
20. N. G. Vassilev, V. S. Dimitrov, *J. Mol. Struc.*, **484**, 39 (1999).
21. N. G. Vassilev, V. S. Dimitrov, *J. Mol. Struc.*, **522**, 37 (2000).
22. K. B. Wiberg, D. J. Rush, *J. Am. Chem. Soc*, **123**, 2038 (2001).
23. M. J. Deetz, C. C. Forbes, M. Jonas, J. P. Malerich, B. D. Smith, O. Wiest, *J. Org. Chem.*, **67**, 3949 (2002).

24. K. B. Wiberg, D. J. Rush, *J. Org. Chem.*, **67**, 826 (2002).
25. N. G. Vassilev, V. S. Dimitrov, *J. Mol. Struc*, **654**, 27 (2003).
26. S. Ilieva, B. Hadjieva, B. Galabov, *J. Mol. Struc*, **476**, 151 (1999).
27. S. Ilieva, B. Hadjieva, B. Galabov, *J. Org. Chem.*, **67**, 6210 (2002).
28. B. Galabov, S. Ilieva, B. Hadjieva, E. Dinchova, *J. Phys. Chem. A*, **107**, 5854 (2003).
29. S. L. Spassov, V. S. Dimitrov, M. Agova, I. Kantschowska, R. Todorova, *Org. Magn. Reson.*, **3**, 551 (1971).
30. K. Spaargaren, P. K. Korver, P. J. van der Haak, T. J. de Boer, *Org. Magn. Reson.*, **3**, 605 (1971).
31. Z. Velkov, Y. Velkov, E. Balabanova, A. Tadjer, *Int. J. Quant. Chem.*, **107**, 1765 (2007).
32. Z. Velkov, E. Balabanova, A. Tadjer, *J. Mol. Struc.: THEOCHEM*, **821**, 133 (2007).
33. M. W. Schmidt, K. K. Baldridge, J. A. Boatz, S. T. Elbert, M. S. Gordon, J. H. Jensen, S. Koseki, N. Matsunaga, K. A. Nguyen, S. J. Su, T. L. Windus, M. Dupuis, J. A. Montgomery, *J. Comput. Chem.*, **14**, 1347 (1993).
34. M. Giambiagi, M. S. D. Giambiagi, D. R. Grempel, C. D. Heymann, *J. Chim. Phys.*, **72**, 15 (1975).
35. I. Mayer, *Chem. Phys. Lett.*, **97**, 270 (1983).
36. I. Mayer, *J. Comput. Chem*., **28**, 204 (2007).
37. W. J. Hehre, L. Radom, P. V. R. Schleyer, J. A. Pople, Ab Initio Molecular Orbital Theory, Wiley, New York, 1986.
38. J. Tomasi, M. Persico, *Chem. Rev.*, **94**, 2027 (1994).

AB INITIO SCF ИЗСЛЕДВАНЕ НА БАРИЕРА НА ВЪТРЕШНА РОТАЦИЯ В N,N-ДИМЕТИЛКАНЕЛЕНИ АМИДИ

Н. Г. Василев

Институт по органична химия с център по фитохимия, Българска академия на науките, ул. „Акад. Г. Бончев“ бл. 9, София 1113

Посветена на акад. Иван Юхновски по повод на 70-та му годишнина

Постъпила на 28 януари 2008 г.; Преработена на 30 януари 2008 г.

(Резюме)

Бариера на вътрешна ротация около амидната C–N връзка в R–C_6H_4–CH=CH–C(O)N$(CH_3)_2$ (R = *p*-NO_2, *m*-NO_2, *m*-Cl, *p*-Cl, *m*-OCH_3, H, *p*-CH_3, *p*-OCH_3) е изследвана на MP2(fc)/6-31+G*//6-31G* ниво на теорията. Ефекта на разтворителя е оценен чрез модела на поляризиран континиум (PCM) и свободната енергия на активиране е сравнена с ЯМР данните в $CHCl_3$. За всички изследвани съединения анти преходното състояние (*anti* TS) е по-стабилно и определя ротационния бариер. Установена е линейна зависимост свързваща височината на бариера и промяната в разликата на C–N порядъка на връзката между anti TS и основно състояние (GS) при заместване в ароматното ядро.

Bulgarian Chemical Communications, Volume 40, Number 4 (pp. 532–537) 2008

Ab initio and DFT study of the structure of metal ion complexes with N-benzalaniline-15-crown-5

V. Enchev[1,*], S. Angelova[1], N. Markova[1], I. Wawer[2], E. Stanoeva[3], M. Mitewa[3]

[1] *Institute of Organic Chemistry with Centre of Phytochemistry, Bulgarian Academy of Sciences, 1113 Sofia, Bulgaria*
[2] *Faculty of Pharmacy, Medical University of Warsaw, Warsaw, Poland*
[3] *Department of Chemistry, University of Sofia, 1 James Bourchier Blv., 1164 Sofia, Bulgaria*

Dedicated to Academician Ivan Juchnovski on the occasion of his 70th birthday

Received January 30, 2008; Revised February 7, 2008

The structures of N-(4-benzalaniline)-15-crown-5 and N-(4'-benzalaniline)-15-crown-5 and their Li^+, Na^+, K^+, Be^{2+}, Mg^{2+}, Ca^{2+}, Sr^{2+} and Ba^{2+} complexes are optimized using *ab initio* and DFT methods. It was found that in all cases the M^{n+}–N distances (n = 1, 2) are longer than the average M^{n+}–O ones in the corresponding complexes and the metal–nitrogen distances in the alkali metal complexes are longer than these in alkaline earth ones. The Li^+, Na^+, Mg^{2+} and Ca^{2+} cations fit to cavity size of the crown while the K^+, Sr^{2+} and Ba^{2+} cations, whose size is greater than the diameter of the macrocycle cavity, protrude from the macrocycle. In all cases the conformation of the crown ether does not change except the Be^{2+} complex, where the conformation of the macrocycle is strongly deformed.

Key words: N-benzalaniline-15-crown-5, *ab initio*, Li^+, Na^+, K^+, Be^{2+}, Mg^{2+}, Ca^{2+}, Sr^{2+}, Ba^{2+} metal ions.

INTRODUCTION

Crown ethers are widely used as complexing agents that can capture selectively metal cations in their cavity. Their ability to bind metal cations depends on the cavity size, the nature of heteroatoms and substituents in the macrocycle. The ability of crown ethers to selectively bind cations makes them valuable components for constructing cation-sensing molecular or supramolecular probes [1]. The effects of metal coordination on the photosensitive and spectral properties of crown ether complexes have been studied [2–6].

During the last decades there is a constant interest in the design of new chromo- and fluoroionophores incorporating a N-phenylaza macrocycle moiety due to the change of their absorption and emission properties upon complexation and thus serving as optical sensors [7–9].

It is suggested that due to conjugation between the lone electron pair of the endocyclic nitrogen atom and the aromatic system a charge transfer (CT) is realized (the chromophoric system usually being acceptor) resulting in the appearance of intense CT band in the UV-Vis spectrum [10–14]. However, the coordination capacity of the macrocycle is lowered and the corresponding stability constants are much lower than these with the parent macrocycle [11, 12]. Taking into account that the conjugation should depend on the acceptor properties of the chromophoric group, we have designed and synthesized new N-benzalaniline-15-crown-5 derivatives, containing a weak acceptor group, namely a Schiff base [15]. The obtained stability constant data confirm the supposition for the formation of relatively stable complexes [15]. The goal of this paper is to study the complexation of these new N-benzalaniline-15-crown-5 derivatives with alkali and alkaline earth metal ions. *Ab initio* and DFT calculations on the structure of N-(4'-benzalaniline)-15-crown-5 and N-(4-benzalaniline)-15-crown-5, and their complexes with alkaline and alkaline earth metal ions were performed and the results obtained are discussed in the present paper.

COMPUTATIONAL DETAILS

Geometry optimization of the structure of the compounds investigated was performed by *ab initio* methods and by density functional theory. The *ab initio* calculations were carried out using the PC GAMESS version [16] of the GAMESS (US) quantum chemistry program package [17]. The structure optimizations for the N-(4-benzalaniline)-15-crown-5 (L1) and N-(4'-benzalaniline)-15-crown-5 (L2) (Fig. 1), and their Li^+, Na^+, K^+, Be^{2+}, Mg^{2+}, Ca^{2+}, Sr^{2+} and Ba^{2+} complexes were performed at a restricted Hartree-Fock (RHF) level without any symmetry constrains (C_1 symmetry was assumed). The mean gradient threshold was 0.0001 hartree/Bohr. The *ab initio* calculations were carried out with the

* To whom all correspondence should be sent:
E-mail: venelin@orgchm.bas.bg

© 2008 Bulgarian Academy of Sciences, Union of Chemists in Bulgaria

Stewens-Basch-Krauss-Jasien effective core potentials (ECP) and their concomitant basis sets for all the atoms (ECP-31G) [18, 19]. The DFT geometry optimizations using Becke's three parameter hybrid functional (B3LYP) [20] and 6-31G(d) basis set [21] were also performed. The DFT geometry optimization was carried out using the Gaussian 98 program package [22]. The Sr^{2+} and Ba^{2+} complexes with L1 have not been optimized at this level of theory because of lack of basis sets for these elements.

^{13}C NMR chemical shieldings were calculated using the GIAO (gauge-including atomic orbitals) approach [23] implemented in Gaussian 03 [24] at DFT level of theory using 6-31+G(d) and 6-31+G(d,p) basis sets. In order to compare with experiment, the calculated absolute shieldings were transformed to chemical shifts using the reference compound tetramethylsilane (TMS): $\delta = \sigma_{calc}(TMS) - \sigma_{calc}$. Both $\sigma_{calc}(TMS)$ and σ_{calc} were evaluated with the same method and basis set.

EXPERIMENTAL

The ^{1}H and ^{13}C NMR spectra and 2D $^{1}H/^{13}C$ heteronuclear correlations for $CDCl_3$ solutions were recorded on a Varian Unity Plus-500 MHz spectrometer. Cross polarization (CP) magic angle spinning (MAS) solid state ^{13}C NMR spectra were recorded on a Bruker MSL-300 instrument at 75.5 MHz. Powder samples were spun at 8.4 kHz in 4 mm ZrO_2 rotor, a contact time of 1-4 ms, a repetition time of 6 s and a spectral width of 20 kHz were used for accumulation of 500-800 scans. Chemical shifts were calibrated indirectly through the glycine CO signal recorded at 176.0 ppm relative to TMS.

N-(4-benzalaniline)-15-crown-5 was synthesized according to a procedure described in Ref. [14].

RESULTS AND DISCUSSION

Structure of N-(4-benzalaniline)-15-crown-5 and N-(4'-benzalaniline)-15-crown-5

The structures of several free arylazacrown ethers have been studied by X-ray diffraction and they can be found in the Cambridge Structural Database [25–31]. We found that the conformation of the optimized structures for N-(4-benzalaniline)-15-crown-5 (L1) and N-(4'-benzalaniline)-15-crown-5 (L2) are close to the experimentally determined ones for aza-15-crown-5.

The optimized structure of N-(4-benzalaniline)-15-crown-5, L1, is shown in Fig. 2. It is evident that the macrocycle is positioned almost perpendicularly to the other part of the molecule. The dihedral angle between the planes of both benzene rings is 30 degrees. The optimized structure of N-(4'-benzalaniline)-15-crown-5, L2, is similar to L1.

The N-(4-benzalaniline)-15-crown-5 was studied by NMR spectroscopy in solid state and in $CDCl_3$ solution. The ^{13}C chemical shifts in the both cases are close because of the similarity in the conformations of the structure investigated in solution and in solid state.

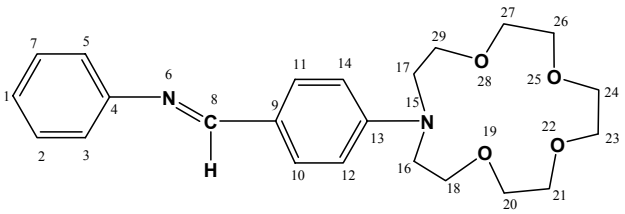

N-(4-benzalaniline)-15-crown-5 (L1)

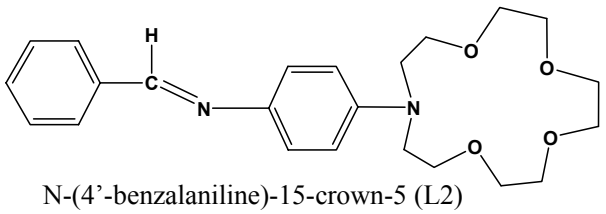

N-(4'-benzalaniline)-15-crown-5 (L2)

Fig. 1. N-(4-benzalaniline)-15-crown-5 (L1) and N-(4'-benzalaniline)-15-crown-5 (L2).

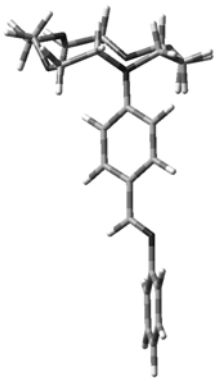

Fig. 2. B3LYP/6-31G(d) optimized structure of N-(4-benzalaniline)-15-crown-5.

The lack of multiple resonances in the ^{13}C NMR CPMAS spectrum of the solid N-(4-benzalaniline)-15-crown-5 indicates that there is one molecule in the asymmetric unit of the crystal. The resonances in the solid-state spectrum were assigned by comparing with solution data and B3LYP/6-31+G(d) and B3LYP/6-31+G(d,p) calculated chemical shifts. The experimental and calculated chemical shifts are collected in Table 1.

The broad signals appearing in the ^{13}C spectrum of L1 indicate that dynamic processes involving aromatic rings are present in the spectra of the solids. The flip motion of the ring gives rise in the spectrum to the equivalence of the *ortho* and *meta* pair of CH resonances in the fast exchange limit. The C1, C4, C9 and C13 resonances are unaffected

by this event, yield narrow resonances in all spectra and thus are easy to recognize. Broad resonances of C2, C7 (at 129.0 ppm) and of C3, C5 (at 120.9 ppm) in the spectrum of L1 indicate that the ring undergoes some reorientation, and these dynamics affect the NMR parameters.

Table 1. Experimental ^{13}C and calculated carbon chemical shifts (ppm) of N-(4-benzalaniline)-15-crown-5. The numbering of the atoms is given in Figure 1.

Atom	Experimental		Calculated	
	$CDCl_3$	Solid state	B3LYP/ 6-31+G(d)	B3LYP/ 6-31+G(d,p)
C1	125.01	126.20	119.48	120.54
C2	129.02	129.00	124.20	125.30
C3	120.93	120.90	110.67	111.70
C4	150.18	150.30	149.49	151.48
C5	120.93	120.90	121.72	122.87
C7	129.02	129.00	123.26	124.33
C8	160.14	161.70	152.49	153.64
C9	124.15	122.60	128.31	130.36
C10	130.68	134.10	128.21	129.23
C11	130.68	127.00	122.92	124.03
C12	111.26	113.50	128.29	129.39
C13	152.75	153.60	145.94	147.82
C14	111.26	113.50	117.45	118.46
C16	52.72	55.00	57.65	58.08
C17	52.72	52.70	56.83	57.12
C18	68.28	66.70	68.96	69.40
C20	70.06	70.10	70.73	71.07
C21	70.25	70.10	72.21	72.61
C23	71.31	72.00	72.08	72.55
C24	71.31	72.00	73.71	74.11
C26	70.25	70.10	73.51	73.93
C27	70.06	70.10	72.13	72.60
C29	68.28	66.70	70.22	70.66

The results obtained with the two basis sets are close. The predictions of chemical shifts of atoms C3, C8, C9 and C12 are with relatively high average deviations because the dynamic processes in solution and in solid state are not taken into account in calculations.

Considering the crown-ether moiety it becomes apparent that the resonances of the two methylene groups linked to the nitrogen atom appear at 52–55 ppm. In the solid state spectrum of L1 separate signals were observed, while in $CDCl_3$ solution only one signal at 52.72 was observed. The predicted values differ by about 1 ppm.

Structure of N-(4-benzalaniline)-15-crown-5 and N-(4'-benzalaniline)-15-crown-5 complexes

The geometry optimization of the complexes with the metal cations was started from the optimized conformation of the free N-(4-benzalaniline)-15-crown-5 and N-(4'-benzalaniline)-15-crown-5. We considered one mode of coordination and the type of cation was varied. The alkaline (Li^+, Na^+, K^+) and alkaline earth (Be^{2+}, Mg^{2+}, Ca^{2+}, Sr^{2+}, Ba^{2+}) metal ions were considered. The metal complexes of the crown ethers are studied in dry acetonitrile, because traces of water destroy the complexes (see [32] and references therein). In our computational study the influence of acetonitrile as solvent on the crown ethers and the complexes was not taken into account. The most important geometrical parameters of the studied complexes, metal-nitrogen and metal-oxygen distances, are presented in Tables 2 and 3.

The size-matching or size-selectivity effect is typical for the crown ethers and is commonly observed in their complexes with alkali and alkaline earth metal ions [34]. This effect is referred to as correspondence between the crown ether cavity size and the ion diameter of preferentially bound cations. Among the alkali cations, lithium and sodium fit best to L1 and L2 while potassium is located above the crown ether ring (the so-called "half-sandwich structure") (Fig. 3).

Table 2. Selected *ab initio* and DFT calculated distances (Å) in N-(4-benzalaniline)-15-crown-5 complexes ($M^{(n)+}$–L1) (n = 1, 2). Available experimental data are also given.

Distances	M = Li^+		M = Na^+		M = K^+		M = Be^{2+}		M = Mg^{2+}		M = Ca^{2+}		M = Sr^{2+}	M = Ba^{2+}
	ECP	DFT	ECP	ECP	DFT	ECP	ECP	DFT	ECP	DFT	ECP	DFT	ECP	ECP
M–N15	2.561	2.437	2.555 (2.658)[a]	2.561	2.437	2.555 (2.658)[a]	1.808	1.788	2.208	2.215	2.467	2.498	2.598	2.867
M–O19	2.159	2.103	2.267 (2.330)[a]	2.159	2.103	2.267 (2.330)[a]	1.647	1.672	2.091	2.119	2.208	2.350	2.366	2.552
M–O22	2.248	2.319	2.369 (2.485)[a]	2.248	2.319	2.369 (2.485)[a]	1.666	1.668	2.112	2.110	2.234	2.386	2.420	2.629
M–O25	2.249	2.244	2.349 (2.443)[a]	2.249	2.244	2.349 (2.443)[a]	2.665	2.664	2.114	2.126	2.238	2.415	2.385	2.554
M–O28	2.214	2.176	2.315 (2.344)[a]	2.214	2.176	2.315 (2.344)[a]	1.667	1.669	2.099	2.127	2.222	2.377	2.393	2.596

a Ref. [33].

Table 3. Selected *ab initio* and DFT calculated distances (Å) in N-(4'-benzalaniline)-15-crown-5 complexes ($M^{(n)+}$–L2), (n = 1, 2).

Distances	$M = Be^{2+}$		$M = Mg^{2+}$		$M = Ca^{2+}$		$M = Li^{+}$		$M = Na^{+}$		$M = K^{+}$	
	ECP	DFT	ECP	ECP	DFT	ECP	ECP	DFT	ECP	DFT	ECP	DFT
M–N15	1.781	1.790	2.275	1.781	1.790	2.275	2.523	2.441	2.551	2.472	3.007	2.921
M–O19	1.645	1.675	2.087	1.645	1.675	2.087	2.158	2.111	2.267	2.318	2.643	2.639
M–O22	1.651	1.673	2.105	1.651	1.673	2.105	2.255	2.283	2.370	2.357	2.753	2.728
M–O25	3.384	2.669	2.109	3.384	2.669	2.109	2.251	2.240	2.346	2.351	2.742	2.739
M–O28	1.640	1.672	2.098	1.640	1.672	2.098	2.219	2.195	2.319	2.318	2.670	2.674

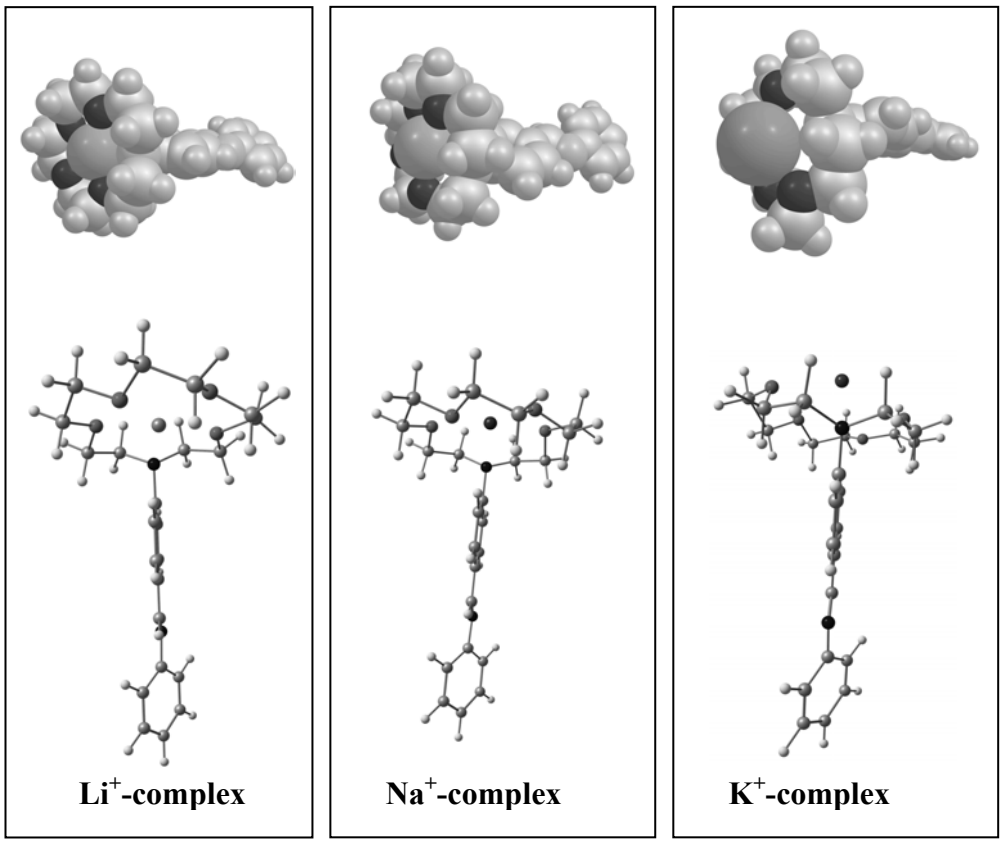

Fig. 3. Two projections of the B3LYP/6-31G(d) calculated structures of N-(4-benzalaniline)-15-crown-5 complexes (M^{+}–L1).

Among the alkaline earth cations, magnesium fits to the cavity size of L1 and L2. Calcium is located somewhat below the crown ether ring. Strontium and barium like potassium are located above the crown ether ring. We found that for the smallest Be^{2+} cation (ion radius 0.27 Å [35]) the macrocycle conformation is changed (Fig. 4).

The calculated M^{n+}–O and M^{n+}–N distances (n = 1, 2) are given in Tables 2 and 3. As can be seen, in all cases the M^{n+}–N bonds are longer than the corresponding average M^{n+}–O bonds. These data are indicative of a weaker interaction of M^{n+} with the nitrogen lone electron pair, e.g. the coordination is realized mainly via the oxygen atoms. It should be mentioned also that in the Be^{2+} complex, one of the oxygen atoms (namely O25) practically is not involved in coordination (Tables 2 and 3).

CONCLUSION

The cations, whose size is equal to the size of the macrocycle (Li^{+}, Na^{+}, Mg^{2+}) fit to cavity size of the crown. The Ca^{2+} is situated slightly below the crown ether ring. The cations, whose size is greater than the diameter of the macrocycle cavity (K^{+}, Sr^{2+}, Ba^{2+}) protrude from the macrocycle. The complexation does not change the conformation of the macrocycle. However, the conformation of the crown ether ring is strongly deformed for the complex of the smallest dication (Be^{2+}). The dications are stronger bound to crown ethers than the monocations. The metal–nitrogen distance in the alkali metal complexes are longer than these in alkaline earth ones.

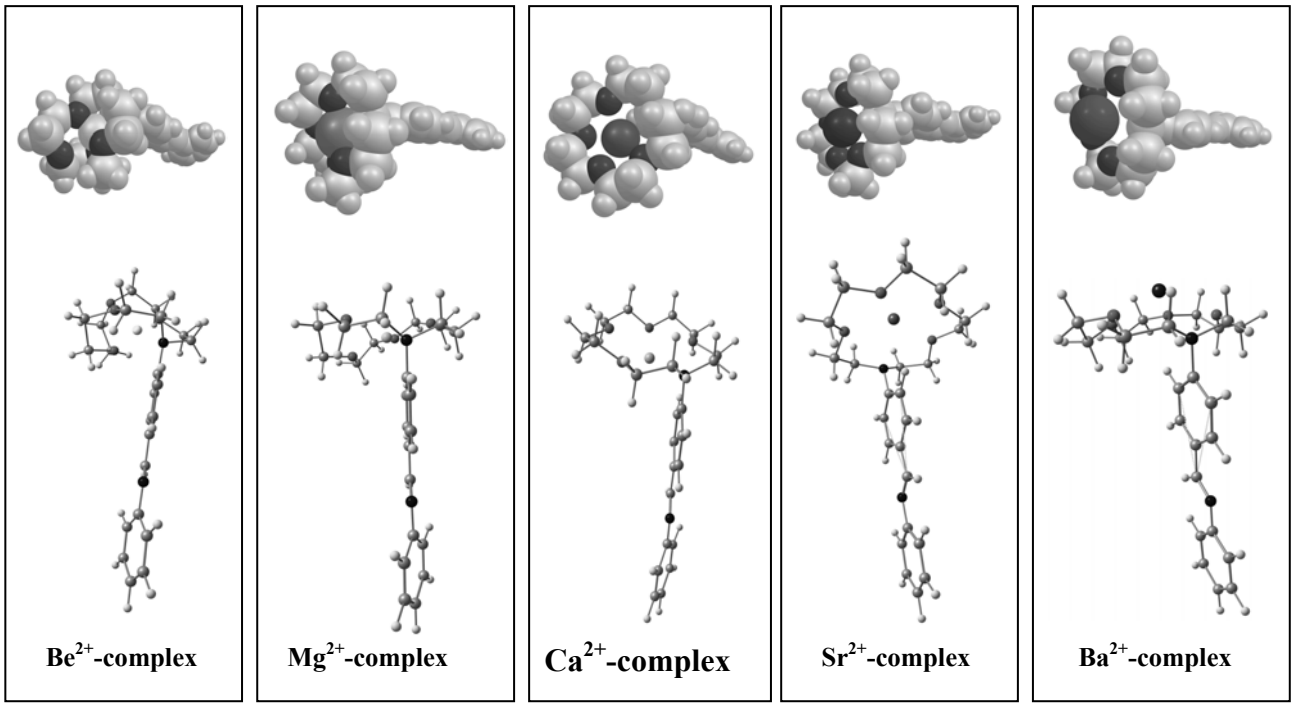

Fig. 4. Two projections of the calculated structures of N-(4-benzalaniline)-15-crown-5 complexes (M^{2+}–L1). Be^{2+}, Mg^{2+} and Ca^{2+} complexes are optimized at B3LYP/6-31G(d) level and Sr^{2+} and Ba^{2+} complexes are optimized at ECP-31G level.

REFERENCES

1. V. Balzani, A. Credi, M. Venturi, *Coord. Chem. Rev.* **171**, 3 (1998).
2. I. K. Lednev, R. E. Hester, J. N. Moore, *J. Phys. Chem. A,* **101**, 7371 (1997).
3. I. K. Lednev, T.-Q. Ye, R. E. Hester, J. N. Moore, *J. Phys. Chem. A,* **101**, 4966 (1997).
4. I. K. Lednev, R. E. Hester, J. N. Moore, *J. Am. Chem. Soc.,* **119**, 3456 (1997).
5. R. Bergonzi, L. Fabrizzi, M. Licchelli, C. Mangano, *Coord. Chem. Rev.,* **170**, 31 (1998).
6. L. F. Lindoy, *Coord. Chem. Rev.,* **174**, 327 (1998).
7. F. Voegtle, Supramolekulare Chemie, 1st Ed., Teubner, Stuttgart, 1989, p. 82.
8. B. Valeur, in: Chemosensors of Ion and Molecule Recognition, Vol. 492, NATO ASI Ser., Ser. C, J.-P. Desvergne, A. W. Czarnik (eds.), Kluwer Academic, Dordrecht, 1997, p. 195.
9. A. P. de Silva, H. Q. N. Gunaratne, T. Gunnlaugsson, A. J. M. Huxley, C. P. McCoy, J. T. Rademacher, T. E. Rice, *Chem. Rev.,* **97**, 1515 (1997).
10. N. Mateeva, V. Enchev, L. Antonov, T. Deligeorgiev, M. Mitewa, *J. Inclusion Phenom. Mol. Recognit. Chem.,* **20**, 323 (1995).
11. A. Boila-Goeckel, W. M. F. Fabian, H. Junek, *Liebigs Ann. Chem.,* 397 (1996).
12. M. Mitewa, N, Mateeva, L. Antonov, *Quim. Anal.,* **16**, 153 (1997).
13. A. Boila-Goeckel, H. Junek, *J. Prakt. Chem.,* **341**, 20 (1999)
14. M. P. Vladimirova, S. D. Simova, E. Stanoeva, M. Mitewa, *Dyes Pigm.*, **50**, 157 (2001).
15. L. Antonov, M. Vladimirova, E. Stanoeva, M. F. F. Fabian, L. Ballester, M. Mitewa, *J. Inclus. Phenom. Macromol. Chem.,* **40**, 23 (2001).
16. A. A. Granovsky, www http://classic.chem.msu.su/gran/gamess/index.html
17. M. W. Schmidt, K. K. Baldridge, J. A. Boatz, S. T. Elbert, M. S. Gordon, J. H. Jensen, S. Koseki, N. Matsunaga, K. A. Nguyen, S. Su, T. L. Windus, M. Dupuis, J. A. Montgomery, *J. Comput. Chem*., **14**, 1347 (1993).
18. W. J. Stevens, H. Basch, M. Krauss, *J. Chem. Phys.,* **81**, 6026 (1984).
19. W. J. Stevens, H. Basch, M. Krauss, P. Jasien, *Can. J. Chem.,* **70**, 612 (1992).
20. A. D. Becke, *J. Chem. Phys.,* **98**, 5648 (1993).
21. R. Ditchfield, W. J. Hehre, J. A. Pople, *J. Chem. Phys.,* **54**, 724 (1971).
22. M. J. Frisch, G. W. Trucks, H. B. Schlegel, G. E. Scuseria, M. A. Robb, J. R. Cheeseman, V. G. Zakrzewski, J. A. Montgomery, Jr., R. E. Stratmann, J. C. Burant, S. Dapprich, J. M. Millam, A. D. Daniels, K. N. Kudin, M. C. Strain, O. Farkas, J. Tomasi, V. Barone, M. Cossi, R. Cammi, B. Mennucci, C. Pomelli, C. Adamo, S. Clifford, J. Ochterski, G. A. Petersson, P. Y. Ayala, Q. Cui, K. Morokuma, P. Salvador, J. J. Dannenberg, D. K. Malick, A. D. Rabuck, K. Raghavachari, J. B. Foresman, J. Cioslowski, J. V. Ortiz, A. G. Baboul, B. B. Stefanov, G. Liu, A. Liashenko, P. Piskorz, I. Komaromi, R. Gomperts, R. L. Martin, D. J. Fox, T. Keith, M. A. Al-Laham, C. Y. Peng, A. Nanayakkara, M. Challacombe, P. M. W. Gill, B. Johnson, W. Chen, M. W. Wong, J. L. Andres, C. Gonzalez, M.

Head-Gordon, E. S. Replogle, J. A. Pople, Gaussian 98, Revision A.11, Gaussian, Inc., Pittsburgh PA, 2001.
23. R. Ditchfield, *Mol. Phys.,* **27**, 789 (1974); K. Wolinski, J. F. Hilton, P. Pulay, *J. Am. Chem. Soc.,* **112**, 8251 (1990).
24. M. J. Frisch, G. W. Trucks, H. B. Schlegel, G. E. Scuseria, M. A. Robb, J. R. Cheeseman, J. A. Montgomery, Jr., T. Vreven, K. N. Kudin, J. C. Burant, J. M. Millam, S. S. Iyengar, J. Tomasi, V. Barone, B. Mennucci, M. Cossi, G. Scalmani, N. Rega, G. A. Petersson, H. Nakatsuji, M. Hada, M. Ehara, K. Toyota, R. Fukuda, J. Hasegawa, M. Ishida, T. Nakajima, Y. Honda, O. Kitao, H. Nakai, M. Klene, X. Li, J. E. Knox, H. P. Hratchian, J. B. Cross, C. Adamo, J. Jaramillo, R. Gomperts, R. E. Stratmann, O. Yazyev, A. J. Austin, R. Cammi, C. Pomelli, J. W. Ochterski, P. Y. Ayala, K. Morokuma, G. A. Voth, P. Salvador, J. J. Dannenberg, V. G. Zakrzewski, S. Dapprich, A. D. Daniels, M. C. Strain, O. Farkas, D. K. Malick, A. D. Rabuck, K. Raghavachari, J. B. Foresman, J. V. Ortiz, Q. Cui, A. G. Baboul, S. Clifford, J. Cioslowski, B. B. Stefanov, G. Liu, A. Liashenko, P. Piskorz, I. Komaromi, R. L. Martin, D. J. Fox, T. Keith, M. A. Al-Laham, C. Y. Peng, A. Nanayakkara, M. Challacombe, P. M. W. Gill, B. Johnson, W. Chen, M. W. Wong, C. Gonzalez, and J. A. Pople, Gaussian 03, Revision B.04, Gaussian, Inc., Pittsburgh PA, 2003.
25. K. Rurack, J. L. Bricks, G. Reck, R. Radeglia, U. Resch-Genger, *J. Phys. Chem. A,* **104**, 3087 (2000).
26. T. Gunnlaugsson, H. Q. N. Gunaratne, M. Nieuwenhuyzen, J. P. Leonard, *J. Chem. Soc. Perkin Trans. 1,* 1954 (2002).
27. M. V. Alfimov, A. V. Churakov, Y. V. Fedorov, O. A. Fedorova, S. P. Gromov, R. E. Hester, J. A. K. Howard, L. G. Kuz'mina, I. K. Lednev, J. N. Moore, *J. Chem. Soc. Perkin Trans. 2,* 2249 (1997).
28. M. Asakawa, P. R. Ashton, S. Iqbal, J. F. Stoddart, N. D. Tinker, A. J. P. White, D. J. Williams, *Chem. Commun.,* 483 (1996).
29. J. T. Bien, M. Shang, B. D. Smith, *Acta Crystallogr. Sect. C,* **52**, 183 (1996).
30. P. D. Beer, Zheng Chen, M. G. B. Drew, A. J. Pilgrim, *Inorg. Chim. Acta,* **225**, 137 (1994).
31. F. D. Sokolov, N. G. Zabirov, V. V. Brusko, D. B. Krivolapov, I. A. Litvinov, *Mendeleev Commun.,* 72 (2003).
32. A. Ya. Freidzon, A. A. Bagatur'yants, S. P. Gromov, M. V. Alfimov, *Int. J. Quant. Chem.,* **100**, 617 (2004).
33. K. Goubitz, C. A. Reiss, D. Heijdenrijk, *Acta Crystall. C*, **45**, 1364 (1989).
34. J. S. Bradshaw, R. M. Izatt, A. V. Bordunov, C. Y. Zhu, J. K. Hathaway, in: Comprehensive Supramolecular Chemistry, Molecular Recognition: Receptors for Cationic Guests, vol. 1, G. W. Gokel (Ed.), Pergamon, Elsevier, Oxford, 1996, Chap. 2,.
35. R. B. Martin, in: Metal Ions in Biological Systems, Vol. 26, H. Siegel, A. Siegel (eds.), Marcel Dekker, NY, 1990, Ch.. 1.

ИЗСЛЕДВАНЕ С МЕТОДИТЕ *AB INITIO* И ТФП НА СТРУКТУРАТА НА КОМПЛЕКСИ НА N-БЕНЗАЛАНИЛИН-15-КРАУН-5 С МЕТАЛНИ ЙОНИ

В. Енчев[1]*, С. Ангелова[1], Н. Маркова[1], Ив. Вавер[2], Ел. Станоева[3], М. Митева[3]

[1] B g k l b l m i h h j] Z g b o q b Z b k y p _ g l t j h n b l h o b f b y e] Z j k Z d Z Z ^ _ f b Z g Z m d, b. 113 K h n b y
[2] N Z j f Z p _ \ l b m q Z g m e, l < Z j r Z \ k f d _ b ^ b p b g m k g Z \ _ j k b k Z l j r Z, \ Z h e r Z
[3] O b f b q _ k Z b m e, l K h n b c k m g b \ _ j k b [m e > ` _ c f k Z m q ^ j 1, 1164 K h n b y

l h k \ _ l _ g Z Z d Z B \ Z g o g h \ k i d h b h \ h g Z 0 - l Z f m] h ^ b r g b g Z

Постъпила на 30 януари 2008 г.; Преработена на 7 февруари 2008 г.

(Резюме)

Структурите на N-(4-бензаланилин)-15-краун-5 и N-(4'-бензаланилин)-15-краун-5 и техните Li^+, Na^+, K^+, Be^{2+}, Mg^{2+}, Ca^{2+}, Sr^{2+} и Ba^{2+} комплекси са оптимизирани чрез използване на методите *ab initio* и ТФП. Намерено е, че във всички случаи разстоянията M^{n+}–N (n = 1, 2) са по-дълги от средните разстояния M^{n+}–O в съответните комплекси и, че разстоянията метал–азот при комплексите на алкалните метали са по-дълги от тези при алкалоземните. Li^+, Na^+, Mg^{2+} и Ca^{2+} катиони пасват на размера на кухината на макроцикъла, докато катионите K^+, Sr^{2+} и Ba^{2+}, чийто размер е по-голям от нейния диаметър, са извън равнината на макроцикъла. Във всички случаи конформацията на коронния етер не се променя. Изключение е комплексът с Be^{2+}, при който макроцикълът е силно деформиран.

Bulgarian Chemical Communications, Volume 40, Number 4 (pp. 538–545) 2008

IR spectra and structure of 3,5,5-trimethyl(cyclohex-2-enylidene) malononitrile and its potassium cyanide and sodium methoxide carbanionic adducts: experimental and B3LYP studies

S. S. Stoyanov*, A. D. Popova, J. A. Tsenov

Department of Structural Organic Analysis, Institute of Organic Chemistry with Centre of Phytochemistry, Bulgarian Academy of Sciences, Acad. G Bonchev St., Block 9, 1113 Sofia, Bulgaria

Dedicated to Academician Ivan Juchnovski on the occasion of his 70th birthday

Received January 31, 2008; Revised February 4, 2008

A combined IR experimental/B3LYP computational approach has been applied to follow the formation and isomerization of potassium cyanide and sodium methoxide carbanionic adducts of 3,5,5-trimethyl(cyclohex-2-enylidene) malononitrile **1.** A good agreement has been found between theoretical and experimental IR data. In agreement between theory and experiment, **1** forms β- and δ-adducts with the above-mentioned nucleophiles. Structural changes, caused by conversion of **1** into β- and δ-adducts, have also been studied. According to the computations, the chemical motive force in the β→ δ isomerization is the much higher stability (by ca. 50 kJ·mol^{-1}) of the δ-adducts compared to β-ones.

Key words: IR, DFT B3LYP, 3,5,5-trimethyl(cyclohex-2-enylidene) malononitrile, adducts, carbanion, isomerization.

INTRODUCTION

3,5,5-trimethyl(cyclohex-2-enylidene) malononitrile (TMCHM, **1**) was prepared by Lemke in 1970 as a precursor in the Knoevenagel-type synthesis of a large series of its 12-ylidene derivatives [1–3].

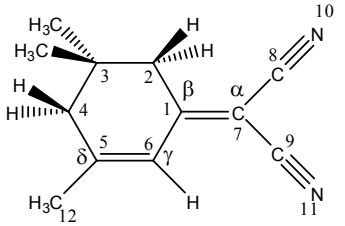

1

These derivates are high-quality dyes for synthetic polymers [4] (and references there in); some of these dyes have solvatochromic properties [1–3]. Nowadays, 12-ylidene derivates of **1** are of special interest as non-linear optical [4–15] and fluorescent [7] materials. We did not find in the literature detailed vibrational studies of **1** itself; some 12-ylidene derivates of **1** have been studied thoroughly by IR [5–7], polarized IR [6] and Raman [5] spectra, B3LYP quantum-chemical calculations [5, 7] and single-crystal X-ray diffraction [8–15].

On the other hand, it is well-known [16] that nucleophilic attacks to C=C bonds are favoured by electron-accepting substitutients, where A, Nu$^-$ and E$^+$ are the acceptor, nucleophile and electrophile, respectively.

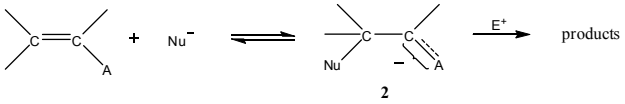

2

When the nucleophilic attacks take place in aprotic solvents (E$^+$ is usually H$^+$), the intermediate adducts **2** have been isolated in many cases [17–23]. Both sodium methoxide (Nu$^-$≡CH$_3$O$^-$) [22-23] and potassium cyanide (Nu$^-$≡CN$^-$) [24–27] carbanionic adducts of benzylidenemalononitrile [22] and other strongly polarized alkenes [21–28], butadienes and hexatrienes [22] have been studied. Nucleophilic attacks by uncharged Lewis bases Nu: result in the formation of zwitterions **3.**

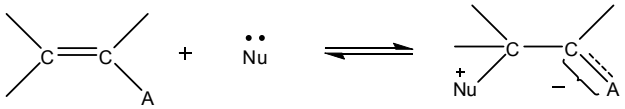

3

This result has been established in cases of tertialy phosphine adducts (**3**, Nu$^-$≡R$_3$P:) of benzylidenemalononitrile by IR [29–31], NMR [32] and confirmed by X-ray diffraction [33]. The heptylamine zwitterionic adduct (Nu$^-$≡C$_7$H$_{15}$NH$_2$) of the same compound has also been studied by IR spectra [24]. Juchnovski *at al*. [22] found 30 years ago that 1,1-dicyano-4-phenylbutadiene **4** and other strongly polarized conjugated butadienes react with CH$_3$O$^-$Na$^+$ to form the β-adduct **5**. Within 24 hours, however, **5** isomerizes spontaneously and practically completely into the corresponding δ-adduct **6**.

* To whom all correspondence should be sent:
E-mail: cacafuego@abv.bg

© 2008 Bulgarian Academy of Sciences, Union of Chemists in Bulgaria

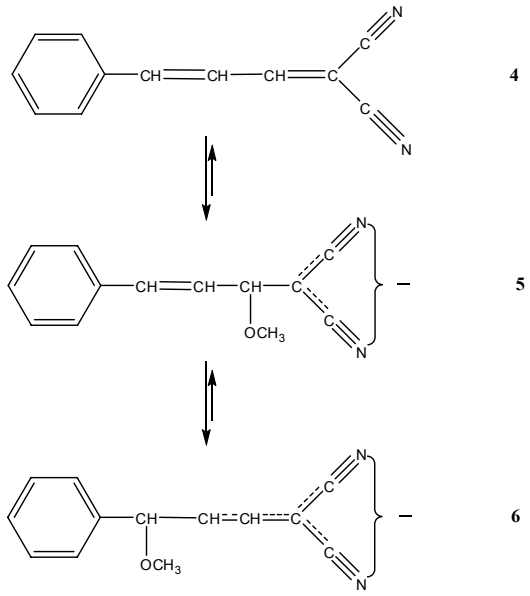

The authors [22] supposed that the **5→6** isomerization was provoked by the higher stability of **6**, due to larger delocalization of the carbanionic charge in **6** compared to **5.** This supposition was confirmed by *ab initio* HF calculations: The δ-adduct **6** is by 28.2 kJ·mol^{-1} more stable than the β-adduct **5**. The title compound **1** is an analogue of **4**, so it was of interest to check whether and what kind of adducts would be formed by the reaction of **4** with potassium cyanide and sodium methoxide.

EXPERIMENTAL

Compound **1** was prepared by the classical Gelmo's method [1] and a sample of it was given to us by Kolev *et al*. [5]. The cyanide and methoxide were prepared by adding DMSO/DMSO-d_6 solutions of **1** to excess of dry KCN and $NaOCH_3$, respectivelly, under argon. After 1 min intense stirring, the reaction mixtures were separated by syringe-filter and the clear adduct solutions were put immediately into a CaF_2 cell of 0.129 mm path length. The IR spectra were recorded on Bruker IFS 113v and Tensor 27 FT spectrometers at a resolution of 1 cm^{-1} and 64 scans.

COMPUTATIONS

The Gaussian 98 program package [34] was used for Density Functional Theory (DFT, full optimization) computations of energies, structures and IR spectra of the species studied. This theory is the groundwork of a series of cost-effective methods to approximate electron correlation effects [35]. We have employed the B3LYP functional, which combines Becke's three-parameter non-local exchange with the correlation functional of Lee, Yang and Parr [36, 37], adopting a 6-31++G** basis set with any symmetry restrictions. For each structure, the stationary points found on the molecular potential energy hypersurfaces were characterized using the standard analytical harmonic procedure. The absence of irrational frequencies or negative eigenvalues of the second-derivative matrix confirmed that the stationary points corresponded to global minima on the potential energy surfaces [35]. A standard least-square program was used for calculating the single-parameter linear regression indices.

RESULTS AND DISCUSSION

Correlation analysis

Comparison of the native B3LYP/6-31++G** vibrational frequencies of TMCHM **1** with those measured in DMSO solvent (see *Spectral analysis* below) resulted in the formation of an excellent (0.99 <R < 1) correlation (Eqn. 1):

$$\nu(\text{exp.}) = 0.93373\ \nu(\text{theor.}) + 55.75\ \ (\text{cm}^{-1}) \quad (1)$$

Correlation coefficient R = 0.99994; Standard deviation S.D. = 8.94 cm^{-1}; Number of data points n = 34.

Eqn. (1) was used for correlational scalling [38] of the theoretical frequencies. As stated in Alcolea's review article [39] (and references therein), the use of scaling equations instead of scaling factors gave better results, especially in the low-frequency region. For more recent works see [40–49] (and references therein).

Spectral analysis

Our theoretical and experimental IR data for **1** are compared in Table 1 together with the approximate description of the corresponding vibrations.

There is nothing special in the data for the CH stretching vibrations, (Nos. 1–14 in Table 1). As it could be expected [50], the ν(=C–H) vibration was the most high-frequency one among them. We found in the experimental spectra a single moderate band in the ν(C≡N) region, without shoulders or satellites, at 2223 cm^{-1}. The calculations predict a small splitting $\Delta\nu(C{\equiv}N)_2 = \nu^{s}(C{\equiv}N)_2 - \nu^{as}(C{\equiv}N)_2$ of 13 cm^{-1} (Table 1, vibrations 15 and 16). The real splitting is probably even smaller, so we assign the band at 2223 cm^{-1} as a superposition of the ν^{s}(C≡N) and ν^{as}(C≡N) bands like in the cases of dozens of ylidenemalonitriles [22–24, 51] (and references therein). The strongest bands in the spectrum of TMCHM at 1614 and 1545 cm^{-1} correspond to the endo- and exocyclic ν(C=C) vibrations (Table 1, vibrations 17 and 18).

Table 1. Theoretical (B3LYP 6-31++G**) and experimental (solvent DMSO / DMSO-d_6) frequencies (ν in cm^{-1}) and integrated intensities (A in $km \cdot mol^{-1}$) of TMCHM molecule **1**.

No.	B3LYP6-31++G**				Experimental data [a]	
	ν	ν [b]	A	Approximate description [c]	ν	A [d]
1	3189	3034	3.7	ν(=C–H)	3030	vw
2	3131	2979	14.8	$\nu^{a}(CH_3)$	- [e]	-
3	3116	2966	25.8	$\nu^{as}(CH_3)$	2962	m
4	3108	2958	40.4	$\nu^{as}(CH_3)$	2962	m
5	3103	2953	11.8	$\nu^{as}(CH_3)$	2962	m
6	3101	2951	21.1	$\nu^{as}(CH_3)$	2962	m
7	3099	2949	3.4	$\nu^{as}(CH_2)$	2962	m
8	3073	2925	11.1	$\nu^{as}(CH_3)$	2936	vw
9	3047	2900	30.7	$\nu^{as}(CH_2)$	2902	w
10	3039	2894	13.8	$\nu^{s}(CH_3)$	2902	w
11	3031	2886	33.0	$\nu^{s}(CH_3)$	2871	w
12	3025	2880	23.0	$\nu^{s}(CH_3)$	2871	w
13	3011	2867	9.9	$\nu^{s}(CH_2)$	- [e]	-
14	2995	2852	18.1	$\nu^{s}(CH_2)$	2828	vw
15	2330	2232	73.3	$\nu^{s}(C\equiv N)_2$	2223	47.5
16	2317	2219	30.1	$\nu^{as}(C\equiv N)_2$	2223	47.5
17	1668	1613	187.5	$\nu(C=C)^{endo}$	1614	78.9
18	1579	1530	148.3	$\nu(C=C)^{exo}$	1545	70.1
19	1517	1473	8.5	$\delta^{as}(CH_3)$	1470	2.1
20	1512	1467	5.4	$\delta^{as}(CH_3)$	- [e]	-
21	1500	1456	5.5	$\delta^{as}(CH_3)$	1450	sh
22	1492	1449	1.8	$\delta^{as}(CH_3)$	- [e]	-
23	1486	1444	15.6	$\delta^{as}(CH_3)$	1439	w
24	1481	1439	11.1	$\delta^{as}(CH_3)$	1439	w
25	1475	1433	2.6	$\delta^{sciss}(CH_2)$	- [e]	-
26	1464	1422	11.2	$\delta^{sciss}(CH_2)$	1416	w
27	1432	1393	5.8	$\delta^{s}(CH_3)$	-[e]	-
28	1419	1381	12.2	$\delta^{s}(CH_3)$	1386	m
29	1411	1373	10.8	$\delta^{s}(CH_3)$	1370	w
30	1404	1367	9.2	δ(CH)	1350	vw
31	1373	1337	7.6	(delocalized)	- [e]	-
32	1352	1318	25.1	ν(C–C)(ring)	1326	m
33	1320	1288	3.5	$\gamma^{wag}(CH_2)$	1286	w
34	1317	1285	3.2	$\gamma^{wag}(CH_2)$	1286	w
35	1285	1256	0.2	ν(C–C)(ring)	- [e]	-
36	1223	1197	2.9	ν(C–CH_3), δ(C–C)(ring)	1201	vw
37	1199	1175	6.8	ν(C–C≡N)	1183	vw
38	1188	1165	4.0	ν(C–C)(ring), $\gamma(CH_2)$	1163	vw
39	1166	1144	5.1	ν(C–CH_3), δ(CC)(ring)	1149	vw
40 [f]	1156	1135	8.1	ν(C–CH_3)	1135	vw

a - Measured after having decomposed the complex bands into components; b - Scaled, according to correlation Eqn. (1); c - Vibrational modes: ν, stretching; δ, in-plane bending; γ, out-of-plane bending; superscripts: s, symmetrical; as, asymmetrical; sciss, scissoring; wag, wagging; endo, endocyclic; exo, exocyclic; d - Relative intensities: m, moderate; w, weak; v, very; sh, shoulder; e - These bands were not detected in the experimental spectrum; f - Followed by 38 lower-frequency vibrations.

TMCHM **1** reacts rapidly with KCN and $NaOCH_3$. The bands of the starting compound **1** disappear and a few new bands appear in the IR spectra. So, let us consider the data in Table 2. The new bands are like the bands in the spectra of adducts of cinnamylidenemalononitrile [22–24]. Immediately after reacting **1** with KCN, we can see in the spectrum four very strong and two weak bands in the ν(C≡N) region (See also Fig. 1). Having in mind that the adduct **A** shows lower-frequency bands than **B** (as predicted by computations) as well as that the bands of **A** fade away on account of these of **B**, we assume that **A** and **B** (Table 2) are β- and δ-cyanide adducts of **1** respectively. The spectra show practically a full conversion of the β-cyanide adduct into the δ-one within 60 min. (Fig. 1). The weak bands above 2200 cm^{-1} of **A** and **B** (Table 2) correspond to the new (added) non-conjugated cyano group.

Table 2. Theoretical (B3LYP 6-31++G**) and experimental (solvent DMSO) cyano stretching IR frequencies (ν in cm^{-1}) and integrated intensities (A in $km \cdot mol^{-1}$) of cyanide and methoxide carbanionic adducts of TMCHM.

No.	B3LYP 6-31++G **				Experimental data [a]	
	ν	ν [b]	A	Approximate description [c]	ν	A [d]
β-cyanide adduct						
15 [e]	2298	2202	43.3	ν(C≡N) [f]	2210	w[g]
16	2242	2149	157.0	$\nu^{s}(C\equiv N)_2$	2163	vs[g]
17 [h]	2192	2103	613.6	$\nu^{as}(C\equiv N)_2$	2101	vs[g]
δ-cyanide adduct						
15 [e]	2307	2210	44.2	$\nu(C\equiv N)_2$	2219	9.7
16	2259	2165	334.4	$\nu^{s}(C\equiv N)_2$	2163	115.7
17 [h]	2217	2126	493.4	$\nu^{as}(C\equiv N)_2$	2119	193.6
β-methoxide adduct						
18 [i]	2241	2148	229.8	$\nu^{s}(C\equiv N)_2$	– [j]	–
19 [k]	2194	2104	603.8	$\nu^{as}(C\equiv N)_2$	– [j]	–
δ-methoxide adduct						
18 [i]	2256	2162	321.1	$\nu^{s}(C\equiv N)_2$	2163	151.0
19 [k]	2214	2123	503.3	$\nu^{as}(C\equiv N)_2$	2120	212.9
6. δ-methoxide adduct of cinnamethylidene-malononitrile [24]						
12 [l]	2445[m]	2183[m]		$\nu^{s}(C\equiv N)_2$	2164	110.1
13 [n]	2398[m]	2141[m]		$\nu^{as}(C\equiv N)_2$	2123	220.4

a - Measured after having decomposed the complex bands into components; b - Scaled, according to correlation Eqn. (1); c - Vibrational modes: ν, stretching; superscripts: s, symmetrical; as, asymmetrical; d - Relative intensities: w, weak; vs, very strong; e - Preceded by 14 ν(C–H) vibrations; f - Bands of the new (additionally introduced) cyano group; g - We have not measured spectra of this adduct with the absence of bands of corresponding δ – cyanide adduct; h - Followed by 67 lower-frequency vibrations; i - Preceded by 17 ν(C–H) vibrations; j - We did not find measurable amounts of this adduct; k - Followed by 74 lower-frequency vibrations; l - Preceded by 11 ν(C–H) vibrations; m - HF/6-31G [24]; n Followed by 63 lower-frequency vibrations.

The formation of **D** or the **C→D** isomerization was so rapid, that we were not able to detect other bands in the spectrum measured immediately after the reaction. In agreement between theory and experiment, the only adduct, registered in this case, was **D** (Table 2). This statement could be confirmed by experimental data for the δ-methoxide adduct of cinnamylidenemalononitrile [24] (**6** in Table 2): **D** and **6** show very close cyano stretching frequencies and close intensities.

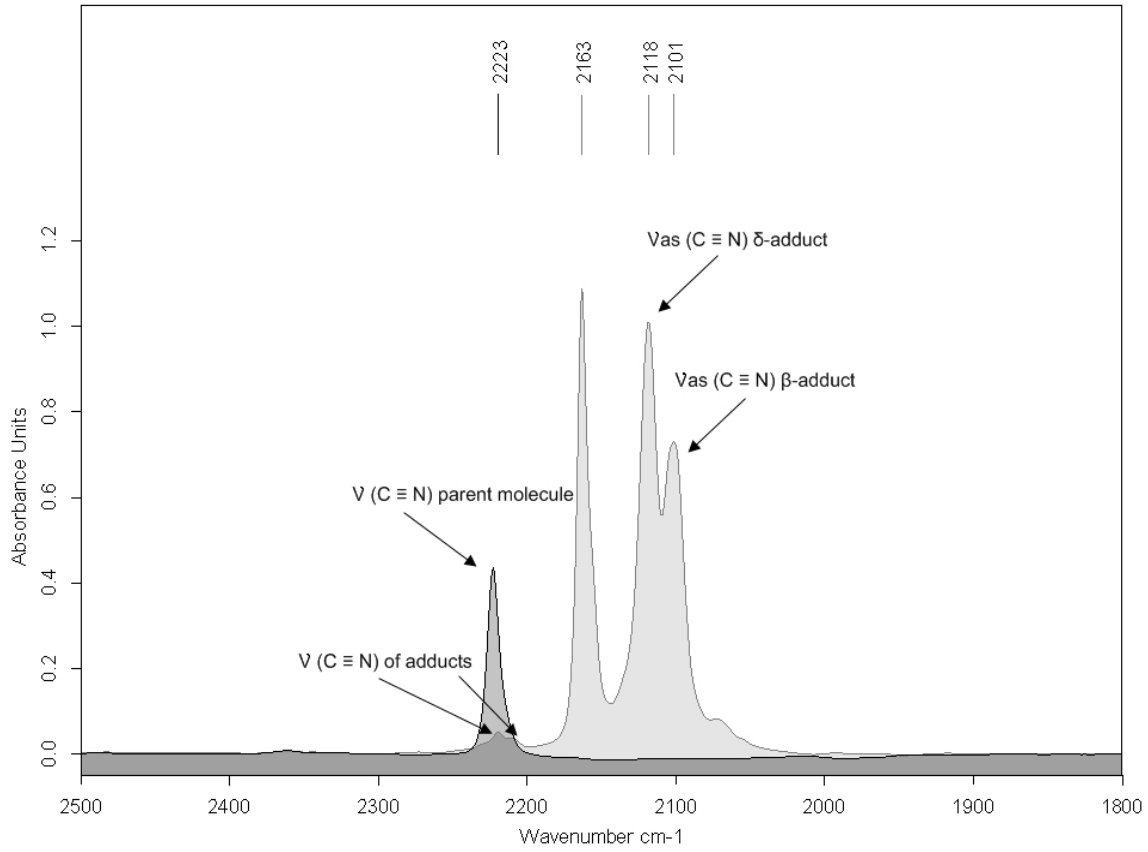

Fig. 1. IR spectra of TMCHM **1** (doubly shaded) and of its β- and δ-cyanide adducts.

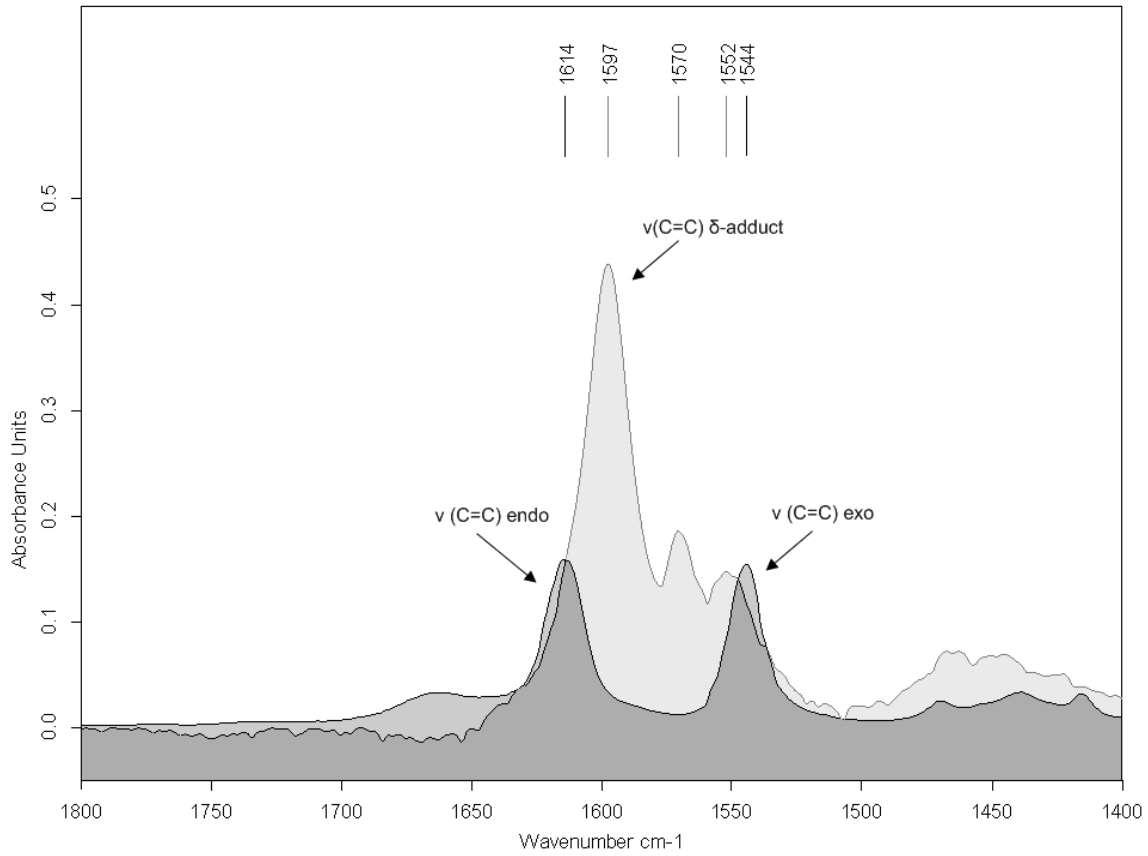

Fig. 2. IR spectra of TMCHM **1** (doubly shaded) and of its δ- methoxide adduct.

Table 3. Theoretical (B3LYP 6-31++G**) and experimenttal (solvent DMSO/DMSO-d_6) frequencies (ν in cm^{-1}) and integrated intensities (A in $km \cdot mol^{-1}$) of δ-methoxide adduct of TMCHM.

No	B3LYP/6-31++G**				Experimental data [a]	
	ν	N [b]	A	Approximate description	ν	A [d]
1	3153	3000	15.5	ν(CH)	3009	w
2	3133	2981	15.8	$\nu^{as}(CH_3)$	- [e]	-
3	3125	2974	33.5	$\nu^{as}(CH_3)$	- [e]	-
4	3103	2953	46.6	$\nu^{as}(CH_3)$	2952	m, br
5	3097	2948	46.4	$\nu^{as}(OCH_3)$	2952	m, br
6	3087	2938	62.7	$\nu^{as}(CH_3)$	- [e]	-
7	3081	2933	76.4	$\nu^{as}(CH_3)$	- [e]	-
8	3076	2928	9.9	$\nu^{as}(CH_3)$	- [e]	-
9	3071	2923	5.3	$\nu^{as}(CH_3)$	- [e]	-
10	3062	2915	19.9	$\nu^{as}(CH_3)$	2910	w, br
11	3053	2906	60.0	$\nu^{as}(CH_3)$	2910	w, br
12	3033	2888	91.9	$\nu^{s}(CH_3)$	- [e]	-
13	3025	2880	66.5	$\nu^{s}(CH_3)$	2865	w
14	3017	2872	46.7	$\nu^{s}(CH_3)$	2865	w
15	3012	2868	29.3	$\nu^{s}(CH_3)$	2865	w
16	3000	2857	30.9	$\nu^{s}(CH_3)$	- [e]	-
17	2972	2831	70.4	$\nu^{s}(OCH_3)$	2823	w
18	2256	2162	321.1	$\nu^{s}(C\equiv N)$	2163	151.0
19	2214	2123	503.3	$\nu^{as}(C\equiv N)$	2118	212.9
20	1634	1582	394.7	ν(C=C)	1598	386.5
					1571 [f]	w
					1552 [f]	w
21	1523	1478	7.2	$\delta^{as}(CH_3)$	- [e]	vw
22	1515	1471	12.0	$\delta^{as}(OCH_3)$	1467	vw
23	1506	1462	4.5	$\delta^{as}(CH_3)$	1463	w
24	1503	1459	6.9	$\delta^{as}(CH_3)$	1463	w
25	1496	1452	1.6	$\delta^{as}(CH_3)$	1451	w
26	1493	1449	2.9	$\delta^{as}(CH_3)$	1451	w
27	1488	1445	5.1	$\delta^{as}(CH_3)$	1451	vw
28	1486	1443	3.2	$\delta^{as}(OCH_3)$	1451	vw
29	1478	1436	1.5	$\delta^{sciss}(CH_2)$	1425	vw
30	1474	1432	2.8	$\delta^{sciss}(CH_2)$	1425	-
31	1459	1418	3.1	$\delta^{s}(OCH_3)$	1425	m
32	1420	1382	2.8	$\delta^{s}(CH_3)$	- [e]	m
33	1401	1364	17.4	$\delta^{s}(CH_3)$	1365	m
34	1397	1361	44.1		1365	w
35	1396	1359	5.3	$\delta^{s}(CH_3)$	1365	vw
36	1375	1340	5.3	δ(CH)	1345	vw
37	1347	1313	5.3	ν(C–C)	1320	vw
38	1315	1283	5.3	$\nu(C–C(CN)_2)$	1302	vw
39	1312	1280	5.3	ν(C–C)	1302	m
40	1294	1264	2.3	ν(C–C)	1270	w
41	1282	1253	115.8	ν(C–C)	1266	vw
42	1255	1228	17.7	$\nu(C–C(CN)_2)$	1226	vw
43	1218	1193	4.7	ν(C–C)	1206	vw
44	1198	1174	30.2	ν(C–C)	1185	vw
45	1193	1170	13.0	ν(C–C)	1148	vw
46	1172	1150	1.4	$\tau(OCH_3)$	1138	vw
47 [g]	1165	1144	10.0	ν(C–C)	1138	vw

a - Measured after having decomposed the complex bands into components; b - Scaled, according to correlation Eqn. (1); c - Vibrational modes: ν, stretching; δ, in-plane bending; γ, out-of-plane bending; τ, torsion; superscripts: s, symmetrical; as, asymmetrical; sciss, scissoring; wag, wagging; d - Relative intensities: m, moderate; w, weak; v, very; sh, shoulder; br, broad; e - These bands were not detected in the experimental spectrum; f - The origin of these bands is not known; g - Followed by 46 lower-frequency vibrations.

Table 3 contains detailed IR data for the δ-methoxide adduct of **1**. We shall put special emphasis on the band at 1598 cm^{-1}. It is the strongest one in the spectrum with A of 386.5 $km \cdot mol^{-1}$ (see also Fig. 2), and corresponds to the vibration of the newly formed quasi-double $C^1{=}{-}{-}{-}C^6$ bond, which is strongly polarized by the $C(CN)_2^-$ group.

Structural analysis

The shapes of TMCHM **1** and of its β- and δ-cyanide adducts are shown on Figure 3.

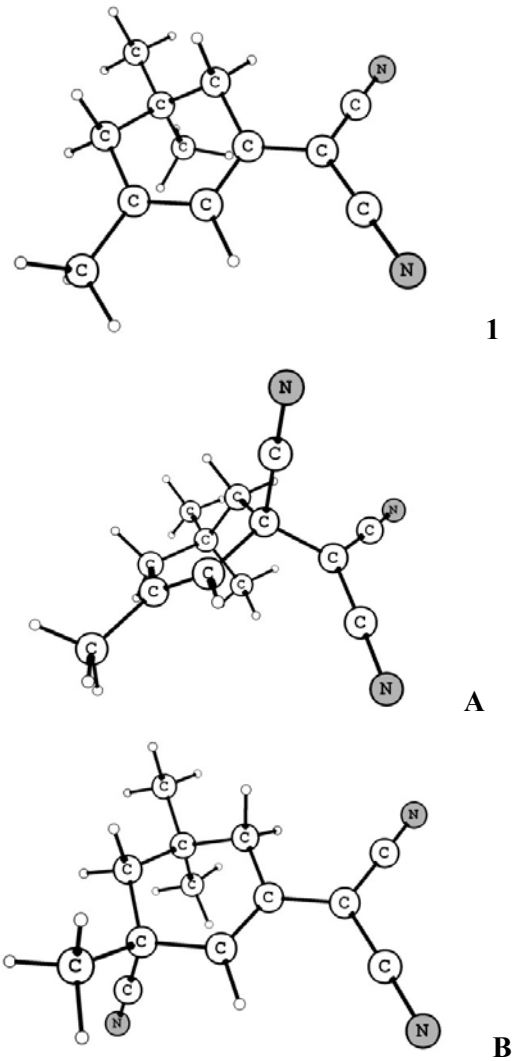

Fig. 3. B3LYP/6-31++G** optimized structures of TMCHM **1** and of its β- and δ-cyanide adducts (**A** and **B** in Table 2).

It is seen there that the conversion of **1** into adducts is not accompanied by essential changes in the general form of the parent molecule. However, the structural elements in the fragment, where the reactions take place, undergo essential variations (Table 4). Big changes in the bond length take place in cases when double or quasi-double bonds become single ones and *vise versa*, *e.g.* R(5,6) and R(1,7).

The biggest bond angle variations take place at atoms, which change their configurations from trigonal (sp^2) into tetrahedral (sp^3), e.g. A(6,1,7) and A(6,5,12).

The net atomic charges (Table 5) are in agreement with the bond length and bond angle variations (cf. Table 4). The largest charge changes take place at those atoms, which alter their configuration in the reaction course (atoms C^1, C^5 and C^6).

Energy analysis

Energy characteristics of the species studied are listed in Table 6. We can see there that δ-adducts of **1** are much more stable than the corresponding β-adducts. The large difference of 49.69 and 53.61 $kJ \cdot mol^{-1}$ between their energies can be assumed as the main groundwork of chemical motive force causing the β→δ isomerizations, like in the case of adducts **6** (Table 2).

Table 4. Selected bond lengths R (Å) and bond angles A (degrees) of TMCHM and its cyanide and methoxide adducts.

Bonds and angles [a]	Mole-cule	β-cyanide adduct	β-methoxide adduct	Δ [b]	δ-cyanide adduct	δ-methoxide adduct	∇ [c]
R(5,6)	1.356	1.339	1.341	–0.017	1.516	1.500	**0.160**
				–0.015			**0.144**
R(5,12)	1.501	1.508	1.509	0.007	1.555	1.538	0.054
				0.008			0.037
R(6,1)	1.445	1.525	1.513	0.080	1.363	1.363	–0.082
				0.068			–0.082
R(1,7)	1.378	1.542	1.510	**0.164**	1.453	1.454	0.075
				0.132			0.076
R(7,8)	1.431	1.399	1.406	–0.032	1.410	1.411	–0.021
				–0.025			–0.020
R(8,10)	1.165	1.179	1.178	0.014	1.176	1.175	0.011
				0.013			0.010
A(1,6,5)	122.4	124.9	125.5	2.5	125.0	125.7	2.6
				3.1			3.3
A(1,7,8)	121.9	119.6	120.2	–2.3	121.7	122.0	–0.2
				–1.7			0.1
A(6,1,7)	121.3	110.9	110.4	**–10.4**	123.3	123.8	2.0
				–10.9			2.5
A(6,5,12)	121.6	121.5	121.9	–0.1	110.3	111.3	**–11.3**
				0.3			**–10.3**

a - Atom numbering according to Formula **1** in Introduction; b - Δ = value (β-adduct) – value (molecule) in the order: cyanide adduct, methoxide adduct; c - ∇ = value (δ-adduct) – value (molecule) in the above order. The largest $|\Delta|$ and $|\nabla|$ values are given in bold.

Table 5. Net Mulliken charges on selected atoms in TMCHM and its adducts.

Atoms	Molecule	β-cyanide adduct	β-methoxide adduct	Δ [b]	δ-cyanide adduct	δ-methoxide adduct	∇ [c]
1	1.30	0.33	0.39	**–0.98**	1.29	1.44	–0.01
				–0.92			0.14
5	0.66	0.43	0.30	–0.23	0.64	0.32	–0.34
				–0.36			**–0.98**
6	–1.01	–0.05	–0.31	**0.96**	–0.36	–0.37	**0.65**
				0.70			**0.64**
7	0.75	0.98	0.20	0.23	0.50	0.48	–0.25
				–0.55			–0.27
8	–0.23	–0.52	–0.39	–0.28	–0.20	–0.34	0.03
				–0.15			–0.11
9	–0.34	–0.23	–0.35	0.12	–0.38	–0.28	–0.04
				–0.01			0.07
10	–0.48	–0.55	–0.60	–0.07	–0.63	–0.64	–0.15
				–0.14			–0.16
11	–0.50	–0.58	–0.61	–0.08	–0.62	–0.62	–0.13
				–0.10			–0.12

a - Atom numbering according to Formula **1** in Introduction; b - Δ = value (β-adduct) – value (molecule) in the order: cyanide adduct, methoxide adduct; c - ∇ = value (δ-adduct) – value (molecule) in the above order. The largest $|\Delta|$ and $|\nabla|$ values are given in bold.

Table 6. Total energies (E in hartree) of TMCHM molecule, its cyanide and methoxide adducts and energy differences (ΔE in kJ·mol^{-1}) between the corresponding β- and δ-adducts.

Species	E	ΔE [a] $= E_\delta - E_\beta$
TMCHM (**1**)	–575.213306	-
TMCHM – β-CN^- adduct	–668.119159	49.69
TMCHM – δ-CN^- adduct	–668.137592	-
TMCHM – β-CH_3O^- adduct	–690.395773	53.61
TMCHM – δ-CH_3O^- adduct	–690.415380	-

a - Corrected with zero-point vibrational energies (ZPVE).

CONCLUSIONS

The combined IR experimental/B3LYP computational approach, applied in the present work, made it possible both to prove the conversion of 3,3,5-trimethyl(cyclohex-2-enylidene)malononitrile into potassium cyanide and sodium methoxide adducts, as well as the chemical motive force which is the main groundwork of the β-adduct→δ-adduct isomerizations: the much higer stability (i.e. lower total energy) of the δ-adducts, compared to the β -ones.

Acknowledgements: *The authors thank the Prof. I. G. Binev for the useful discussion. The authors also thank Prof. Ts. M. Kolev, Dr. D. Y. Yancheva and Dr. B. A. Stamboliyska for providing us with a sample of* ***1****. The financial support by the Bulgarian Council of Scientific Research for Project Chem. – 1510 is gratefully acknowledged.*

REFERENCES

1. R. Lemke, *Chem. Ber*., **103,** 1168 (1970).
2. R. Lemke, *Chem. Ber.*, **103,** 1894 (1970).
3. R. Lemke, *Synthesis,* 359 (1974).
4. D. Y. Yancheva, Ph.D.Thesis*,* Inst. Org. Chem., Bulg. Acad. Sci., Sofia, 2003.
5. T. M. Kolev, D. Y. Yancheva, B. A. Stamboliyska, *Spectrochim. Acta. A*, **59**, 3325 (2003).
6. B. B. Ivanova, *Spectrochim. Acta Part A,* **65**, 1035 (2006).
7. X, Liu, H. Ju, X. Zhao, X. Tao, W. Bian, M. Jiang, *J. Mol. Struct. (TEOCHEM),* **770**, 73 (2006).
8. T. M. Kolev, D. Y. Yancheva, D. C. Kleb, *Z. Krist.-New Cryst. ST,* **216,** 67 (2001).
9. T. Kolev, Z. Glavcheva, D. Yancheva, M. Schuerman, D. C. Cleb, H. Prent, P. Bleckmann, *Acta Crystallogr.,* **E57**, 561 (2001).
10. T. Kolev, Z. Glavcheva, D. Yancheva, *Acta Crystallogr.,* **E57**, 760 (2001).
11. T. Kolev, Z. Glavcheva, M. Schuerman, *Acta Crystallogr.,* **E57**, 964 (2001).
12. T. Kolev, Z. Glavcheva, D. Yancheva, *Acta Crystallogr.,* **E57**, 966 (2001).
13. T. Kolev, Z. Glavcheva, M. Schuerman, *Acta Crystallogr.,* **E57**, 1166 (2001).
14. T. Kolev, D. Yancheva, M. Schuerman, *Acta Crystallogr.,* **E58**, 1093 (2002).
15. T. Kolev, D. Yancheva, B. Shivachev, R. Petrova, M. Spiteler, *Acta Crystallogr.,* **E58**, 1093 (2002).
16. S. Patai, Z. Rappoport, in: The Chemistry of the Alkenes, S. Patai (Ed.), Interscience, London, 1964, Ch. 8.
17. D. J. Kroeger, R. Stewart, *Can. J. Chem.,* **45**, 2163 (1967).
18. R. Stewart, D. J. Kroeger, *Can. J. Chem.,* **45**, 2173 (1967).
19. C. A. Fyfe, *Can. J. Chem.,* **47**, 2331 (1969).
20. I. N. Juchnovski, I. G. Binev, *Tetrahedron Lett.,* 3645 (1974).
21. I. G. Binev, I. N. Juchnovski, *Commun. Dept. Chem. Bulg. Acad. Sci.,* **9**, 33 (1976).
22. I. N. Juchnovski, I. G. Binev, *Bull. Soc. Chim. Belg.* **86**, 793 (1977).
23. I. N. Juchnovski, V. B. Radomirska I. G. Binev, *Commun. Dept. Chem. Bulg. Acad. Sci.*, **14**, 147 (1981).
24. I. G. Binev, Y. I. Binev, B. A. Stamboliyska, I. N. Juchnovski, *J. Mol. Struct.,* **435,** 235 (1997).
25. E. A. Velcheva, I. E. Bineva, I. N. Juchnovski, C. R. *Acad. Bulg. Sci.*, **51,** 41 (1998).
26. E. A. Velcheva, Y. I. Binev, M. J. Petrova, *J. Mol. Struct.,* **475**, 65 (1999).
27. E. A. Velcheva, *Bulg. Chem. Commun.* **32**, 162 (2000).
28. Z. I. Demireva, I. G. Binev, I. N. Juchnovski, *Tetrahedron Lett.,* 1713 (1972).
29. Z. Rappoport, S. Gerter, *J. Chem. Soc.*, 1360 (1964).
30. D. A. Scola, J. S. Adams, Jr., *J. Chem. Eng. Data,* **15**, 349 (1970).
31. B. A. Arbuzov, N. A Poleznaev, V. S. Vinogradova, I. I. Saydashev, *Izv. Akad. Nauk SSSR, Ser. Khim*., 2762 (1971).
32. C. A. Fyfe, M. Zbozny, *Can. J. Chem.*, **50**, 1713 (1972).
33. G. Ferguson, C. A. Fyfe, W. C. March, *Can. J. Chem.*, **51**, 2794 (1973).
34. M. J. Frisch, G. W. Trucks, H. B. Schlegel, G. E. Scuseria, M. A. Robb, J. R. Cheeseman, V. G. Zakrzewski, J. A. Montgomery, Jr., R. E. Stratmann, J. C. Burant, S. Dapprich, J. M. Millam, A. D. Daniels, K. N. Kudin, M. C. Strain, O. Farkas, J. Tomasi, V. Barone, M. Cossi, R. Cammi, B. Mennucci, C. Pomelli, C. Adamo, S. Clifford, J. Ochterski, G. A. Petersson, P. Y. Ayala, Q. Cui, K. Morokuma, D. K. Malick, A. D. Rabuck, K. Raghavachari, J. B. Foresman, J. Cioslowski, J. V. Ortiz, A. G. Baboul, B. B. Stefanov, G. Liu, A. Liashenko, P. Piskorz, I. Komaromi, R. Gomperts, R. L. Martin, D. J. Fox, T. Keith, M. A. Al-Laham, C. Y. Peng, A. Nanayakkara, C. Gonzalez, M. Challacombe, P. M. W. Gill, B. Johnson, W. Chen, M. W. Wong, J. L. Andres, C. Gonzalez, M. Head-Gordon, E. S. Replogle, J. A. Pople, Gaussian 98, revision A.7; Gaussian, Inc.; Pittsburgh, PA, 1998.
35. T. M. Kolev, E. A. Velcheva, B. A. Stamboliyska, *Int. J. Quant. Chem.,* **102**, 1069 (2005).

36. A. D. Becke, *J. Chem. Phys.* **98**, 5648 (1993).
37. C. Lee, W. Yang, G. R. Parr, *Phys. Rev. Part B,* **37**, 785 (1988).
38. I. G. Binev, J. A. Tsenov, E. A. Velcheva, I. N. Juchnovski, *J. Mol. Struct.,* **344**, 205 (1995).
39. A. Alcolea Palafox, *Recent Res. Dev. Phys*. *Chem.*, **2**, 213 (1998).
40. I. D. Reva, S. V. Ilieva, R. Fausto, *Phys. Chem. Chem. Phys.*, **3**, 4235 (2001).
41. O. Sala, N. S. Gonsalves, L. K. Nada, *J. Mol. Struct.,* **565-566,** 411 (2001).
42. M. K. Georgieva, *Bulg. Chem. Commun.,* **32**, 195 (2003).
43. M. Alcolea Palafox, V. K. Rastogi, L. Mittal, *Int. J. Quant. Chem.,* **94**, 198 (2003).
44. M. K. Georgieva, P. A. Angelova, I. G. Binev, *J. Mol. Struct.*, **692**, 23 (2003).
45. M. K. Georgieva, N. B. Nedelchev, I. N. Juchnovski, *Bulg. Chem. Commun*., **37**, 235 (2005)
46. L. I. Daskalova, I. G. Binev, *Int. J. Quant. Chem.*, **106**, 1338 (2006).
47. A. D. Popova, M. K. Georgieva, O. I. Petrov, K. V. Petrova, E. A. Velcheva, *Int. J. Quant. Chem.*, **107**, 1752 (2007).
48. L. I. Daskalova, E. A. Velcheva, I. G. Binev, *J. Mol. Struct*., **826**, 198 (2007).
49. L. I. Daskalova, *J. Mol. Struct. (THEOCHEM)*, **848**, 9 (2008)
50. G. N. Andreev, Molecular spectroscopy, Plovdiv University Press, 1999 (in Bulgarian).
51. I. G. Binev, E. A. Velcheva, *Spectrosc. Lett.*, **32**, 793 (1999).

ИЧ СПЕКТРИ И СТРУКТУРА НА 3,5,5-ТРИМЕТИЛ(ЦИКЛОХЕКС-2-ЕНИЛИДЕН) МАЛОНОНИТРИЛ И НЕГОВИТЕ КАЛИЕВО-ЦИАНИДНИ И НАТРИЕВО-МЕТОКСИДНИ КАРБАНИОННИ АДУКТИ. ЕКСПЕРИМЕНТАЛНО И B3LYP ИЗСЛЕДВАНЕ

С. С. Стоянов*, Анг. Д. Попова, Й. Ан. Ценов

Лаборатория „Структурен органичен анализ“, Институт по органична химия с център по фитохимия, Българска академия на науките, ул. „Акад. Г. Бончев“ бл. 9, 1113 София

Посветена на акад. Иван Юхновски по повод на 70-та му годишнина

Постъпила на 31 януари 2008 г.; Преработена на 4 февруари 2008 г.

(Резюме)

Приложен е, комбиниран ИЧ експериментален/B3LYP теоретичен подход, за изучаване на получаването и изомеризацията на калиево-цианидни и натриево-метоксидни карбанионни адукти на 3,5,5-триметил(цикло-хекс-2-енилиден) малононитрил **1**. Установено е добро съответствие между теоретичните и експерименталните ИЧ данни. В съответствие между теория и експеримент, **1** образува β- и δ-адукти с посочените по-горе нуклеофили. Структурните промени, породени от превръщането на **1** в β- и δ-адукти, също са изучени. Според изчисленията, химически движеща сила на β→δ изомеризацията е по-високата стабилност (с около 50 $kJ \cdot mol^{-1}$) на δ-адуктите, в сравнение с β-адуктите.

Bulgarian Chemical Communications, Volume 40, Number 4 (pp. 546–555) 2008

Chain-breaking antioxidant activity of two new chalcones from propolis of El Salvador in homogeneous and micellar media

V. D. Kancheva*, V. S. Bankova

Institute of Organic Chemistry with Centre of Phytochemistry, Bulgarian Academy of Sciences, 1113 Sofia, Bulgaria

Dedicated to Academician Ivan Juchnovski on the occasion of his 70th birthday

Received January 31, 2008; Revised February 11, 2008

The chain-breaking antioxidant activities of two new chalcones from propolis of El Salvador 2',3'-dihydroxy-4,4'-dimethoxy chalcone (AH_2) and 2',3',4-trihydroxy-4'-methoxy chalcon*e* (BH_2) were determined by applying three oxidation kinetic models in homogeneous and micellar systems: model 1 - chemiluminescence of cumene in homogeneous solution; model 2 - oxidation of methyl linoneate and ethylbenzene in homogeneous solution; and model 3 - oxidation of methyl linoneate in sodium dodecyl sulfate (SDS) micelles. The oxidation was carried out at a constant and well-controlled rate of radical generation. The results demonstrated that AH_2 and BH_2 showed moderate chain-breaking activities, higher than naringenin, but lower that caffeic acid, 2,6-di-*tert*-butyl-4-methylphenol (BHT) and DL-α-tocopherol in peroxidation in SDS micellar solution. The moderate chain-breaking activity of the chalcones obtained in homogeneous solution, was similar to that for BHT, but lower than those of caffeic and sinapic acids, and higher than *p*-coumaric and ferulic acids. Full geometric optimization of AH_2 and BH_2 and three-dimensional structures filed as Z matrices were obtained with Chem 3D MOPAC energy minimization at the AM1/RHF level. The determination of the hyperfine coupling constants was carried out with density-functional theory (DFT) calculations, using the B3LYP hybrid function, the CPCM option for considering the solvent effect for the mostly dissociated aroxyl radicals and the basis sets 6-311 G* and 6-311G** of the Gaussian 98 program.

Key words: Antioxidants, propolis, kinetics, methyl linoleate, chalcones.

INTRODUCTION

Chalcones are natural precursors of flavones and flavanones. These polyphenolics are multifunctional and can act as reducing agents (free radical terminators), metal chelators, and singlet oxygen quenchers [1–4] (Fig. 1). It is amazing that propolis samples of different geographic and plant origin and with different chemical composition possess pronounced antioxidant properties. The beneficial effects of antioxidant activity of propolis against oxidation stress and cancer, i.e. the important role of propolis on human health, have been proven by experimental, chemical and epidemiological data [3–5]. Two new chalcones (AH_2 and BH_2, Fig. 2), isolated from El Salvador propolis [6], display pronounced biological activity, particularly signifycant antibacterial and antifungal activity and moderate toxicity to *Artemia salina nauplii*. This observation, as well as the fact that these chalcones are rather accessible substances of low-toxicity, makes the idea intriguing to apply them as stabilizers with antioxidative action for food, cosmetics and other lipid-containing products.

The chain-breaking antioxidative abilities of chalcones were determined by applying three kinetic models:

Model 1: chemiluminescence of cumene in homogeneous solution;

Model 2: oxidation of methyl linoneate (ML) and ethylbenzene (EB) in homogeneous solution;

Model 3: oxidation of ML in sodium dodecyl sulfate (SDS) micelles.

The oxidation was carried out at a constant and well-controlled rate of free radical generation in all models by using free-radical initiators: lipid-soluble azo compound 2,2'-azobisisobutyronitrile (AIBN) for models 1 and 2 and the water-soluble 2,2'-azo-bis(4-carboxyisovalero)-nitrile (ACVN) for micellar model 3 (this model imitated peroxidation in heterogeneous lipid systems and under *in vivo* conditions). Antioxidant activity of new chalcones AH_2 and BH_2 studied are compared at the same molar concentration with the flavonoid naringenin (Ng) possessing a similar structure and with the following reference compounds: 2,6-di-*tert*-butyl-4-methyl-

* To whom all correspondence should be sent:
E-mail: vedeka@abv.bg

© 2008 Bulgarian Academy of Sciences, Union of Chemists in Bulgaria

phenol (BHT), DL-α-Tocopherol (TOH), caffeic (CA), ferulic (FA), sinapic (SA) and *p*-coumaric (*p*-CA) acids.

AH_2 and BH_2 have quite different structures in comparison with previous chalcones from the propolis reported. There are no literature data (for comparison) concerning their full geometry optimization as well as hyperfine coupling constants for such a kind of chalcones (neither theoretical, nor experimental). This study illustrates the possibility of using two new chalcones from propolis of El Salvador as effective chain-breaking antioxidants during lipid peroxidation in homogeneous and micellar systems.

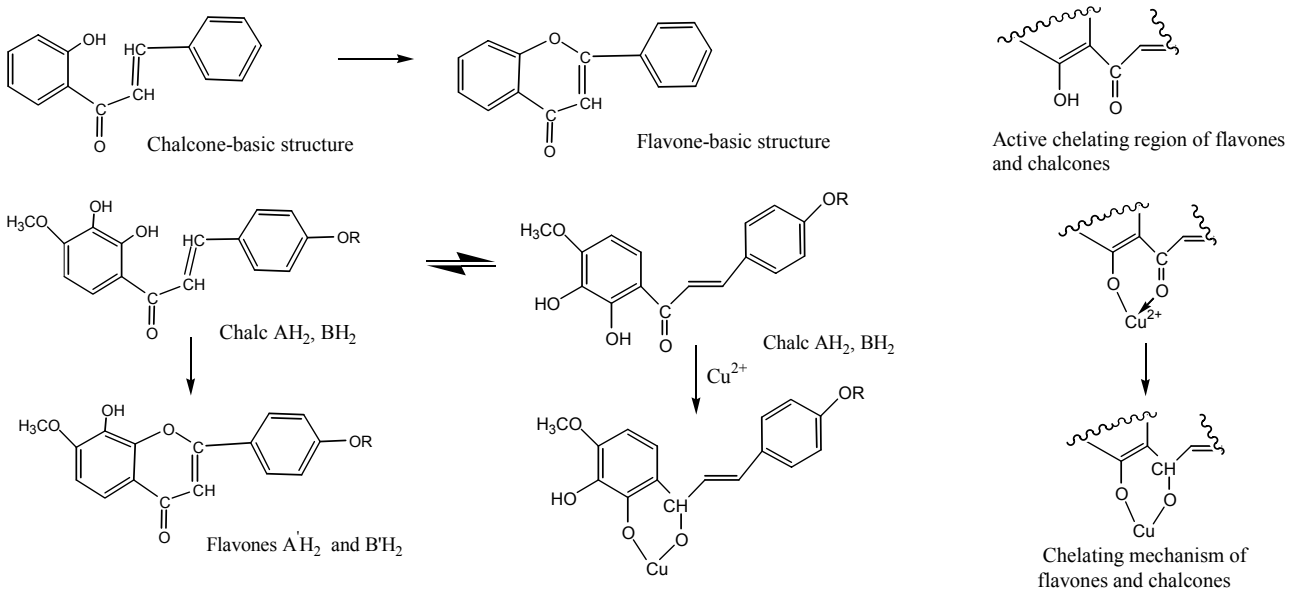

Fig.1. Structure of chalcones and flavones.

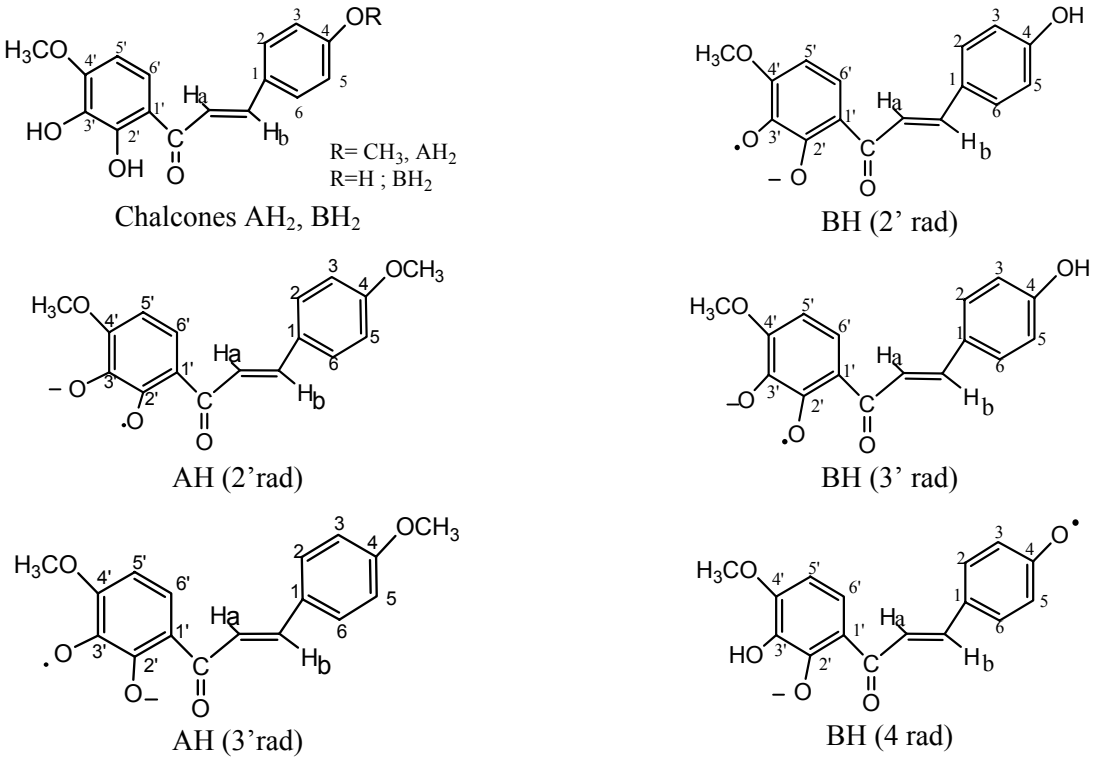

Fig. 2. Structure of chalcones and all possible aroxyl-anion radicals.

EXPERIMENTAL

2',3'-dihydroxy-4,4'-dimethoxychalcone (AH_2) and 2',3',4-trihydroxy-4'-methoxy-chalcone (BH_2) were isolated from propolis of El Salvador and characterized by mass spectra, UV, ^{1}H- and ^{13}C-NMR spectra. The isolation procedure was described in Popova *et al*. [6]. All chemicals were of highest quality and were purchased from Merck (Germany): anhydrous sodium phosphates, Na_2HPO_4 and Na_2PO_4, the initiator AIBN, the chemiluminescence activator 9,10-dibromantracene, cumene, ethylbenzene and chlorobenzene were purified by standard methods. Methyl linoleate (Sigma, Germany) and ACVN (Deisenhofen, Germany) were used as received.

Model 1: The inhibited cumene oxidation was studied by means of a chemiluminescence method (CL) that is known to be one of the most sensitive and informative methods to explore the reactivity of chain-breaking antioxidants [7–9]. The oxidation of cumene (3.6 M) was carried out in chlorobenzene as a solvent in 1:1 ratio, at 60ºC, under air atmosphere. AIBN was used as a free radical initiator. The rate of free radical generation (R_i) was determined in every experiment from the induction period, IP, caused by adding the strong inhibitor 2,2,5,7,8-pentamethyl-6-chromanol (chroman C1, a synthetic analogue of TOH) at known concentration [7–9].

Model 2: The kinetics of oxygen consumption during the oxidation of chlorobenzene solutions of methyl linoleate, ML, and ethylbenzene, EB, (60 ± 0.1ºC, air, 10 mM AIBN as a free-radical initiator, volume of sample tested of 2.0 mL) was studied by using a homemade glass-capillary micro-volumometer of high sensitivity with a cell construction that allowed addition of the required components without opening the cell [10, 11]. A kinetic run was started by measuring the rate of oxidation in the absence of antioxidants (non-inhibited oxidation, R_0) and rate of initiation, R_i. After the determination of R_0 and R_i, chalcones or other phenols at various concentrations were added. Oxygen consumption monitoring started 3–5 min after adding the antioxidant.

Model 3: The oxidation of 0.02 M ML in 0.2 M SDS micelles was studied in 0.05 M Na phosphate buffer, pH 7.40 ± 0.02, at 37.0 ± 0.2ºC in the presence of 50 mM ACVN as an initiator [12]. Under these conditions, ML peroxidation was found to be a chain process with a kinetic chain length of about 40. Chalcones AH_2 and BH_2 were used as stock solutions, depending on solubility, in dimethyl sulfoxide, chlorobenzene, water, or in mixture of these solvents. The kinetics of oxygen consumption was studied with a Yellow Springs Instrument Co. (Yellow Springs, OH) Model 5300 Biological Oxygen Monitor with a Clark electrode as sensor. Similar to the study of the oxidation of homogeneous solutions of ML, the run started with the determination of R_0 and R_i, then, aliquots of a stock solution of chalcones were added without suspending [O_2] monitoring by using microsyringe with long needle.

Quantum chemical calculations: All aroxyl radicals (at 2', 3' and 4 positions) formed from AH_2 and BH_2 and three-dimensional structures filed as Z-matrices were obtained with Chem 3D MOPAC energy minimization at the AM1/RHF level (CambridgeSoft, Cambridge, MA). The determination of the coupling constants was carried out with density-functional theory calculations, using the B3LYP hybrid function, the CPCM option for considering the solvent effect for the mostly dissociated aroxyl radicals and the basis sets 6-311G* and 6-311G** of the Gaussian98 program [13].

RESULTS AND DISCUSSION

Kinetic study

Determination of the chain-breaking antioxidant activity of chalcones during the oxidation of cumene in homogeneous (chlorobenzene) solution (Model 1). It is known that during the recombination of peroxyl radicals in an oxidation system, electronically excited states of carbonyl compounds are generated with a certain probability [7–9]. As a result of their relaxation to the ground state, light emission is observed (chemiluminescence, CL) that can be registered using very sensitive photomultipliers [14, 15]. The mechanism of oxidation of cumene (RH), initiated by a free radical initiator, AIBN, in the presence of an antioxidant, AH_2, may be described by the following kinetic Scheme 1:

Chain generation (i)

$$\text{AIBN} + (O_2, \text{RH}) \rightarrow RO_2^{\bullet} \qquad R_i$$

Chain propagation (p)

$$RO_2^{\bullet} + \text{RH} \rightarrow \text{ROOH} + R^{\bullet} \; (+O_2 \rightarrow RO_2^{\bullet}) \qquad k_p$$

Chain termination (t)

$$RO_2^{\bullet} + RO_2^{\bullet} \rightarrow \text{P*} \rightarrow \text{P} + h\nu \qquad k_t$$

Inhibition 1 (A)

$$RO_2^{\bullet} + AH_2 \rightarrow \text{ROOH} + \text{AH} \qquad k_A$$

Inhibition 2 (A')

$$RO_2^{\bullet} + \text{AH} \rightarrow \text{products} \qquad k_{kA'}$$

Disproportionation (A'')

$$\text{AH} + \text{AH} \rightarrow AH_2 + \text{A} \qquad k_{A''}$$

Scheme 1.

where $RO_2^{\bullet}$ is the cumene peroxyl radical, P* - the

molecule of the oxidation product in excited state, AH is an aroxyl radical, and A – a quinone.

The CL intensity (I) is proportional to the chain termination rate, i.e. to the square of the peroxyl radicals' concentration in the system [7–9]:

$$I = \varphi\,(2k_t\,[RO_2^\bullet]^2) \qquad (1)$$

where φ is a proportional coefficient which depends on chemiluminescence parameters of the system oxidized and on the parameters of photometer device.

The determination of k_A actually involves the evaluation of the competition between reaction of chain termination (k_t) and inhibition 1 (k_A) (see Scheme 1). The antiradical activity of an inhibitor is characterized by the stoichiometric coefficient (***n***) that is equal to the number of free radicals scavenged by one inhibitor's molecule. The key rate constant of inhibited oxidation (k_A) may be calculated from the kinetic curves of CL of the inhibited oxidation from the value of the minimum intensity of CL (I_{min}) in the presence of the inhibitor, AH_2,

$$k_{A(min)} = (1 - I_{min})\,(2R_i\,k_t)^{0.5}/\{\boldsymbol{n}[AH_2]\,(I_{min}^{0.5})\}, \qquad (2)$$

and the stoichiometric coefficient of inhibition, ***n***, is determined according to [8–10]:

$$\boldsymbol{n} = R_i\,IP/[AH_2]_0 \qquad (3)$$

In real experiments, IP is equal to the time from the moment of the inhibitors' injection to the moment of 50% restoration of the CL intensity. It is known that ***n*** for chroman C1, is equal to 2 [7–9]. Thus, the CL method allows the direct determination both of the rate constant of inhibition, k_A, and the stoichiometric coefficient of inhibition, ***n***, from one and the same CL curve.

The kinetic parameters, obtained during the CL oxidation of cumene, in the presence of different concentrations of both chalcones, are presented in Table 1. It could be seen that the rate constants for inhibiting (k_A) for both chalcones are almost the same, but the stoichiometric coefficients are quite different. It means that the mechanism of action of the chalcones differs from BH_2 to AH_2.

Table 1. Kinetic parameters characterizing the chain-breaking activity of chalcones AH_2 and BH_2 at various concentrations during the oxidation of cumene at 60ºC.

Chalcone type	Chalcone concentration, M	R_i, M/s	k_A, $(M{\cdot}s)^{-1}$	***n***
AH_2	2.08×10^{-6}	2.45×10^{-8}	1.20×10^{4}	0.3
AH_2	4.95×10^{-6}	2.33×10^{-8}	1.27×10^{4}	0.5
BH_2	4.50×10^{-6}	3.23×10^{-8}	1.46×10^{4}	1.9
BH_2	8.70×10^{-6}	3.12×10^{-8}	1.04×10^{4}	2.0

The moderate chain-breaking antioxidant activity and the decrease of the stoichiometric coefficient ***n*** are due to the increased contribution of the following side reactions [8, 11, 12]:

$$AH + ROOH \rightarrow AH_2 + RO_2^\bullet \qquad (4)$$

$$AH + O_2 \rightarrow A + HO_2^\bullet \qquad (5)$$

$$AH + RH + O_2 \rightarrow AH_2 + RO_2^\bullet \qquad (6)$$

$$AH \rightarrow \text{product "r"}(+O_2) \rightarrow rO_2^\bullet \qquad (7)$$

"r" denotes undefined structure derived from the original aroxyl radical. Belyakov *et al*. [8] suggested that reaction (7) of the monomolecular transformation of AH (dissociation or isomerization) seems to be the most probable reason for the lower values of the stoichiometric coefficient ***n*** of some polyphenols.

The comparison of the chain-breaking activity of the two studied chalcones with known and standard antioxidants at the same experimental conditions and antioxidant's concentrations is presented in Table 2. The results obtained demonstrated that the chain-breaking antioxidant activity of AH_2 and BH_2 in reaction with peroxide radicals, k_A in a homogeneous solution is similar to those obtained for BHT, but lower than those of caffeic (CA) and sinapic (SA) acids, and higher than *p*-coumaric (*p*-CA) and ferulic (FA) acids. It could be seen that k_A decreases in the following sequence:
CrC_1 (1.2×10^5) > CA (8.3×10^4) > SA (2.5×10^4) > > BH_2 (1.5×10^4) ≥ BHT (1.4×10^4) ≥ AH_2 (1.3×10^4) > FA (0.8×10^4) > *p*-CA (0.7×10^4).

Table 2. The values of the rate constant (k_A) and the stoichiometric coefficient (***n***) obtained from the kinetics of cumene oxidation in presence of AIBN, 60ºC, for known antioxidants (*p*-CA, FA, SA, CA, BHT and Croman C_1) as well as for the tested chalcones AH_2 and BH_2.

Phenolic antioxidant	k_{inh} $(Ms)^{0.5}$	***n***	Refs.
p-Coumaric acid (*p*-CA)	0.7×10^4	1.9	[9]
Ferulic acid (FA)	0.8×10^4	3.5	[9]
Sinapic acid (SA)	2.5×10^4	2.6	[9]
Caffeic acid (CA)	8.3×10^4	2.5	[9]
Butylated hydroxyl toluene (BHT)	1.4×10^4	2.0	[9]
Chroman C_1 (CrC_1)	11.6×10^4	2.0	[9]
Chalcone BH_2	1.46×10^4	1.9	This work
Chalcone AH_2	1.27×10^4	0.5	This work

Kinetics of oxygen consumption during oxidation of ML and EB in homogeneous (chlorobenzene) solutions and in the presence of chalcones (Model 2). The basic kinetic scheme of lipid (LH) oxidation under conditions of a constant rate of free-radical

generation due to the thermo-decompositions of a free-radical initiator, Y, in the presence of an antioxidant (AH_2) is presented in Scheme 2 [12]:

(i) Y (+LH,+O_2) → $LO_2^•$ R_i
Chain generation

(p) $LO_2^•$ +LH (+O_2) → LOOH + $LO_2^•$ k_p
Chain propagation

(t) $LO_2^•$ + $LO_2^•$ → products k_t
Chain termination

(A) $LO_2^•$ + AH_2 → LOOH + AH k_A
Inhibition 1

(A') AH+ $LO_2^•$ → AH-OOL $k_{A'}$
Inhibition 2

(A") AH+ AH → AH_2 + A $k_{A"}$
Disproportionation

Scheme 2.

where $LO_2^•$ are the lipid peroxide radicals, LOOH – lipid hydroperoxides. In the absence of antioxidants, the rate of chain oxidation is as follows:

$$R_0 = d[O_2]/dt = d[LOOH]/dt = k_p[LH](R_i/k_t)^{1/2} \quad (8)$$

In the presence of an antioxidant when k_A[PhOH] is high enough so that $R << R_0$, the system is in the induction period. The duration of the induction period, IP, and the rate of chain inhibited oxidation R_A are given by:

$$IP = \boldsymbol{n}[AH_2]_0/R_i \quad (9)$$

$$R_A = k_pR_i[LH]/\boldsymbol{n}.k_A[AH_2]_0 \quad (10)$$

where $[AH_2]_0$ is the starting concentration of inhibitor. In the classic variant under consideration, a value of $\boldsymbol{n}$ for phenolic antioxidants containing only one active –OH group is generally equal to two without reference to whether AH decays in the reaction of chain inhibition 1 and 2. When AH decays by reaction of chain inhibition 2, Eqn. (10) remains valid, but n changes from 2 to 1 [11, 12]. In conclusion, for a classic phenol IP increases directly with $[AH_2]_0$ and R_A decreases inversely with $[AH_2]_0$. Eqns. (9) and (10) have been confirmed experimentally many times for a phenol with two –OH groups, as well as for many flavonoids and other catechol derivatives.

Table 3 presents the experimental conditions and the main kinetic parameters obtained during lipid (ML) and model hydrocarbon (EB) oxidation in the presence of BH_2. It could be seen that chalcone BH_2 demonstrates also moderate chain-breaking activity, which is almost the same in the both oxidizing systems (ML and EB). It is also evident that the value of k_A of BH_2 in ML is lower than in EB. Roginsky [16] reported that k_A has a lower value in ML than in hydrocarbons (cumene, ethylbenzene, *etc*.) and explained this phenomena with the possible H-bond formation between carbonyl group (C=O) of ML and OH-group of the phenol. The maximal effect of the k_A decrease in ML oxidation was obtained for 4-methoxyphenol (a phenol without substitutions in *ortho*- position). Under these conditions, the chain length (ν) of ML and EB oxidation process was found to be 72 for ML and 8 for EB, respectively.

Table 3. Kinetic parameters, characterizing the chain-breaking activity of chalcone BH_2 obtained from the kinetics of oxygen absorption in methyl linoleate and ethyl benzene in presence of an initiator AIBN, 60ºC.

Substrate	$[BH_2]$, M	R_i, M/s	R_0/R_{A-}	k_A $(Ms)^{0.5}$	$\nu = R_0/Ri$
Methyl linoleate	0.1	$5.0\ 10^{-8}$	4.5	1.5×10^4	72
Ethylbenzene	0.1	$1.0\ 10^{-7}$	4.0	2.0×10^4	8

Determination of the inhibiting activities of chalcones during the oxidation of ML in SDS micelles (Model 3). This model imitates peroxidation in heterogeneous lipid systems and under in vivo conditions. With this model, it is possible to determine an inhibiting activity of both lipid- and water-soluble chain-breaking antioxidants. In contrast to ML oxidation in homogeneous (chlorobenzene) solution, where R is proportional to $(R_i)^{1/2}$, reflecting the bimolecular chain termination ($LO_2^•$ + $LO_2^•$ → products), in SDS micellar solutions, R is nearly proportional to R_i [12]. The latter means that chain termination occurs by first-order reaction with respect to $[LO_2^•]$ [12]:

$LO_2^•$ → products $k_{t'}$ (t').

For this reason, the kinetic scheme under consideration includes reactions (i), (p), (t'), (A), (A'). The following system of differential equations corresponds to this scheme:

$$d[LO_2^•]/dt = R_i - k_{t'}[LO_2^•] - k_A[LO_2^•][AH_2] - -k_{A'}[LO_2^•][AH] \quad (11)$$

$$d[AH]/dt = k_A[LO_2^•][\ AH_2] - k_{A'}[LO_2^•][AH] \quad (12)$$

$$-d[AH_2]/dt = k_A[LO_2^•][AH_2] \quad (13)$$

The rate of non-inhibited oxidation equals

$$R_0 = k_p[LH]R_i/k_{t'} \quad (14)$$

The rate of inhibited oxidation and the relative rate of oxidation are:

$$R = k_p[LO_2^•][LH] \quad (15)$$

$$R/R_0 = k_{t'}[LO_2^•]/R_i \quad (16)$$

The solution is given for quasi-stationary approximation for all free radicals. Combining Eqns. (14), (15) and (16) results in:

$$R_i - k_{t'}[LO_2^\bullet] - 2k_A[LO_2^\bullet][AH_2] = 0 \qquad (17)$$

and the k_A/k_p ratio, which determines actually the inhibiting ability of phenols during the oxidation of ML, may be calculated from the kinetics of oxygen consumption with the help of Eqn. (18):

$$F = R_0/R - 1 = 2k_A R_0[AH_2]/k_p R_i[LH] + \text{const} \qquad (18)$$

The tested chalcones AH_2 and BH_2 displayed an ability to depress ML chain oxidation in the system under consideration. The values of k_A/k_p calculated from the slope of the line by using Eqn. (18) (the plot of F *vs* [AH_2], resp. [BH_2] – see Fig. 3) are listed in Table 4. Structure-activity relationship was studied by using comparable kinetic analysis with other antioxidants, studied at the same experimental conditions. For that reason, the chain-breaking antioxidant activity of the studied chalcones (AH_2 and BH_2) is compared at the same molar concentration with the flavonoid naringenin (Ng) of similar structure and with the reference compounds: 2,6-di-*tert*-butyl-4-methylphenol (BHT), DL-α-Tocopherol (TOH). The data shown in Fig. 3 and Table 4 demonstrate the moderate chain breaking antioxidant activity of AH_2 (2.3) and BH_2 (7.7), which is higher than naringenin (0.5), but lower than CA (23.0), BHT (240.0) and TOH (290.0).

The antioxidant activity of chalcones is based mainly on the chalcone-chalcone-quinone redox system (Fig. 4). Chalcones (AH_2 and BH_2) may act as radical scavengers and produce chalcone-semiquinone radicals (AH, BH). The bimolecular recombination with disproportionation reaction of these two chalcone-semiquinone radicals (AH, BH, Fig. 4) may form a molecule of chalcone-quinone (A, B) and regenerated molecule of chalcone (AH_2, BH_2). Figures 4a and 4b present the reactivity, transformation and degradation products of AH_2 and BH_2 during the oxidation process.

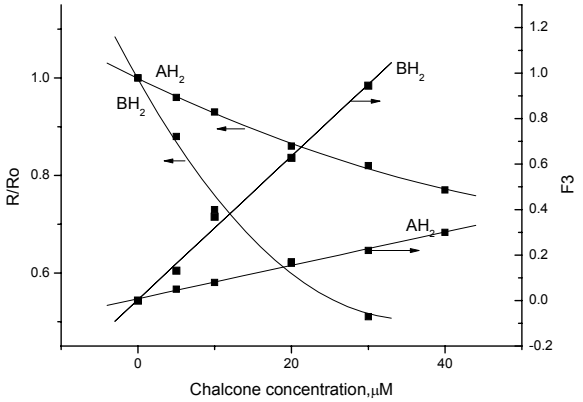

Fig. 3. Kinetics of oxygen consumption during the oxidation of 0.02 M methyl linoleate in 0.2 M SDS micellar solution in 0.05 M Na phosphate buffer pH = 7.40 at 37ºC ($R_i = 1.65 \cdot 10^{-9}$ M/s) in the presence of AH_2 and BH_2.

Table 4. Kinetic parameters characterizing the chain breaking activity of chalcones AH_2 and BH_2 and known antioxidants during the methyl linoleate oxidation in SDS micellar solution, 37ºC.

Antioxidant	k_A/k_P	Ref.	Antioxidant	k_A/k_P	Ref.
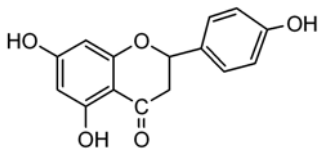 Naringenin	0.5	[12]	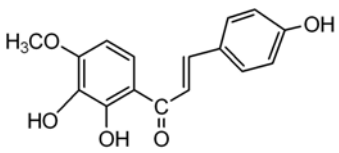 BH_2	7.7	This work
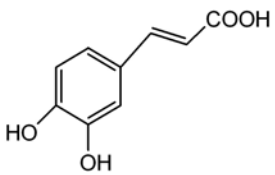 Cafeic acid	23	[12]	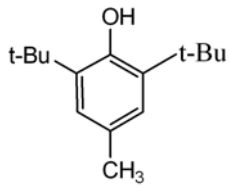 BHT	240	[12]
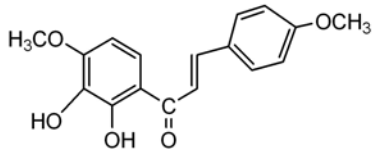 AH_2	2.3	This work	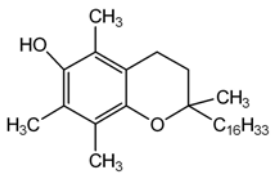 Tocopherol	290	[12]

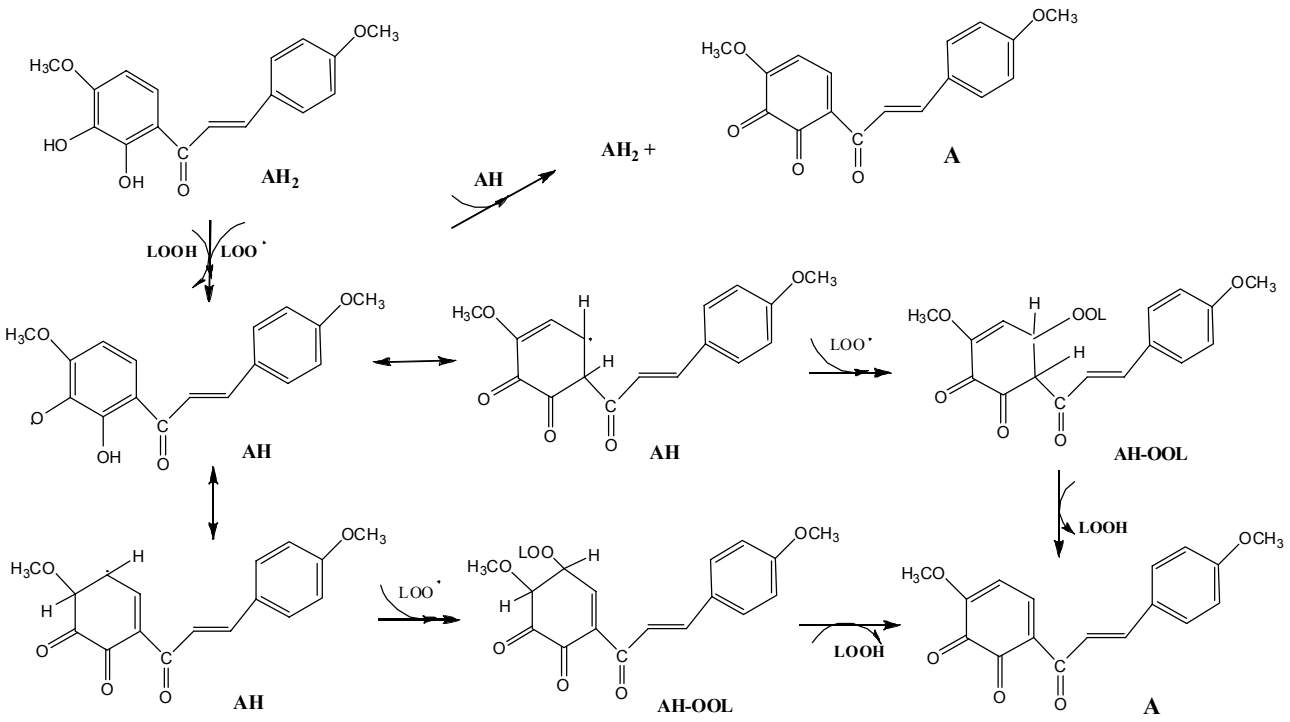

Fig. 4a. Reactivity, transformation and degradation products for chalcone AH_2.

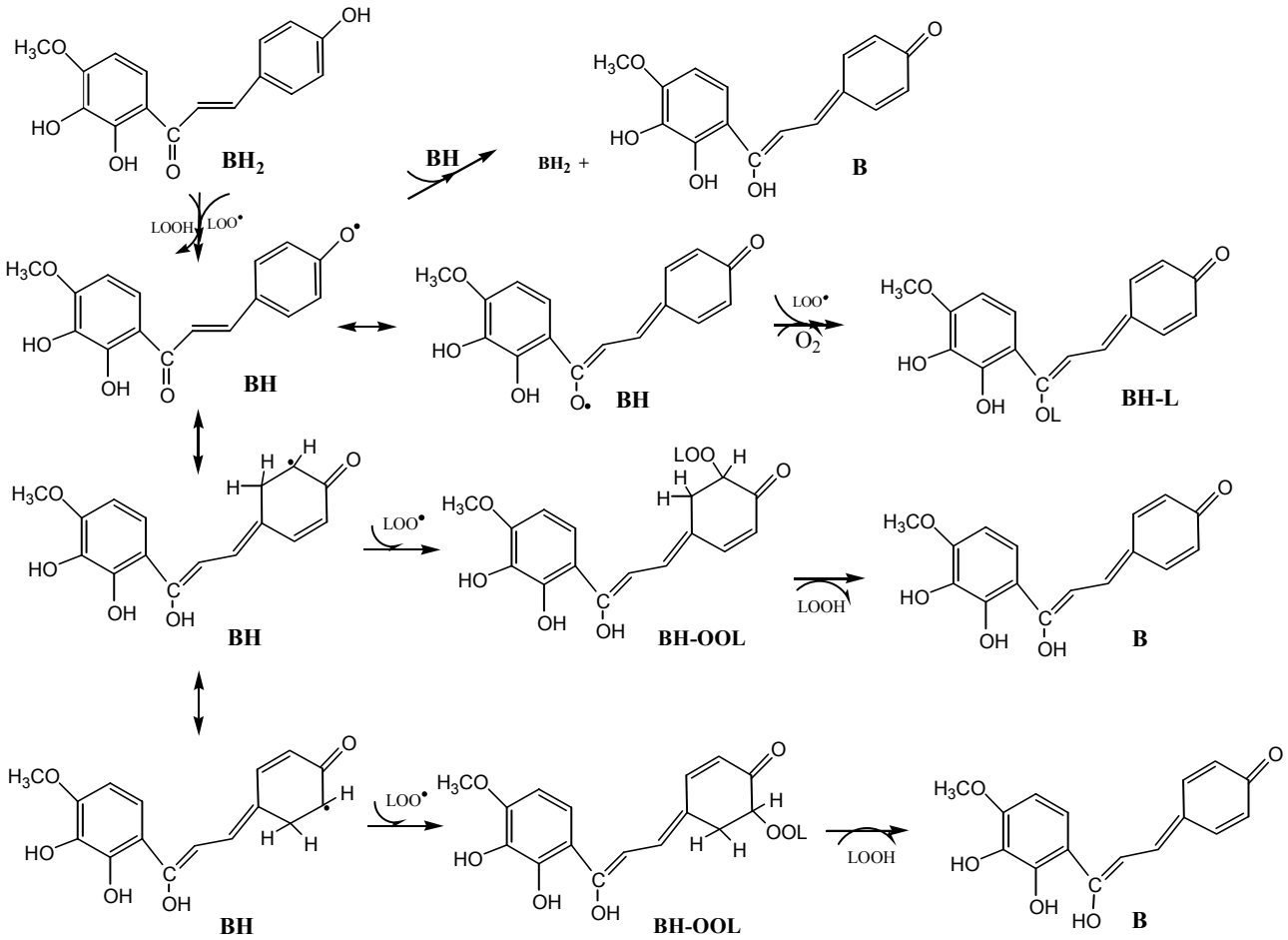

Fig. 4b. Reactivity, transformation and degradation products for chalcone BH_2.

Table 5. Theoretical coupling constants of aroxyl radicals from new chalcones of El Salvador propolis.

Substance		$H_{6'}$	$H_{1'}$	H_α	H_β	H_2	H_3	H_5	H_6	Comments
BH_2 rad2'	CA	4.6903	1.2380	0.2464	0.0180	0.0065	0.0029	0.0020	0.0074	CPCM mode, 6-311G*
	CB	4.5682	1.2143	0.2474	0.0185	0.0066	0.0029	0.0020	0.0076	CPCM mode, 6-311G**
BH_2 rad3'	CA	4.7419	1.2047	0.2662	0.0100	0.0031	0.0031	0.0007	0.0029	CPCM mode, 6-311G*
	CB	4.6192	1.1817	0.2675	0.0106	0.0033	0.0032	0.0007	0.0030	CPCM mode, 6-311G**
BH_2 rad4	CA	0.8403	0.0031	3.4360	7.4023	1.8274	5.2172	4.7962	1.7516	CPCM mode, 6-311G*
	CB	0.8556	0.0022	3.3627	7.2074	1.7743	5.1104	4.6988	1.7012	CPCM mode, 6-311G**
	PA	0.8615	0.0022	3.4246	7.3813	1.8212	5.2190	4.7943	1.7516	PCM mode, 6-311G*
AH_2 rad2'	CA	4.7017	1.2324	0.2457	0.0181	0.0069	0.0026	0.0024	0.0071	CPCM mode, 6-311G*
	CB	4.5788	1.2091	0.2466	0.0187	0.0070	0.0026	0.0025	0.0073	CPCM mode, 6-311G**
AH_2 rad3'	CA	4.7390	1.2022	0.2652	0.0127	0.0038	0.0034	0.0010	0.0031	CPCM mode, 6-311G*
	CB	4.6161	1.1796	0.2664	0.0133	0.0040	0.0034	0.0010	0.0032	CPCM mode, 6-311G**

Quantum chemical calculations

Calculated coupling constants for all possible aroxyl radical-anions formed from AH_2 and BH_2 (see Fig. 2) are shown in Table 5. It is no doubt that the chalcones AH_2 will produce aroxyl radicals only in ring a. The calculated hyperfine coupling constants for aroxyl radicals in positions 2' and 3' for chalcone BH_2 showed no differences. Therefore, it is impossible to predict which kind of aroxyl radical (in which position of the same ring) will be formed on the base of DFT calculations.From the point of view of theory of phenol antioxidant's efficiency, it seems to be more easily the formation of aroxyl radical AH in position 3' than in position 2'. It is well-known, that the addition of electron-donating constituents on *ortho*-position increases the hydrogen abstraction (respectively to the radical formation) of the phenol group. In our case, the hydrogen abstraction in position 3' (ring a) is much possible than in position 2', due to the double substituents $–OCH_3$ and –OH existing in *ortho*-position of 3' phenol group. It must be noted that the reactivity of OH groups in ring **a** is expected to be much lower that of OH group in ring **b** [1, 8, 11, 12].

From the calculated hyperfine coupling constants of AH radical in position 4 (ring **b**), it is evident that they are drastically different in comparison with those of aroxyl radicals formed in ring **a** (see the data in Table 5). It is clear that the formation of an aroxyl radical in ring **b** for the chalcone BH_2 demonstrated a stronger effect on the calculated hyperfine coupling constants of α and β hydrogen atoms than the effect observed in the case of aroxyl radicals (2' or 3') formed in ring **a**. No differences were observed for the both chalcones AH_2 and BH_2 in the coupling constants of hydrogen atoms near to the radicals formed in ring **a**. The differences for the calculated hyperfine coupling constants of aroxyl radicals formed in ring **a** and **b** (in the case of chalcone BH_2) are significant.

AM1/MOPAC full geometry optimization of the geometry of these chalcones and the corresponding aroxyl radicals is shown in Figure 5. A formation of hydrogen bonding between H and OH group in position 2' and oxygen from the neighbouring C=O group (close distance is about 1.42 Å) for the chalcone BH_2 is observed. In contrast, in case of AH_2, the two rings are turned on about 30º and there is no possible formation of hydrogen bond (close distance in this case is almost 2.52 Å).

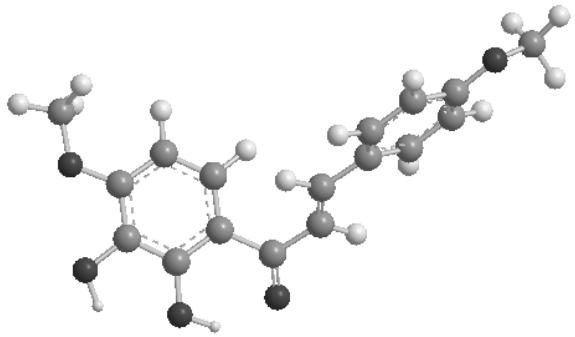

Chalcone AH_2

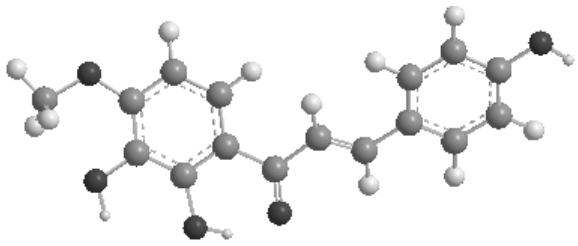

Chalcone-BH_2

Fig. 5a. Optimized 3D structures of the studied chalcones.

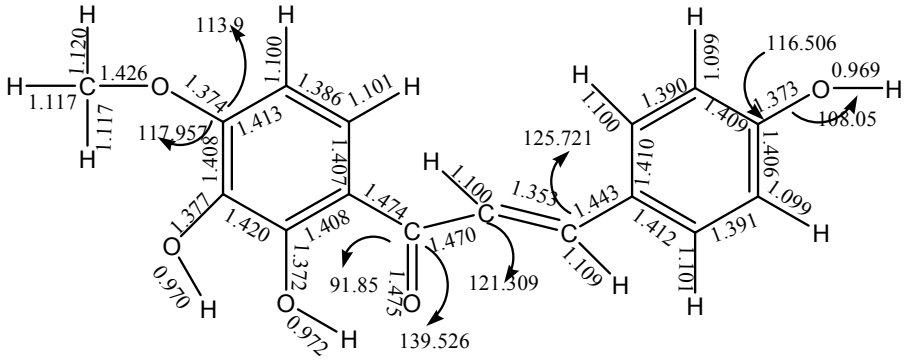

Chalcone BH_2

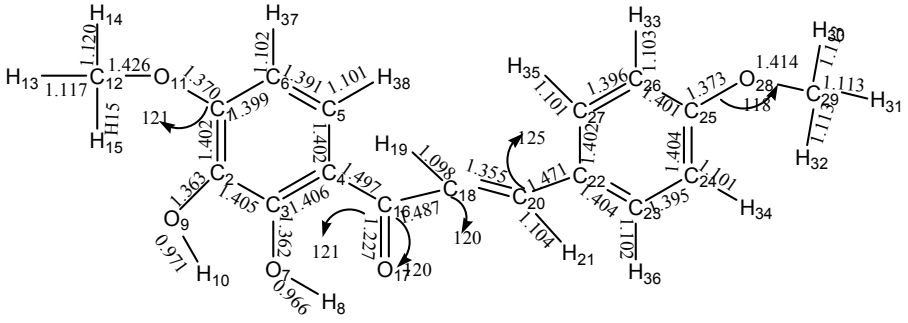

Chalcone AH_2

Fig. 5b. Equilibrium structural parameters for the chalcones AH_2 and BH_2.

CONCLUSIONS

New data demonstrate a moderate chain-breaking antioxidant activity of the new chalcones AH_2 and BH_2 isolated from propolis of El Salvador in homogeneous and in SDS micellar systems. At the present time it is difficult to suggest either mechanism as the only reason for the moderate antioxidative capability of both chalcones. Most likely, all arguments presented are valid, but their real contributions still have not be determined. The calculations of the theoretical coupling constants of aroxyl-anion radicals by density-functional theory, allow to show the absolutely different type of aroxyl radical-anions, formed from the tested chalcones. Further run of EPR experiments will allow also permitting which type of these aroxyl radicals are indeed formed from the two chalcones. These new data about the chain-breaking antioxidant activity for both chalcones are important, especially from the point of view of their possible application as bio-antioxidants for stabilization of lipids and lipid-containing products.

Acknowledgements: *We are thankful for the financial support of Deutsche Forschungs Gemeinschaft (DFG Grant 436BUL 112/16/01) for V. D. K. We appreciate the stimulating discussion with Prof. Dr. V. A. Roginsky and Dr. W. Bors as well as the possibility to run a part of these experiments in the Yellow Springs Instrument Co. at the laboratory of Prof. Roginsky, Semenov Institute of Chemical Physics, Russian Academy of Sciences and quantum-chemical calculations in the GSF National Research Center for Environment and Human Health, Germany. Partial support of this work from the National Fund for Scientific Research at the Bulgarian Ministry of Education (Contract BIn 4/04) is gratefully acknowledged.*

REFERENCES

1. F. Shahidi, P. K. J. P. D. Wanasundara, *Food Sci. Nutr.*, **32**, 67 (1992).
2. S. M. Barlow, in: Food Antioxidants, B. J. Hudson (Ed.), Elsevier, Amsterdam, 1990, p. 253.
3. S. Z.Dziedzic, B. J. F. Hudson, *Food Chem*., **12**, 205 (1983).
4. V. Kortenska-Kancheva, V. Bankova, *Recent Prog. Med. Plants*, **14**, 81 (2006).
5. V. D. Kortenska-Kancheva, V. S. Bankova, M. P. Popova; *Oxid. Commun*., **28**, 525 (2005).
6. M. Popova, V. Bankova, S. Spassov, I. Tsvetkova, Ch. Naydenski, M. V. Silva, M. Tsartsarova, *Z. Naturforsch*., **56c**, 593 (2001).
7. V. Ja. Shlyapintoch, O. N. Karpuchin, L. M. Postnikov, I. V. Zacharov, A. A. Vitchunski, V. F. Chepalov, Chemiluminescence Methods for Studies of Slow Chemical Processes, Nauka, Moscow, 1966 (in Russian).
8. V. A. Belyakov, V. A. Roginsky, W. Bors, *J. Chem. Soc. Perkin Trans*., **2**, 2319 (1995).
9. I. F. Rusina, M. I. Boneva, O. T. Kasaikina, V. D. Kortenska, N. V. Yanishlieva, *Oxid. Commun*., **27**, 562 (2004).
10. V. F. Tsepalov, V. A. Charitonova, G. P. Gladyshev,

N. M. Emanuel', *Kinet. Katal*., **18**, 1261 (1977).
11. V. A. Roginsky, Phenolic Antioxidants – Efficiency and Reactivity, Nauka, Moscow, 1988 (in Russ.).
12. V. A. Roginsky, T. K. Barsukova, A. A. Remorova, W. Bors, *J. Am. Oil Chem. Soc*., **73,** 777 (1996).
13. M. J. Frisch, G. W. Trucks, H. B. Schlegel, G. E. Scuseria, M. A. Robb, J. R. Cheeseman, V. G. Zakrzewski, J. A. Montgomery Jr., R. E. Stratmann, J. C. Burant, S. Dapprich, J. M. Millam, A. D. Daniels, K. N. Kudin, M. C. Strain, Ö. Farkas, J. Tomasi, V. Barone, M. Cossi, R. Cammi, B. Mennucci, C. Pomelli, C. Adamo, S. Clifford, J. Ochterski, G. A. Petersson, P. Y. Ayala, Q. Cui, K. Morokuma, P. Salvador, J. J. Dannenberg, D. K. Malick, A. D. Rabuck, K. Raghavachari, J. B. Foresman, J. Cioslowski, J. V. Ortiz, A. G. Baboul, B. B. Stefanov, G. Liu, A. Liashenko, P. Piskorz, I. Komáromi, R. Gomperts, R. L. Martin, D. J. Fox, T. Keith, M. A. Al-Laham, C. Y. Peng, A. Nanayakkara, M. Challacombe, P. M. W. Gill, B. Johnson, W. Chen, M. W. Wong, J. L. Andres, C. Gonzalez, M. Head-Gordon, E. S. Replogle, J. A. Pople, Gaussian 98, Gaussian, Inc., Pittsburgh, PA, 1998.
14. V. A. Belyakov, E. L. Shanina, V. A. Roginsky, V. B. Miller, *Izv. Akad. Nauk SSSR*, **12**, 2685 (1975).
15. A. M. Jimenes, M. J. Navas, *Grasas y Aceitas*, **53**, 64, (2002).
16. V. A. Roginsky, *Biol. Membr. (Eng. Transl.),* **4**, 437 (1990).

ПРЕКЪСВАЩА ВЕРИГИТЕ АНТИОКСИДАНТНА АКТИВНОСТ НА НОВИ ХАЛКОНИ ОТ ПРОПОЛИС ОТ ЕЛ САЛВАДОР В ХОМОГЕННА И МИЦЕЛАРНА СРЕДА

В. Д. Кънчева*, В. С. Банкова

Институт по органична химия с център по фитохимия, Българска академия на науките, 1113 София

Посветена на акад. Иван Юхновски по повод на 70-та му годишнина

Постъпила на 31 януари 2008 г.; Преработена на 11 февруари 2008 г.

(Резюме)

Прекъсващата веригите антиоксидантна активност на два нови халкона от прополис на Ел Салвадор 2',3'-дихидрокси-4,4'-диметокси халкон (AH2) и 2',3',4-трихидрокси-4'-метокси халкон (BH2) е определена чрез прилагане на три кинетични модела на окисление в хомогенна и мицеларна среда: модел 1 – хеми-луминисценция на кумол в хомогенен разтвор, модел 2 – окисление на метиллинолеат и етилбензол в хомогенен разтвор, и модел 3 – окисление на метиллинолеат в мицели на натриев додецилсулфат (SDS). Окислението е проведено при постоянна и добре контролирана скорост на инициране, т.е. на зараждане на радикали. Резултатите показват, че при окислението в разтвор на SDS мицели AH_2 и BH_2 проявяват умерена антиоксидантна активност, прекъсваща веригите, по-висока от тази на нарингенина, но по-ниска от тази на кафеената киселина и по-висока от тази на 2,6-ди-*трет*-бутил-4-метилфенол (BHT) и DL-α-токоферола. Умерена прекъсваща окислителните вериги активност е наблюдавана също така за халконите в хомогенни разтвори, подобно на тази за BHT, но по-ниска от тази на кафеена и синапова киселини, и по-висока от тази на р-кумарова и ферулова киселини. Чрез прилагане на Chem 3D MOPAC минимална енергия при ниво AM1/RHF е получена пълната оптимизация на геометрията на AH_2 and BH_2 и три-дименсионалните им структури като Z матрици. Определянето на свръхфините константи на взаимодействие са получени като са използвани изчисления с плътностно-фунционалната теория (DFT) и е приложена B3LYP хибридна функция и CPCM опция за отчитане на ефекта на разтворителя за дисоциираните ароксилни радикали и базовите мрежи 6-311 G* и 6-311G** на програма Gaussian 98.

Bulgarian Chemical Communications, Volume 40, Number 4 (pp. 556–560) 2008

Implementation and testing of routine procedure for mixture analysis by search in infrared spectral library

P. N. Penchev, V. L. Miteva, A. N. Sohou, N. T. Kochev, G. N. Andreev*

Department of Analytical Chemistry, Faculty of Chemistry, University of Plovdiv, 24 Tsar Assen St., Plovdiv 4000, Bulgaria

Dedicated to Academician Ivan Juchnovski on the occasion of his 70th birthday

Receved February 4, 2008; Revised February 14, 2008

A routine procedure for mixture analysis by searching in infrared spectral library using spectra subtraction was implemented and tested. The peak search parameters were optimized to improve the mixture components identification. Four new heuristics have been devised that improved the identification of mixture components.

Key words: infrared spectra, library search, mixture analysis.

INTRODUCTION

The infrared (IR) spectrum reflects to a great extent the compound structure, therefore, it is well suited for the process of structure elucidation [1]. Library search systems are currently commercially available from both the instrument manufacturers and chemical software businesses. Also, spectral libraries containing several hundreds to thousands of spectra can be obtained [2]. Despite that, the number of collected spectra is much smaller than the number of currently known compounds, in some cases a correct identification of a compound or mixture components can be achieved which makes the further study in this field sensible.

The library search in spectral databases has two main goals [3]:

(1) identification of an unknown compound if its spectrum is among the reference spectra (identity search), or

(2) obtaining a list of compounds (called hitlist) whose spectra are most similar to that of the unknown (similarity search). Since the IR spectrum is a function of the structure of the compound, the result hitlist can be used for deriving some conclusions for the unknown's structure, which is usually done through manual inspection of the hit structures by the chemist or with the aid of some computer algorithms as that of maximum common substructure [4].

In this work the identification of mixture components through a search in an IR spectral library is studied. A well-known procedure [5, 6] that uses spectra subtraction is implemented and studied. The procedure is optimized and several heuristics improving considerably the identification of mixture components have been defined.

EXPERIMENTAL

Measurements and Processing of Spectra

The IR spectra were registered on a Perkin-Elmer 1750 FT-IR Spectrometer from 4000 cm^{-1} to 450 cm^{-1} at a resolution 4 cm^{-1} with 16 scans. The solid samples were recorded in KBr pellets and the liquids as thin films, so that the strongest band in the 4000-450 cm^{-1} wavenumber range gave approximately 10% transmittance (T). All spectra were subjected to curvilinear baseline correction and were transferred to an IBM compatible computer with the standard protocol for data exchange KERMIT [7]. The original spectral data were converted by a smoothing procedure based on weights from a normal distribution.

SPECTRAL LIBRARY AND SOFTWARE

SpecInfo Library

The IR database of this system contains 1000 full-curve spectra together with chemical structures and was available for this work in JCAMP-DX format [8]. The original spectral range is 4000 to 400 cm^{-1}, with a sampling interval of 1.93 cm^{-1}. The IR spectra, structural data, molecular formulas, and compound names were converted for use in the software product IRIS.

* To whom all correspondence should be sent:
E-mail: andreev@uni-plovdiv.bg

© 2008 Bulgarian Academy of Sciences, Union of Chemists in Bulgaria

IRIS

This is a Windows-based program for searching in libraries of IR spectra [9, 10]. Six different algorithms for comparison of IR spectra are implemented: two methods for peak matching and four methods for comparing full spectral curves. IRIS uses the spectral range from 3700 to 500 cm^{-1}, with a sampling interval of 4 cm^{-1}, corresponding to 801 data points. Furthermore, IRIS contains software tools for the import of IR spectra in JCAMP-DX format, for peak picking, and for an interactive analysis of IR spectra of mixtures based on multiple linear regression.

METHODS

Peak Matching

Peak search algorithms described in Ref. [3] can be generally divided into two types: (1) forward one used for identification of pure compounds, and (2) reverse one applied for identification of the components of organic mixtures. The corresponding spectra similarity measures, or hit quality indices (HQIs), were implemented as it was described in Sadtler IR library [6]:

forward: $HQI_F = ABC$

reverse: $HQI_R = BAC$;

where A, B and C are calculated as it is described below.

If the unknown spectrum contains N peaks, the reference spectrum contains M peaks, and K is the number of matched peaks, then

$A = 9K/N$; $B = 9K/M$;

$C = 9[1 - \Sigma \left| \nu_U^K - \nu_R^K \right| /(K\,\Delta\nu)]$;

where $\Delta\nu$ is the tolerance in peak shift at the abscissa (wavenumber), the sum in C is taken for all matched peaks, and A, B and C are rounded to integers.

In the applied spectroscopy a full coincidence of peaks is rather accidental even for two different IR spectra of the same compound. That is why the peak matching is done with tolerances defined by the user. In IRIS program two tolerances are used: one along the abscissa (wavenumber), $\Delta\nu$, and the other along the ordinate (absorbance), ΔA. The coincidence of a peak from unknown and a peak from reference spectrum means that the peak in the unknown is within a rectangle with sides' lengths $2\Delta\nu$ and $2\Delta A$ and a center in the top of the reference peak (Figure 1).

For comparative purposes, four additional measures were applied to describe the similarity of IR spectra: (1) sum of the squared absorbance differences, (2) sum of the absolute absorbance differences, (3) normalized scalar product of two spectral vectors, and (4) correlation coefficient between spectral vectors. These four measures compare full spectral curves, and the corresponding HQIs (HQI_1 to HQI_4) were described earlier [4].

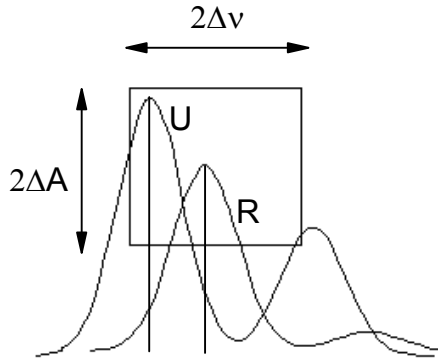

Fig. 1. Matching two peaks, one from the unknown spectrum (U), another from the reference one (R), using tolerances along the abscissa and the ordinate.

Mixture Analysis Procedure

The main requirement for the application of this procedure is that all mixture components are members of the library. At the beginning, the mixture spectrum is searched in the library. The first hit is assumed as one of the mixture components and its spectrum is subtracted from the mixture spectrum, see Eqn. (1). Further, the negative values of the remainder spectrum are truncated, normalized and then it is searched in the library. The first hit in this newly obtained hitlist is supposed to be the second component [5, 6].

$$\text{Remainder} = \text{Mixture} - \text{Coefficient} \times \text{“Hit \#1”} \quad (1)$$

Described in this way, the procedure looks pretty straightforward, but even for a mixture of components with quite different spectra it could fail and give erroneous results. There are no recommenddations in the literature to what extent the subtraction is performed, except that one or more selected spectral bands of the mixture spectrum have to be nullified. Another complication can arise if the mixture components have similar spectra with overlapping bands (because of their similar structures) thus leading to an over-subtraction – and as a result of it – the second component might not be the first hit in the hitlist that results from the second library search.

To test the procedure and to make it robust and reliable, ten mathematically composed mixture spectra and ten recorded mixture spectra are analyzed: all spectra are registered in our laboratory and searched in the SpecInfo library. Since our spectra are not identical with those of SpecInfo, the mathe-

matically composed spectra have all features of the spectra of real samples: they differ from the reference ones in the level of baseline and the band widths, and they are also recorded by quite a different sample path and spectral resolution. Five of them are composed of samples recorded in KBr pellet and this fact has additionally complicated the subtraction.

RESULTS AND DISCUSSION

Optimization of Tolerances

The full spectrum search was studied earlier [11] and proved to be better than the peak search if applied to spectra of pure compounds. Since a mixture spectrum is nearly an algebraic sum of components spectra, the comparison of full spectra gives inadequate result and components spectra are not at the first two positions in the hitlist. On the other side, the tolerance values optimized for identification of pure compounds [9] are expected to be unsuitable for identification of mixture components because the relative intensity of spectral bands decreases in the mixture spectrum and appeared as shifted alongside the wavenumber by the overlapping bands of the components. Because of this, new values of the tolerances have to be established when mixture spectra are searched in the library.

To find the optimal tolerances, ten mixture spectra recorded in our laboratory were searched in the SpecInfo library. They are five mixtures of butanol and 2-methyl-1-propanol (*iso*-butanol) with volume ratio of 1:9, 1:4, 1:1, 4:1 and 9:1 v/v, and five mixtures of pyridine and benzene with volume ratio of 1:9, 1:4, 1:1 v, 4:1 and 9:1 v/v. There IR spectra were searched with $\Delta\nu$ varying from 3 to 20 cm^{-1}; the threshold of peak-picking applied to mixture spectrum was 0.01 a.u. in order to find most of the peaks of the component with smaller concentration. The usage of ΔA less than 1.0 a.u. proved to be unfavorable when there was a component with smaller concentration. In this way, the found optimal tolerances are ΔA = 1.0 a.u. and $\Delta\nu$ in the range of 8 to 11 cm^{-1}: the latter is a little wider than the optimal $\Delta\nu$ found by the pure compound identification (7 cm^{-1}). The HQI_R was better suited than HQI_F for mixture components identification.

The four full spectrum HQIs were also tested for mixture identification. As expected, they performed worse than peak search HQIs.

Identification of Mixture Components

One of the authors (P.N.P) composed five mixture spectra of 2-nitrobenzaldehyde and indole-3-carboxaldehyde with volume ratio of 1:9, 1:4, 1:1, 4:1 and 9:1 v/v, and five mixture spectra of 3,3-dimethyl-2-butanone and propiophenone with volume ratio of 1:9, 1:4, 1:1, 4:1 and 9:1 v/v. For the first five mixtures the components spectra were recorded in KBr pellet and for the next five as thin films. These ten spectra were searched in random order by another author (V.L.M.) who knew neither the components nor the composition of the mixtures. The threshold by pick-peaking from mixture spectra and remainder spectrum is 0.01 a.u., and the reverse peak search was used with $\Delta\nu$ = 9 cm^{-1} and ΔA = 1.0 a.u. The routine procedure described in the Mixture Analysis Procedure section was applied. As expected, the component identification was not a straightforward one, and in eight cases the second component was not identified. The two mixtures with correctly identified components have a volume ratio of 1:1 v/v.

The detail analysis showed several reasons for that misidentification. First, the difference spectrum is too noisy and has some kind of "wings" that result from the different band widths of the component spectrum and the reference one. Second, the spectroscopist selects usually one band from the mixture spectrum and tries to nullify it by subtracting the first hit spectrum. There is no warranty that the selected "nullified" band is not present in the second component spectrum or severely overlaps with one of its bands: in this case, substantial spectral information is lost in the remainder. Third, an unambiguous criterion when to stop the subtraction was not used. The smaller the coefficient from Eqn. (1), the more spectral features remain from the first hit; the bigger the coefficient, the less spectral features remain from the spectrum of the second component. The presence of some "wings", positive or negative – see Fig. 2, is unavoidable and they harm the search. That is why it is better to minimize their magnitude.

To overcome these problems three heuristics were formulated and applied by the next test searches of other ten mixture spectra. They are:

(1) By the second search, i.e. by the search of the remainder, a higher threshold is applied by the peak-picking procedure. Our experiments proved that instead of 0.01 a.u., the threshold has to be between 0.03 and 0.05 a.u.

(2) Several bands (not only one) are supervised by the subtraction. These are the bands which have close relative intensities in the mixture spectrum and in the reference one.

(3) The subtraction is done till the bands selected by heuristic 2 give equal positive and negative "wings" as is shown in Fig. 2.

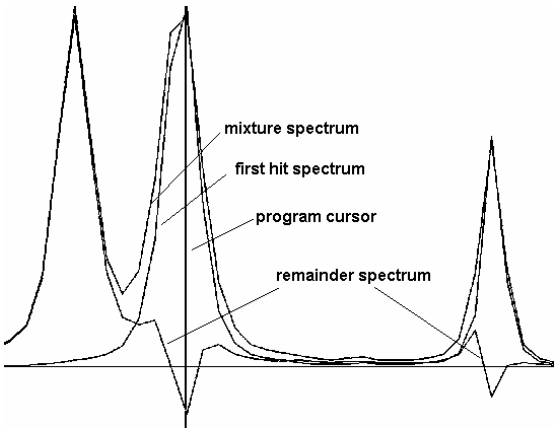

Fig. 2. Illustration of the third heuristic.

To test the significance of these heuristics ten mixture spectra recorded in our laboratory were searched in random order by one of the authors (V.L.M.) who knew neither the components nor the composition of the mixtures. The thresholds by pick-peaking from mixture spectra and remainder spectrum were, respectively, 0.01 a.u. and 0.05 a.u., and the reverse peak search was used with $\Delta\nu = 9$ cm^{-1} and $\Delta A = 1.0$ a.u. The routine procedure described in the Mixture Analysis Procedure section was applied. The results are presented in Table 1.

For seven out of ten mixtures, both components were correctly identified. Not surprisingly, the failed identification is for mixtures 1 and 4. Mixture 1 gives nearly "null" (flat) spectrum after the subtraction, and that illustrates the limits of the routine to the range of concentration of the components. The second component, *o*-xylene, of mixture 8 was also not identified: it was positioned at the 43 place in the second hitlist. One possible explanation might be that the spectrum of *o*-xylene is a subset of the spectrum of the *iso*-propylbenzene (first identified component). The most intensive band of *iso*-propylbenzene spectrum is at 700 cm^{-1} and it is not overlapping with any *o*-xylene bands. This band was used by subtraction and the other bands of *o*-xylene disappeared obviously in the remainder. Mixture 2 was successfully analyzed: it has a coefficient of 0.99 despite the predominant component has volume percentage of 80%. The normalization of a spectrum (unknown or reference) in IRIS is between 0.0 a.u. (for the background) and 1.00 a.u. (for the most intensive band). In a mixture spectrum, the most intensive band can solely be the band of one of the components. That is why by an idealized spectrum measurement, when the path lengths of mixture sample and reference spectrum sample are equal, the coefficient from Table 1 has to be close to 1.00. This could be regarded as another heuristic by performing the spectra subtraction.

As the remainder spectrum (see Eqn. (1)) is very noisy, one could expect that the full spectral HQIs will give better results when applied only to the second search. This did not happen, and one possible explanation is the partially remaining spectrum of the first identified component.

Table 1. Mixture component identification. The component is considered as identified if it was the first hit by the corresponding search. In parentheses the corresponding HQI is given.

#	Mixture	Volume ratio (v/v)	Found 1 component and (HQI)	Coefficient from Eqn. 1	Found 2 component and (HQI)
1	Butanol and *iso*-butanol	1:9	*iso*-butanol (979)	1.02	- [1)]
2	Butanol and *iso*-butanol	1:4	*iso*-butanol (978)	0.99	butanol (648)
3	butanol and *iso*-butanol	1:1	*iso*-butanol (877)	1.01	butanol (648)
4	butanol and *iso*-butanol	4:1	butanol (968)	0.96	-
5	*o*-xylene and *m*-xylene	1:1	*o*-xylene (949)	0.86	*m*-Xylene (888)
6	*o*-xylene and *p*-xylene	1:1	*p*-xylene (948)	1.06	*o*-Xylene (778)
7	*m*-xylene and *p*-xylene	1:1	*m*-xylene (938)	1.10	*p*-Xylene (879)
8	*iso*-propylbenzene and *o*-xylene	1:1	*iso*-propylbenzene (949)	1.15	-
9	*iso*-propylbenzene and *m*-xylene	1:1	*iso*-propylbenzene (958)	1.08	*m*-Xylene (848)
10	*iso*-propylbenzene and *p*-xylene	1:1	*iso*-propylbenzene (948)	1.13	*m*-Xylene (878)

[1)] the component was not found as the first hit by the corresponding search.

CONCLUSIONS

A routine procedure for mixture analysis by searching in infrared spectral library was implemented and tested. The peak search parameters were optimized to improve the mixture components identification. The procedure that uses spectra subtraction appeared to be not a straightforward one; that is why four new heuristics were devised that improved the identification of mixture components:

(1) A higher threshold has to be applied by the peak-picking procedure of the remainder;

(2) Several bands have to be supervised by the subtraction;

(3) The subtraction has to be performed until the bands selected by heuristic 2 give equal positive and negative "wings";

(4) Values near to 1.00 of the coefficient from Eqn. (1) have to be expected.

REFERENCES

1. H. J. Luinge, *Vib. Spectrosc*., **1**, 3 (1990).
2. W. A. Warr, *Anal. Chem*., **65**, A1087 (1993).
3. J. T. Clerc, in: Computer-Enhanced Analytical Spectroscopy, H. L. C. Meuzelaar, T. L. Isenhour (Eds.), Plenum Press, New York, 1987, pp. 145-162.
4. K. Varmuza, P. Penchev, H. Scsibrany, *J. Chem. Inf. Comp. Sci*., **38**, 420 (1998).
5. H. Somberg; Qualitative Mixture Analysis by Use of an Infrared Library Search System, Brucker Reports, 1988.
6. The Sadtler IR Search Software Manual, Sadtler Research Labs, Division of Bio-Rad Laboratories, Inc, 1988.
7. D. L. Eisner, C. S. Mayfield, IDRIS KERMIT, version 1.0, Perkin-Elmer Corp., July, 1985.
8. SpecInfo: Spectroscopic Information System, vers. 3.1, 1996; Available from: Chemical Concepts, P.O. Box 100202, D-69442 Weinheim, Germany.
9. P. N. Penchev, PhD. Thesis, University of Plovdiv, 1998.
10. IRIS can be downloaded together with a small demo library and all used mixture spectra from http://www.kosnos.com/spectroscopy/iris.
11. P. N. Penchev, A. N. Sohou, G. N. Andreev, *Spectrosc. Lett*., **29**, 1513 (1996).

РЕАЛИЗИРАНЕ И ПРОВЕРКА НА РУТИННА ПРОЦЕДУРА ЗА АНАЛИЗ НА СМЕСИ С ПОМОЩТА НА БИБЛИОТЕКА ОТ ИНФРАЧЕРВЕНИ СПЕКТРИ

П. Н. Пенчев, В. Л. Митева, А. Н. Сохоу, Н. Т. Кочев, Г. Н. Андреев*

Катедра „Аналитична химия", Химически факултет, Пловдивски университет, ул. „Цар Асен" № 24, Пловдив 4000

Посветена на акад. Иван Юхновски по повод на 70-та му годишнина

Постъпила на 4 февруари 2008 г.; Преработена на 14 февруари 2008 г.

(Резюме)

В статията е реализирана и проверена рутинна процедура за анализ на смеси с помощта на библиотека от инфрачервени спектри. Параметрите за търсене по пикове са оптимизирани за да подобрят идентификацията на компонентите на смеси. Формулирани са четири нови евристики, които подобряват идентификацията на компонентите на смеси.

Bulgarian Chemical Communications, Volume 40, Number 4 (pp. 561–567) 2008

Characteristics of pectic polysaccharides from leek obtained through consecutive extraction with various reaction agents

M. Kratchanova[1]*, M. Gocheva[1], E. Pavlova[1], I. Yanakieva[1], D. Nedelcheva[2], V. Kussovski[3], A. Slavov[4]

[1] *Laboratory of Biologically Active Substances, Institute of Organic Chemistry with Centre of Phytochemistry, Bulgarian Academy of Sciences, 95 V. Aprilov Blv., P.O.Box 27, 4002 Plovdiv, Bulgaria;*
[2] *Analytical Laboratory of Instrumental Chromatography and Mass Spectrometry, Institute of Organic Chemistry with Centre of Phytochemistry, Bulgarian Academy of Sciences, Acad. G. Bonchev St., Block 9, 1113 Sofia, Bulgaria;*
[3] *Institute of Microbiology, Bulgarian Academy of Sciences, Acad. G. Bonchev St., Block 26, 1113 Sofia, Bulgaria;*
[4] *University of Food Technology, 26 Maritza Blv., 4002 Plovdiv, Bulgaria*

Dedicated to Academician Ivan Juchnovski on the occasion of his 70th birthday

Received February 7, 2008; Revised March 18, 2008

Five polysaccharide fractions of commensurable by yield, but different in composition were obtained through consecutive extraction with water, solutions of ammonium oxalate, sodium carbonate, hydrochloric acid and sodium hydroxide from the alcohol-insoluble residue (AIR) of leek. In the polyuronide part of these fractions besides galacturonic acid was found also glucuronic acid. In the neutral sugar fraction, the prevailing sugar was galactose, followed by rhamnose. The water-extractable pectic polysaccharide was highly homogenous (93.3% of it had molecular mass of 1.3×10^6 kDa) and protein content of 8% (the highest compared to the other extracted polysaccharides). Extraction with diluted hydrochloric acid yielded polysaccharide with the highest neutral sugar content of 71.1% and a low uronic acids content. The water- and chelate-extractable fractions had a lower L-rhamnose content (2.7% and 2.9%, respectively) and the other polysaccharide fractions from leek were characterized by a high L-rhamnose content (from 14 to 28%). The pectic polysaccharides obtained from leek have shown good immunostimulating properties. The highest immunostimulating activity has been shown by the water- and chelate-extractable polysaccharides, which are also characterized by a high polyuronic acid content and polysaccharides with molecular mass over 10^6 Da.

Key words: leek, pectic polysaccharides, consecutive extractions, chemical compositions, immunological activity.

INTRODUCTION

Pectic polysaccharides along with cellulose, hemicelluloses, glycoproteins, proteins and lignin build up the plant cell wall [2–6]. The pectic polysaccharides are complex biopolymers made up of α-(1→4) bound residues of D-galacturonic acid, the so-called "smooth region" or homogalacturonan and branched regions of rhamnogalacturonans. Rhamnogalacturonans contain side chains of neutral sugars such as arabinans, galactans, arabinogalactans, *etc*., which account for the haired layout ("hairy region") of the pectic macromolecule [1].

The branched pectic molecules are highly entwined in the cell wall, which hampers their extraction from the plant material. Various approaches for isolation of pectic substances have been applied. Voragen *et al*. [1] have introduced a method for obtaining pectic polysaccharides through consecutive extraction with water, chelate substances, acids and alkali. The scheme for consecutive fractional extraction also gives information on the type of bonding of the isolated pectic polysaccharides with the other components in the cell wall [1, 7, 8].

The leek is a vegetable known from hoary antiquity. It has been used for food, which is beneficial for the human health. The influence of some of the components of leek, such as polysaccharides, flavonoids, saponins, sulphur-containing compounds, minerals and vitamins, on the human health is well known, but there is a lack of information for the composition and biological importance of pectic polysaccharides [9].

It has been found that pectic polysaccharides isolated from different plant sources have diverse biological properties. They and their derivatives have antitumour, anticomplement, antiinflamatory, immunological and antivirus activity [10].

The aim of the present investigation is the isolation of pectic polysaccharides from AIR of leek through consecutive fractional extraction, their

* To whom all correspondence should be sent:
E-mail: lbas@plov.omega.bg (M. Krachanova)

© 2008 Bulgarian Academy of Sciences, Union of Chemists in Bulgaria

characterization and determination of their immunostimulating activity.

EXPERIMENTAL

Obtaining of alcohol-insoluble substance (AIS) from leek: Extraction and characterization of the pectic polysaccharides were conducted with leek (*Allium porrum*) from the region of Plovdiv, Bulgaria. 1 kg fresh leek was cut into small pieces of 8–10 mm and mixed with 96% ethanol pre-heated to 65ºC. The ratio between the raw materials and alcohol was 1:2.5. The obtained mass was kept for 1 h at 65ºC and for 24 h at room temperature. Then it was filtered through cloth and washed twice with 200 ml 96% ethanol. The obtained alcohol-insoluble substance was dried at 60ºC.

Fractionation of pectic polysaccharides from leek by means of consecutive extraction with various extractants (Figure 1):

1. Water extraction – carried out twice. As a first step, 70 g AIS from leek were extracted with 1400 ml water at 80ºC at continuous stirring for 45 min. The obtained mixture was filtered through cloth. A second extraction was applied for 20 min with 700 ml water, at 80ºC and then the mixture was filtered again. The two combined filtrates of pH~6 were precipitated with ethanol to isolate the water soluble pectic polysaccharide from leek;

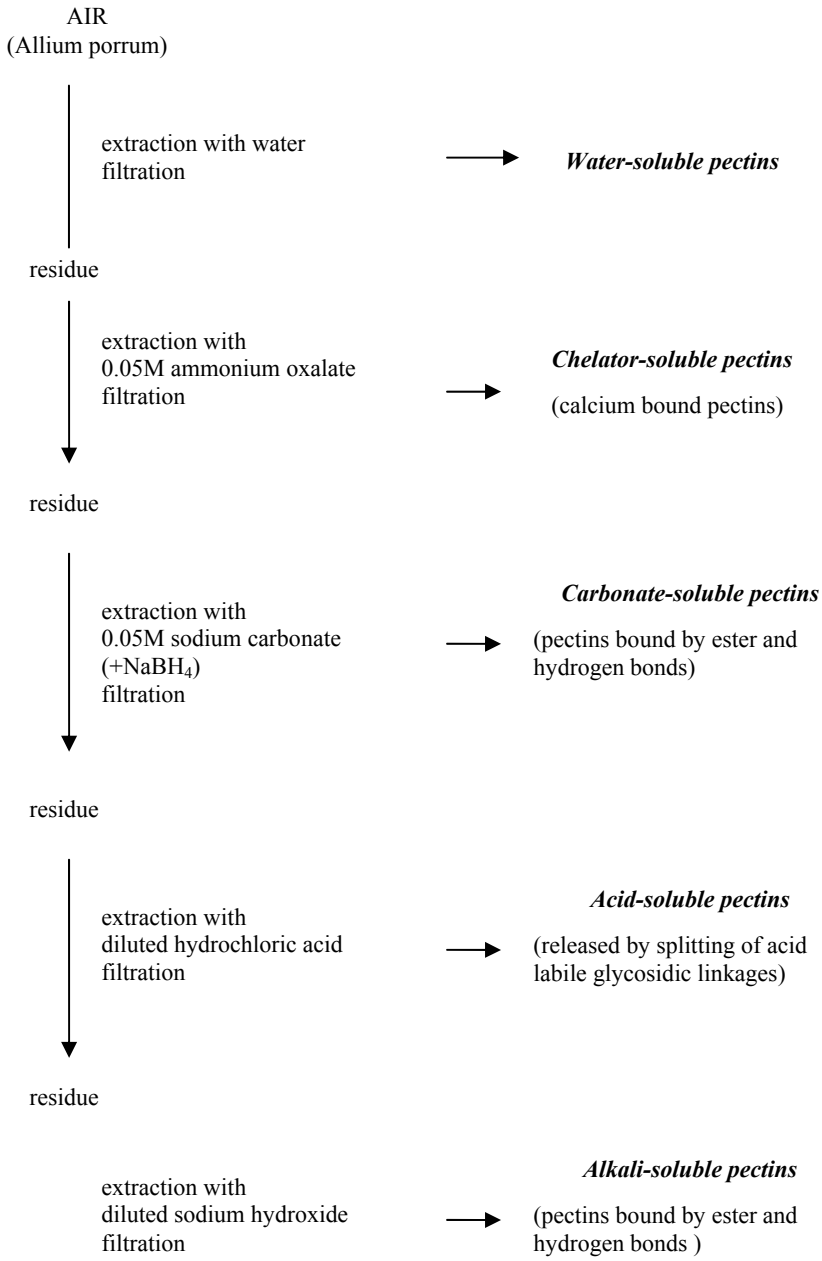

Fig. 1. Scheme for extraction of pectins proposed by Voragen *et al*. [1].

2. Chelate extraction – for this purpose 930 ml 0.05 M aqueous solution of ammonium oxalate was added to the residue obtained after the water extraction. The extraction took place for 4 h at 20ºC followed by continuous stirring at pH~6. The obtained mixture was filtered through cloth. The residue was subjected to a second extraction with 760 ml 0.05 M aqueous solution of ammonium oxalate for 30 min at the same temperature. The combined filtrates were precipitated with ethanol to obtain the chelate-extractable pectic polysaccharide;

3. Carbonate extraction – it was conducted twice with 0.05 M aqueous solution of sodium carbonate. 930 ml were added to the residue from the chelate extraction at 1ºC followed by continuous stirring for 17h at pH~10. The first extraction with carbonates was conducted in the presence of 280 mg sodium borehydride ($NaBH_4$). The obtained mixture was filtered through cloth. A second extraction was conducted for 3 h with 885 ml 0.05 M solution of sodium carbonate at 20ºC, but without sodium borehydride. The obtained mixture was filtered through cloth. The residue from the second extraction with sodium carbonate was washed with H_2O at a ratio of 1:10 (470 ml water, respectively) for 20 min at room temperature at stirring. The combined filtrates were precipitated with ethanol to obtain the carbonate-soluble pectic polysaccharide;

4. Acid extraction was performed twice. The first extraction was conducted with 930 ml 0.1 M solution of hydrochloric acid added to the residue from the previous extraction for 1 h followed by continuous stirring, at 80ºC and pH~1.5. The obtained mixture was filtered through cloth. A second extraction was conducted with 450 ml water for 30 min at 80ºC. The combined filtrates were precipitated with ethanol to obtain the acid-soluble pectic polysaccharide;

5. Extraction with alkali – conducted with 0.05 M solution of sodium hydroxide (590 ml) added to the residue from the previous extraction at 0ºC followed by continuous stirring for 17 h at pH~11.8. The obtained mixture was filtered through cloth and the filtrate was precipitated with ethanol to obtain alkaline-soluble pectic polysaccharide.

Isolation of the polysaccharides: Each of the obtained filtrates was precipitated with 96% ethanol at a ratio of 1:1 for 1h. The coagulated polysaccharides were isolated after filtration through cloth. The obtained pectic polysaccharides were washed consecutively with 100 ml 70% hydrochloric ethanol, with 70% ethanol to a neutral reaction and with 100 ml 96% ethanol. The washed pectic polysaccharides from leek were dried at 60ºC.

Determination of polyuronic content, degree of esterification and protein content: The assay of polyuronic content (PUC) and degree of esterification (DE) of the polysaccharides was determined by the method of Owens *et al*. [11], the protein content of leek – by Kjlthal and the polysaccharides – by Lowry [12].

Determination of monosaccharide composition: Neutral sugars were measured as alditol acetates after hydrolysis of samples. The crude extracted pectic polysaccharides (20 mg) were pretreated with 2 M trifluoroacetic acid (TFA) for 3 h at 120°C before conversion to alditol acetates according to the method described in [13].

The monosaccharide composition of pectic polysaccharides was assessed on a gas-mass chromatography system 6890 GC System Plus/5793 Mass Selective Detector (Hewlett Packard) with a column SP-2380 Supelco, 200°C for 3 min, then 5°C/min to 250°C; injector temperature 250°C, detector temperature 280°C; helium as a carrier gas at a flow rate of 1 ml/min. Peak identification was based on retention times, using myo-inositole as an internal standard.

Determination of molar mass: The molar masses of the crude polysaccharides were assayed through HPSEC on a Waters (Millipore) system. The assay was made on Ultrahydrogel™ 120 and Ultrahydrogel™ 500 column (7.8×300 mm, Waters) with bidistilled water as eluent at an eluation rate of 0.8 ml/min. The column was calibrated using the Shodex standard P-82 (Showa DENKO, Japan).

Determination of biological activity: The immunological activity of pectic polysaccharides was assayed applying the following biological tests: protective activity of the polysaccharides in an experimental bacterial infection, killing capacity of the peritoneal macrophages obtained from mice treated with polysaccharides [14] and activation of the complement system in blood serum by a classical pathway [15] and by an alternative pathway [16].

RESULTS AND DISCUSSION

The analysis of AIR obtained from leek, crop 2002, from the region of Plovdiv, Bulgaria showed that the major polysaccharides in the leek were pectic substances – 23.3%, which had a high degree of esterification (73–74%) and cellulose – 21.7%. The protein content of the leek was 24%. The results from the consecutive fractional extraction of AIR from leek carried out following the scheme used by

Voragen [1] showed that five pectic polysaccharide fractions of commensurate yields (2.4 – 3%) were obtained (Table 1). The obtained pectins differed in their polyuronic content, degree of esterification, neutral sugar content and protein content. The highest PUC was observed in the water- and chelate-extractable fractions. The acid- and alkaline-extractable pectic polysaccharides contained about 30% uronic acids. In the polysaccharide fractions, a presence of glucuronic acid was observed. Its content was about 10% of the total polyuronic acid content. Only the first two fractions had a high degree of esterification: 76.59 and 61.53%. The first fraction had also very high protein content (8%). In the other polysaccharides the protein content was between 1.3 and 2.2%.

Table 1. Yield and characteristics of pectic polysaccharides obtained by a consecutive extraction with different reaction agents from AIS of leek.

Polysaccharides*	yield, per100 g AIR	Polyuronic content, %	Degree of esterification, %	Neutral sugar, %	Protein by Lowry, %
A	3.39	73.6	76.6	18.4	8.0
B	3.11	64.1	61.5	34.3	1.6
C	3.60	49.3	32.1	48.5	2.2
D	3.60	27.5	26.1	71.1	1.5
E	2.94	28.0	12.6	70.8	1.3

* A – water-extractable pectic polysaccharide, B – chelate-extractable pectic polysaccharide, C – carbonate-extractable pectic polysaccharide, D – acid-extractable pectic polysaccharide, E – alkaline-extractable pectic polysaccharide.

Interesting data on the neutral sugars in the obtained pectic polysaccharides were found as it is seen in Table 2. It is assumed that the extraction with water and chelate reagents was not destructive and, therefore, the amount of the neutral sugars in the first two polysaccharide fractions was lower (less than 35%). It must be noted, however, that the polysaccharide obtained with a chelate extractant (ammonium oxalate) had almost twofold more neutral sugars than the water-extractable pectic polysaccharide. Twice as high was the content of galactose (increased from 13 to 24%), arabinose (1.6 and 3.7%) and glucose (1.9 and 3.4%). It is well known that polysaccharides extracted by aqueous solutions of chelate extractants are mostly pectic chains of homogalacturonan linked to each other through calcium bridges, which form the so called "egg-box" systems in the cell walls of plants [1, 17]. Obviously, in our case the degradation of these "egg-box" systems through the linkage of Ca^{2+} by the chelating extractant and the degradation of homogalacturonan, were accompanied by the degradation of part of the rhamnogalacturonan, containing galactose and arabinose. This led to a relative increase in the amount of the neutral sugars in the second fraction and probably to a higher molecular heterogeneity of this fraction (Figure 2). During the extraction of pectin from tomatoes with a chelating extractant, Round et al. have also found out that the extracted pectic polysaccharide contains ~15% of the branched part of the pectic molecule [18].

Table 2. Monosaccharide composition of pectic polysaccharides from leek, obtained through a consecutive extraction with different extractants (as % of the total amount of carbohydrates).

Monosaccharides*	A	B	C	D	E
rhamnose	2.4	3.0	14.4	17.0	28.3
fucose	-	-	1.1	-	-
ribose	0.8	-	1.2	-	-
arabinose	1.6	3.7	9.5	5.1	5.9
xylose	0.1	0.2	0.3	2.1	2.2
manose	trace	trace	trace	trace	trace
galactose	13.2	24.7	20.0	45.0	30.7
glucose	1.9	3.4	3.3	3.2	4.7
Σ neutral sugar	20.0	35.0	49.8	72.4	71.8
Σ uronic acid	80.0	65.0	50.2	27.6	28.2
GalA	68.2	50.2	40.3	19.3	18.4
GluA	11.8	14.8	9.9	8.3	9.8
GalA/Rha	28.4	16.7	2.8	1.1	0.7

* A – water-extractable pectic polysaccharide, B – chelate-extractable pectic polysaccharide, C – carbonate-extractable pectic polysaccharide, D – acid-extractable pectic polysaccharide, E – alkaline-extractable pectic polysaccharide.

The pectic polysaccharides in the residue after the second extraction were more strongly linked to the cell wall and because of that, they could be extracted only using hydrolyzing extracting agents. By extraction with sodium carbonate, a pectic fraction containing higher amount of neutral sugars was obtained, as the content of L-arabinose and particularly that of L-rhamnose sharply increased. Presence of fucose and ribose was also observed (Table 2). The molecular mass of this polysaccharide was lower compared to the chelate-extractable polysaccharide (Figure 2), but it was more homogenous (80% of it had 1.55×10^6 Da) in comparison with the next two pectic polysaccharides. According to Selvendran and O'Neill [17], during extraction with aqueous solution of sodium carbonate, pectins, bound to the other components of the cell wall through ester and hydrogen bonds, are released.

During As a result of extraction with dilute solution of hydrochloric acid (0.1 M), a pectic polysaccharide with a low polyuronic content (27.5%) and a very high amount of neutral sugars (71.1%) was obtained. This fraction was characterized by the highest galactose content and by the higher amount of L-rhamnose and xylose compared to the previous polysaccharide fractions, while the amount of arabinose was lower (Table 2). Apparently, the use

of hydrochloric acid for the purposes of extraction led to a breakage of the bonds of the pectin molecule with other components of the cell wall. In parallel, a hydrolysis of the glycosidic bonds in the macromolecule itself took place, which was registered by the decrease in the molecular mass (Figure 2). This observation was in correspondence with the different stability of glycosidic bonds observed at heating the pectic polysaccharides with a solution of dilute mineral acid, established by BeMiller [19] and Neukom et al. [20]. In pectins, particularly, the arabinofuranosyl linkages are most labile, followed by the glycosidic linkages between the other neutral sugar residues as well as between the neutral sugars and the galacturonic acid residues (pseudo-aldobiuronic acid linkages), glycosidic linkages between the galacturonic acid and the neutral sugars residues (aldobiuronic acid linkages). The most stable are those between the galacturonic acid residues.

As a result of the extraction with diluted solution of sodium hydroxide (at pH~11.8), a polysaccharide with a high content of neutral sugars, low content of uronide and the lowest amount of protein was obtained (Table 1). There was a considerable increase in the amount of L-rhamnose in comparison with the other pectic fractions (Table 2). This polysaccharide contained similar amounts of uronic acids (28%), L-rhamnose (27.9%) and galactose (30.3%). At these conditions, degradation also took place in terms by hemicellulose breakdown [6]. This was confirmed by the data on the relative increase of the amount of glucose and xylose as compared to the other pectic polysaccharides. The molecular mass (Figure 2) of the alkaline-extractable polysaccharide from leek was between 4.0×10^6 and 2.9×10^4 Da.

The data presented in Table 2 show that when water and chelating extractants were used, pectic fractions with a smaller content of L-rhamnose were obtained, as the ratio GalA/Rha varied from 16.7 to 28.4. According to Redgwell and Selvendran [9], under these conditions the pectic polysaccharides from the middle lamella of the plant cell wall dissolved. With the other extraction agents, pectic polysaccharides from the primary cell wall were isolated. Their content of L-rhamnose increased, as the ratio GalA/Rha became between 2.8 and 0.7. These facts gave us ground to assume that the pectin macromolecule of leek had areas of different composition, which also differed in terms of linking to the cell wall of leek.

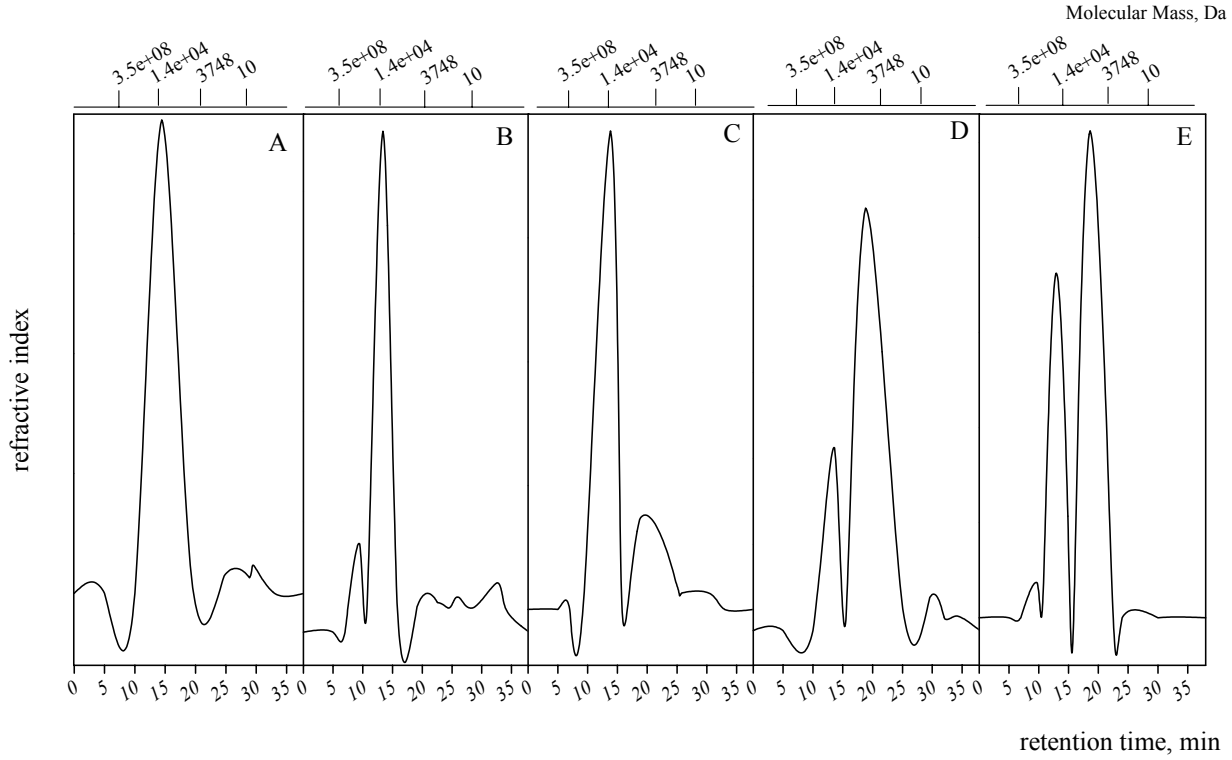

Fig. 2: HPSEC elution patterns of fractionated pectic polysaccharides from leek by means of consecutive extraction with various extractants: A - water extraction; B - chelate extraction; C - carbonate extraction; D - acid extraction; E - alkali extraction.

Table 3. Biological activity of pectic polysaccharides from leek obtained through consecutive extraction with various extractants.

Polysaccharide*	Survivability, days	Complement activation, % inhibition of the hemolysis					Killing index
		Alternative pathway			Classical pathway		
		1000 μg/ml	500 μg/ml	250 μg/ml	1000 μg/ml	500 μg/ml	
A	17.2±3.2	95.9±3.8	35.4±4.1	19.6±2.3	34.7±2.4	0	12.5±1.8
B	12.2±2.5	62.1±8.2	27.4±4.2	9.3±1.5	18.8±4.2	0	10.5±1.6
C	14.8±3.4	79.9±11.4	28.9±4.4	0	6.7±0.8	0	13.8±1.2
D	11.8±2.1	25.3±3.5	6.5±0.8	0	11.2±3.9	0	14.4±3.2
Control	6.6±2.1						5.4±0.9

A – water-extractable pectic polysaccharide, B – chelate-extractable pectic polysaccharide, C – carbonate-extractable pectic polysaccharide, D – acid-extractable pectic polysaccharide.

The obtained five pectic polysaccharides were biologically active. The data presented in Table 3 show that they are good immunostimulators. Treating a test mice with the pectic polysaccharides caused a significant increase in the number of the peritoneal macrophages, which are effector cells of the natural resistance, unlike the control, non-treated mice. The data correlate with the observed protection in the experimental salmonella infection manifested in increased survivability of the mice treated with polysaccharides. At a concentration of 1000 μg/ml, the polysaccharides resulted in a considerable activation of the serum complement, which was more distinct in the alternative rather than in the classical pathway. Trials with a reducing concentration of the polysaccharides distinguished the water- and chelate-extractable polysaccharides, characterized by the highest PUC and molecular mass, as most strongly activating the complement.

CONCLUSION

The approach of consecutive extraction of AIR from leek led to obtaining pectic polysaccharides of different composition. Water- and chelate-extractable polysaccharides present in the middle lamella had the highest polyuronic acid content and molecular mass. Extraction with solution of sodium carbonate led to obtaining pectic polysaccharides with increased total amount of monosaccharides and higher homogeneity than the chelate-extractable polysaccharide. Application of hydrochloric acid as extracting reagent showed a sharp increase in the amount of neutral sugars. In each fraction the prevailing monosaccharide was galactose and its content increased with every extraction step. It can be assumed that this is due to the presence of polysaccharide built by galactose residues in the cell wall of leek bound to the pectin macromolecule. The glucuronic acid could be found in every isolated fraction.

This investigation demonstrated also the heterogeneity of the pectic molecule. The pectic polysaccharides isolated from leek had sections differing in terms of composition. In some of them, the galacturonic acid prevailed, as the ratio between GalA/Rha in water- and chelate-extractable polysaccharides varied from 28.4 to 16.7 and in the other isolated polysaccharides it was between 2.8 and 0.7.

The pectic polysaccharides isolated through consecutive extraction from the cell wall of leek possess biological activity and are good stimulators of the immune system. Pectic polysaccharides with a higher uronic content and molecular mass show also higher immunostimulating activity.

REFERENCES

1. A. G. J Voragen, W. Pilnik, J. Thibault, M. A. Axelos, C. M. G. C. Renard, in: Food Polysaccharides and Their Applications, A. M. Stephen (ed), Marsel Dekker, Inc., New York, Basel, Hong Kong, 1995, p. 287.
2. A. Showalter, *Plant Cell*, **5**, 9 (1993).
3. R. R. Selvendran, B. J. H. Stevens, O'Neill, in: Biochemistry of Plant Cell Walls, C. T. Bret, J. R. Hillman (Eds.), Cambridge University Press, 1985, p. 39.
4. S. Fry, *Ann. Rev. Plant Physiol*. **37**, 165 (1986).
5. S. Fry, *New Phytol.*, **161**, 641 (2004).
6. E Kerr, S. Fry, *Planta*, **219**, 73 (2004)
7. C. M. G. C. Renard, PhD Thesis, University of Nantes, France, 1989.
8. D. E. Wechsler, G. R. Strasser, R. Amado, in: Pectin and Pectinases (Progress in Biotechnology, vol 14), J. Visser, A. G. J. Voragen (Eds), Elsevier Science B.V., Amsterdam, 1996, p. 651 .
9. R. Redgweel, R. Selvendran, *Carbohydr. Res*., **157**, 183 (1986).
10. R. Srivastava, D. K. Kulshreshtha, *Phytochem*., **28**, 2877 (1989).
11. H. S. Owens, R. M. McCready, A. D. Shepherd, T. H. Schultz, E. L. Pipen, N. A. Swenson, J. C. Milers, F. R. Erlander, W. D. Maclay, AIC Report 340, Western Regional Research, Albany, CA (1952).
12. O. H. Lowry, N. J. Rosenbrough, A. L. Farr, R. L. Randall, *J. Biol. Chem*., **193**, 265 (1951).
13. A. Blakeney, P. Harris, R. Henry, B. Stony,

Carbohydr. Res., **113**, 291 (1983).
14. L. G. Vissar, A. Annema, R. van Furth, *Infect. Immun.*, 63, 2570 (1995).
15. J. P. A. M. Klerx, C. J. Beukiman, H. van Dijk, J. M. N. Willers, *J. Immunol. Meth*., **63**, 215 (1983)
16. J. P. A. M. Klerx, C. J. Beukelman, H. van Dijk, F. J. Van Overveld, W. J. van der Maaden, J. M. N. Willers, *Infect. Immun.*, **49**, 841 (1985).
17. R. R. Selvendran, M. A. O'Neill, *Methods Biochem. Anal*., **32**, 153 (1987).
18. A. N. Round, N. M. Rigby, A. J. MacDougall, S. C. Ring, V. J. Morrus, *Carbohydr. Res*., **331**, 337 (2001).
19. J. N. BeMiller, *Adv. Carbohydr. Chem. Biochem.,* **22**, 25 (1967).
20. H. Neukom, R. Amado, M. Plister, *Lebensm. Wiss. u. Technol*., **13**, 1 (1980).

ХАРАКТЕРИЗИРАНЕ НА ПЕКТИНОВИ ПОЛИЗАХАРИДИ ОТ ПРАЗ ПОЛУЧЕНИ ЧРЕЗ ПОСЛЕДОВАТЕЛНО ЕКСТРАХИРАНЕ С РАЗЛИЧНИ РЕАГЕНТИ

М. Крачанова[1]*, М. Гочева[1], Е. Павлова[1], Ир. Янакиева[1], Д. Неделчева[2], В. Късовски[3], А. Славов[4]

[1] Лаборатория „Биологично активни вещества", Институт по органична химия с център по фитохимия, Българска академия на науките, бул. „Васил Априлов" № 95, ПК 27, 4002 Пловдив
[2] Аналитична лаборатория по инструментална хроматография и мас-спектрометрия, Институт по органична химия с център по фитохимия, Българска академия на науките, ул. „Акад. Г. Бончев" бл. 9, 1113 София
[3] Институт по микробиология, Българска академия на науките, ул. „акад. Г. Бончев" бл. 26, 1113 София
[4] Университет по хранителни технологии, бул. „Марица" № 26, 4002 Пловдив

Посветена на акад. Иван Юхновски по повод на 70-та му годишнина

Постъпила на 7 февруари 2008 г.; Преработена на 18 март 2008 г.

(Резюме)

Получени са пет съизмерими по добив, но различни по състав пектинови полизахаридни фракции чрез последователна екстракция с вода, разтвори на амониев оксалат, натриев карбонат, солна киселина и натриева основа от алкохолно неразтворима част (АНЧ) на праз. В полиуронидния състав на тези фракции освен галактуронова киселина се открива и наличие на глюкуронова киселина. В състава на неутралните захари (НЗ) доминира галактозата последвана от рамнозата. Водно-екстрахируемият пектинов полизахарид е високо хомогенен (93.3% с молекулна маса 1.3×10^6 Da) и с белтъчно съдържание 8% (най-високо в сравнение с останалите полизахариди). При екстракцията с разредена солна киселина се получава полизахарид с най-високо съдържание на НЗ (71.1%) и ниско количество на уронови киселини. Водно- и хелатно-екстрахируемите фракции имат по-ниско съдържание на L-рамноза (съответно 2.7% и 2.9%), а останалите полизахаридни фракции от праз се отличават с високо съдържание на L-рамноза(от 14 до 28%). Пектиновите полизахариди на праза са добри имуностимулатори. Най-висока имуностимулираща активност показват водно- и хелатно-екстрахируемите полизахариди, които се характеризират с високо съдържание на полиуроними и молекулна маса над 10^6 Da.

Bulgarian Chemical Communications, Volume 40, Number 4 (pp. 568–571) 2008

Stereocontrolled intramolecular cyclization of *anti*-β-aminonitriles. Convenient access to *trans*-azetidin-2-imines

Tz. Gospodova, J. R. Rashkova, L. Z. Viteva*

Institute of Organic Chemistry with Centre of Phytochemistry, Bulgarian Academy of Sciences, 1113 Sofia, Bulgaria

Dedicated to Academician Ivan Juchnovski on the occasion of his 70th birthday

Received February 13, 2008; Revised March 6, 2008

We have developed a convenient approach to synthesis of *trans*-azetidin-2-imines, consisting in stereocontrolled cyclization of *anti*-*β*-amino nitriles in boiling ethanol in the presence of hydrochloric acid.

Key words: azetidin-2-imine, intramolecular cyclization, *β*-amino nitrile

INTRODUCTION

In spite of the amount of research addressed to synthesis of β-lactams, one of the most successful groups of antibiotics, very few studies have been devoted to the preparation of the corresponding imine derivatives.

The first examples of the azetidine 2-imine small-ring heterocyclic system have been reported in the early 1975 [1]. The products have been obtained in reaction of N-isopropylallenimine with organic azides. Later on, Gaudemare *et al*. demonstrated that the addition of organozinc reagents of α-bromonitriles to aldimines in THF resulted in formation of substituted azetidine 2-imines in good yields [2].

Ghosez *et al*. [3] developed a general approach to synthesis of azetidin-2-iminium salts, which have been used as valuable precursors in synthesis of various four-membered heterocycles like 2-amino-azetines [4, 5], β-lactams and their sulphur analogues azetidine-2-thiones [6–8] and azetidine-2-imines [8].

Data concerning the stereochemical course in the cyclization reaction are scarce [7, 9] and to the best of our knowledge only one paper deals with the preferential formation of *cis* or *trans* product as a function of the steric and electronic demands of the reactants [7].

Recently, in our study on the diastereoselectivity in addition of lithiated nitriles to Schiff bases we observed fast proton shift in the initially formed azanion, resulting in a prochiral carbanionic intermediate with an adjacent chiral centre [10]. The subsequent one-pot alkylation reaction was found to proceed with high to outstanding level of anti diastereoselectivity, thus giving convenient access to relatively complex molecules with definite configuration.

In an attempt for acidic hydrolysis of a casually selected example of the alkylated compounds, more precisely *anti*-2-methyl-2,3-diphenyl-3-phenylamino-propionitrile instead of the corresponding β-amino-acid, we isolated a product which was specified as 3-methyl-1,3,4-triphenylazetidine-2-imine.

Taking into account this finding and with readily available *anti*-β-aminonitriles in hands, it was of interest to explore the applicability of the above-mentioned approach to the synthesis of new representatives of this small, scarcely presented in the chemical structural space heterocycle. An additional reason to perform this study was our anticipation that starting from stereochemically pure β-amino-nitriles with *anti*-configuration, we would obtain stereochemically pure azetidine-2-imines as a result of a stereocontrolled cyclization.

Herein we present our study on the cyclization of some β-aminonitriles to differently functionalized azetidine-2-imines under acidic conditions.

RESULTS AND DISCUSSION

The synthesis (Scheme 1) was performed in boiling methanol in the presence of conc. hydrochloric acid for 4 hours. The target compounds were isolated after a common work-up procedure, followed by purification with flash chromatography on silica gel (see Experimental section). In all cases studied, only one of the two possible isomers was isolated. The structure of all new products was unambiguously proved using a set of spectral techniques and elemental analysis.

* To whom all correspondence should be sent:
E-mail: lilia@orgchm.bas.bg

© 2008 Bulgarian Academy of Sciences, Union of Chemists in Bulgaria

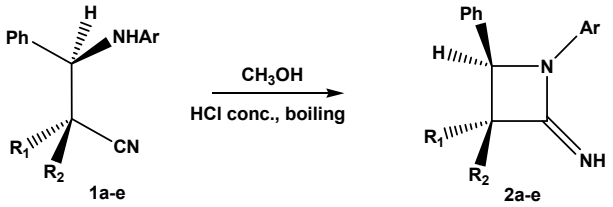

	Ar	R_1	R_2
a	Ph	Ph	CH_3
b	β-naphthyl	Ph	CH_3
c	Ph	Ph	$CH_2CH{=}CH_2$
d	β-naphthyl	Ph	$CH_2CH{=}CH_2$
e	Ph		CH_3

Scheme 1: Synthesis of azetidine-2-imines **2**a–**2**e.

The reaction occurs with good to moderate yields. The optimal reaction time was determined by monitoring the reaction using ^{1}H NMR and TLC analysis. It was clearly demonstrated that the prolongation of the reaction duration above 4 hours resulted not in an increase of the reaction yields, but in decomposition of the starting β-aminonitriles as shown in Scheme 2.

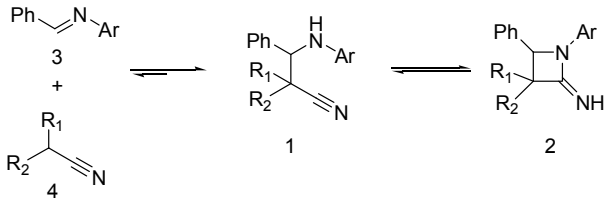

Scheme 2: Cyclization and decomposition of β-aminonitriles.

To realize the stereochemical course of the reaction, we took in mind the following consideration. Since the cyclization does not concern the existing stereogenic centres, the configuration of the cyclic azetidine-2-imines must be in immediate relation with the configuration of the β-aminonitrile precursors. Hence, starting from configurationally pure *anti*-isomers **1a**–**1e** we should obtain *trans*-azetidin-2-imines **2a**–**2e**. This presumption was undoubtedly confirmed by ^{1}H NMR analysis of the crude reaction mixtures where no signals for the second possible *cis*-stereoisomer were detected. An attempt for visualization of the relationship between the stereochemistry of the starting adducts and the resulting azetidine-2-imines is presented in Scheme 1.

Thus, the assigned *trans*-configuration was confirmed in an independent way by the NOESY experiments, carried out in the case of **2e**. The experiments proved unambiguously the *trans*-location of the phenyl group and the R_2 substituent at the adjacent stereogenic centres. Some characteristic NOESY correlations are presented in Fig. 1.

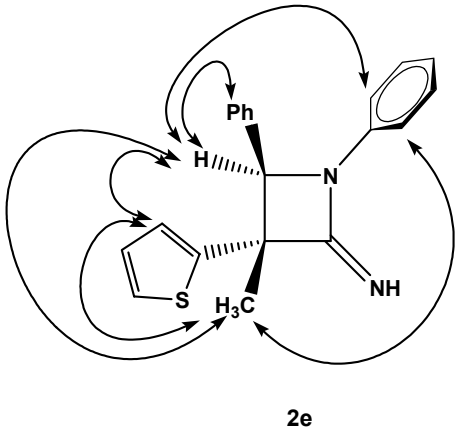

Fig. 1. Arrows indicate the important NOE effects in compound 2e.

As reported, cyclization occurs in the presence of hydrochloric acid, e.g. under acidic conditions. Our attempts to perform the synthesis in neutral medium were unsuccessful. As could be expected, protonation of the nitrile group increases its electrophilicity and makes possible closing of the azethidin-2-imine heterocycle. The probable mechanism of cylization is depicted in Sheme 3:

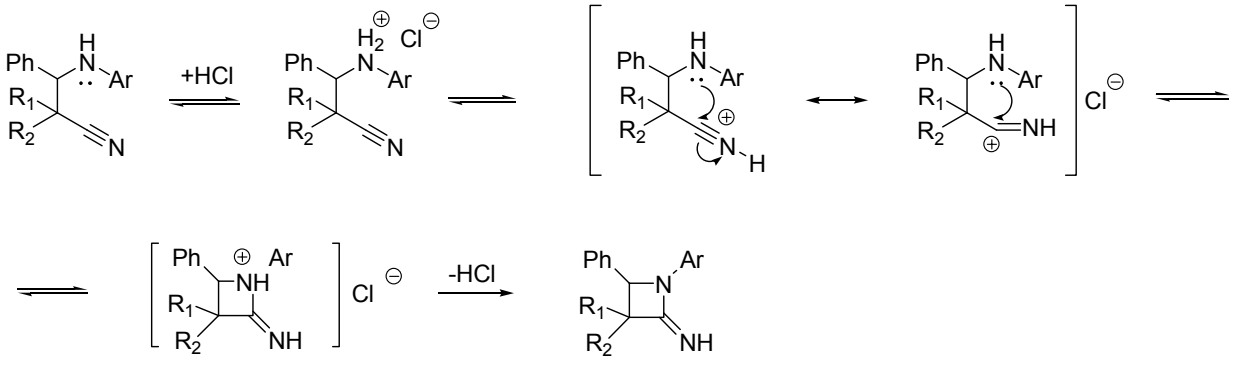

Scheme 3. Probable reaction mechanism of the cyclization reaction.

In conclusion, the present paper reports a new and convenient approach to synthesis of differently functionalized *trans*-azetidie-2-imines, consisting in stereocontrolled cyclization of *anti*-β-aminonitiles in acidic medium. The paper contributes to the synthetic diversity of scarcely presented azetidine-2-imine small heterocyclic system.

EXPERIMENTAL

The solvents were commercially available and used without further purification. The starting *anti*-β-aminonitiles **1a**–**1e** were synthesized as described [10]. Compound **1e** is newly prepared for the purposes of the present investigation and described in Experimental. Flash chromatography was carried out using Fluka silica gel 60 (0.04–0.063 mm). Analytical thin-layer chromatography (TLC) was performed on Merck 60 F254 plates. Melting points were determined on a Kofler apparatus and were not corrected. IR spectra were recorded on a Bruker FTR-113 V spectrometer using KBr pellets and only partial data are reported. ^{1}H and ^{13}C NMR spectra were recorded on a Bruker DRX-250 spectrometer using TMS as an internal standard. The chemical shifts are reported in ppm on the δ scale relative to TMS (tetramethylsilane, δ = 0 ppm); J = Hz; C-multiplicities were assigned by DEPT techniques. EI-MS (30 eV) were recorded on a Hewlett Packard 5973 device. Elemental analysis was performed by the Micro-analytical service Laboratory of the Institute of Organic Chemistry, Bulgarian Academy of Sciences.

Anti-2-methyl-3-phenyl-3-(phenylamino)-2-(thiophen-2-yl)propanenitrile (**1e**): The starting compound **1e** was obtained for the purposes of the present study as described [10]. Thus, from 2-thiophenyl-acetonitrile (123 mg, 1 mmol), benzylideneaniline (181 mg, 1 mmol) and methyl iodide (213 mg, 1.5 mmol) the title compound *anti*-**1e** was isolated by recrystallization (EtOH) (150 mg, 47%). M.p. 104–106ºC. R_f = 0.3 (Et_2O/hexane = 1:3). $C_{20}H_{18}N_2S$ (318.44): calcd. C 75.44; H 5.70; N 8.80; S 10.07; found: C 75.30, H 5.43, N 8.43, S 9.84. MS (EI, 30eV): m/z = 318 $[M]^+$. ^{1}H NMR ($CDCl_3$):1.69 (s, 3H, CH_3), 4.29 (d, J = 6.5, 1H, NH), 4.53 (d, J = 6.5, 1H, CH), 6.42–6.46 (m, 2H, $CH_{thienyl}$), 6.62–6.68 (m, 1H, $CH_{thienyl}$), 6.96–7.06 (m, 3H, CH_{phenyl}), 7.25–7.30 (m, 1H, CH_{phenyl}), 7.30–7.42 (m, 6H, CH_{phenyl}). ^{13}C NMR ($CDCl_3$): 26.9 (CH_3), 45.8 (C_q), 66.7 (CH), 114.2, 118.6 (CH), 120.8 (CN), 126.0, 126.8, 126.83, 128.11, 128.58, 128.65, 129.0, 137.7 (C_q), 142.1 (C_q), 146.25 (C_q).

*General experimental procedure for synthesis of 1,3,4 substituted azetidin-2-imines **2a-e***

The starting β-aminonitrile (1 mmol) was dissolved in methanol (20 ml). Conc. hydrochloric acid (3 ml) was then added and the reaction mixture was kept under reflux for 4 hours. After cooling, the solvent was removed under reduced pressure to half of the volume, diluted with cold water and neutralized to pH = 7 with solid Na_2CO_3. The solution was extracted with CH_2Cl_2, the combined organic layer was dried over Na_2SO_4, filtered and the solvent was evaporated under vacuum. The target compounds were purified by column chromatography on silica gel. Thus isolated products are spectroscopically and analitycally pure. Additional recrystallisation from EtOH decreases significantly the reaction yields without appreciable effect on the product purity.

Trans-3-methyl-1,3,4-triphenylazetidin-2-imine (**2a**): Following the general experimental procedure, starting from 1a (312 mg, 1 mmol) the title compound *trans*-**2a** (187 mg, 60%) was isolated after purification by column chromatography (silica gel, Et_2O/hexane = 1:1). Recrystallization (EtOH) afforded **2a** (140 mg, 40%) as white crystals, m.p. 134–136ºC. R_f = 0.29 (Et_2O/hexane = 1:1). $C_{22}H_{20}N_2$ (312.41): calcd. C 84.58, H 6.45, N 8.97, found C 84.39, H 6.33, N 8.78. MS: m/z = 312 $[M]^+$. IR: ν = 1675 cm^{-1}. ^{1}H NMR ($CDCl_3$): 1.23 (s, 3 H, CH_3), 5.13 (s, 1H, CH), 6.95–7.44 (m, 15H, 3×Ph). ^{13}C NMR ($CDCl_3$): 18.8 (CH_3); 57.7 (C_q); 70.6 (CH–Ph); 116.7, 122.1, 125.8, 126.8, 127.3, 128.0, 128.6 and 128.9 (CH_{arom}); 135.4, 139.6 and 142.3 (C_q), 169.1 (C=NH).

Trans-3-methyl-1-(naphthalen-2-yl)-3,4-diphenylazetidin-2-imine (**2**b): Following the general experimental procedure, starting from **1b** (362 mg, 1 mmol) the title compound *trans*-**2b** (238 mg, 66%) was isolated after purification by column chromatography (silica gel, Et_2O/hexane = 1:1). Recrystallization (EtOH) afforded **2b** (144 mg, 40%) as white crystals. M.p. 185–187ºC, R_f = 0.32 (Et_2O/hexane = 1:1). $C_{26}H_{22}N_2$ (362.47):calcd. C 86.15, H 6.12, N 7.73, found C 86.02, H 5.93, N 7.51. MS: m/z = 362 $[M]^+$. IR: ν = 1679 cm^{-1}. ^{1}H NMR ($CDCl_3$): 1.19 (s, 3H, CH_3), 5.19 (s, 1H, CH), 7.18–7.70 (m, 17H, H_{arom}). ^{13}C NMR ($CDCl_3$): 18.8 (CH_3); 57.8 (C_q); 70.9 (CH–Ph); 112.9, 117.5, 124.2, 125.8, 126.4, 126.9, 127.2, 127.4, 127.6, 128.1, 128.7, 128.8, 129.0 and 129.5 (CH_{arom}); 133.8, 135.4, 137.2 and 142.2 (C_q); 169.3 (C=NH).

3-Allyl-1,3,4-triphenylazetidin-2-imine (**2c**): Following the general experimental procedure, starting from **1c** (338 mg, 1 mmol) the general experimental procedure afforded the title compound *trans*-**2c** (100 mg, 30%) after purification by column chromatography (silica gel, Et_2O/hexane = 1:1). Recrystallization (EtOH) gave access to **2c** (50 mg, 15%) as white crystals. M.p. 152–154ºC. R_f = 0.35 (Et_2O/hexane = 1:1). $C_{24}H_{22}N_2$ (338.44): calcd. C 85.17, H 6.55, N 8.28, found C 84.94, H 6.42, N 8.00. MS: m/z = 338 $[M]^+$. IR: ν = 1669 cm^{-1}. ^1H NMR ($CDCl_3$): 1.56 (br., NH), 2.22–2.40 (m, 2H, CH_2), 4.92–5.01 (m, 2H, CH_2=), 5.12 (s, 1H, CH–Ph), 5.40–5.55 (m, 1H, CH=), 6.93–7.56 (m, 15H, 3×Ph). ^{13}C NMR ($CDCl_3$): 38.25 (CH_2); 60.42 (C_q); 70.58 (CH–Ph); 116.74 (CH); 118.95 (CH_2=); 122.05, 126.49, 127.08, 127.36, 128.25, 128.76, 128.83, 129.04 and 132.94 (CH_{arom}), 135.28, 139.68 and 140.48 (C_q); 167.11 (C=NH).

3-Allyl-1-(naphthalen-2-yl)-3,4-diphenylazetidin-2-imine (**2d**): Following the general experimental procedure, starting from **1d** (388 mg, 1 mmol) the title compound *trans*-**2d** (116 mg, 30%) was isolated after purification by column chromatography (silica gel, Et_2O/hexane = 1:1). Recrystallization (EtOH) afforded **2d** (70 mg, 18%) as white crystals. M.p. 166–168ºC. R_f = 0.48 (Et_2O/hexane = 1:1). $C_{28}H_{24}N_2$ (388.5): calcd. C 86.56, H 6.23, N 7.21; found C 86.33, H 6.00, N 6.99. MS: m/z = 388 $[M]^+$. IR: ν = 1669 cm^{-1}. ^1H NMR ($CDCl_3$): 2.27–2.44 (m, 2H, CH_2), 4.95–5.05 (m, 2H, CH_2=), 5.26 (s, 1H, CH), 5.46–5.52 (m, 1H, CH=), 7.35–7.73 (m, 17H, CH_{arom}). ^{13}C ($CDCl_3$+$DMSO_{d6}$): 36.3 (CH=); 57.7 (CH_2); 71.5 (CH–Ph); 117.8 and 118.5 (CH), 118.8 (CH_2=); 126.0, 126.4, 126.5, 127.0, 127.2, 127.4, 128.1, 128.2, 128.5, 128.8 and 128.9 (CH_{arom}); 130.5, 130.7, 131.1, 132.1 and 135.9 (C_q); 165.8 (C=NH).

3-Methyl-1,4-diphenyl-3-(thiophen-2-yl)azetidin-2-imine (**2e**): Following the general experimental procedure, starting from **1e** (318 mg, 1 mmol) the title compound *trans*-**2e** (130 mg, 41%) was isolated after purification by column chromatography (silica gel, Et_2O/hexane = 1:1). Recrystallization (EtOH) afforded **2e** (60 mg, 19%) as white crystals. M.p. 134–136ºC. R_f = 0.27 (Et_2O/hexane = 1:1). $C_{20}H_{18}N_2S$ (318.44): calcd. C 75.44, H 5.70, N 8.80, S 10.07, found 75.39, H 5.49, N 8.63, S 9.90. MS: m/z = 318 $[M]^+$. IR: ν = 1673 cm^{-1}. ^1H NMR ($CDCl_3$): 1.26 (s, 3H, CH_3), 5.24 (s, 1H, CH), 6.99–7.08 (m, 3H, $CH_{thiophene}$), 7.24–7.30 (m, 5H, CH_{arom}), 7.33–7.40 (m, 5H, CH_{arom}). ^{13}C ($CDCl_3$): 20.3 (CH_3); 55.3 (2-C) C_q; 71.2, 116.9, 122.3, 123.9, 124.7, 126.8, 127.2, 128.2, 128.7 and 128.9, (CH), 135.0, 139.7 and 146.1 (C_q); 168.3 (C=NH).

REFERENCES

1. K. Grandall, L. C. Crawley, J. B. Komin, *J. Org. Chem*., **40**, 2045 (1975).
2. N. Goasdoue, M. Gaudemare, *J. Organomet. Chem*., **125**, 9, (1977).
3. J. Marchand-Brynaert, M. De Poortere, L. Ghosez, *Angew. Chem., Int. Ed. Engl*., **13**, 267, (1974).
4. J. Marchand-Brynaert, M. Moya-Portugues, D. Lesuisse, L. Ghosez, *J. Chem. Soc., Chem. Comm*., 173, (1980).
5. F. Stierli, R. Prewo, J. H. Bieri, H. Heimgartner, *Helv. Chem. Acta*, **67**, 927, (1980).
6. M. I. Page, P. Webster, S. Bogdan, B. Tremerie, L. Ghosez, *J. Chem. Soc., Chem. Comm*., 318 (1987).
7. G. Barbaro, A. Battaglia, C. Bruno, P. Giorgianni, A. Guerrini, *J. Org. Chem*., **61**, 8480 (1996).
8. J. Marchand-Brynaert, M. Moya-Portugues, I. Huber, L. Ghosez, *J. Chem. Soc., Chem. Comm*., 818, (1983).
9. A. van Camp, D. Goossens, M. Moya-Portugues, J. Marchand-Brynaert, L. Ghosez, *J. Tetrahedron Lett*., **21**, 3081, (1980).
10. L. Viteva, Tz. Gospodova, Y. Stefanovsky, S. Simova, *Tetrahedron*, **61**, 5855, (2005).

СТЕРЕОКОНТРОЛИРАНА ВЪТРЕШНОМОЛЕКУЛНА ЦИКЛИЗАЦИЯ НА *анти*-β-АМИНО-НИТРИЛИ. УДОБНА СИНТЕЗА НА *транс*-АЗЕТИДИН-2-ИМИНИ

Цв. Сп. Господова, Ж. Р. Рашкова, Л. Зл. Витева*

Институт по органична химия с център по фитохимия, Българска академия на науките, 1113 София

Посветена на акад. Иван Юхновски по повод на 70-та му годишнина

Постъпила на 13 февруари 2008 г.; Преработена на 6 март 2008 г.

(Резюме)

Разработен е удобен метод за получаване на *транс*-азетидин-2-имини, включващ стереоконтролирана циклизация на *анти*-β-амино нитрили в кипящ етанол в присъствие на солна киселина.

AUTHOR INDEX

AbdEl-Lateef S., See M. A. El-Badawi et al. …… 70
Afify A. A. E., See Madkour H. M. F. et al. ……147
Alhamed Y. A., Phenol removal using granular activated carbon from dates' stones …….. 26
Altun Ö., See Gavazov K. B. et al. …… 65
Amutha P., See Selvambigai K. et al. ……36
Anastasov A. I., See A. T. Georgieva, et al.: …… 13
Anastasov A. I., See A. T. Georgieva, et al.: …… 19
Anastasov A. I., See A. T. Georgieva, et al.: ……. 3
Andreev G. N., See Penchev P. N. et al. ……. 556
Angelova S., See Enchev V. et al. ……... 532
Arnaudova M., See Hristova E. et al. ……. 291
Atanasov Y., See Ilieva S. et al. ……. 401
Atanasova G., See Guergova D. et al. ……. 227
Atanassova P., See Petrov K. et al. …… 333
Avgouropoulos G., See Tabakova T. et al. …….. 42
Avramova I., See Guergova D. et al. …….. 227
Babu B. H., B. V. Babu, C. N. Raju, Synthesis and bio-activity of 6-alkoxy/aryl/aryloxy-4,8-di(*tert*-butyl) 2,10-dimethyl-12*H*-6λ^5-dibenzo[d,g][1,3,2] dioxa-phosphocin-6-ones/thiones/selenones …….. 160
Babu B. V., See Babu B. H. et al. ……160
Bachvarov V., See Raicheff R. et al. ……... 244
Bakalova S. M., J. Kaneti, O. Castaño, Computational study of the electronic spectra of some B–N dyes ……..... 450
Bankova V. S., See Kancheva V. D. et al. …….. 546
Batovska D. I., See Ivanova D. I. et al. ……....440
Belov K., See Mladenov M. et al. ……. 360
Binev I., A. Popova, Ivan Nikolov Juchnovski – Biographical and professional data ……. 373
Binev I. G., See Popova A. D. et al. …… 512
Binev I. G., See Tsenov J. A. et al. ……..520
Binev I. G., See Velcheva E. A. et al. ……. 433
Binev Y. I., See Popova A. D. et al. …… 512
Blagoeva I. B., E. P. Ignatova-Avramova, A. H. Koedjikov, I. G. Pojarlieff, L. I. Proevska, V. T. Rachina, N. G. Vassilev, Linear free energy relationships of the gem-dimethyl (gem-dialkyl) effect ……386
Blaskov V., See Ljutzkanov L. et al. 109
Bojinov M. S., See Karastoyanov V. I. et al. ……. 267
Bojinov M. S., See Tzvetkov B. Tz. et al. …….. 261
Bontchev R. P., See Simeonov S. P. et al. ……. 409
Boshkov N. S., See Raichevski G. M. et al. …….. 281
Brougham D. F., See Ivanova G. I. et al. …… 464
Budevski E., See Petrov K. et al. …… 122
Budinova T., M. Krzesinska, B. Tsyntarski, J. Zachariasz, N. Petrov, Activated carbon produced from bamboo pellets for removal of arcenic(iii) ions from water …….. 166
Buess-Herman C., See Stoyanova A. R. et al. …….. 185
Cabrita E. J., See Ivanova G. I. et al. …….. 464
Castaño O., See Bakalova S. M. et al. ……. 450
Chernev G. E., See Raicheff R. G. et al. 295
Cherneva E. D., Ts. M. Kolev, Solid-state polarized IR-spectroscopic study of high temperature red phase of 5-amino-2-methoxypyridine ester amide of squaric acid ethyl ester …… 477
Damyanov M., See Lukanova R. et al. …….. 340
Dardanova I. D., See Petkov L. N. et al. ……. 323
Daskalova L. I., Y. Dimitrova, Theoretical study of structures and stability of hydrogen-bonded systems between pyridine-3-carboxamide (nicotinamide) and DMSO ……..... 426
De Rosa S., Z. Kamenarska, K. Seizova, C. Iodice, A. Petrova, D. Nedelcheva, K. Stefanov, S. Popov, Volatile and polar compounds from Geodia cydonium and two Tedania species ……..... 48
Dimcheva N., See Horozova E. et al. ……. 233
Dimcheva N., See Horozova E. et al. …….. 129
Dimitrova Y., Hydrogen bonding in ionic systems of 1,5,7- triazabicyclo[4.4.0]dec-5-ene (TBD) with 4-cyanophenol: *ab initio* and DFT studies of their structures ……. 418
Dimitrova Y., See Daskalova L. I. et al. 426
Djambaski P. R., See Raicheff R. G. et al. 295
Djambova A. G., See Popova A. K. et al. ……300
Dobrev Ts. M., M. Chr. Monev, Iv. N. Krastev, R. P. Zlatev, Electrochemical methods for evaluation of the protective ability of electroplated coatings and conversion films …….. 198
Dobrev Ts. M., See Stefanov Y. S. et al. …… 277
Dobrovolska Ts., R. Kowalik, P. Zabinski, I. Krastev, Investigations of the surface morphology of electrodeposited Ag-In coatings by means of optical, scanning-electron and atomic-force microscopy …….. 254
Dobrovolska Ts., See Nineva S. et al. ……. 248
Dodevska T., See Horozova E. et al. …….. 233
El-Badawi M. A., H. F. Rizk, S. AbdEl-Lateef, M. A. El-Borai, Synthesis and reactivity of some pyridyl isoxazol-5-ones …….. 70
El-Borai M. A., See M. A. El-Badawi et al. ……. 70
Enchev V., S. Angelova, N. Markova, I. Wawer, E. Stanoeva, M. Mitewa, *Ab initio* and DFT study of the structure of metal ion complexes with N-benz-alaniline-15-crown-5 …… 532
Eustace A. J., See Ivanova G. I. et al. ……..... 464
Fachikov L., Y. Tumbaleva, D. Ivanova, Phosphating of ferro-carbon alloys by modifying zinc-phosphate solutions ……355
Farhi O. A., See Yanev Y. S. et al. ……..330
Gabrielli C., See Mirkova L. et al. …….. 240
Galabov B., See Ilieva S. et al. …….. 401
Gamburzev S., See Petrov K. et al. ……..333
Gavazov K. B., M. Türkyilmaz, Ö. Altun, Extractive-spectrophotometric investigations on ternary ion-associated complexes between the vanadium(V)–4-(2-pyridylazo)-resorcinol anionic chelate and some methoxyditetrazolium cations ……. 65

Georgiev D. P., S. D. Vlaev, Effect of inclined-blade impeller design on mixing and aeration in stirred vessels ……..173
Georgieva A. T., A. I. Anastasov, An investigation of the resources of a conventional catalyst O 4-25 calcined under special conditions for oxidation of o-xylene to phtalic anhydride. Part I: Calcination and working characteristics of the catalyst ……. 3
Georgieva A. T., A. I. Anastasov, An investigation of the resources of a conventional catalyst O 4-25 calcined under special conditions for oxidation of *o*-xylene to phtalic anhydride. Part II: Formation of dual catalyst bed in the case of operation with low inlet reagent concentration …….. 13
Georgieva A. T., A. I. Anastasov, An investigation of the resources of a conventional catalyst O 4-25 calcined under special conditions for oxidation of o-xylene to phtalic anhydride. Part III: Characteristics of the bed in the case of operation with high inlet reagent concentrations …….. 19
Gerwann J., See Kozhukharov V. et al. …….. 310
Girginov A. A., See Tzvetkov B. Tz. et al. ……..261
Girish Kumar S., See Gomathi Devi L. et al. ……. 114
Gocheva M., See Kratchanova M., et al. ……. 561
Gomathi Devi L., S. Girish Kumar, Role of oxidising agent in photocatalytic degradation of benzene and its influence on kinetic and adsorption mechanism ……..... 114
Gospodova Tz., J. R. Rashkova, L. Z. Viteva, Stereocontrolled intramolecular cyclization of *anti*-β-aminonitriles. Convenient access to *trans*-azetidin-2-imines …… 568
Guergova D., E. Stoyanova, D. Stoychev, G. Atanasova, I. Avramova, P. Stefanov, Influence of calcination of stainless steel OC4004 covered with alumina or ceria carrier layers on their passive state in different acid media ……. 227
Hampden-Smith M., See Petrov K. et al. …… 333
Horozova E., N. Dimcheva, M. Miteva, Z. Jordanova, Rhodium deposits on graphite: The impact of the graphite pad on the electrocatalytic activity towards the electrooxidation of formic acid ... 129
Horozova E., T. Dodevska, N. Dimcheva, Modified graphite electrodes as catalysts for electroreduction of hydrogen peroxide …… 233
Hristov G., M. Mitov, R. Rashkov, S. Hristov, A. Popov, Electrooxidation of alkaline borohydrides on metal hydride electrodes …….. 306
Hristov Hr., See Petrov K. et al. ……. 122
Hristov S. M., Amperometric biosensors ……. 204
Hristov S., See Hristov G. et al. ……. 306
Hristova E., M. Mitov, R. Rashkov, M. Arnaudova, A. Popov, Sulphide oxidation on electrodeposited Ni-Mo-W catalysts …… 291
Idakiev V., See Tabakova T. et al. …….. 42
Ignatova-Avramova E. P., See Blagoeva I. B. et al. …386
Iliev P. Ts., See Tsanev A. S. et al. ……. 348
Iliev P., See Petrov K. et al. …… 122
Ilieva S., Y. Atanasov, B. Galabov, Mechanism of the aminolysis of phenyl acetate: a computational study …… 401
Ioannides T., See Tabakova T. et al. …… 42
Iodice C., See De Rosa et al. …… 48
Ivanov P. M., See Kotev M. I. et al. …… 505
Ivanova D. I., I. I. Timtcheva, B. A. Stamboliyska, D. I. Batovska, UV-VIS absorption and fluorescent characteristics of some substituted in the styril fragment synthetic chalcones ……... 440
Ivanova D. I., See Raicheff R. G. et al. 295
Ivanova D., See Fachikov L. et al. …….. 355
Ivanova G. I., E. J. Cabrita, R. O´Connor, A. J. Eustace, D. F. Brougham, Application of diffusion- ordered spectroscopy for the analysis of cancer related biological samples …… 464
Jagannadham V., How do we synthesize acyclic mixed (O,S)-acetals? A physical-organic chemistry approach ……. 144
John Appleby A., See Petrov K. et al. …… 333
Jordanova Z., See Horozova E. et al. …….. 129
Kamenarska Z., See De Rosa et al. …….. 48
Kancheva V. D., V. S. Bankova, Chain-breaking antioxidant activity of two new chalcones from propolis of El Salvador in homogeneous and micellar media …… 546
Kaneti J., See Bakalova S. M. et al. …… 450
Karastoyanov V. I., M. S. Bojinov, Conduction mechanism of anodic oxide films on tungsten – effect of the electrolyte pH ……. 267
Kochev N. T., See Penchev P. N. et al. …….. 556
Koedjikov A. H., See Blagoeva I. B. et al. ……. 386
Kolev Ts. M., See Cherneva E. D. et al. ……..477
Kolev Ts. M., See Stamboliyska B. A. et al. …….. 498
Kolev Ts. M., See Tsanev Ts. D. et al. …….. 483
Koleva B. B., Solid-state IR-LD spectroscopy of L-tryptophan-containing dipeptides L-tryptophyl-L-methionine (*H-Trp-Met-OH*), L-methionyl-L-tryptophan (*H-Met-Trp-OH*) and glycyl-L-tryptophan dihydrate (*H-Gly-Trp-OH.2*H_2O) …… 456
Kotev M. I., P. M. Ivanov, Molecular mechanics (MM3(π)) conformational analysis of molecules containing conjugated π-electron fragments: a molecular tweezer …… 505
Kovacheva D., See Mladenov M. et al. …….. 360
Kowalik R., See Dobrovolska Ts. et al. 254
Kozhukharov S., See Kozhukharov V. et al. …….. 310
Kozhukharov V., S. Kozhukharov, G. Tsaneva, J. Gerwann, M. Schem, T. Schmidt, M. Veith, Investigation on the corrosion protection ability of nanocomposite hybrid coatings ……310
Kraicheva I., Iv. Tsacheva, K. Troev, Poly(oxyethylene aminophosphonate)s – novel promising biologically active polymers and drug carriers. Design and NMR characterization …… .54
Krastev I., See Dobrovolska Ts. et al. 254
Krastev I., See Nineva S. et al. …… 248
Krastev Iv. N., See Dobrev Ts. M. et al. ……..198
Kratchanova M., M. Gocheva, E. Pavlova, I. Yanakieva, D. Nedelcheva, V. Kussovski, A. Slavov, Characteristics of pectic polysaccharides from leek obtained through consecutive extraction with

various reaction agents …… 561
Krishna A. B., See Kumar B. S. et al. …….. 59
Krzesinska M., See Budinova T. et al. 166
Kumar B. S., A. U. R. Sankar, M. V. Reddy, A. B. Krishna, C. S. Reddy, One-pot synthesis and antimicrobial activity of a new class of α-amino-phosphonic acid esters ……... 59
Kurteva V. B., See Simeonov S. P. et al. ……409
Kussovski V., See Kratchanova M., et al. ……... 561
Ljutzkanov L., I. Stambolova, V. Blaskov, S. Vassilev, V. Petkova, Ts. Tsacheva, D. Mehandjiev, Synthesis of nanosized TiO_2 particles on activated carbon …….. 109
Lukanova R., E. Stoyanova, M. Damyanov, D. Stoychev, Formation of protective films on Al in electrolytes containing no Cr^{6+} ions ……340
Lutov L., See Raichevski G. M. et al. ……. 281
M. D. Marinova, B. P. Tchorbanov, Brassicaceae plants as a new source of food grade peptidases …… 397
Machkova M. S., See Popova A. K. et al. …….. 300
Madkour H. M. F., A. A. E. Afify, G. A. E. Sayed, M. S. Salem, Synthetic utility of enaminonitrile moiety in heterocyclic synthesis ……..... 147
Magaeva S. D., See Stefanov Y. S. et al. …… 277
Manolova N. E., See Spasova M. G. et al. 469
Manolova N., See Stoilova O. et al. 491
Marcheva Y. S., R. G. Raicheff, Comparison of stress-corrosion cracking susceptibility of mild and low alloy steels in phosphate environments …… 318
Markova N., See Enchev V. et al. …… 532
Maurin G., See Mirkova L. et al. ……240
Meenakshi K. M., K. Vasant Kumar Pai, K. N. Mohana, R. Ramachandrappa, Kinetics and mechanism of oxidation of pyrazinamide with Bromamine-T in perchloric acid medium …….. 137
Mehandjiev D., See Ljutzkanov L. et al. 109
Minkova K., See Raichevski G. M. et al. …… 281
Miranda Salvado I. M., See Raicheff R. G. et al. 295
Mirkova L., G. Maurin, C. Gabrielli, Hydrogen permeation through Ni layers deposited from Watts' electrolyte ……240
Miteva M., See Horozova E. et al. ……. 129
Miteva V. L., See Penchev P. N. et al. …… 556
Mitewa M., See Enchev V. et al. ……532
Mitov M., See Hristov G. et al. ……306
Mitov M., See Hristova E. et al. ……. 291
Mladenov M., P. Zlatilova, R. Raicheff, S. Vassilev, N. Petrov, K. Belov, V. Trenev, D. Kovacheva, Synthesis and characterization of novel nanostructured carbon for supercapacitors on the basis of biomaterials ……... 360
Mladenova E., See Petrov K. et al. ……. 333
Mohana K. N., See Meenakshi K. M. et al. ……137
Monev M. Chr., See Dobrev Ts. M. et al. ……... 198
Nagarajan S., See Selvambigai K. et al. …… 36
Najdenov V., See Petrov K. et al. …… 122
Napolitano P., See Petrov K. et al. …….. 333
Nedelcheva D., See De Rosa et al. …….. 48
Nedelcheva D., See Kratchanova M., et al. …… 561
Nikolova V., See Petrov K. et al. …… 122
Nineva S., Ts. Dobrovolska, I. Krastev, Electrodeposition of silver-cobalt coatings ……. 248
O´Connor R., See Ivanova G. I. et al. …… 464
Paneva D. P., See Spasova M. G. et al. 469
Papavasiliou J., See Tabakova T. et al. …… 42
Pavlova E., See Kratchanova M., et al. …….. 561
Peev T. M., Electrochemical processes in magnetic field ……. 190
Penchev H., See Stoilova O. et al. 491
Penchev P. N., V. L. Miteva, A. N. Sohou, N. T. Kochev, G. N. Andreev, Implementation and testing of routine procedure for mixture analysis by search in infrared spectral library …… 556
Petkov L. N., I. D. Dardanova, Mathematical modelling of electrolysis processes …….. 323
Petkova V., See Ljutzkanov L. et al. 109
Petrov K., E. Mladenova, S. Gamburzev, A. John Appleby, P. Napolitano, P. Atanassova, M. Hampden-Smith, Evaluation of polymer electrolyte fuel cell catalysts using gas diffusion electrodes in aqueous electrolytes ……... 333
Petrov K., V. Najdenov, V. Nikolova, P. Iliev, Hr. Hristov, T. Vitanov, E. Budevski, "ELCOX" laboratory and pilot devices for purification of industrial waste gases from sulfur dioxide: optimization and real tests in "Pirdop" copper factory ……. 122
Petrov N., See Budinova T. et al. 166
Petrov N., See Mladenov M. et al. …….. 360
Petrov K. M., See Tsanev A. S. et al. …….. 348
Petrova A., See De Rosa et al. …….. 48
Pojarlieff I. G., See Blagoeva I. B. et al. …… 386
Popov A., See Hristov G. et al. ……306
Popov A., See Hristova E. et al. …….. 291
Popov S., See De Rosa et al. …….. 48
Popova A. See Binev I. et al. …….. 373
Popova A. D., See Stamboliyska B. A. et al. ……. 445
Popova A. D., See Stoyanov S. S. et al. ……. 538
Popova A. D., Y. I. Binev, P. J. Vassileva-Boyadjieva, I. G. Binev, Experimental IR, and computa-tional *ab initio* and DFT B3LYP studies on spectral and structural changes, caused by the conversion of methyl cyanoacetate into carbanion ……. 512
Popova A. K., M. S. Machkova, A. G. Djambova, A. Zwetanova, S. N. Raicheva, Relationship between chemical structure parameters and inhibitor efficiency of some azoles ……. 300
Proevska L. I., See Blagoeva I. B. et al. ……. 386
Rachina V. T., See Blagoeva I. B. et al. ……. 386
Raicheff R. G., G. E. Chernev, V. G. Zaprianova, D. I. Ivanova, P. R. Djambaski, B. I. Samuneva, I. M. Miranda Salvado, Electrochemical corrosion behaviour of silica hybrid sol-gel coatings …...295
Raicheff R. G., See Marcheva Y. S. et al. …….. 318
Raicheff R. G., See Raichevski G. M. et al. …….. 281
Raicheff R., G. Raichevski, V. Bachvarov, Inhibitor composition for corrosion protection of steels in water systems based on polymers and inorganic salts …….. 244
Raicheff R., See Mladenov M. et al. ……... 360
Raicheva S. N., See Popova A. K. et al. ……. 300

Raichevski G. M., N. D. Tsvetkova, N. S. Boshkov, R. G. Raicheff, K. Minkova, I. Topalova, L. Lutov, Corrosion and electrochemical investigations of low-alloyed and austenitic stainless steel used in the steam generators of Kozloduy nuclear power plant ……..... 281
Raichevski G., See Raicheff R. et al. …… 244
Raju C. N., See Babu B. H. et al. …… 160
Ramachandrappa R., See Meenakshi K. M. et al. …. 137
Rashkov I. B., See Spasova M. G. et al. 469
Rashkov I., See Stoilova O. et al. 491
Rashkov R., See Hristov G. et al. …… 306
Rashkov R., See Hristova E. et al. ……...291
Rashkov R., Synthesis and characterization of novel electrodeposited catalytic materials for hydrogen evolution reaction ……211
Rashkova J. R., See Gospodova Tz. et al. …….. 568
Reddy C. S., See Kumar B. S. et al. ……. 59
Reddy M. V., See Kumar B. S. et al. ……59
Revanasiddappa H. D., M. A. Veena, Facile and validated spectrophotometric methods for the determination of ascorbic acid …… 104
Rizk H. F., See M. A. El-Badawi et al. ……. 70
Ruskov T., See Stoilova O. et al. 491
Salem M. S., See Madkour H. M. F. et al. …… 147
Samuneva B. I., See Raicheff R. G. et al. 295
Sankar A. U. R., See Kumar B. S. et al. …… 59
Sayed G. A. E., See Madkour H. M. F. et al. ……. 147
Schem M., See Kozhukharov V. et al. …….. 310
Schmidt T., See Kozhukharov V. et al. …….. 310
Seizova K., See De Rosa et al. …….. 48
Selvambigai K., P. Amutha, S. Nagarajan, Inclusion complexes of 3,4-dihydropyrimidin-2-(1H)-ones with β-cyclodextrin …… 36
Simeonov S. P., V. B. Kurteva, R. P. Bontchev, One-pot solvent-free synthesis of symmetrical azines under microwave irradiation …… 409
Slavov A., See Kratchanova M., et al. …… 561
Sohou A. N., See Penchev P. N. et al. …… 556
Spasova M. G., D. P. Paneva, N. E. Manolova, I. B. Rashkov, Preparation of novel chitosan-containing micro- and nanofibrous materials by electro-spinning …… 469
Spirov I., See Stoilova O. et al. 491
Stamboliyska B. A., A. D. Popova, E. A. Velcheva, Theoretical study of the conformational preference of N-[(4-aminophenyl) sulphonyl]acetamide (sulphacetamide) and its azanion ……. 445
Stamboliyska B. A., D. Y. Yancheva, Ts. M. Kolev, A theoretical investigation on the structure, electronic spectra and nonlinear optical properties of pyridinium-betaines of squaric acid …….. 498
Stamboliyska B. A., See Ivanova D. I. et al. …….. 440
Stambolova I., See Ljutzkanov L. et al. 109
Stanoeva E., See Enchev V. et al. ……. 532
Stefanov K., See De Rosa et al. …… 48
Stefanov P. K., See Tsanev A. S. et al. ……348
Stefanov P., See Guergova D. et al. ……227
Stefanov Y. S., I. D. Valchanova, S. D. Magaeva, Ts. M. Dobrev, Investigations of composite coatings used as anodes for zinc electroextraction from sulphate electrolytes ……277
Stoilova O., H. Penchev, T. Ruskov, I. Spirov, N. Manolova, I. Rashkov, One-pot preparation of magnetic chitosan beads ……...491
Stoyanov S. S., A. D. Popova, J. A. Tsenov, IR Spectra and structure of 3,5,5-trimethyl(cyclohex-2-enylidene) malononitrile and its potassium cyanide and sodium methoxide carbanionic adducts: experimental and B3lYP studies …… 538
Stoyanov S. S., See Tsenov J. A. et al. ……. 520
Stoyanova A. R., C. Buess-Herman, V. Ts. Tsakova, Copper-modified conducting polymer layers for electroanalytic applications in neutral solutions ……... 185
Stoyanova A. R., V. Ts. Tsakova, Electrooxidation of glucose on copper-modified polyaniline layers in alkaline solution …….. 286
Stoyanova E., Contemporary aspects in the surface treatment of aluminium..... 85
Stoyanova E., See Guergova D. et al. ……. 227
Stoyanova E., See Lukanova R. et al. ……...340
Stoychev D. S., See Tsanev A. S. et al. ……... 348
Stoychev D., See Guergova D. et al. …….. 227
Stoychev D., See Lukanova R. et al. …….. 340
Stoynov Z., 40 Years of Experience and Excellence .. 183
Tabakova T., V. Idakiev, J. Papavasiliou, G. Avgouropoulos, T. Ioannides, Impact of the preparation method on the water-gas shift activity of CuO/doped-ceria catalysts …… 42
Tchorbanov B. P., See Marinova M. D. et al. ……. 397
Timtcheva I. I., See Ivanova D. I. et al. …….. 440
Topalova I., See Raichevski G. M. et al. ……. 281
Trenev V., See Mladenov M. et al. ……. 360
Trifonova A. V., Modified carbon matrix – high energy anode for lithium ion battery ……..... 219
Troev K., See Kraicheva I. et al. ……..... 54
Tsacheva Iv., See Kraicheva I. et al. ……..... 54
Tsacheva Ts., See Ljutzkanov L. et al. 109
Tsakova V. Ts., See Stoyanova A. R. et al. …… 185
Tsakova V. Ts., See Stoyanova A. R. et al. …… 286
Tsanev Ts. D., Ts. M. Kolev, Spectroscopic elucidation of hydrogensquarate and ester amide of squaric acid of 2-chloro-3-aminopyridine …… 483
Tsanev A. S., P. Ts. Iliev, K. M. Petrov, P. K. Stefanov, D. S. Stoychev, Electrocatalytic activity of electrochemically deposited Zr-Ce-Y/Ni and Co/Zr-Ce-Y/Ni oxide systems during evolution of hydrogen and oxygen ……... 348
Tsaneva G., See Kozhukharov V. et al. …….. 310
Tsenov J. A., S. S. Stoyanov, I. G. Binev, IR spectral and structural changes, caused by the conversion of 4-cyanobenzamide into azanion: a combined experimental/computational approach ……... 520
Tsenov J. A., See Stoyanov S. S. et al. ……538
Tsvetkova N. D., See Raichevski G. M. et al. ……. 281
Tsyntarski B., See Budinova T. et al. 166
Tumbaleva Y., See Fachikov L. et al. ……...355
Türkyilmaz M., See Gavazov K. B. et al. ……..65

Tzvetkov B. Tz., M. S. Bojinov, A. A. Girginov, Study of anodic films on niobium by scanning electron microscopy …….. 261
Valchanova I. D., See Stefanov Y. S. et al. ……. 277
Vasant Kumar Pai K., See Meenakshi K. M. et al. …. 137
Vassilev N. G., *Ab initio* SCF study of the barrier to internal rotation in N,N-dimethylcinnamamides ……..... 526
Vassilev N. G., See Blagoeva I. B. et al. …….. 386
Vassilev S., See Ljutzkanov L. et al. 109
Vassilev S., See Mladenov M. et al. …… 360
Vassileva-Boyadjieva P. J., See Popova A. D. et al. .. 512
Vassileva-Boyadjieva P. J., See Velcheva E. A. et al. .433
Veena M. A., See Revanasiddappa H. D. et al. …….. 104
Veith M., See Kozhukharov V. et al. ……. 310
Velcheva E. A., P. J. Vassileva-Boyadjieva, I. G. Binev, Experimental and DFT studies on IR spectral and structural changes arising from the conversion of 1H-indole-2,3-dione (isatin) into azanion …… 433
Velcheva E. A., See Stamboliyska B. A. et al. …….. 445
Vitanov T., See Petrov K. et al. …… 122
Viteva L. Z., See Gospodova Tz. et al. …… 568
Vlaev S. D., See Georgiev D. P. et al. …….. 173
Wawer I., See Enchev V. et al. ……. 532
Yanakieva I., See Kratchanova M., et al. …….. 561
Yancheva D. Y., See Stamboliyska B. A. et al. …… 498
Yanev Y. S., O. A. Farhi, Microcontroller converter of corrosion rate with current output …….. 330
Zabinski P., See Dobrovolska Ts. et al. 254
Zachariasz J., See Budinova T. et al. 166
Zaprianova V. G., See Raicheff R. G. et al. 295
Zlatev R. P., See Dobrev Ts. M. et al. …….. 198
Zlatilova P., See Mladenov M. et al. ……. 360
Zwetanova A., See Popova A. K. et al. …… 300

SUBJECT INDEX

ab initio
and DFT studies of their structures. Hydrogen bonding in ionic systems of 1,5,7- triaza-bicyclo[4.4.0]dec-5-ene (TBD) with 4-cyano-phenol: ……. 418
and DFT study of the structure of metal ion complexes with N-benzalaniline-15-crown-5 . 532
computational, and DFT B3LYP studies on spectral and structural changes, caused by the conversion of methyl cyanoacetate into carb-anion. Experimental IR and ……. 512
SCF study of the barrier to internal rotation in N,N-dimethylcinnamamides …… 526
acetals
acyclic mixed (O,S), How do we synthesize, ? A physical-organic chemistry approach ……. 144
activated carbon
granular, from dates' stones Phenol removal using ……. 26
produced from bamboo pellets for removal of arcenic(iii) ions from water …….. 166
Synthesis of nanosized TiO_2 particles on …. 109
activity
Chain-breaking antioxidant, of two new chalcones from propolis of El Salvador in homogeneous and micellar media …….. 546
Electrocatalytic, of electrochemically deposited Zr-Ce-Y/Ni and Co/Zr-Ce-Y/Ni oxide systems during evolution of hydrogen and oxygen .348
acyclic mixed (O,S)-acetals
How do we synthesize? A physical-organic chemistry approach …… 144
adsorption
mechanism and kinetic. Role of oxidising agent in photocatalytic degradation of benzene and its influence on ……..... 114
aeration
and mixing in stirred vessels, Effect of inclined-blade impeller design on …….. 173
Ag-In coatings,
electrodeposited, Investigations of the surface morphology of, by means of optical, scanning-electron and atomic-force microscopy …….. 254
Al
Formation of protective films on, in electrolytes containing no Cr^{6+} ions …… 340
alumina
Influence of calcination of stainless steel OC4004 covered with, or ceria carrier layers on their passive state in different acid media …….. 227
aluminium
Contemporary aspects in the surface treatment of 85
aminolysis
of phenyl acetate, Mechanism of the : a computational study …… 401
5-amino-2-methoxypyridine ester amide
of squaric acid ethyl ester. Solid-state polarized IR-spectroscopic study of high temperature red phase of …… 477
anti-β-aminonitriles
Stereocontrolled intramolecular cyclization of. Convenient access to *trans*-azetidin-2-imines .568
α-aminophosphonic acid esters
One-pot synthesis and antimicrobial activity of a new class of ……59
anodes
for zinc electroextraction from sulphate electrolytes. Investigations of composite coatings used as ……...277
anodic films
on niobium, Study of, by scanning electron

microscopy …… 261
anodic oxide films
on tungsten – effect of the electrolyte pH. Conduction mechanism of ……. 267
arcenic(iii)
ions, removal of, from water. Activated carbon produced from bamboo pellets for …… 166
ascorbic acid
Facile and validated spectrophotometric methods for the determination of ……. 104
atomic-force microscopy
Investigations of the surface morphology of electrodeposited Ag-In coatings by means of optical, scanning-electron and ……254
azanion
Experimental and DFT studies on IR spectral and structural changes arising from the conversion of 1H-indole-2,3-dione (isatin) into ……433
IR spectral and structural changes, caused by the conversion of 4-cyanobenzamide into: a combined experimental/computational approach ……. 520
Theoretical study of the conformational preference of N-[(4-aminophenyl) sulphonyl]acetamide (sulphacetamide) and its …… 445
trans-azetidin-2-imines
Stereocontrolled intramolecular cyclization of *anti*-β-aminonitriles. Convenient access to …. 568
azines
symmetrical, One-pot solvent-free synthesis of, under microwave irradiation …… 409
azoles
Relationship between chemical structure parameters and inhibitor efficiency of some …….. 300
N-benzalaniline-15-crown-5
Ab initio and DFT study of the structure of metal ion complexes with ……. 532
benzene
Role of oxidising agent in photocatalytic degradation of, and its influence on kinetic and adsorption mechanism …….....114
biomaterials
Synthesis and characterization of novel nanostructured carbon for supercapacitors on the basis of ……. 360
biosensors
Amperometric …… 204
B–N dyes
Computational study of the electronic spectra of some …….. 450
borohydrides
alkaline, Electrooxidation of, on metal hydride electrodes …….. 306
Brassicaceae plants
as a new source of food grade peptidases …. 397
Bromamine-T
Kinetics and mechanism of oxidation of pyrazinamide with, in perchloric acid medium …….. 137
cancer
related biological samples. Application of diffusion-ordered spectroscopy for the analysis of 464
carbanionic adducts
IR Spectra and structure of 3,5,5-trimethyl(cyclohex-2-enylidene) malononitrile and its potassium cyanide and sodium methoxide, : experimental and B3lYP studies …… 538
carbon
matrix, Modified, – high energy anode for lithium ion battery …….....219
nanostructured, novel, for supercapacitors on the basis of biomaterials. Synthesis and characterization of, ……. 360
catalyst
CuO/doped-ceria. Impact of the preparation method on the water-gas shift activity of …. 42
for electroreduction of hydrogen peroxide. Modified graphite electrodes as …….. 233
Ni-Mo-W, Sulphide oxidation on electrodeposited ……. 291
O 4-25 calcined under special conditions for oxidation of *o*-xylene to phtalic anhydride. Part I: Calcination and working characteristics of the catalyst. An investigation of the resources of a conventional …… 3
polymer electrolyte fuel cell, Evaluation of, using gas diffusion electrodes in aqueous electrolytes ……. 333
catalytic materials
novel electrodeposited, Synthesis and characterization of for hydrogen evolution reaction …… 211
ceria
Influence of calcination of stainless steel OC4004 covered with alumina or, carrier layers on their passive state in different acid media …… 227
chalcones
synthetic, substituted in the styril fragment, UV-VIS absorption and fluorescent characteristics of some …….. 440
two new, from propolis of El Salvador, Chain-breaking antioxidant activity of, in homogeneous and micellar media. ……. 546
chitosan
-containing micro- and nanofibrous materials, novel, Preparation of, by electrospinning …… 469
2-chloro-3-aminopyridine
Spectroscopic elucidation of hydrogensquarate and ester amide of squaric acid of …….. 483
Co/Zr-Ce-Y/Ni
and Zr-Ce-Y/Ni oxide systems, Electrocatalytic activity of electrochemically deposited, during evolution of hydrogen and oxygen …….. 348
cobalt
-silver coatings Electrodeposition of …….. 248
complexes
Inclusion, of 3,4-dihydropyrimidin-2-(1H)-ones with β-cyclodextrin …… 36
ternary ion-associated, Extractive-spectrophotometric investigations on, between the vanadium(V)–4-(2-pyridylazo)-resorcinol anionic

chelate and some methoxyditetrazolium cations …….. 65
composite coatings
used as anodes for zinc electroextraction from sulphate electrolytes. Investigations of, ……. 277
Computational study
of the electronic spectra of some B–N dyes … 450
conducting polymer
layers, Copper-modified, for electroanalytic applications in neutral solutions …….. 185
conversion films
Electrochemical methods for evaluation of the protective ability of electroplated coatings and …….. 198
Copper
-modified conducting polymer layers for electroanalytic applications in neutral solutions …185
-modified polyaniline layers, Electrooxidation of glucose on, in alkaline solution …….. 286
Corrosion
and electrochemical investigations of low-alloyed and austenitic stainless steel used in the steam generators of Kozloduy nuclear power plant ……...281
corrosion
protection ability of nanocomposite hybrid coatings. Investigation on the …… 310
protection of steels in water systems based on polymers and inorganic salts. Inhibitor composition for …… 244
rate, Microcontroller converter of, with current output ……. 330
Cr^{6+} ions
Formation of protective films on Al in electrolytes containing no …….. 340
CuO
/doped-ceria catalysts. Impact of the preparation method on the water-gas shift activity of ……. 42
4-cyanobenzamide
IR spectral and structural changes, caused by the conversion of, into azanion: a combined experimental/computational approach …….. 520
4-cyanophenol
Hydrogen bonding in ionic systems of 1,5,7-triazabicyclo[4.4.0]dec-5-ene (TBD) with: *ab initio* and DFT studies of their structures …….. 418
β-cyclodextrin
Inclusion complexes of 3,4-dihydropyrimidin-2-(1H)-ones with ……36
DFT
and *ab initio* studies of their structures. Hydrogen bonding in ionic systems of 1,5,7-triazabicyclo[4.4.0]dec-5-ene (TBD) with 4-cyanophenol: …….. 418
and *ab initio* study of the structure of metal ion complexes with N-benzalaniline-15-crown-5 ……. 532
and experimental studies on IR spectral and structural changes arising from the conversion of 1H-indole-2,3-dione (isatin) into azanion …… 433
B3LYP and computational *ab initio* studies on spectral and structural changes, caused by the conversion of methyl cyanoacetate into carbanion. Experimental IR and …… 512
diffusion-ordered spectroscopy
Application of, for the analysis of cancer related biological samples …….. 464
3,4-dihydropyrimidin-2-(1H)-ones
Inclusion complexes of, with β-cyclodextrin … 36
drug carriers
Poly(oxyethylene aminophosphonate)s – novel promising biologically active polymers and, Design and NMR characterization ……... 54
dual catalyst bed
Characteristics of, in the case of operation with high inlet reagent concentrations. An investigation of the resources of a conventional catalyst O 4-25 calcined under special conditions for oxidation of *o*-xylene to phtalic anhydride. Part III: ……..19
Formation of, in the case of operation with low inlet reagent concentration. An investigation of the resources of a conventional catalyst O 4-25 calcined under special conditions for oxidation of *o*-xylene to phtalic anhydride. Part II: …. 13
Electrocatalytic activity
of electrochemically deposited Zr-Ce-Y/Ni and Co/Zr-Ce-Y/Ni oxide systems during evolution of hydrogen and oxygen ……. 348
towards the electrooxidation of formic acid. Rhodium deposits on graphite: The impact of the graphite pad on the 129
Electrochemical corrosion
behaviour of silica hybrid sol-gel coatings … 295
Electrochemical methods
for evaluation of the protective ability of electroplated coatings and conversion films ……... 198
Electrochemical processes
in magnetic field ……. 190
Electrodeposition
of silver-cobalt coatings …….. 248
electroextraction
of zinc from sulphate electrolytes. Investigations of composite coatings used as anodes for ….. 277
electrolysis processes
Mathematical modelling of ……. 323
Electrooxidation
of alkaline borohydrides on metal hydride electrodes …….. 306
of formic acid. Rhodium deposits on graphite: The impact of the graphite pad on the electrocatalytic activity towards the..... 129
of glucose on copper-modified polyaniline layers in alkaline solution …… 286
electroplated coatings
and conversion films. Electrochemical methods for evaluation of the protective ability of …… 198

electrospinning
Preparation of novel chitosan-containing micro- and nanofibrous materials by …….. 469
enaminonitrile
moiety in heterocyclic synthesis, Synthetic utility of ……..... 147
Experience and Excellence
40 Years of …….. 183
Extractive-spectrophotometric investigations
on ternary ion-associated complexes between the vanadium(V)–4-(2-pyridylazo)-resorcinol anionic chelate and some methoxyditetrazolium cations 65
ferro-carbon alloys,
Phosphating of, by modifying zinc-phosphate solutions ……. 355
fluorescent characteristics
and UV-VIS absorption of some substituted in the styril fragment synthetic chalcones ……. 440
formic acid
Rhodium deposits on graphite: The impact of the graphite pad on the electrocatalytic activity towards the electrooxidation of 129
gas diffusion electrodes
Evaluation of polymer electrolyte fuel cell catalysts using, in aqueous electrolytes …….. 333
gem-dimethyl
(gem-dialkyl) effect. Linear free energy relationships of the ……386
Geodia cydonium
Volatile and polar compounds from, and two *Tedania* species ……..... 48
glucose
Electrooxidation of, on copper-modified polyaniline layers in alkaline solution …….. 286
glycyl-L-tryptophan dihydrate (*H-Gly-Trp-OH.2H$_2$O*)
L-tryptophyl-L-methionine (*H-Trp-Met-OH*) and L-methionyl-L-tryptophan (*H-Met-Trp-OH*). Solid-state IR-LD spectroscopy of L-tryptophan-containing dipeptides ……. 456
graphite
electrodes, Modified, as catalysts for electroreduction of hydrogen peroxide …….. 233
Rhodium deposits on, : The impact of the graphite pad on the electrocatalytic activity towards the electrooxidation of formic acid 129
high energy anode
for lithium ion battery. Modified carbon matrix – ……..... 219
Hydrogen
bonding in ionic systems of 1,5,7- triazabicyclo [4.4.0]dec-5-ene (TBD) with 4-cyanophenol: *ab initio* and DFT studies of their structures …… 418
evolution reaction. Synthesis and characterization of novel electrodeposited catalytic materials for ……211
permeation through Ni layers deposited from Watts' electrolyte ……240
hydrogen-bonded systems
between pyridine-3-carboxamide (nicotinamide) and DMSO. Theoretical study of structures and stability of ……..... 426
hydrogen peroxide
Modified graphite electrodes as catalysts for electroreduction of …….. 233
hydrogensquarate
and ester amide of squaric acid of 2-chloro-3-aminopyridine. Spectroscopic elucidation of .. 483
inclined-blade impeller
design, Effect of, on mixing and aeration in stirred vessels …….. 173
1H-indole-2,3-dione (isatin)
Experimental and DFT studies on IR spectral and structural changes arising from the conversion of, into azanion ……. 433
industrial waste gases
from sulfur dioxide, "ELCOX" laboratory and pilot devices for purification of: optimization and real tests in "Pirdop" copper factory ……. 122
infrared spectral library
Implementation and testing of routine procedure for mixture analysis by search in …… 556
Inhibitor
composition for corrosion protection of steels in water systems based on polymers and inorganic salts ……244
efficiency of some azoles. Relationship between chemical structure parameters and ……. 300
internal rotation
in N,N-dimethylcinnamamides. *Ab initio* SCF study of the barrier to …….. 526
intramolecular cyclization
Stereocontrolled, of *anti*-β-aminonitriles. Convenient access to *trans*-azetidin-2-imines …….. 568
Ivan Nikolov Juchnovski
– Biographical and professional data …….. 373
kinetic
and adsorption mechanism. Role of oxidising agent in photocatalytic degradation of benzene and its influence on ……..... 114
Kinetics
and mechanism of oxidation of pyrazinamide with Bromamine-T in perchloric acid medium …… 137
leek
Characteristics of pectic polysaccharides from, obtained through consecutive extraction with various reaction agents …… 561
Linear free energy
relationships of the gem-dimethyl (gem-dialkyl) effect ……386
lithium ion battery
Modified carbon matrix – high energy anode for ……..... 219
magnetic chitosan beads
One-pot preparation of …… 491
magnetic field
Electrochemical processes in …….. 190
mechanism
and kinetics of oxidation of pyrazinamide with Bromamine-T in perchloric acid medium…137

of the aminolysis of phenyl acetate: a computational study ……..401
metal hydride electrodes
Electrooxidation of alkaline borohydrides on .. 306
L-methionyl-L-tryptophan (*H-Met-Trp-OH*)
L-tryptophyl-L-methionine (*H-Trp-Met-OH*), and glycyl-L-tryptophan dihydrate (*H-Gly-Trp-OH.2H$_2$O*). Solid-state IR-LD spectroscopy of L-tryptophan-containing dipeptides …… 456
methoxyditetrazolium cations
Extractive-spectrophotometric investigations on ternary ion-associated complexes between the vanadium(V)–4-(2-pyridylazo)-resorcinol anionic chelate and some …… 65
methyl cyanoacetate
Experimental IR, and computational *ab initio* and DFT B3LYP studies on spectral and structural changes, caused by the conversion of, into carbanion …….. 512
Microcontroller
converter of corrosion rate with current output 330
microwave irradiation
One-pot solvent-free synthesis of symmetrical azines under ……. 409
mixture analysis
Implementation and testing of routine procedure for, by search in infrared spectral library …… 556
Mo
-Ni-W catalysts, Sulphide oxidation on electrodeposited …….. 291
modelling
Mathematical, of electrolysis processes …….. 323
Molecular mechanics (MM3(π)) conformational analysis of molecules containing conjugated π-electron fragments: a molecular tweezer …….. 505
molecular tweezer
Molecular mechanics (MM3(π)) conformational analysis of molecules containing conjugated π-electron fragments: a …… 505
N,N-dimethylcinnamamides
Ab initio SCF study of the barrier to internal rotation in …… 526
N-[(4-aminophenyl) sulphonyl]acetamide
(sulphacetamide) and its azanion. Theoretical study of the conformational preference of ……445
nanocomposite
hybrid coatings. Investigation on the corrosion protection ability of …….. 310
Ni
layers deposited from Watts' electrolyte. Hydrogen permeation through …… 240
-Mo-W catalysts, Sulphide oxidation on electrodeposited …… 291
niobium
Study of anodic films on, by scanning electron microscopy …….. 261
oxidation
Kinetics and mechanism of, of pyrazinamide with Bromamine-T in perchloric acid medium…137
of *o*-xylene to phtalic anhydride. An investigation of the resources of a conventional catalyst O 4-25 calcined under special conditions for, Part I: Calcination and working characteristics of the catalyst ……. 3
polysaccharides
pectic, from leek obtained through consecutive extraction with various reaction agents. Characteristics of ……. 561
peptidases
Brassicaceae plants as a new source of food grade …….. 397
Phenol
removal using granular activated carbon from dates' stones …….. 26
phenyl acetate
Mechanism of the aminolysis of: a computational study …… 401
Phosphating
of ferro-carbon alloys by modifying zinc-phosphate solutions ……. 355
photocatalytic degradation
of benzene and its influence on kinetic and adsorption mechanism. Role of oxidising agent in … 114
phtalic anhydride
An investigation of the resources of a conventional catalyst O 4-25 calcined under special conditions for oxidation of *o*-xylene to. Part I: Calcination and working characteristics of the catalyst ……. 3
Poly(oxyethylene aminophosphonate)s
– novel promising biologically active polymers and drug carriers. Design and NMR characterization ……..... 54
polymer electrolyte fuel cell
catalysts using gas diffusion electrodes in aqueous electrolytes. Evaluation of ……..…….. 333
propolis
of El Salvador, Chain-breaking antioxidant activity of two new chalcones from, in homogeneous and micellar media ……. 546
protective films
Formation of, on Al in electrolytes containing no Cr^{6+} ions ……340
pyrazinamide
Kinetics and mechanism of oxidation of, with Bromamine-T in perchloric acid medium …… 137
pyridine-3-carboxamide
(nicotinamide) and DMSO. Theoretical study of structures and stability of hydrogen-bonded systems between ……..... 426
pyridinium-betaines
of squaric acid A theoretical investigation on the structure, electronic spectra and nonlinear optical properties of ……..498
4-(2-pyridylazo)-resorcinol
–vanadium(V) anionic chelate and some methoxyditetrazolium cations. Extractive-spectrophotometric investigations on ternary ion-associated complexes between the …….. 65

pyridyl isoxazol-5-ones
Synthesis and reactivity of some …… 70
Rhodium
deposits on graphite: The impact of the graphite pad on the electrocatalytic activity towards the electrooxidation of formic acid 129
scanning electron microscopy
Study of anodic films on niobium by ……. 261
selenones
Synthesis and bioactivity of 6-alkoxy/aryl/aryloxy-4,8-di(*tert*-butyl)2,10-dimethyl-12*H*-6λ^5-dibenzo[d,g][1,3,2]dioxaphosphocin-6-ones/thiones/ …….. 160
silica
hybrid sol-gel coatings. Electrochemical corrosion behaviour of ……. 295
silver
-cobalt coatings Electrodeposition of ……. 248
Solid-state IR-LD spectroscopy
of L-tryptophan-containing dipeptides L-tryptophyl-L-methionine (*H-Trp-Met-OH*), L-methionyl-L-tryptophan (*H-Met-Trp-OH*) and glycyl-L-tryptophan dihydrate (*H-Gly-Trp-OH.2H$_2$O*) .. 456
Solid-state polarized IR
-spectroscopic study of high temperature red phase of 5-amino-2-methoxypyridine ester amide of squaric acid ethyl ester …… 477
spectra
electronic, of some B–N dyes. Computational study of the …….. 450
spectrophotometric methods
Facile and validated, for the determination of ascorbic acid ……. 104
squaric acid
A theoretical investigation on the structure, electronic spectra and nonlinear optical properties of pyridinium-betaines of ……. 498
squaric acid ethyl ester
Solid-state polarized IR-spectroscopic study of high temperature red phase of 5-amino-2-methoxypyridine ester amide of ……. 477
stability
and structures of hydrogen-bonded systems between pyridine-3-carboxamide (nicotinamide) and DMSO. Theoretical study of ……..... 426
stainless steel
OC4004 covered with alumina or ceria carrier layers, Influence of calcination of, on their passive state in different acid media …… 227
used in the steam generators of Kozloduy nuclear power plant. Corrosion and electrochemical investigations of low-alloyed and austenitic …….....281
steels
Inhibitor composition for corrosion protection of, in water systems based on polymers and inorganic salts …… 244
mild and low alloy, Comparison of stress-corrosion cracking susceptibility of, in phosphate environments ……. 318
stress-corrosion
cracking susceptibility of mild and low alloy steels in phosphate environments. Comparison of … 318
sulfur dioxide
"ELCOX" laboratory and pilot devices for purification of industrial waste gases from, : optimization and real tests in "Pirdop" copper factory .. 122
supercapacitors
on the basis of biomaterials. Synthesis and characterization of novel nanostructured carbon for …… 360
surface morphology
of electrodeposited Ag-In coatings by means of optical, scanning-electron and atomic-force microscopy. Investigations of the, …….. 254
Synthesis
and bioactivity of 6-alkoxy/aryl/aryloxy-4,8-di(*tert*-butyl)2,10-dimethyl-12*H*-6λ^5-dibenzo [d,g][1,3,2]dioxaphosphocin-6-ones/thiones/ selenones …… 160
and characterization of novel electrodeposited catalytic materials for hydrogen evolution reaction ……211
and characterization of novel nanostructured carbon for supercapacitors on the basis of biomaterials …… 360
and reactivity of some pyridyl isoxazol-5-ones . 70
heterocyclic, Synthetic utility of enaminonitrile moiety in ……..... 147
One-pot solvent-free, of symmetrical azines under microwave irradiation ……409
One-pot, and antimicrobial activity of a new class of α-aminophosphonic acid esters …… 59
Tedania
species. Volatile and polar compounds from *Geodia cydonium* and two ……..... 48
thiones
Synthesis and bioactivity of 6-alkoxy/aryl/aryloxy-4,8-di(*tert*-butyl)2,10-dimethyl-12*H*-6λ^5-dibenzo[d,g][1,3,2]dioxaphosphocin-6-ones/, selenones …….. 160
TiO_2
nanosized particles, Synthesis of, on activated carbon …….. 109
1,5,7-triazabicyclo[4.4.0]dec-5-ene (TBD)
Hydrogen bonding in ionic systems of, with 4-cyanophenol: *ab initio* and DFT studies of their structures …… 418
3,5,5-trimethyl(cyclohex-2-enylidene) malononitrile
and its potassium cyanide and sodium methoxide carbanionic adducts, IR Spectra and structure of: experimental and B3lYP studies ……. 538
L-tryptophan
-containing dipeptides L-tryptophyl-L-methionine (*H-Trp-Met-OH*), L-methionyl-L-tryptophan (*H-Met-Trp-OH*) and glycyl-L-tryptophan dihydrate (*H-Gly-Trp-OH.2H$_2$O*). Solid-state IR-LD spectroscopy of …… 456
L-tryptophyl-L-methionine (*H-Trp-Met-OH*),
L-methionyl-L-tryptophan (*H-Met-Trp-OH*) and

glycyl-L-tryptophan dihydrate (*H-Gly-Trp-OH.2H$_2$O*). Solid-state IR-LD spectroscopy of L-tryptophan-containing dipeptides …… 456
tungsten
Conduction mechanism of anodic oxide films on, – effect of the electrolyte pH …….. 267
vanadium(V)
–4-(2-pyridylazo)-resorcinol anionic chelate and some methoxyditetrazolium cations. Extractive-spectrophotometric investigations on ternary ion-associated complexes between the …… 65
W
-Ni-Mo catalysts, Sulphide oxidation on electro-deposited …….. 291
water-gas
shift activity of CuO/doped-ceria catalysts. Impact of the preparation method on the ……42
Watts' electrolyte
Hydrogen permeation through Ni layers deposited from …….. 240
zinc
electroextraction from sulphate electrolytes. Investigations of composite coatings used as anodes for ……. 277
Zr-Ce-Y/Ni
and Co/Zr-Ce-Y/Ni oxide systems, Electrocatalytic activity of electrochemically deposited, during evolution of hydrogen and oxygen ….. 348

АВТОРЕН УКАЗАТЕЛ

Авгуропулос Г., Виж Табакова Т. и др. 47
Аврамова Ив., Виж Гергова Д. и др. 232
Алтън О., Виж Гавазов К. Б. и др. 69
Алхамед Я. А., Отстраняване на фенол с гранулиран активен въглен от костилки на фурми 35
Амута П., Виж К. Селвамбигай, и др. 41
Анастасов Ас. Ив., Виж Георгиева Ан. Т. и др. 12
Анастасов Ас. Ив., Виж Георгиева Ан. Т. и др. 18
Анастасов Ас. Ив., Виж Георгиева Ан. Т. и др. 25
Ангелова С., Виж Енчев В. и др. 537
Андреев Г. Н., Виж Пенчев П. Н. и др. 560
Арнаудова М., Виж Христова Ел. и др. 294
Атанасов Я., Виж Илиева С. и др. 408
Атанасова Г., Виж Гергова Д. и др. 232
Атанасова П., Виж Петров К. и др. 339
Афифи А. А. Е., Виж Мадкур Х. М. Ф. и др. 159
Бакалова Сн. М., Х. Ян. Канети, Об. Д. Кастаньо, Изчислително моделиране на електронните спектри на някои багрила, съдържащи връзката B–N 455
Банкова В. С., Виж Кънчева В. Д. и др..... 555
Белов К., Виж Младенов М. и др. 366
Бинев Ив. Г., Виж Велчева Ев. А. и др..... 439
Бинев Ив. Г., Виж Попова Ан. Д. и др..... 519
Бинев Ив. Г., Виж Ценов Й. Ан. и др..... 525
Бинев Юр. Ив., Виж Попова Ан. Д. и др..... 519
Благоева Ив. Б., Ел. П. Игнатова-Аврамова, Ас. Х. Коеджиков, Ив. Г. Пожарлиев, Л. И. Проевска, В. Т. Рачина, Н. Г. Василев, Линейни зависимости на свободните енергии на гем-диметил ефекта (гем-диалкил ефекта)..... 396
Блъсков В., Виж Люцканов Л. и др. 113
Божинов М., Виж Цветков Б. и др. 266
Божинов М. С., Виж Карастоянов В. И. и др. 276
Божков Н. С., Виж Райчевски Г. М. и др. 285
Бончев Р. П., Виж Симеонов Св. и др. 417
Броухам Д. Ф., Виж Иванова Г. Ив. и др..... 468
Будевски Ев., Виж Петров К. и др. 128
Будинова Т., М. Кшешинска, Б. Цинцарски, Ю. Закариаш, Н. Петров, Получаване на активен въглен от бамбук за извличане на As(III) от водни разтвори 172
Бътовска Д. И., Виж Иванова Д. И. и др. 444
Бъчваров В., Виж Райчев Р. и др. 247
Бюес-Ерман К., Виж Стоянова Ан. Р. и др. 189
Вавер Ив., Виж Енчев В. и др. 537
Вайт М., Виж Кожухаров В. и др. 317
Васант Кумар Пай К., Виж Меенакши К. М. и др. 143
Василев Н. Г., *Ab initio* SCF изследване на бариера на вътрешна ротация в N,N-диметилканелени амиди 531
Василев Н. Г., Виж Благоева Ив. Б. и др. 396
Василев С., Виж Люцканов Л. и др. 113
Василев С., Виж Младенов М. и др. 366
Василева-Бояджиева П. Ж., Виж Велчева Ев. А. и др. 439
Василева-Бояджиева П. Ж., Виж Попова Ан. Д. и др. 519
Веена М. А., Виж Реванасидапа Х. Д. и др. 108
Велчева Е. А., Виж Стамболийска Б. А. и др..... 449
Велчева Ев. А., П. Ж. Василева-Бояджиева, Ив. Г. Бинев, Експериментално и DFT изследване на ИЧ спектрални и структурни промени произтичащи от превръщането на 1H-индол-2,3-дион (изатин) в азанион 439
Вену Бабу Б., Виж Хари Бабу Б. и др. 165
Витанов Т., Виж Петров К. и др. 128
Витева Л. Зл., Виж Господова Цв. Сп. и др. 571
Влаев С. Д., Виж Георгиев Д. П. и др. 177
Вълчанова Ив., Виж Стефанов Яв. и др. 280
Габриели К., Виж Миркова Л. и др. 243
Гавазов К. Б., М. Тюркилмаз, О. Алтън, Екстракционно-спектрофотометрични изследвания на тройни йонно-асоциирани комплекси между анионния хелат на ванадий(V) с 4-(2-пиридилазо)-резорцин и някои метокси-бис(тетразолиеви) катиони 69
Гамбурцев С., Виж Петров К. и др. 339
Георгиев Д. П., С. Д. Влаев, Влияние на формата на импелер с наклонени лопатки върху характеристиките на смесване и аерация в съдове с разбъркване 177
Георгиева Ан. Т., Ас. Ив. Анастасов, Изследване възможностите на накаляван при специални условия конвенционален катализатор О 4-25 за окисление на *о*-ксилол до фталов анхидрид. Част 1. Накаляване и работни характеристики на катализатора 12
Георгиева Ан. Т., Ас. Ив. Анастасов, Изследване на възможностите на накаляван при специални условия конвенционален катализатор О 4-25 за окисление на *о*-ксилол до фталов анхидрид. Част 2. Организиране на двоен катализаторен слой при работа с ниска начална концентрация на реагента 18
Георгиева Ан. Т., Ас. Ив. Анастасов, Изследване на възможностите на накален при специални условия конвенционален катализатор О 4-25 за окисление на *о*-ксилол до фталов анхидрид. Част III. Особености на катализаторния слой при работа с високи начални концентрации на реагента 25
Герван Й., Виж Кожухаров В. и др. 317
Гергова Д., Ем. Стоянова, Д. Стойчев, Г. Атанасова, Ив. Аврамова, П. Стефанов, Влияние на термичната обработка на електроотложени алуминиев и цериев оксиди върху пасивното състояние на неръждаема стомана ОС4004 в кисели среди 232
Гиргинов Ас., Виж Цветков Б. и др. 266

Гириш Кумар С., Виж Гомати Деви Л. и др. 121
Гомати Деви Л., С. Гириш Кумар, Роля на окислителния агент при фотокаталитично разлагане на бензен и неговото влияние върху кинетиката и механизма на адсорбция 121
Господова Цв. Сп., Ж. Р. Рашкова, Л. Зл. Витева, Стереоконтролирана вътрешномолекулна циклизация на анти-β-амино-нитрили. Удобна синтеза на транс-азетидин-2-имини 571
Гочева М., Виж Крачанова М. и др. 567
Гълъбов Б., Виж Илиева С. и др. 408
Дамянов М., Виж Луканова Р. и др. 347
Дарданова Ив. Д., Виж Петков Л. Н. и др. 329
Даскалова Л. Ив., Й. Димитрова, Теоретично изследване на структури и стабилност на водородно-свързани системи между пиридин-3-карбоксамид (никотинамид) и ДМСО 432
Де Роса С., З. Каменарска, К. Сеизова, К. Йодисе, Ас. Петрова, Д. Неделчева, К. Стефанов, С. Попов, Летливи и полярни вещества в Geodia cydonium и два вида Tedania 53
Джаганадхам В., Как да синтезираме един ацикличен смесен (O,S) ацетал? Подход на физичната органична химия 146
Джамбова Ан. Г., Виж К. Попова Ан. и др. 305
Джон Апълби А., Виж Петров К. и др. 339
Димитрова Й., Виж Даскалова Л. Ив. и др..... 432
Димитрова Й., Водородно свързване в йонни системи на 1,5,7-триазабицикло[4.4.0]дец-5-ен с 4-цианофенол. Изследвания на структурите им с методите *ab initio* и ТФП 425
Димчева Н., Виж Хорозова Е. и др. 239
Димчева Н., Виж Хорозова Ел. и др. 136
Добрев Цв. М., М. Хр. Монев, Ив. Н. Кръстев, Р. П. Златев, Електрохимични методи за оценка на защитната способност на галванични покрития и конверсионни филми 203
Добрев Цв., Виж Стефанов Яв. и др. 280
Доброволска Ц., Виж Нинева С. и др. 253
Доброволска Ц., Р. Ковалик, П. Забински, Ив. Кръстев, Изследвания на повърхностната морфология на електролитно отложени Ag-In покрития чрез оптична, сканираща електронна и атомно-силова , Ив.

Кръстев, Изследвания на повърхностната морфология на електролитно отложени Ag-In покрития чрез оптична, сканираща електронна и атомно-силова , Ив.

Изследвания на повърхностната
ия на електролитно

получени чрез последователно екстрахиране с различни реагенти 567
Кришна А. Б., Виж Кумар Б. С. и др. 64
Кръстев Ив., Виж Доброволска Ц. и др. 260
Кръстев Ив. Н., Виж Добрев Цв. М. и др. 203
Кръстев Ив., Виж Нинева С. и др. 253
Кумар Б. С., А. Ю. Р. Санкар, М. В. Реди, А. Б. Кришна, К. С. Реди, Синтез в един реактор и антимикробна активност на нов клас естери на α-аминофосфорната киселина 64
Куртева В. Б., Виж Симеонов Св. и др. 417
Кшешинска М., Виж Будинова Т. и др. 172
Кънчева В. Д., В. С. Банкова, Прекъсваща веригите антиоксидантна активност на нови халкони от прополис от Ел Салвадор в хомогенна и мицеларна среда 555
Късовски В., Виж Крачанова М. и др. 567
Луканова Р., Ем. Стоянова, М. Дамянов, Д. Стойчев, Формиране на защитни филми върху алуминий от несъдържащи Cr^{6+} електролити 347
Лютов Л., Виж Райчевски Г. М. и др. 285
Люцканов Л., Ир. Стамболова, В. Блъсков, С. Василев, В. Петкова, Ц. Цачева, Д. Механджиев, Получаване на наноразмерни частици от TiO_2 нанесени върху активен въглен 113
Магаева Сн., Виж Стефанов Яв. и др. 280
Мадкур Х. М. Ф., А. А. Е. Афифи, Г. А. Елсайед, М. С. Салем, Приложимост на енаминонитрилен фрагмент в хетероциклени синтези 159
Манолова Н., Виж Стоилова О. и др. 497
Манолова Н. Ем., Виж Спасова М. Г. и др. 476
Маринова М. Д., Б. П. Чорбанов, Растенията от сем. Brassicaceae като източник на хранителни пептидази 400
Маркова Н., Виж Енчев В. и др. 537
Марчева Й., Р. Райчев, Сравнение на склонността към корозионно напукване на ниско-въглеродна и нисколегирана стомани във фосфатни среди 322
Мачкова М. С., Виж К. Попова Ан. и др. 305
Меенакши К. М., К. Васант Кумар Пай, К. Н. Мохана, Р. Рамачандрапа, Кинетика и механизъм на окисление на пиразинамид с бромамин-Т в среда на перхлорна киселина 143
Механджиев Д., Виж Люцканов Л. и др. 113
Минкова К., Виж Райчевски Г. М. и др. 285
Миркова Л., Г. Морен, К. Габриели, Проникване на водород в Ni слоеве отложени от Уотсов електролит 243
Митева В. Л., Виж Пенчев П. Н. и др. 560
Митева М., Виж Енчев В. и др. 537
Митева М., Виж Хорозова Ел. и др. 136
Митов М., Виж Христов Г. и др. 309
Митов М., Виж Христова Ел. и др. 294
Младенов М., П. Златилова, Р. Райчев, С. Василев, Н. Петров, К. Белов, В. Тренев, Д. Ковачева, Синтез и характеризиране на нов наноструктуриран въглен за суперкондензатори на основата на биоматериали 366
Младенова Е., Виж Петров К. и др. 339
Монев М. Хр., Виж Добрев Цв. М. и др. 203
Морен Г., Виж Миркова Л. и др. 243
Мохан Ч., Виж Хари Бабу Б. и др. 165
Мохана К. Н., Виж Меенакши К. М. и др. 143
Нага Раджу К., Виж Хари Бабу Б. и др. 165
Нагараджан С., Виж К. Селвамбигай, и др. 41
Найденов В., Виж Петров К. и др. 128
Наполитано П., Виж Петров К. и др. 339
Неделчева Д., Виж Де Роса С. и др. 53
Неделчева Д., Виж Крачанова М. и др. 567
Николов Ив., Виж Петров К. и др. 128
Николова В., Виж Петров К. и др. 128
Нинева С., Ц. Доброволска, Ив. Кръстев, Електролитно отлагане на сребърно-кобалтови покрития 253
О´Конор Р., Виж Иванова Г. Ив. и др. 468
Павлова Е., Виж Крачанова М. и др. 567
Панева Д. П., Виж Спасова М. Г. и др. 476
Папавасилиу Й., Виж Табакова Т. и др. 47
Пеев Т. М., Електрохимични процеси в магнитно поле..... 197
Пенчев П. Н., В. Л. Митева, А. Н. Сохоу, Н. Т. Кочев, Г. Н. Андреев, Реализиране и проверка на рутинна процедура за анализ на смеси с помощта на библиотека от инфрачервени спектри 560
Пенчев Хр., Виж Стоилова О. и др. 497
Петков Л. Н., Ив. Д. Дарданова, Математическо моделиране на електролизни процеси 329
Петкова В., Виж Люцканов Л. и др. 113
Петров К., В. Найденов, В. Николова, П. Илиев, Хр. Христов, Т. Витанов, Ив. Николов, Ев. Будевски, „ELCOX“ лабораторна и пилотна инсталации за очистване на серен диоксид от отпадни газове: оптимизационни и промишлени изпитания в медодобивен завод „Пирдоп“ 128
Петров К., Е. Младенова, С. Гамбурцев, А. Джон Апълби, П. Наполитано, П. Атанасова, М. Хампдем-Смит, Използване на газодифузионни електроди в алкален електролит за определяне активността на катализатори в полимерен електролит 339
Петров К. М., Виж Цанев Ал. С. и др. 354
Петров Н., Виж Будинова Т. и др. 172
Петров Н., Виж Младенов М. и др. 366
Петрова Ас., Виж Де Роса С. и др. 53
Пожарлиев Ив. Г., Виж Благоева Ив. Б. и др. 396
Попов А., Виж Христов Г. и др. 309
Попов Ал., Виж Христова Ел. и др. 294
Попов С., Виж Де Роса С. и др. 53
Попова А. Д., Виж Стамболийска Б. А. и др. 449
Попова Ан. Д., Юр. Ив. Бинев, П. И. Василева-Бояджиева, Ив. Г. Бинев, Експериментални ИЧ и теоретични ab initio ХФ и ТФП B3LYP изследвания на спектралните и структурните промени, причинени от превръщането на метилцианоацетата в карбанион 519
Попова Ан. К., М. С. Мачкова, Ан. Г. Джамбова, Ал. Цветанова, Св. Н. Райчева, Връзка между

параметри на химичната структура и степента на корозионна защита на някои азоли 305
Попова Анг. Д., Виж Стоянов С. С. и др. 545
Проевска Л. И., Виж Благоева Ив. Б. и др. 396
Райчев Р. Г., Виж Райчевски Г. М. и др. 285
Райчев Р., Виж Марчева Й. и др. 322
Райчев Р., Виж Младенов М. и др. 366
Райчев Р., Г. Райчевски, В. Бъчваров, Инхибиторна композиция на базата на полимери и неорганични соли за защита на стомана от корозия във водни системи 247
Райчев Р., Г. Чернев, В. Запрянова, Д. Иванова, П. Джамбазки, Б. Самунева, Из. М. Миранда Салвадо, Корозионно-електрохимични отнасяния на зол-гелни хибридни покрития 299
Райчева Св. Н., Виж К. Попова Ан. и др. 305
Райчевски Г., Виж Райчев Р. и др. 247
Райчевски Г. М., Н. Д. Цветкова, Н. С. Божков, Р. Г. Райчев, К. Минкова, Ин. Топалова, Л. Лютов, Корозионни и електрохимични изследвания на нисколегирани и аустенитни неръждаеми стомани използвани в парогенераторите на АЕЦ „Козлодуй“ 285
Рамачандрапа Р., Виж Меенакши К. М. и др. 143
Рачина В. Т., Виж Благоева Ив. Б. и др. 396
Рашков Ил., Виж Стоилова О. и др. 497
Рашков Ил. Б., Виж Спасова М. Г. и др. 476
Рашков Р., Виж Христов Г. и др. 309
Рашков Р., Виж Христова Ел. и др. 294
Рашков Р., Синтез и охарактеризиране на електрохимично отложени нови материали катализиращи отделянето на водород 218
Рашкова Ж. Р., Виж Господова Цв. Сп. и др. 571
Реванасидапа Х. Д., М. А. Веена, Прост и валидиран спектрофотометричен метод за определяне на аскорбинова киселина 108
Реди К. С., Виж Кумар Б. С. и др. 64
Реди М. В., Виж Кумар Б. С. и др. 64
Ризк Х. Ф., Виж Ел-Бадауи М. А. и др. 77
Русков Т., Виж Стоилова О. и др. 497
Салем М. С., Виж Мадкур Х. М. Ф. и др. 159
Санкар А. Ю. Р., Виж Кумар Б. С. и др. 64
Сеизова К., Виж Де Роса С. и др. 53
Селвамбигай К., П. Амута, С. Нагараджан, Комплекси на включване на 3,4 дихидропиримидин-2-(1Н)-они с β-циклодекстрин 41
Симеонов Св., В. Б. Куртева, Р. П. Бончев, Едностадиен синтез на симетрични азини под дей-ствие на микровълни в отсъствие на разтворители 417
Славов А., Виж Крачанова М. и др. 567
Сохоу А. Н., Виж Пенчев П. Н. и др. 560
Спасова М. Г., Д. П. Панева, Н. Ем. Манолова, Ил. Б. Рашков, Получаване на нови хитозан-съдържащи микро- и нановлакнести материали чрез електроовлакняване 476
Спиров Ив., Виж Стоилова О. и др. 497
Стамболийска Б. А., А. Д. Попова, Е. А. Велчева, Теоретично изследване на конформационните предпочитания на N-[(4-аминофенил)сулфонил]ацетамид (сулфацетамид) и неговия азанион 449
Стамболийска Б. А., Виж Иванова Д. И. и др. 444
Стамболийска Б. А., Д. Я. Янчева, Ц. М. Колев, Теоретично изследване на структурата, електронните спектри и нелинейните оптични свойства на пиридин-бетаините на квадратната киселина 504
Стамболова Ир., Виж Люцканов Л. и др. 113
Станоева Ел., Виж Енчев В. и др. 537
Стефанов К., Виж Де Роса С. и др. 53
Стефанов П. К., Виж Цанев Ал. С. и др. 354
Стефанов П., Виж Гергова Д. и др. 232
Стефанов Яв., Ив. Вълчанова, Сн. Магаева, Цв. Добрев, Изследване на композитни покрития, предназначени за аноди при електроекстракция на цинк от сулфатни електролити 280
Стоилова О., Хр. Пенчев, Т. Русков, Ив. Спиров, Н. Манолова, Ил. Рашков, Едноетапно получаване на магнитни хитозанови сфери 497
Стойчев Д., Виж Гергова Д. и др. 232
Стойчев Д., Виж Луканова Р. и др. 347
Стойчев Д. С., Виж Цанев Ал. С. и др. 354
Стоянов С. С., Анг. Д. Попова, Й. Ан. Ценов, ИЧ спектри и структура на 3,5,5-триметил(циклохекс-2-енилиден) малононитрил и неговите калиево-цианидни и натриево-метоксидни карбанионни адукти. Експериментално и B3LYP изследване 545
Стоянов С. С., Виж Ценов Й. Ан. и др. 525
Стоянова Ем., Виж Гергова Д. и др. 232
Стоянова Ан. Р., В. Ц. Цакова, Електроокисление на глюкоза върху модифицирани с мед полианилинови слоеве в алкални разтвори 290
Стоянова Ан. Р., К. Бюес-Ерман, В. Ц. Цакова, Модифицирани с мед проводящи полимерни слоеве за електроанализ в неутрални разтвори 189
Стоянова Ем., Виж Луканова Р. и др. 347
Стоянова Ем., Съвременни аспекти в повърхностната обработка на алуминий 103
Табакова Т., В. Идакиев, Й. Папавасилиу, Г. Авгуропулос, Т. Йоанидес, Влияние на метода на получаване върху активността в реакцията на конверсия на CO с водна пара на катализатори CuO/дотиран CeO_2 47
Тимчева Ил. И., Виж Иванова Д. И. и др. 444
Топалова Ин., Виж Райчевски Г. М. и др. 285
Тренев В., Виж Младенов М. и др. 366
Трифонова Ат. В., Модифицирана въглеродна матрица – високоенергиен анод за литиево-йонна батерия 226
Троев, К. Виж Крайчева Ив. и др. 58
Тумбалева Я., Виж Фачиков Л. и др. 359
Тюркилмаз М., Виж Гавазов К. Б. и др. 69
Фархи О. А., Виж Янев Ян. С. и др. 332
Фачиков Л., Я. Тумбалева, Д. Иванова, Фосфатиране на желязовъглеродни сплави в модифицирани цинкови препарати 359
Хампдем-Смит М., Виж Петров К. и др..... 339

Хари Бабу Б., Б. Вену Бабу, Ч. Мохан, К. Нага Раджу, Синтез и биологична активност на 6-ал-кокси/арил/арилокси-4,8-ди(трет-бутил)2,10-диметил-12*H*-6λ^5-дибензо[d,g][1,3,2]ди-окса-фосфоцин-6-они/тиони/селенони 165
Хорозова Е., Т. Додевска, Н. Димчева, Модифицирани графитови електроди като катализатори за електроредукция на водороден

ствие на микровълни в отсъствие на разтворители 417
азоли
Връзка между параметри на химичната структура и степента на корозионна защита на някои 305
активен въглен,
гранулиран, от костилки на фурми. Отстраняване на фенол с..... 35
Получаване на наноразмерни частици от TiO_2 нанесени върху 113
Получаване на, от бамбук за извличане на As(III) от водни разтвори 172
активност
антиоксидантна, Прекъсваща веригите, на нови халкони от прополис от Ел Салвадор в хомогенна и мицеларна среда 555
Електрокаталитична, на електрохимично отложени Zr-Ce-Y/Ni и Co/Zr-Ce-Y/Ni оксидни системи при отделянето на водород и кислород 354
алуминиев оксид
и цериев оксид, електроотложени, Влияние на термичната обработка на, върху пасивното състояние на неръждаема стомана ОС4004 в кисели среди 232
алуминий
Съвременни аспекти в повърхностната обработка на 103
Формиране на защитни филми върху, от несъдържащи Cr^{6+} електролити 347
амиди
N,N-диметилканелени, *Ab initio* SCF изследване на бариера на вътрешна ротация в 531
аминолиза
на фенилацетат. Теоретично изследване на механизма на 408
5-амино-2-метоксипиридин естер амид
на етиловия естер на квадратната киселина. Поларизационно ИЧ-спектрално изследване на високотемпературната “червена” фаза на 482
анти-β-аминонитрили
Стереоконтролирана вътрешномолекулна циклизация на,. Удобна синтеза на *транс*-азетидин-2-имини 571
N-[(4-аминофенил)сулфонил]ацетамид
(сулфацетамид) и неговия азанион. Теоретично изследване на конформационните предпочитания на 449
α-аминофосфорна киселина
Синтез в един реактор и антимикробна активност на нов клас естери на 64
анализ
Молекулно-механичен (ММ3(π)) конформационен, на молекули съдържащи спрегнати π-електронни фрагменти: молекулна пинсета 511
на ракови биологични проби. Приложение на дифузионно подредена спектроскопия за 468
на смеси с помощта на библиотека от инфра червени спектри. Реализиране и про верка на рутинна процедура за 560
анод
високоенергиен, за литиево-йонна батерия. Модифицирана въглеродна матрица –..... 226
аноди
при електроекстракция на цинк от сулфатни електролити. Изследване на композитни покрития, предназначени за 280
анодни филми
върху ниобий, Изследване със сканираща електронна микроскопия 266
оксидни, върху волфрам. Влияние на pH на електролита върху механизма на проводимост на 276
аскорбинова киселина
Прост и валидиран спектрофотометричен метод за определяне на 108
атомно-силова микроскопия
Изследвания на повърхностната морфология на електролитно отложени Ag-In покрития чрез оптична, сканираща електронна и 260
ацикличен смесен (O,S) ацетал
Как да синтезираме един? Подход на физичната органична химия 146
багрила
съдържащи връзката B–N. Изчислително моделиране на електронните спектри на някои... 455
N-бензаланилин-15-краун-5
Изследване с методите *ab initio* и ТФП на структурата на комплекси на, с метални йони 537
бензен
фотокаталитично разлагане на, Роля на окислителния агент при, и неговото влияние върху кинетиката и механизма на адсорбция 121
биологична активност
Синтез и, на 6-алкокси/арил/арилокси-4,8-ди(трет-бутил)2,10-диметил-12*H*-6λ^5-дибензо[d,g][1,3,2]ди-оксафосфоцин-6-они/тиони/селенони 165
биологично активни полимери
и носители на лекарства. Поли(оксиетилен аминофосфонат)и – нови перспективни. Дизайн и ЯМР спектроскопска характеристика 58
биоматериали
Синтез и характеризиране на нов наноструктуриран въглен за суперкондензатори на основата на 366
биосензори
Амперометрични 210
борхидриди
алкални, Електроокисление на, върху метал хидридни електроди 309
бромамин-Т
Кинетика и механизъм на окисление на пиразинамид с, в среда на перхлорна киселина . 143
ванадий(V)
Екстракционно-спектрофотометрични изслед-

вания на тройни йонно-асоциирани комплекси между анионния хелат на, с 4-(2-пиридилазо)-резорцин и някои метоксибис(тетразолиеви) катиони 69
водород
и кислород. Електрокаталитична активност на електрохимично отложени Zr-Ce-Y/Ni и Co/Zr-Ce-Y/Ni оксидни системи при отделянето на 354
Проникване на, в Ni слоеве отложени от Уотсов електролит 243
Синтез и охарактеризиране на електрохимично отложени нови материали катализиращи отделянето на 218
водороден пероксид
Модифицирани графитови електроди като катализатори за електроредукция на 239
Водородно свързване
в йонни системи на 1,5,7-триазабицикло[4.4.0] дец-5-ен с 4-цианофенол. Изследвания на структурите им с методите *ab initio* и ТФП 425
системи между пиридин-3-карбоксамид (никотинамид) и ДМСО. Теоретично изследване на структури и стабилност на 432
волфрам
Влияние на pH на електролита върху механизма на проводимост на анодните оксидни филми върху 276
въглен
нов наноструктуриран, за суперкондензатори на основата на биоматериали. Синтез и характеризиране на 366
въглеродна матрица
Модифицирана, – високоенергиен анод за литиево-йонна батерия 226
вътрешномолекулна циклизация
Стереоконтролирана, на *анти*-β-аминонитрили. Удобна синтеза на *транс*-азетидин-2-имини 571
галванични покрития
и конверсионни филми. Електрохимични методи за оценка на защитната способност на ... 203
гем-диметил ефект
(гем-диалкил ефект). Линейни зависимости на свободните енергии на 396
глицил-L-триптофан дихидрат (H-Gly-Trp-OH.2H_2O)
L-триптофил-L-метионин (H-Trp-Met-OH) и L-метионил-L-триптофан (H-Met-Trp-OH).
Твърдотелна линейно-дихроична ИЧ спектроскопия на L-триптофан-съдържащи дипептиди 463
глюкоза
Електроокисление на, върху модифицирани с мед полианилинови слоеве в алкални разтвори 290
графит
Родиеви отложения върху: Влияние на графитовата подложка върху електрокаталитичната активност при електро-окисление на мравчена киселина 136
графитови електроди
Модифицирани, като катализатори за електроредукция на водороден пероксид 239
двоен катализаторен слой
Организиране на, при работа с ниска начална концентрация на реагента. Изследване на възможностите на накаляван при специални условия конвенционален катализатор О 4-25 за окисление на *о*-ксилол до фталов анхидрид. Част 2..... 18
дипептиди
Твърдотелна линейно-дихроична ИЧ спектроскопия на L-триптофан-съдържащи, L-триптофил-L-метионин (H-Trp-Met-OH), L-метионил-L-триптофан (H-Met-Trp-OH) и глицил-L-триптофан дихидрат (H-Gly-Trp-OH.2H_2O) 463
дифузионно подредена спектроскопия
Приложение на, за анализ на ракови биологични проби 468
3,4-дихидропиримидин-2-(1H)-они
Комплекси на включване на, с β-циклодекстрин..... 41
електроанализ
в неутрални разтвори. Модифицирани с мед проводящи полимерни слоеве за 189
електроди
газодифузионни, Използване на, в алкален електролит за определяне активността на катализатори в полимерен електролит .. 339
графитови, Модифицирани, като катализатори за електроредукция на водороден пероксид 239
метал хидридни, Електроокисление на алкални борхидриди върху 309
електроекстракция
на цинк от сулфатни електролити. Изследване на композитни покрития, предназначени за аноди при 280
електролизни процеси
Математическо моделиране на. 329
електролит
алкален, за определяне активността на катализатори в полимерен електролит. Използване на газодифузионни електроди в 339
полимерен, Използване на газодифузионни електроди в алкален електролит за определяне активността на катализатори в 339
електролити
несъдържащи Cr^{6+}, Формиране на защитни филми върху алуминий от 347
електролитно отлагане
Ag-In покрития, Изследвания на повърхностната морфология на, чрез оптична, сканираща електронна и атомно-силова микроскопия .. 260
Електролитно отлагане
на сребърно-кобалтови покрития 253

електронни спектри
на някои багрила, съдържащи връзката B–N. Изчислително моделиране на 455
структура и нелинейни оптични свойства на пиридин-бетаините на квадратната киселина. Теоретично изследване на, ... 504
електроовлакняване
Получаване на нови хитозан-съдържащи микро- и нановлакнести материали чрез 476
Електроокисление
на алкални борхидриди върху метал хидридни електроди 309
на глюкоза върху модифицирани с мед полианилинови слоеве в алкални разтвори ... 290
на мравчена киселина. Родиеви отложения върху графит: Влияние на графитовата подложка върху електрокаталитичната активност при 136
електроредукция
на водороден пероксид. Модифицирани графитови електроди като катализатори за 239
електрохимични изследвания
и Корозионни, на нисколегирани и аустенитни неръждаеми стомани използвани в парогенераторите на АЕЦ „Козлодуй“ 285
Електрохимични методи
за оценка на защитната способност на галванични покрития и конверсионни филми 203
електрохимични отнасяния
Корозионно-, на зол-гелни хибридни покрития 299
Електрохимични процеси
в магнитно поле 197
електрохимично отлагане
Zr-Ce-Y/Ni и Co/Zr-Ce-Y/Ni оксидни системи, Електрокаталитична активност на, при отделянето на водород и кислород 354
на нови материали катализиращи отделянето на водород. Синтез и охарактеризиране 218
енаминонитрилен фрагмент
Приложимост на, в хетероциклени синтези . 159
естери
нов клас, на α-аминофосфорната киселина. Синтез в един реактор и антимикробна активност на 64
защитни филми
върху алуминий от несъдържащи Cr^{6+} електролити. Формиране на, ... 347
импелер с наклонени лопатки
Влияние на формата на, върху характеристиките на смесване и аерация в съдове с разбъркване 177
1H-индол-2,3-дион (изатин)
Експериментално и DFT изследване на ИЧ спектрални и структурни промени произтичащи от превръщането на, в азанион 439
инсталации
за очистване на серен диоксид от отпадни газове, „ELCOX“ лабораторна и пилотна: оптимизационни и промишлени изпитания в медодобивен завод „Пирдоп“ 128
инфрачервени спектри
библиотека от, Реализиране и проверка на рутинна процедура за анализ на смеси с помощта на 560
Инхибиторна композиция
на базата на полимери и неорганични соли за защита на стомана от корозия във водни системи 247
ИЧ спектри
и структура на 3,5,5-триметил(цикло-хекс-2-енилиден) малононитрил и неговите калиево-цианидни и натриево-метоксидни карбанионни адукти. Експериментално и B3LYP изследване 545
йонни системи
Водородно свързване в, на 1,5,7-триазабицикло [4.4.0]дец-5-ен с 4-цианофенол. Изследвания на структурите им с методите *ab initio* и ТФП 425
карбанион
Експериментални ИЧ и теоретични *ab initio* ХФ и ТФП B3LYP изследвания на спектралните и структурните промени, причинени от превръщането на метилцианоацетата в 519
карбанионни адукти
ИЧ спектри и структура на 3,5,5-триметил (цикло-хекс-2-енилиден) малононитрил и неговите калиево-цианидни и натриево-метоксидни,. Експериментално и B3LYP изследване 545
катализатор
конвенционален, О 4-25, за окисление на *о*-ксилол до фталов анхидрид. Изследване възможностите на накаляван при специални условия. Част 1. Накаляване и работни характеристики на катализатора 12
катализаторен слой
Особености на, при работа с високи начални концентрации на реагента. Изследване на възможностите на накален при специални условия конвенционален катализатор О 4-25 за окисление на *о*-ксилол до фталов анхидрид. Част III. 25
катализатори
Ni-Mo-W, електроотложени, Окисление на сулфиди върху 294
в полимерен електролит. Използване на газодифузионни електроди в алкален електролит за определяне активността на 339
за електроредукция на водороден пероксид. Модифицирани графитови електроди като 239
квадратна киселина
Поляризационно ИЧ-спектрално изследване на високотемпературната “червена” фаза на 5-амино-2-метоксипиридин естер амид на етиловия естер на 482
квадратна киселина
Спектрално охарактеризиране на хидроген-скварат и естер амид на, с 2-хлор-3-амино-

окисление
на *о*-ксилол до фталов анхидрид. Изследване възможностите на накаляван при специални условия конвенционален катализатор О 4-25 за, . Част 1. Накаляване и работни характеристики на катализатора 12
на пиразинамид с бромамин-Т в среда на перхлорна киселина Кинетика и механизъм на 143
на сулфиди върху електроотложени Ni-Mo-W катализатори 294
пептидази
хранителни, Растенията от сем. Brassicaceae като източник на 400
пиразинамид
Кинетика и механизъм на окисление на, с бромамин-Т в среда на перхлорна киселина 143
4-(2-пиридилазо)-резорцин
Екстракционно-спектрофотометрични изследвания на тройни йонно-асоциирани комплекси между анионния хелат на ванадий(V) с, и някои метоксибис(тетразолиеви) катиони ... 69
пиридилизоксазол-5-они
Синтез и реактивоспособност на някои 77
пиридин-3-карбоксамид (никотинамид)
и ДМСО. Теоретично изследване на структури и стабилност на водородно-свързани системи между 432
пиридин-бетаините
на квадрат-ната киселина. Теоретично изследване на структурата, електронните спектри и нелинейните оптични свойства на 504
покрития
електролитно отложени Ag-In, Изследвания на повърхностната морфология на, чрез оптична, сканираща електронна и атомно-силова микроскопия 260
сребърно-кобалтови, Електролитно отлагане на 253
хибридни, зол-гелни, Корозионно-електрохимични отнасяния на 299
Поларизационна ИЧ
-спектрално изследване на високотемпературната “червена” фаза на 5-амино-2-метокси-пиридин естер амид на етиловия естер на квадратната киселина 482
Поли(оксиетилен аминофосфонат)и
– нови перспективни биологично активни полимери и носители на лекарства. Дизайн и ЯМР спектроскопска характеристика 58
полизахариди
пектинови, от праз получени чрез последователно екстрахиране с различни реагенти. Характеризиране на 567
праз
Характеризиране на пектинови полизахариди от, получени чрез последователно екстрахиране с различни реагенти 567
преобразовател
Микроконтролерен, на ниво на корозия с токов изход 332
проводимост
на анодните оксидни филми върху волфрам. Влияние на pH на електролита върху механизма на 276
проводящи полимерни слоеве
Модифицирани с мед, за електроанализ в неутрални разтвори 189
прополис
от Ел Салвадор, Прекъсваща веригите антиоксидантна активност на нови халкони от, в хомогенна и мицеларна среда 555
Растения
от сем. Brassicaceae като източник на хранителни пептидази 400
Родий
отложения върху графит: Влияние на графитовата подложка върху електрокаталитичната активност при електро-окисление на мравчена киселина 136
CuO
/дотиран CeO_2. Влияние на метода на получаване върху активността в реакцията на конверсия на CO с водна пара на катализатори . 47
свободни енергии
на гем-диметил ефекта (гем-диалкил ефекта) Линейни зависимости на 396
серен диоксид
очистване на, от отпадни газове. „ELCOX“ лабораторна и пилотна инсталации за : оптимизационни и промишлени изпитания в медодобивен завод „Пирдоп“ 128
синтез
Едностадиен, на симетрични азини под действие на микровълни в отсъствие на разтворители 417
и биологична активност на 6-алкокси/арил/арилокси-4,8-ди(трет-бутил)2,10-диметил-12*H*-6λ^5-дибензо[d,g][1,3,2]ди-оксафосфоцин-6-они/тиони/селенони 165
и охарактеризиране на електрохимично отложени нови материали катализиращи отделянето на водород 218
и реактивоспособност на някои пиридилизоксазол-5-они 77
и характеризиране на нов наноструктуриран въглен за суперкондензатори на основата на биоматериали 366
синтеза
Удобна, на *транс*-азетидин-2-имини. Стереоконтролирана вътрешномолекулна циклизация на *анти*-β-амино-нитрили 571
синтези
хетероциклени. Приложимост на енаминонитрилен фрагмент в 159
сканираща електронна микроскопия
Изследване на анодни филми върху ниобий със 266

смесване и аерация
в съдове с разбъркване. Влияние на формата на импелер с наклонени лопатки върху характеристиките на 177
спектрофотометричен метод
Прост и валидиран, за определяне на аскорбинова киселина 108
сплави
желязовъглеродни, Фосфатиране на, в модифицирани цинкови препарати 359
стомана
защита на, от корозия във водни системи. Инхибиторна композиция на базата на полимери и неорганични соли за 247
неръждаема, ОС4004 в кисели среди. Влияние на термичната обработка на електроотложени алуминиев и цериев оксиди върху пасивното състояние на 232
стомани
неръждаеми, нисколегирани и аустенитни, използвани в парогенераторите на АЕЦ „Козлодуй“. Корозионни и електрохимични изследвания на 285
ниско-въглеродна и нисколегирана, Сравнение на склонността към корозионно напукване на, във фосфатни среди 322
сулфиди
Окисление на, върху електроотложени Ni-Mo-W катализатори, ... 294
суперкондензатори
на основата на биоматериали. Синтез и характеризиране на нов наноструктуриран въглен за 366
Теоретично изследване
на конформационните предпочитания на N-[(4-аминофенил)сулфонил]ацетамид (сулфацетамид) и неговия азанион 449
на структурата, електронните спектри и нелинейните оптични свойства на пиридин-бетаините на квадратната киселина 504
на структури и стабилност на водородно-свързани системи между пиридин-3-карбоксамид (никотинамид) и ДМСО 432
3,5,5-триметил(цикло-хекс-2-енилиден) малононитрил
и неговите калиево-цианидни и натриево-метоксидни карбанионни адукти. ИЧ спектри и структура на, Експериментално и B3LYP изследване 545
L-триптофан
-съдържащи дипептиди L-триптофил-L-метионин (H-Trp-Met-OH), L-метионил-L-триптофан (H-Met-Trp-OH) и глицил-L-триптофан дихидрат (H-Gly-Trp-OH.2H_2O). Твърдотелна линейно-дихроична ИЧ спектроскопия на .. 463
L-триптофил-L-метионин (H-Trp-Met-OH),
L-метионил-L-триптофан (H-Met-Trp-OH) и глицил-L-триптофан дихидрат (H-Gly-Trp-OH.2H_2O). Твърдотелна линейно-дихроична ИЧ спектроскопия на L-триптофан-съдържащи дипептиди 463
ТФП
B3LYP и *ab initio* ХФ изследвания, Експериментални ИЧ и теоретични, на спектралните и структурните промени, причинени от превръщането на метилцианоацетата в карбанион 519
Водородно свързване в йонни системи на 1,5,7-триазабицикло[4.4.0]дец-5-ен с 4-цианофенол. Изследвания на структурите им с методите *ab initio* и 425
Изследване с методите *ab initio* и, на структурата на комплекси на N-бензаланилин-15-краун-5 с метални йони 537
изследване, Експериментално и, на ИЧ спектрални и структурни промени произтичащи от превръщането на 1H-индол-2,3-дион (изатин) в азанион 439
Уотсов електролит
Проникване на водород в Ni слоеве отложени от 243
фенилацетат
Теоретично изследване на механизма на аминолизата на 408
фенол
Отстраняване на, с гранулиран активен въглен от костилки на фурми 35
флуоресцентни характеристики
и Абсорбционни, в УВ-видимата област на някои заместени в стирилния фрагмент синтетични халкони 444
Фосфатиране
на желязовъглеродни сплави в модифицирани цинкови препарати 359
фотокаталитично
разлагане на бензен и неговото влияние върху кинетиката и механизма на адсорбция. Роля на окислителния агент при 121
фталов анхидрид
Изследване възможностите на накаляван при специални условия конвенционален катализатор О 4-25 за окисление на *о*-ксилол до . Част 1. Накаляване и работни характеристики на катализатора 12
халкони
нови, от прополис от Ел Салвадор, Прекъсваща веригите антиоксидантна активност на, в хомогенна и мицеларна среда 555
синтетични. Абсорбционни и флуоресцентни характеристики в УВ-видимата област на някои заместени в стирилния фрагмент 444
хибридни покрития,
нанокомпозитни, Изследвания върху корозионно-защитната способност на 317
хидрогенскварат
Спектрално охарактеризиране на, и естер амид на квадратната киселина с 2-хлор-3-аминопиридин 490

хитозан
-съдържащи микро- и нановлакнести материали, Получаване на нови, чрез електроовлакняване 476
хитозанови сфери
магнитни, Едноетапно получаване на 497
2-хлор-3-аминопиридин
Спектрално охарактеризиране на хидрогенскварат и естер амид на квадратната киселина с 490
цериев диоксид
дотиран. Влияние на метода на получаване върху активността в реакцията на конверсия на CO с водна пара на катализатори CuO/ 47
цериев оксид
и алуминиев оксид, електроотложени, Влияние на термичната обработка на, върху пасивното състояние на неръждаема стомана ОС4004 в кисели среди 232
4-цианобензамид
ИЧ-спектрални и структурни промени, породени от превръщането на, в азанион. Комбиниран експериментално-теоретичен подход 525
β-циклодекстрин
Комплекси на включване на 3,4-дихидропиримидин-2-(1H)-они с 41
цинк
електроекстракция на, от сулфатни електролити. Изследване на композитни покрития, предназначени за аноди при 280

CONTENTS

Editorial …… 372

I. Binev, A. Popova, Ivan Nikolov Juchnovski – Biographical and professional data ……..…….. 373

I. B. Blagoeva, E. P. Ignatova-Avramova, A. Hadjikov, I. G. Pojarlieff, L. I. Proevska, V. T. Rachina, N. G. Vassilev, Linear free energy relationships of the gem-dimethyl (gem-dialkyl) effect …… 386

M. D. Marinova, B. P. Tchorbanov, Brassicaceae plants as a new source of food grade peptidases …. 397

S. Ilieva, Y. Atanasov, B. Galabov, Mechanism of the aminolysis of phenyl acetate: a computational study ……. 401

S. P. Simeonov, V. B. Kurteva, R. P. Bontchev, One-pot solvent-free synthesis of symmetrical azines under microwave irradiation …… 409

Y. Dimitrova, Hydrogen bonding in ionic systems of 1,5,7-triazabicyclo[4.4.0]dec-5-ene (TBD) with 4-cyanophenol: ab initio and DFT studies of their structures ……. 418

L. I. Daskalova, Y. Dimitrova, Theoretical study of structures and stability of hydrogen-bonded systems between pyridine-3-carboxamide (nicotinamide) and DMSO ……... 426

E. A. Velcheva, P. J. Vassileva-Boyadjieva, I. G. Binev, Experimental and DFT studies on IR spectral and structural changes arising from the conversion of 1H-indole-2,3-dione (isatin) into azanion …… 433

D. I. Ivanova, I. I. Timtcheva, B. A. Stamboliyska, D. I. Batovska, UV-VIS absorption and fluorescent characteristics of some substituted in the styril fragment synthetic chalcones …… 440

B. A. Stamboliyska, A. D. Popova, E. A. Velcheva, Theoretical study of the conformational preference of N-[(4-aminophenyl) sulphonyl]acetamide (sulphacetamide) and its azanion ……. 445

S. M. Bakalova, J. Kaneti, O. Castaño, Computational study of the electronic spectra of some B–N dyes …….. 450

B. B. Koleva, Solid-state IR-LD spectroscopy of L-tryptophan-containing dipeptides L-tryptophyl-L-methionine (H-Trp-Met-OH), L-methionyl-L-tryptophan (H-Met-Trp-OH) and glycyl-L-tryptophan dihydrate (H-Gly-Trp-OH.2H_2O) …… 456

G. I. Ivanova, E. J. Cabrita, R. O´Connor, A. J. Eustace, D. F. Brougham, Application of diffusion-ordered spectroscopy for the analysis of cancer related biological samples …… 464

M. G. Spasova, D. P. Paneva, N. E. Manolova, I. B. Rashkov, Preparation of novel chitosan-containing micro- and nanofibrous materials by electrospinning ……. 469

E. D. Cherneva, Ts. M. Kolev, Solid-state polarized IR-spectroscopic study of high temperature red phase of 5-amino-2-methoxypyridine ester amide of squaric acid ethyl ester …… 477

Ts. D. Tsanev, Ts. M. Kolev, Spectroscopic elucidation of hydrogensquarate and ester amide of squaric acid of 2-chloro-3-aminopyridine …… 483

O. Stoilova, H. Penchev, T. Ruskov, I. Spirov, N. Manolova, I. Rashkov, One-pot preparation of magnetic chitosan beads …….. 491

B. A. Stamboliyska, D. Y. Yancheva, Ts. M. Kolev, Theoretical investigation on the structure, electronic spectra and nonlinear optical properties of pyridinium-betaines of squaric acid …….. 498

M. I. Kotev, P. M. Ivanov, Molecular mechanics (MM3(π)) conformational analysis of molecules containing conjugated π-electron fragments: a molecular tweezer …….. 505

A. D. Popova, Y. I. Binev, P. J. Vassileva-Boyadjieva, I. G. Binev, Experimental IR, and computational ab initio and DFT B3LYP studies on spectral and structural changes, caused by the conversion of methyl cyanoacetate into carbanion ……. 512

J. A. Tsenov, S. S. Stoyanov, I. G. Binev, IR spectral and structural changes, caused by the conversion of 4-cyanobenzamide into azanion: a combined experimental/computational approach …… 520

N. G. Vassilev, Ab initio SCF study of the barrier to internal rotation in N,N-dimethylcinnamamides .. 526

V. Enchev, S. Angelova, N. Markova, V. Wawer, E. Stanoeva, M. Mitewa, Ab initio and DFT study of

В. Енчев, *С. Ангелова*, *Н. Маркова*, *Ив. Вавер*, *Ел. Станоева*, М. Митева, Изследване с методите ab initio и ТФП на структурата на комплекси на N-бензаланилин-15-краун-5 с метални йони 537
С. С. Стоянов, *Анг. Д. Попова*, *Й. Ан. Ценов*, ИЧ спектри и структура на 3,5,5-триметил(цикло-хекс-2-енилиден) малононитрил и неговите калиево-цианидни и натриево-метоксидни карбанионни адукти. Експериментално и B3LYP изследване 545
В. Д. Кънчева, *В. С. Банкова*, Прекъсваща веригите антиоксидантна активност на нови халкони от прополис от Ел Салвадор в хомогенна и мицеларна среда 555
П. Н. Пенчев, *В. Л. Митева*, *А. Н. Сохоу*, *Н. Т. Кочев*, *Г. Н. Андреев*, Реализиране и проверка на рутинна процедура за анализ на смеси с помощта на библиотека от инфрачервени спектри 560
М. Крачанова, *М. Гочева*, *Е. Павлова*, *Ир. Янакиева*, *Д. Неделчева*, *В. Късовски*, *А. Славов*, Характеризиране на пектинови полизахариди от праз получени чрез последователно екстрахиране с различни реагенти 567
Цв. Сп. Господова, *Ж. Р. Рашкова*, *Л. Зл. Витева*, Стереоконтролирана вътрешномолекулна циклизация на *анти*-β-амино-нитрили. Удобна синтеза на *транс*-азетидин-2-имини 571
Авторен указател 583
Предметен указател 587